



IEA
SOLAR R&D

INTERNATIONAL ENERGY AGENCY

**solar heating and
cooling programme**

TASK IX-

**Solar Radiation
and
Pyranometer Studies**

RECENT ADVANCES IN PYRANOMETRY

**S.M.H.I. NORRKOPING, SWEDEN
JANUARY 1984**

SYMPOSIUM PROCEEDINGS



Environment
Canada

Environnement
Canada

Atmospheric
Environment
Service

Service
de l'environnement
atmosphérique

Canada

Task IX
Solar Radiation and Pyranometry Studies

RECENT ADVANCES IN PYRANOMETRY

Swedish Meteorological and Hydrological Institute

Norrköping, Sweden

January 1984

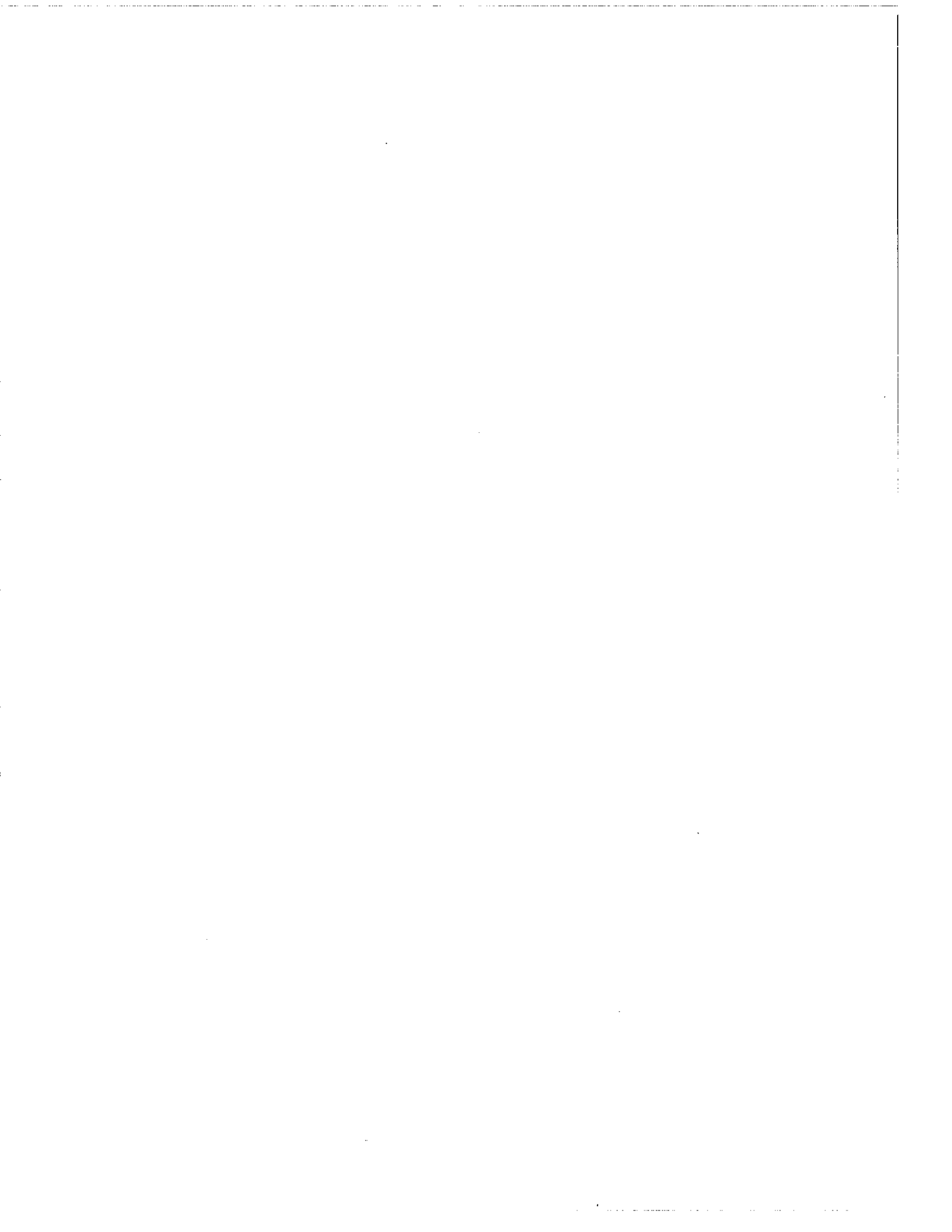
Symposium Proceedings

Edited by D.I. Wardle & D.C. McKay
Atmospheric Environment Service
Canada

Additional copies may be obtained from:

Atmospheric Environment Service
4905 Dufferin Street
Downsview, Ontario
CANADA
M3H 5T4

Price: \$15.00 Cdn.



PREFACE

In March 1981 a group of pyranometry experts met in Boulder, Co., USA to address the problem of accurate irradiance measurements required for the performance testing of solar collectors. From that meeting it became clear that a more complete and detailed characterization study of pyranometers used for solar collector performance testing was necessary to achieve the desired accuracy in the irradiance measurements.

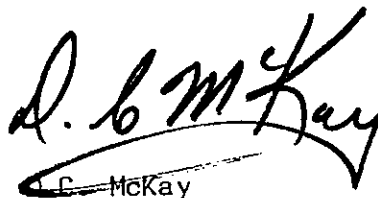
To undertake this pyranometer characterization the IEA Solar Heating and Cooling Program established in 1982 a new Task, Task IX, Solar Radiation and Pyranometry Studies with one of its mandates to demonstrate improvements in irradiance measurements for solar collector testing that can be achieved with detailed characterization of pyranometer responsiveness.

In January 1984 twenty-three pyranometry experts representing government, universities and manufacturers took part in a symposium in Norrköping, Sweden to review progress in the subject of pyranometry that had been achieved since the USA meeting. The report presents papers given at the symposium, the results of the various discussions and a list of the major areas where further research is needed.

The coordinators would like to take this opportunity to thank all those who took part in the symposium and made it a success. Special thanks are due to Dr. L. Dahlgren and his organization, the Swedish Meteorological and Hydrological Institute for hosting the symposium. Una Ellis and Krystyna Czaja of the Atmospheric Environment Service meticulously maintained a high quality in the text and diagrams of this volume. Their work is very gratefully acknowledged.



D.I. Wardle



D. B. McKay



EXECUTIVE SUMMARY

From January 23 to 25, 1984 a pyranometry symposium sponsored by the IEA Solar Heating and Cooling Programme Task IX was held in Norrköping, Sweden. The purpose of the symposium was to review progress in the subject of pyranometry that had been achieved since the last IEA pyranometry meeting held in the United States of America in 1981 and to plan for the future.

The objective set out to be addressed by the participants were:

- to review current practices in pyranometry in the context of requirements for solar energy development;
- to consolidate recent work sponsored by the IEA and others;
- to identify those areas of pyranometry most in need of further research and development.

To meet these objectives the symposium was organized into six sessions which covered the following topics:

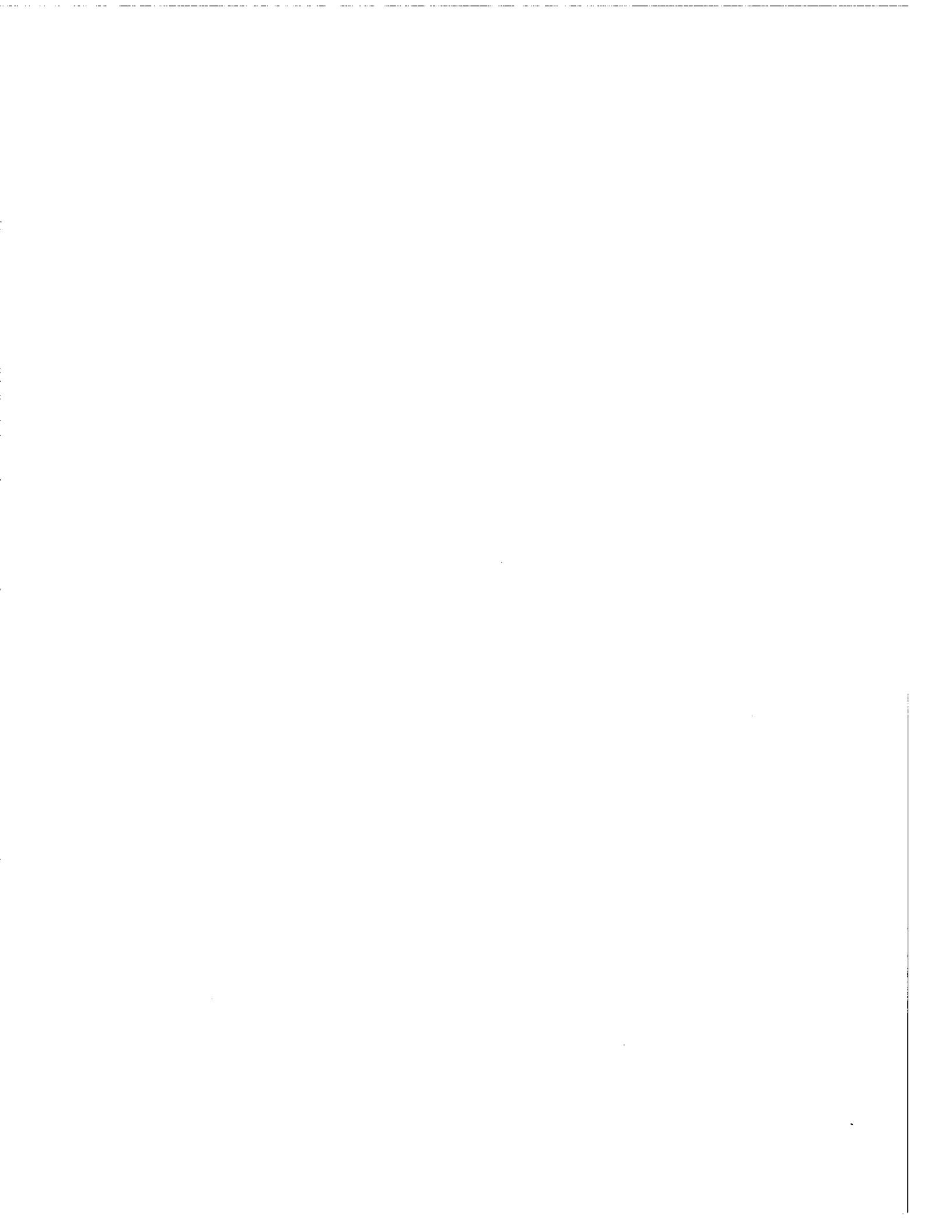
- Session 1** Operational Practices in National Networks
- Session 2** Laboratory Characterization: methods and intercomparisons of results
- Session 3** Physics of Pyranometers
- Session 4** Field Characterization
- Session 5** Field Performance and Accuracy
- Session 6** General Discussion

In total twenty presentations were given within the first five sessions.

At the end of the symposium the following major areas of need were indicated:

- a better understanding of the physics of pyranometers;
- a mechanism for relating field tests to laboratory tests;
- clear and precise documentation of calibration procedures and results, including a common formatting for reporting;
- a set of guidelines in the use of pyranometers which can be used by the solar energy engineer.

All the above areas are being addressed by the Task IX experts and it is the intent to have the needs fulfilled at the end of the Task.



SYMPOSIUM PROCEEDINGS

Session 1 Operational Practices in National Networks Chairman: D.C. McKay

	<u>Page</u>	
1.A A. Zelenka	13	The Swiss Automatic Network (including calibration transfer).
1.B O. Motschka and E. Wessely	15	The Austrian Radiation Network
1.C D.I. Wardle	23	The Canadian Radiation Network
1.D J.H. Seymour	35	Recent work in the UK Radiation Network
1.E W. Josefsson	41	The Solar Radiation Measuring Program in Sweden

Session 2 Laboratory Characterization Chairman: L. Dahlgren

2.A P.-M. Nast	51	Methods for determination of sensitivity and angle dependence at DFVLR Stuttgart
2.B B. Petersen and G.J. van den Brinke	57	Calibration and comparison of pyranometers
2.C K. Dehne	61	Tilt effect on pyranometers: A Review
2.D L. Liedquist	65	Pyranometer characterization measurement methods at the Statens Provingsanstalt, Borås and results from the IEA measurements in Borås 1982.
2.E L.F. van Wely and G.J. van den Brinke	95	Presentation of some of the IEA Instrument characteristics
2.F L.F. van Wely and G.J. van den Brinke	107	Manufacturer's indoor calibration procedure on the Kipp and Zonen CM 11
2.G H.D. Talarek	117	Indoor and Outdoor Pyranometer comparisons

Session 3 Physics of Pyranometers: ageing, ventilation, manufacturing techniques, etc.
Chairman: H.E.B. Andersson

	<u>Page</u>	
3.A P.M. Nast	123	Measurements of transients: irradiance, temperature, ageing
3.B Y. Miyake	129	New thermal model of the pyranometer and its characteristics
3.C J.R. Hickey, A.R. Karoli R.G. Frieden	137	Self-calibration cavity radiometers at the Eppley Laboratory: capabilities and applications
3.D O. Motschka	151	Time variability of angular dependence of a pyranometer: error estimation and test equipment
3.E C.V. Wells	157	An ageing test for pyranometers - a proposal

Session 4 Field Characterization
Chairman: D.C. McKay

4.A C. Frohlich	163	The need for characterization of pyranometers
4.B D.V. Barton D.I. Wardle	171	An investigation of the stability, accuracy and linearity of an Epply Normal Incidence Pyrheliometer based on a field comparison with a cavity radiometer
4.C G. Zerlaut	181	The New River intercomparisons of absolute cavity pyrheliometers, (NRIP I-VI)

Session 5 Field Performance and Accuracy
Chairman: H.E.G. Andersson

5.A G. Zerlaut G.D. Maybee	193	The intercomparison of pyranometers at horizontal, 45° tilt and normal incidence
5.B A. Zelenka	217	Accuracy checks on pyranometers in the Swiss ANETZ network

	<u>Page</u>	
5.C E. Flowers	221	Solar radiation measurements
5.D L. Dahlgren	251	Some examples of field evaluation of pyranometers
5.E J.L. Plazy R. Coudert M. Gregoire J. Olivieri	255	Comparison of standard pyranometers of EEC member countries
5.F D. Lala	269	Photochemical measurements of ultra-violet solar radiation
5.G B. Karlsson	285	Correlation between the performance of a concentrating collector and the direct radiation derived from pyranometric measurements

Session 6 General Discussion
 - requirements for further research
 - Task IX pyranometry work plan
 Chairman: D.I. Wardle

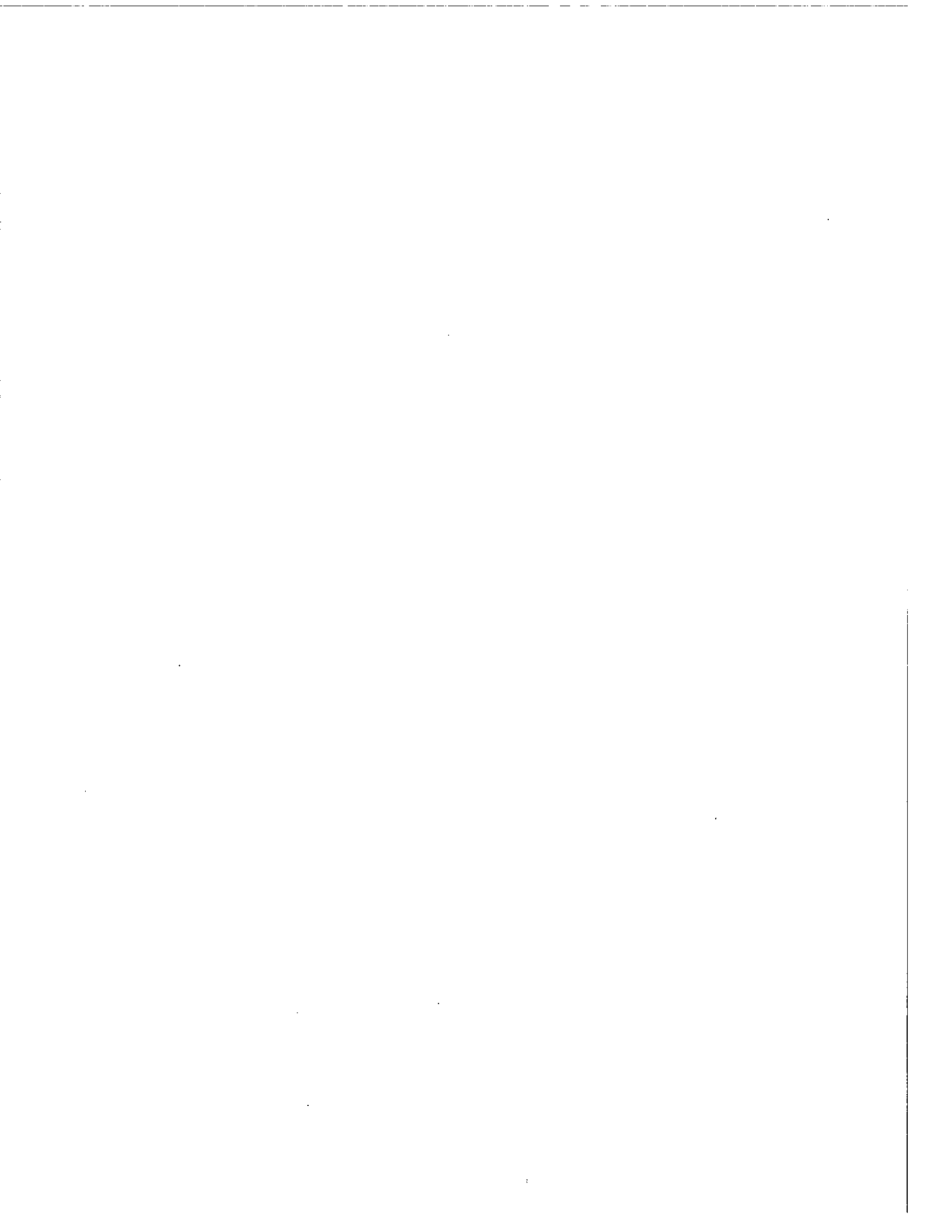
6.A D.C. McKay	295	Summary of the discussion
6.B E. Flowers	299	An open letter on pyranometry calibration

Written contributions on current status, etc.

6.C K. Dehne	317
6.D F. Kasten	319
6.E Y. Miyake	321
6.F B. Petersen	323
6.G C.A. Velds	325

Extra Contributions

7.A P.M. Nast	329	Outdoor and laboratory transient response of the Epply PSP - a short note
7.B K. Dehne R. Trapp	335	Preliminary report on the results of the first test loop of four pyranometers within IEA Task IX
7.C G.J. van den Brink	371	Preliminary presentation of characteristics of IEA pyranometers



Dr. Jean-Louis Plazy
Agence Francaise pour Maitrise de l'Energie
Route des Lucioles
Sophia - Antipolis
F - 06565 Valbonne, Cedex
France

Telex. 461357 F+

F.R. GERMANY

Dr. Klaus Dehne
Deutscher Wetterdienst
Meteorologisches Observatorium Hamburg
Frahredder 95
D-2000 Hamburg 65
F.R. Germany
Tel. 040-6017924

Telex. 02162912 DWSA D

Dr. F. Kasten
Deutscher Wetterdienst
Meteorologisches Observatorium Hamburg
Frahredder 95
D-2000 Hamburg 65
F.R. Germany
Tel: 040-6017096

Telex. 02162912 DWSA D

Dr. Erwin Memmert
D.I.N.
Burggrafenstrasse 4-7
D-1000 Berlin 30
F.R. Germany
Tel: 030-2601350

Telex. 184273 dna d

Dr. H.D. Talarek
Solar Energy Branch/IKP
Kernforschungsanlage Jülich
Postfach 1913
D170 Jülich
F.R. Germany
Tel: 02461/61-4640

Telex. 833 556 kfa d

Dr. P.-M. Nast
DFVLR
Pfaffenwaldring 38-40
D-7000, Stuttgart 80
F.R. Germany
Tel: 711 783485/429

Telex. 7255689 dfvs

ITALY

Prof. Salvatore Barbaro
Istituto Fisica Technical
Fac. Ingegneria
Dell'Universita
Viale Delle Scienze
90128 Palermo
Italy
Tel: 091/488780

Telex. 910235 Facing

JAPAN

Mr. Y. Miyake
EKO Instruments Trading Co. Ltd.
21-8 Hatagaya 1 Chome
Shibuya-Ku 151, Tokyo
Japan
Tel: (03)469-4511-6

Telex. EKOTRA J25364

NETHERLANDS

Dr. C.A. Velds
Royal Netherlands Meteorological Institute
P.O. Box 201
3730 AE De Bilt
Netherlands
Tel: (030)766911

Telex. 47067 nl

Dr. Gert-Jaap Van den Brink
Institute of Applied Physics, TNO-IH
P.O. Box 155
2600 A.D. Delft
Netherlands
Tel: (015)787113

NORWAY

Dr. Jan Olseth
Geofysisk Institut
Avd. B
Universitetet i Bergen
Bergen, Norway
Tel: 05-320040-2892

SWEDEN

Dr. Lars Dahlgren
Swedish Meteorological and Hydrological Institute
S-60176 Norrköping
Sweden
Tel: 11/158186

Telex. 644 00 smhi S

Mr. Weine Josefsson
Swedish Meteorological and Hydrological Institute
S-60176 Norrköping
Sweden
Tel: 11/158000 Telex. 644 00 smhi S

Dr. Hans E.B. Andersson
Swedish Council for Building Research
St. Göransgatan 66
S-11233, Stockholm
Sweden
Tel: 8/540640 Telex. 10398 bfr s

Mr. Leif Liedquist
National Testing Institute
Box 857
S-50115, Borås
Sweden
Tel: 033/165000/5448 Telex. 36252 testing S

Dr. Darwish Lala
The National Swedish Institute for Building Research
Box 785
S-80129, Gävle
Sweden
Tel: 026-100220

Dr. Björn Karlsson
Swedish State Power Board
Alvkarlebylaboratoriet
S-81071, Alvkarleby
Sweden
Tel: 026-72300

SWITZERLAND

Dr. A. Zelenka
Schweiz. Meteorologische Zentralanstalt
Krähbühlstrasse 58
CH-8044 Zürich
Schweiz
Tel: 01-2569376 Telex. 52202 metzuch

Dr. C. Fröhlich
World Radiation Centre/PMOD
Dorfstrasse 33
Postfach 173
CH 7260 Davos Dorf
Switzerland
Tel: 183/52131 Telex. 74732 pmod ch

UNITED KINGDOM

Mr. J. Seymour
UK Meteorological Office
Headquarters Annex, Room T21
Eastern Road, Bracknell, Berks RG12 2UR
UK
Tel: 344 20242 ex 2538 Telex. 84160

UNITED STATES

Mr. E.C. Flowers
NOAA
Solar Radiation Facility
325 Broadway
Boulder, CO. 80803
U.S.A.
Tel: 303 497-6662

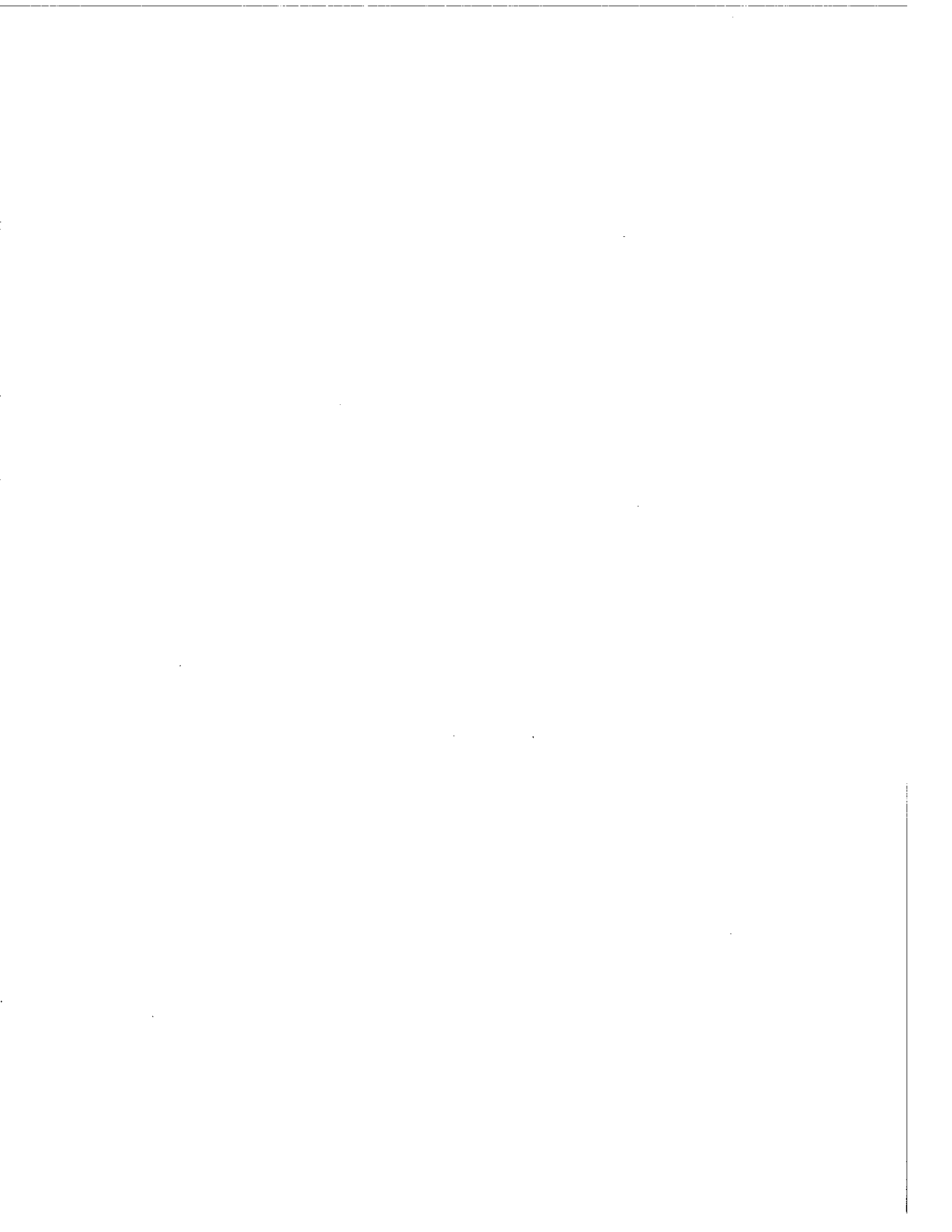
Mr. Chester V. Wells
Renewable Resources Assessment and Instrument Branch
Bldg. 16/3 Branch 215
Solar Energy Research Institute
1617 Cole Boulevard
Golden, CO. 80401
U.S.A.
Tel: 303 231-1981 Telex. 910 937-0738
wlsogglrn

Mr. G. Zerlaut
DSET Laboratories, Inc.
Box 1850
Black Canyon Stage
Phoenix, Arizona 85029
U.S.A.
Tel: 602 465-7356 Telex. 910-950-4681
DSET PHX



SESSION 1

Operational Practices in National Networks



1.A THE SWISS AUTOMATIC NETWORK

A. Zelenka

Swiss Meteorological Institute, Zurich

THE SWISS AUTOMATIC NETWORK

The Swiss Meteorological Institute operates a network (ANETZ) comprising 61 automatic stations, most of which (59) record 15-25 elements including global horizontal irradiation over 10 minute intervals.

The mean spatial coverage is one station per 680 km², corresponding to a mean grid of 26 km x 26 km. Altitudes range from 197 m to 3580 m above sea level.

Each station is equipped with a ventilated Kipp and Zonen CM6 pyranometer. The interface, command and transmission unit (ASTA) operates with an external power supply, but a NiCd battery can keep it operating one week long (without heating power). The output voltage of the pyranometer is continuously integrated. The offset is determined between 0:00 and 2:40 U.T., the counter is reset at 0:00 U.T. The counter status is stored into local memory every 10 minutes. The stored values are called for by a central station (AZEN) operated in tandem. Conversion into physical units (according to the individual characteristics of each instrument) is performed by the AZEN, which also operates an initial quality control of the data and signal breakdowns.

For the pyranometers, the failure frequency per station lies around once every 5 years. Six technical teams provide repairs within two days at most. The cyclic maintenance includes characterization of the pyranometer by calibration transferred once per year.

The calibration transfer procedure and the construction of the pertaining apparatus follow from a compromise between the needs of simple handling, low power demand, high stability, long life and versatility. The last condition allows for calibration of sunshine duration and daylight sensors. The characterization encompasses the whole circuit, from sensor to central station.

A self-stabilised (Si-diode) iodine quartz lamp, in conjunction with a heat-filter, reproduces very roughly the spectral distribution of sunlight. The optics provide a homogeneous illumination of the sensors. Heat is ventilated as far as possible away from the pyranometer.

The whole device is tuned to induce a response of 400 Wm⁻² at a secondary standard (CM6, calibrated in Davos) mounted on a monitoring ANETZ station. The set-up is reproduced at each site. The beginning, and end of the calibration period are communicated via ASTA to the AZEN. There, the response of the counter is compared to the one which should hold for 400 Wm⁻², the correction factor, if necessary, is stored on the file of the characteristics of the individual stations, and applied until the next calibration.

1.B THE AUSTRIAN RADIATION NETWORK

O. Motschka and E. Wessely

Zentralanstalt f. Met. u. Geod., Wien

THE AUSTRIAN RADIATION NETWORK

The Austrian Radiation Network began in 1950. A greater expansion of the Network was initiated within the scope of the IGY, 1957.

The Network

At the end of 1983, 34 stations over Austria were established. The distances between the different stations are not equal, see Figure 1. The interesting radiation-climatological regions are well described: there are stations between the sea levels of 200 m up to 3100 m near to each other; and stations in the North and the South of the Alps; stations in the most important valleys and basins. Details can be seen in Table 1.

The Applied Measuring Techniques

All of the 34 stations are instrumented uniformly with Starpyranometers. Recording systems used are as follows:

- a) at 3 stations strip chart recorders with moving coil systems are in use; the scantimes are 20 seconds and the repetition times are 20, 40 and 60 seconds;
- b) for 16 stations semi-automatic-climatic stations with digital measuring systems are used. Every 2 seconds a reading will be taken. The readings are integrated over an hour and will be divided by the number of readings of the hour. The result is an hourly mean of radiation in mV;
- c) integrators are used at 14 stations. The output of the pyranometers is digitated by a voltage-frequency-converter: 10 mV over 1 hour are equal to 600 pulses per hour;
- d) at the station in Vienna a Commodore computer provided with scanner, ADC, printer and floppy disk is used; the scantime is 2 seconds, the repetition time is greater than 2 seconds and depends on the number of radiation sensors connected to the system;
- e) 3 stations are provided with data logger systems for a synoptic meteorological network in a first network test. The 3 stations have a full radiation measurement program without direct solar radiation sensors. The stations are not named in Table 1.

20 of the 34 global radiation stations are additionally provided with shadow bands (uniformly) for the measuring of diffuse sky radiation. At 4 stations, in addition to the named radiation sensors, net radiation balance meters and for the appointment of the short wave radiation-balance albedometers are installed. Only from one station of the four stations are these data published and sent to the world data center at Leningrad.

All measuring equipments have an accuracy of 0.1 mV or better. This gives $0.25 \text{ J/cm}^2 \text{ (min)}$, if the sensitivity of the starpyranometers is $2.5 \text{ mV/Jcm}^{-2} \text{ (min)}$.

The Observation Time

The data loggers for radiation measurements are working with true solar time. Some others use the mean local time, i.e. for climatological purposes.

It could be possible to provide software for the computer systems which consider different observation times. But in most cases, people get trouble with the capacity of the used microcomputers. On the other hand, it is necessary to have the same observation times, for example, to correlate air temperature with radiation. That means a discussion about the different observation times in meteorology is necessary and to try and find a solution.

The Elevation of the Horizon

To get maximum information about a station we measure the elevation angles of the surrounding horizon at each of the radiation stations. Out of this we get sunrise and sunset and we have the possibility to estimate the part of energy coming down by the surrounding hills, etc. especially in wintertime (see Figure 2).

Calibration Method

The global radiation pyranometers for each station are calibrated twice per year against a substandard pyranometer (comparison). Pyranometers connected to digital equipment are checked with respect to their EMF, connected to the moving coil systems the whole system will be calibrated. The same procedure is done for the albedometers. The calibration of the radiation balance meters is only to be done outdoors using the direct solar radiation (shading disk method). The calibration of the diffuse sky radiation is divergent: if the dates are in the computer, then we will use all days with global radiation sums below 40% of cloudless daily sums and the measured sunshine duration as second parameter to estimate the calibration factors for the diffuse sky radiation. This method will be advanced in a second step to the hourly totals. Our assumption is, that it gives no case with sky radiation greater than global radiation. The sky radiation only could be equal to the global radiation in the overcast situation. Using this method, you get the calibration factors for the sky radiation with respect to the errors due to the shadow band.

Data Checks

The mean hourly values of the global radiation (dimension mV) multiplied by the calibration factors estimated by the comparison quoted above are the basic data for the following data checks.

From a semi-empirical curve for maximum daily global radiation for each station of the network 3 intensity intervals are defined: 85-95%, 96-105%, greater than 106%. Measured global radiation values falling into this interval will be checked against sunshine duration, neighbouring stations and the meteorological conditions.

Publications

The most radiation data are published annually in "Ergebnisse von Strahlungsmessungen in Osterreich", Publikation Nr. 271 der Zentralanstalt f. Met. u. Geod., Wien.

The content of this publication is: description of the stations, daily totals of global radiation and sky radiation and daily values of sunshine duration, the mean monthly diurnal variations, the maximum hourly totals of each day over the year with time, frequency intervals, the daily hourly totals for global, sky and net radiation.

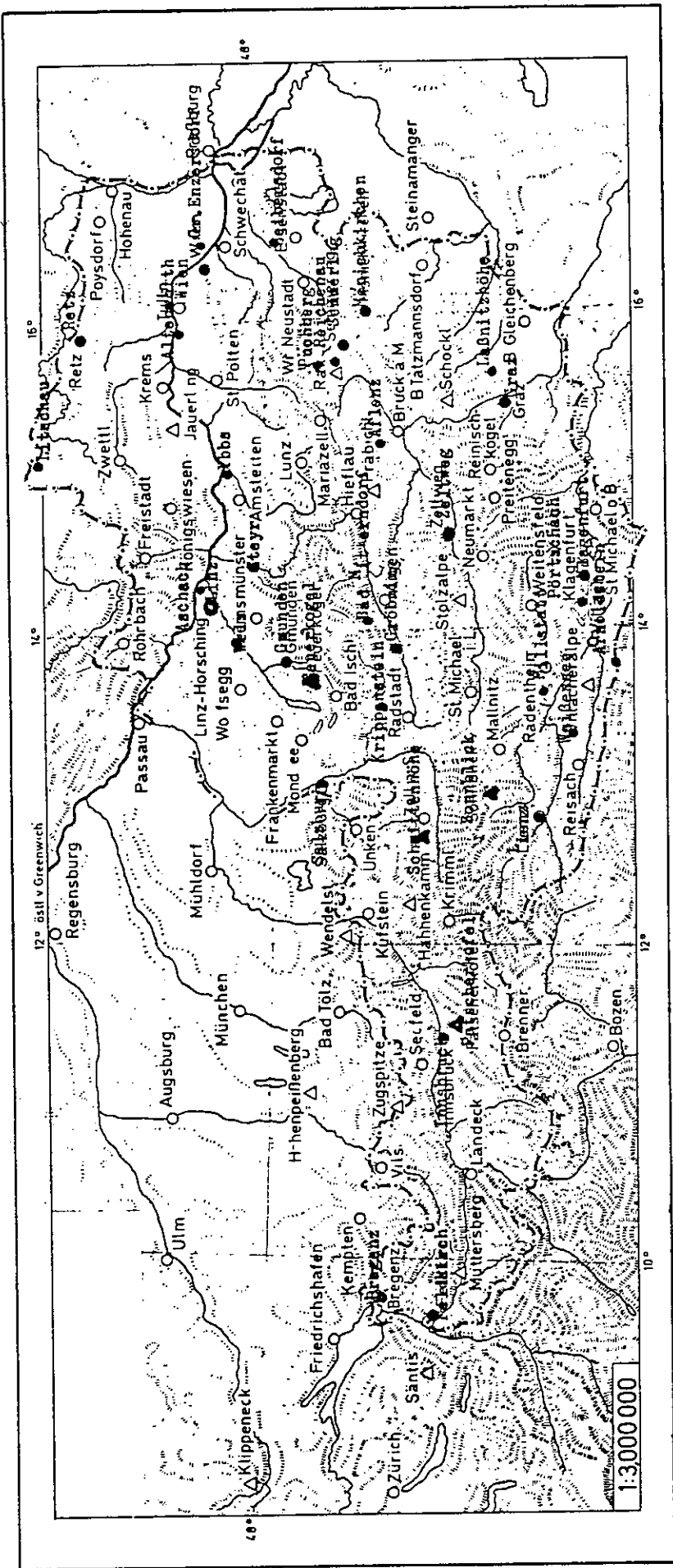


FIGURE 1

LIENZ

GEO. BREITE : 46.49 LAENGE : 12.47 KORR. MEZ/MOZ : 8.9 MIN.

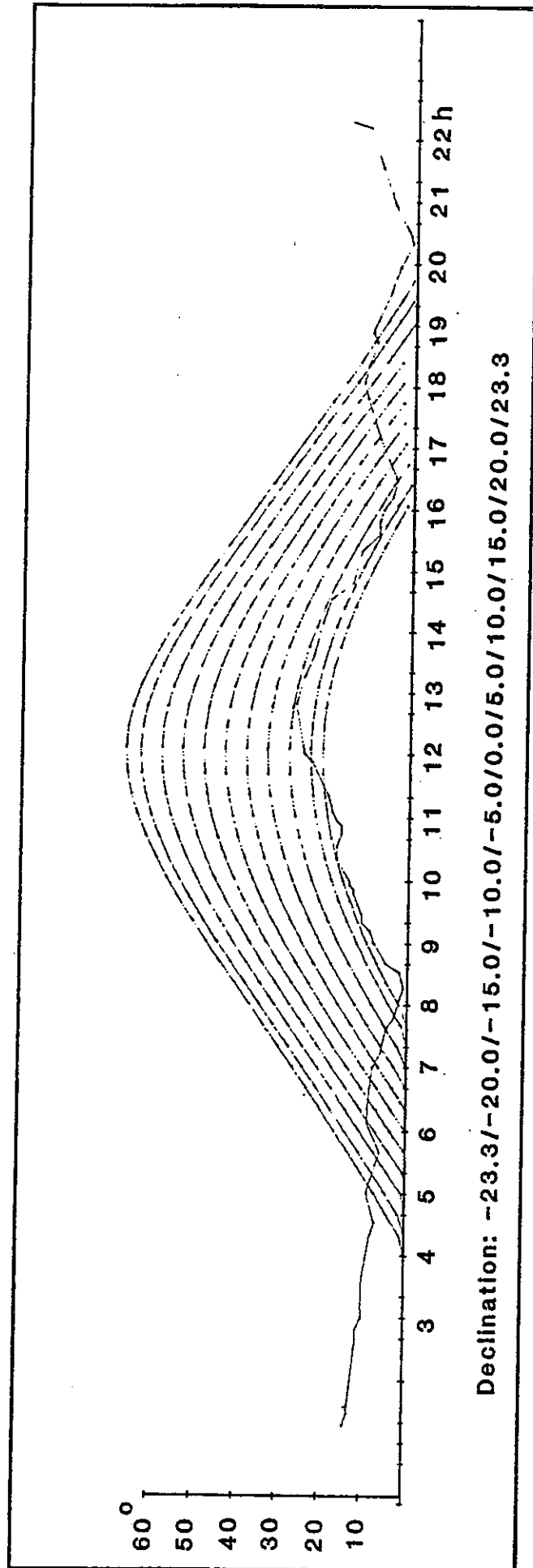


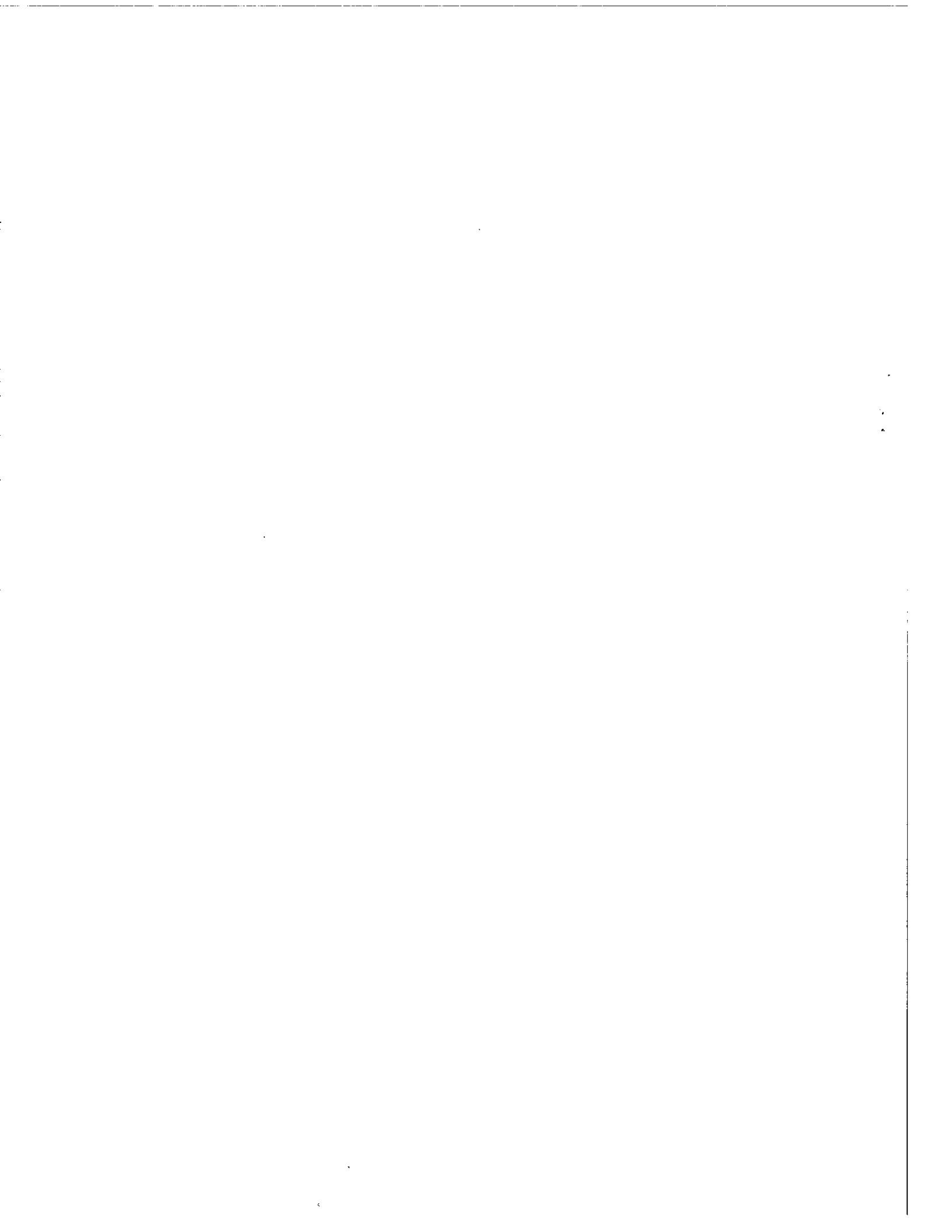
FIGURE 2

TABLE 1
Station in Radiation Network

	MSL	λ	ϕ			
Altenwoerth	190	15.01	48.23	INTEG.	G	
Aflenz	784	15.14	47.33	TAKLIS	G H	S
Arnoldstein	555	13.42	46.33	ANALOG	G	
Aschach	291	14.02	48.23	INTEG.	G	
Bad Aussee	665	13.47	47.37	TAKLIS	G H	S
Bad Mitterndorf	804	13.57	47.33	TAKLIS	G H	S
Baden	249	16.14	48.01	TAKLIS	G	S
Feldkirch	439	9.36	47.16	INTEG.	G	S
Feuerkogel	1598	13.44	47.49	INTEG.	G	S
Gmunden	425	13.47	47.55	TAKLIS	G H	S
Graz	342	15.27	46.59	INTEG.	G H A	SB S
Groebming	770	13.54	47.27	TAKLIS	G H	S
Innsbruck FLH	579	11.21	47.16	INTEG.	G A	SB S
Innsbruck UNI	582	11.24	47.16	G		S
Klagenfurt	452	14.20	46.39	INTEG.	G	S
Krippenstein	2050	13.42	47.31	INTEG.	G	S
Lasnitzhoehe	543	15.35	47.05	INTEG.	G H	S
Lienz	670	12.47	46.49	INTEG.	G	S
Litschau	570	15.02	48.58	TAKLIS	G H	S
Millstadt	791	13.35	46.48	TAKLIS	G H	S
Moenichkirchen	998	16.02	47.29	TAKLIS	G H	S
Obersiebenbrunn	150	16.43	48.16	INTEG.	G H A	SB S
Poertschach	447	14.10	46.37	TAKLIS	G H	S
Puchberg	584	15.55	47.47	TAKLIS	G H	S
Reichenau	486	15.51	47.42	TAKLIS	G H	S
Retz	243	15.58	48.46	INTEG.	G	S
Salzburg	435	13.00	47.48	INTEG.	G H A	SB S
Schmittenhoehe	1973	12.44	47.20	TAKLIS	G	S
Seibersdorf	185	16.30	47.59	TAKLIS	G H	S
Sonnblick	3106	12.57	47.03	ANALOG	G H	S
Steyr	309	14.26	48.04	ANALOG	G	S
Wels-Schleiszheim	312	14.04	48.10	TAKLIS	G	S
Wien	202	16.22	48.15	CBM	G H	S
YBBS Persenbeug	228	15.04	48.11	INTEG.	G	

λ longitude
 ϕ latitude
 G Global radiation
 H Sky radiation
 A Short wave radiation reflected
 SB Net radiation
 S Sunshine duration

TAKLIS data logger system
 INTEG integrator
 ANALOG moving coil system
 CMB personal computer adapted



1.C THE CANADIAN RADIATION NETWORK

D.I. Wardle

Atmospheric Environment Service
4905 Dufferin Street
Downsview, Ontario
M3H 5T4
CANADA

THE CANADIAN RADIATION NETWORK

SUMMARY

This paper briefly describes the instruments, deployment and data management used in the Canadian Network. Certain aspects of calibration and possible long term drift are considered in more detail. It is shown that Kipp and Zonen CM5/6 and Eppley PSP (and Model 2) pyranometers do not lose or gain sensitivity when exposed horizontally as is usual in meteorological monitoring. A steadily increasing and ultimately large error during the 1970's in the Kipp & Zonen manufacturer's calibration factors is identified. Also a difference of about 3% between Eppley calibration factors and the Canadian values is evident for most of the period.

EXTENT AND INSTRUMENTATION

The present network was built up during the 1960's under the direction of J.R. Latimer. There are 49 stations where at least global irradiance is measured. At 9 of these diffuse irradiance is measured using a pyranometer with a shade ring, at 5 the reflected short-wave irradiance and at 23 the total net radiation are measured. The net pyrradiometers are Middleton CN2's (Funk type). The pyranometers are mostly Kipp & Zonen CM5's except for the global instruments installed north of 60°N. These are Eppley PSP or its prototype the Eppley Model 2. All instruments are calibrated at 2 year intervals.

The global instruments are equipped with ventilators which enclose all the instrument except the dome. Air is forced up from below then passes around the instrument and exists at the base of the dome moving somewhat inwards. These ventilators have all but eliminated problems with condensation and frost. Also they tend to keep the domes clean and free of snow and rain.

DATA MANAGEMENT

Currently the data is recorded on site as hourly integrations based on local solar time using a printing ball and disc integrator; a chart recording is also made and used for quality control. The chart recording and printout from the integrator are sent to Downsview every month. The chart is scrutinized for timing errors, effects of dew, frost or snow on the sensor domes or shadows of local objects. Appropriate corrections are made to the hourly integrations. Some further quality control is done automatically by comparison with computer clear sky values.

The diffuse irradiance is evaluated using a calibration factor which is set for each month so that on fully overcast days in that month the diffuse total is equal to the global. There is also a crude but small correction made for the non-isotropic radiation distribution in clear conditions. An amount $f \times 2\%$ is added to all diffuse measurements on any particular day

where f is the fraction of that day during which it was sunny. The measurements have been published since 1960 in the "Monthly Radiation Summary".

The data management system will be replaced during 1986. The quality control techniques in the new system will include the inspection of daily data on a high resolution display (1 minute \times 2 Wm^{-2}) by qualified observers.

RADIATION STANDARDS AND CALIBRATION

Maintaining standard pyrhemometers, calibrating pyrhemometers and calibrating pyranometers are all part of the function of the National Atmospheric Research Centre (NARC) which is also a WMO regional radiation centre. The pyranometer calibrations depend on the NARC pyrhemometers which are often intercompared among themselves and have been taken to several international pyrhemometer comparison (IPC II (1964), IPC III (1970), IPC IV (1975), IPC V (1980) all in Switzerland and the Table Mountain Washington comparisons in 1959 and 1960).

The following table lists the more important standard pyrhemometers used by NARC during the past 25 years. It also shows during which periods, if any, each instrument was the primary standard for NARC.

Manufacturer and Serial Number	Acquired by NARC	Origin of Calibration	Used on NARC Prime Standard
Hickey-Frieden No. 17750	1979	Manufacturer's absolute	1979 - present
Eppley-Kendall No. 11399	1972	Manufacturer's absolute	1974 - 1979
Eppley-Angstrom EA9001	1968	Eppley	--
Abbot silver disc T7	1964	From SI14 confirmed by PACRAD* at IPC III	1971 - 1974
SMHI-Angstrom A210, A208	1960	Manufacturer (Stockholm)	--
Lindbald-Angstrom A149, A150	1954	Manufacturer (Stockholm)	--
Smithsonian silver disc SI14 (repaired 1960)	1937	From Table Mountain SI5 No. in 1960	1960 - 1965

* The primary absolute cavity radiometer of J.M. Kendall No. Smithsonian Institution Silver-Disk No. 5

The relation of these standards to the current World Radiometric Reference (WRR) can be summarized as follows:

- a) from the present back to 1970/06/01 the standards were within 0.3% of the WRR;
- b) between 1970/06/01 and sometime early in 1965 (probably January) the standard was 1.25% \pm 0.3% lower than WRR;
- c) prior to 1965 the standard was 0.25% \pm 0.5% lower than WRR.

With the benefit of hindsight it has been possible to make this fairly simple summary. However, one must recognize that in the past and especially prior to 1970, the situation was very confusing. The Eppley-Angstrom EA9001, for example, had a manufacturer's calibration 2.6% different from SI14 and the precision of comparison measurements was not so high as with today's instruments. It is to the credit of J.R. Latimer, who was then in charge of NARC, that the standards were kept so constantly; reference (1) is his review of the situation in the early seventies.

PYRANOMETER CALIBRATIONS

Because pyranometers must respond to radiation from a wide range of incidence angles ($\mp\pi/2$) their calibration factors are less well defined and are nearly always less precisely determined than those of pyrhemometers. For example, a step change of 1.25% such as occurred in the NARC pyrhemometer standard, would until recently be difficult to recognize in pyranometer calibration.

Since 1970, the Canadian network pyranometers have been calibrated against reference instruments of like manufacture every two years in the NARC diffuse radiation sphere. The pyranometer to be calibrated together with one or two reference pyranometers is put into the sphere where all are subjected to the same irradiance. The calibration factor is determined as the product of the calibration on the reference pyranometer with the ratio of signals from microvolts per watt square meter ($\mu\text{V}\cdot\text{W}^{-1}\text{m}^2$).

The sphere reference instruments (Kipp 2498, Eppley 10037 and 11671) have assigned calibration factors based on many out-door occultation measurements. The intention was to choose calibration factors suitable for the Canadian Network. This is nominally achieved by taking an average of all calibration measurements between 8 a.m. and 4 p.m. on clear July days from the site at Mt. Kobau (50°N, 1870 m alt.).

The factor for the Kipp reference has been changed occasionally in response either to changes in the pyrhemometer standard (June 1971) or to better determination of the calibration factor (September 1974). In the case of the Eppley reference, there was a purely clerical error of 2.3% which was corrected in January 1974.

STABILITY OF PYRANOMETER CALIBRATIONS

Figure 1 and Figure 5 show the relation of the original manufacturer's calibration (KM) to the NARC calibration (KC) of the same pyranometer plotted against the date of the NARC calibration. Most pyranometers are represented by several points each corresponding to different NARC calibrations over the period 1970-1983. These data are derived using today's (post 1974) calibration factors for the reference instruments. The actual factors in use prior to 1974 are indicated by the thin solid lines and have already been discussed in relation to changes in the pyrhelimeter standard, recalibration and the "clerical error". No attempt has been made to modify the manufacturer's factors in relation to the change from IPS to WRR, or for any other reason.

The data are remarkable for the wide spread of discrepancy between each manufacturer and NARC. The Kipp discrepancies range from -10% to +7%, while the Eppley ones ranges between -7% and 0%. It may be noticed that, prior to the 1974, the NARC "clerical error" caused a fortuitous agreement between NARC and Eppley.

Figure 2 and Figure 6 show the same data as 1 and 5 but rearranged according to the date of manufacturer's calibration. Figure 2 demonstrates an upward drift of 10% in the Kipp calibration between 1970 and 1980. Figure 7 shows a mean discrepancy of from 3% to 4% but no long term drift. The writer has been informed by Dr. John Hickey that Eppley reference was changed in 1981 by about 3%; thus the Eppley NARC discrepancy will likely be smaller in future. As well, the Kipp factory calibration was changed in 1980.

Figure 3, 4, 7 and 8 have nothing to do with manufacturer's calibration. The ordinate in every case is a NARC calibration factor (KC) on a particular instrument compared with the first NARC calibration (KCO) on that instrument. There are two versions of the abscissa, either the date of the first calibration, or date of any subsequent calibration. In the writer's opinion these four graphs show conclusively that the NARC calibration factors are not drifting.

To investigate the possibility of drift numerically, the sphere calibration data were analyzed to estimate a hypothesized linear drift between the field instruments as a group and the reference instruments. The results are as follows:

**Drift of References vs. Field Instruments
1970 - 1983**

KIPP CM5		EPPLEY PSP
682	No. Calibrations	289
219	No. Instruments	74
.059	Drift in	-0.064
+/- .007	% per annum	+/- .011
0.45%	RMS Scatter of each calibration < 2 years	0.49%

Thus the estimated drifts are in the region of only 1.0% during 13 years and in opposing directions for the CM5 and PSP. These are very small and one must conclude that the Canadian network pyranometers are not subject to ageing. Yet clear evidence of ageing has been presented by other workers (Ref. 2). It seems likely to the writer that ageing only happens when some threshold of temperature and/or irradiance is exceeded for a sustained period. Perhaps these conditions are encountered more often when pyranometers are mounted sloping towards the sun or on solar tracking tables.

The analysis also yields a value for the effective noise in sphere calibrations - it is about 0.5% both for the Kipp and Eppley pyranometers. A more obvious measure of the variability of sphere calibrations is given by the discrepancies between each calibration and the previous one (KPO) on that pyranometer. Figures 9 and 10 show the distribution of discrepancies. The histogram display takes no account of the time between successive calibrations which ranges from 2 to 10 years. The r.m.s. spreads are 0.7% for Kipp pyranometers and 0.8% for Eppley pyranometers.

REFERENCES

1. Latimer, J.R., Tellus XXV (1973), 6. p. 586-592.
2. Zerlaut, G.A.: Proceedings of the IEA Conference on pyranometer measurements, 16-20 March 1981, Boulder, Colorado, p. 104-123.

CALIBRATION SCATTER PLOT FOR KIPP CM-5/6

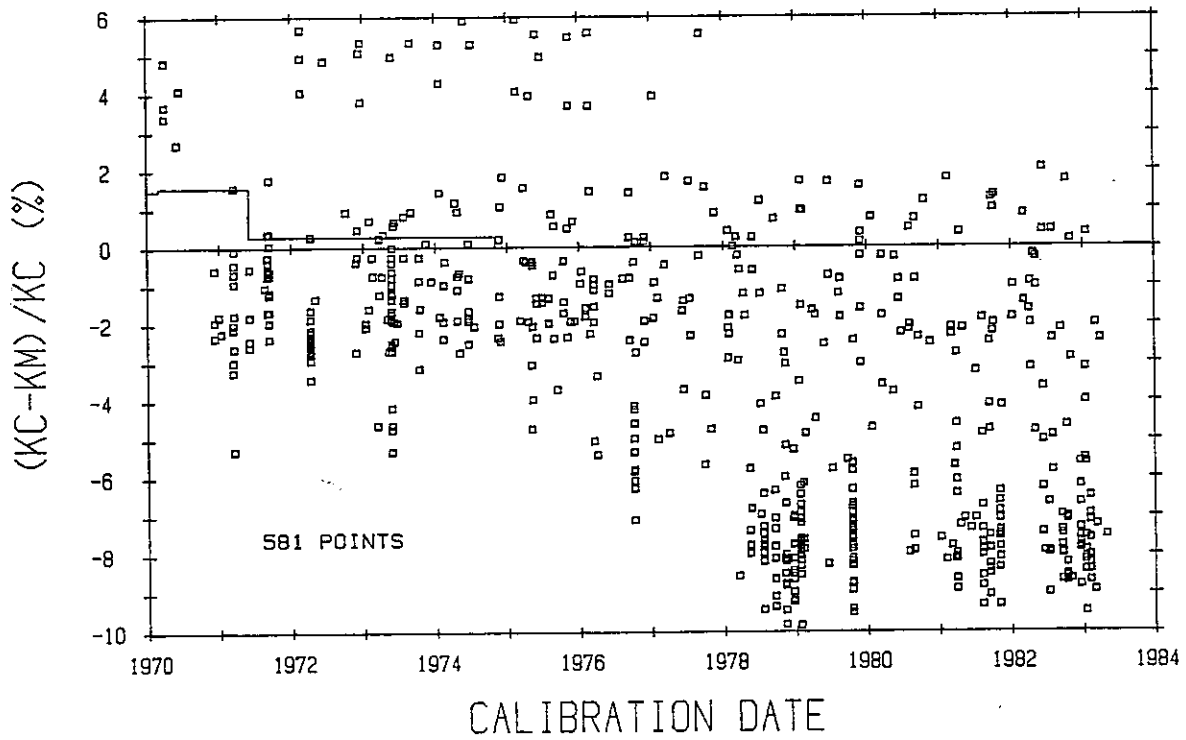


Figure 1

CALIBRATION SCATTER PLOT FOR KIPP CM-5/6.

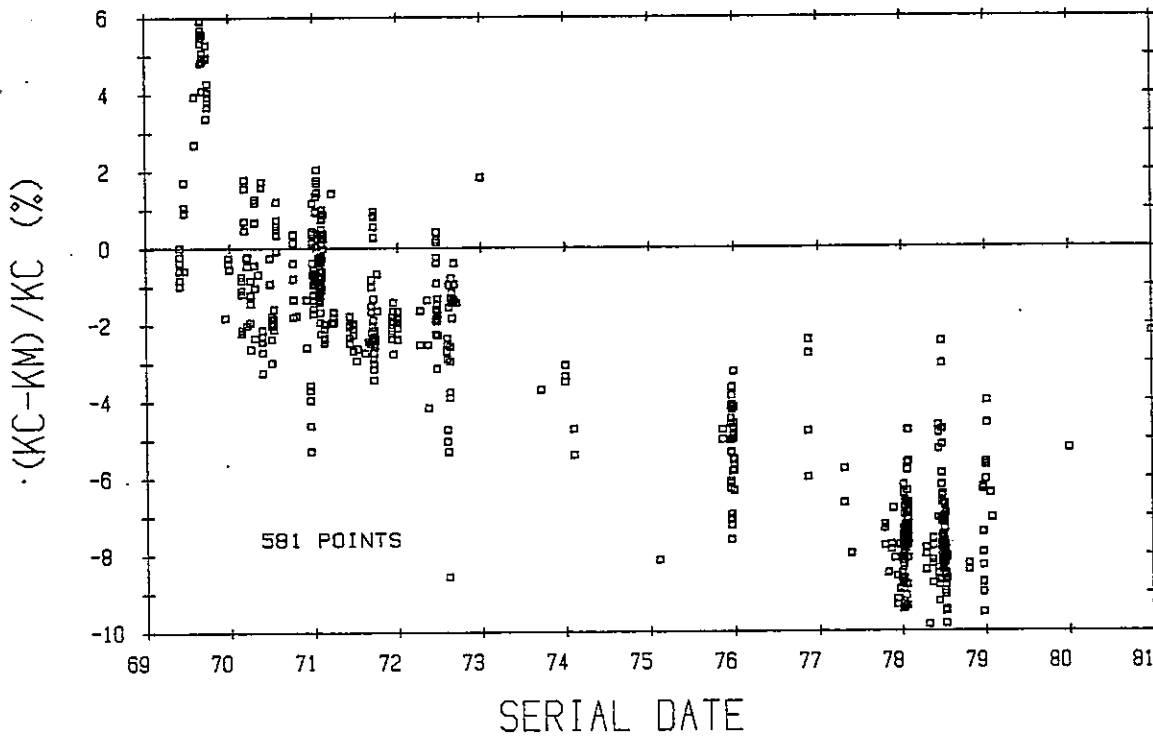


Figure 2

CALIBRATION SCATTER PLOT FOR KIPP CM-5/6

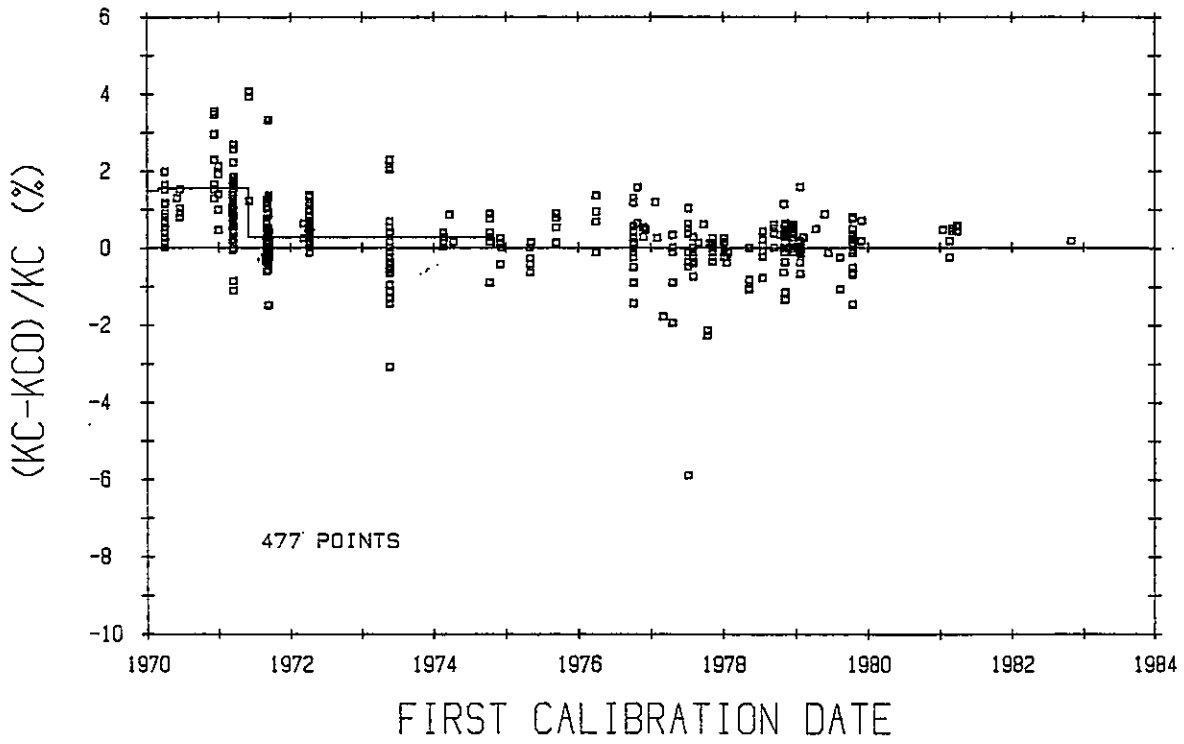


Figure 3

CALIBRATION SCATTER PLOT FOR KIPP CM-5/6

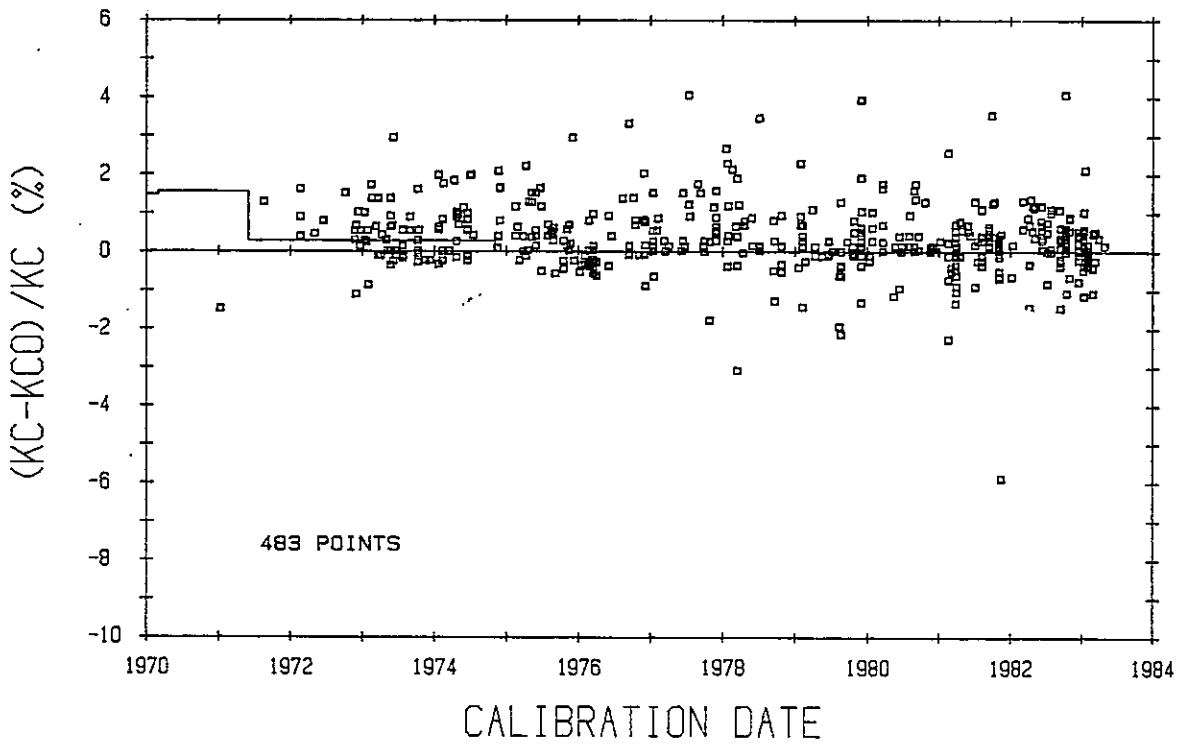


Figure 4

CALIBRATION SCATTER PLOT FOR EPPLEY PSP & MODEL 2

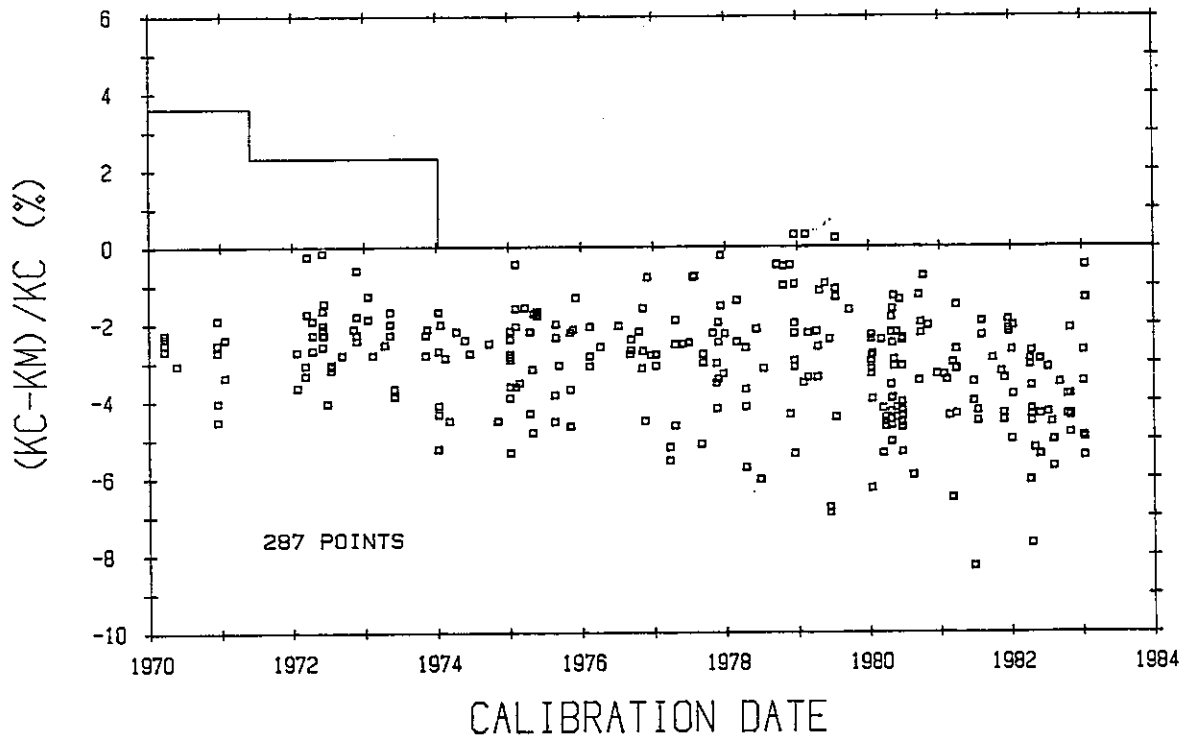


Figure 5

CALIBRATION SCATTER PLOT FOR EPPLEY PSP & MODEL 2

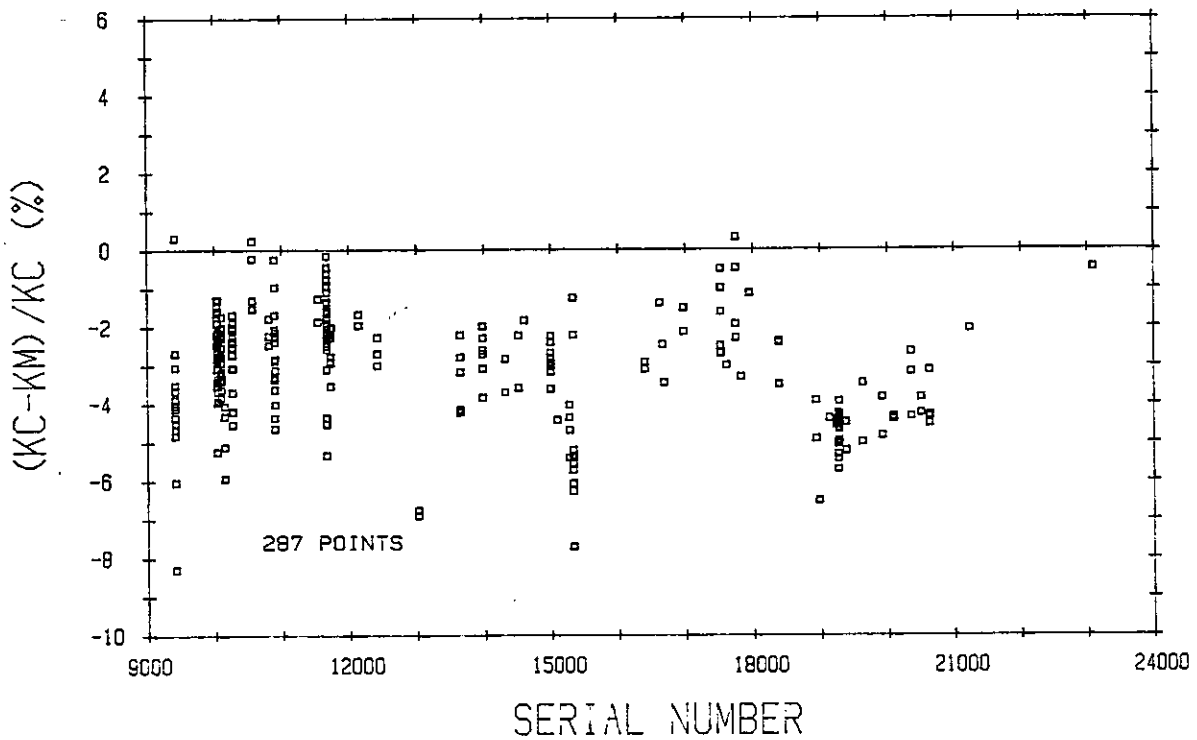


Figure 6

CALIBRATION SCATTER PLOT FOR EPPLEY PSP & MODEL 2

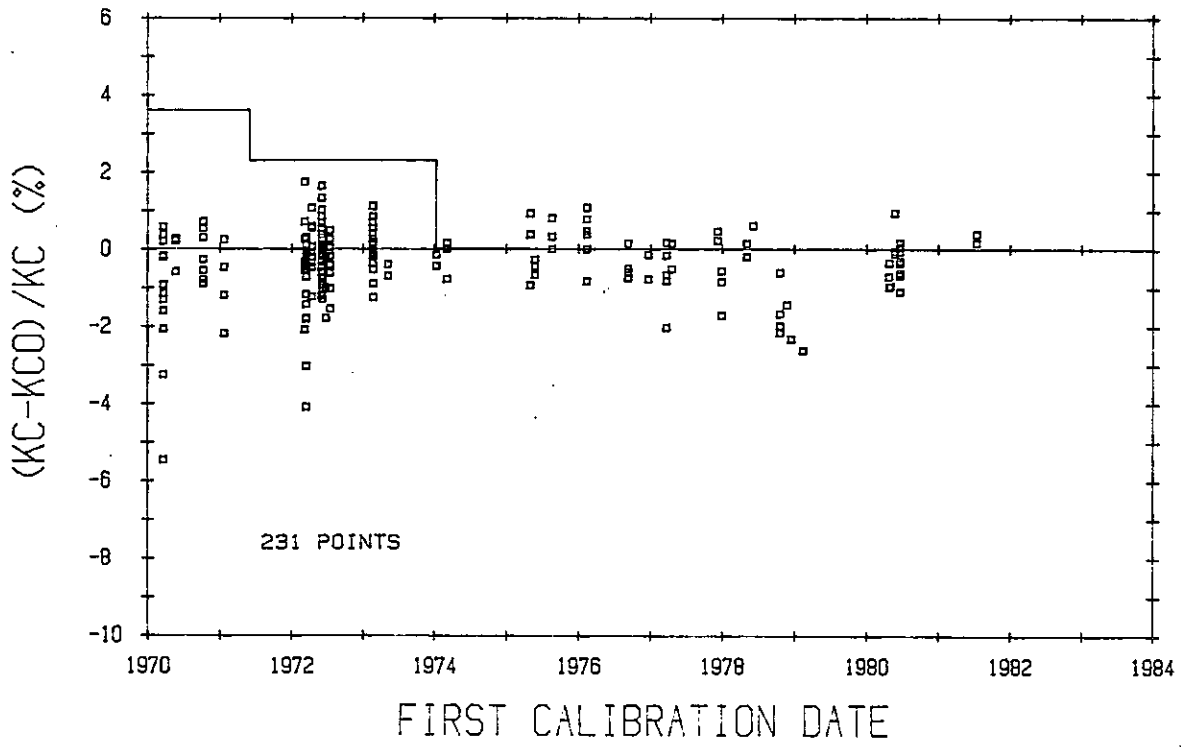


Figure 7

CALIBRATION SCATTER PLOT FOR EPPLEY PSP & MODEL 2

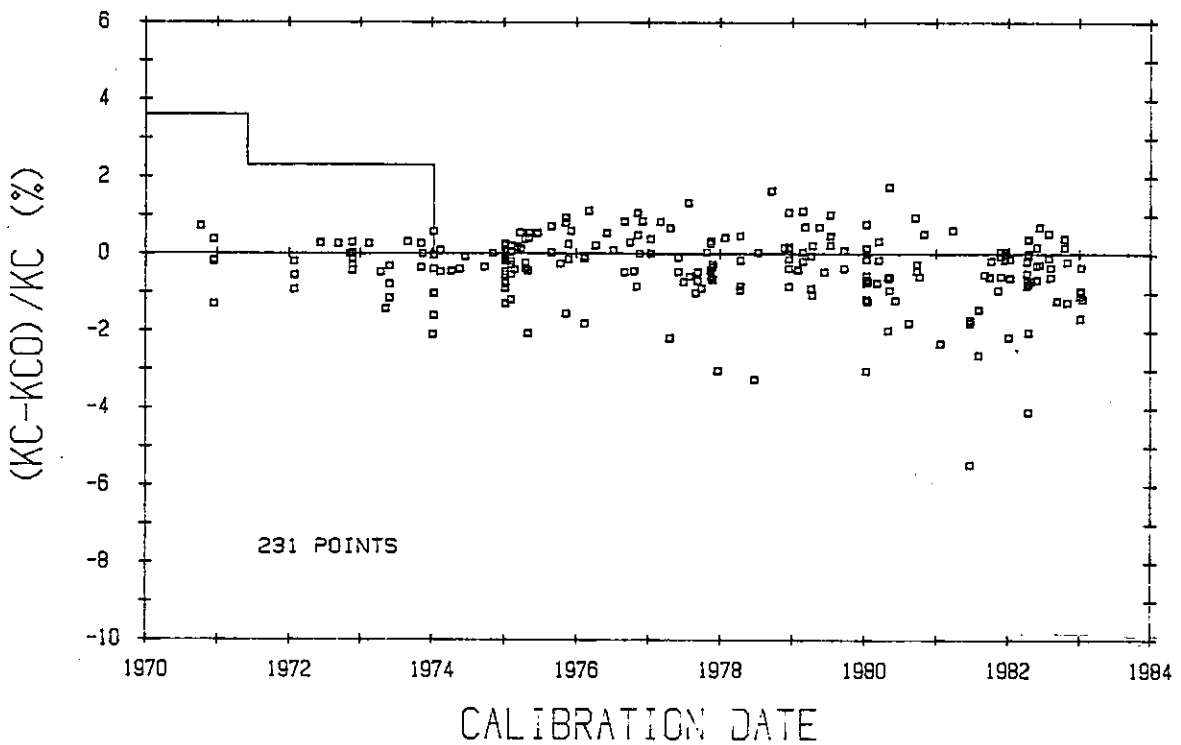


Figure 8

HISTOGRAM OF KIPP CM-5/6 CALIBRATIONS

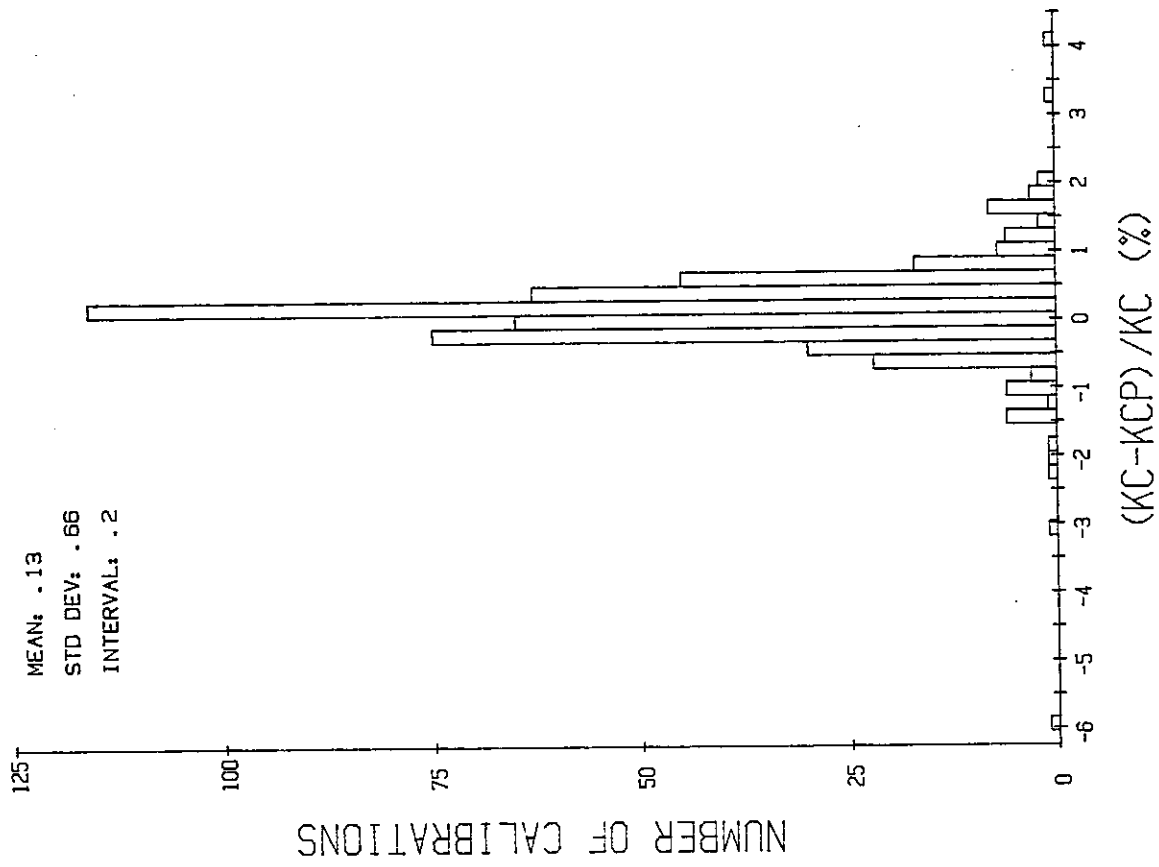


Figure 9

HISTOGRAM OF EPPLEY PSP/2 CALIBRATIONS

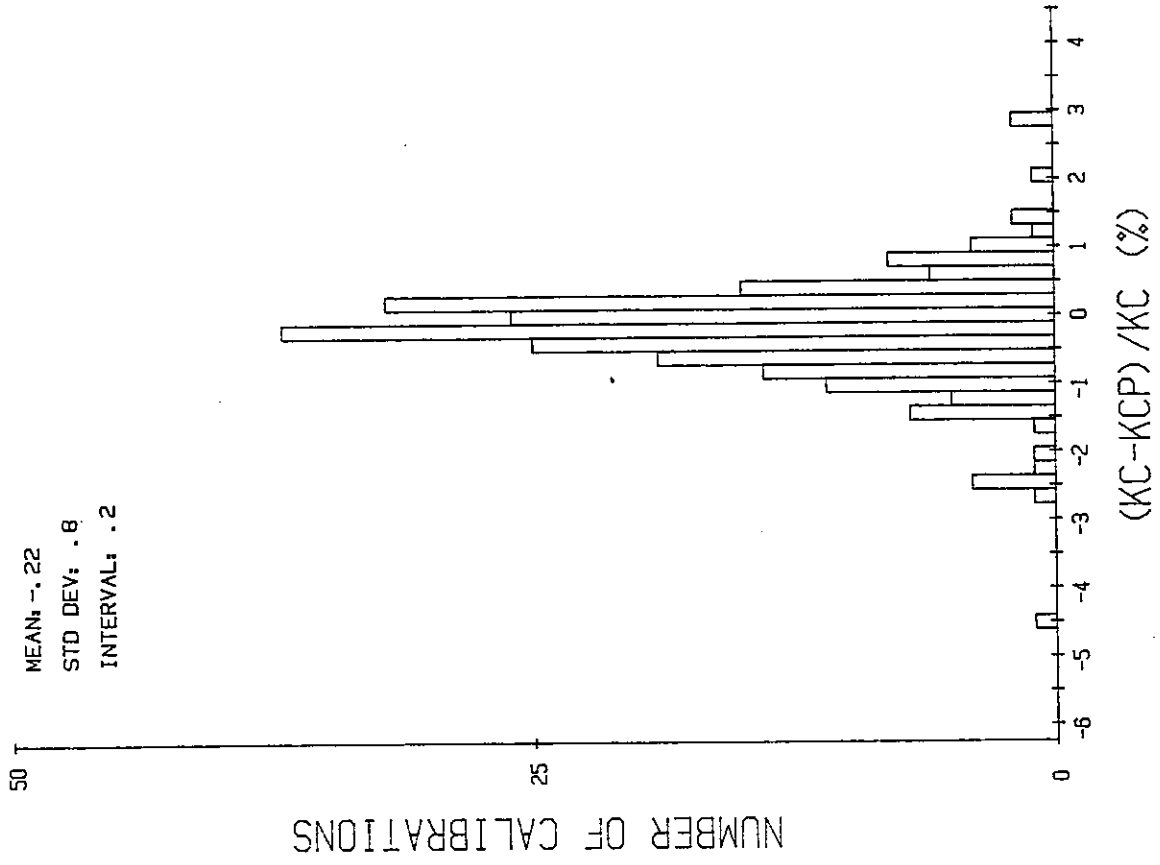


Figure 10



1.D RECENT WORK IN THE UK RADIATION NETWORK

J.H. Seymour

Meteorological Office, Bracknell, UK

RECENT WORK IN THE UK RADIATION NETWORK

The UK Network

The work within the radiation network is co-ordinated by the National Radiation Centre (NRC) which is part of the National Meteorological Service based at Bracknell. A total of 14 stations operated by the Met Office make measurements of radiation - each one being equipped to measure global and diffuse (shadow band) radiation on a horizontal surface. In addition 3 have Eppley NIPs for direct beam monitoring, 2 have Eko sunphotometers for turbidity measurements, 2 have pyranometers on vertical and inclined surface and 3 have net radiometers. Kipp CM5 pyranometers are used almost exclusively although the NRC also makes some broadband spectral measurements using Eppley PSPs. At all stations data are recorded every minute on magnetic tape with a resolution of $10\mu\text{V}$. In addition to the main data logger a strip chart recorder is used in parallel to provide a backup system and to provide a visual output for station staff. The magnetic tapes are returned to Bracknell every two weeks and processed on the IBM mainframe computer. Hourly mean values are archived as the basic data set after quality control has been performed, however more recently we have been archiving the minute data as well.

In addition to these 14 stations there are 24 which belong to co-operating bodies such as universities, agricultural institutes and water authorities. Most of these supply daily global data using voltage integrators, 6 however, give hourly means and 2 also supply diffuse data. The distribution of the stations is depicted in Figure 1 and is seen to be asymmetric with a heavy bias toward the southeast of the country. We are planning further extensions to the network using synoptic automatic weather stations to help fill some of the gaps on the map.

Instrument Calibration

The reference pyrhelimeter used at the NRC is a TMI cavity radiometer and the calibration is transferred to a group of reference pyranometers using the shading disc technique. The NRC also maintains a pair of short tube Angstrom pyrhelimeter which were the reference instruments before the cavity radiometer was acquired. Transfer standard instruments for each type of pyranometer used in the UK, by outside users as well as the network, are calibrated against the reference instruments under a variety of sky conditions outdoors. Network instruments, after undergoing physical checks, are calibrated in an integrating sphere which gives an intensity of about 500 Wm^{-2} at the thermopile using 6 quartz-halogen lamps mounted below the instrument horizon. The platform carrying one transfer standard and two test pyranometers is rotated through 360° in 10 minutes once in each direction with the instrument outputs being sampled every 10 seconds. The whole system is under the control of a micro-computer and a calibration certificate is produced at the end of each test. Whenever possible a check calibration is also carried out outdoors as well and there is very often a difference of

the order of 1% between the two values, the outdoor one usually being the higher. Whenever there is a consistent difference the final figure given is biased towards that obtained outdoors as this should be more representative of conditions of actual use.

Shade Ring Correction

In common with other meteorological services the diffuse pyranometer measurements are corrected, for over-shading by the ring, during the processing of the raw data by using the assumption of an isotropic distribution for the diffuse radiation. For overcast conditions this assumption is close to the truth but with other sky states the diffuse field can be strongly anisotropic and errors of a few per cent can be achieved. Under these conditions the best way of measuring the diffuse is by subtraction of the direct beam component from the global radiation, however tracking pyrhelimeter are expensive and most networks use the shade ring method for diffuse measurements. Following the work of Dehne at Hamburg and McWilliams at Valentia within the EEC Solar Energy programme it was decided to investigate the additional corrections required using a second pyranometer alongside the shade ring instrument but shaded by an occulting disc ($7.9^\circ \times 5.4^\circ$). This represents what we call the "true" diffuse measurement. Data were collected during the period June to December 1983 and a preliminary analysis undertaken on the lines followed by the other investigations, i.e. finding an empirical relationship between the extra correction required and the ratio of ring diffuse to global radiation and the solar declination. The results of the first analysis produced the relationship (for hourly mean values).

$$\frac{D_D}{D_R} = 1.098 - .127 \frac{D_{MR}}{G} - .008(\delta)$$

(correlation coefficient = .84)

where

- D_D = Disc Diffuse radiation
- D_R = Ring Diffuse radiation (with isotropic correction)
- D_{MR} = Ring Diffuse radiation (without isotropic correction)
- G = Ring Global Radiation
- δ = Solar declination

Further work is being undertaken to refine this relationship for Bracknell and to test it on independent data during the coming year.

Zero Offset Corrections

The pyranometer zero offset associated with clear sky conditions is treated in the operational (Met Office) network by taking the mean value for the three hours at each end of the daylight period and assuming that this applies throughout the day. This intuitive approach obviously has limitations but it has always been felt that this was a better method than ignoring the offset. During a recent trial of some voltage integrators an

opportunity arose to check the value of making these corrections. A ventilated and an unventilated pyranometer were each connected to the operational data logger and to a parallel integrator. The integrators do not respond to negative inputs and therefore the recorded daily irradiances do not take account of any offsets.

During the period October/November 1983 the night time correction for the ventilated instrument was always $0 \pm 1/2 \text{ Wm}^{-2}$ (the resolution is limited by the data logger), we can therefore call this the truth against which to reference the other measurements.

- If: V_L = Daily irradiation recorded on the logger (ventilated)
- V_I = Daily irradiation recorded on the integrator (ventilated)
- G_L = Daily irradiation recorded on the logger (unventilated)
- G_I = Daily irradiation recorded on the integrator (unventilated)

actual (mean) σ

We would expect

$\frac{V_L}{G_L} = 1$.9998	.01 (56 days)
$\frac{V_I}{V_L} = 1$.9995	.004
$\frac{G_I}{G_L} < 1$.9823	.009
$\frac{G_I + \text{Corrections}}{G_L} = 1$.9933	.007

Tentative conclusions are therefore:

- a) If zero offsets are not taken into account then errors of 1-2% in daily sums can be expected during the winter half of the year at Bracknell;
- b) The correction method used at present seems to produce answers that are realistic;
- c) Ventilating the pyranometer significantly improves the data quality by removing the offset problem as well as preventing the formation of dew and frost.

Again this work will continue through the Winter and Spring of 1984.

THE UK METEOROLOGICAL OFFICE RADIATION NETWORK, SEPTEMBER 1983.

● LERWICK

● STATIONS OPERATING (MET. OFFICE)

x CO-OPERATING STATIONS

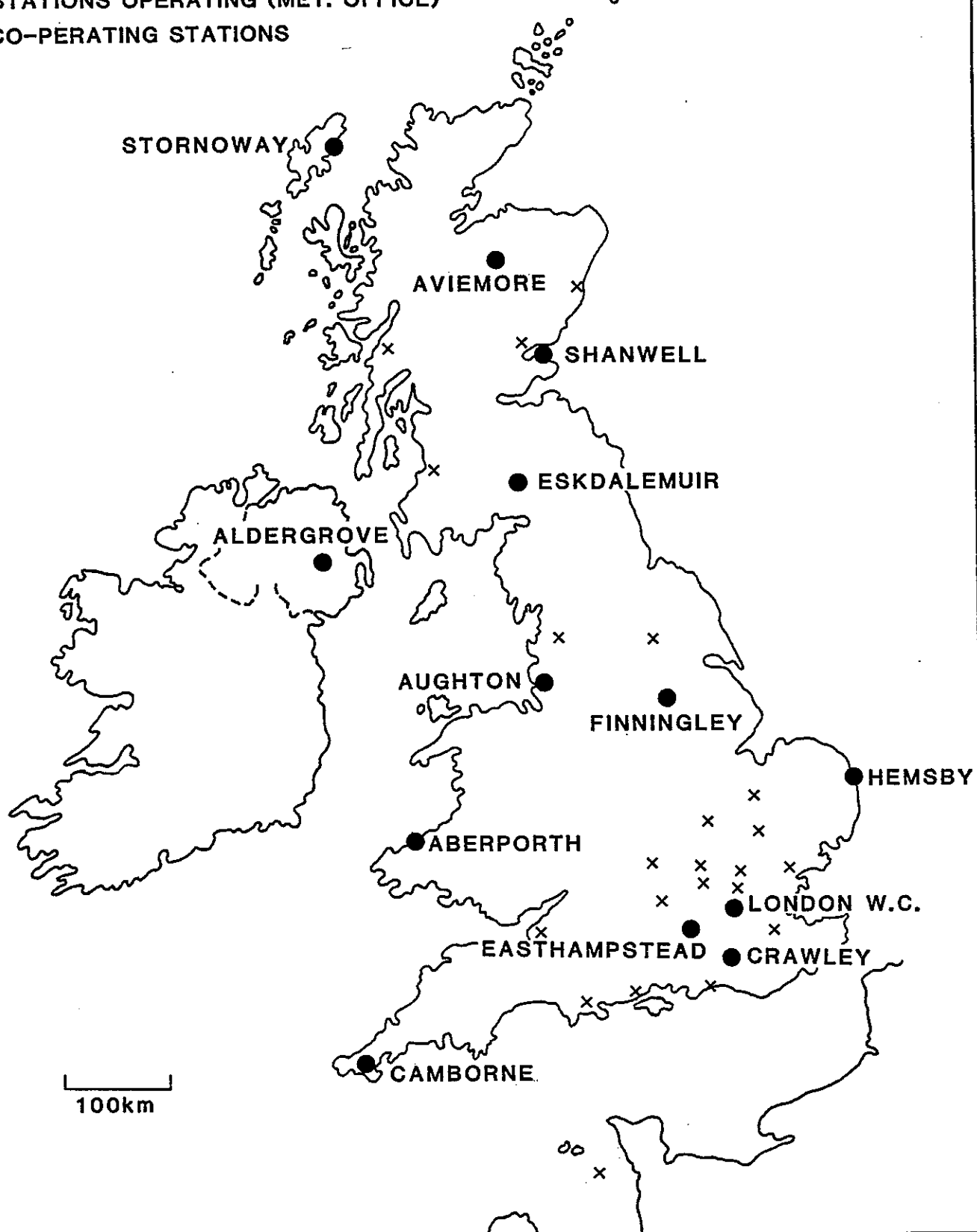
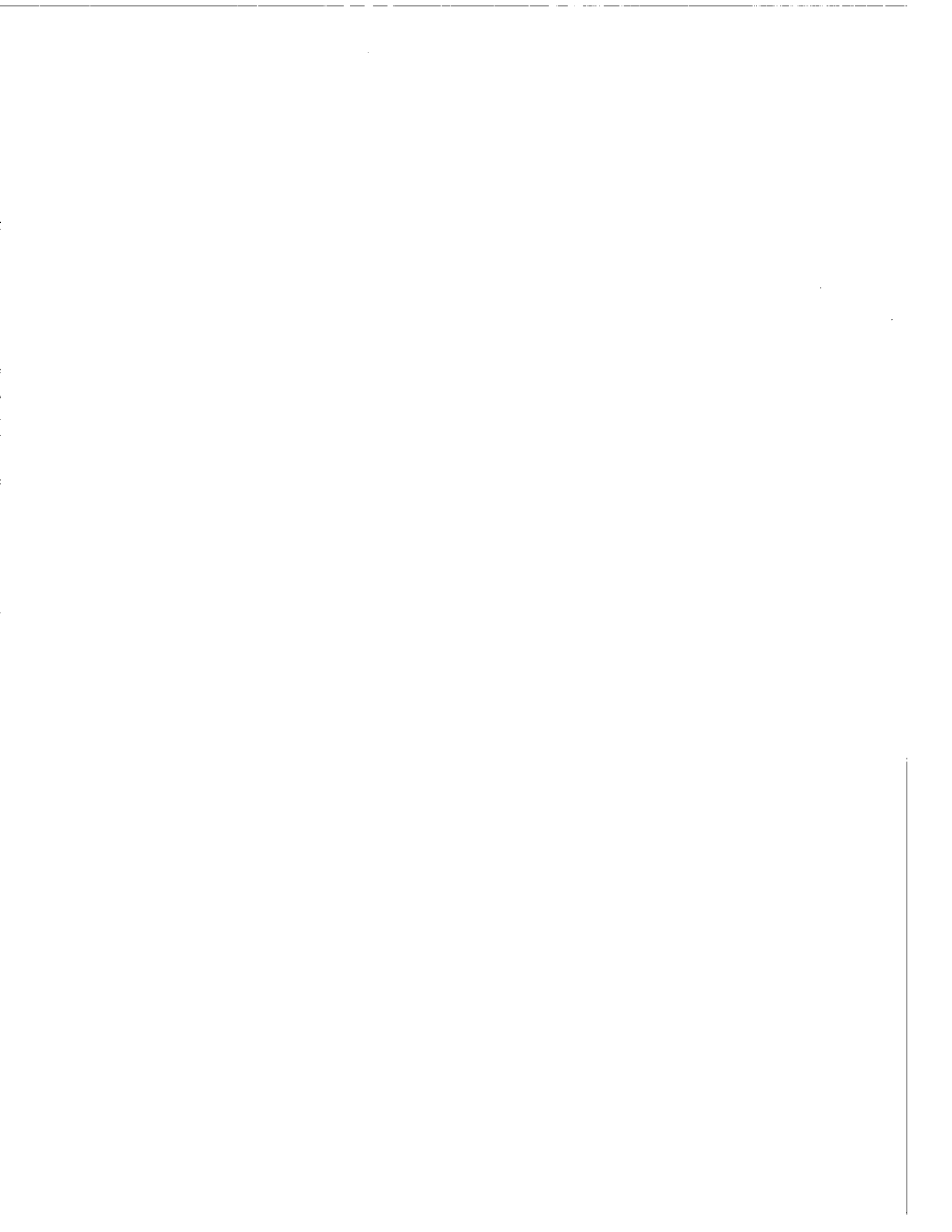


Figure 1



**1.E THE SOLAR RADIATION
MEASURING PROGRAM IN SWEDEN**

W. Josefsson

THE SOLAR RADIATION MEASURING PROGRAM IN SWEDEN

In 1982 the Swedish Meteorological and Hydrological Institute (SMHI) began the installation of a new solar radiation network. This network consisting of twelve stations is using a fully automatic data acquisition system developed and designed by the Swedish company ASEA and SMHI. The present Swedish automatic station network consist of approximately 50 stations, 12 of which are measuring solar radiation. Many stations are situated in remote areas where other observing techniques are out of the question.

Another advantage with the automatic station is the possibility of measuring many parameters very frequently and the ability of processing and storing of data.

The solar radiation network is measuring the following parameters:

-	wind direction	DD
-	wind speed	FF
-	air temperature	TT
-	relative humidity	RH
-	direct solar-radiation	I
-	global radiation	G
-	sunshine duration	SS

in addition some station are measuring:

-	atmospheric radiation	L+
	global radiation on inclined surface	
-	30° towards south	G30S
-	60° towards south	G60S
-	90° towards south	G90S
-	ultraviolet radiation	UV

The data can be stored in the memory of the station for four hours. Usually data are transferred via the telephone network twice an hour to the control-centre at SMHI in Norrköping. Direct access to real time data is possible by calling the station. At stations situated at airports or at university institutions this option is used to present real time data on a screen or to get relevant data as an input to e.g. solar heating systems.

The radiation instruments are ultimately calibrated against the Angström pyrheliometer No. 171 and the values are referred to the World Radiometric Reference. For each hour the diffuse solar radiation is computed from the measured global and direct solar radiation. The global radiation on vertical surfaces facing south, east, west and north together with a south facing surface inclined 60° are computed in routine for each station. As mentioned some stations also measure the global radiation on three different sloped surfaces. In both cases the ground reflected

component is not included. When measuring with tilted pyranometers the ground reflected radiation is eliminated by a series of black slats.

SMHI The Swedish solar radiation network

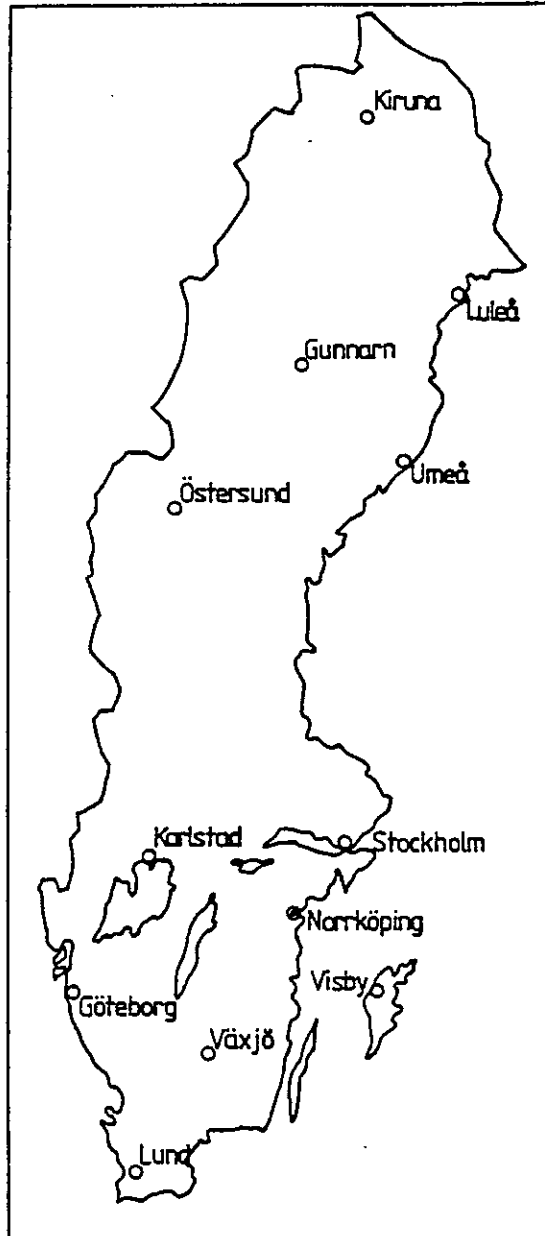


FIGURE II

Measured and calculated daily values from the automatic stations

DAILY VALUES

SMHI

Station: Stockholm-KTH 02483

IAT: N 59.35 Degrees LONG: E 18.07 Degrees

December 1983

Day	FF	TT	RH	SS	I	GO	D	G60S*	G90S*	G90R*	G90N*	G90E*	L+
1	2.0*	- 8.0*	93.0*	123*	903*	443*	339	1223	1221	326	154	354	3612+
2	4.8	- 2.4	80.3	0	0	92	92	69	46	46	46	46	6757
3	5.3	2.6	91.3	0	0	82	82	61	41	41	41	41	8358
4	3.3	2.6	98.8	0	63	220	212	253	209	137	103	103	7379
5	5.5	6.3	88.8	0	0	93	93	69	46	46	46	46	7777
6	2.7	0.5	95.1	12	184	255	242	384	346	232	118	118	7031
7	2.9	- 2.9	87.9	5	113	253	244	376	337	156	115	148	6629
8	5.1	0.9	86.6	0	0	74	74	55	37	37	37	37	6977
9	3.8	- 0.3	92.5	0	0	124	124	93	62	62	62	62	6599
10	2.7	- 9.5	92.6	0	46	243	242	239	187	163	120	120	4900
11	3.4	-10.8	90.0	85	547	304	246	783	777	279	115	129	3124
12	3.1	- 6.8*	88.0	267	1768	405	222	1852	1947	366	102	358	3057+
13	4.0	- 0.6	86.2	0	0	130	130	97	65	65	65	65	4671
14	5.2	0.3	69.0	0	0	167	167	125	83	83	83	83	5909
15	4.4	- 0.3	87.4	0	465	294	248	731	723	234	115	171	6030
16	3.4	- 0.5	90.2	12	418	271	228	656	646	230	106	126	5304
17	3.0	- 0.8	93.8	0	0	89	89	67	44	44	44	44	3533
18	1.9	- 3.7	97.3	0	0	165	165	124	82	82	82	82	2587
19	2.5	- 0.7	99.3	0	0	65	65	49	33	33	33	33	2888
20	2.9	1.0	100.0	0	0	29	29	22	15	15	15	15	2788
21	1.8	0.9	100.0	0	0	46	46	35	23	23	23	23	2489
22	3.4	2.4	98.0	0	0	113	113	84	56	56	56	56	2602
23	3.9	3.1	95.8	0	0	51	51	38	25	25	25	25	2553
24	6.1*	- 0.2*	74.5*	135*	895*	243*	238	1100	1130	226	110	282	1608+
25	2.7	- 3.5*	85.2*	0*	146*	237*	225	397	366	154	105	141	1689+
26	4.6	0.7	92.0	0	0	66	66	49	33	33	33	33	1976
27	4.7*	- 0.7*	87.1*	0	0	82	82	61	41	41	41	41	1669+
28	6.3	4.2	76.0*	244	1488	367	213	1604	1682	316	98	299	1928+
29	5.6	1.9	66.1*	241	1423	377	234	1563	1632	323	108	321	1822+
30	7.3	2.5	88.4	0	0	45	45	34	22	22	22	22	1446
31	6.0	0.8	69.0	0	1346*	350	206	1460	1534	241	94	316	1401
SUM	4.0	- 0.7	88.4	1124	9804	5854	4854	13760	13491	4134	2314	3738	126093

FIGURE III

A routine compilation of statistical data based on measured and calculated values from an automatic station

SMHI

Station: Stockholm-KTH 02483

IAT: N 59.35 Degrees LONG: E 18.07 Degrees

December 1983

	DD	FF	TT	RH	SS	I	GO	D	G60S*	G90S*	G90W*	G90N*	G90E*	L+
Mean/sun		4.0	-0.7	88.4	1124	9804	5854	4854	13760	13491	4134	2314	3738	126093
Daily:														
Max		7.3	6.3	100.0	267	1768	443	339	1852	1947	366	154	358	7777
Min		1.8	-10.8	66.1	0	0	29	29	22	15	15	15	15	1401
No. of Missing Days	0	0	0	0	0	0	0	0	0	0	0	0	0	7
Hourly:														
Abs. Max.		13.3	7.9	100.0	60	435	103	77	468	490	155	35	146	333
Ave. Max.		5.6	1.6	97.1	12	95	49	39	126	125	46	18	40	189
Ave. Min.		2.5	-2.9	79.1	0	0	0	0	0	0	0	0	0	158
Abs. Min.		0.6	-13.4	50.0	0	0	0	0	0	0	0	0	0	50
Number of Hours														
Measured	725	727	727	726	730	724	732	0	0	0	0	0	0	722
Int/comp	19	17	17	18	14	20	12	744	744	744	744	744	744	0
Missed	0	0	0	0	0	0	0	0	0	0	0	0	0	22
Total	744	744	744	744	744	744	744	744	744	744	744	744	744	744
Frequency Observed	FF	FF	FF	FF		TT	TT	TT	TT	TT	TT		SS	SS
No. of Hours	=0	>0	>5	>10		←-20	←-10	<0	>0	>10	>=20		=0	=60
	0	546	191	7		0	31	329	384	0	0		709	9
Irradiation	<100	<200	<300	<400	<500	<600	<700	<800	<900	<1000	<1100	Six. Min.	I	GO
GO :	743	744	744	744	744	744	744	744	744	744	744	Abs. Max.	443	116
I :	708	722	733	741	744	744	744	744	744	744	744			
*G60S :	702	720	730	739	744	744	744	744	744	744	744			
*G90S :	702	720	729	737	744	744	744	744	744	744	744			
Wind direction	Calm	N	NE	E	SE	S	SW	W	NW					
	2	31	55	29	28	149	151	214	85					

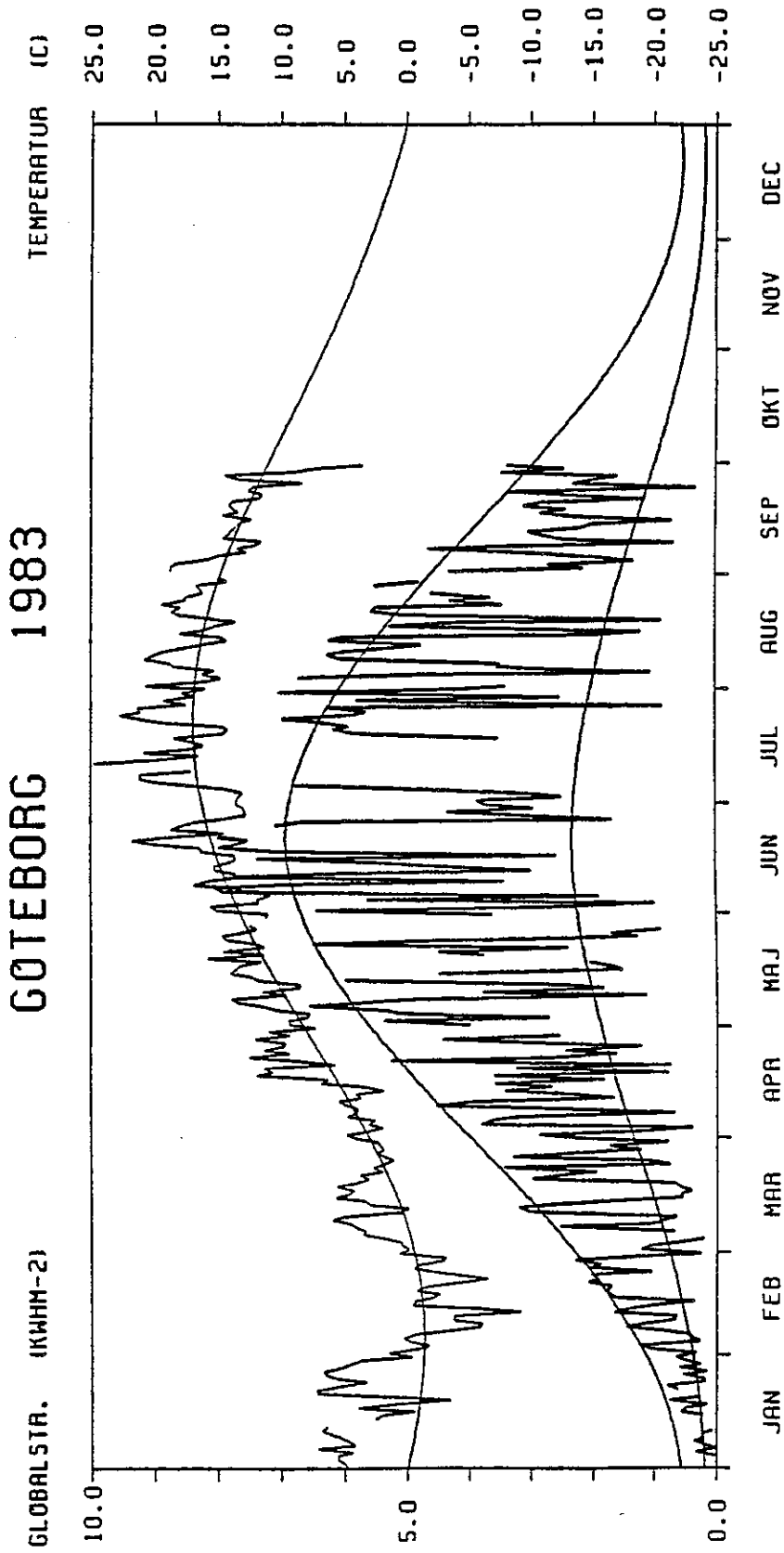
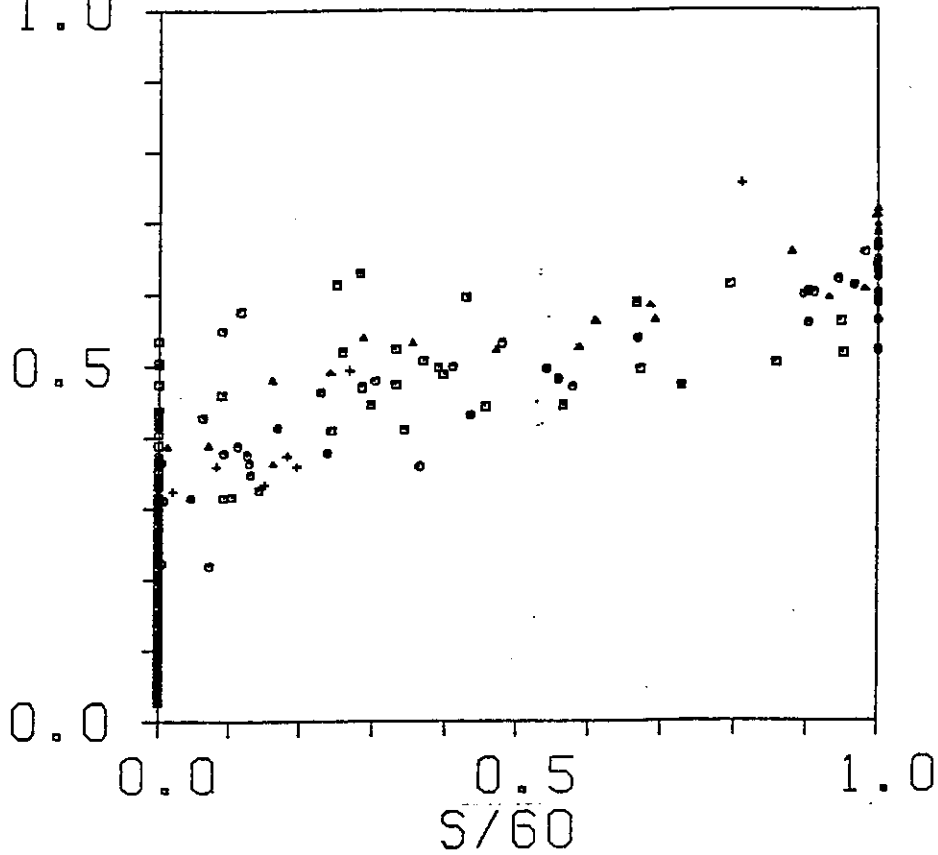


Figure 4 Daily values of the global radiation and the temperature

GÖTEBORG JANUARY-MARCH 1983

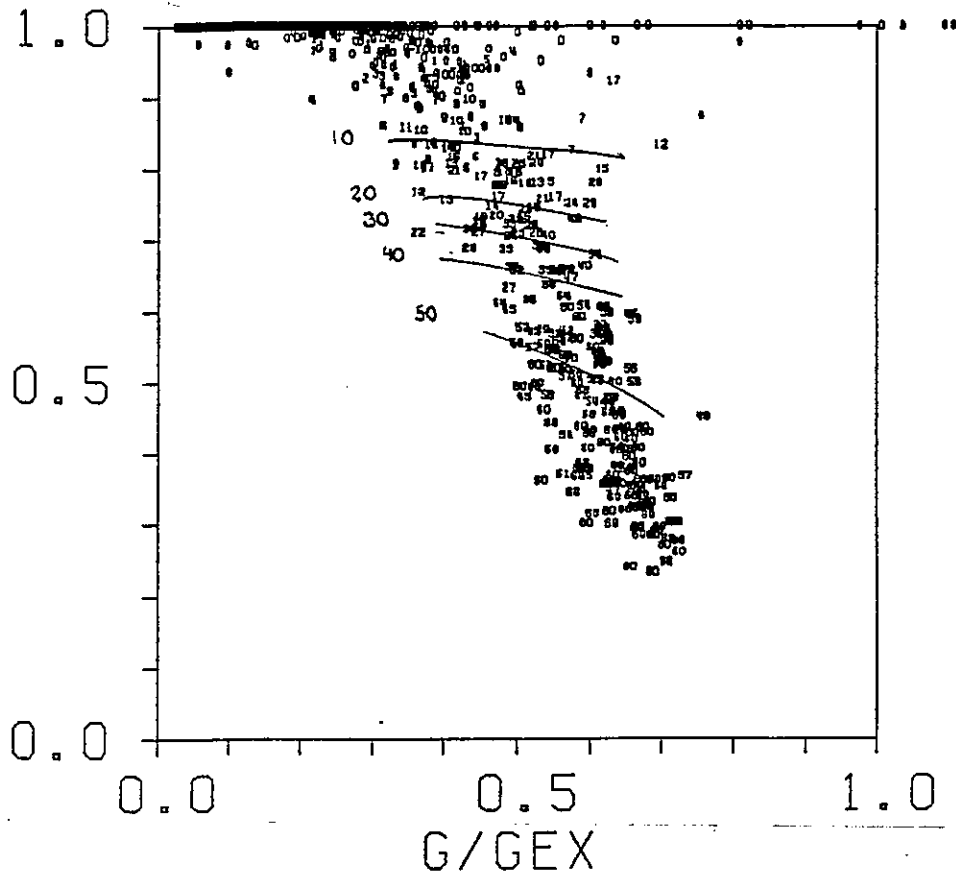
G/GEX
1.0

PARAMETER: SOLAR ALTITUDE



D/G
1.0

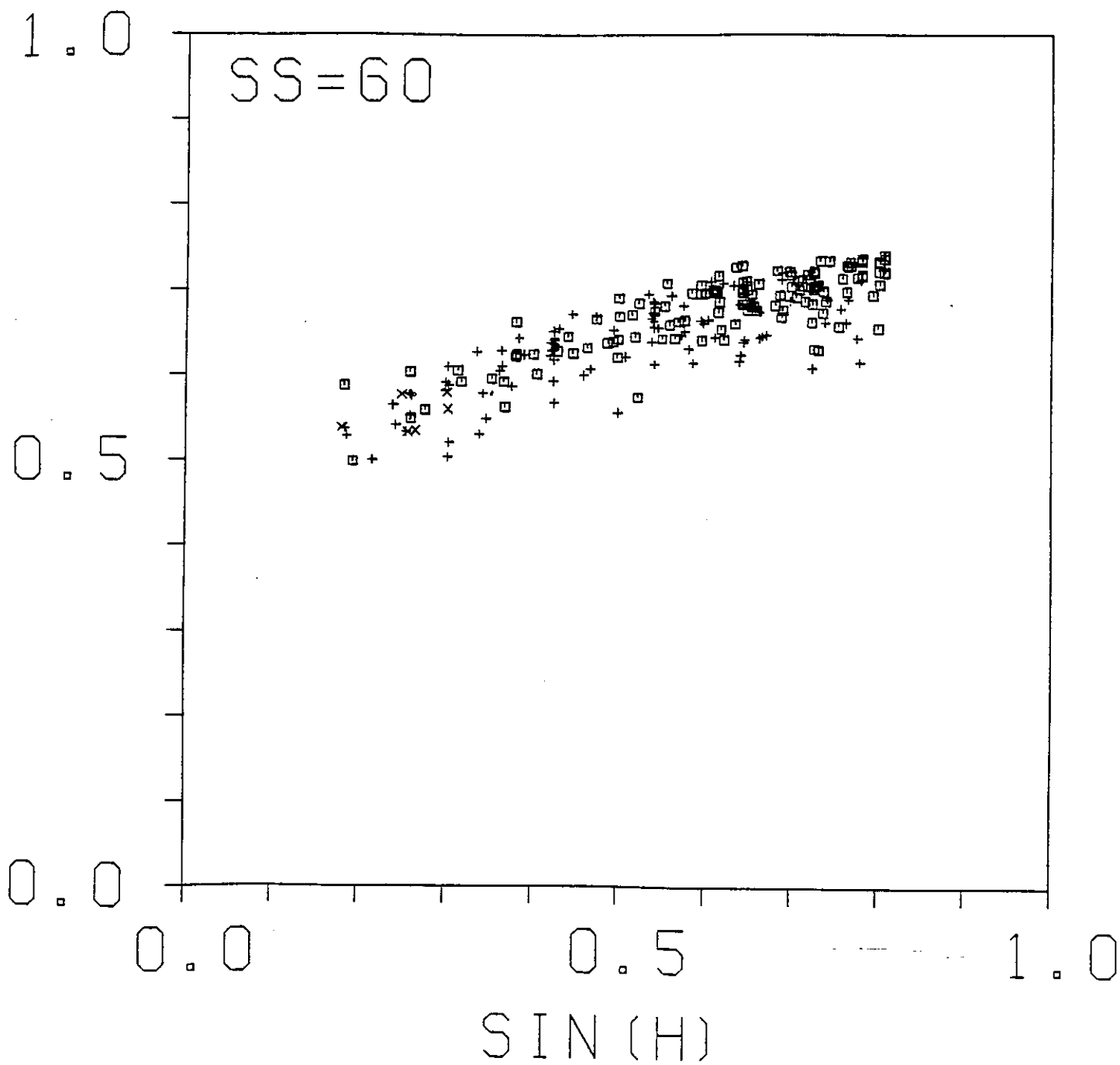
PARAMETER: SUNSHINE DURATION



STOCKHOLM APRIL-JUNE 1983

□ RH < 50%
+ 50 ≤ RH ≤ 80%
x 80 < RH

G/GEX



SESSION 2

Laboratory Characterization



**2.A METHODS FOR DETERMINATION OF SENSITIVITY
AND ANGLE DEPENDENCE AT DFVLR STUTTGART**

P.M. Nast

DFVLR, Institute for Technical Physics
D 7000 Stuttgart 80, F.R.G.

METHODS FOR DETERMINATION OF SENSITIVITY AND ANGLE DEPENDENCE AT DFVLR STUTT GART

The sensitivities of the pyranometers are determined outdoors. Partly using a HF-cavity pyr heliometer as reference and partly by comparison to a pyranometer (PSP 18376) used as working standard. The determination of $\cos\theta$ -effect results from indoor measurements. Special attention is given to the response time of the pyranometers.

The $\cos\theta$ -effect is determined by means of the apparatus shown in Figure 1. Its detailed description is found elsewhere*. The following measuring sequence is used. Measurements start with the determination of the zero point when the halogen lamp is shaded. Then readings are taken starting with $\theta = 85^\circ$ and ending with normal incidence. Then the sequence is repeated starting with $\theta = -85^\circ$. The mean of both sequences is the result. The times between the readings are decreasing during the sequence and were selected according to the measured response times. For the PSPs the readings for $\theta = 85^\circ$ are taken after 90 seconds. This time is reduced till 30 s for normal incidence. The selected sequence should give maximum accuracy despite the relatively short intervals between the readings. The calibration of the sensitivity of the working standard is done using the shading disk method. The pyranometer is mounted on a tracking platform. So the sensitivity for normal incidence is determined. Calibrations take only place on days with clear skies. Readings of the diffuse or the global irradiance are taken at least 5 minutes after the shading or the unshading. Changes of the diffuse irradiance during the waiting times are monitored by a siliconcell pyranometer. Most of the other pyranometers calibrated in Stuttgart have been compared to the working standard.

Some alternative methods for calibration have been tested (Figure 2). Shown are results of calibrations relative to the calibration factors specified by the manufacturer. The different methods compared are:

- using a second pyranometer of known sensitivity to monitor the diffuse radiation;
- change of attachment to the tracking device. The body of the pyranometer was thermally isolated from the frame of the tracking platform;
- shading disk method in a horizontal position of the pyranometer. Sensitivity for normal incidence is obtained by applying corrections for the $\cos\theta$ -effect (Elevations of the sun were between 35° and 50°)

* P.M. Nast, Measurements on the accuracy of pyranometers, Solar Energy, Vol. 31, No. 3, pp. 279-282, 1983

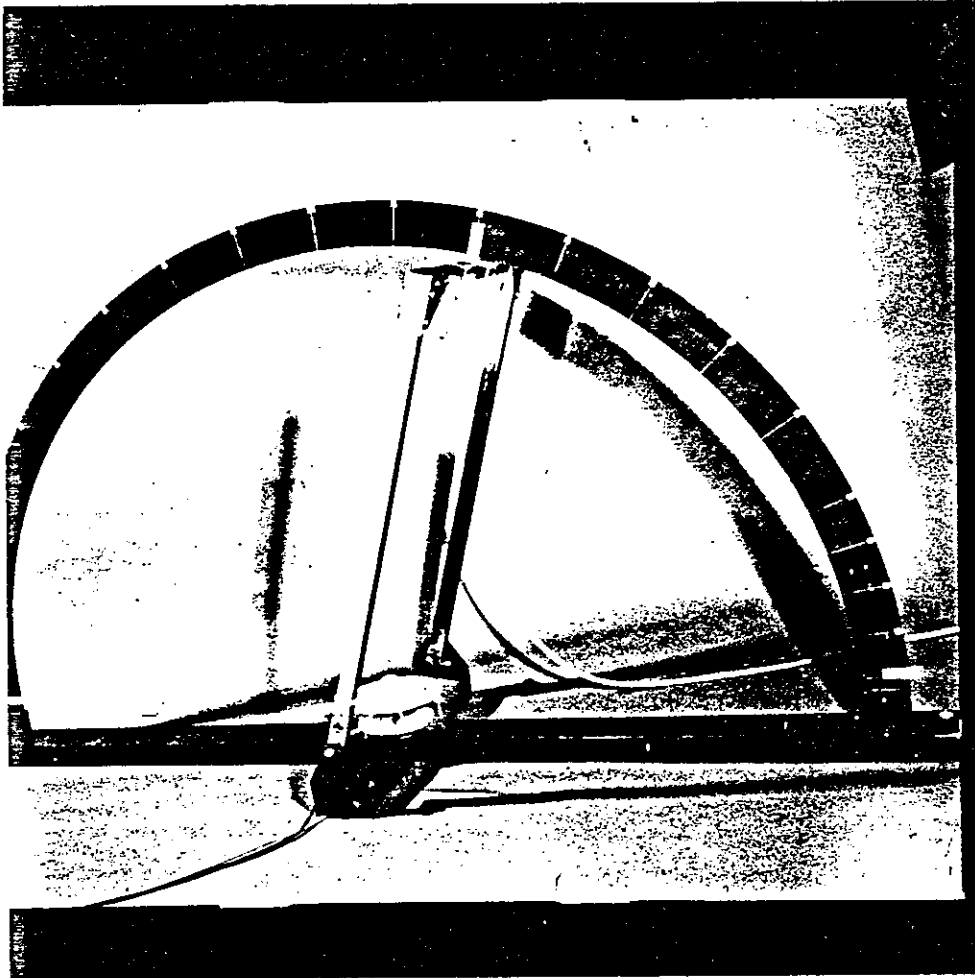


Figure 1

COMPARISON OF ALTERNATIVE METHODS FOR CALIBRATIONS

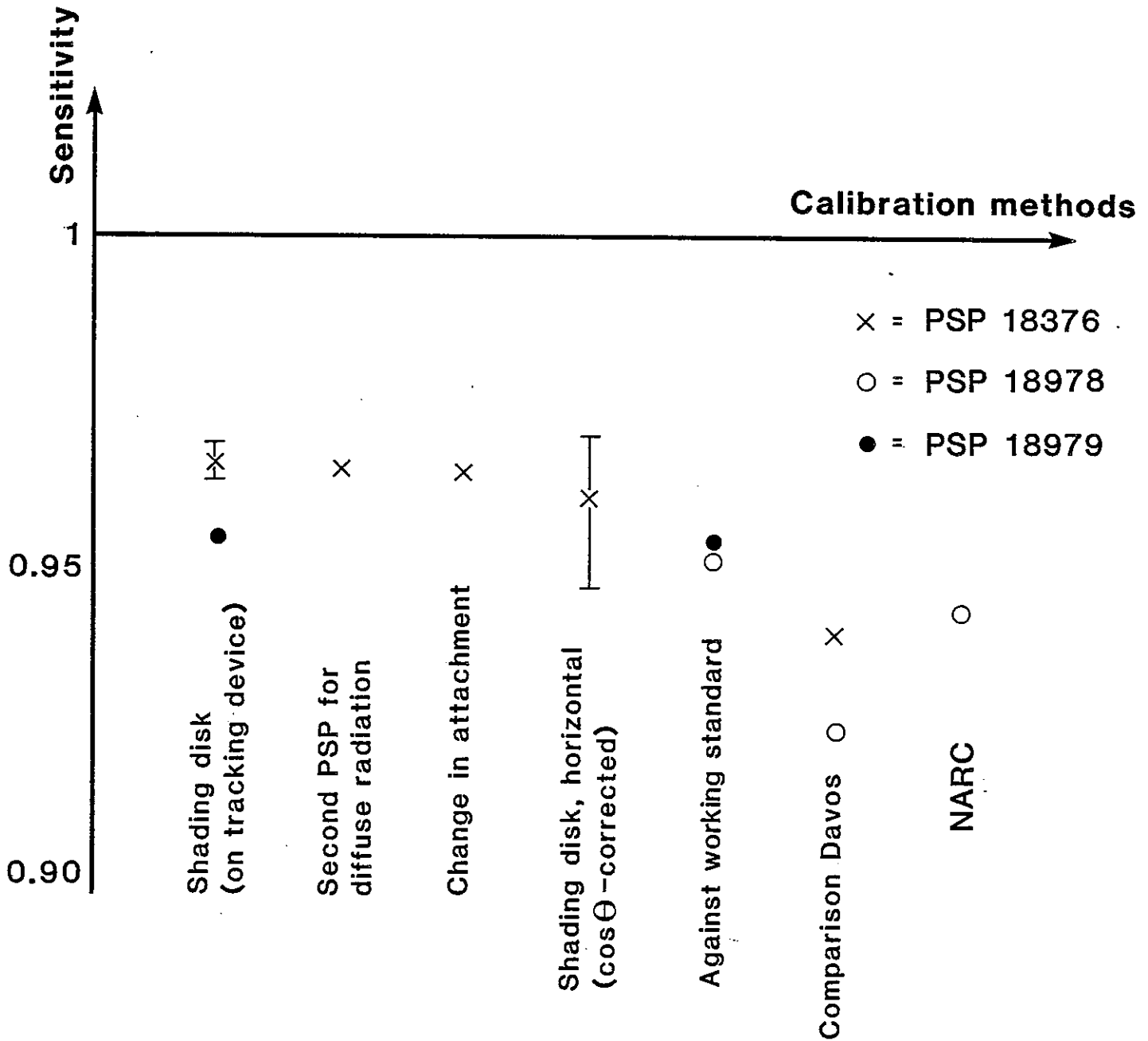


Figure 2

- calibration by comparison with a working standard that has been calibrated by the shading disc method;
- result of the pyranometer comparison in Davos, March 5/6, 1980;
- result of calibration at NARC, March 1981.

The data show that for Stuttgart the resulting sensitivities are fairly independent of the method used. The error bars in Figure 2 suggest, that methods using the tracking platform are to be preferred because they do not need corrections for the $\cos\theta$ -effects resulting in a better reproducibility.

The sensitivities measured in Stuttgart are markedly different from that determined by other laboratories. Only the agreement with the results of NARC is fairly good and the remaining differences might be caused by the angle dependence of the pyranometer.

As primary standard a HF-cavity pyrhelimeter from Eppley is used. In 1983 its accuracy has been checked against two pyrhelimeters Kendall MK6. All three gauges gave exactly the same readings.



2.8 CALIBRATION AND COMPARISON OF PYRANOMETERS

B. Petersen
Kipp & Zonen
Mercuriusweg 1
Delft - NL

G.J. van den Brink
Technisch Physische Dienst TNO-TH
(Institute of Applied Physics TNO-TH)
Stieltjesweg 1
Delft - NL

CALIBRATION AND COMPARISON OF PYRANOMETERS

INTRODUCTION

Pyranometers have been in use for quite a long time. The required accuracy of the sensitivity of the instruments has increased in the last few years. The irradiance should be known within about five percent for meteorological purposes, whereas a significant higher accuracy is required for solar energy applications. Usually a constant calibration factor is used for calculation of the irradiance from the voltage output of the pyranometer. The output of the instrument is however influenced by:

- time response;
- sudden temperature changes (thermal shocks);
- temperature (of instrument and ambient air);
- irradiance (linearity);
- tilt;
- cosine response;
- azimuth response;
- wavelength responsitivity.

It is important for the user of a pyranometer to know the dependency of the instruments output on the possible working conditions.

One should be able to make a good choice between different instruments for particular applications. A possible tilt dependency for instance is not important if the instrument is only used on a horizontal surface. A correction can be made on the calibration factor for an instrument used on a tilted surface, if the tilt dependency is known and not influenced by other working conditions.

Furthermore the manufacturer of the pyranometer should know the sensitivity dependency on the working conditions since this is indispensable for improving the instrument.

CHARACTERIZATION

Actually each pyranometer should be completely characterized by the manufacturer: the dependency on the different working conditions should be known.

A complete characterization of each individual instrument is however too time consuming and therefore too expensive. Nevertheless, it is not necessary to do all tests for determination of the characteristics on each individual pyranometer. The main parts of the characteristics are comparable to each other for different instruments of one type.

Therefore, only one of the instruments of a certain type (the working reference) has to be characterized completely in general, whereas for the

other instruments only a part of the characteristics has to be measured, supplemented by those of the working standard.

Especially the cosine response and azimuth response and the somewhat less important temperature dependency are different for the individual pyranometers. At least the first two should therefore be measured for each instrument.

CALIBRATION

Calibration of a pyranometer involves in most cases at least two steps, since it is practically impossible to calibrate each individual instrument against a pyrheliometer:

- a) calibration of a "working standard" pyranometer against a pyrheliometer as reference;
- b) transfer of the working standard calibration to the pyranometer to be used in the field.

A characterization is required of both the working standard and the field instrument for this transfer.

It is essential to present apart from the sensitivity all working conditions of the calibration procedure which might influence the sensitivity as well as a complete characterization of the instrument. A general format or calibration/characterization certificate should be developed for this presentation.

It would be very useful to present the sensitivity of a pyranometer under certain well defined conditions as well. The sensitivity can be given for instance for normal incident irradiance and/or for a uniformly isotropic illumination using a sphere. The intensity, light source, temperature level, tilt etc. should be prescribed. A direct comparison of calibration factors found by different institutes is then possible and changes of sensitivity in time can be detected easily.

Special attention should be given to outdoor measurements, taken during a whole day. It is usually not correct to calculate the sensitivity as a mean value over the day, unless "working standard" and "field instrument" have the same characteristics, since the working conditions (sun elevation, azimuth, temperature etc.) are not constant. Theoretically every incremental measurement should be normalized before taking the mean value.

The calibration factor presented under normalized conditions can be adjusted for an instrument used in the field by manufacturer or user for the actual working conditions if a complete calibration/characterization has been carried out. The adjustment of the calibration factor may be strongly dependent on the climatic circumstances under which the instrument is used.

CONCLUDING REMARKS

- Characterization of pyranometers is of the utmost importance for manufacturers to improve the instruments and for the user in the field.
- Presentation of the sensitivity of the pyranometer under uniformly well defined conditions is useful.
- A general format or calibration/characterization certificate should be developed for the presentation of the calibration factor of the pyranometer under well defined conditions, the characteristics of the instrument under different working conditions and the methods used for the determination.

2.C TILT EFFECT ON PYRANOMETERS: A REVIEW

Klaus Dehne

Deutscher Wetterdienst
Meteorologisches Observatorium Hamburg

CONTRIBUTION TO TASK IX PYRANOMETRY SYMPOSIUM AT NORRKÖPING 1984

Tilt Effect on Pyranometers: A Review

The dependence on tilt angle of pyranometer response may be caused by the following effects:

- a) The convective heat losses of the receiver surfaces depend on their inclinations (1);
- b) The infrared irradiance on the receiver of sky and ground is different at different tilt angles;
- c) The warming by direct solar radiation of the pyranometer body depends on the orientation of the pyranometer with respect to the direction to the sun.

The effect a) has been investigated in different laboratories. The results for different types of pyranometers are compiled in Table 1 which are not claimed to be complete. The sequence of the authors follows the year of publication. Four different types of test devices has been used. The results are given as relative change of sensitivity (in percentage) for the worse case if the pyranometers are tilted from the horizontal to the vertical position. The comparability of the results of different authors is restricted since the applied irradiance and the orientation of the thermopiles of the pyranometers are often not specified as indicated by the question marks.

Nevertheless, looking for a preliminary summarizing result for the above mentioned worse case of tilting the pyranometers (irradiated by 1000 Wm^{-2}), the following relative changes of sensitivity may be extracted from Table 1.

Pyranometer	%	Remarks
PSP	<.5	
CM 11	<.5	
CM 5	-2	Best case: Cable outlet parallel to tilt axis
STAR	(-2)	orientation?
EKO	(-2)	"
8-48	(-7)	"
HOLLIS	(<.5)	

While the results for the first three pyranometers have a high level of confidence, the results for the four other pyranometers should be confirmed by further tests.

The effect b) has been tested by the author in the laboratory using hemispherical blackbody radiators. Accordingly the tilting from the horizon-

tal to the vertical position of field pyranometers of the type CM 5, CM 11 and PSP should deliver after 15-30 minutes irradiation outdoors an infrared generated excess signal equivalent to 15-20 Wm^{-2} when the temperature difference between sky and ground is of the order of 30 K. Natural and artificial ventilation of the pyranometer dome may reduce this effect by more than a factor 5. Therefore, for accurate measurements at calm the artificial ventilation will be necessary.

The effect c) has not yet been investigated thoroughly. It depends on the heat conduction and the painting of the pyranometer body as well as on the wind velocity. By special screens for tilted pyranometers this effect can be prevented.

Field tests are more realistic than laboratory tests but are less well defined and reproducible (see (2) for instance). The duration of a field test is limited by the variation of the sun position and changing atmospheric conditions. Nevertheless, field tests are considered to be necessary for verifying the results of laboratory tests on realistic conditions, and should be performed at selected sites. "Clean" results may be expected from field experiments which can be described as "sun and shade" calibration of sun-tracking pyranometers. Such experiments carried out by DSET Laboratories (Phoenix) and by NARC (Toronto) for instance, should verify the results of the indoor tests which lead to the conclusion that a ventilated, well screened pyranometer with a "cold" thermobattery has a tilt effect less than 0.5%.

REFERENCES

- Dehne, K.: Dependency on tilt angle of pyranometer sensitivity. In: Proceedings of the CIE-Symposium on Light and Radiation Measurement '81, Hajduszoboszlo, 27-28 May 1981. Hungarian National Committee of the CIE, Budapest, 1981.
- Stoffel, T.: Preliminary analysis of IEA Pyranometer performance comparisons: an outdoor tilt table study, in Appendix M. In: Proceedings of the International Energy Agency Conference on Pyranometer Measurements. 16-20 March 1981, Boulder, Colorado. Solar Energy Research Institute, October 1982.

TABLE 1
Laboratory Tests of Tilt Effect

Authors	Institution	Year of Publ.	Type of Test device	Tested Pyranometer	Results $M(90^\circ)/M(0^\circ) - 1$	at Wm^{-2}	Thermopile orientation
Norris	CSIRO, Division of Mechanical Engineering	1974	Rotating arm & mirror	K & Z CM5 Eppley PSP	10% 10%	?	? ?
Flowers	NOAA, SRF, Boulder	1977	Rotating boom	Eppley PSP Eppley 8-48 (B&W) K & Z CM5 Kahl Star	0.5% -0.25% 0% -0.5%	450	?
Pimpel	DVFLR, Oberpfaffenhofen, FR Germany	1977	Rotating boom	Eppley PSP K & Z CM5	< 0.5% -3%	mixed	?
Dehne	Met. Obs. Hamburg	1978	Rotating drum	K & Z CM5 Eppley PSP	-4% -2% -2% -1% < 0.5%	1400 450 1400 450 1400	cable \perp axis cable / axis cable \parallel axis cable axis cable \perp axis
Dehne	Met. Obs. Hamburg	1980	Rotating drum	K & Z CM10	< -0.5%	1000	cable \perp axis
Ichiki & Ikeda	Aerological Observatory & Abasheri District Met. Obs. Japan	1979	Tilt box	EIKO-Eppley K & Z CM5	-0.5% -4%	? ?	? ?
Mohr, Dahlberg & Dirnhirn	Utah University	1979	Rotating boom	Schenk Star 8101	+1%	?	?
Goldberg	Smithsonian Radiation Biology Laboratory	1980	Rotating boom	Eppley PSP	+1%	1000	?
Petersen & van Wely	Kipp & Zonen, Delft	1981	Rotating arm & mirror	Kipp & Zonen CM11	< 0.5%	1000	?
Andersson et. al.	Statens Provningsanstalt, Boras	1981	Rotating boom	Eppley PSP K & Z CM5 Schenk Star 8101 Hollis MR-5	0% -1.5% -3% 0%	1000 & 450	?
Andersson et. al.	Statens Provningsanstalt, Boras	1982 (not yet published)	Rotating boom	K & Z CM10 EKO	0% -1% ... -3%	1000	cable \parallel axis
Nast	DVFLR, Stuttgart	1983	Rotating boom	Eppley PSP K & Z CM5 K & Z CM10 Eppley 8-48 (B&W)	0% -2% 0% -7%	800	?

2.D PYRANOMETER CHARACTERIZATION MEASUREMENT METHODS AT THE
STATENS PROVNINGSANSTALT, BORAS
AND RESULTS FROM THE IEA MEASUREMENTS IN BORAS 1982

Lief Liedquist

PYRANOMETER CHARACTERIZATION MEASUREMENT METHODS AT THE
STATENS PROVNINGSANSTALT, BORÅS
AND RESULTS FROM THE IEA MEASUREMENTS IN BORÅS 1982

GENERAL

At Statens provningsanstalt (National Testing Institute) in Borås we have methods for indoor measurements of four pyranometer characterization parameters: cosine dependence, tilt effect, linearity and temperature dependence. Measurement of azimuth dependence is included in the cosine measurements. We have also facilities for outdoor calibration of pyranometers.

Our indoor methods are indeed very simple. Actually so simple that we assemble and disassemble the measurement set-up before and after every measurement period. As a solar simulator we use an ordinary small picture slide projector, Kodak Carousel, which is slightly modified for DC power operation of its lamp: a 250 W 24 V tungsten halogen lamp. We use this projector as a source for all indoor measurements except for the linearity measurements where we use two identical projectors which are very similar to the Kodak projector but are made by another manufacturer. Heat filter (infrared cut-off-filter) is used except for the temperature dependence measurements where we had problems to get enough irradiance on the pyranometer. With the filter we get a spectral irradiance wavelength distribution as in Figure 1. The dotted curve in Figure 1 shows the solar irradiance at ground level passing two airmasses. The irradiance center wavelength is 581 nm for the projector radiation and 711 nm for the solar radiation. As the pyranometers we so far have measured with these methods are total absorbing temperature sensing devices this should mean that the difference between the two spectral distributions (and also other ground level solar distributions) are not very significant for the measurement unaccuracy.

COSINE DEPENDENCE

For the cosine dependence measurements we mount the pyranometer on a rotational stage. The stage and pyranometer we then mount on another rotational stage (Figure 2) whose surface is horizontal (vertical axis). The top stage has an horizontal axis of rotation. We adjust the position of the top stage so the sensitive surface of the pyranometer which is vertical will have its vertical diameter coinciding with the rotational axis of the bottom stage.

We make this adjustment very carefully using a microscope. The projector source is placed about one meter from the pyranometer surface and positioned so the pyranometer is irradiated along an horizontal optical axis. Three screens are used to reduce stray radiation to the surrounding which is in black material. A shutter is also placed in the optical path. The projector is operated without the objective lens. This set-up gives a very uniform irradiation over the pyranometer surface also in cases where the sensitive area is rather large. We measured the luminance distribution across a surface corresponding to that of the Schenk Star pyranometer to be

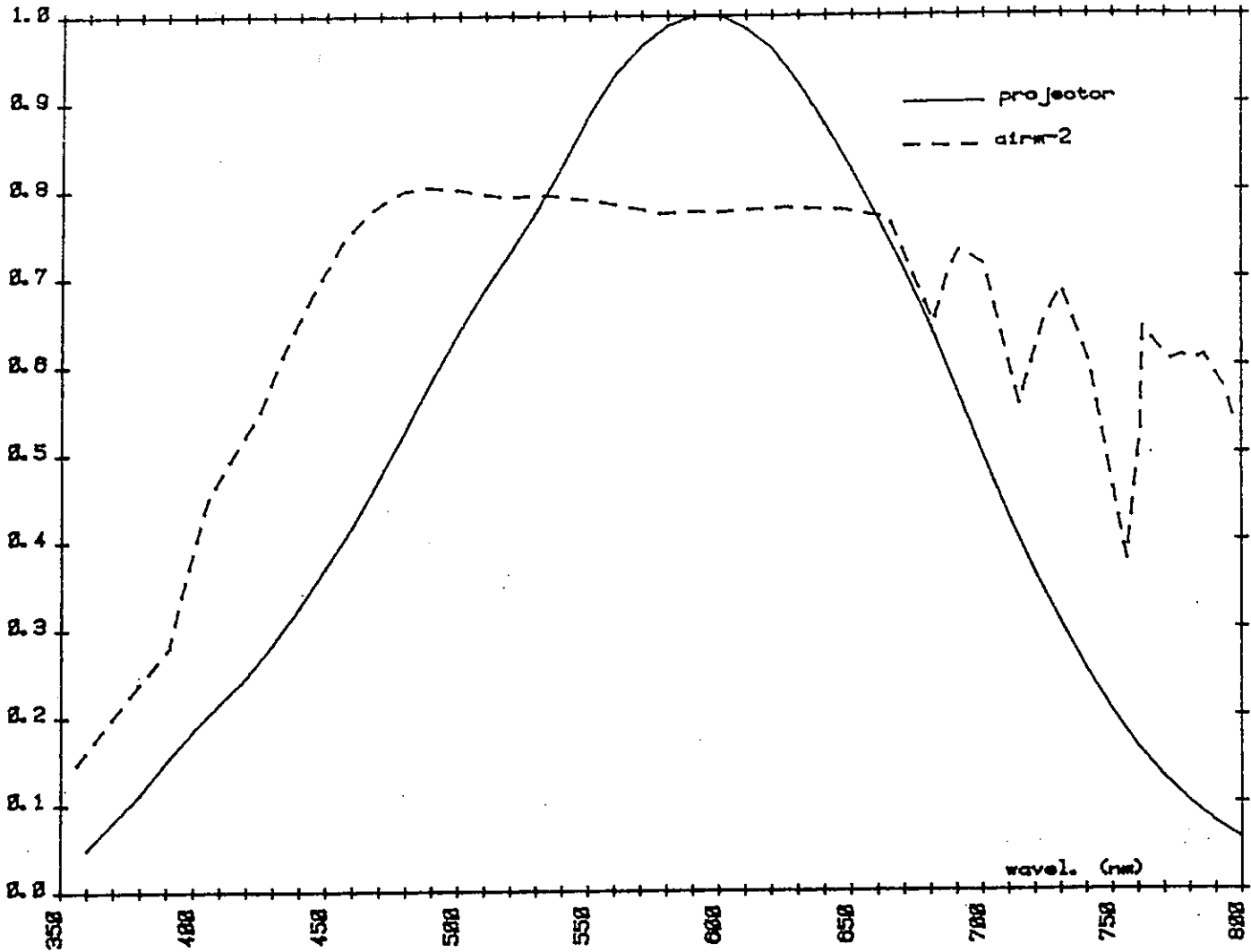


Figure 1. The radiation spectrum of the projector compared with airmass-2 solar spectrum

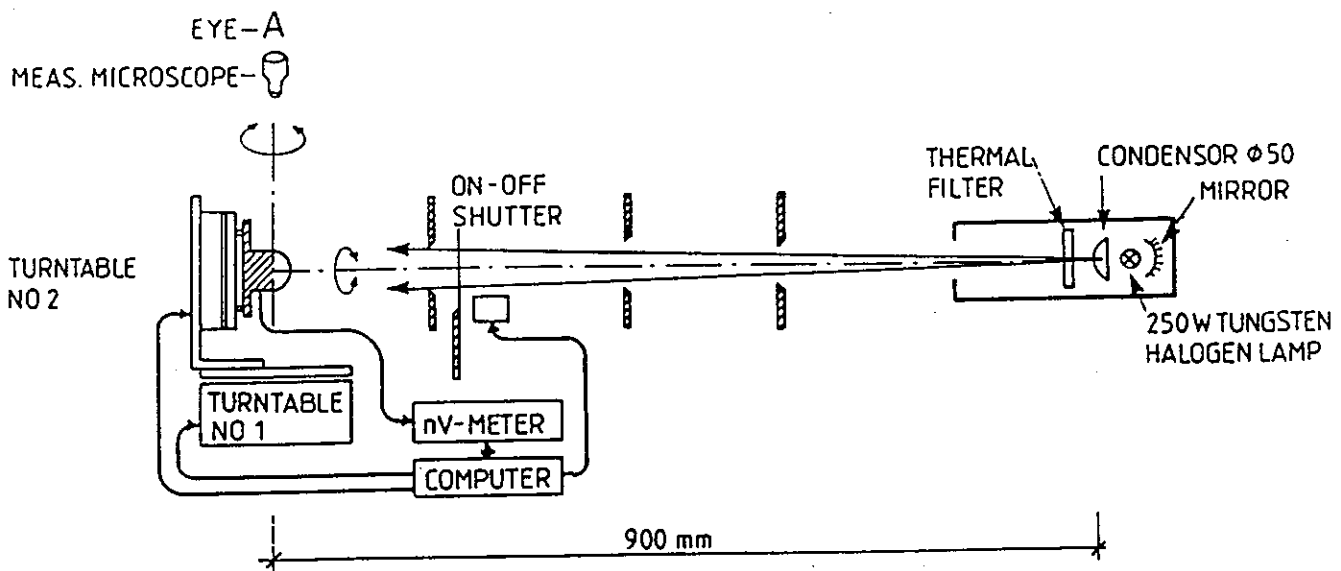


Figure 2. Cosine dependance measurements

within $\pm 0.5\%$ and within $\pm 0.1\%$ for the Eppley PSP surface size. The irradiance is rather low: about 50 W/m^2 . The whole outer glass dome is irradiated.

Before mounting the pyranometer it was carefully positioned "parallel" to the upper rotational stage surface using its spirit level. This was done to check the accuracy of the spirit level from the measured cosine dependence angular distributions.

The bottom stage is rotated so the light reflex from the vertical stage surface reentered the source. This angle of the stage defines the zero angle of incidence.

Both rotational stages are computer controlled and so is the shutter. The pyranometer output which is very small, just a few hundreds of microvolts, and is measured by a digital nanovolt meter, made by Keithley, is fed into the computer.

The bottom stage is rotated $\pm 90^\circ$ and measurements are taken every 2° . Reference measurements are taken at 0° before, in the middle and after the sweep for correction of source instabilities. Then the measurements are repeated with the upper stage and pyranometer rotated in 30° steps until cosine dependence has been measured in six different polar planes which gives 12 azimuth directions. At each angular position the difference is measured between the pyranometer output when irradiated and the output when shaded by the shutter. But both voltages are recorded.

The whole measurement is automatic and takes different time depending of the time constant of the pyranometer. A complete cosine measurement of a Kipp & Zonen CM5 pyranometer takes about 18 hours while an Eppley PSP is measured in about 8 hours.

The result is given in a table like Figure 3 for the 12 azimuth directions.

TILT EFFECT

For measuring the tilt effect we mount the projector and the pyranometer on an optical bench like Figure 4. The bench is mounted on a tripod with a tilting head. With the bench horizontal the pyranometer is mounted vertical. The irradiance is adjusted to 1000 W/m^2 . The whole outer glass dome is irradiated.

The irradiance change a little during the tilting and therefore a reference detector is mounted into the radiation beam by means of a beam splitter. The reference detector is adjusted so geometrically about the same radiation falls on its surface as falls on the pyranometer sensing area. It is a silicon detector with a radiometric filter.

FIGURE 3

Cosine/azimuth table

Responsivity Deviation Per Mile from Cosinus Response
at Different Azimuth Planes

Pyranometer: CM11-810181

Azimuth: Polar Angle	0	30	60	90	120	150	180	210	240	270	300	330
1	0	0	0	0	0	0	0	0	0	0	0	0
2	0	-0	-0	-0	-1	-1	0	0	-0	0	-0	0
4	0	0	-0	-0	-0	-1	0	0	-0	-0	-0	-0
6	0	-0	0	-0	-0	-1	0	0	-0	0	-0	0
8	0	-0	-0	-0	-1	-1	0	0	0	-0	-1	-0
10	0	-0	0	-0	-1	-1	0	1	-0	-0	-0	-0
12	-0	-0	0	0	-1	-1	0	1	-0	-0	-1	-0
14	-0	-0	0	0	-0	-1	0	0	0	-1	-1	-0
16	0	0	1	0	-0	-0	1	1	-0	-1	-1	-0
18	0	0	1	0	-0	-1	1	1	0	-1	-1	-0
20	0	1	1	1	-0	-0	1	1	0	-1	-1	-0
22	0	0	1	1	0	-0	1	1	0	-1	-0	0
24	0	1	1	1	-0	0	1	2	0	-1	-0	0
26	1	0	2	1	0	0	2	2	1	-0	-0	1
28	1	1	2	1	0	1	2	2	1	-1	-0	1
30	1	1	2	1	1	1	2	3	1	-0	-0	1
32	1	1	2	1	1	1	3	3	1	-1	0	1
34	1	1	2	2	1	1	3	3	1	-0	0	1
36	2	1	2	2	1	1	3	4	1	-0	1	2
38	2	2	3	2	1	1	3	4	1	-0	1	2
40	2	2	3	2	1	1	3	4	1	0	1	2
42	2	2	3	3	1	2	4	4	1	0	2	2
44	2	2	3	3	1	2	4	5	2	1	2	2
46	2	2	3	2	1	2	4	5	2	1	2	2
48	3	2	3	2	1	1	4	5	2	1	3	1
50	3	2	3	2	1	2	4	6	3	2	3	1
52	4	2	3	3	1	1	4	6	3	2	3	2
54	4	3	3	2	1	2	4	6	3	2	3	1
56	5	4	4	3	2	2	4	6	3	2	3	1
58	6	4	4	3	2	3	3	6	2	2	3	1
60	6	5	5	4	2	2	3	6	2	1	3	1
62	7	5	5	4	2	2	2	5	3	1	3	1
64	8	6	6	4	2	3	2	5	3	1	3	1
66	9	7	7	4	2	3	3	6	3	1	4	1
68	9	7	8	4	2	3	2	6	4	1	4	2
70	11	10	9	5	3	5	3	7	5	2	6	4
72	14	12	12	6	4	8	4	9	8	6	8	7
74	19	17	17	10	7	14	5	11	10	7	0	9
76	26	22	21	14	11	21	8	16	16	13	15	13
78	35	29	30	20	18	28	11	21	22	18	21	22
80	50	38	41	29	25	37	16	30	32	30	33	36
82	73	56	54	43	31	43	16	39	48	51	54	55
84	103	72	59	46	29	40	13	42	64	77	80	71
86	147	109	92	77	56	73	28	64	85	110	121	98
88	305	239	214	197	161	194	119	118	214	246	261	224
90	---	---	---	---	---	---	---	---	---	---	---	---
Offset	.10	.02	.03	.04	.05	.02	.10	.02	.03	.04	.05	.02

The ratio of the pyranometer output voltage and the reference detector short circuit current is taken every 10° tilting of the bench from 0° to 90° and back again.

Before the measurements the pyranometer is stabilized at 1000 W/m^2 irradiance for about 5 minutes. The stabilization time used at each tilt position is 10-20 seconds.

The tilt position is set manually but the readings of the detector outputs are taken directly into a computer in order to save time. The result is got directly by taking the mean values of the two measured ratios at each tilting position and then normalizing the mean values to one at 0° tilt angle of the pyranometer.

LINEARITY

For measuring the linearity of a pyranometer the pyranometer is placed horizontally and irradiated from two projectors as in Figure 5. This projector set-up was actually developed for measuring linearity of photodetectors and radiometers vertically mounted on an 11 meter optical bench. But we want to measure the pyranometers in horizontal position and therefore we place a mirror on top of it. The mirror is concave and focussing the radiation so we can get 1000 W/m^2 irradiation (500 W/m^2 from each projector). The projector outputs are adjusted to give approximately the same pyranometer output voltages. The irradiance on the pyranometer surface is in this measurement not very uniform.

The DC power to the projector lamps is controlled by a computer which also controls the individual shutters in the projectors. The computer also reads the detector output.

The following measurements are made of the pyranometer output: both projectors closed, projector A open, both closed, both open, both closed, B open and both closed. With the zero values subtracted from the readings the ratio is taken of the detector outputs with both projectors open and the sum of the two outputs with single projector. The ratio shall be equal to one if the pyranometer is linear (by the principle of superposition).

These measurements are repeated three times and a mean value is calculated.

Then the DC voltage of the lamps is adjusted to give half of the previous irradiance level on the pyranometer. This of course gives a change in the spectral distribution of the irradiance but we assume that the linearity is independent of those changes in distributions we get, which may be true or not.

The lamps must be stabilized at each new power level. Also a stabilizing period is needed before taking a pyranometer output reading after changing the irradiance. The latter time is different for different pyranometer types.

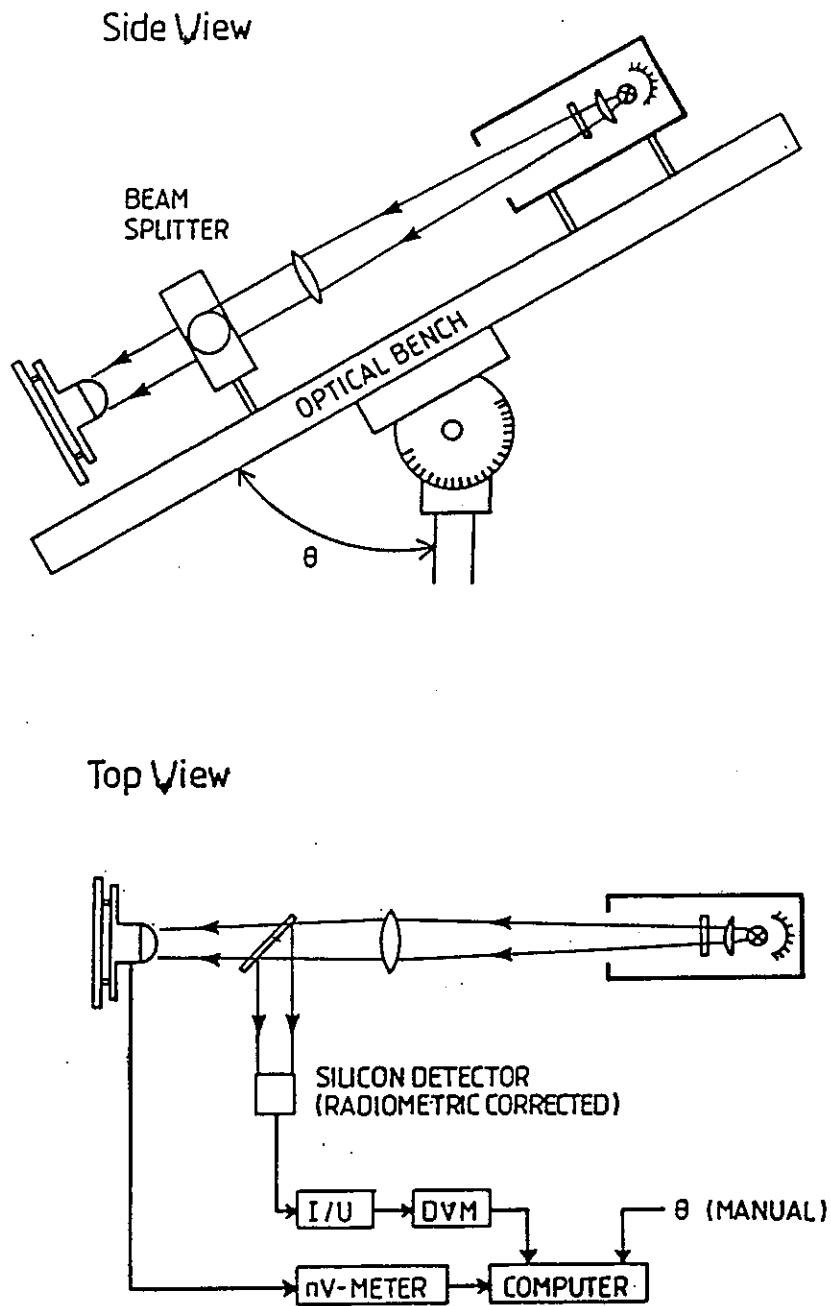


Figure 4. Tilt effect measurements

The measurement of the linearity is automatic, taking several hours to complete mostly depending on the time constant of the pyranometer.

The result is normalized to one at 500 W/m² and is presented as the responsivity R(E) as a function of the irradiance level E on the pyranometer. With the measured ratios r(E) the responsivity is given by:

$$R(1000) = r(1000)$$

$$R(E/2) = R(E)/r(E)$$

TEMPERATURE DEPENDENCE

For measuring the temperature dependence the pyranometer is placed inside a temperature chamber with a hole in its roof through which the radiation is transferred from outside to the pyranometer (Figure 6). A reference detector similar to that for the tilt measurements keeps track of the irradiance level during the measurement period.

A thermocouple is carefully attached with aluminium tape to the base of the pyranometer. We also use silicon grease to get good thermal contact which is very important.

The temperature setting from -25°C to +35°C in 15°C step is controlled by a computer which also reads the thermocouple output, the reference detector output and the pyranometer output. When the temperature is found stable within a given degree measurements are taken of the detector outputs. 5°C is taken to be reference temperature and the measurements at the different temperatures are made in the following order: 5°, -10°, 5°, -35°, 5°, 20°, 5°, 35°, 5°.

All these measurements are automatic. The measuring time depends to a large extent on the heat capacity of the pyranometer body. Normally, it is about 7 hours which means that we can measure two pyranometers per 24 hours.

The mean detector output at each temperature divided by the 5°C mean output is calculated. No zero values of the pyranometers were taken.

OUTDOOR CALIBRATION

Finally, we also make outdoor calibration of pyranometers. I think this is outside the theme of this lecture but I will mention it very briefly for completeness. We can calibrate up to 25 pyranometers simultaneously on the roof of one of our buildings. Readings of all 25 is taken simultaneously each minute during daytime in a 4 second integration period with a voltage to frequency converter for each pyranometer. A mean value weighted with the irradiance level is taken for about 5 days measurements with the pyranometers horizontally mounted and another 5 days with the pyranometers tilted 50° towards south. We also take readings from a reference pyranometer. Correction (very small) for temperature variations and cosine dependence of

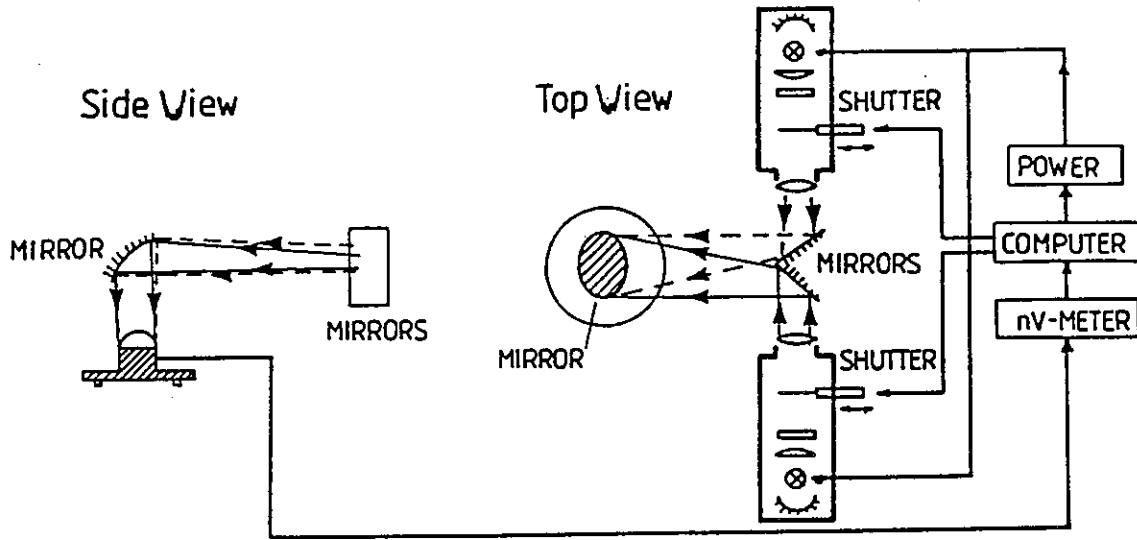


Figure 5. Linearity measurements

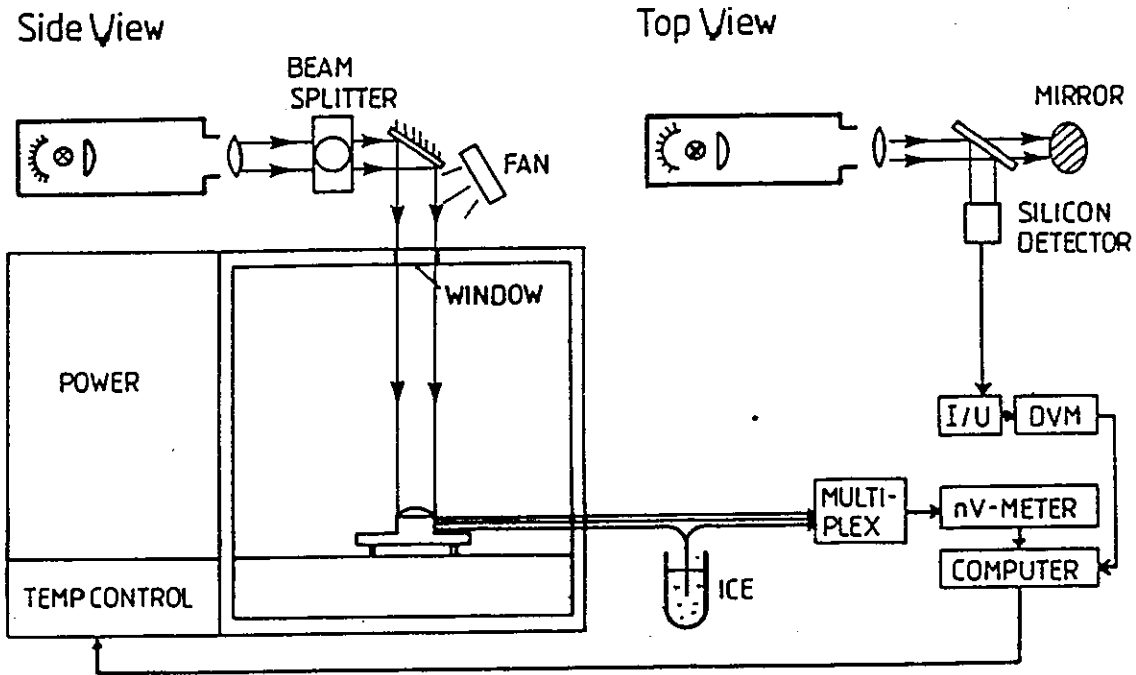


Figure 6. Temperature coefficient measurements

SOLAR IRRADIANCE RELATIVE EPPLEY PSP 15835F3 (8.75 mV/kW/m²)
Pyranometers: Eppley PSP 15835F3 with responsivity 8.7 mV/kW/m²
Horizontally mounted
Borås, Sweden 2-7 juni 1983

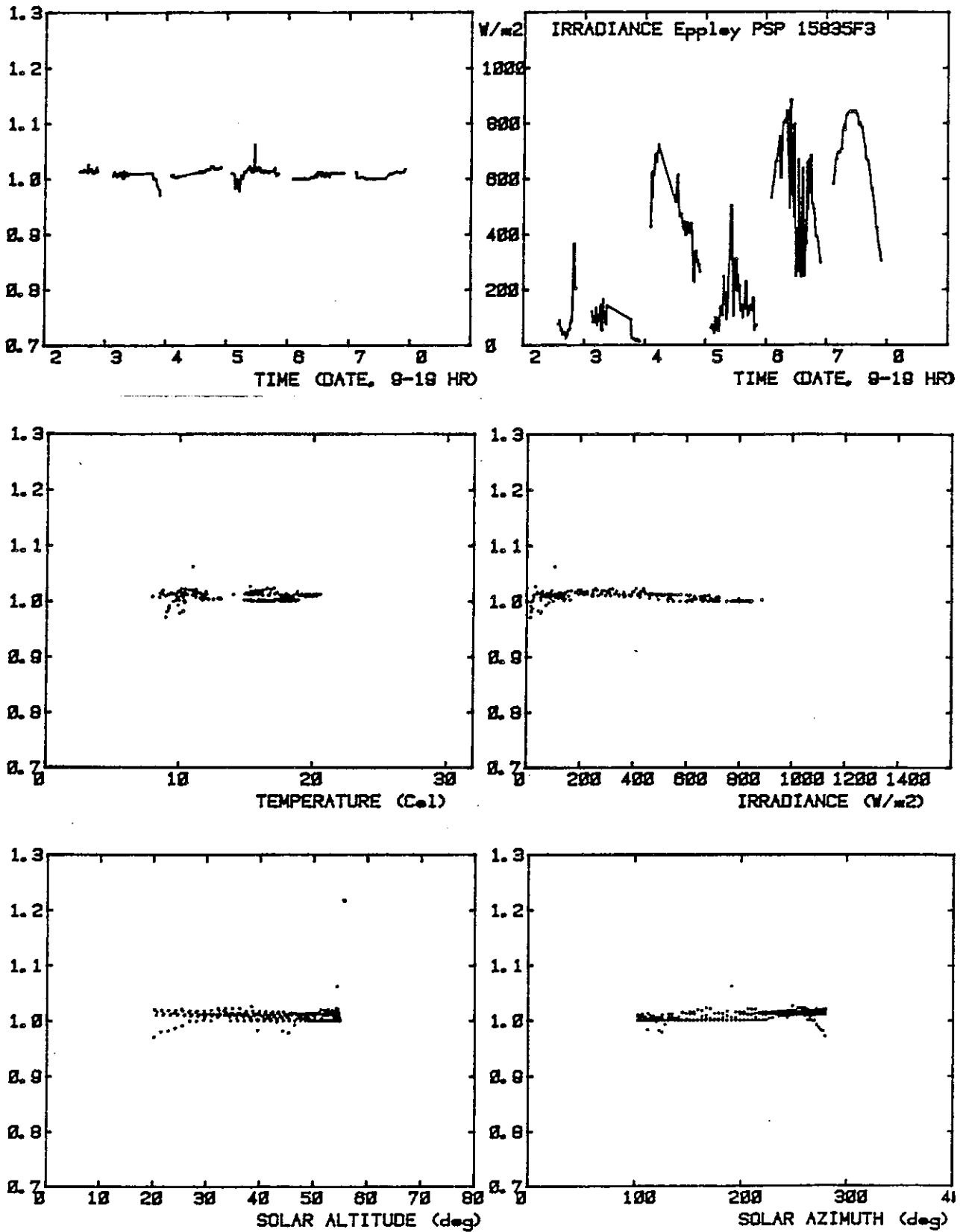


Figure 7. Result from outdoor calibration

the reference pyranometer as we use shading technique when we absolute calibrate it against a pyr heliometer. The voltage to frequency converters are calibrated electrically before each 5 day period. The result of the measurements looks like Figure 7 which shows diagrams for the radiation situation during the period of measurement. Each point in the diagram represents a 10 minute mean value.

IEA MEASUREMENTS IN BORÅS 1982

The indoor characterization parameters of 33 pyranometers was measured in Borås 1982 within the IEA work. Cosine dependence, tilt effect, linearity and temperature dependence was measured on 6 items EKO, 6 items Eppley RSP, 5 items Kipp & Zonen CM5, 5 items Kipp & Zonen CM10, 5 items Schenk Star, 3 items Swissteco SS-25 and 3 of the World Radiation Center pyranometers.

Figure 8-12 show the result of these measurements where each diagram represent one type of instruments with the result from each individual instrument of the type plotted.

Figure 8 shows the temperature dependence. The behaviour of the instruments of each type are very close except for the EKO instruments. Also one of the older PSP and the very oldest CM10 differs significantly.

Figure 9 shows the pyranometer responsivity with the irradiance level. In general the instruments of each type are behaving the same. Eppley PSP has negligible temperature dependence.

Figure 10 shows the tilt effect. Swissteco SS-25, Eppley PSP and Kipp & Zonen has negligible tilt effect. EKO has different tilt effect for different orientations of the black and white fields. Smaller tilt effect was measured for EKO No. 81901 and No. 81903 which have a black field upwards while the other ones have a black/white field upwards. Cable connection to the pyranometer defines the north (up) direction.

Figure 11 shows deviations from ideal cosine dependence in N-S direction. Kipp & Zonen CM10 was found to have the best cosine dependence of the measured types. The spread of the cosine characteristics of the other types are very large.

Figure 12 shows azimuth variations of responsivity calculated from the cosine measurements with 70° incident angle of radiation. The behaviour of the individual instruments are very random. Only the periodicity of responsivity with the azimuth angle is consistent within each type of pyranometers.

The measured values are also compared with corresponding indoor measurements at WRC, NARC and Kipp & Zonen:

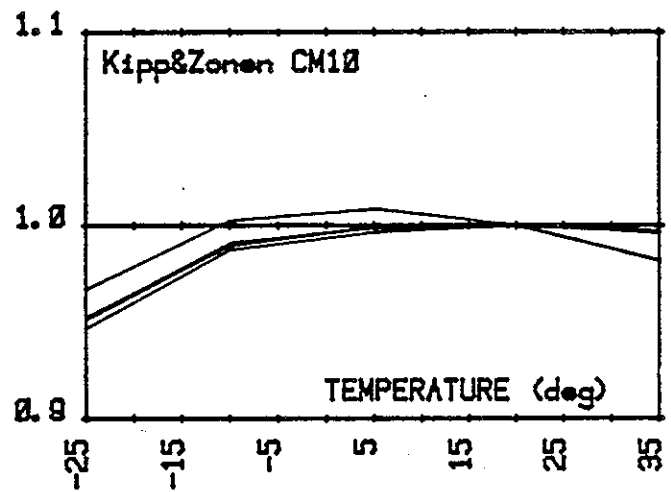
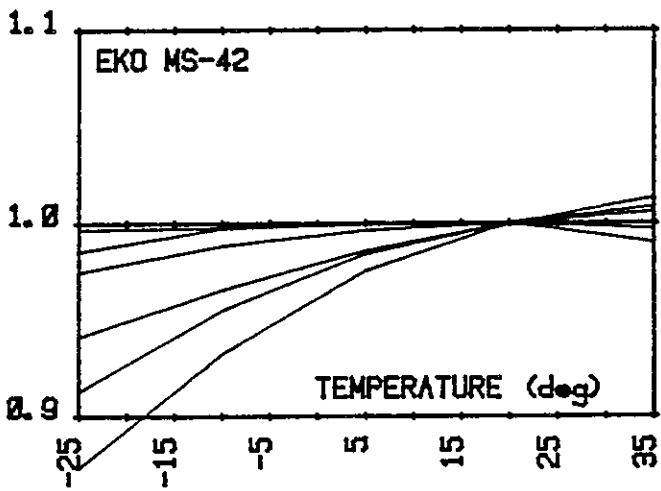
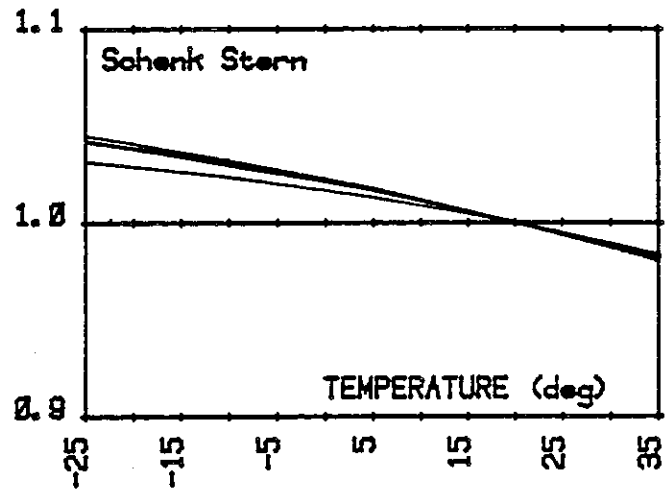
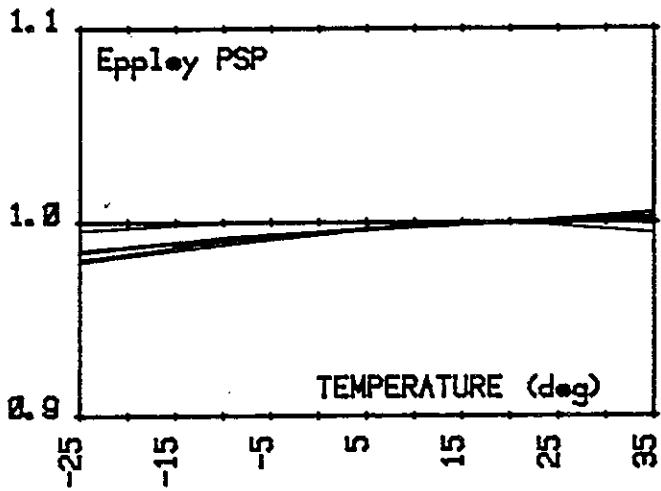
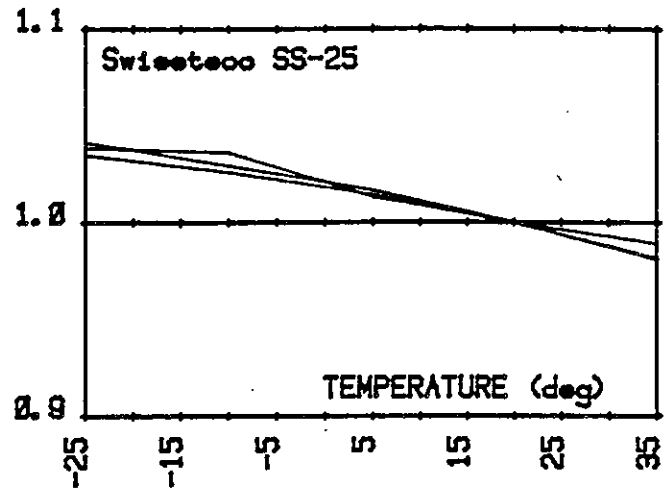
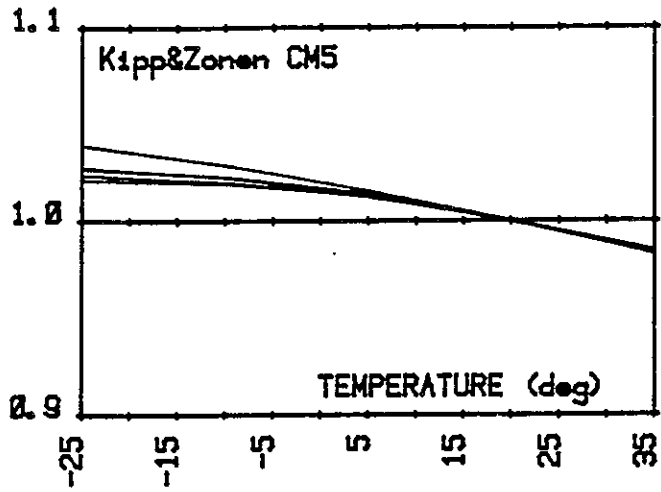


Figure 8.

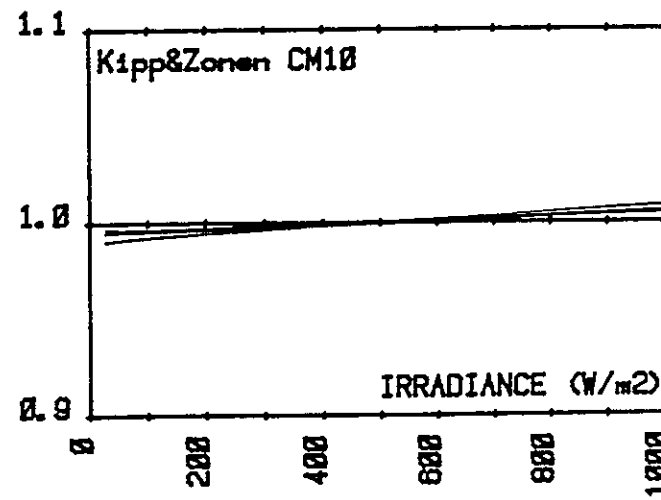
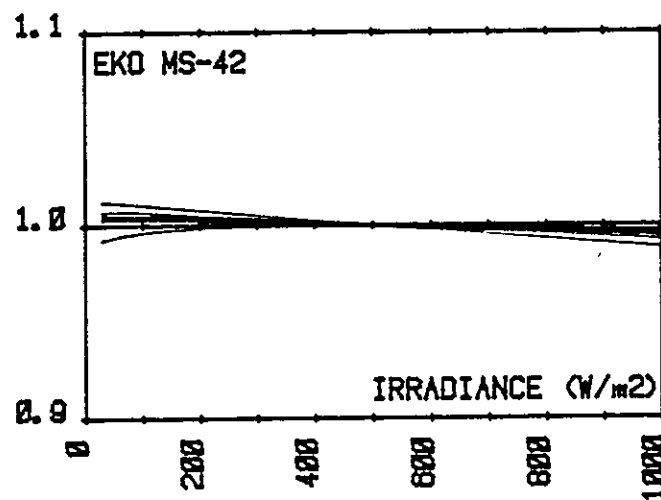
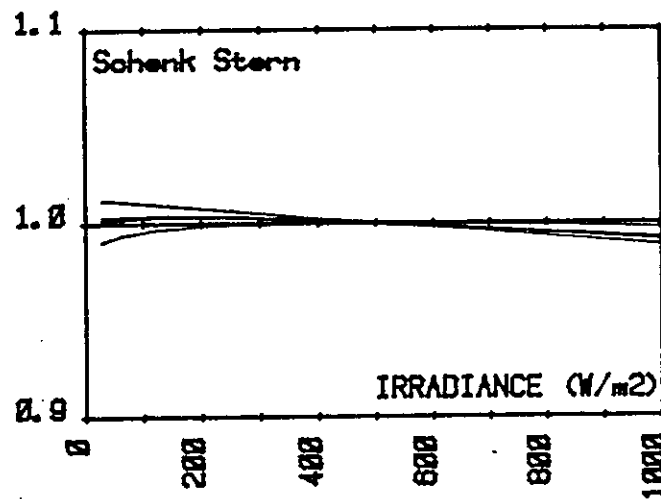
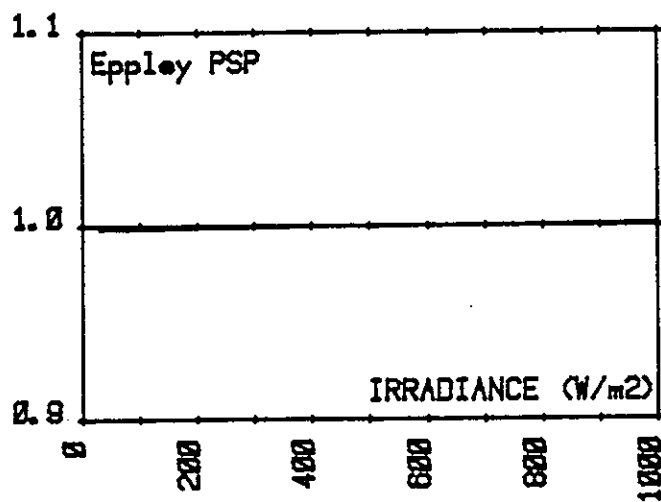
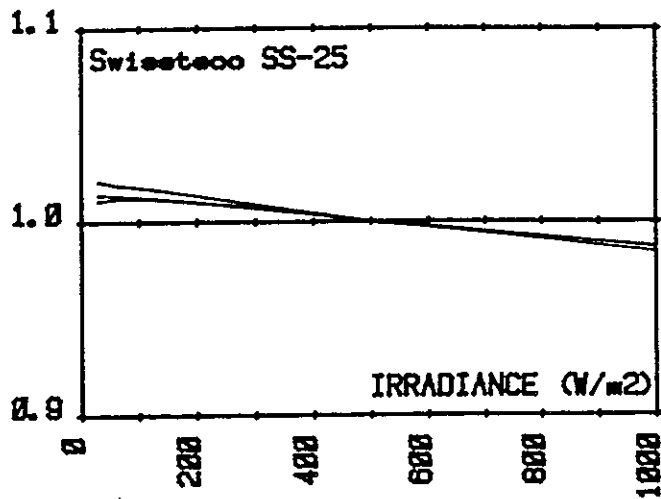
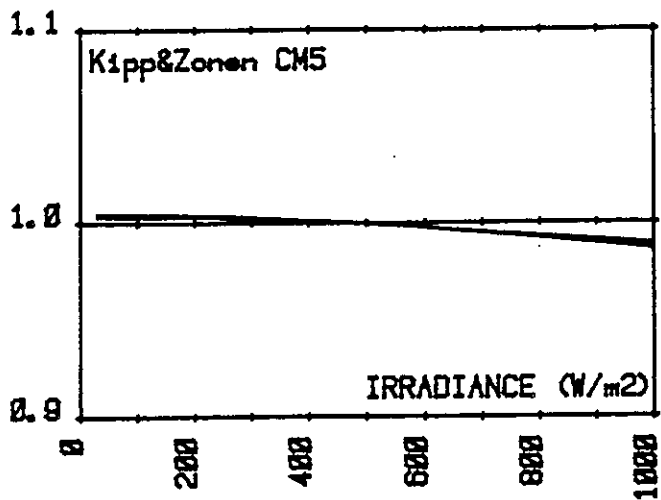


Figure 9.

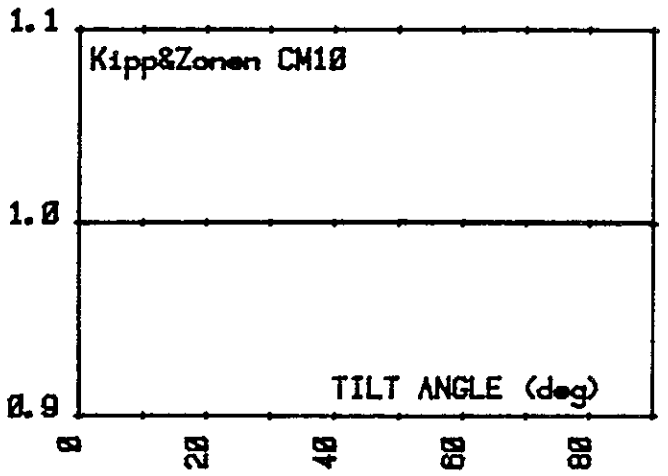
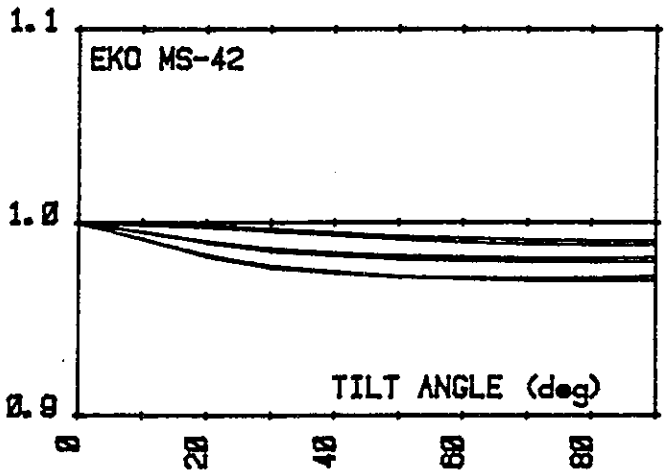
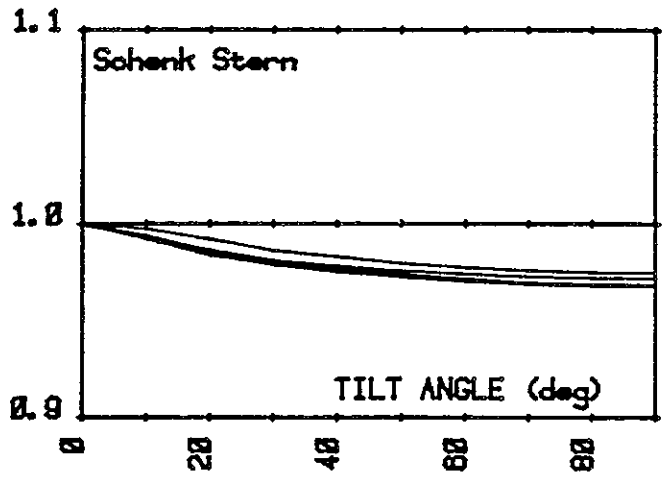
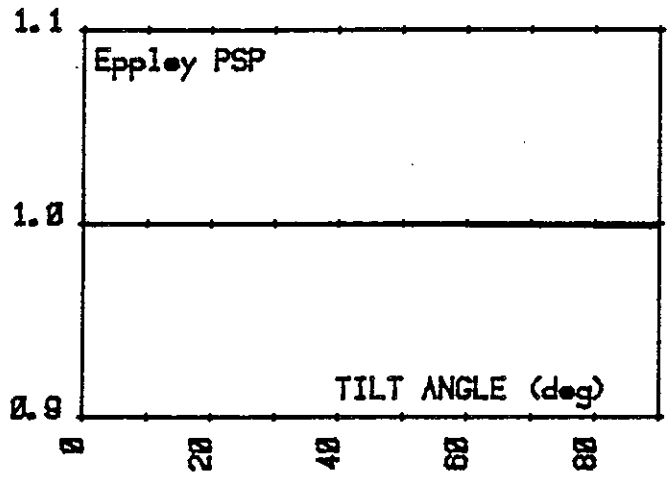
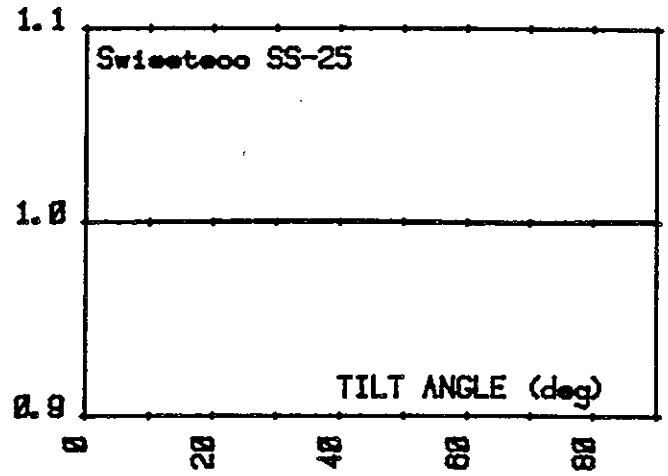
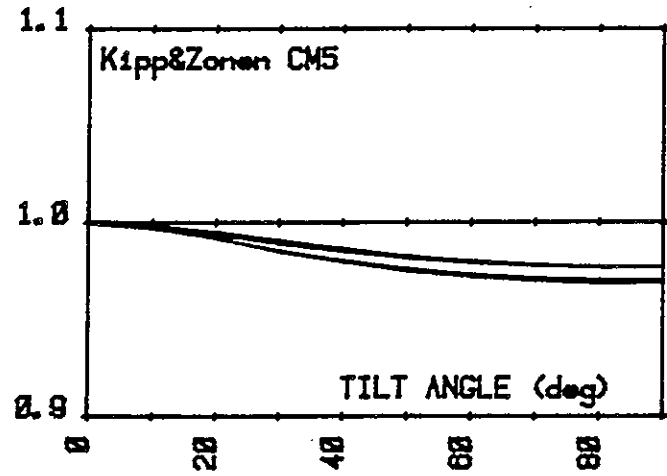


Figure 10.

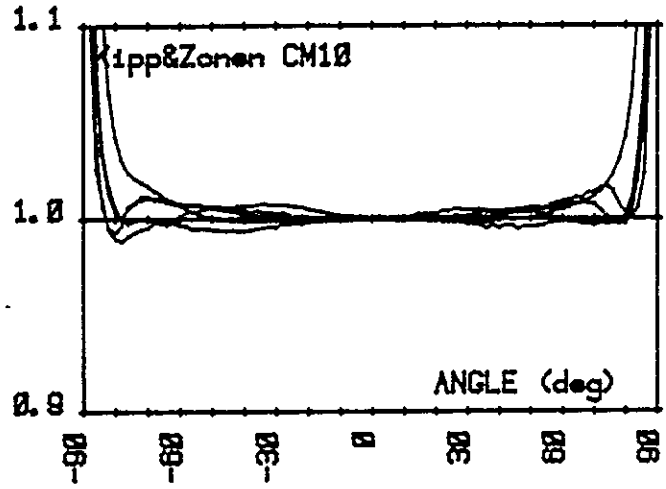
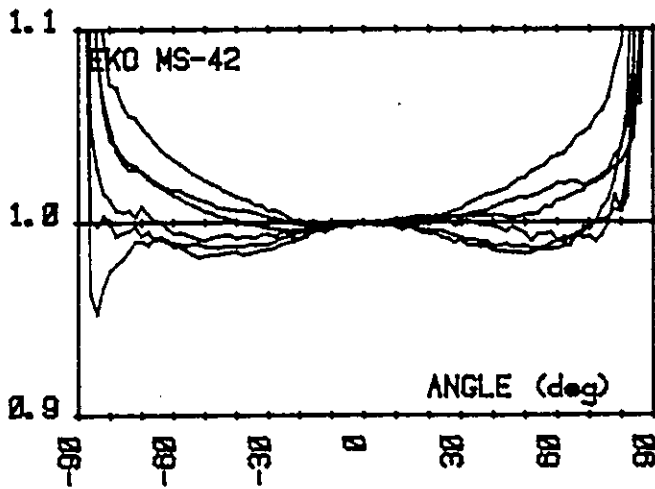
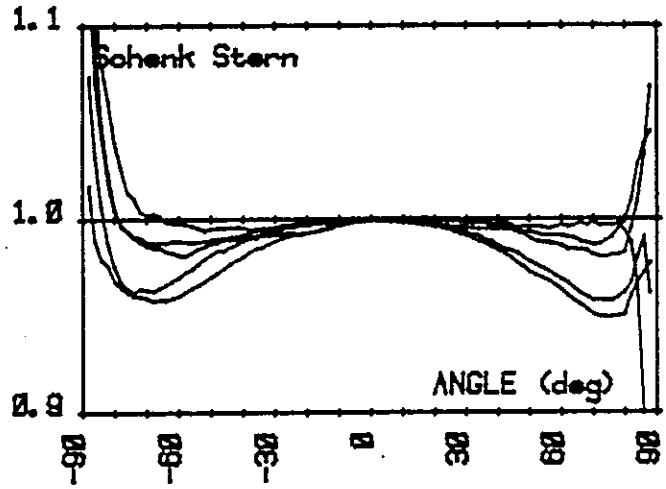
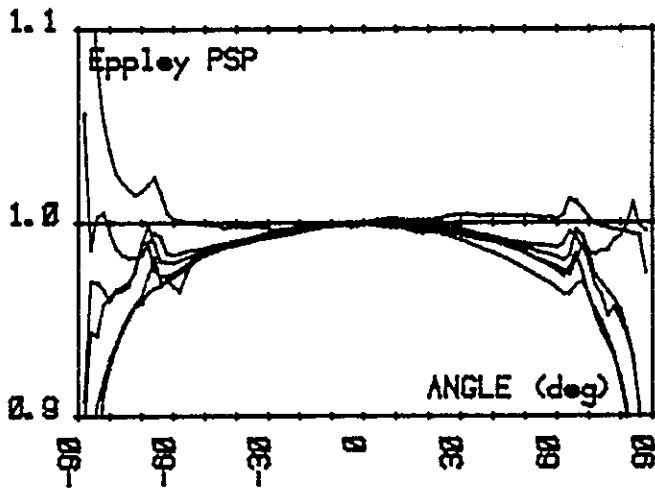
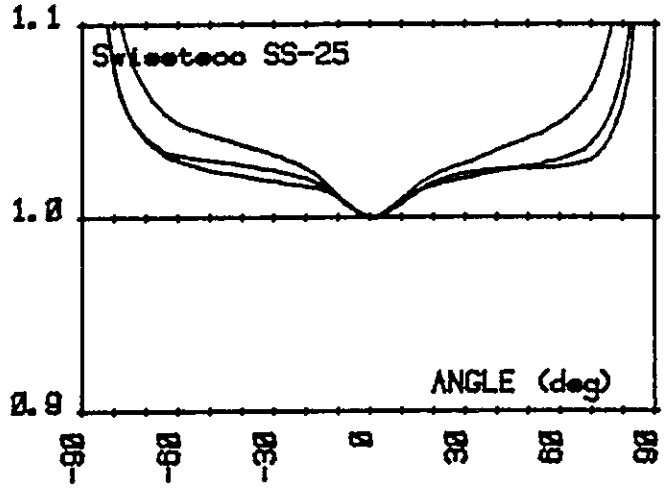
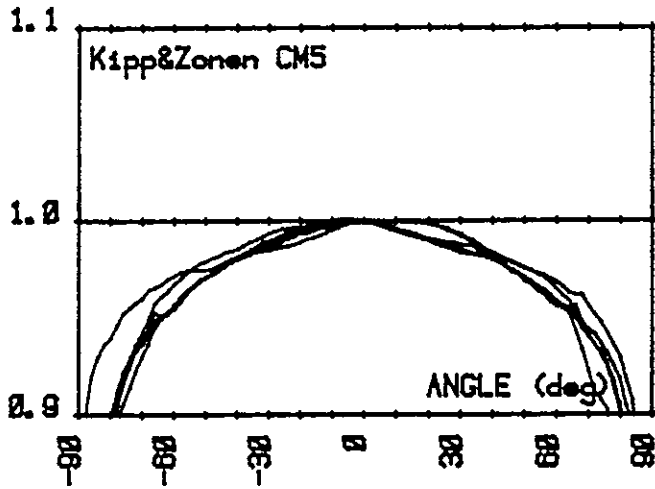


Figure 11.

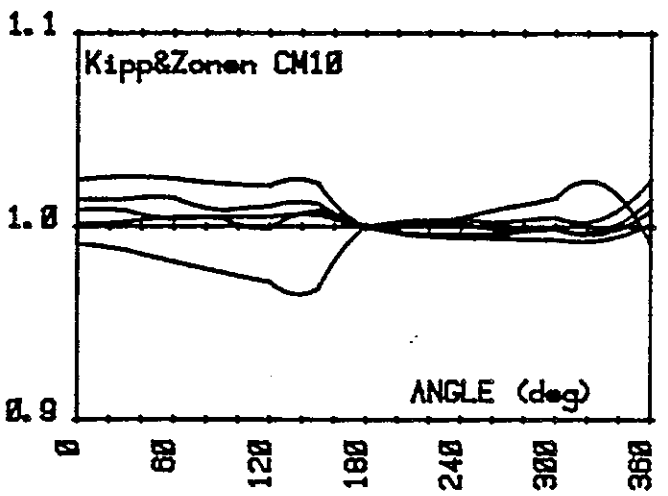
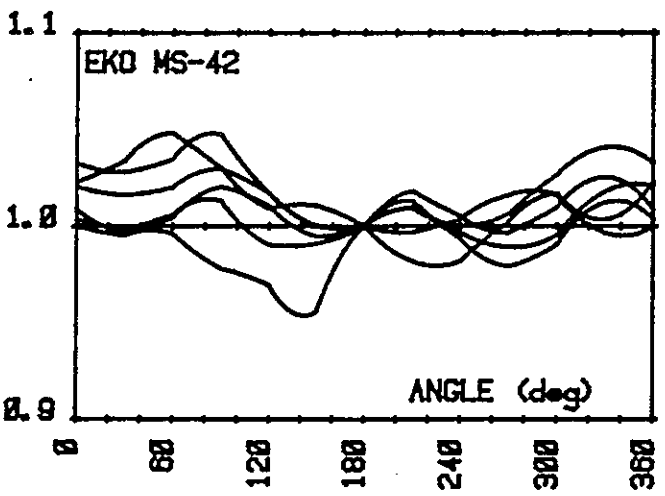
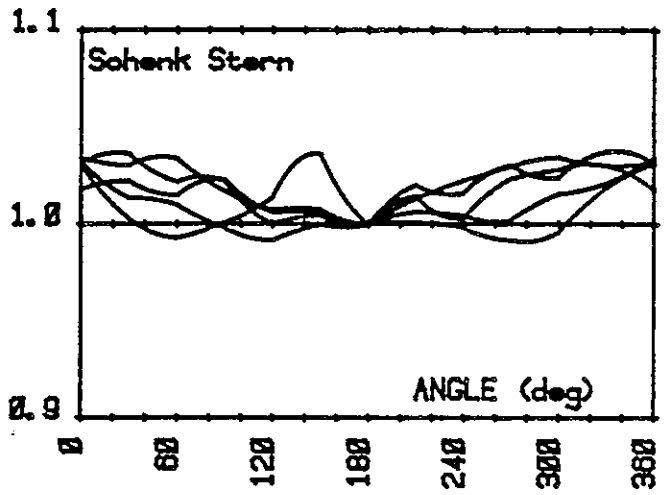
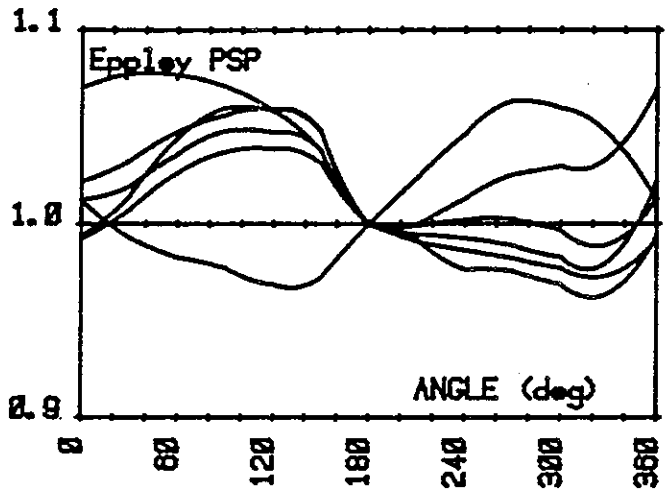
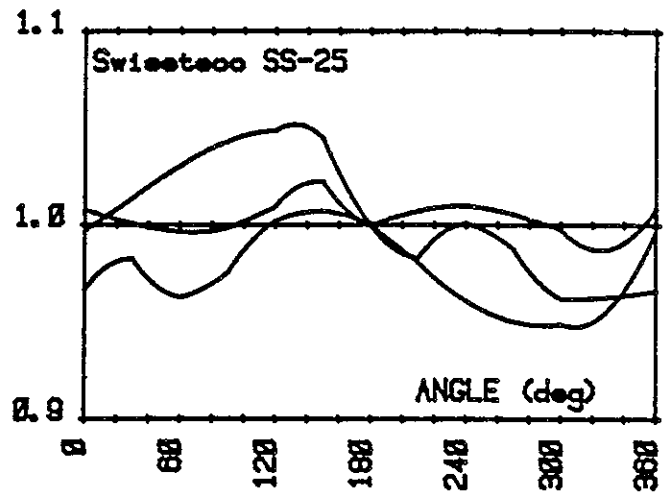
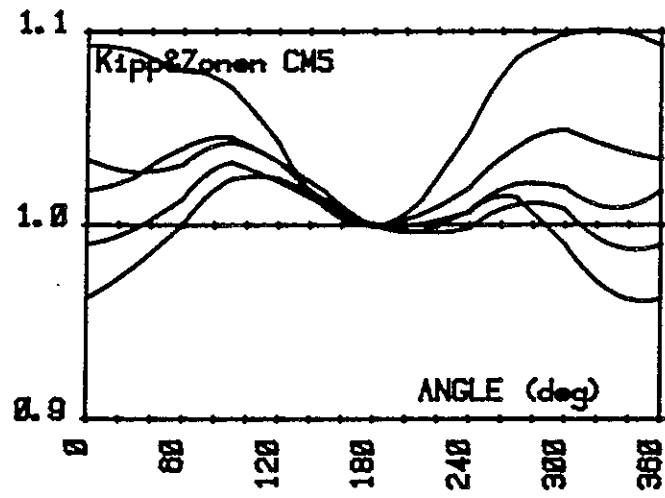


Figure 12.

Figure 13-16 show a comparison of cosine measurements between SP-NARC-WRC. Figure 13-14 in S-N direction and Figure 15-16 in W-E direction. The agreement was very poor except for the CM10 type where SP and NARC agreed very well.

Figure 17-18 shows a comparison of cosine measurements between SP-K&Z-WRC. Only on the CM10 type. The agreement between SP and Kipp & Zonen was very good.

Figure 19-20 show a comparison of temperature dependence measurements at SP and NARC. The same general shape of temperature characteristics was achieved at both laboratories with good agreement on the PSP and CM10 types.

Finally, a calculation was performed using the measured data to see how much the deviation from an ideal pyranometer would be for the individual pyranometers on two specific sunny days in Davos 1981-07-30 7h-18h and 1982-01-13 11h-15h measuring the time integrated irradiance (energy) and taking account cosine dependence, non linearity and tilt effect. The calculations were performed according to Appendix 1. The result is given in Figure 21-22. CM10 type gives the best result with about 0.5% deviation from an ideal pyranometer.

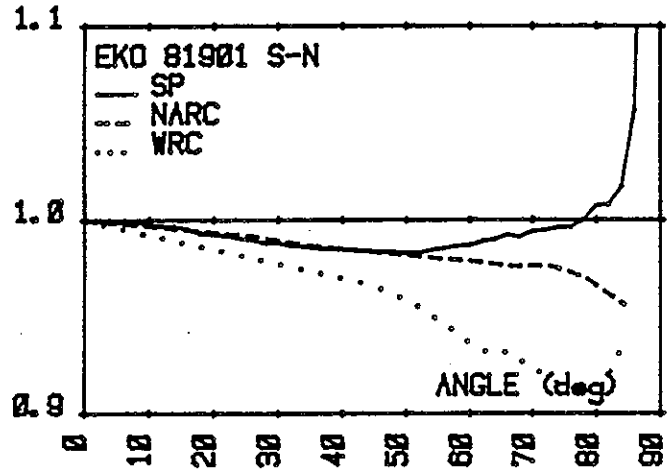
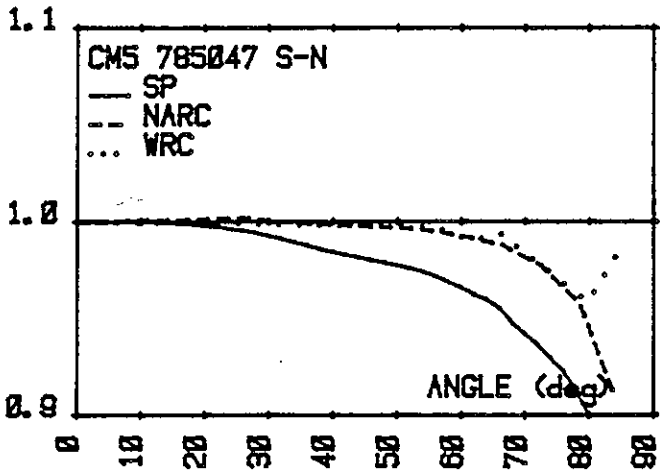
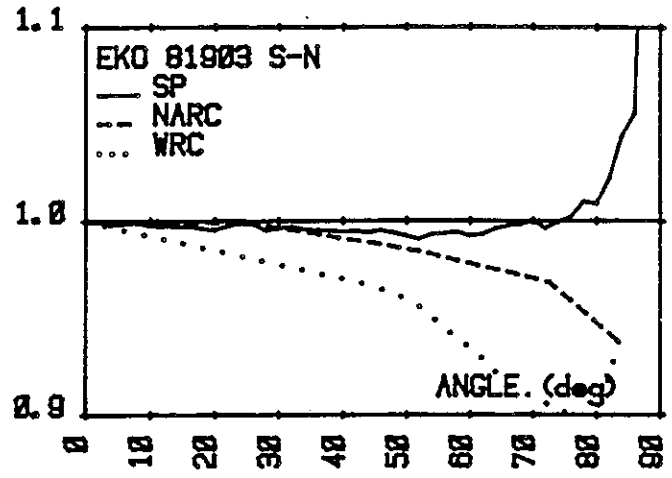
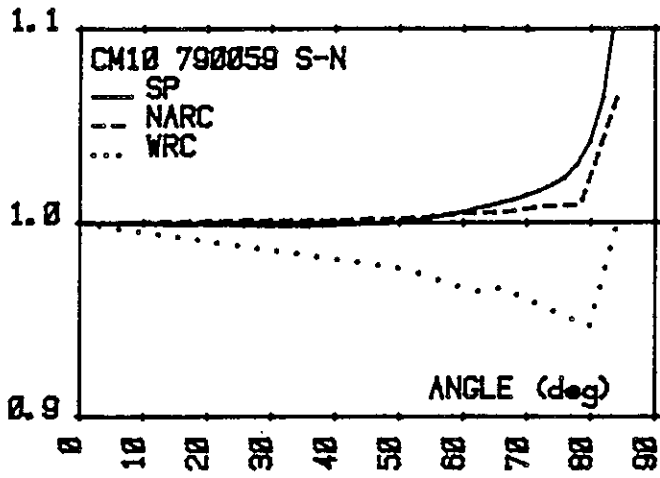


Figure 13.

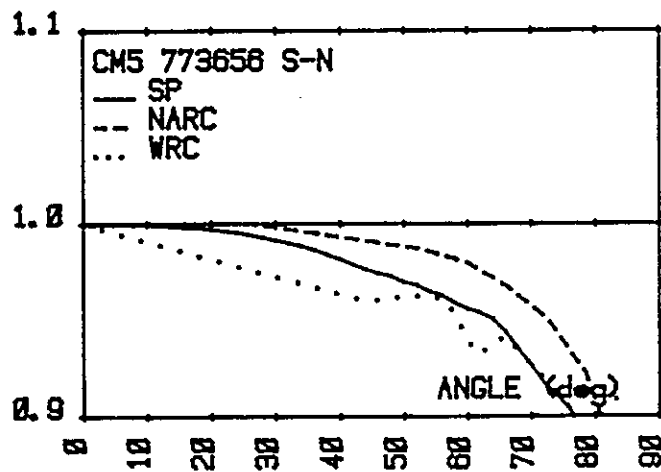
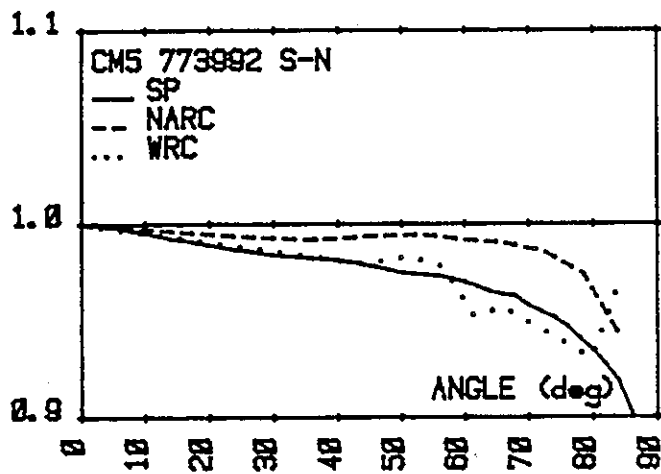
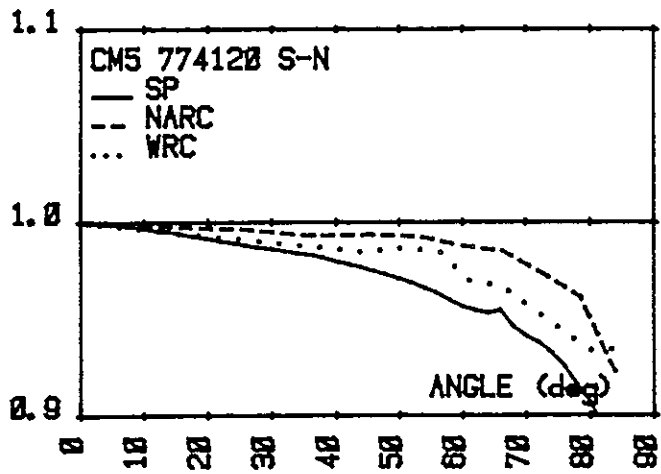


Figure 14.

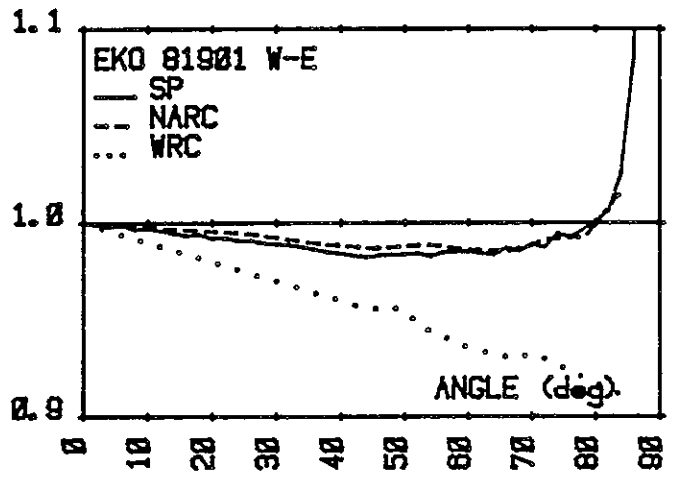
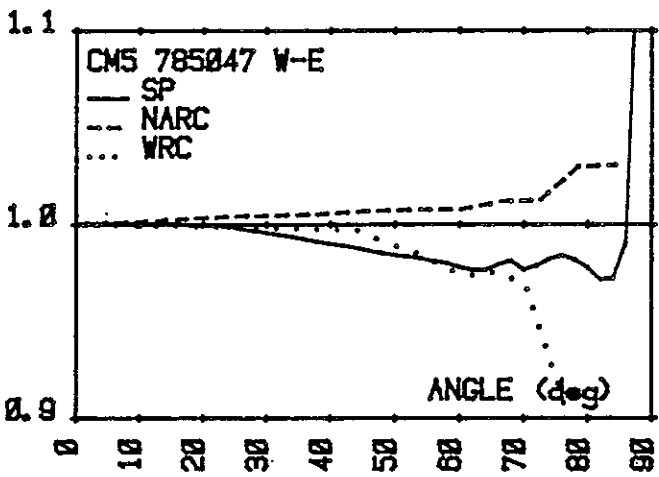
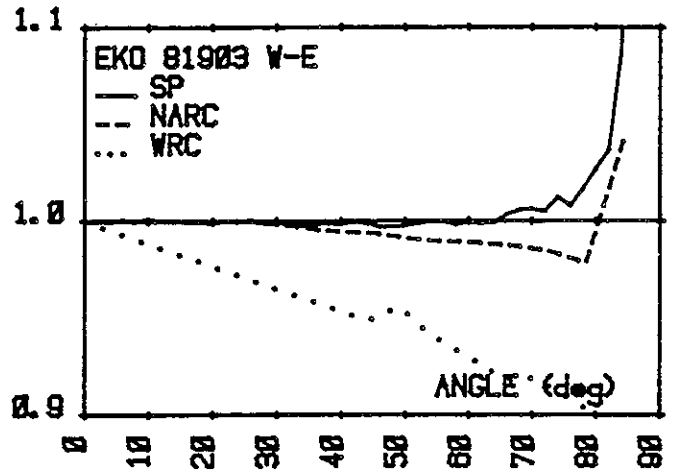
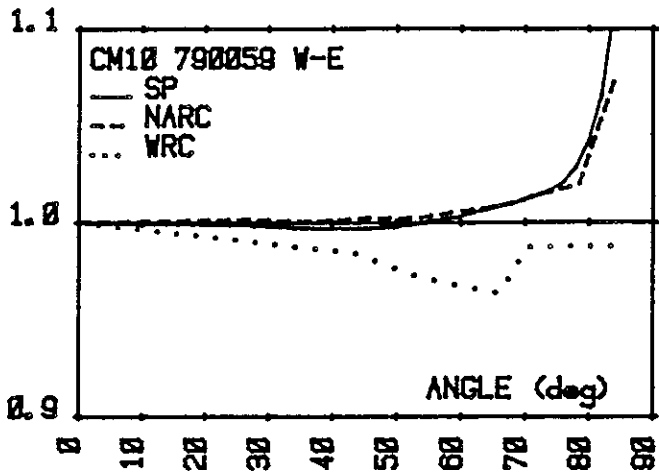


Figure 15.

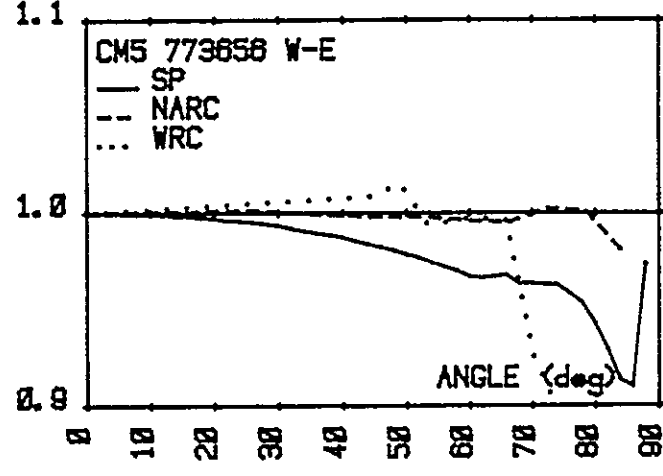
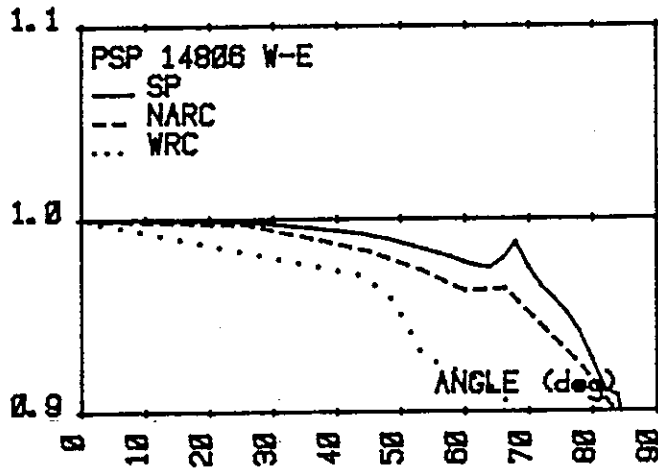
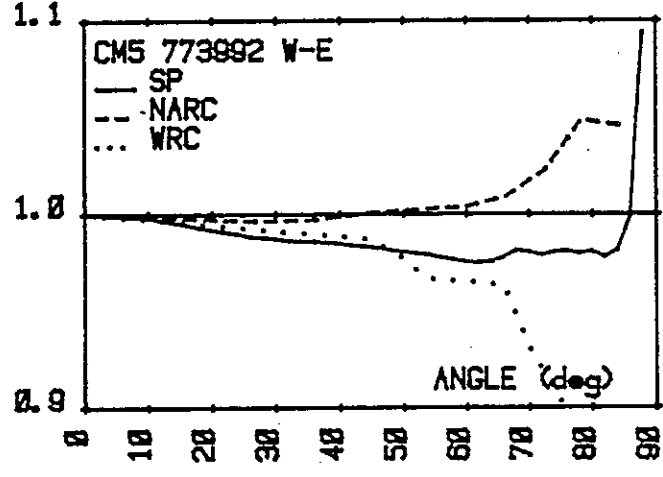
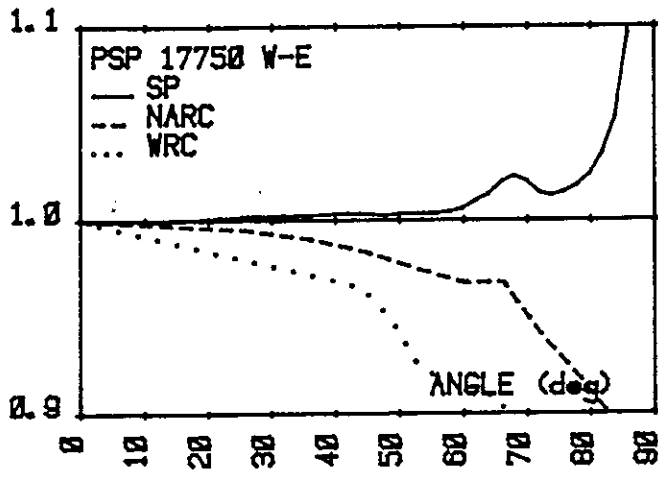
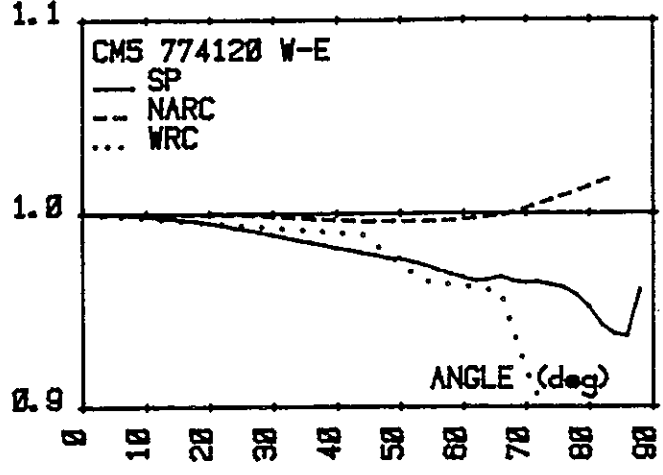
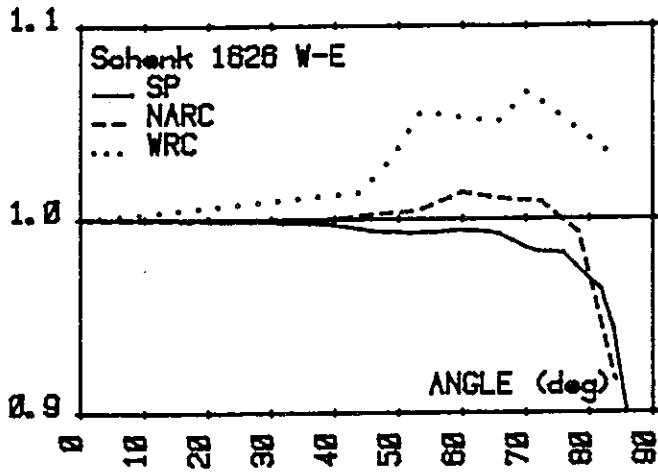


Figure 16.

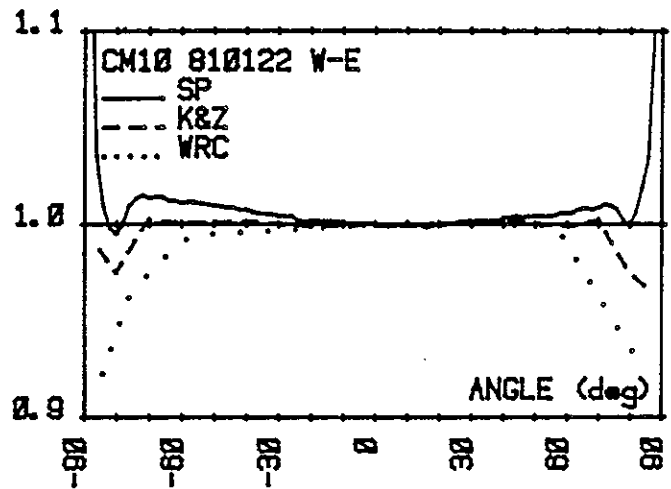
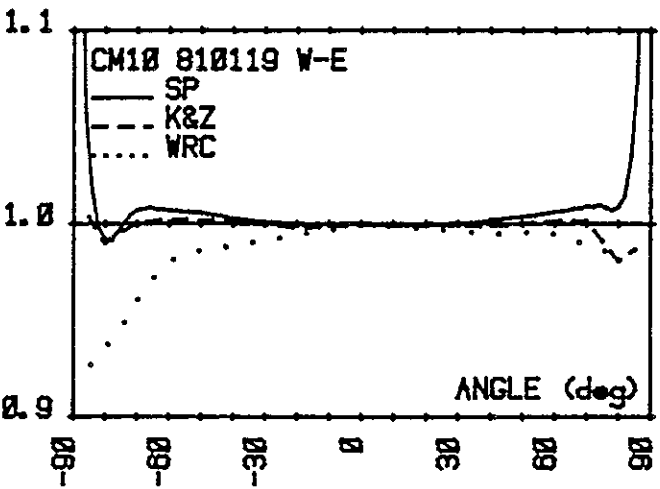
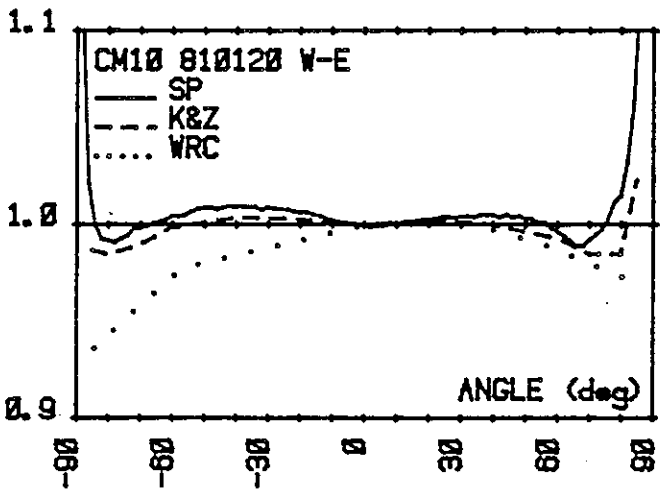
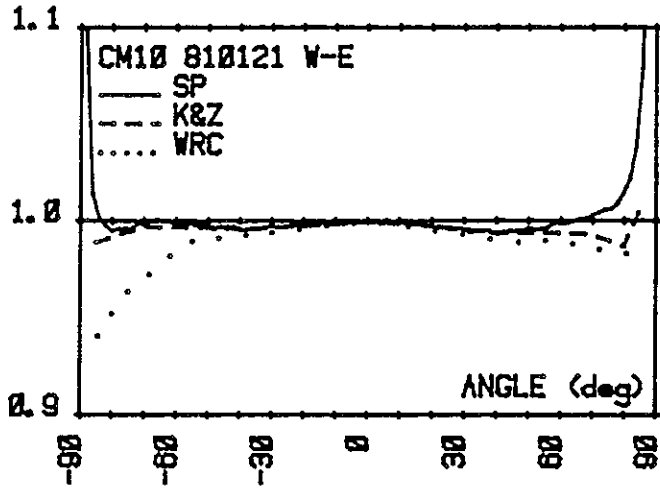


Figure 17.

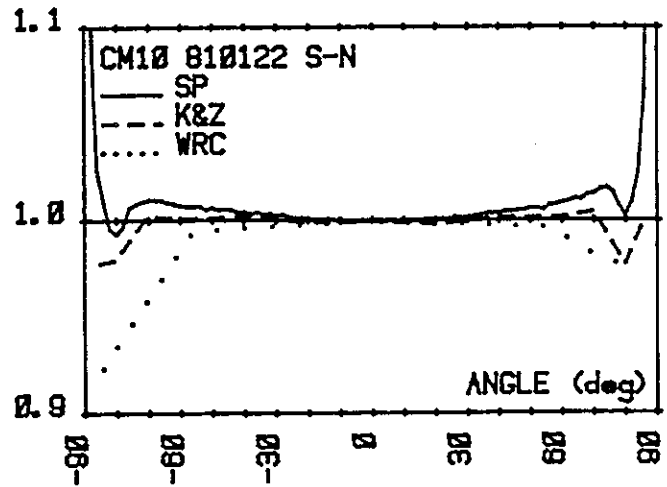
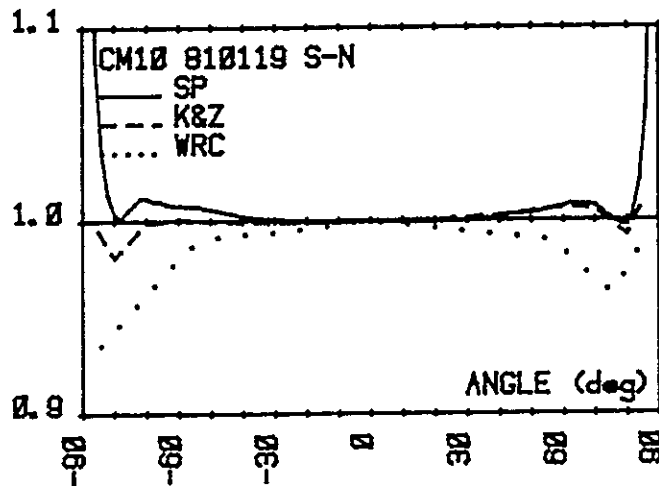
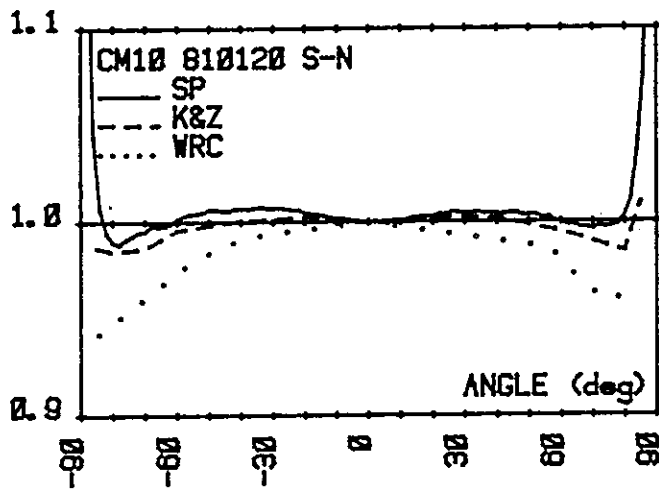
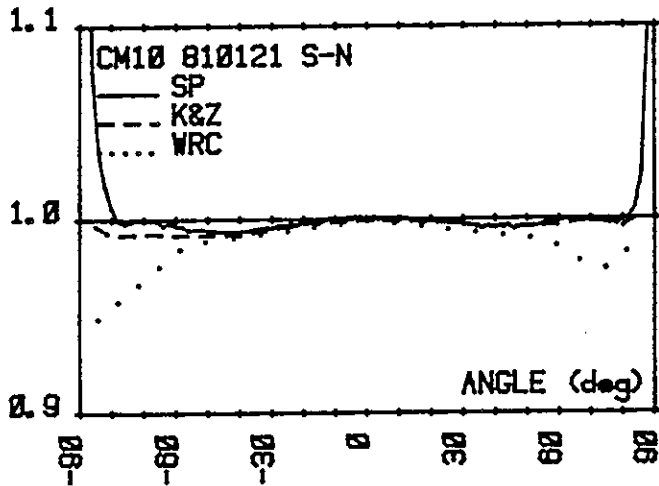


Figure 18.

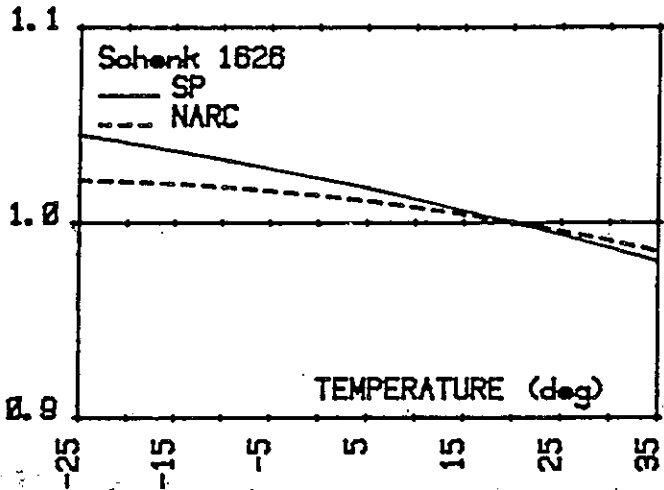


Fig. z₅a

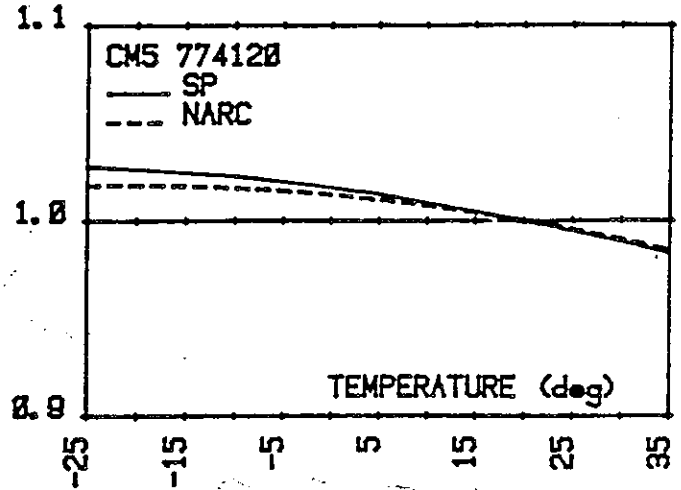


Fig. z₅b

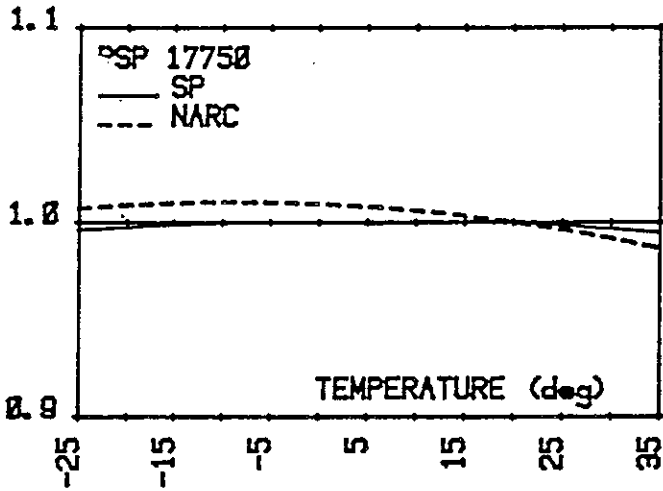


Fig. z₅c

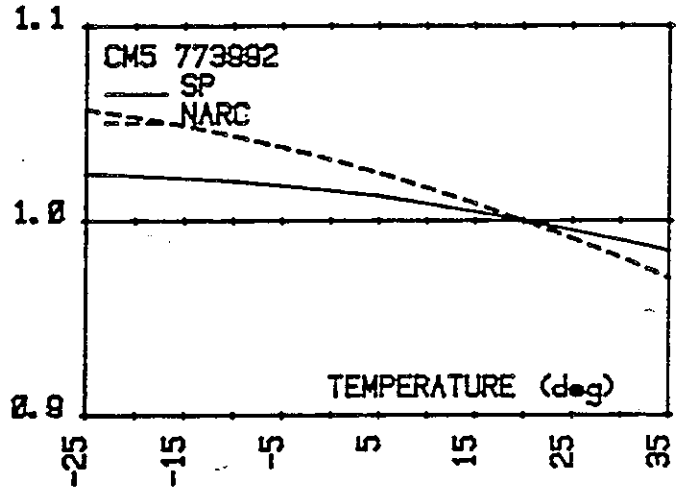


Fig. z₅d

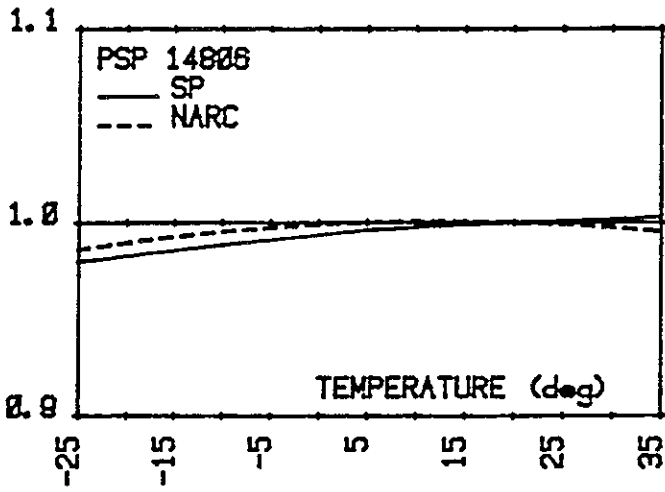


Fig. z₅e

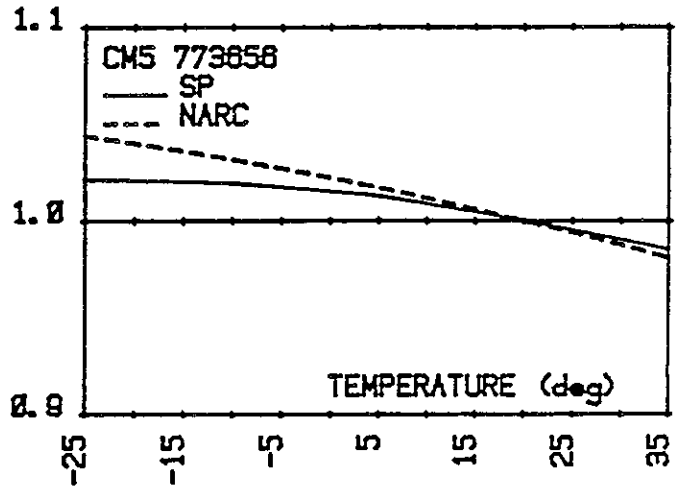


Fig. z₅f

Figure 19.

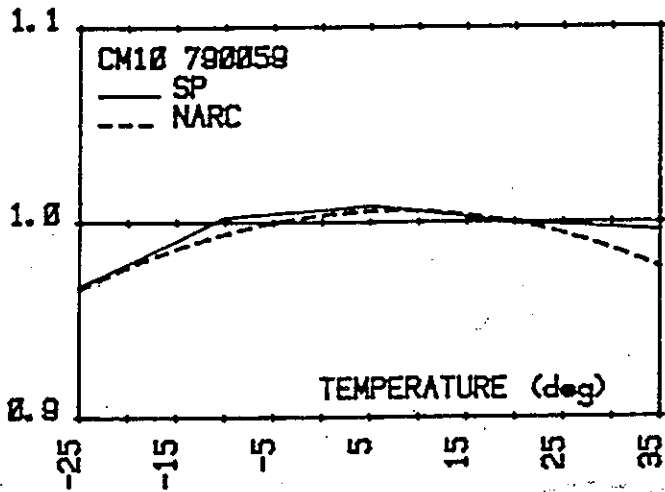


Fig. z_{5g}

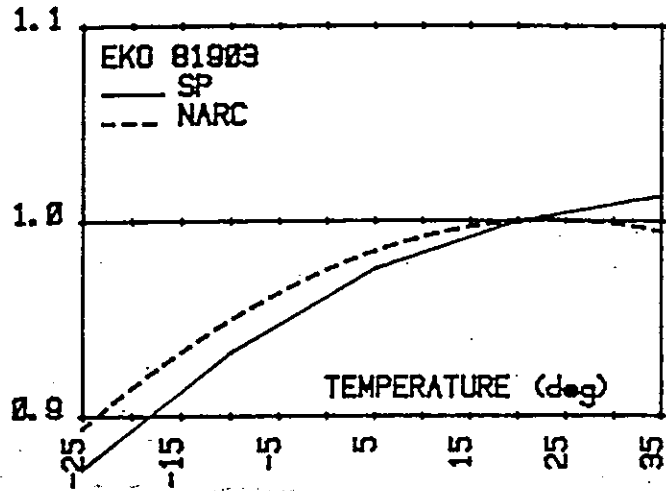


Fig. z_{5h}

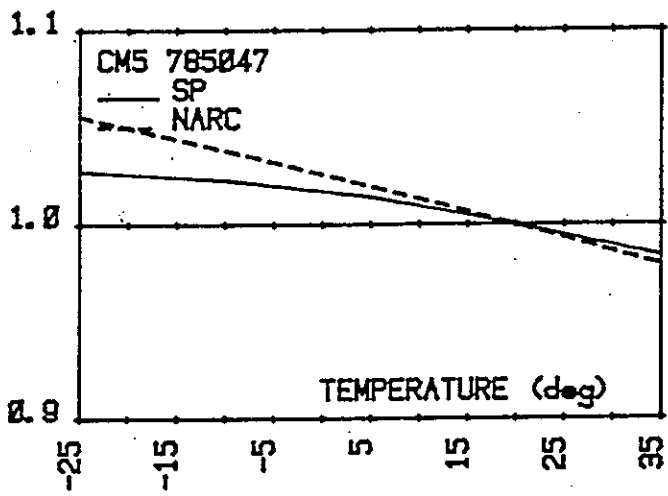


Fig. z_{5i}

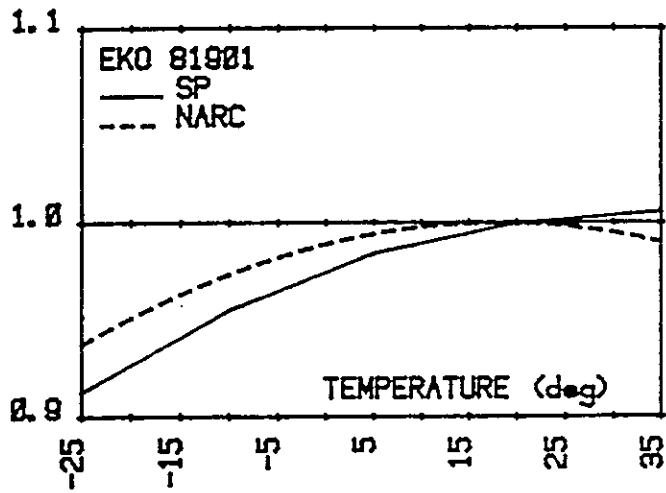


Fig. z_{5j}

Figure 20.

FIGURE 21

Integrated Irradiance 820113 11h-15h and 810730 7h-18h
Deviation from Ideal Pyranometer in Percent Covered by
Cosine Error, Nonlinearity and Tilt Effect

Tilt toward south (deg): 30

	82-01-03	81-07-30
Ideal pyranometer	0.00	0.00
IEA EKO 81901 /4	-1.55	-0.91
IEA EKO 81903 /5	-0.53	-0.16
IEA EKO 81906 /6	0.70	0.50
IEA EKO 81907 /7	-1.02	-0.54
IEA EKO 81908 /8	0.02	0.03
IEA EKO 81909 /9	1.39	0.88
IEA Eppley PSP 14806 /10:2	-1.00	-0.70
IEA Eppley PSP 17750F3 /11	-0.02	0.31
IEA Eppley PSP 18135F3 /12	-0.79	-0.22
IEA Eppley PSP 20523F3 /13	-0.96	-0.50
IEA Eppley PSP 20524F3 /14	-1.26	-0.93
IEA Eppley PSP 20655F3 /15	-1.04	-0.59
IEA Kipp & Zonen CM5-773656 /16	-1.74	-1.52
IEA Kipp & Zonen CM5-773992 /17	-1.60	-1.44
IEA Kipp & Zonen CM5-774120 /18	-1.76	-1.66
IEA Kipp & Zonen CM5-785017 /19	-1.81	-1.61
IEA Kipp & Zonen CM5-785047 /20	-1.33	-1.18
IEA Kipp & Zonen CM10-790059 /21	0.05	0.42
IEA Kipp & Zonen CM10-810119 /22	0.42	0.59
IEA Kipp & Zonen CM10-810120 /23	0.56	0.58
IEA Kipp & Zonen CM10-810121 /24	-0.31	0.12
IEA Kipp & Zonen CM10-810122 /25	0.60	0.68
IEA Schenk Star 1626 /26	-0.32	-0.53
IEA Schenk Stern 2186 /27	-1.18	-1.24
IEA Schenk Stern 2209 /28	-1.96	-1.55
IEA Schenk Stern 2217 /29	-0.79	-0.55
IEA Schenk Stern 2221 /30	-0.60	-0.73
IEA Swissteco SS-25 113 /31	3.20	1.93
IEA Swissteco SS-25 114 /32	1.70	0.95
IEA Swissteco SS-25 115 /33	2.09	1.04
IEA WRC AV-1 /1	0.53	0.30
IEA WRC AV-2 /2	-1.79	-0.73
IEA WRC 6703-A /3	-1.09	-0.85
CM11-810181	0.32	0.14
PSP&35	-0.15	-0.02
Exposure on ideal pyran, Ws/m ²	5637	16584
Mean irradiance, W/m ²	564	691

The instruments calibrated at 500 W/m²
and 45° tilt angle.

FIGURE 22

Integrated Irradiance 820113 11h-15h and 810730 7h-18h
 Deviation from Ideal Pyranometer in Percent Covered by
 Cosine Error, Nonlinearity and Tilt Effect

Tilt toward south (deg): 45

	82-01-03	81-07-30
Ideal pyranometer	0.00	0.00
IEA EKO 81901 /4	-1.38	-1.21
IEA EKO 81903 /5	-0.56	-0.41
IEA EKO 81906 /6	-0.17	0.29
IEA EKO 81907 /7	-0.93	-0.91
IEA EKO 81908 /8	-0.64	-0.31
IEA EKO 81909 /9	0.26	0.83
IEA Eppley PSP 14806 /10:2	-0.34	-0.89
IEA Eppley PSP 17750F3 /11	-0.07	0.27
IEA Eppley PSP 18135F3 /12	-0.36	-0.33
IEA Eppley PSP 20523F3 /13	-0.53	-0.66
IEA Eppley PSP 20524F3 /14	-0.58	-1.14
IEA Eppley PSP 20655F3 /15	-0.50	-0.73
IEA Kipp & Zonen CM5-773656 /16	-1.41	-2.28
IEA Kipp & Zonen CM5-773992 /17	-1.84	-2.20
IEA Kipp & Zonen CM5-774120 /18	-1.58	-2.38
IEA Kipp & Zonen CM5-785017 /19	-1.54	-2.34
IEA Kipp & Zonen CM5-785047 /20	-1.22	-1.92
IEA Kipp & Zonen CM10-790059 /21	0.12	0.42
IEA Kipp & Zonen CM10-810119 /22	0.33	0.56
IEA Kipp & Zonen CM10-810120 /23	0.72	0.61
IEA Kipp & Zonen CM10-810121 /24	-0.08	0.03
IEA Kipp & Zonen CM10-810122 /25	0.55	0.70
IEA Schenk Star 1626 /26	-0.74	-1.00
IEA Schenk Stern 2186 /27	-1.01	-1.76
IEA Schenk Stern 2209 /28	-1.60	-2.24
IEA Schenk Stern 2217 /29	-1.04	-1.05
IEA Schenk Stern 2221 /30	-0.79	-1.13
IEA Swissteco SS-25 113 /31	2.35	2.66
IEA Swissteco SS-25 114 /32	1.16	1.34
IEA Swissteco SS-25 115 /33	1.48	1.57
IEA WRC AV-1 /1	0.52	0.69
IEA WRC AV-2 /2	-0.59	-0.99
IEA WRC 6703-A /3	-0.55	-0.99
CM11-810181	0.17	0.20
PSP&35	0.08	0.03
Exposure on ideal pyran, Ws/m ²	6523	15428
Mean irradiance, W/m ²	652	643

The instruments calibrated at 500 W/m²
 and 45° tilt angle.

APPENDIX 1

Integrated all day irradiation on a tilted surface

The deviation from ideal cosine response, the tilt effect, the nonlinearity and the temperature effect on the responsivity all course errors in the measurement of all day irradiation. This effect has been calculated using the following formalism.

The pyranometer is supposed to be mounted in a position tilted towards south, the tilt angle being β degrees.

The sun is traversing the sky in a terrestrial coordinate system (x, y, z) . The pyranometer is mounted in a coordinate system (x', y', z') which is rotated the angle β in the (x, y, z) -system. The pyranometer is positioned in the common origin of the two systems.

Let (r, θ, ψ) and (r', θ', ψ') be spherical coordinates in the respective systems.

The coordinate axis have the following orientations:

x and x' are pointing west
 y is pointing south
 z is pointing towards zenith

The angles have the following meaning:

θ is the solar elevation
 $\psi = \phi - 180^\circ$
 ϕ is the azimuth angle, 0° to the north and positive angle towards east
 β is the tilt angle of the pyranometer

The following relationships are then valid in the respective system.

$$\begin{cases} x = r \cos \theta \cdot \sin \psi \\ y = r \cos \theta \cos \psi \\ z = r \sin \theta \end{cases} \quad (1)$$

$$\begin{cases} x' = r \cos \theta' \cdot \sin \psi' \\ y' = r \cos \theta' \cdot \cos \psi' \\ z' = r \sin \theta' \end{cases} \quad (2)$$

The rotation of the (x', y', z') -systems around the x -axis gives the following equations:

$$\begin{cases} y' = y \cos \beta - z \sin \beta \\ z' = y \sin \beta + z \cos \beta \\ x' = x \end{cases} \quad (3)$$

Equations (1), (2) and (3) give the solar elevation, θ' , and solar azimuth, ϕ' , in the pyranometer system.

$$\begin{cases} \cot(\phi' - 180^\circ) = \cot \psi \cos \beta - \frac{\tan \theta}{\sin \psi} \sin \beta \\ \sin \theta' = \cos \theta \cos \psi \sin \beta + \sin \theta \cos \beta \end{cases} \quad (4)$$

The total radiation has been divided in beam radiation and diffuse radiation according to a formalism in ref. x₁.

The extraterrestrial radiation, G_0 , is given by

$$G_0 = G_{SC} \left(1 + 0.033 \cos \left(\frac{360 n}{365} \right) \right) \sin \theta \quad (5)$$

where G_{SC} is the solar constant and n is the day of the year.

The atmospheric transmittance for beam radiation at clear sky is

$$\tau_b = a_0 + a_1 e^{-k/\sin \theta} \quad (6)$$

where $a_0 = r_0 a_0^*$; $a_1 = r_1 a_1^*$; $k = r_k k^*$

and $a_0^* = 0.4237 - 0.00821 (6-A)^2$

$a_1^* = 0.5055 + 0.00595 (6.5-A)^2$

$k^* = 0.2711 + 0.01858 (2.5-A)^2$

where A is the altitude in kilometers.

r_0 , r_1 and r_k are climatic correction factors given in Table y.

Table y. Correction factors for climate types

Climate type	r_0	r_1	r_k
Tropical	0.95	0.98	1.02
Mid-Latitude Summer	0.97	0.99	1.02
Subarctic Summer	0.99	0.99	1.01
Mid-Latitude Winter	1.03	1.01	1.00

The transmittance for diffuse radiation at clear sky is given by

$$\tau_d = 0.2710 - 0.2939 \tau_b \quad (7)$$

In the calculations the diffuse radiation is assumed to be isotropic.

The radiation as measured by the pyranometer can then be calculated as

$$G = G_b + G_d$$

or

$$G = G_0 \left[\tau_b \epsilon_c(\theta', \phi') + \frac{\tau_d}{2\pi} \int_{\Omega} \epsilon_c(\theta', \phi') d\Omega \right] \epsilon_l(G) \epsilon_{\beta}(\beta) \epsilon_t(t) \quad (8)$$

where ϵ is an error function

and $\epsilon_c(\theta', \phi')$ indicates cosine dependence

$\epsilon_l(G)$ indicates linearity dependence

$\epsilon_{\beta}(\beta)$ indicates tilt angle dependence

$\epsilon_t(t)$ indicates temperature dependence

Equation (8) has been used to integrate the all day irradiation by summing each half hour over the day. The integral in Equation (8) has been replaced by a sum over the 540 measured directions across the pyranometer hemisphere.

In the computations $\epsilon_t(t) = 1$ in lack of data.

LITERATURE

- x₁ Duffie, J.A. and Beckman, W.A.
Solar engineering of thermal processes, John Wiley & Sons, New York, 1980.

2.E PRESENTATION OF SOME OF THE IEA-INSTRUMENT CHARACTERISTICS

L.F. Lan Wely
Kipp & Zonen
Mercuriusweg 1
Delft - NL

G.J. van den Brink
Technisch Physische Dienst TNO-TH
(Institute of Applied Physics TNO-TH)
Stieltjesweg 1
Delft - NL

PRESENTATION OF SOME OF THE IEA-INSTRUMENT CHARACTERISTICS

SUMMARY

The characterized pyranometers are part of a larger group of instruments that are being tested at several laboratories in different countries. The objective of the characterizations is to compare the techniques and results of the manufacturers and the independent laboratories. In this paper are presented the measurements of the time response, thermal shock response, linearity and tilt dependency, as well as the influence of the radiation source on calibrations.

TIME RESPONSE MEASUREMENTS

Test facility

The Xenon-lamp test facility is described in detail in the paper "Manufacturers indoor calibration procedure of Kipp & Zonen CM 11", which is included in the proceedings as well.

The Xenon-lamp beam is reflected downwards on the horizontally placed pyranometer with the mirror device which is mounted on the vertical table of the goniometer.

The normal incident radiation on the pyranometer is approximately 500 W/m², with a short term stability of $\pm 0.2\%$. The room temperature was between 16 and 20°C.

A three channel Kipp & Zonen X-T recorder (type BD 100) is used for registration of the signal.

Test Procedure

The recorder pen was set between 99 and 100% of the full scale with the variable setting of the span after illuminating the pyranometer for several minutes. The pyranometer was then shaded by turning the light part of the rotating sector in the beam until the signal was below 0.25% of the full scale. The pyranometer is illuminated for three minutes then shaded again.

Results

The response of the pyranometers for illumination during three minutes and shading afterwards is shown in Figure 1 and in Table 1. Table 1 shows the response relative to the response after three minutes illumination.

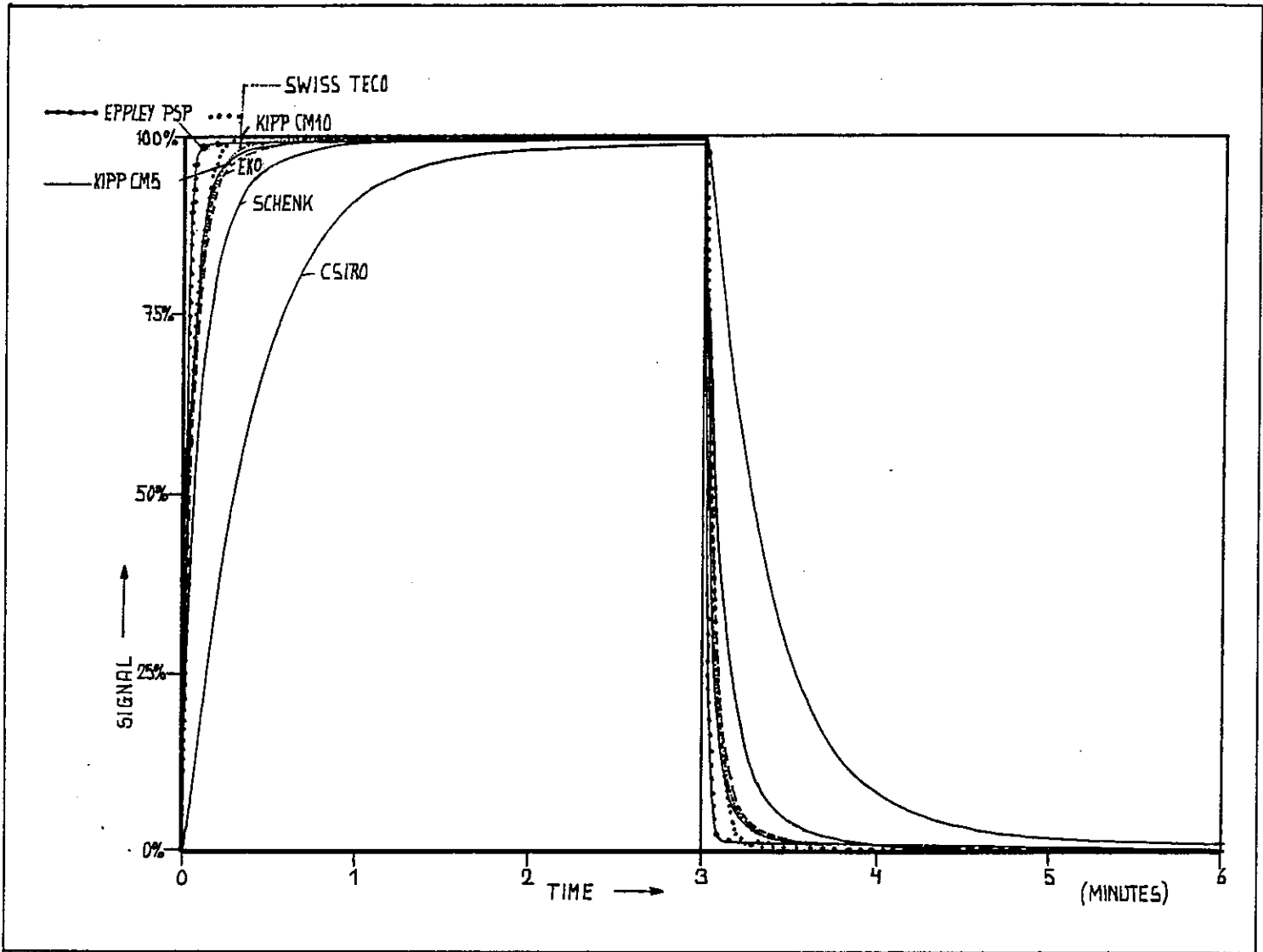


Figure 1. Time response of pyranometers

TABLE 1
Time Response

Instrument		Percentage of final value after:				
Type	Number	10 s.	30 s.	60 s.	120 s.	180 s.
Eppley PSP	20524 F3	99.0	99.3	99.5	99.6	100.0 by definition
Kipp CM 10	810121	95.3	100.0	100.0	100.0	
Kipp CM 5	773656	93.0	99.0	99.8	100.0	
Schenk	2209	77.0	96.0	99.2	99.9	
Swissteco	114 A	90.0	99.4	99.5	99.9	
CSIRO	HBR 115	32.0	73.8	92.7	98.9	
Eko	A 81908	90.7	98.8	99.9	100.0	

Pyranometers have multiple time constants as most thermal devices. The time response is firstly influenced by the inertia of the sensor caused by its thermal capacity, secondly by the net infra-red radiation between inner dome and sensor and thirdly by a change in the temperature of the housing. Each of these influences has its own time constant, the first has the smallest. Further research on these responses is going on.

Table 2 shows the time constant ($1/e$) of the first response, which is influenced by the thermal capacity of the sensor. Furtheron, the suggested settling time (t_s) is given. This is the time after which the voltage output is read out in the characterization tests (linearity, tilt, etc.). The first response is suspected to have its final value within 0.1 percent after this settling time. This response will almost turn to zero by shading off for the same period.

A possible stable second and third response can be determined now, they are together the remaining signal. Subtracting the rest signal after shading for the settling time from the signal after illuminating for the settling time will yield results close to the actual response to the irradiance.

THERMAL SHOCK RESPONSE

Test Facility

A climatic chamber (Vötsch 125 1) with built-in ventilator is used for heating the pyranometers (Figure 2). The cooling is achieved in a normal darkened room by using a ventilator, producing wind over a wooden table. The output of the pyranometers is measured with a three-channel Kipp & Zonen recorder (BD 100).

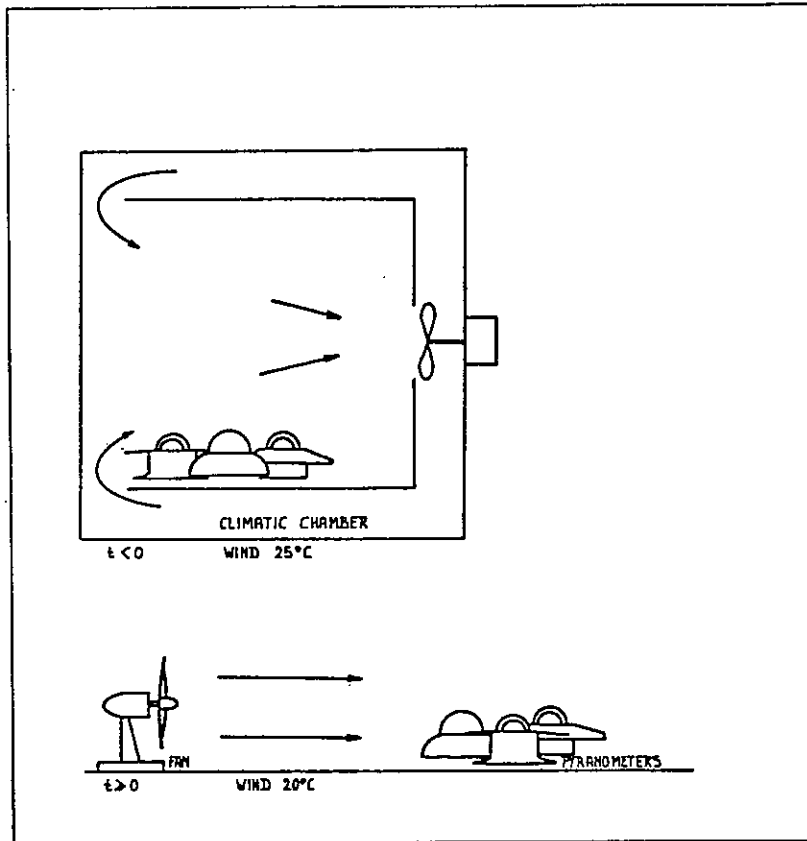


Figure 2. Test facility for thermal shock tests

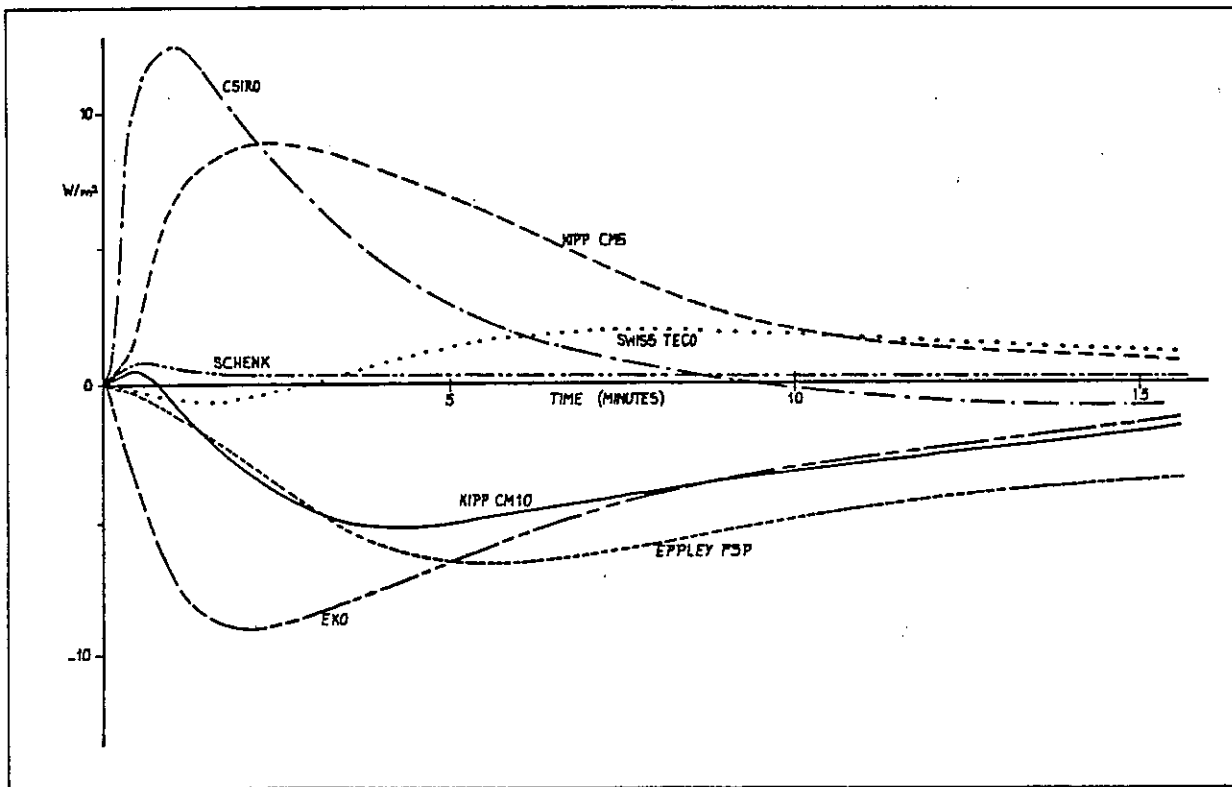


Figure 3. Response to an abrupt change in air temperature 25 → 20° C

TABLE 2
Time constant and settling time

Instrument		Time Constant (s)	Settling Time (s)
Type	Number		
Eppley PSP	20524 F3	1	60
Kipp CM 10	810121	4	60
Kipp CM 5	773656	3	60
Schenk	2209	6.5	120
Swissteco	114 A	4	90
CSIRO	HBR 115	22	180
Eko	A 81908	4	90

Test Procedure

The pyranometers have been placed in groups of three instruments in the climatic chamber. The temperature was 25°C. The built-in ventilator guarantees a good heat transfer from the air to the pyranometers. When their signal had decreased below 1 W/m² the instruments were placed outside the climatic chamber in front of a ventilator in triangular arrangement. The room temperature was about 20°C. The signal of the instruments was recorded for 20 minutes. In the mean time the next group of pyranometers was warmed up.

This test has been carried out twice on the Eppley PSP and Kipp CM 10.

Results

The responses of the pyranometers on a thermal shock are presented in Figure 3. The curves are corrected for the zero offset which was still present when the instruments were placed in front of the ventilator. The two sources of the instrument outputs are the infrared radiation between the inner dome and the sensor and the temperature change of the body. It is obvious that the different pyranometer constructions yield very different behaviours.

The reproducibility of the tests on the Eppley PSP and the Kipp CM 10 was within 10 percent.

LINEARITY AND TILT EFFECTS

Test Facility

The Xenon-lamp test facility is used for the measurement of linearity and tilt effects. The mirror device is mounted on the vertical table of the goniometer, allowing a horizontal operation of the pyranometer for the

linearity tests. Tilt effects can be measured by rotating the mirror device and pyranometer over its horizontal axis. A disadvantage of this method is that by tilting the pyranometer, the light beam rotates around its axis in relation to the pyranometer. Errors will be made if the beam is not homogeneous and if the sensor is not rotationally symmetric. Measurements have shown that the homogeneity of the irradiance is within 2 percent over an area with a diameter of 40 mm.

The maximum irradiance of the instrument is approximately 1000 W/m². Other irradiance levels are realized by using a rotating sector which transmits 50.0 percent or 25.0 percent.

Using both rotating sector and mirror device, measurements can be made on linearity, tilt and combined linearity and tilt effects. The voltage output of the pyranometers is measured with a Keithley 177 digital volt meter.

Test Procedure

The pyranometers are placed in the middle of the light bundle. They were shifted or rotated a little until no tilt effects were found at the low irradiance level of 100 W/m². This procedure guarantees that no influence shall be found which is caused by the small inhomogeneity of the light bundle combined with a rotationally asymmetric sensor. Only the Schenk and the Eko pyranometer showed a small tilt effect (maximum 0.3 percent) at this low irradiance level.

Table 3 shows the measurement routine for the Schenk pyranometer. The measurement routine for the other pyranometers was alike, only having different settling times.

The zero offset is measured before and after each series of tests at a certain irradiance level. The measurements are compensated for this zero offset. The effect of a linear lamp drift and zero offset drift is reduced by taking the averages of the measured output of the first and the second half of a series of tests.

The series of tests started and ended with a 500 W/m² period to obtain a good definition of the 500 W/m² horizontal response. It appeared that the 250 W/m² series should precede the 1000 W/m² series to minimize the zero offset drift.

Results

Figure 4 shows the measured irradiance on the pyranometers (calculated using the constant calibration factor for 500 W/m² on a horizontal sensor) divided by the actual irradiance on the instrument as a function of the irradiance level for different tilt angles (the relative response).

The Kipp CM 5, Schenk and Eko pyranometers show an interaction between linearity and tilt dependency.

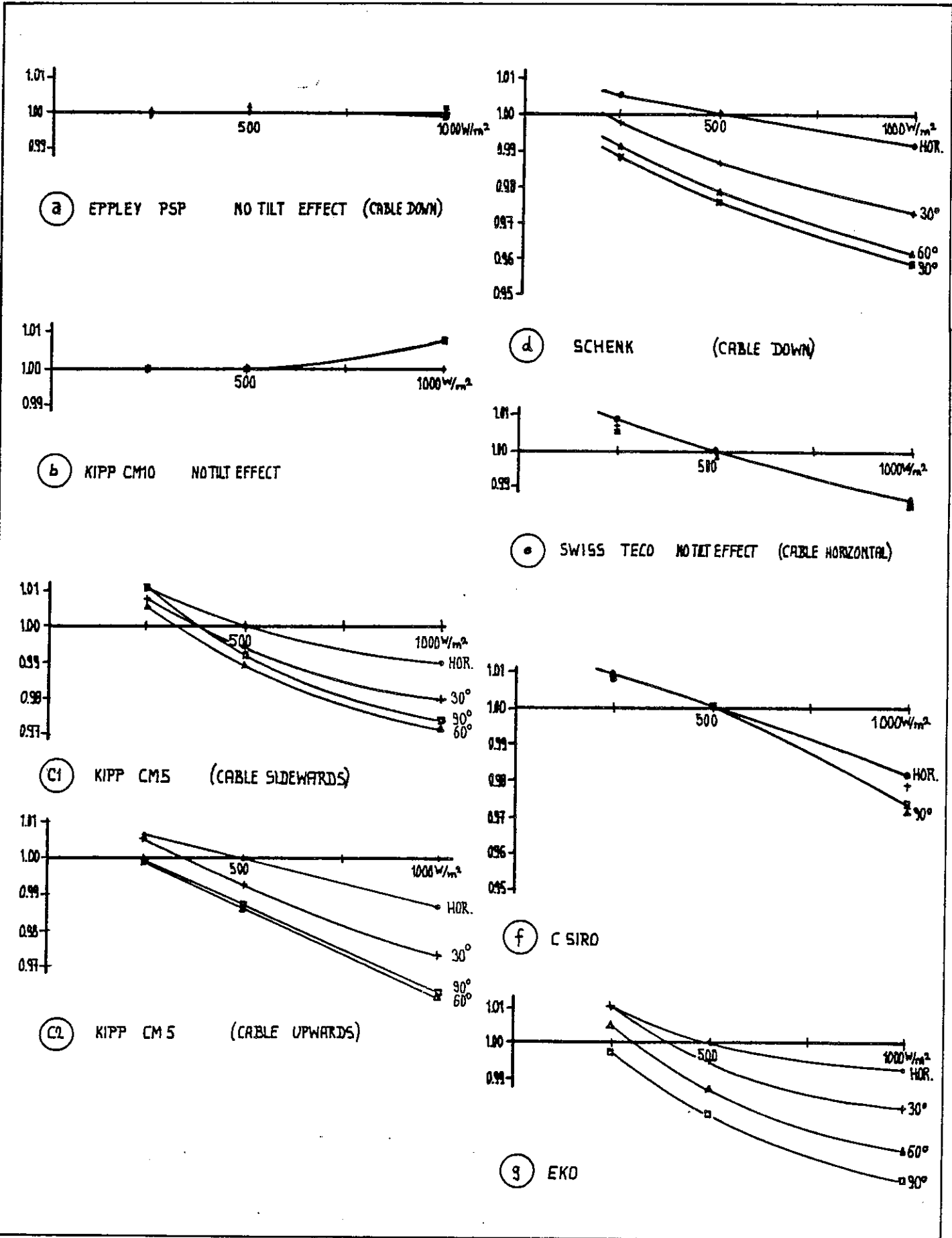


Figure 4. Linearity as a function of irradiance level and tilt angle

TABLE 3
Measurement routine for the Schenk pyranometer.

Test Number	Time (Min.)	Irradiance level (W/m ²)	Tilt (degrees)
1	0	shaded	0
2	2	500	0
3	3	500	30
4	4	500	60
5	5	500	90
6	6	500	60
7	7	500	30
8	8	500	0
9	10	shaded	0
10	12	250	0
11	13	250	30
12	14	250	60
13	15	250	90
14	16	250	60
15	17	250	30
16	18	250	0
17	20	shaded	0
18	22	1000	0
19	23	1000	30
20	24	1000	60
21	25	1000	90
22	26	1000	60
23	27	1000	30
24	28	1000	0
25	30	shaded	0
26	32	500	0
27	33	500	30
28	34	500	60
29	35	500	90
30	36	500	60
31	37	500	30
32	38	500	0
33	40	shaded	0

INFLUENCE OF RADIATION SOURCE ON CALIBRATION

The wavelength responsivity of the pyranometers is influenced by the type of glass of the domes and the surface material of the sensor. The influence of the radiation source will be small if two instruments of one type are calibrated to each other. There is however, a strong influence of

the radiation source if two different type of instruments with for example different types of glass are calibrated to each other.

Test Facility

The Xenon-lamp facility and tungsten-halogen lamp test facility have been described before.

The short term stability of the 500 W/m² irradiance was ± 0.2 percent. The room temperature was between 19 and 22°C.

The output of the pyranometers was measured with a Keithley 177 digital voltmeter.

Test Procedure

Each pyranometer was compared with the Kipp & Zonen CM 11 working standard (nr. 820078). Firstly, the IEA-pyranometer was illuminated for the settling time (Table 2) and compensated for zero offset which was measured after shading for the settling time.

Then the working standard was illuminated for one minute and compensated for 1 minute shading. Thirdly, the IEA-pyranometer was illuminated for another time and offset compensated. The reproducibility of the first and last measurement was within 0.5 percent.

Results

Table 4 shows the calibration factors of the IEA-instruments using the Kipp & Zonen CM 11 working standard for both the Xenon-lamp and Halogen-lamp as the light source. The calibration factors are relative to the level which is in use at Kipp & Zonen at this moment. The traceability with other levels is shown in the paper "Manufacturers indoor calibration procedure of Kipp & Zonen CM 11".

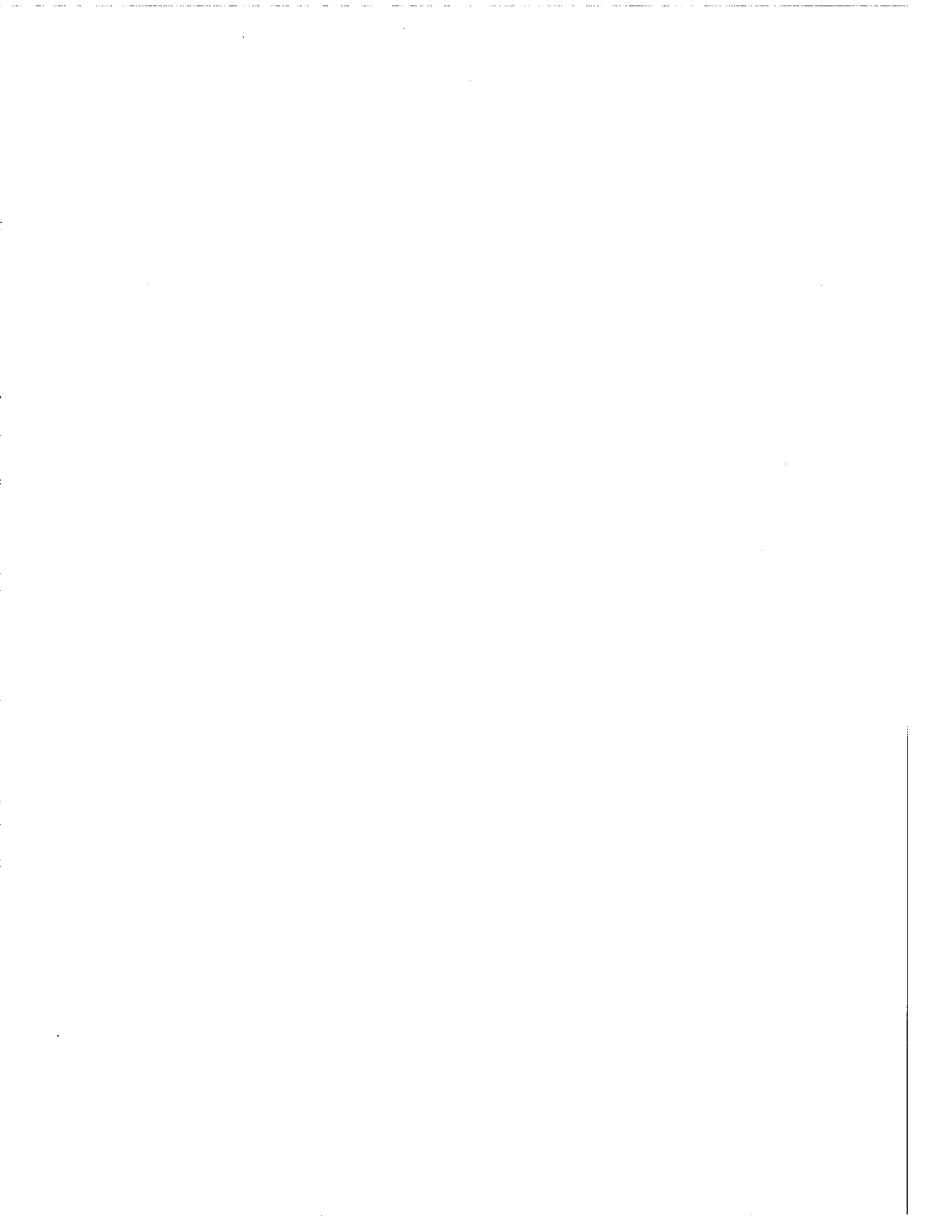
TABLE 4
Calibration Factor

Instrument		Calibration factor			S_{Xenon} <hr/> S_{Halogen}
Type	Number	Manufacturer ($\mu\text{V/W m}^{-2}$)	Xenon-lamp ($\mu\text{V/Wm}^{-2}$)	Halogen-lamp ($\mu\text{V/Wm}^{-2}$)	
Eppley PSP	20524 F3	10.10	10.16	9.79	1.038
Kipp CM 10	810121	4.68	4.69	4.69	1.000
Kipp CM 5	773656	11.74	11.87	11.77	1.008
Schenk	2209	-	15.55	15.03	1.034
Swissteco SS.25	114 A	-	15.70	14.96	1.049
Csiro Mk.2	HBR 115	-	3.85	3.61	1.067
Eko	A 81908	-	9.69	8.84	1.096

The difference between Xenon and Halogen calibration is probably caused by a difference in spectrum. The spectrum of the Xenon-lamp test facility is from 350 nm to 2700 nm. About 10 percent of the irradiance of Halogen-lamp test facility has a wavelength of more than 2700 nm (infrared).

Comparison of an Eppley PSP and a Kipp CM 10 under outdoor conditions showed a very close agreement to the Xenon-lamp calibration (within 1%). Comparison of an Eppley PSP and a Kipp CM 10 with the halogen test facility using a water filter (wavelength transmission up to 1100 nm) showed good agreement with the Xenon-lamp calibration as well (within 1%).

It is shown clearly that special care has to be taken for intercomparison of different types of instruments.



2.F MANUFACTURERS INDOOR CALIBRATION PROCEDURE OF KIPP & ZONEN CM 11

L.F. Lan Wely
Kipp & Zonen
Mercuriusweg 1
Delft - NL

G.J. van den Brink
Technisch Fysische Dienst TNO-TH
(Institute of Applied Physics TNO-TH)
Stieltjesweg 1
Delft - NL

MANUFACTURERS INDOOR CALIBRATION PROCEDURE OF KIPP & ZONEN CM 11

INTRODUCTION

The electrical output of a pyranometer is dependent upon the characteristics (linearity, tilt dependency, etc.) of the instrument. The total set of characteristics is different for different pyranometers. Some of the characteristics are however, almost the same for instruments of one series. The time response, thermal shock response, linearity, tilt dependency, wavelength responsivity and zero offset (I.R. radiation) are almost independent on the pyranometer taken from the series of instruments of the type Kipp & Zonen CM 11. Some small differences can be found for the temperature response. The most important characteristics of the Kipp & Zonen CM 11 are the cosine response, azimuth response and of course the calibration factor.

The cosine error and azimuth error are mainly caused by imperfect polishing of the domes, reflection at the inner side of the domes, reflections at the absorber, roughness of the absorber and wrong levelling of the absorber. Each Kipp & Zonen CM 11 pyranometer is checked for cosine and azimuth error before leaving the factory. The instrument is modified if too large errors are encountered.

The calibration factor is found by comparison of the output with a "working standard" of the same type of instruments, which has been calibrated externally.

DETERMINATION OF COSINE ERROR AND AZIMUTH ERROR

Test Facility

The Kipp & Zonen sun simulator is used for the determination of the cosine and azimuth error. The test facility is shown in Figure 1a. The light source is a Xenon-lamp which is fed by a 2500 Watt stabilized power supply. A photo-cell feedback control is applied. The short term stability of the lamp remains within 0.2%. The condensor forms an image of the Xenon-arc at a small flat mirror (Figure 1b). A concave mirror projects an image of this circular flat mirror at infinity, being an almost true sun image. The angle subtended by the artificial sun as seen from the pyranometer can be varied by using different dimensions of the small mirror. The maximum irradiance on the pyranometer is dependent on the size of the small mirror. A minimum irradiance of 1000 W/m^2 is required on the pyranometer for linearity tests, resulting in an angle subtended by the artificial sun of about 1 degree. This angle has the realistic value of 0.5 degrees for the determination of cosine error and azimuth error. The irradiance on the pyranometer is then approximately 250 W/m^2 at normal incidence. The irradiance is now approximately 43 W/m^2 for an azimuth angle of 80 degrees. No linearity problems occur for irradiance levels up to 500 W/m^2 .



Figure 1a. Photo of Kipp & Zonen sun simulator

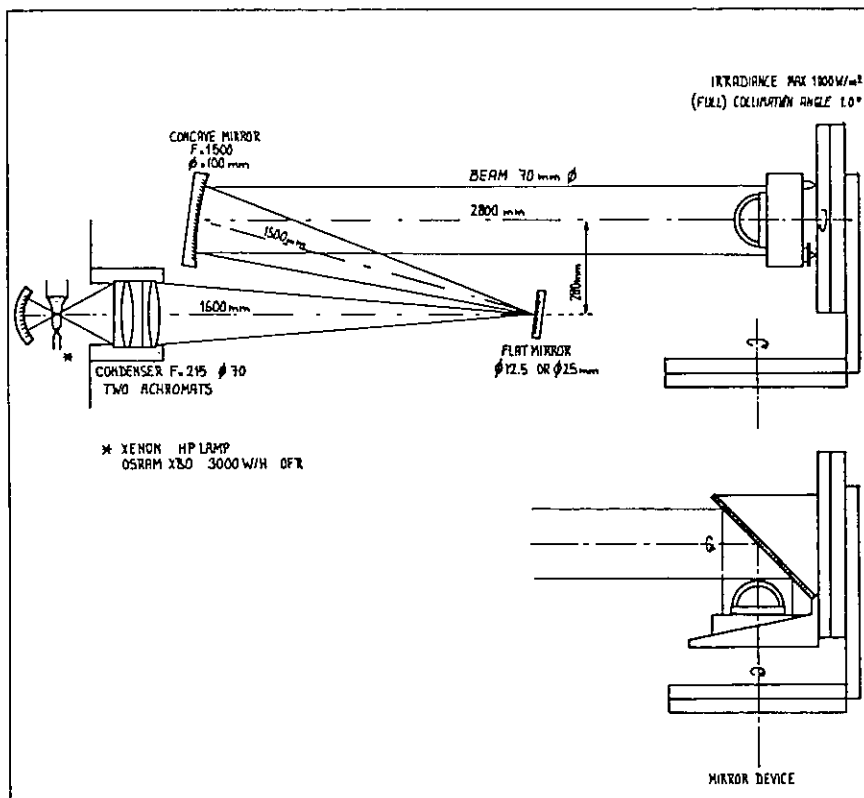


Figure 1b. Kipp & Zonen sun simulation

The output voltage of the pyranometer was measured with a Keithley digital multimeter model 177.

Test Procedure

The horizontal and vertical turntables are used for the determination of the cosine and azimuth error. The errors introduced by the turntables are negligible. The wobble in the vertical turntable is within ± 0.05 degrees over a complete revolution. The horizontal turntable can be adjusted within ± 0.1 degrees.

The pyranometer is mounted on the vertical turntable. The spirit level is parallel to this table. No inaccuracies are introduced by measuring with the pyranometer in the vertical position since the CM 11 does not have a tilt dependency.

All possible combinations of azimuth and zenith angle can be made by rotating the horizontal and vertical turntables.

TABLE 1
Measurements for determination of cosine and azimuth response
of Kipp CM 11

Number	Azimuth	Zenith Angle	Illumination or shading time seconds
1	-	0°	60
2	shaded		60
3	west	40°	60
4	west	60°	30
5	west	70°	30
6	north	70°	30
7	north	80°	30
8	south	80°	60
9	south	70°	30
10	east	70°	30
11	east	60°	30
12	east	40°	30
13	shaded		60
14	-	0°	60

The measurement series starts with determining the output of the pyranometer at normal incidence. The read-out is after one minute. The zero offset is determined by shading for a minute. There is always some zero offset, maybe caused by infrared radiation from the inner dome to the sensor.

The horizontal turntable is rotated 40 degrees clockwise. The connection cable is pointing downwards, which is by definition north. Therefore, the azimuth angle is now west.

The horizontal turntable is rotated another 20 resp. 10 degrees. The read-out time is for both measurements half a minute. The vertical turntable is rotated 90 degrees clockwise for the next measurement. The azimuth angle changes from west towards north, the zenith angle does not change, etc.

After measurement 12 the zero offset is determined again after shading for 60 seconds. Finally, the output of the pyranometer is measured a second time as a check on changes in the irradiance level.

Calculation Procedure and Quality Control

The mean zero offset and mean irradiance at normal incidence are calculated from measurements 2 & 13, respectively 1 & 14. The measurement data are compensated for this zero offset.

The cosine errors are calculated from the averages of the outputs of measurements 3 & 12, 4 & 11, 5 & 10, 6 & 9, and 7 & 8 by relating these averages to the mean output from 1 & 14 at normal incidence. This calculation procedure reduces the effect of zero offset and lamp output drift. The consequence is that the cosine errors are given with respect to the plane of the sensor and are therefore only valid for a radio-metrically levelled instrument.

A small azimuth error can exist for a normally levelled instrument, since the spirit level is not perfectly coplanar with the sensor. The azimuth error for the north, west, south and east direction is detected from the measurements 5, 6, 8 & 9 and 7 & 8. Differences of maximum 2 percent are allowed for the measurements 5, 6, 8 & 9, and a maximum of 3 percent for the measurements 7 & 8.

The alignment of the set-up is checked for larger discrepancies and the procedure is repeated. The instrument is modified if there is still a too large discrepancy.

The quality of the instrument is guaranteed by this procedure.

The cosine errors are presented on the calibration certificate of each individual pyranometer.

DETERMINATION OF CALIBRATION FACTOR

Test Facility

The artificial sun is a 1000 W tungsten-halogen film sun (Osram) with compact filament, fed by an AC voltage stabilizer. The color temperature is about 3300 K. The built-in ventilator allows a continuous operation

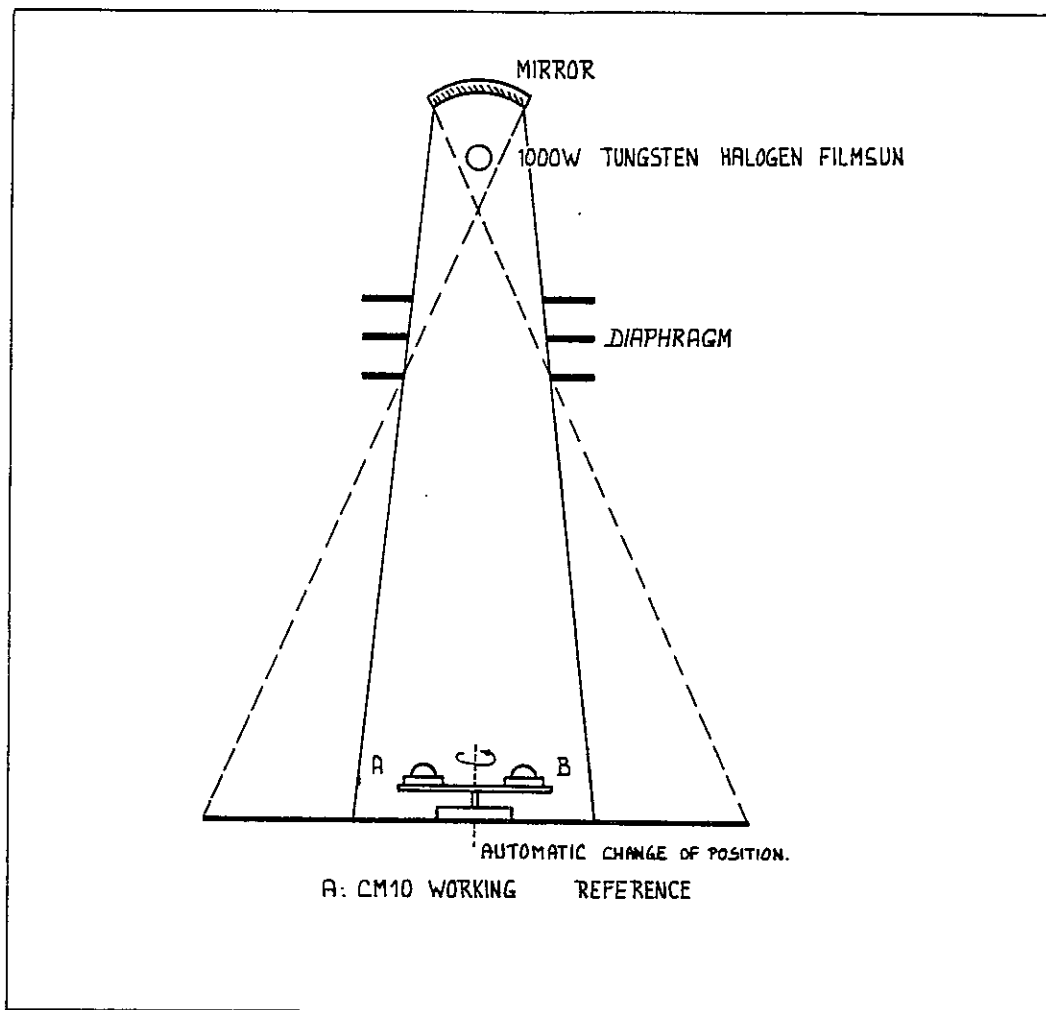


Figure 2. Calibration facility

(Figure 2). A diffuse reflector with a diameter of 7.5 cm is placed above the lamp. The reflector is 1.2 m over the pyranometers, resulting in an angle subtended by the sun of 3.5 degrees. The light on the working table is limited to a small cone around the two pyranometers by using diaphragms, for minimizing the stray light. The irradiance level is approximately 500 W/m².

The pyranometers are to be placed on a small table which can rotate to interchange the positions of the instruments. The lamp is centred on the rotation axis of this table.

The pyranometers are placed on their base. The inaccuracy caused by sensor and base not being parallel can be ignored at nearly normal incidence.

Test Procedure

The pyranometer (A) which has to be calibrated is placed next to the Kipp & Zonen CM 10 working reference (B) on the special table. The outputs of the instruments are measured shortly after each other after illuminating them for one minute. An accurate digital voltmeter with a sensitivity of 1 μ V per digit is used.

The zero offset of both pyranometers is read-out after shading the instruments for one minute with an inside blackened hat. The zero offset problem shall be described further on in this paper.

This zero offset has to be subtracted from the measured output voltages by illumination to get the correct responses R_A and R_B respectively.

The irradiance on both pyranometers might be slightly different from each other due to the lamp optics etc. Therefore, the instruments are interchanged automatically and the whole procedure is repeated, resulting in responses R'_A and R'_B .

Calculation Procedure

The sensitivity of pyranometer A is calculated from the known sensitivity of the working reference B from:

$$S_A = \frac{R_A + R'_A}{R_B + R'_B} \times S_B$$

The irradiance during the calibration is calculated from:

$$I = \frac{R_B + R'_B}{2 \times S_B}$$

The error in the sensitivity of A caused by asymmetry of the lamp optics (< 5%) and drift of the lamp output (< 0.5%) remains within 0.01%. A special check is made for possible errors made in reading of the voltage output. The calibration procedure is supposed to be correct if:

$$0.995 < \frac{R_A \cdot R_B}{R'_A \cdot R'_B} < 1.005$$

Otherwise the calibration procedure is repeated.

Another inaccuracy is introduced by the temperature difference of the pyranometer and the working standard. The temperature dependency of the sensitivity is not known accurately for each individual instrument. The determination of this dependency for each pyranometer is too time consuming and therefore too expensive.

The temperature of the working reference increases somewhat during a set of calibration. It can be up to 5°C warmer than the pyranometer which has to be calibrated. No correction is applied for this temperature difference. A maximum error of half a percent is introduced.

Zero Offset

The glass domes of the pyranometers are heated by absorption of the long wave infrared radiation emitted by the lamp house and diaphragms. A small signal of 10-30µV remains after shading the pyranometers for one minute, due to long wave infrared radiation from the domes to the sensor. This zero offset fades away with a time constant of about 4 minutes.

Such a zero offset is part of the read-out response after one minute illumination as well. The zero offset after one minute shading is subtracted to correct for this undesired response.

Secondly, the pyranometer body is heated a little during the illumination. A negative zero offset is produced by a small heat flow to the center of the sensor. This heat flow stops when the instrument is shaded. The CM 11 pyranometers have a second non-illuminated sensor to compensate for this zero effect. Measurements show a signal up to -30µV without the use of a compensation element, which reduces to a few microvolts when the compensation element is used; it is therefore negligible.

Traceability to World Radiometric Reference

Several working standard pyranometers are maintained at Kipp & Zonen. Up to September 1981 a Kipp & Zonen G-18 has been used as working standard. The calibration factor of this instrument has undergone several changes. In January 1981 the change of IPS 1956 scale to WRR scale resulted in a correction of 2.2%. In May 1981 the calibration factor has been changed another 2% after comparison with Davos-measurements. A Kipp & Zonen CM 10 is in use as

working standard since September 1, 1981. The sensitivity as given by the manufacturer in the past years for the manufactured pyranometers is somewhat different from the sensitivity as it should be given at this moment, due to changes of the calibration factor of the working references which were not caused by changes of the actual sensitivity.

The factor by which the sensitivity (given in $\mu\text{V}/(\text{W m}^{-2})$) has to be multiplied is dependent on the actual date of calibration, it is given in Table 1.

TABLE 1
Sensitivity Multiplication Factor 1

Period of Calibration	Multiplication Factor	Working Standard Pyranometer
1977 - January 1981	0.962	Kipp & Zonen G-18 (nr. 938)
January 1981 - May 11, 1981	0.984	Kipp & Zonen G-18 (nr. 938) (IPS 1956 scale WRR scale)
May 11, 1981 - September 1, 1981	1.004	Kipp & Zonen G-18 (nr. 938)
September 1, 1981 - September 1983	1.000	Kipp & Zonen CM 10 (nr. 800065)
September 1983 - now	1.000	Kipp & Zonen CM 10 (nr. 800074)

As an example, the sensitivity of an instrument calibrated in 1980 of e.g. $10 \mu\text{V}/(\text{W m}^{-2})$ should be changed to $9.62 \mu\text{V}/(\text{W m}^{-2})$ to make it comparable to the calibrations of this moment.

The above described correction is only relative to the calibration of this moment, which itself is not an absolute calibration. At this moment it is not completely sure which correction should be applied to come to an absolute correct value. The calibration factor which is used as reference at this moment was measured at the World Radiation Center (WRC) in Davos in 1981. A first telex from Davos shows a sensitivity of $4.50 \mu\text{V}/(\text{W m}^{-2})$ of the CM 10 (nr. 800065). This value is at this moment in use as reference. However, a correction has been made by WRC shortly after, resulting in a sensitivity of $4.40 \mu\text{V}/(\text{W m}^{-2})$. Working standard reference pyranometers have been calibrated as well by the Deutsche Wetterdienst (DWD) in Hamburg and by DSET laboratories in Phoenix Arizona (USA). The measurements gave different results. Therefore, the calibration factors as given by Kipp & Zonen for its pyranometers should be adjusted, dependent on which international calibration is seen as "Absolute".

Table 2 shows the factor by which the present give sensitivity (in $\mu\text{V}/(\text{Wm}^{-2})$) should be multiplied to have a sensitivity related to the corresponding calibration.

TABLE 2
Sensitivity Multiplication Factor 2

Laboratory	Date	CM 10/11 Number	Multiplication Factor	Circumstances
WRC	July 1981	800065	1.000	First telex
WRC	July 1981	800065	0.978	Second telex
DWD	February 1981	800074	0.989	Indoor calibration
DWD	April 1981	800074	0.993	Outdoor measurements
DSET	May 1982	820078	0.981	Outdoor, tilted, normal incidence
DSET	November 1983	800065	0.982	Outdoor, tilted normal incidence

As an example, the sensitivity of a recently calibrated instrument with a sensitivity of e.g. $10\mu\text{V}/(\text{W m}^{-2})$ should be changed in $9.93\mu\text{V}/(\text{W m}^{-2})$ to make it comparable to the outdoor measurement at the Deutsche Wetterdienst of April 1981.

From Table 2 it seems reasonable to decrease the sensitivity (in $\mu\text{V}/(\text{W m}^{-2})$) by about 1 to 2 percent. The calibration factor of the working standard shall be adjusted as soon as a better international agreement is made on which of the above mentioned multiplication factors should be used.

2.6 INDOOR AND OUTDOOR PYRANOMETER COMPARISONS

H.D. Talarek
Kernforschungsanlage Julich GmbH
Julich, Federal Republic of Germany

INDOOR AND OUTDOOR PYRANOMETER COMPARISON

This project was organized and executed by the solar collector testing experts of Task III of the IEA Solar Heating and Cooling Program.

A total of 30 pyranometers comprising six different models from five different manufacturers were tested. During 1981 the pyranometers were exposed in various outdoor configurations on 26 days at the Davos World Radiation Centre in Switzerland. The pyranometers were later characterized in the laboratories of the Statens Provningsansalt in Boras, Sweden. Results from other laboratories investigating these pyranometers are also referred to.

An aim of the project was to attempt validation of indoor characterization with outdoor results. The following is a summary of the project findings, recommendations and conclusions. The project is completely described in Reference 1.

OUTDOOR TESTING

- check of calibration constants
 - new Eppley PSP) agreement better than + 1%
 - K & Z CM 10)
 - EKO star scatter of + 1.5% to ±3%
 - Schenk star scatter of ± 1.5%
 - Old K & Z CM 5 bias of + 2% to + 3%
- day-long variability
consistent with findings about the calibration constants
- tilt effects (day-long variability)
 - Eppley PSP) not resolved
 - K & Z CM10)
 - K & Z CM5 moderate effect (tilt: 30°
sensitivity: -1-2%)
 - Eko star)
 - Schenk star) "natural" temperature coefficient
 - Swissteco)
 - Eppley PSP) not detectable
 - K & Z CM10)

INDOOR TESTING

- tilt
confirmation of outdoor findings
- dependence on ambient air temperature
confirmation of outdoor findings
- deviation from a linear response
Eppley PSP: excellent linearity
others: less than 1% for 100 W/m² - 1000 W/m²
- directional response
deviation from cosine response at all angles
measurements from different laboratories
do not compare at all (angles 60°)

RECOMMENDATIONS

- We would not recommend using pyranometers which show a tilt dependence (calibration in an inclined position is no remedy because of the cross-correlated dependence on the level of irradiance).
- From those instruments that were tested only the Eppley PSP and the K&Z CM10 can be accepted in solar energy applications for testing and monitoring.
- We would recommend a standardized certification by the manufacturer's laboratory for the individual instrument with respect to the:
 - calibration constant
 - temperature coefficient
 - tilt effects
 - linearity

Angular dependence should only be investigated for angles less than 60°.

CONCLUSIONS

- Remarkable correspondence between indoor and outdoor test qualitatively.
- Measurements of directional response are not reliable (uncertainty of cross correlation with level of irradiance).
- Correction of outdoor performance based on indoor laboratory data can improve measurement accuracy. However, if correction are small they tend to be inconsistent within a small band of uncertainty.

- Accounting for seasonal variations and for uncertainties of the calibration procedure we claim for short term values of irradiance on accuracy of ± 2.5 to $\pm 3\%$ for the group of the best instruments.

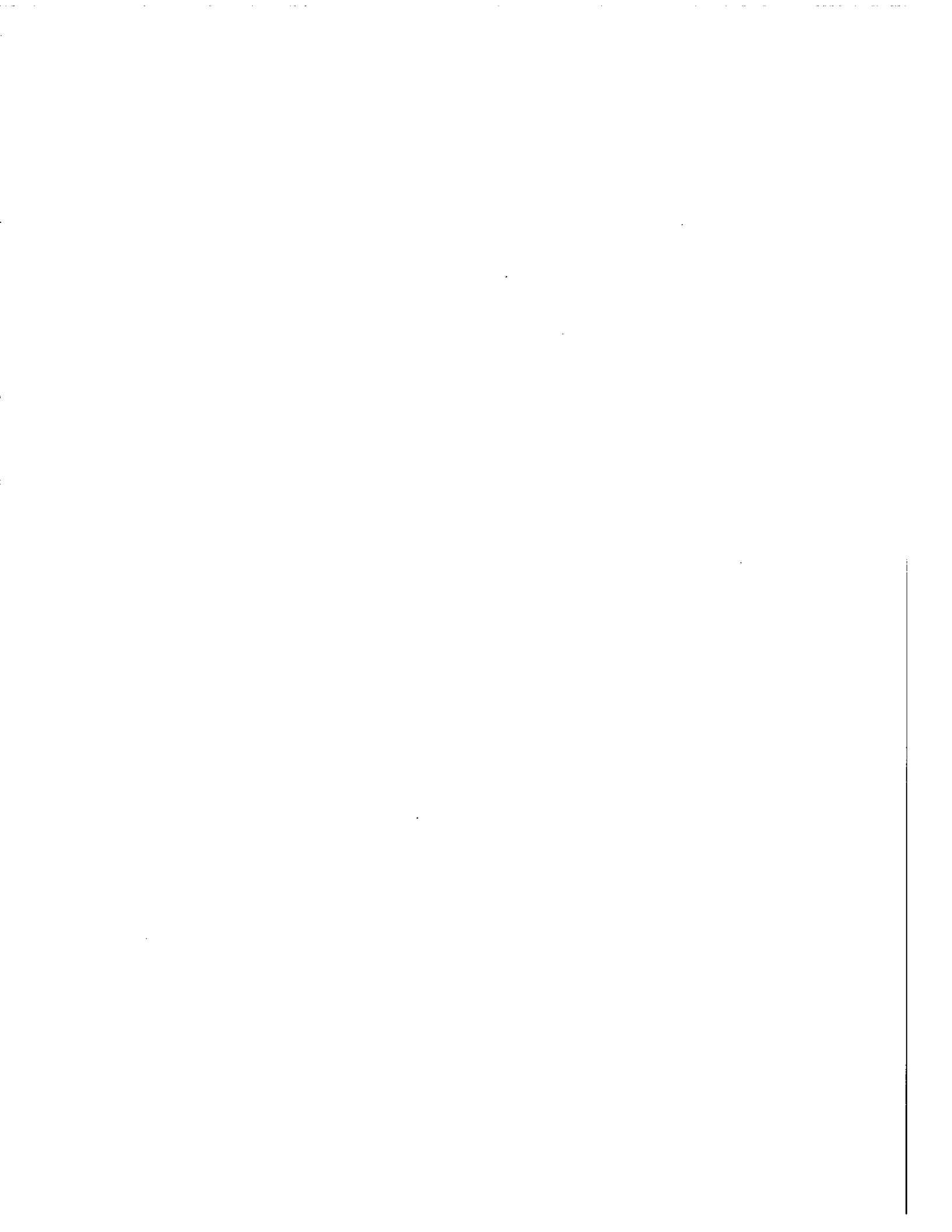
REFERENCE

Ambrosetti, P., H.E.B. Andersson, D. Frohlich and H.D. Talarck: Results of an outdoor and indoor comparison of pyranometers - IEA Document No. IIIA3 Solar Heating and Cooling Program.

SESSION 3

Physics of Pyranometers:

Ageing, ventilation, manufacturing techniques, etc.



**3.A MEASUREMENTS OF TRANSIENTS:
IRRADIANCE, TEMPERATURE, AGEING**

P.-M. Nast

DFVLR, Institute for Technical Physics
D 7000 Stuttgart 80, F.R.G.

MEASUREMENTS OF TRANSIENTS: IRRADIANCE, TEMPERATURE, AGEING

One condition for the classification of a calibration method is the knowledge of the transient behaviour of the pyranometers. Results of calibrations should apply for equilibrium conditions. Therefore prior to calibrations one should know when equilibrium is reached.

The most important transient is the response of the pyranometer to a sudden change in irradiance. Figure 1 gives this response for four different types of pyranometers. From the figure it is seen, that for accurate measurements one has to take into account more time constants than the short response time that is specified by the manufacturer. For example, calibrations of a PSP with the shading disk method will be erroneous by more than 2% when readings are taken within one minute after shading or unshading of the pyranometer.

Figure 2 gives the transient behaviour of four types of pyranometers with respect to temperature. The pyranometers were brought from a temperature of -14°C to a dark laboratory at 20°C where the output was monitored. For all types the time constant ($1/e$) of the signal was about 45 minutes. For the CM 11 and the PSP a maximum signal of about 34 W/m^2 was measured. Assuming linear behaviour this corresponds to a sensitivity of $1 \text{ W/m}^2/^{\circ}\text{C}$ for sudden changes in temperature. This effect has to be taken into account when changes between outdoor and indoor measurements are necessary.

The data available in Stuttgart, that reflect the ageing of two PSP are shown in Figure 3. The PSP 18376 is the working standard in Stuttgart and has been used indoors and outdoors. The PSP 20820 was in the field for 8 months in Baja California Sur, Mexico. For both pyranometers there is no sign of ageing with reference to sensitivity.

For the CM 11 and the PSP the influence of the attached white screen on the sensitivity to normal irradiance has been investigated. For the PSP a decrease of about .6% in sensitivity has been found without the screen. For the CM 11 the corresponding figure is .2%.

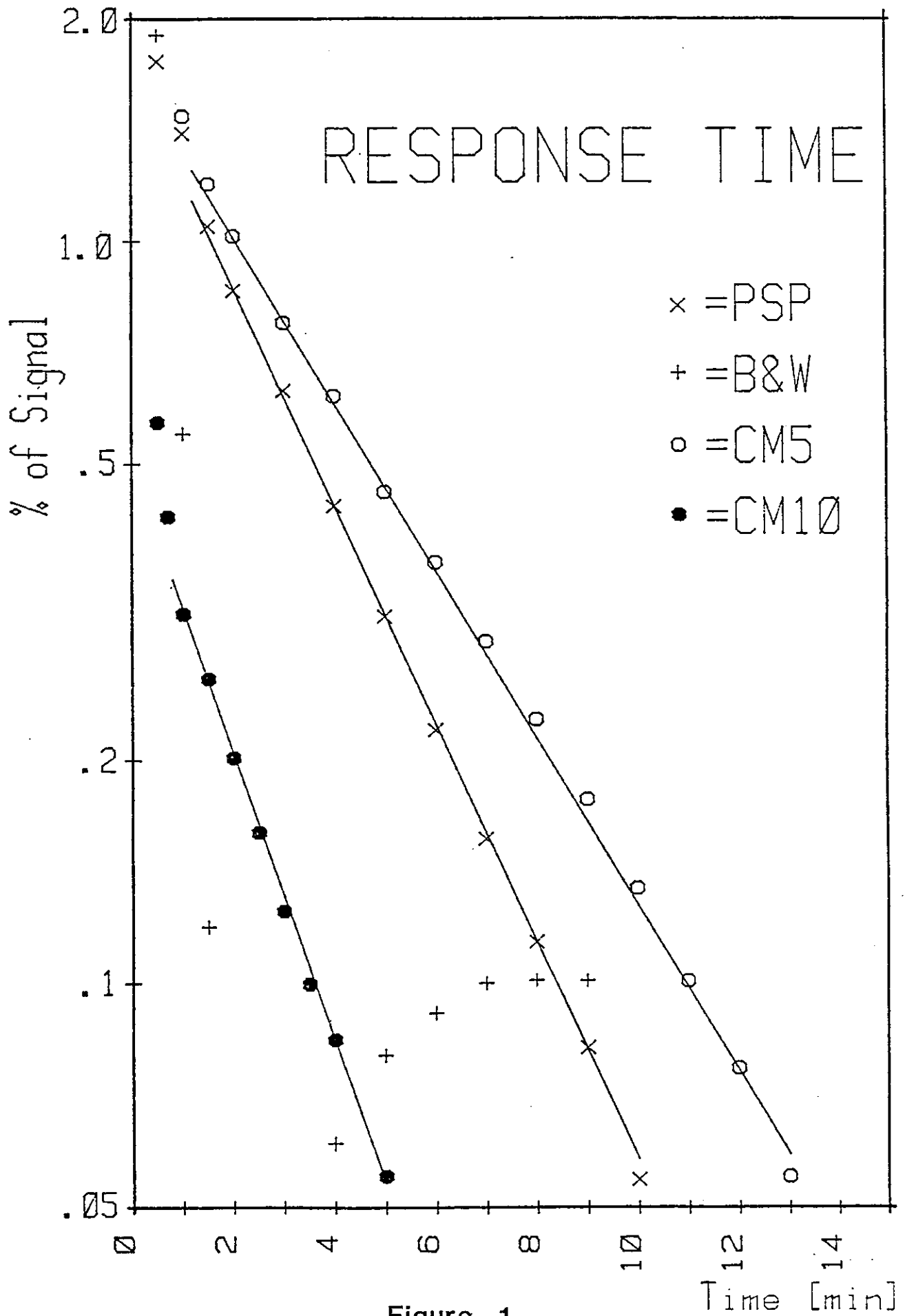


Figure 1

RESPONSE TO CHANGES IN TEMPERATURE

(from -14°C to 20°C)

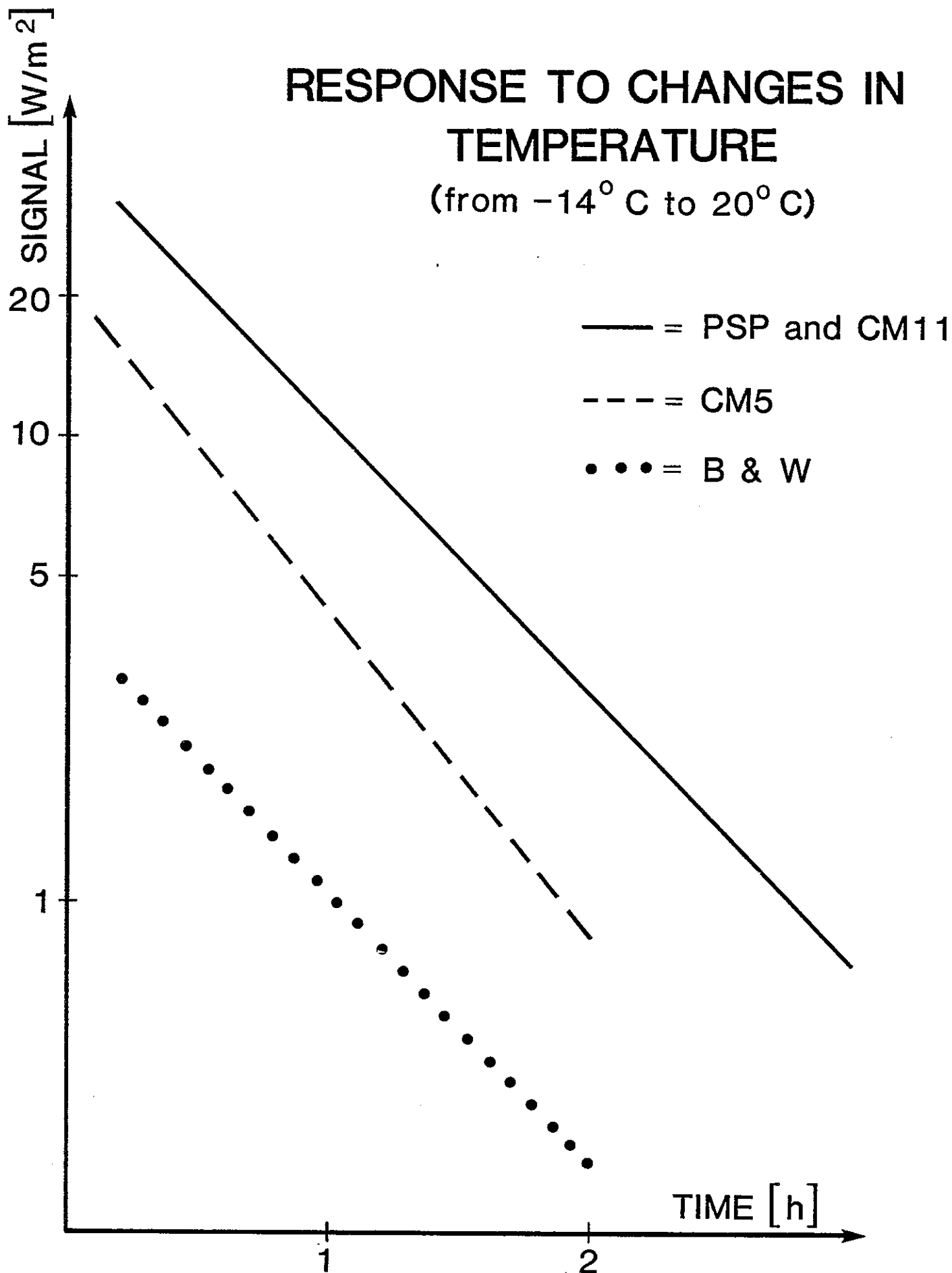


Figure 2

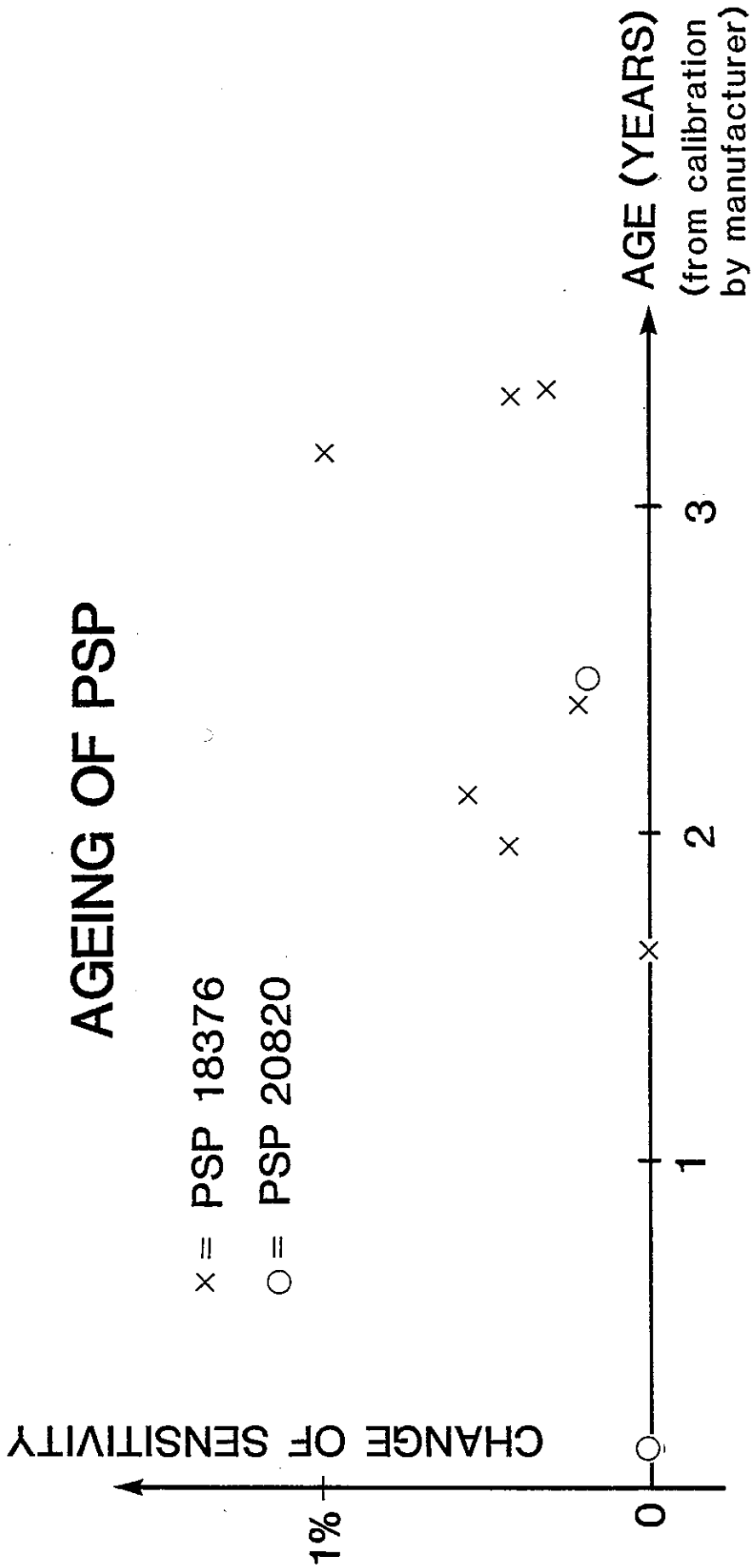


Figure 3.



3.B NEW THERMAL MODEL OF THE PYRANOMETER AND ITS CHARACTERISTICS

Yukiharu Miyake
Executive Director
EKO Instruments Trading Co., Ltd., Tokyo

NEW THERMAL MODEL OF THE PYRANOMETER AND ITS CHARACTERISTICS

PREFACE

The reasons for the difficulties in the establishment of thermal design of a pyranometer are as follows:

- a) The characteristics of the pyranometer should not be influenced by weather conditions such as wind, temperature, etc.;
- b) The angular incidence of the global solar radiation is bidirectional;
- c) The spectral distribution of the solar radiation is very wide;
- d) The phenomena mentioned in b) and c) change depending on time.

In addition to the above difficulties common instrumental quality such as linearity, ageing, etc. are required for the purpose of measurement. In this report advantage and disadvantage of various thermal models of a pyranometer are described and further the characteristics of a new pyranometer which is not yet made public is shown.

MODELS OF THERMAL DETECTION ON PYRANOMETER

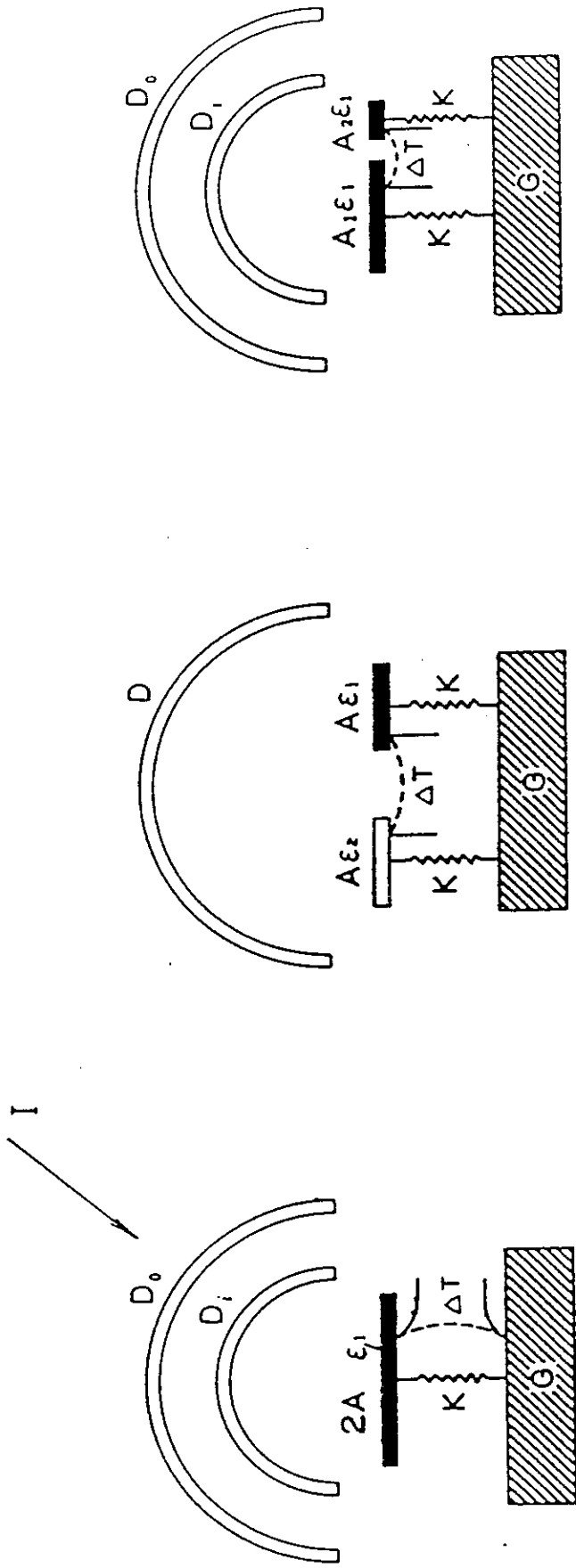
Three models are considered as Figure 1 shows. Supposed that the incoming solar radiation to a pyranometer is "I", absorptivity of the receiving plate " α ", its area "A", its temperature " θ_1 ", base plate temperature " θ_0 " respectively, the thermal balance on the receiving plate at model 1 is as follows:

$$I\alpha A = K(\theta_1 - \theta_0) + \Delta Q \quad \dots (1)$$

where, "K" is the thermal conductance between the receiving plate and the base plate and " ΔQ " the heat loss amount transferred to other places than the plate. The output of a pyranometer is actually detected as temperature balance by the following equation:

$$\theta_1 - \theta_0 = \frac{1}{K} (\alpha AI - \Delta Q) \quad \dots (2)$$

An ideal pyranometer requires that " $\frac{\alpha A}{c}$ " and " θ_0 " are constant and yet $\Delta Q = 0$. However, these conditions cannot be satisfied actually due to limitations in the constitution, so that various methods are commonly considered. For example, " ΔQ " is minimized by making the pyranometer dome double shield.



MODEL 1

$$I = \frac{K}{2A\epsilon_1} \Delta T$$

MODEL 2

$$I = \frac{K}{A(\epsilon_1 - \epsilon_2)} \Delta T$$

MODEL 3

$$I = \frac{K}{\epsilon(A_1 - A_2)} \Delta T$$

I : Incident Radiation

ΔT : Temp. Difference

D: Glass Dome

G: Base Plate

K: Thermal Conductance

ϵ : Emissivity (Absorptivity)

A: Area

Fig.1 Basic Thermal Model of Pyranometer

The second model is to detect solar radiation by means of the difference of absorptivity in 2 receiving plates. The detection principle in this case is given by following equation:

$$\theta_1 - \theta_2 = \frac{1}{K} A(\alpha_1 - \alpha_2)I - (\Delta Q_1 - \Delta Q_2) \quad \dots (3)$$

where, the subscripts "1" and "2" show each receiving plate.

When comparing equation (3) and equation (2) it is known that ΔQ is small as it is given as the balance. On the other hand, however, it is required to make the balance of absorptivity " $\alpha_1 - \alpha_2$ " constant. Viewing this from optical point its realization is very difficult.

Model 3 is the same as model 2 in that the balance is taken out, but this method takes out an output by means of areal difference instead of the difference in absorptivity. Therefore, the solar radiation is determined by the equation.

$$\theta_1 - \theta_2 = \frac{1}{K} \alpha(A_1 - A_2) - \Delta Q_1 - \Delta Q_2 \quad \dots (4)$$

The equation is based upon the idea that making areal difference " $A_1 - A_2$ " constant is technically easier than making absorptivity difference constant. Because the commonly used white paint has the disadvantages that its spectral response is not homogenous in all wave-length range, that its angular response slips out of cosine law and that it ages.

On the contrary the areal difference is effected not by optical conditions but only by geometric form, therefore, Model 3 would be more constant than Model 2 for various conditions mentioned as pos. 1. As we examined Model 3 from various aspects, the results are reported below.

IMPROVEMENTS OF PYRANOMETER AND EVALUATION OF ITS CHARACTERISTICS

There are two ways in the improvement of pyranometer. One is to pursue an ideal model from the principle point and the other is to eliminate the disadvantage of the principal model technically.

We have employed Model 3 for improvement of pyranometer and in addition have made the dome double. It goes without saying that the pyranometer manufactured in such away must be measured as precisely as possible in its characteristics. The evaluation of the characteristics can of course be carried at outdoor but the correct performance is difficult as various conditions must be taken into consideration as referred at pos. 1.

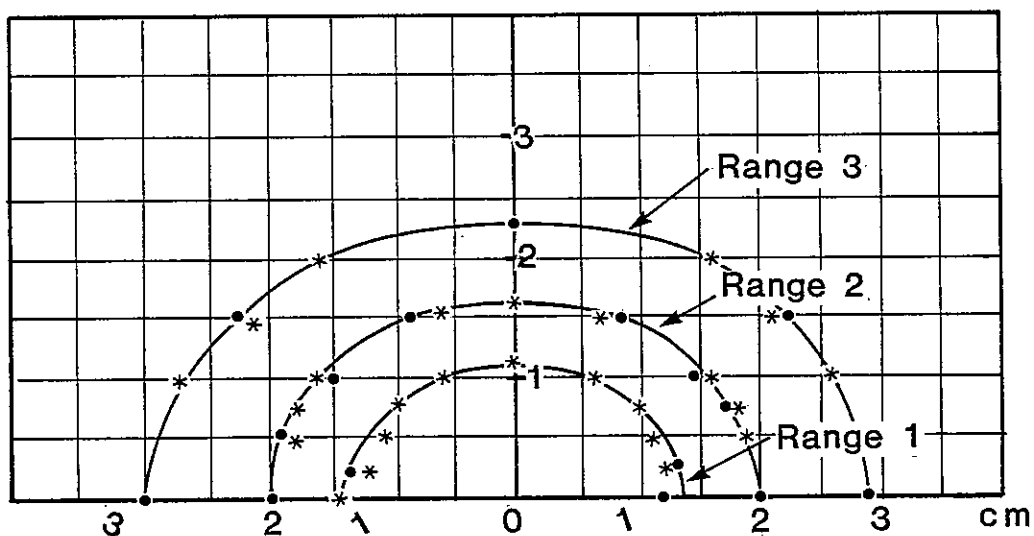


Figure 2A Intensity distribution on an irradiated plane

- Range 1: Distribution within 0.25% 2.2x2.7cm
- Range 2: Distribution within 0.5 % 3.2x4.0cm
- Range 3: Distribution within 1 % 4.5x5.8cm

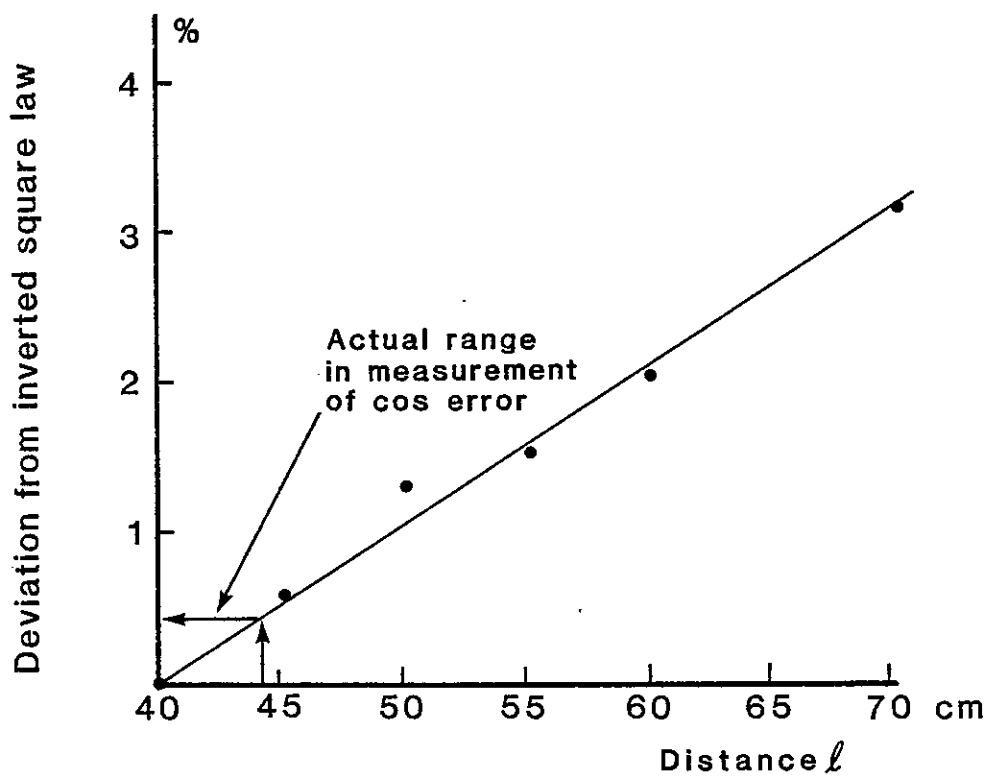


Figure 2B Deviation from inverted square law of the artificial lamp

Under the circumstances we have used a special artificial light source* for the evaluation. The features of the light are that the light intensity is homogenous on an irradiated plane and that the inverted square law of the light intensity is given as per Figure 2. In case of a common artificial light source one of the above mentioned features is in short. We have measured cosine error and azimuth error of our new pyranometer setting the above light source on an optical bench. Also, we have measured the linearity by adding a rotating attenuator to the device.

As for other characteristics such as temperature coefficient, tilt error, etc. we evaluated them with by ordinary methods. The results are as per Figure 3. The remarkable point in the data is the fact that the linearity and temperature coefficient have been improved to a large extent. The two characteristics can further be improved if one of pyranometry constitution problems is solved. Also our new pyranometer has no electric compensation circuit to correct temperature coefficient.

In order to examine zero stability (drift) and influence of natural wind we have recorded the output data of the pyranometer during clear night time (Figure 4). As can be shown from Figure 4 the prementioned ΔQ is very small in case of Model 3.

CONCLUSION

I have classified in this report constitution of pyranometer into three models and referred respective advantages and disadvantages, and further have introduced our new development of pyranometer of Model 3 (areal difference type) mainly in its evaluation of characteristics. The remaining subject for us is to compare the characteristics between pyranometers of other models.

* Supplied by Optronics Laboratories, Orland, FL 32809 USA

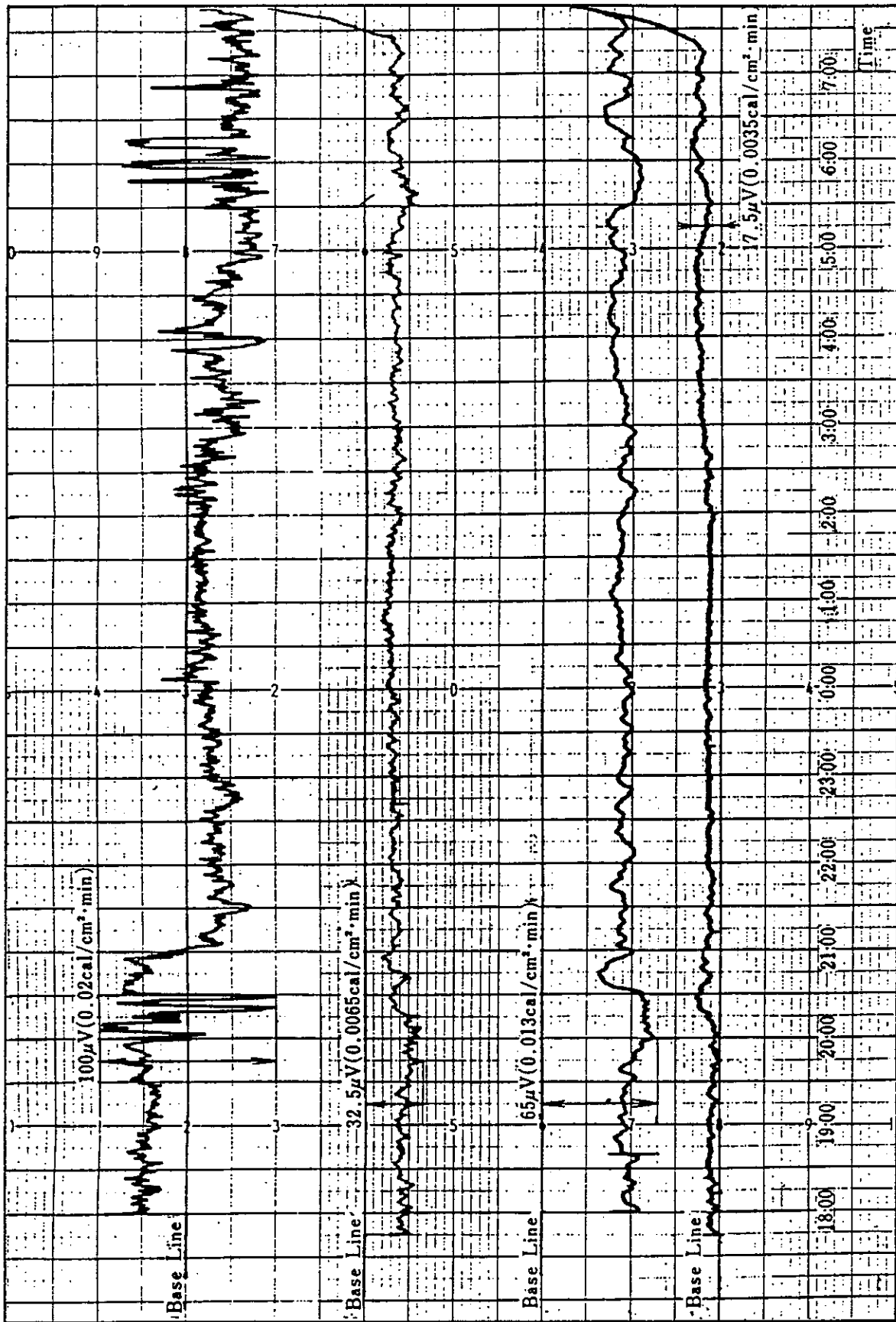


Fig.4 Zero-stability of Pyranometer

- A: Black & White (Non symmetry)
- B: Black & White (Radial Symmetry)
- C: Black
- D: Areal Difference



**3.C SELF-CALIBRATING CAVITY RADIOMETERS AT THE EPPLEY LABORATORY:
CAPABILITIES AND APPLICATIONS**

Alton R. Karoli,
John R. Hickey and
Roger G. Frieden

The Eppley Laboratory, Inc.
12 Sheffield Ave.
Newport, RI 02840
(401)847-1020

SELF-CALIBRATING CAVITY RADIOMETERS AT THE EPPLEY LABORATORY: CAPABILITIES AND APPLICATIONS

ABSTRACT

Considerable effort at the Eppley Laboratory Inc., over the past decade has been directed toward the accurate measurement of solar irradiance and the design and development of low temperature blackbodies. Additionally, we have been involved with the design and production of thermopile-type sensors for special applications. The implications of referring all relevant measurements to a unified reference scale or radiation are always of concern. In this paper, self-calibrating radiometers with cavitated receivers which can be designed for a number of total irradiance measurement tasks will be described. Among these tasks are the measurement of solar irradiance, both direct beam and over larger fields-of-view, and the measurement of earth emitted flux (generally from satellites), for which the low temperature blackbodies act as simulators. The radiometer can also be adapted to a number of laboratory measurements such as the output of lamp or laser sources. The basic type of sensor employed in the Eppley radiometers is a circular, wirewound and plated thermopile, sometimes called totidal thermopile. Self-calibration is performed using a heater on the cavity receiver which is employed in an electrical substitution mode. The difference in response produced by the heater to that produced by the radiation source is called the "nonequivalence". Determination and application of the correction factors including the components of the nonequivalence term will be discussed. Results of intercomparisons with other self-calibrating radiometers will be presented.

INTRODUCTION

One of the most elusive goals of absolute radiometry is the establishment of a universal reference or standard. Such a device would have to operate over a large range of radiative flux and over the entire spectral range of interest. The device must have a firm theoretical basis and yet be practical in its use. Possibly the biggest obstacle to the development of such a device is the requirement to operate over a range of geometrical conditions. The nature of radiometric detectors possessing cavitated receivers allows for self-calibration by employing the electrical substitution method and spectral flatness based on the enhanced absorptance of the cavity. There remains the problem of non-equivalence of response to electrical, as opposed to radiative, power dissipation which must be addressed by thermal transfer analysis.

In this paper we wish to discuss some aspects of the design, construction and utilization of cavity radiometers at The Eppley Laboratory.

BASIC CONSIDERATIONS

There are a number of ways of categorizing cavity radiometers. They are:

1. Self-calibration capability and technique;
 - 1.1 Not self-calibrating
 - 1.2 Self-calibrating
 - 1.1.1 Active
 - 1.2.2 Passive
2. Intended use
 - 2.1 Source of radiation
 - 2.1.1 Point source or narrow field-of-view
 - 2.1.2 Extended source or wide field-of-view
 - 2.1.3 Intermediate size sources
 - 2.2 Intensity range required
 - 2.3 Environment of operation
3. Detection method (temperature difference)
 - 3.1 Thermoelectric (Thermopile)
 - 3.2 Resistance thermometry
 - 3.3 Pyroelectric
 - 3.4 Quartz crystal thermometers
4. Cavity geometry
 - 4.1 Classical cone
 - 4.2 Classical cone with trap
 - 4.3 Inverted cone (within a cylinder ("W"))
 - 4.4 Modified "W" geometries
 - 4.5 Truncated double cone: base to base

PARAMETERIZATION

The important characteristics of any cavity radiometer device include:

- a) Absorptivity of the cavity receiver;
- b) Area of the precision aperture;
- c) Knowledge of the absolute electrical power during calibration, including the corrections for measurement leads;
- d) Non-equivalence;
- e) Linearity;
- f) Responsivity;

- g) Speed of response (time constant);
- h) Field-of-view;
- i) Spectral flatness.

Non-equivalence is the term employed to describe any of the design and/or fabrication parameters which cause the same signal output to be obtained for different levels of measured radiant power and self-calibrating electrical power. This is related to the difference of the thermal transfer characteristics of the instrument (radiative, conductive and convective) for two sources of power input. The knowledge of the changes in this characteristic for the various measurement conditions is critical to the question of unique reference scale as will be appreciated from the following paragraphs.

APPLICATIONS

The intended applications of these devices usually dictate the design. It follows that an instrument designed for one type of application may not necessarily be useable for others, or that it may be used "absolutely" only if changes are made in the data reduction equations. That is, the non-equivalence may be different for a given device for different measurement applications, even if all other parameters are unchanged. Generally speaking, this will be the result of the geometry of the measurement situation, although other factors such as induced temperature gradients by the environment or thermal transients may also cause errors.

At the Eppley Laboratory, the general areas of interest include solar radiation measurement and measurement of earth emitted radiation, the geophysical radiation parameters¹. The simulation of these by various sources is also addressed. A number of laboratory types of radiometric investigation are also considered. The latter are concerned with calibration of sources, such as lamps of various types, and general source characteristics for other emitters such as laser and solid state devices. Probably the most significant area requiring a unified radiation reference or scale is the study of earth radiation budget. The radiative elements include:

- a) The incoming (extraterrestrial) solar irradiance;
- b) The outgoing radiation consisting of:
 - reflected solar radiation (albedo)
 - emitted infrared radiation

In order to determine the heat balance of the earth to a high precision, the measurements must be of comparable high accuracy. While the problems of sampling theory, both temporal and spatial, are significant in such studies, we will address only the measurement equipment here.

THE SENSOR

The basic sensor² chosen for use by the Eppley Laboratory is a plated thermopile. A continuous constantan wire is plated with copper to form the

junctions. Since one of the most important characteristics of the completed radiometer is uniformity of response over the receiving area and since a circular cross section of the incident beam is generally sensed, the wire is wound on a doughnut shaped support in the form of a toroid. Junctions are plated on both sides of the device to create a balanced unit. The side facing the incoming beam is the "active junction" side while the side facing into the housing is the "reference junction" side. These sensors are usually employed for net radiant input measurements, so the active side is generally called the "hot junction". This does not eliminate the possibility of use either as a Net radiation emitter or as a differential radiometer.

It is the mounting of the cavity receiver to this basic sensor that creates the radiometer. Figure 1 shows how the cavity pieces fit to both sides of the thermopile. At Eppley the "W" shaped inverted-cone-within-a cylinder type of cavity construction is employed. Both the inverted cone and the cylinder have electrical heater wires wound on them. The interior cavity surfaces are painted with a specularly reflecting black paint. The exterior surfaces are goldplated or left uncoated. The cylinder and cone are made of silver foil. The precision aperture is placed in front of the opening of the cylinder. Generally these are made of invar because of its low thermal expansion coefficient, which may be stated conversely as dimensional stability of the opening area over a wide temperature range.

It should be noted that the selection of this type of construction was also based on the ability to meet the stringent vibration specifications of spacecraft and rocket missions. The responsivity can be varied over a range of values by changing a number of parameters including the number of junctions, the wire size, the dimensions of the body of the unit, the plating parameters and the thermal impedance (conductance) to the base. While most of these methods are considered proprietary, the special thermal conductor is shown schematically in Figure 2. This is essentially a piece of the supporting base which extends up beneath the wire at the point where the bottom of the cavity receiver is affixed to the plated junctions which allows a certain amount of the heat present at the ring of junctions to flow to the base without flowing through the wires of the sensor. If all other parameters are held constant, the response can be varied by a factor of 10 by adjusting this thermal conductor. The maximum response is obtained with the conductor removed completely so the heat does flow through the wires.

In retrospect, we see that the output of the thermopile is a measure of the temperature differential between the base of the cavity on the hot junctions and that at the base of the cavity on the cold junctions. One of the most significant reasons for the employment of the thermal conductor is to keep this differential to a minimum for a given application which will prevent the device from entering non-linear regions with respect to the Seebeck coefficient and the differential radiation loss term. This may be restated as a goal to obtain the lowest possible temperature rise in the sensor consistent with the capability of the external electronics to process the signal to a high accuracy. It should be noted here that for the sensor itself this limit is set by the Johnson noise of the resistance of the windings.

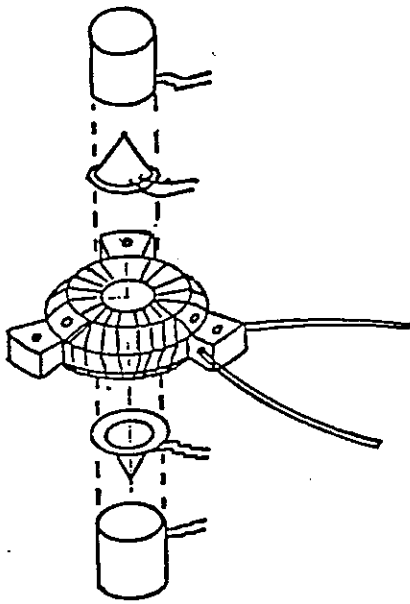


Fig. 1 Self-calibrating cavity to thermopile construction

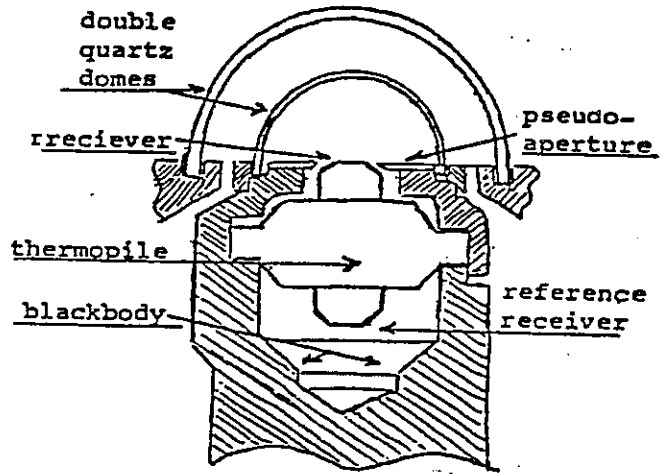


Fig. 3 Self-calibrating radiometer with flat receiver

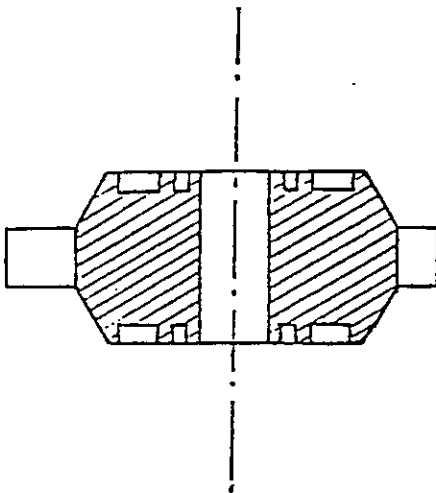


Fig. 2 Thermopile body (conductor) design

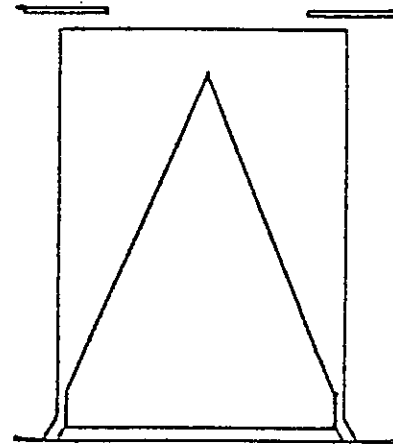


Fig. 4 Cavity with light trap

The sensor assembly is mounted into a goldplated copper case with a precision aperture mounted to each side. This is called a sensor module. The three legs of the basic sensor are sandwiched by the two sides of the copper case to allow good heat flow to and from the sensor body to the module case which acts as a massive heat sink. A 4 to 1 aspect ratio black body is mounted behind the precision aperture as an ambient temperature radiation reference for the reference receiver.

The final external casing depends upon the intended use.

BASIC EQUATIONS

The nature of the self calibration is to equate electrical power to equivalent radiant power, However, the desired result is usually irradiance. The sensed radiant power, P_R , is related to the irradiance at the precision aperture, H_R , by:

$$P_R = H_R \alpha A \gamma \quad \dots (1)$$

where α is the absorbance of the cavity, A is the area of the aperture and γ is a stray light factor related to any view tube employed. Electrical power is calculated from the measured voltage and current

$$P_e = I (V - V_C) \quad \dots (2)$$

where V_C is the voltage drop in the connection leads, expressed as:

$$V_C = I R_C \quad \dots (3)$$

where R_C is the lead correction resistance. R_C is measured during manufacture for each instrument.

The signal generated for both a radiation measurement and an electrical calibration (with the instrument shuttered) are proportional to the respective power terms if the cautions mentioned previously are adhered to relative to linearity. These may be expressed as:

$$E_R = K_R P_R \quad \dots (4)$$

$$E_e = K_e P_e \quad \dots (5)$$

where K_R and K_e are not equal both are related by $K_e = L K_R$... (6)

where L is the non-equivalence term. Equating the signal output terms in (4) and (5) yields

$$K_R H_R \alpha A \gamma = K_e I (V - I R_C) \quad \dots (7)$$

which may be expressed in terms of the measured irradiance as:

$$H_R = L I (V - I R_C) / \alpha A \gamma \quad \dots (8)$$

or by combining constants as

$$H_R = C I (V - I R_C) \quad \dots (9)$$

where the instrument - application constant

$$C = L / \alpha A \gamma \quad \dots (10)$$

This simplified derivation assumes that the non-equivalence, L , is truly a constant. In fact it is only a constant for that condition for which it was measured or calculated. As mentioned previously this parameter depends on the thermal analysis of the different heat paths from source to sensor between the measurement and calibration conditions. One of the factors of the term is the temperature drop across the paint of the receiver. Since the radiation is absorbed at one side of the paint and the electrical heat dissipated on the other side, the path for these is obviously different. Also, the conduction and convection terms may vary slightly if the device is either oriented differently or shuttered between the two relevant measurements. It is still considered the best operating procedure to set the signal output at the same level during measurement and calibration. If this is done automatically by servo or other feedback techniques, the mode is said to be "active". If it is done by manually resetting the heater power to the measured signal, it is called "passive". The thermopile-type devices have the advantage and capability of being employed in either mode. Another is the advantage of linearity, if employed for the measurement of the design criteria. This allows the device to be electrically calibrated at a different time over the intensity (power) range of the intended measurement. That is it can be characterized for a range of conditions prior to the radiation measurements. For these devices, linearity has been proven many times.

CHARACTERIZATION

The evaluation of the constants of the instrument factor and R_C is called the characterization. The aperture area must be measured to a very high accuracy using optical or mechanical metrology. The absorptivity is generally measured using laser reflectivity techniques. This is somewhat limited in wavelength range but has proven satisfactory. Cavitation enhances spectral flatness as well as total absorption. Values for α of 0.999 have been achieved. The difficult term to evaluate is L . One method that we have used to reduce the uncertainty is to remove the convection and air conduction terms by testing in vacuum. In this way the mathematical analysis need apply on to vacuum conditions. The corrections to the terms required for operation at atmospheric pressure can then be applied using test results. The device is operated for both radiant and electrical power conditions in

vacuum and then without any change to the experimental set up, the tests are repeated in air. The ratios for both radiant and electrical response are evaluated. The difference in the two vacuum/air ratios is the change in non-equivalence caused by the air conduction and convection processes.

This technique has also been employed to evaluate cavity to aperture spacing. This is critical for determining the maximum field-of-view which can be achieved for operation at atmospheric pressure (see reason below). When the vacuum/air ratio is minimum as a function of aperture distance, then the minimum loss factor has been achieved.

Characterization must be extended for sensors to be used in space programs. The dynamic environment of the orbital temperatures must be considered. That is, the temperature transient terms must be considered as well as the static temperature terms. There are two types of thermal transients to be considered, radiative and conductive. Since the only conductive term (in vacuum) is the transfer of heat via the sensors mounting legs, the device design criterial of balanced active and reference (hot and cold) junctions may now be appreciated. This balance allows heat to flow to or from the sensor without affecting the signal output. Radiative transients are more difficult to characterize since they are caused by differential (with time) gradients between the sensor and the external elements of the view limiting components.

SOLAR RADIATION MEASUREMENTS

Two types of solar radiation measurements are generally made from ground based stations, direct beam and global. The direct beam measurements are made by instruments having a 5° opening angle (10 to 1 length to aperture ratio) which are mounted on solar trackers. These instruments are called pyrhemometers. Global measurements are made of the total radiation, direct beam plus diffuse sky, over the entire upper hemisphere. The instruments used for this measurement are call pyranometers. Sometimes pyranometers have a 180° field. While it is not difficult to characterize a cavity pyrhemometer, it is very difficult to design a pyranometer which has 180° field and a cavity sensor. Because of the highly variable nature of the geometry of the incoming beam, the amount of radiation striking each part of the receiver varies with solar altitudes and azimuth and the latitude and meteorological conditions. Also, the difficulty of placing the aperture close to the receiver to obtain a 180° field must be considered, even if the losses mentioned previously can be assessed. Solar radiation measurements were discussed in SPIE proceedings previously³. Albedo measurements are made from the ground and aircraft using inverted pyranometers. These measurements present low irradiance levels since the sun is never in the field.

From space both direct beam and albedo measurements have been performed. Space applications offer the advantage of a reduced field-of-view requirement (about 130°) for the pyranometer-type measurements, but the non-uniform (non-homogeneous) source function is still present. The spectral nature of global shortwave measurements must be addressed. With wide angle

sensors there is significant infrared exchange. The spectral range is usually limited by a glass or quartz hemisphere to the solar range of approximately 0.3 to 3 micrometers on the ground, and 0.2 to 5 micrometers in space. These hemispheric filters also contribute to the problems of characterization both for static and transient infrared radiative effects.

As mentioned previously, the most difficult instrument to design is a pyranometer for measurement of shortwave flux in the upper hemisphere. While such instruments have been built, there are problems in interpreting the results. Since the instruments require filter hemispheres, they can never be truly absolute and self calibrating because of the losses caused by the domes both in intensity and in spectral content. As a minimum, there is an additional necessary term in the instrument constant

$$H_m = H_R \tau$$

where τ is the effective transmittance of the domes and H_m now represents the measured radiation while H_R is the desired result, incident radiation. However, the biggest problem is related to the field-of-view, in two ways:

- a) The inability to achieve a 180° field with an aperture - cavity geometry common to absolute instruments;
- b) The difficulty of achieving a non-equivalence which is independent of the measurement conditions.

One way of minimizing the first problem is to evacuate this instrument in order to reduce the conduction and convection losses between the cavity and the aperture. Most users are unwilling to go to this expense for routine measurements. The only practical way to treat the second problem is to prove that the device has a perfect cosine response by an alternate method; then show that the self-calibration heater will produce an unambiguous signal output for various distributions of sun and sky radiation. In other words: 1) at low sun angles, on clear days, the sunlight strikes the cylinder; 2) on clear days, at low latitudes (or with the pyranometer tilted), the sunlight strikes the inverted cone as in a pyr heliometer; 3) on overcast days, the diffuse radiation, not necessarily homogeneous, strikes all parts of the cavity. The only method of assuring that non-equivalence in scene-insensitive is to show that light striking any part of the cavity yields the same signal; while for calibration signals, a different division of power dissipation between cylinder and cone will produce the same signal for the same total power. It can be seen that the evaluation of a cavity pyranometer depends on the use of a self-calibrating cavity pyr heliometer. This raises the question as to why there is a need for an absolute pyranometer at all. Our approach now is to build a self-calibrating but non cavity device. Using the same sensor technology the receiver is changed from a cavity to a shaped receiver mounted to the top of the cylinder as shown in Figure 3. A pseudo-precision aperture is retained in the design. The shaping of the receiver is to allow the capture of all rays entering the precision aperture and to aid

in achieving true cosine response. Work is continuing on development and testing of these units.

EARTH FLUX MEASUREMENTS

These measurements, made from satellites, determine the earth emitted longwave (infrared) radiation. In a previous SPIE paper³ we have discussed the calibration of such sensors using blackbody sources. Since blackbody sources have a theoretical basis for their radiation emissions, this is one of the few cases for which an absolute sensor can be compared to an absolute source. Agreement in the 0.7% range was achieved. However, in actuality this measurement can be made only when the dark side of the earth fills the field-of-view since on the sunlit side the shortwave reflected energy will be present and the measurement will be of the total radiation. For this it has been shown that a trap must be added to the cavity design (Figure 4) to retain the absorptivity with the wide field-of-view. Also, this heater must be arrayed differently on the cavity to minimize non-equivalence.

INTERCOMPARISONS OF PYRHeliometers

There are two levels that can be discussed here: ground and space. Intercomparisons are conducted at the World Radiation Center in Davos, Switzerland every five years. The last meeting, IPC V, was held in 1980⁴. There were 26 absolute radiometers of at least 9 different types represented. Six of these were of the type discussed earlier here. The ratio of these instruments to reference instrument ranged from 0.9979 to 1.0011 or from -0.21% to +0.11%. The range for all instruments was from 0.9923 to 1.0055. In the U.S. there have been five intercomparisons since 1978. All have been held at New River, Arizona, outside Phoenix. The results of the first four have been summarized⁵ by Estey and Seaman. The fifth has been reported by Zerlaut⁶. The results of all five have been summarized by Zerlaut⁷. A total of twenty-six instruments have participated in the NRIP's. Of these only three were at all five intercomparisons, six at four, and eight were present for only one. Eight of the instruments had been at the IPC's either in 1975 or 1980. Five different types of instruments have participated. For the type described here the range of ratios to the group mean ranged from 0.9970 to 1.0026 with standard deviations ranging from 0.9967 to 1.0079. These results show the high stability that the self-calibrating cavity pyrhelometers possess. The intercomparison results for so many different types and designs of instruments show that characterization of all types have been successful.

In space there is only one possible intercomparison of cavity pyrhelometers. The instrument aboard Nimbus 7⁸ has been measuring total extraterrestrial solar radiation since November 1978 and is still operating. The ACRIM instrument developed by Dr. R. Willson⁹ of JPL has been performing similar measurements from the Solar Maximum Mission satellite since February 1980 through September 1980. For the 165 coincident daily mean values available, the ratio the SMM results to the Nimbus results is 0.9981⁰. For a 508-day period using preliminary Nimbus results, the ratio is 0.9978. This

agreement of 0.2% is the proof that both the space instruments are functioning properly.

SUMMARY

In this paper we have attempted to discuss the various aspects of self-calibrating cavity radiometers. Certain elements of the design and fabrication have been explained. More detailed explanations would require further information relative to materials considerations and the thermal analysis computer techniques for evaluating instrument performance. It has been concluded that cavity instruments perform well for narrow angle shortwave measurements such as pyr heliometry and wide angle longwave measurements such as for extended infrared sources. The matter of practical wide angle shortwave measurements is yet to be proven in an acceptable instrument.

Intercomparison data for direct solar measurements by different instruments and techniques both on the earth at atmospheric pressure and in space agree on the order of a few tenths of a percent. The longterm stability of such instruments appears to be in the order of hundredths of a percent per year.

REFERENCES

1. Hickey, J.R.: "Solar Radiation Measurements: Terrestrial and Extraterrestrial", Proceedings of SPIE, Vol. 68, pp. 53-61, San Diego, CA. August 1975.
2. Hickey, J.R., R.G. Frieden, F.J. Griffin, S.A. Cone, R.H. Maschoff and J. Gniady: "The Self-calibrating Sensor of the Eclectic Satellite Pyr heliometer (ESP) Program", Proceedings of the 1977 Annual Meeting of the International Solar Energy Society, Vol. 1, Section 15-1, June 1977.
3. Hickey, J.R., A.R. Karoli and B.M. Alton: "Experimental Evaluation of Self-calibrating Radiometers Used in Earth Flux Radiation Balance Measurements from Satellites", Proceedings of SPIE, Vol. 308, pp. 114-121, San Diego, CA. August 1981.
4. Fifth International Pyr heliometric Comparisons and Absolute Radiometer Comparisons (IPC V), 1980, Working Report No. 94, Swiss Meteorological Institute, Zurich, February 1981.
5. Estey, R.S. and C.H. Seaman: "Four Absolute Cavity Radiometer (Pyr heliometer) Intercomparisons at New River, Arizona, JPL Publication 81-60, Jet Propulsion Laboratory, Pasadena, CA. 1981.
6. Zerlaut, G.A.: "Solar Radiation Measurements: Calibration and Standardization Efforts", Advances in Solar Energy, U.S. Section, Int. Solar Energy Society, Boulder, CO. 1983.

7. Zerlaut, G.A.: "The Fifth New River Intercomparisons of Absolute Cavity Pyrheliometers", DSET Report 82-1201E, DSET Laboratories, Phoenix, Arizona 1982.
8. Hickey, J.R., L.L. Stowe, H. Jacobowitz, P. Pellegrina, R.H. Maschhoff, F. House and T.H. VanderHaar: "Initial Solar Irradiance Determinations from Nimbus 7 Cavity Radiometer Measurements", Science 208, 281-283. 1980.
9. Willson, R.C., S. Gulkis, M. Janssen, H.S. Hudson and G.A. Chapman: "Observations of Solar Irradiance Variability", Science 211, 700-702. 1981.
10. Hickey, J.R., B.M. Alton, F.J. Griffin, H. Jacobowitz, P. Pellegrino, R.H. Maschhoff, E.A. Smith and T.H. VanderHaar: "Extraterrestrial Solar Irradiance Variability", Solar Energy 29, 125-127. 1982.



3.D TIME VARIABILITY OF ANGULAR DEPENDENCE OF A PYRANOMETER AND
ERROR-ESTIMATION OF ANGULAR-DEPENDENCE-TEST EQUIPMENT

Dr. G. Motschka

Zentralanstalt f. Met. u. Geod., Wien

**TIME VARIABILITY OF ANGULAR DEPENDENCE OF A PYRANOMETER AND
ERROR-ESTIMATION OF ANGULAR-DEPENDENCE-TEST EQUIPMENT**

Tests on a number of pyranometers were made first in the laboratory in 1981 and then outdoors over 2 years. Tests in the laboratory again were made at the end of 1983. One of the results was, that the cosine and azimuth response of one of these instruments shows an ageing effect. Figure 1 shows the angular dependence measured in 1981. The last tests, shown in Figure 2, compared with the older results give an opposite result. The reason could be an ageing effect or different arrangements of the pyranometer into the test equipment. Therefore a test in this direction was made. The cosine test equipment consists of a fixed pyranometer and turning lamp. The system was not changed in anyway from 1981 to 1984.

To find out the errors due to the arrangement of a pyranometer some incorrect arrangements were made (see Figure 3). The results of these tests are shown in Figure 4, small deviations in the vertical arrangement after accurate positioning of the pyranometer using the light beam and a small diaphragm give only minimal errors in cosine response. Greater deviations occur at higher zenith angles. Surprising all errors in the arrangement are within the error, due to a uncertainty of ± 1 degree of the position of the lamp. This results surely is transferable to cosine test equipment using fixed lamp and turning the pyranometer. Under this aspect we have to see more or less all results especially for cosine response measurements.

On the other hand it is shown, that for this special pyranometer an ageing effect for cosine response exists.

GERÄT Nr.2244 (STAR)

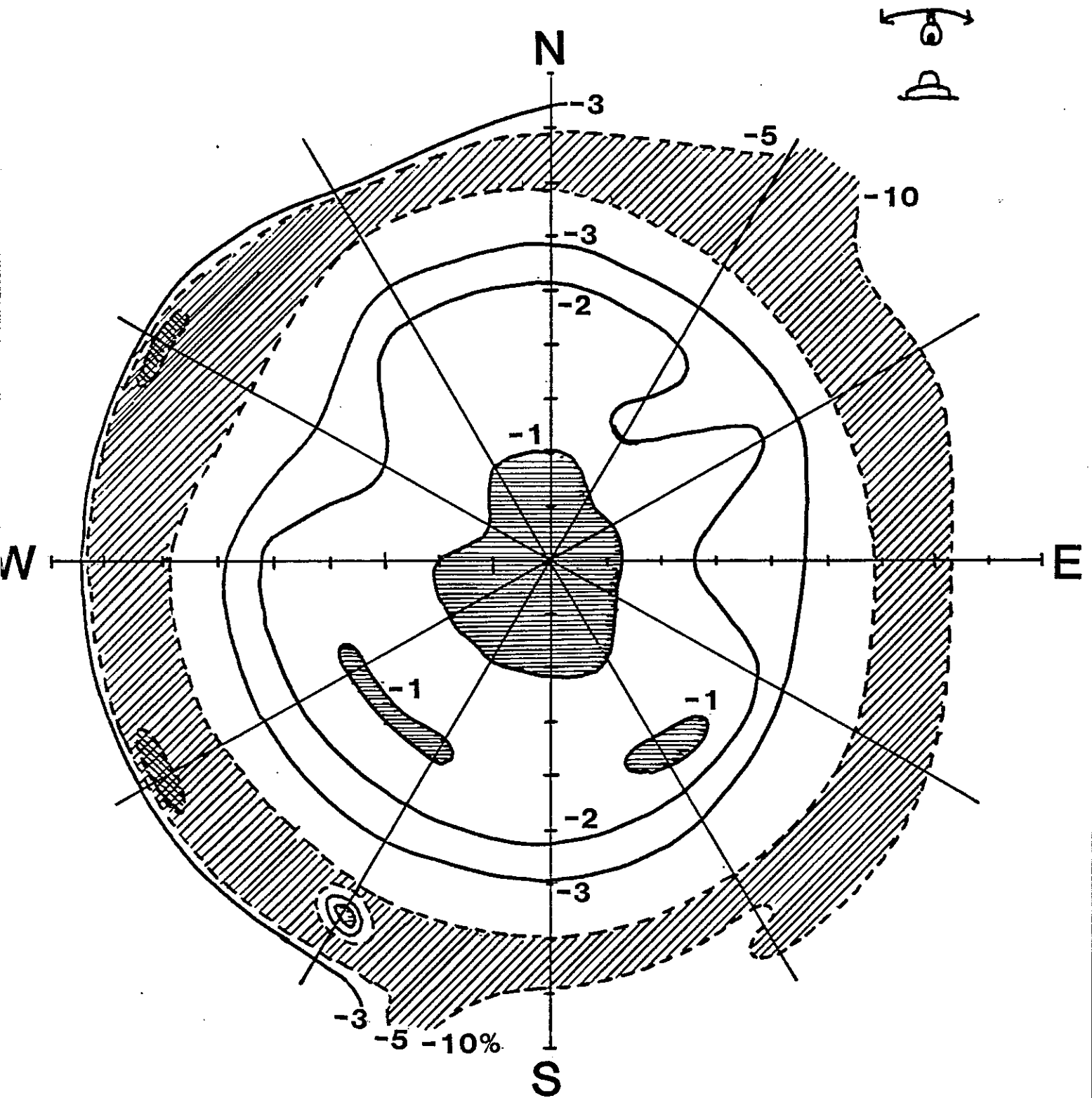


Figure 1 Cosine-Response September 1981

STARPYRANOMETER 2244

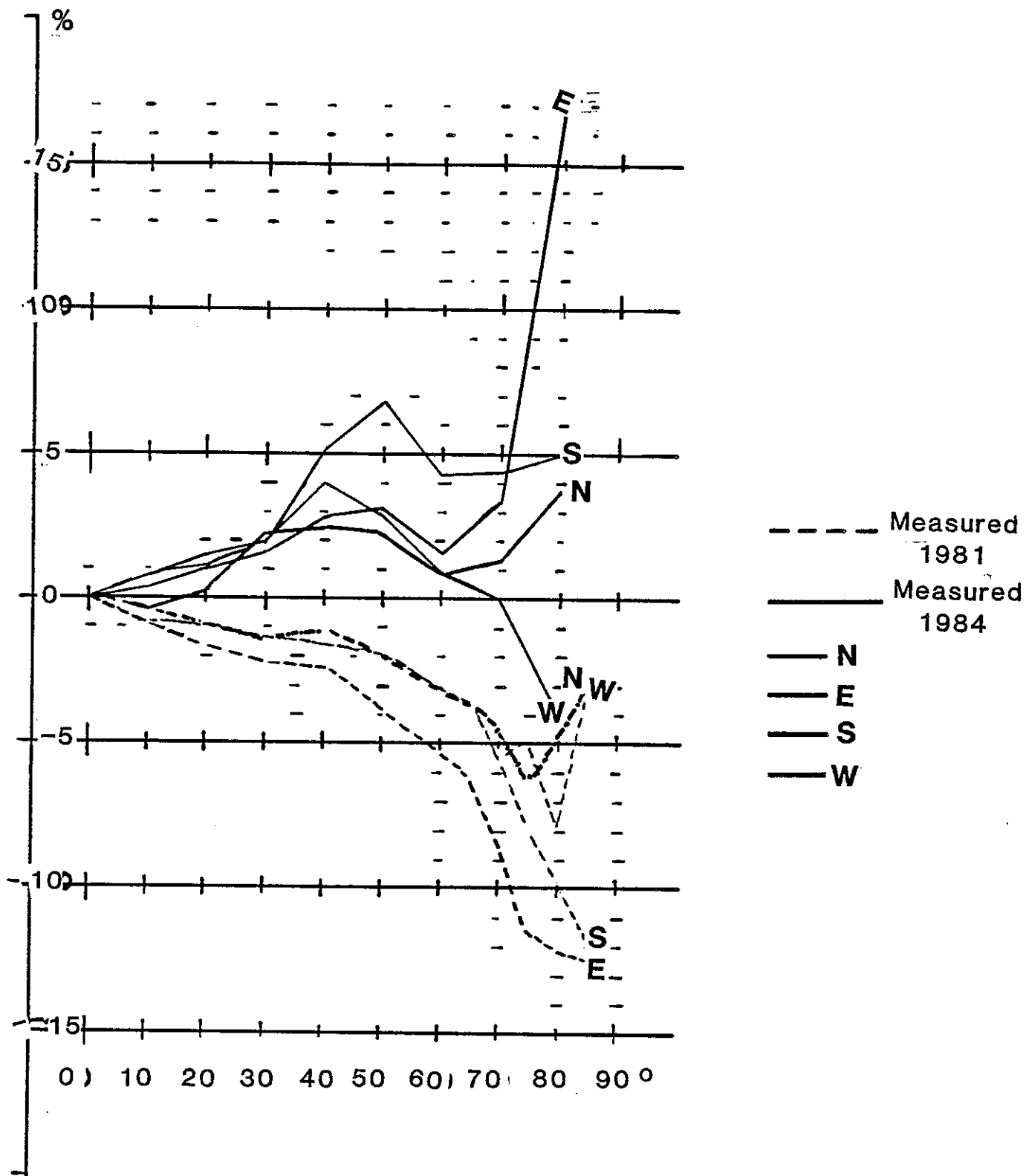


Figure 2. Cosine Response

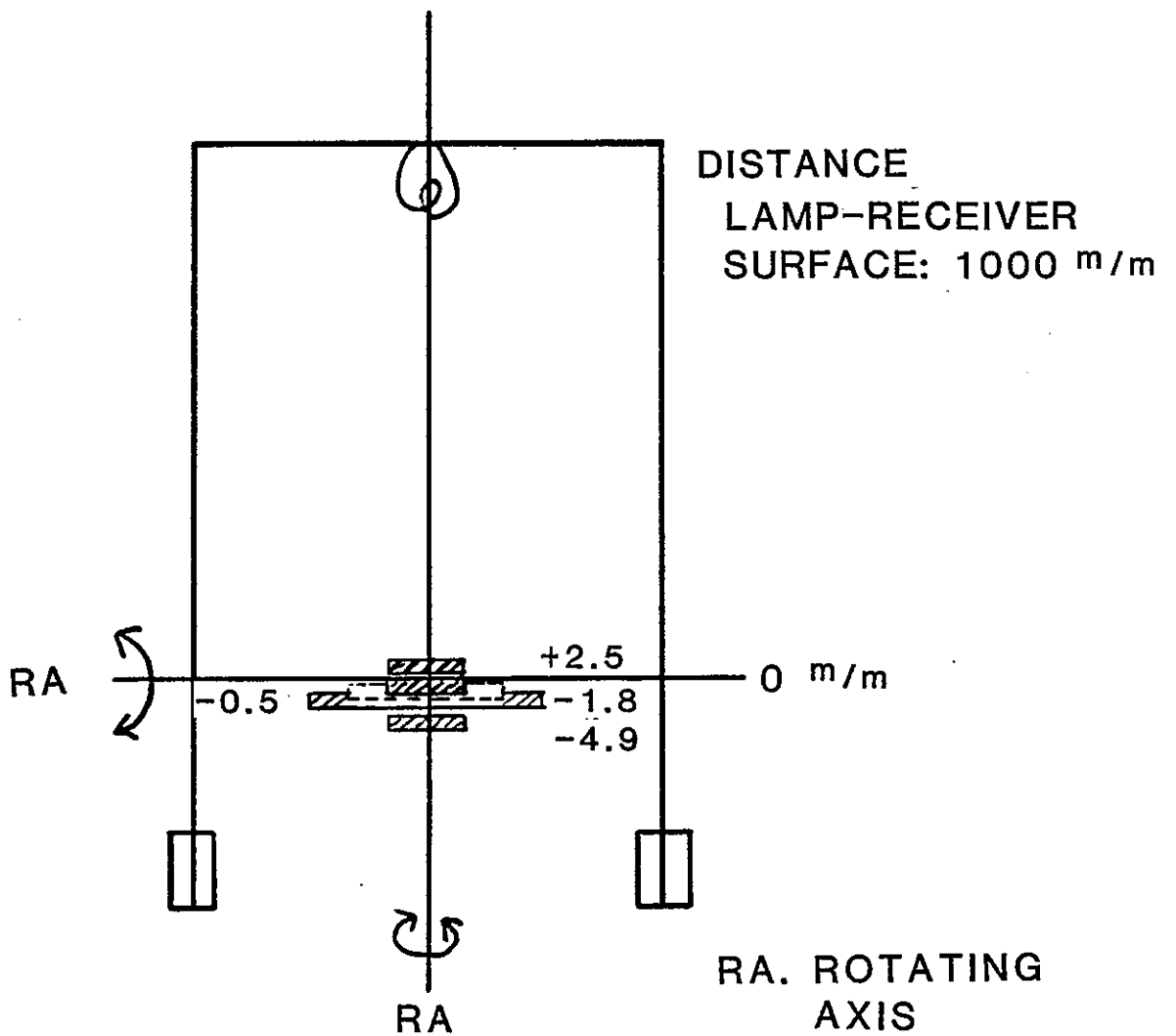


Figure 3

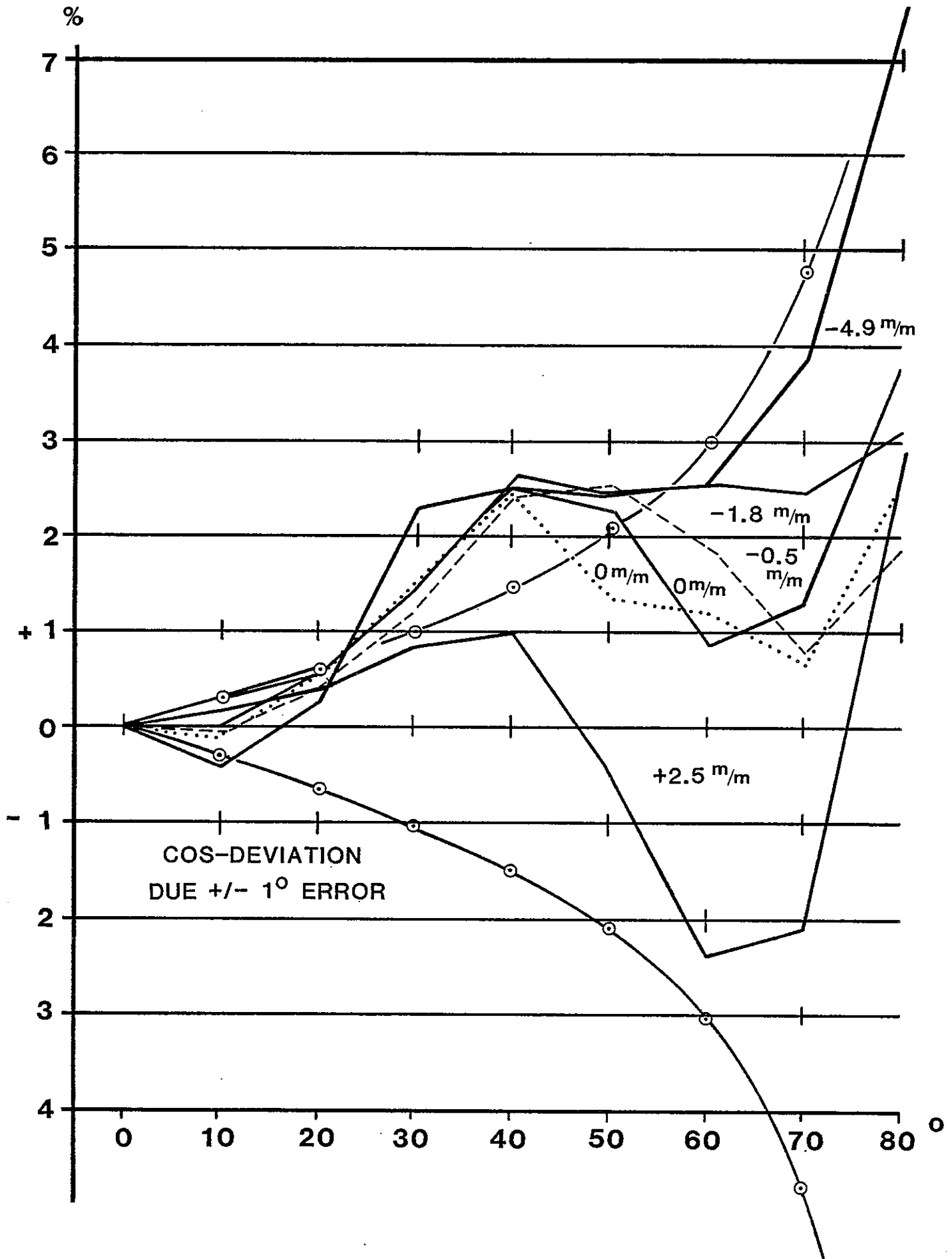


Figure 4.

3.E AN AGEING TEST OF PYRANOMETERS

- A PROPOSAL -

Chester V. Wells

Solar Energy Research Institute
1617 Cole Boulevard
Golden, Colorado 80401 U.S.A.

AN AGEING TEST OF PYRANOMETERS

ABSTRACT

There are many characteristics of pyranometers which are measured by various laboratories around the world. Yet one of the characteristics that can have a significant impact on the measurement results obtained with pyranometers over the long term is not often determined, for a variety of reasons. That characteristic is the **long-term stability** or the **ageing** of pyranometers.

Now is an ideal time, in the midst of pursuing improved pyranometry, to conduct a carefully constructed test to **determine the effect of solar and weather exposure** on the long-term stability and measuring performance of pyranometers. This paper outlines a proposed test program which is being designed to measure, in the shortest possible time, the degradation of performance of pyranometers with solar and weather exposure.

The planned test program will consist of several parts:

- a) A thorough characterization of the pyranometers before and after the solar exposure;
- b) Repeated calibrations of the pyranometers during the solar exposure period;
- c) A program of careful measurements and documentation of the UV, VISible, and IR dosage in the solar exposure;
- d) Use of accelerated exposure techniques without reciprocity failure to gain maximum information in minimum time (two or three years); and
- e) Careful statistical evaluation and controls on the experiments to ensure quality results.

DISCUSSION

Many sources of errors in pyranometers have been identified over the years of their use. But the source that may be overlooked the most often, and takes the longest period of time to identify and measure, is the long-term stability of the pyranometer. By longterm stability is meant the constance of the characteristics of the pyranometer so that it performs identically from year-to-year. A principal factor of concern is the instability of the sensitivity of the pyranometer with time and solar and weather exposure, or ageing of the pyranometer. This concern has been reported and discussed at various times [Ref. 1-4], but no specific research has been conducted and reported that I am aware of.

This ageing test and experiment is being proposed (and funding requested) for the Solar Energy Research Institute to conduct over the next three years, during the time that major efforts in pyranometry research are being conducted within the IEA. The ageing test experiments will involve the participation of several laboratories and manufacturers.

The long-term solar exposures will be conducted at the New River, Arizona facilities of DSET Laboratories (formerly called Desert Sunshine Exposure Tests, Inc.). The pyranometers will be exposed in a direct normal attitude using a tracking equatorial mount, thus gaining about a two times greater total energy exposure (compared to a horizontal position) without submitting the pyranometers to greater than a "one sun" irradiance at any time.

Testing of the pyranometers will be conducted before, during and following the solar exposure at SERI, NOAA, DSET, and at possible other laboratories. These tests will be conducted:

- a) Shading disk calibrations against absolute cavity radiometers;
- b) Intercomparison against reference pyranometers at normal incidence, 45 degree tilt, and horizontal - one full day at each exposure attitude;
- c) Comparison against reference pyranometers for daily total energy (probably at beginning and end of test only);
- d) Static temperature coefficient of sensitivity (at the beginning and end of test only);
- e) Linearity of sensitivity with irradiance, and variation in sensitivity with tilt and irradiance - if an adequate test is developed (at beginning and end only);
- f) Transmission characteristics of domes, as a function of wavelength - if an adequate test can be performed (at beginning and end of test only);
- g) Angular dependence of sensitivity - cosine and azimuth errors (at beginning and end only);
- h) Determination of sensitivity in a sphere and/or hemisphere (at beginning and end only); and
- i) Application of transfer function - if an adequate transfer function can be derived (at beginning and end only).

A portion of the instruments for this extensive ageing tests will be sought by loan from the manufacturers (those to be giving the long-term exposure), while an equal number of control instruments will be purchased.

The "exposed" loaned instruments will be returned to the manufacturers for their final analysis and retention.

Funding to conduct the entire ageing experiment is being sought, and it is hoped such an experiment could begin by summer of 1984, and testing be completed by the summer of 1987 at the latest (or a two year testing program completed in 1986). Funding for this experiment is not available under SERI's normal IEA source of funds. Therefore, separate funding of a research effort is being pursued to support this agency test, as well as development of characterization and calibration techniques for all uses of pyranometers in energy research, resource assessment and meteorology.

Comments and suggestions to improve this ageing experiment are most welcome, including inputs of data and applicable test procedures, and offers of assistance. Obviously, the total cooperation and participation of the manufacturers is needed to make this research and experiment successful.

REFERENCES

1. Flowers, E.C.: The "So-Called" Parson's Black Problem with Old-Style Eppley Pyranometers"; Report and Recommendations of the Solar Energy Data Workshop Held November 29-30, 1973. Charles Turner, Editor; NSF-RA-N-74-062, September 1974; pp. 28-30.
2. Flowers, E.C.: Hourly Solar Radiation-Surface Meteorological Observations; SOLMET Volume 2 - Final Report TD-9724; Department of Energy, Division of Solar Technology, Environmental and Resource Assessment Branch; pp. 2-67.
3. Riches, M.R., T.L. Stoffel and C.V. Wells: Proceedings of the International Energy Agency Conference on Pyranometer Measurements - Final Report, Solar Energy Research Institute, SERI/TR-642-1156R; October 1982.
4. Thacher, P.D.: Private communication to C.V. Wells and D.R. Myers, 16-20 March 1981, Boulder, Colorado. November 1983; Phoenix, Arizona.

SESSION 4

Field Characterization



4.A THE NEED FOR CHARACTERIZATION OF PYRANOMETERS

Claus Fröhlich

Physikalisch-Meteorologisches Observatorium
World Radiation Center
Davos, Switzerland

THE NEED FOR CHARACTERIZATION OF PYRANOMETERS

INTRODUCTION

Outdoor and indoor tests have been performed in order to improve our knowledge of the performance of pyranometers. A very exhaustive investigation has been completed recently (1) during which the behaviour of more than 30 instruments of eight different types was explored. The outdoor tests covered a wide range of conditions: winter, summer, clear skies, cloudy skies and overcast skies. In the laboratory the temperature dependence, linearity, influence of tilt and directional response (cosine law) were measured for all instruments. The ultimate goal of the trial was to determine how accurate or how variable pyranometers can be under different conditions and if the accuracy can be substantially improved by introducing corrections based on the laboratory results.

In the following the behaviour of different types of pyranometers is presented as it is seen from the results of the indoor characterization. Some insight is sought into the outdoor performance. Furthermore, some guidelines are given for future developments. This investigation will only treat black receivers and not black and white type pyranometers, because of their inherently more complicated performance and less important use for very accurate solar measurements. On the other hand, some results will be presented for cavity pyranometers recently developed by the PMOD/WRC.

RESULTS OF OUTDOOR CALIBRATIONS

In Figure 1 and 2 the results of the calibrations for a wide range of temperature intensity and incident angle are shown for two instruments. An Eppley PSP and a Kipp & Zonen CM-5 are taken as arbitrarily chosen examples to illustrate the behaviour of two quite different classes of pyranometers: a modern high precision type and a traditional one of lower price. From the results it is quite obvious that the Eppley PSP performs better than the CM-5 and allows measurements within 2-3 per cent over a very large range of conditions. But for both instruments it is not clear from the plots against temperature, intensity and incident angle, which one of these effects affect the reading most. It is obvious, that the temperature compensation of the PSP improves the behaviour, but the deviations from linearity and directional response characteristics are for both type of instruments of some importance, although less for the PSP than the CM-5. A similar qualitative behaviour can be found for all other types of instruments examined in the trial (1). The discomfort with these results is that no obvious physical explanation for the variability can be given.

RESULTS OF INDOOR CALIBRATIONS

In order to understand the variability of the outdoor performance the indoor measurements have to be examined in more detail. The advantage of these measurements is that only the influence of one parameter can be

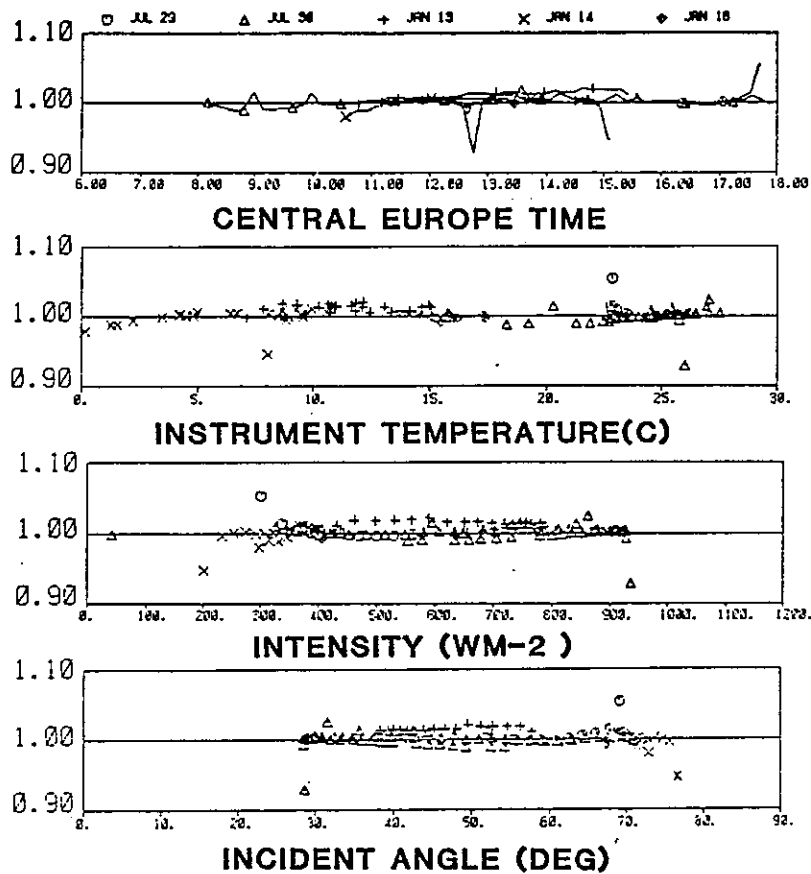


Figure 1. Results of the absolute calibrations of the Eppley PSP-20655 during the 5 days 1981/ 82 indicated at the top

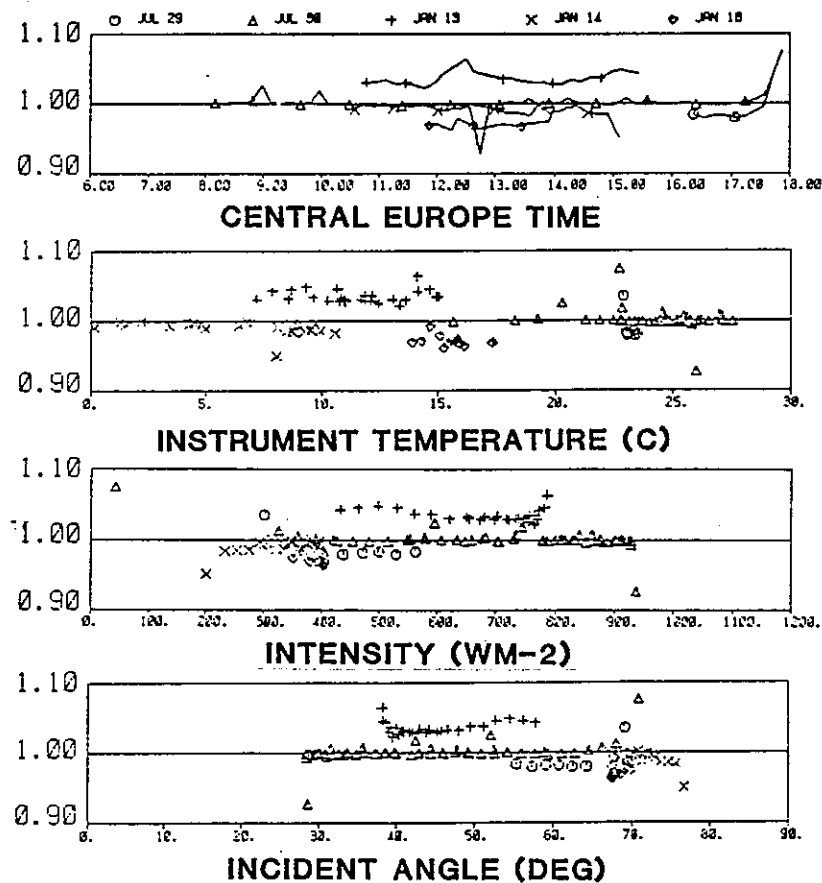


Figure 2. Same as Fig.1 but for the Kipp & Zonen CM-5 785047

examined at a time. The disadvantage is that the cross effects seen in the outdoor results are difficult to assess. This disadvantage can be somewhat compensated by the improvement to the understanding of the physical mechanisms responsible for each dependence of the sensitivity. In the following an attempt will be made in this direction with the results of the indoor measurements done in the framework of (1) by the Statens Provningsanstalt, Borås, Sweden, and the PMOD/WRC, Davos.

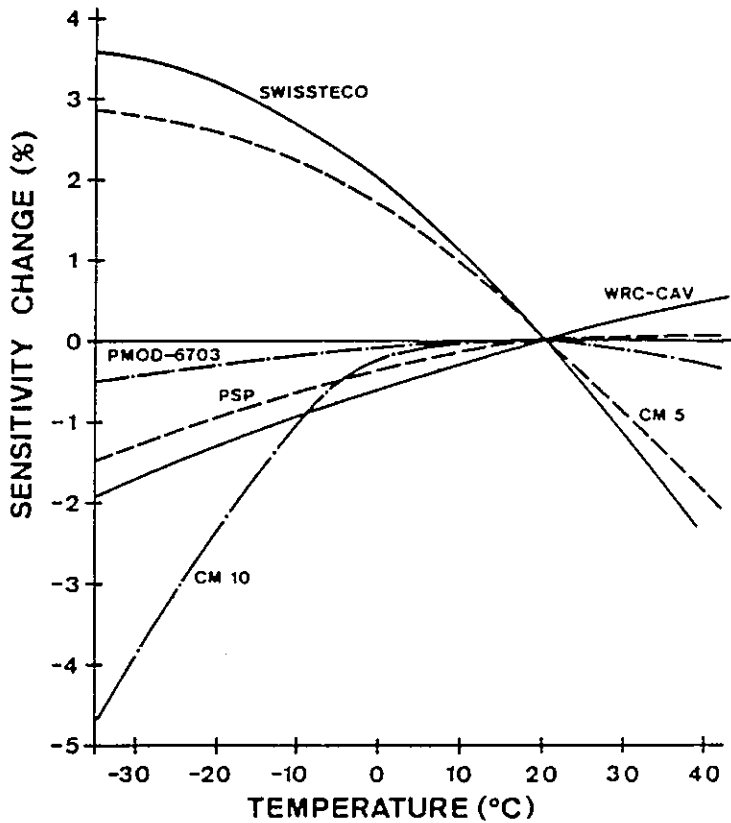


FIGURE 3 Temperature dependence of the sensitivity of 6 types of pyranometers. The measurements were performed at Borås.

Figure 3 shows the results of the measurements of the temperature dependence of the sensitivity of different types of instruments. The difference between the one with temperature compensation and the traditional ones is obvious. The traditional instruments CM-5 and Swissteco show a behaviour which reflects the typical temperature dependence of a copper-constantan thermopile. The PMOD-6703 is a special case, where the dimensions of the copper and constantan legs of the thermopile are chosen in such a way, that the overall temperature dependence of the thermal conductance to the thermopile is equal to the temperature dependence of the thermal EMF between copper and constantan. Thus the combined temperature dependence is very small over a wide range of temperatures. The WRC-Cavity seems to be overcompensated and shows a more pronounced temperature dependence than the PMOD-6703. The PSP and CM-10 have an electrical temperature compensation by means of a

temperature dependent loading of the thermopile, which is the instrument behaviour not as well suited as the physical compensation described above. Furthermore, the CM-10 becomes suddenly rather big below 0°.

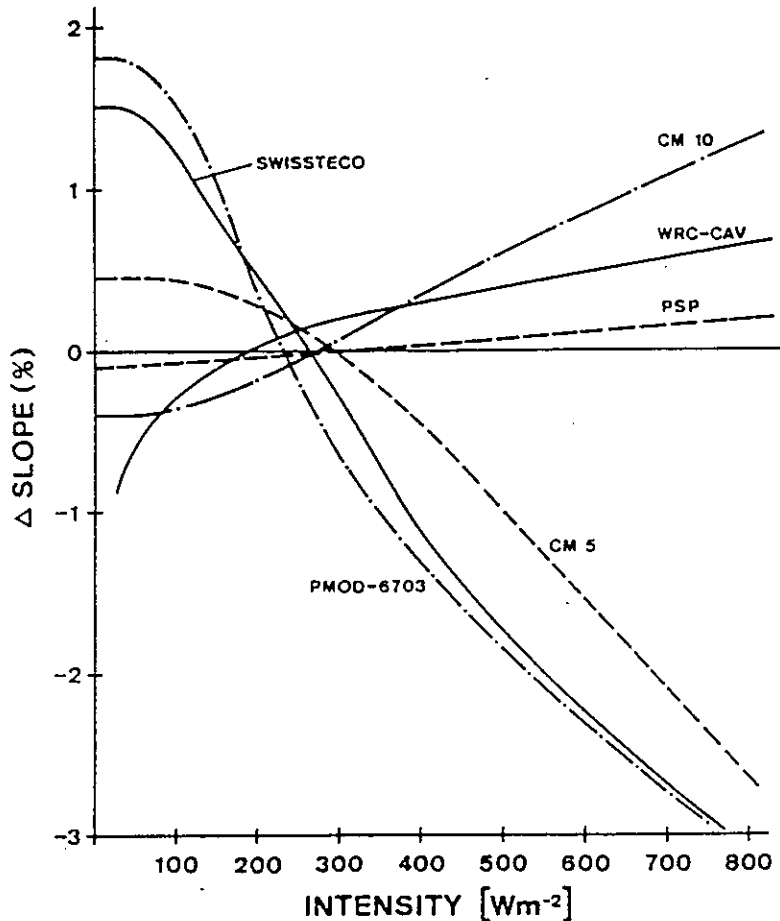


FIGURE 4 Deviation from linearity of 6 types of pyranometers. The data are based on measurements made at Borås.

In Figure 4 the results of the laboratory determinations of the linearity for a number of instruments is shown. The linearity is influenced by three terms and is related to the temperature behaviour of the sensor:

$$V_{out} = K \cdot Q \cdot \sigma_1 - Q \cdot \left(\frac{d(\ln \lambda)}{dT} - \frac{d(\ln V)}{dT} - \frac{d(\ln \alpha)}{d(\Delta T)} \right) \xi$$

The classical, non-compensated instruments, such as CM-5, Swissteco and the PMOD-6703 show a behaviour determined by the temperature coefficient and strongly influenced by the convective losses at high intensities, due to the rather high temperature increase of the thermopile's hot junctions. The electrically compensated instruments show a completely different behaviour: their sensitivity increases with increasing intensity. This increase is

influenced by how well the temperature compensation is achieved and changes from one individual instrument to another. On the other hand the non-linearity of the traditional instruments - although big - is very similar for all individual instruments. A complete different behaviour is shown by the WRC-Cavity, where the sensitivity increases very rapidly with increasing intensity at low intensities. The behaviour looks very much like a square or higher order root dependence, which is found in the temperature difference dependence of convection. In contrast to the traditional instruments, where the behaviour is determined by the increased loss due to convection, the WRC-Cavity instruments shows an increased overall gain, which is due to a more pronounced increase of the loss of the compensating cavity. This effect could give a handle to construct a highly linear instrument by adjusting the geometrical dimensions between the sensors and the surroundings.

TABLE 1

Azimuth dependence of the sensitivity as a function of the angle of incidence. In the experimental set-up this angle is changed by changing the tilt of the instruments as the illuminating beam is horizontal. The dependence is given in terms of peak-to-peak variation.

The data have been taken at Davos.

Instrument Type	Tilt Angle				%
	90°	60°	45°	30°	
PMOD-6703	4.2	5.7	2.5	4.5	%
WRC-Cavity	0.3	2.3	4.0	4.2	%
PSP	0.8	1.1	2.0	4.8	%
CM-5	1.6	2.0	6.2	4.2	%
CM-10	0.4	0.8	0.8	1.1	%
Swissteco	0.4	3.1	2.8	3.9	%

Another effect, which influences the behaviour of the pyranometers is the variation of its sensitivity as function of the azimuth of the incoming radiation. This effect is summarized for the same instruments in Table 1. Two types of behaviour can be recognized: a variability which is independent of the tilt or in this context the angle of incident and a variability, which increases with decreasing angle. The first effect is inherent to the thermopile, the other due to a misalignments of the normal on the surface of the thermopile and the axis of the instrument. The second effect can easily be cured by an appropriate geometrical alignment procedure, the first is more difficult to deal with. However, all types of instruments are influenced by some of the first effect and it would seem worth to look into the possible reasons for it more closely. The smallest influence is found in the cavity instrument, probably because the receiving surface is a hole and not a painted and thus not necessarily very flat surface.

A further influence on the sensitivity of tilting the instrument out of its horizontal position. This effect is due to changes of the convective losses of the surface of the thermopile to the surroundings, mainly the glass dome. Table 2 lists the averaged values found for the different

instruments. The least influenced instruments are the PSP, CM-10, Swissteco and the WRC-Cavity. It is obvious that instruments such as the PMOD-6703 or the CM-5 have more pronounced effects because their convective losses are big as shown by the behaviour of the non-linearity. It is, however, not clear why the Swissteco has such a small effect although the non-linearity would also indicate substantial convective losses. This point deserves more attention in the future.

TABLE 2
Change of the Sensitivity upon tilt of the instrument.
The data were taken at Borås.

Instrument Type	Tilt Angle				
	0°	30°	60°	90°	
PMOD-6703	0.0	-1.7	-2.5	-2.6	%
WRC-Cavity	0.0	-0.1	0.0	-0.1	%
PSP	0.0	0.0	-0.1	-0.2	%
CM-5	0.0	-1.2	-2.3	-2.6	%
CM-10	0.0	0.0	0.1	0.1	%
Swissteco	0.0	0.1	0.0	0.2	%

The most controversial effect is the deviation from the ideal cosine response. Both institutes have determined this deviation in the course of their investigations in (1). The methods used were quite different: in Borås a halogen lamp was used with an intensity at the receiver of less than 100 Wm^{-2} and in Davos a Xenon arc lamp illuminated the detectors with more than 700 Wm^{-2} . Therefore, the level of irradiance and the colour temperature of the source is different. Some of the results at 56° and 84° are given in Table 3. At the low angles the differences are small, but at the high angles there seems to be a systematic difference of more than 5 per cent, with the Borås readings being always higher in intensity. The same effect is present at smaller angles, but much less pronounced (ca. 0.8 per cent). As the difference seems to be depend on the type of instrument it cannot be explained by the non-linearity effects measured at normal incidence as shown in Figure 4. It may be due to some of these suspected cross effects: the linearity may depend on the angle of incidence. The differences may also be artifact of the set-up of one or both experiments or influenced by the different spectral distribution of the sources. In any case, it seems to be a difficult parameter to be assessed and it may be, that the difficulty is inherent to the instruments and thus important for any further investigations.

TABLE 3

Deviations from the ideal cosine law. The first number in each column are the results of Davos, the second the ones of Borås. The uncertainties indicate the standard deviation as function of the azimuth.

Instrument Type	Incident Angle				
	56°			84°	
PMOD-6703	-1.7±1.2	-1.8±1.2	-16.1±5.2	- 8.6±5.0	%
WRC-Cavity	-1.6±1.2	-2.2±2.6	- 4.5±3.0	- 2.4±7.3	%
PSP	-4.4±0.8	-2.2±1.6	-19.0±3.8	- 8.5±6.3	%
CM-5	-2.0±0.7	-3.4±0.6	-14.5±6.3	-11.8±5.5	%
CM-10	-1.4±0.4	0.2±0.5	- 5.5±1.7	1.7±3.7	%
Swissteco	1.4±1.1	2.7±1.2	1.9±3.8	10.8±4.8	%

CONCLUSIONS

Although the laboratory investigation cannot yet answer all the questions about the physical mechanisms governing the behaviour of a pyranometer, they can give insight in the problems to be solved in order to improve the instruments in future. An important result from the laboratory investigations is that they help to understand the instrument, but are not sufficient to improve outdoor data substantially by applying corrections according to indoor results. Moreover, the results indicate, that possible developments in the direction of the use of cavities and more sensitive electronics available today give some hope, that the pyranometer may achieve in future accuracies comparable to normal incidence radiometers. But as for the absolute radiometers reliable methods for their accurate characterization are needed. The direction to go in indicated, but the methods and the instruments have to be improved.

REFERENCES

- 1) "Results of an Outdoor and Indoor Pyranometer Comparison", Draft IEA-Report of Task III (Performance Testing of Solar Collectors), Document III.A.3 Jülich, April 1984.

4.B AN INVESTIGATION OF THE STABILITY, ACCURACY AND LINEARITY
OF AN EPPLEY NORMAL INCIDENCE PYRHELIOMETER BASED ON A
FIELD COMPARISON WITH A CAVITY RADIOMETER

D.V. Barton and D.I. Wardle

AN INVESTIGATION OF THE STABILITY, ACCURACY AND LINEARITY
OF AN EPPLEY NORMAL INCIDENCE PYRHELIOMETER BASED ON A
FIELD COMPARISON WITH A CAVITY RADIOMETER

SUMMARY

Comparison measurements on direct irradiance for a total of 980 hours distributed within a 20 month period were acquired from an Eppley NIP and a Hickey-Frieden cavity radiometer. Analysis of the data, treating the cavity radiometer as the reference, shows that (i) the NIP calibration factor is fairly stable (within about 1.0%); (ii) that 10 minute mean measurements have an r.m.s. spread or standard error of $3-5 \text{ Wm}^{-2}$ around a mean response; (iii) there is a small but definite departure for simple linearity which, if neglected, causes errors in the range $+3$ to -4 Wm^{-2} .

INTRODUCTION

Ideally, one would use an absolute pyrhelimeter to calibrate a pyranometer, but in practice there are several reasons to substitute a non-absolute pyrhelimeter such as the Eppley Normal Incidence Pyrhelimeter (NIP). The NIP is not damaged by being left out in the rain or snow, and if it were broken it would be much cheaper to replace. Also, the signal from the NIP is continuous. Thus, though the NIP is less accurate than an absolute pyrhelimeter, its use allows more calibration data to be collected. This is particularly relevant when the calibration data to be collected. This is particularly relevant when the calibration method does not require the presence of an observer as with automated intermittent occultation or with the Frohlich two pyranometer methods. However, the NIP itself needs calibration or possibly characterization.

MEASUREMENT ROUTINE

The NARC field characterization experiment of 1983 was arranged so as to take advantage of the permanent emplacement of two NIP's and every effort was made to compare the NIP's with the NARC absolute standard cavity radiometer HF 18747. Whenever the day appeared to promise clear sky conditions with little chance of rain, the cavity pyrhelimeter was put on the sun-tracker which already carried the NIP's. It was put back under cover in the evening. During the period March '83 to October '83 it was run for a total of 720 hours. During November '83, June and October '84 a further 260 hours of comparison data were taken.

The cavity radiometer was run on a 30 minute schedule. It was shaded from the sun during the first eight minutes and the calibration electric power was applied during minutes 4, 5, 6 and 7. The recorded data were minute averages from 5 samples taken at 12 second intervals during the minute (this is the data form for all the 45 pyranometer/pyrhelimeter signals and for the 15 thermistor resistances). The voltage, current and thermopile readings during minute 3 and 7 were taken to calibrate the HF 18747 for the

TABLE 1

Calibration of NIP No. 20202 Against Hickey-Frieden No. 18747
1983/1984 AES Roof at Downsview

	Data Points	Rejects	Slope (K)	Intercept (err)	Scatter	K 1000	K 750	K 500
83/01/25/12/00 tape 1	62	3	834	081 (011)	37	841	845	848
83/04/02/13/10 tape 2	317	4	833	095 (005)	23	842	846	852
83/06/03/08/20 tape 3	737	6	834	062 (003)	26	840	843	846
83/08/05/13/50 tape 4	319	19	835	067 (008)	38	842	845	848
83/10/07/08/00 tape 5	58	6	838	071 (015)	34	845	849	852
83/12/30/18/30 tape 6								
84/03/07/14/00 tape 7	57	1	831	142 (016)	42	845	852	859
84/05/10/15/30 tape 8	81	24	828	127 (018)	41	841	847	851
84/07/05/17/30 tape 9								
84/09/04/16/00 tape 10	64	7	840	053 (017)	43	845	848	851
84/11/03/05/50								
Means weighted by number of data points			834			841	844	849

Note: Units for slope and calibration factor K are $\mu\text{V}\cdot\text{W}^{-1}\text{m}^2 \times 100$. Units for intercept and r.m.s. scatter are μV . Each data point is a comparison of 10 minute means.

SQUARE ROOT FIT

$$\text{Signal (in } \mu\text{V)} = A1 \cdot I + A2 \cdot \sqrt{I} \quad (\text{I is in } \text{Wm}^{-2} / 100)$$

	A2	A1	r.m.s. scatter	K 1000	K 750	K 500
tape 1	081	815	37	841	845	851
tape 2	086	815	23	842	846	852
tape 3	056	822	26	840	842	847
tape 4	063	821	38	841	844	849
tape 5	067	822	35	843	846	852
tape 7	140	799	41	843	850	862
tape 8	116	803	39	840	845	855
tape 10	056	827	42	845	847	852
weighted means as above				841	844	850

remainder of the 30 minute schedule. The mean signals obtained from the NIP and the cavity radiometer during the two ten minute periods - minute 10 through 19 and minute 20 through 29 - were used for the comparison. The NIP measurements were corrected for temperature. Only the data with irradiance greater than 100 Wm^{-2} were used in the following analysis; for most of the data the irradiance is greater than 500 Wm^{-2} .

DATA ANALYSIS

Figure 1 is a plot of the NIP signal versus the irradiance measured by HF 18747 during June, July and August '83 and Figure 2 shows the same data with seven of the 743 points rejected. The parameters shown on the graph are the slope in $\mu\text{V}\cdot\text{W}^{-1}\text{m}^{-2}$, the vertical intercept and the scatter in millivolts of the points about the regression line. The fourth and fifth parameters are the slope of a regression through zero and the r.m.s. scatter about the regression. The quantities in brackets are standard error estimates.

The important property of Figure 2 is the the estimate intercept is significantly different from zero (-0.062 ± 0.003) and equivalently that the r.m.s. scatter about the single parameter regression line ($32 \mu\text{M}$) is definitely larger than about the non-zero intercept line ($26 \mu\text{V}$).

Thus the offset linear response function fits the data better than the simple zero intercept linear function. However, the zero irradiance signal of a NIP is undoubtedly within a few microvolts of zero and a form of the response function which automatically passes through zero might be expected to fit the data better than the offset linear one. Accordingly a form in which the offset was replaced with a term proportional to the square root of irradiance was also fitted into the data. The r.m.s. scatter about this function was the same ($26 \mu\text{V}$) as with the offset linear function.

The calibration factor of the NIP derived from the offset-linear parameters of Figure 2 is given by:

$$K_{\text{NIP}} = (8.34 + 62/I) \mu\text{V} \cdot \text{W}^{-1}\text{m}^{-2}$$

where I is the irradiance in $\text{W} \cdot \text{m}^{-2}$. Similarly the square foot fit gives:

$$K_{\text{NIP}} = (8.22 + 5.6/\sqrt{I}) \mu\text{V} \cdot \text{W}^{-1}\text{m}^2$$

Over the range $500 < I < 1000$, these are not significantly different.

Table 1 lists the parameters of linear fitting and of the square root fit derived from 8 separate periods over the total span of 20 months. The computed calibration factors at 1000, 750 and 500 Wm^{-2} from both the offset linear and from the square root functions are also given for each period.

DISCUSSION

During all the periods the offset linear and the square root response functions give similar or identical answers for r.m.s. scatter and calibration factors in the range $500 < I < 1000$. The following further conclusions can be drawn from Table 1.

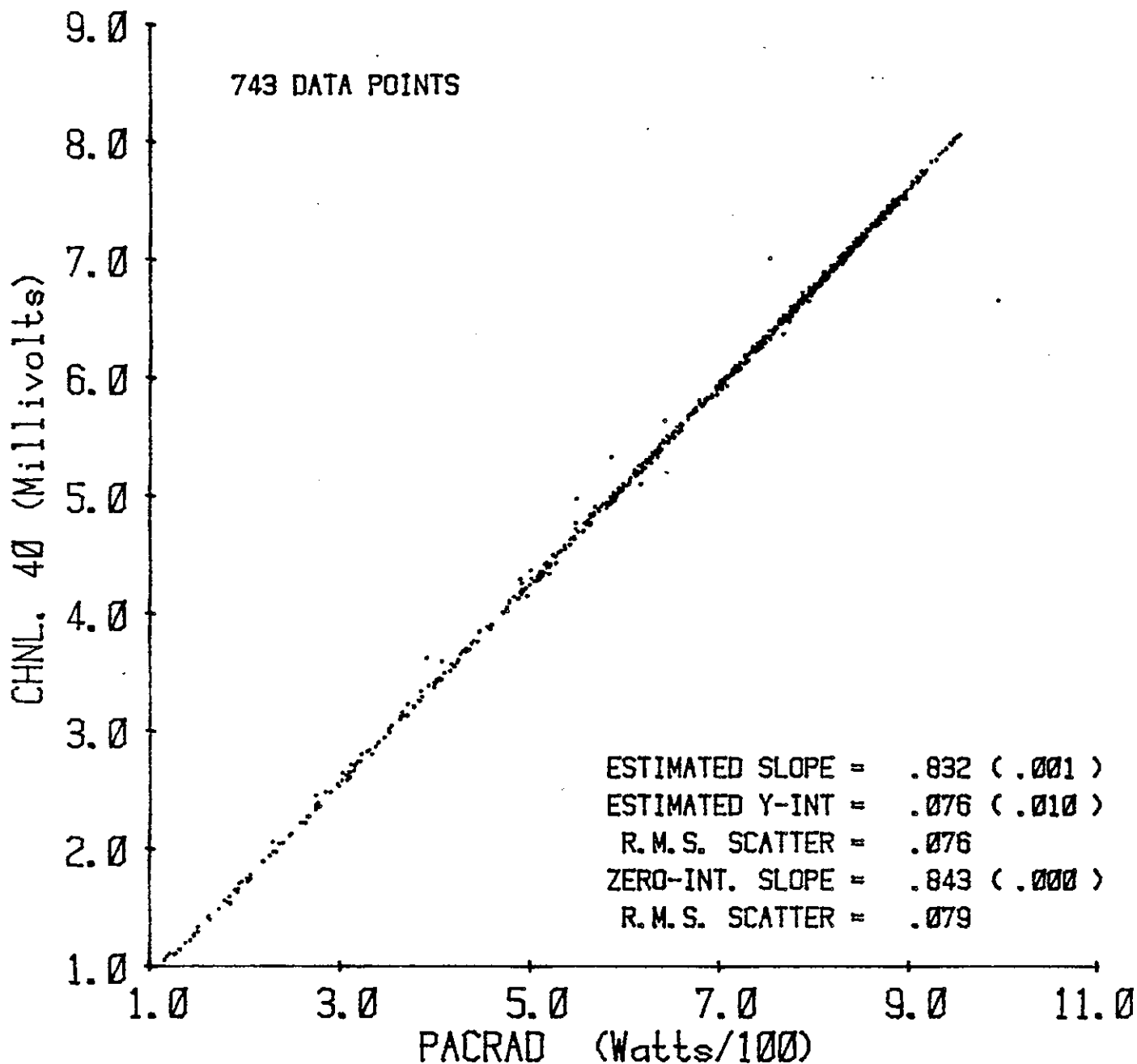
- a) The derived calibration factors are quite reproducible between the different periods. The spreads between the highest and lowest values at 1000, 750 and 500 Wm^{-2} are respectively 0.6%, 1.1% and 1.3%. An earlier calibration of this instrument in 1980 yielded $8.45 \mu\text{V}\cdot\text{W}^{-1}\text{m}^2$ for irradiance values in the range 600-900 Wm^{-2} , which is very close to the weighted mean for the whole 83/84 period at 750 Wm^{-2} ($8.44 \mu\text{V}\cdot\text{W}^{-1}\text{m}^2$).
- b) The r.m.s. scatter of individual 10-minute data points about the regressions lines varies from 24 μV to 43 μV which corresponds to irradiance values in the range 3-5 Wm^{-2} .
- c) In every period the intercept is significantly different from zero, and consequently the sensitivities change with irradiance level. The overall mean sensitivity is 0.4% less at 1000 Wm^{-2} and 0.6% more at 500 Wm^{-2} than at 750 Wm^{-2} . (-4 Wm^{-2} at 1000 Wm^{-2} , $+3 \text{ Wm}^{-2}$ at 500 Wm^{-2}).

Similar conclusions can be drawn from Figures 3 and 4 which contain respectively data from the whole 20 month duration and data just from the Tape 3/Figure 2 period of two months. They show the distribution of errors when irradiance is calculated in the usual manner by dividing the NIP signal by a single constant calibration factor ($8.45 \mu\text{V} \cdot \text{W}^{-1}\text{m}^2$),

We have considered the following possible causes of the clear departure from the simple zero-intercept linear response:

- i) intrinsic non-linearity of the NIP thermopile;
- ii) an effect of different secondary time constants of the NIP and the cavity radiometer;
- iii) spectral absorption of the glass window of the NIP.

At this time we are not able to rule out any of these causes. The other NIP which we have tested (No. 21945) shows the same non-linearity.



SCATTERGRAM OF RATIOS BETWEEN TWO RADIOMETERS

Figure 1

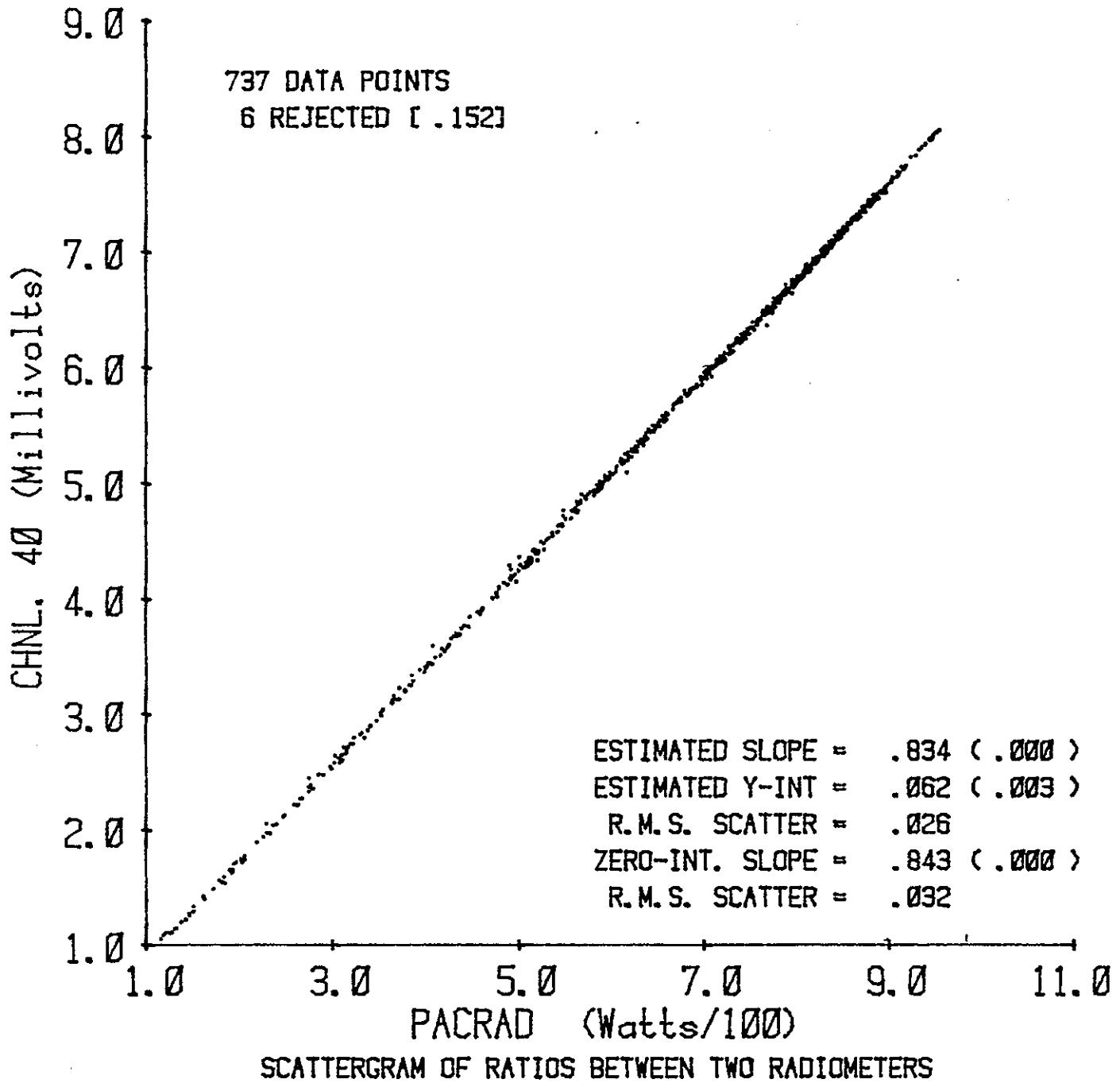


Figure 2

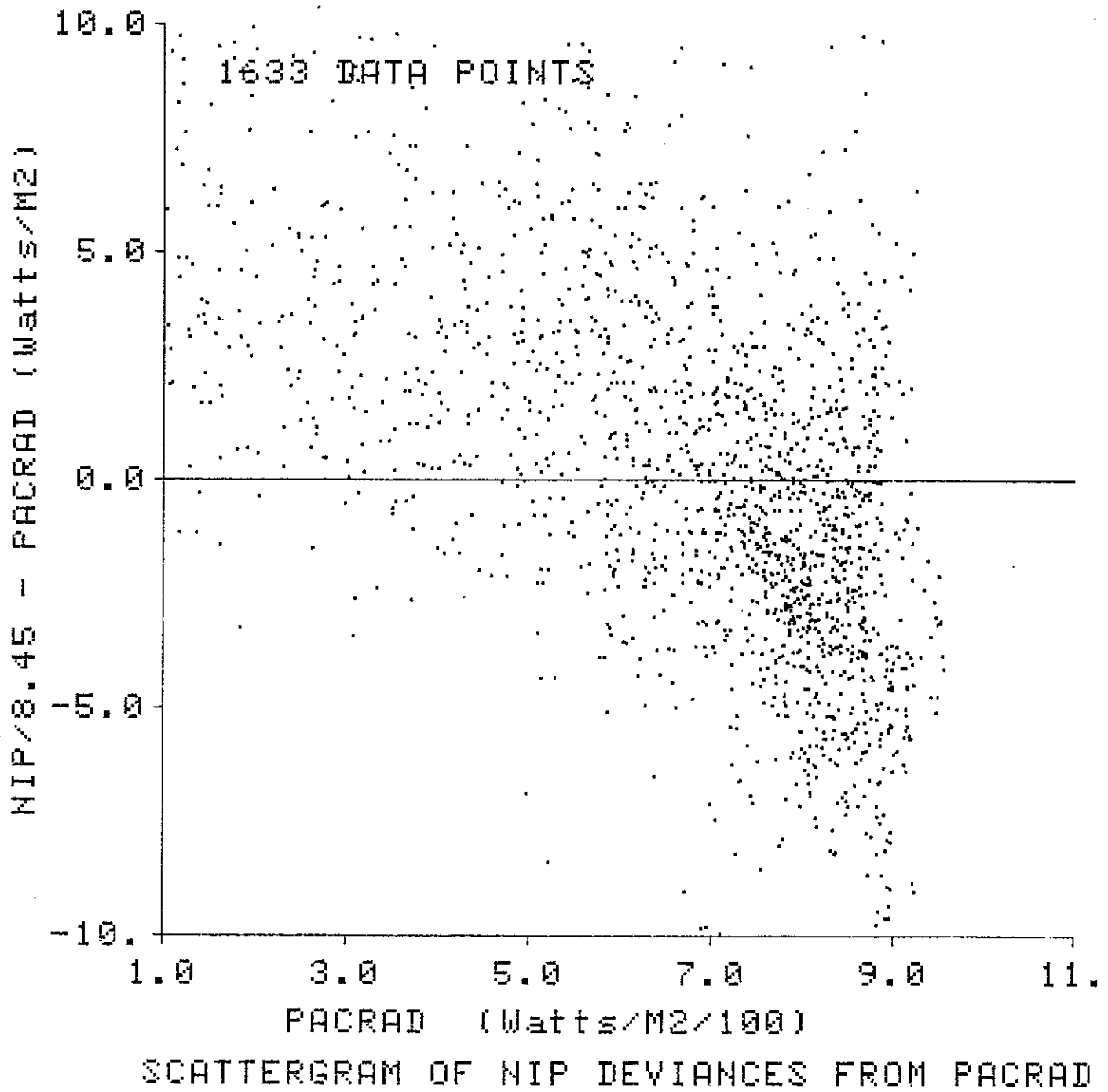
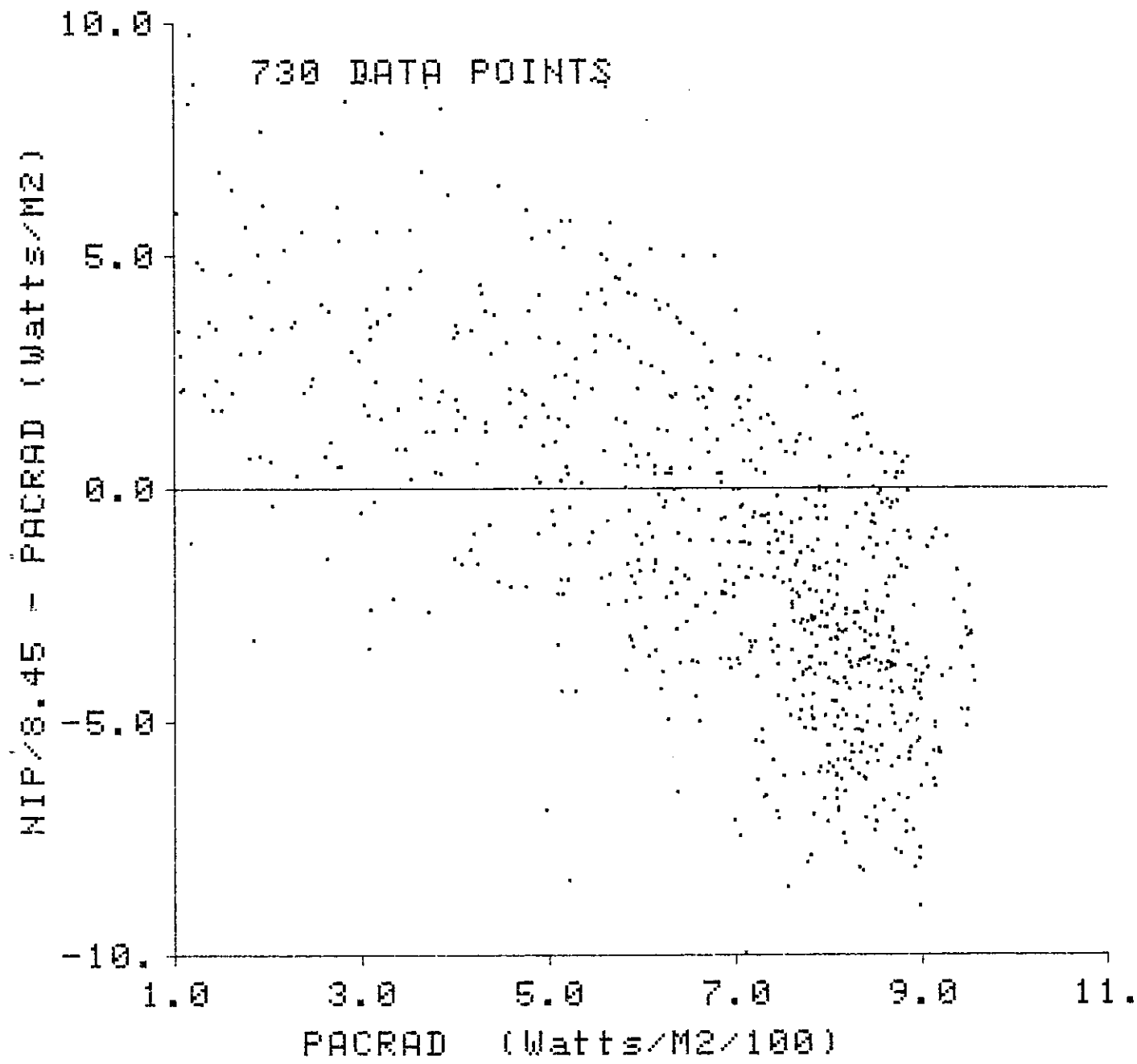


Figure 3



SCATTERGRAM OF NIP DEVIANCES FROM PACRAD

Figure 4



4.C THE NEW RIVER INTERCOMPARISONS OF ABSOLUTE CAVITY
PYRHELIOMETERS (NRIP I - VI)

Gene A. Zerlaut

DSET Laboratories, Inc.
Phoenix, Arizona 85029

THE NEW RIVER INTERCOMPARISONS OF ABSOLUTE CAVITY PYRHELIOMETERS (NRIP I - VI)

ABSTRACT

The genesis of the New River Intercomparisons and their operation are discussed in detail. NRIP I (November 1978) came about as a result of a need to establish a basis for transfer of calibration from primary standard pyrheiliometers to field pyranometers (and field pyrheiliometers) for use in solar device testing. NRIP VI, with 15 cavities participating, as held in late November, 1983. The six intercomparisons held to date have involved a total of 31 different absolute cavities from five countries. Dates of the intercomparisons are selected to insure the greatest probability of cloud- and haze-free conditions in the northern Sonoran desert of Arizona. Simultaneous instantaneous readings are organized into ten-minute sequences of 21 readings in 30-second intervals. Between 30 and 40 runs are obtained in each intercomparison, requiring no more than four days at the site selected. The advantages and disadvantages of the procedures employed in the NRIP's, which require that the normal readout electronics associated with a given instrument are a part of the intercomparison, are discussed in terms of procedures employed in the International Pyrheiliometric Conferences. Results of the comparisons are presented in aggregate. Agreement for the more than 40,000 instantaneous measurements is within .25% for the 31 cavities intercompared.

INTRODUCTION

Largely as a result of our early assessment of the disparate results of the first U.S. National Bureau of Standards-sponsored Round Robin tests of the thermal performance of solar hot water collectors¹, and our own independent observations of pyranometer-to-pyranometer difference among a large group of so-called WMO Class I instruments, DSET Laboratories purchased an Eppley Model H-F absolute cavity pyrheiliometer in January 1977. This particular instrument was the first terrestrial version of the Hickey-Frieden absolute cavity radiometer that was developed for the Nimbus satellite series. In early 1979 we obtained a second Model H-F cavity radiometer, SN 17142.

In the summer of 1977 we began periodic shading disk calibrations of our family of Eppley Model PSP pyranometers at test angles of interest, but predominantly at normal incidence employing an altazimuth tracking mount. Altazimuth tracking is the most widely used altitude employed in the U.S. to test solar collectors for thermal performance. Calibration transfers are made directly from the H-F cavity radiometers.

Because of the need for a U.S. reference base to provide material continuity and traceability for legal purposes (in terms of product certification testing), we proposed hosting the first regional intercomparison of absolute cavity radiometers at DSET's New River, Arizona site. The facilities and generally superior environmental conditions that prevail in the

northern Great Sonoran Desert north of Phoenix resulted in a consensus agreement among participants to hold subsequent intercomparisons in New River. These three-to-five day intercomparisons, known as the New River Intercomparisons of Absolute Cavity Pyrheliometers (NRIPs), have been co-sponsored by DSET Laboratories, the National Weather Service's Solar Radiation Laboratory (NOAA), and the Solar Energy Research Institute (DOE). In May 1982, in conjunction with NRIP V, the New River intercomparisons became partially self-supporting on a participating fee basis. NRIP VI was held in November 1983 and future intercomparisons are planned for November 1985, and thereafter on a biannual basis.

The success of the NRIPs has been largely due to the helpful support and enthusiasm of Mr. Edwin Flowers of NWS/SRL/NOAA, Mr. John Hickey of The Eppley Laboratory, Mr. James Kendall of the Jet Propulsion Laboratory, and Mr. Chester Wells of the Solar Energy Research Institute.

OPERATION OF THE NRIPs

More than 40,000 individual instantaneous irradiance readings have been accumulated by five different absolute cavity radiometers in NRIP I through VI, as shown in Table 1. Five different cavity designs from the United States, Canada, Switzerland, Italy and the People's Republic of China have contributed to this data base.

TABLE 1
NRIP Instrument Breakdown

Intercomparison	Date	New	Total	Solar Observations
NRIP I	Nov. 1-5, 1978	14	14	315
NRIP II	May 2-5, 1979	4	12	441
NRIP III	Nov. 5-9, 1979	4	17	550
NRIP IV	Nov. 17-19, 1980	4	15	465
NRIP V	May 3-5, 1982	2	7	798
NRIP VI	Nov. 14-18, 1983	3	16	525

Dates for the intercomparisons are selected to ensure the greatest probability of cloud- and haze-free conditions. The site at New River, Arizona is distinguished by a combination of moderate temperatures, low average humidity, clear sky conditions, and high average daily sunshine for the times of year chosen.

Outdoor laboratory facilities were constructed specially for the NRIP experiments. They consist of three permanent double-tiered instrument benches, with the upper table serving as the cavity mounting deck, which in turn shades a lower electronic shelf that also doubles as working desk space. Each table accommodates eight experimenters, making it possible to intercompare 24 cavity radiometers at a time.

Instantaneous readings are organized into 10-minute sequences of 21 readings at 30-second intervals (some ACR-type instruments obtained 11 readings at 1-minute intervals). Readings for all instruments are sensed within less than 1 second of each other to minimize scatter between instruments due to rapidly changing sky conditions. Calibrations are usually performed both before and after each experimental sequence with the apertures shuttered. A complete description of the NRIP comparisons has been published by Estey and Seaman², and a summary by Zerlaut³.

Direct beam spectral measurements were obtained during NRIP V (May 1982) and NRIP VI (November 1983) employing DSET's Scanning Solar Spectroradiometer. The spectroradiometer design has been described previously⁴; it is based on a Leiss dual-prism quartz monochromator with source optics consisting of a pyrheliometer comparison tube/integrating sphere receiver. Complete solar spectral measurements were obtained in the 300 to 2500 nm region in a 4-minute period. The field of view and slope angle of the occulting tube match exactly those of the Eppley Model NIP Pyrheliometer. Data obtained represented a band pass resolution of from 4 nm in the middle ultraviolet to 50 nm in the 2300 nm wavelength region.

SUMMARY OF NRIP I THROUGH NRIP VI

Summary results of NRIP I through V have been compiled by the author³. These data have been updated by adding results of the recently completed NRIP VI and are presented in Table 2. The standard deviation (S.D.) shown is the statistical average of the S.D. computed for each intercomparison in which the instrument was involved. The standard deviation of all readings (weighted average of the individual S.D.'s) is 0.0011.

The excellent agreement obtained between all absolute cavity instruments (with the agreement being to within 0.25% for more than 40,000 instantaneous measurements) is attributed principally to (1) the excellent quality of currently available absolute cavity instruments, (2) the quality of the environmental conditions obtained at New River for the times of the year chosen for the intercomparisons, and (3) the improved techniques with which the experimenters themselves operate their respective instruments as a result of the experience gained.

COMPARISON OF NRIP INSTRUMENTS TO SN 67502

Data for each intercomparison are also obtained by ratioing the irradiance of each instrument to that of the agreed upon reference instrument -- NOAA/SRL's SN 67502. The set values are given in Table 3 for these instruments that have participated in most of the NRIP's. Also, the ratios to SN 67502 are given for the results of IPC V (Davos, 1980) for those instruments that have participated in both. This was done by normalizing IPC V data⁵ to SN 67502 results for those instruments.

TABLE 2
Results of NRIP I through NRIP VI with Ratio of
Each Instrument to Group Mean

Model	SN	Participant	NRIPs	N	Weighted Mean Ratio	S.D.x
EPAC	11399	AES, Canada	1,3	40	0.9997	+0.0021
*EPAC	11402	The Eppley Lab.	1	15	1.0008	0.0018
*EPAC	12843	NOAA	3,4	50	0.9968	0.0042
∞H-F	14915	The Eppley Lab.	1 thru 6	140	1.0010	0.0009
H-F	14917	NASA-Lewis	2	22	0.9995	0.0004
*H-F	15745	NOAA (SRL)	1,2,3,4,6	122	0.9973	0.0007
∞H-F	17142	DSET Labs	2 thru 6	137	1.0006	0.0013
∞H-F	18747	AES, Canada	3	25	0.9990	0.0007
H-F	18748	The Eppley Lab.	3,4	44	1.0026	0.0009
H-F	19743	Peop. Rep. China Met.	6	22	0.9973	0.0008
H-F	20294	Peop. Rep. China Met.	6	25	0.9992	0.0010
ACR	501	Boeing Aerospace	1,5,6	59	0.9966	0.0027
ACR	601	NOAA	3	24	1.0067	0.0028
ACR	904	Battelle Mem. Inst.	5	23	1.0027	0.0018
ACR	1104	Lawrence Berkeley Lab.	4	31	1.0079	0.0028
∞*PMO	PMO2	PMOD/Davos, Switz.	3	29	1.0008	0.0007
MK VI	001	Jet Propulsion Lab.	2,3,4	74	1.0027	0.0017
∞MK VI	67401	Tech. Measurements	1,2,3,4,6	117	0.9997	0.0010
∞*MK VI	67502	NOAA (SRL)	1 thru 6	160	1.0005	0.0010
MK VI	67603	Sandia Natl. Lab.	1,2,3,6	84	0.9999	0.0011
∞MK VI	67702	Jet Propulsion Lab.	1,2,3,4,6	116	1.0011	0.0009
MK VI	67706	So. Cal. Edison	1,2,3,4,6	118	1.0004	0.0010
MK VI	67707	Utah State Univ.	1	15	1.0000	0.0011
MK VI	67811	Sandia Natl. Lab.	2	11	0.9997	0.0006
MK VI	67812	Ga. Institute of Tech.	1,3	40	0.9980	0.0007
∞MK VI	67814	SERI	1 thru 6	162	0.9990	0.0006
MK VI	68017	SERI	4	27	0.9989	0.0006
MK VI	68018	SERI	4,5,6	94	1.0017	0.0009
MK VI	68020	Martin Marietta	4	31	0.9990	0.0006
MK VI	68021	Stazione Astron. Italy	6	24	0.9978	0.0009
MK VI	68022	Sandia Natl. Lab.	6	13	1.0012	0.0005

N = Number of 21-reading sets (runs) in which each instrument has participated

* = Also compared in IPC IV, Davos, November 1975

∞ = Also compared in IPC V, Davos, November 1980

These data are plotted in Figure 1 and 2 to show instrument trends. All instruments show a general trend to greater sensitivity compared to SN 67502. The marked similarities in data for NRIPs I, II and III leads to speculation that the reference instrument SN 67502 exhibited a decrease in sensitivity of about 0.15% in the period since May 1979. Also, one of the most important attributes of the frequency and procedures employed in the NRIPs is manifest in the behaviour of SN 17142 (the author's instrument). As a result of the nearly 0.5% apparent decrease in sensitivity of this instrument in NRIP V, the cavity was examined and several large dust particles were observed. After removal by blowing with an optics bulb, the apparent sensitivity increased and the instrument again essentially assumed its historical position among its peer group.

TABLE 3
Ratio of Each Instrument to the NOAA/SRL
Reference Cavity, SN 67502

Inst.SN	NRIP			Davos IPC	NRIP		
	1	2	3	V	4	5	6
14915	0.9984	0.9984	1.0013	1.0005	1.0011	1.0016	1.0006
15745	0.9963	0.9955	0.9971	---	0.9971	---	0.9975
17142	---	1.0008	1.0012	1.0005	1.0019	0.9971	1.0009
67401	0.9968	0.9956	1.0019	1.0004	0.9996	---	1.0006
67502	1.0000	1.0000	1.0000	1.0000	1.0000	1.0000	1.0000
67603	0.9966	0.9980	0.9999	---	---	---	0.9998
67702	0.9940	0.9996	1.0023	1.0005	1.0019	---	1.0020
67706	0.9992	0.9983	1.0003	---	1.0002	---	1.0010
67814	9.9978	0.9968	0.9989	0.9974	0.9988	0.9989	0.9986
68018	---	---	---	---	1.0021	1.0013	1.0014

COMPARISON OF THE NRIPs WITH IPC IV AND V

Unlike the WMO-sanctioned intercomparisons held every five years at Davos where only the cavity is compared, the New River intercomparisons compare the cavity and its associated electronic data logging and readout equipment. The advantages of the NRIP-type comparisons are that the actual equipment compared is the same as employed by the participants when they use absolute cavity radiometers as primary reference instruments in their own laboratories. Hence, the performance of individual instruments compare in NRIPs has greater reference significance, if not greater credibility, than the same instruments compared at Davos.

The advantages of the NRIP intercomparisons relate to the de facto maintenance of the SI Radiometric Scale (WRR) in the U.S. by this peer group of instruments. To the reference quality of the intercomparisons for citation and traceability purposes, and to the availability of representatives of the peer grouping for the calibration and quality control purposes of any given organization.

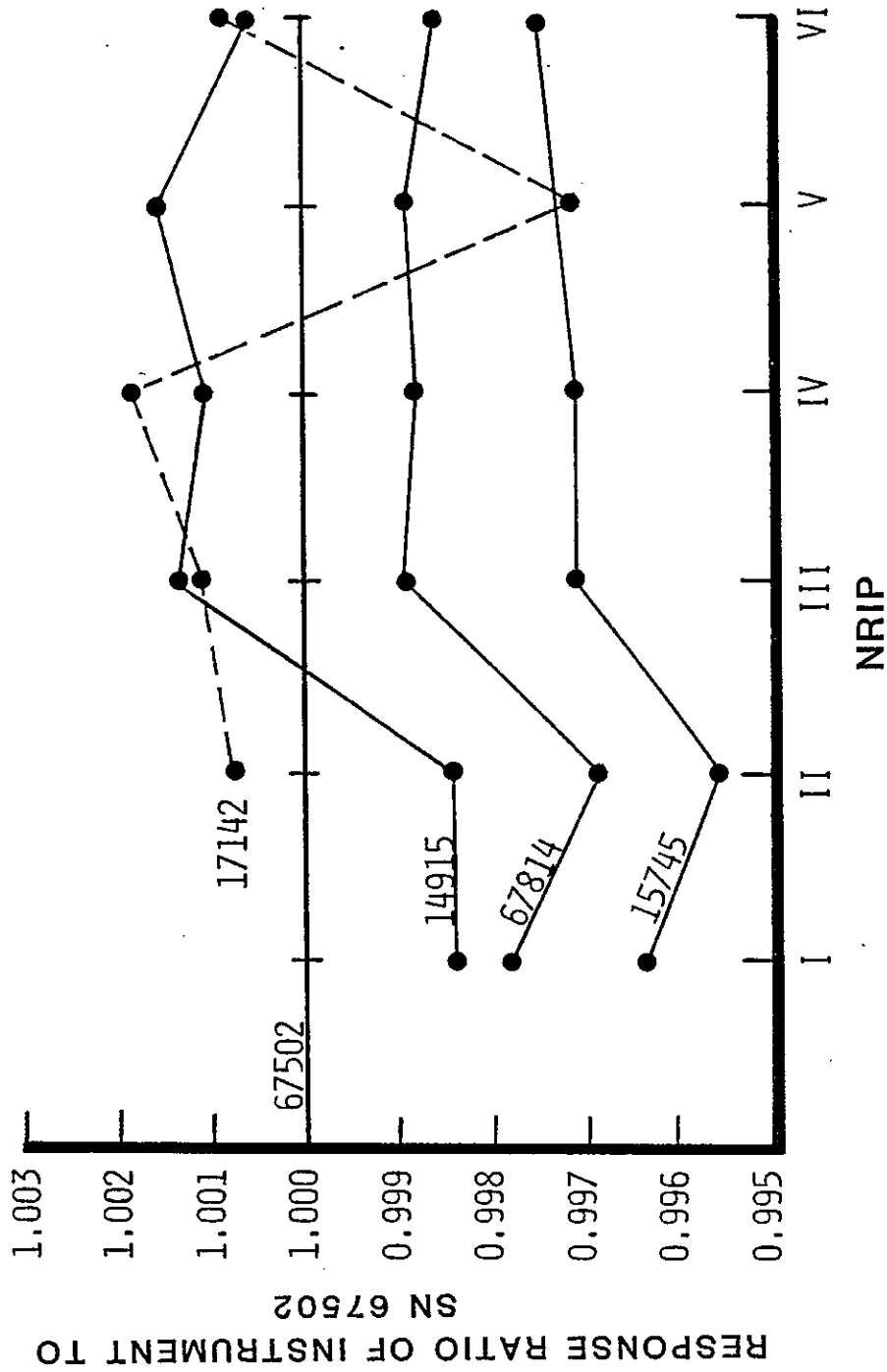


Figure 1. Comparison of several NRIP cavities to the NOAA reference, SN 67502.

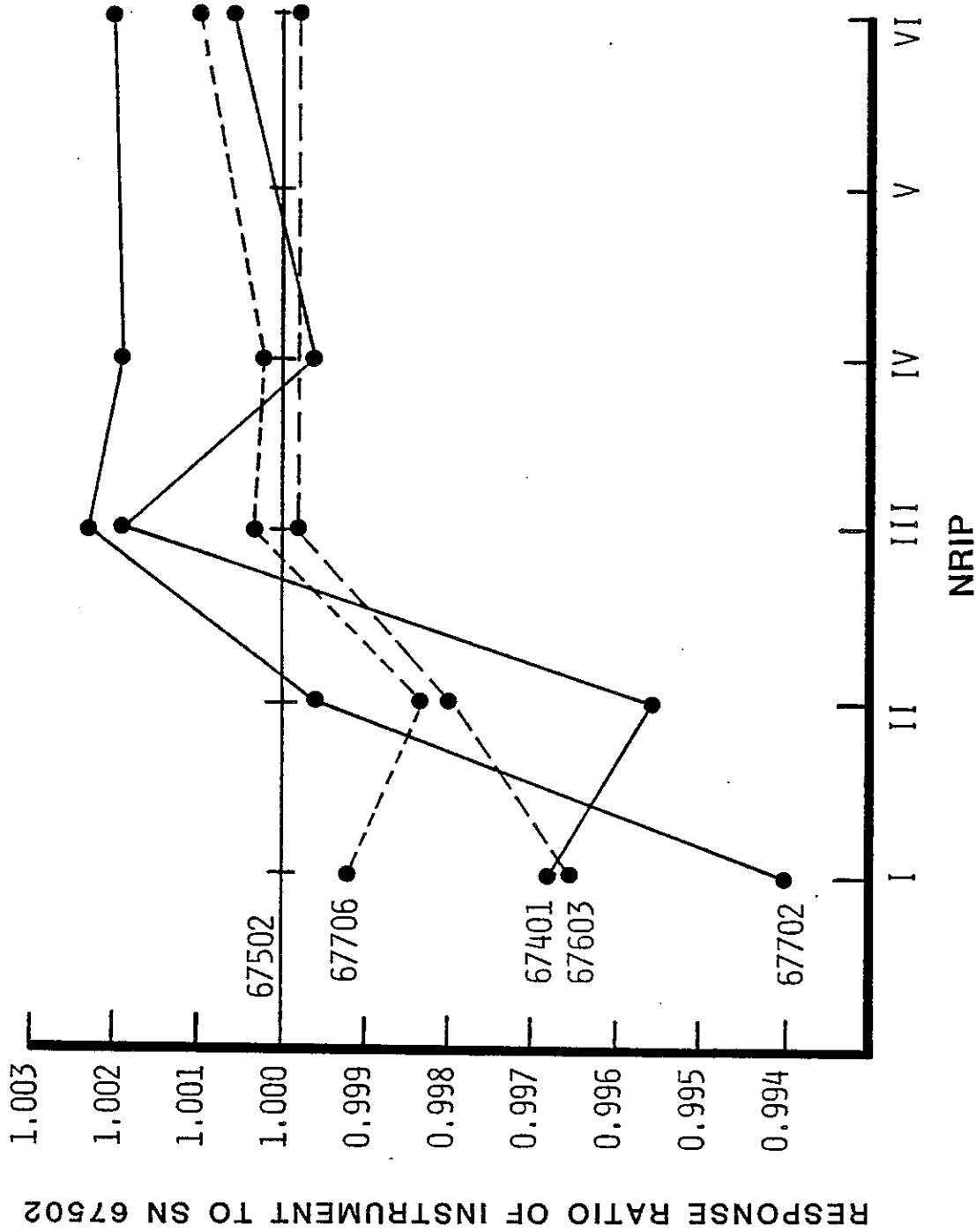


Figure 2. Comparison of several NRIP cavities to the NOAA reference, SN 67502

ACKNOWLEDGEMENTS

The author wishes to thank Ms. Claudene Fliegel for data entry and computer analyses that made this report possible.

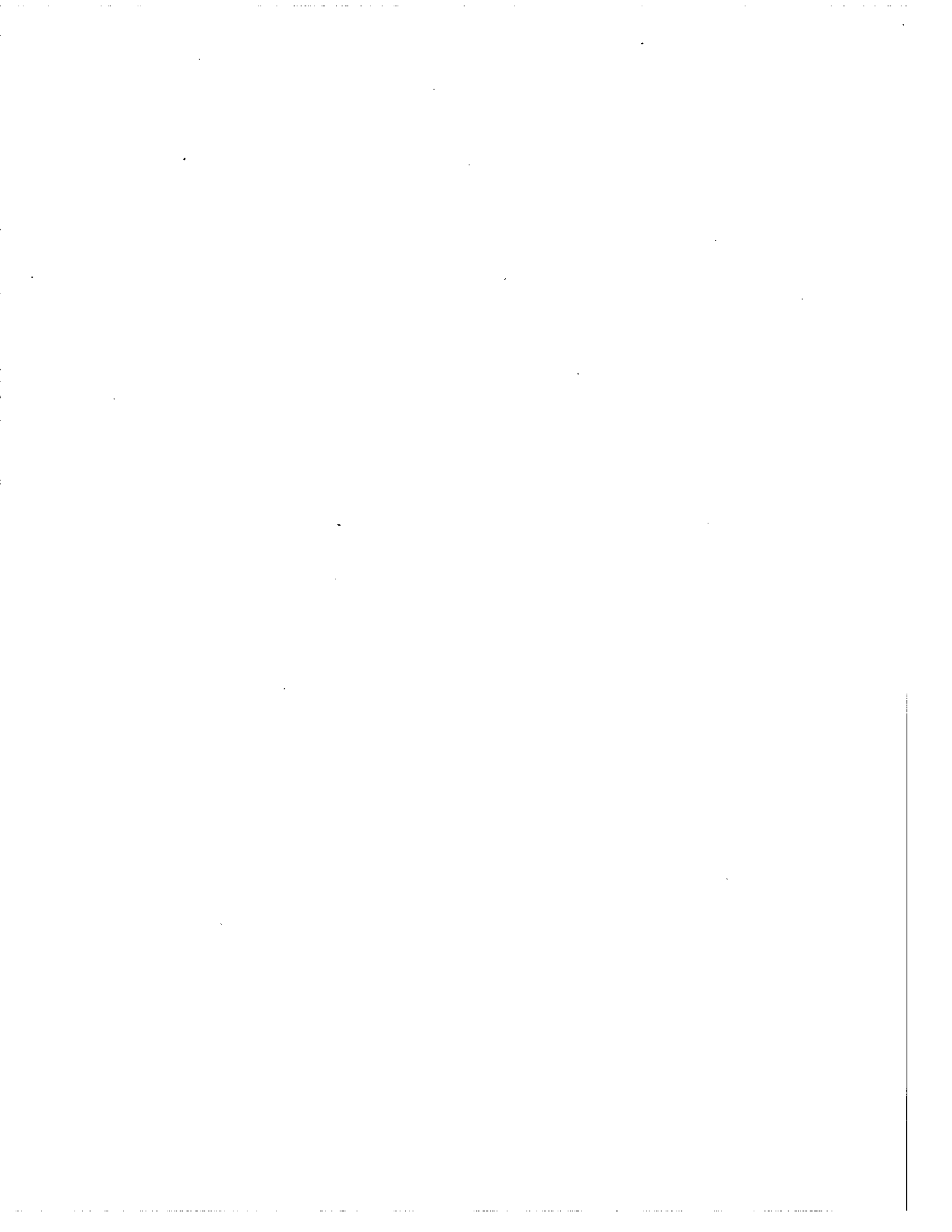
REFERENCES

1. Streed, E.R., et. al., 1978: Results and Analysis of a Round Robin Test Program for Liquid-heating Flat-plate Solar Collectors. NBS-975. Washington, D.C.
2. Estey, R.S. and C.H. Seaman, 1971: Four Absolute Cavity Radiometer (Pyrheliometer) Intercomparisons at New River, Arizona. JPL Publication 81-60. Jet Propulsion Laboratory. July 1971.
3. Zerlaut, G.A. 1982: Solar Radiation Measurements: Calibration and Standardization Efforts, pp. 19-60, Advances in Solar Energy, An Annual Review of Research and Development, Volume 1. Karl W. Böer and John A. Duffie, eds., American Solar Energy Society, Inc.
4. Zerlaut, G.A. and J.D. Maybee, 1982: Spectroradiometer Measurements in Support of Photovoltaic Device Testing. Solar Cells. November 1982.



SESSION 5

Field Performance and Accuracy



5A. THE INTERCOMPARISON OF PYRANOMETERS AT HORIZONTAL
45° TILT, AND NORMAL INCIDENCE

Gene A. Zerlaut and Gerald D. Maybee

DSET Laboratories, Inc.
Phoenix, Arizona 85029

THE INTERCOMPARISON OF PYRANOMETERS AT HORIZONTAL 45° TILT, AND NORMAL INCIDENCE

ABSTRACT

Three comparisons of pyranometers have been held at New River, Arizona since the fall of 1981. Except for the first, they have been in conjunction with the more widely known New River Intercomparisons of Absolute Cavity Pyrheliometers (NRIP's). These comparisons, designated the New River Comparisons of Pyranometers and Pyrheliometers, have defined a number of problems that arise in assessing data, and have suggested an outdoor approach to the characterization of pyranometers. Participating pyranometers are co-mounted on a large platform in order that they may be moved in unison from tilt tables to horizontal to altazimuth amounts for comparison. Data are taken every 30 seconds and are organized into 10-minute sets of 21 measurements each. Various techniques for analyzing data are discussed, as are general results. The comparisons are performed in compliance with ASTM Standard E 824. Each instrument is compared both to the mean of all instruments and to the mean of a set of three reference instruments. The three reference instruments utilized are SN 19129 (DSET Laboratories, Inc.), SN 19917 (NOAA/NWS/SRF), and SN 21017 (The Eppley Laboratory).

INTRODUCTION

The purpose of the first New River Comparison of Pyranometers, held in November 1981, was to elucidate the extent to which a substantially large set of instruments deviated from each other when compared at 0° horizontal, 45° south, and at normal incidence on an altazimuth tracking mount. Results of the first comparison confirmed the expectation that a wide difference in irradiance would be observed. The off-angle response at 0° horizontal and 45° south was determined by computer analysis of the data obtained at these orientations.

The second comparison, held in May 1982, included 23 pyranometers and, like the first, utilized the same reference set of three specially selected pyranometers that were calibrated by the shade method at the three tilt modes 0° horizontal, 45° south, and normal incidence. However, a new shade technique (described in subsequent paragraphs) was utilized for the first time. These shading calibrations were performed immediately after the pyranometer comparisons. As in the first comparisons, the off-angle response of all instruments compared at horizontal and 45° south was determined.

Eighteen instruments participated in the third comparison, which was concluded in early December 1983. Like the first two, the third involved comparisons at three orientations and utilized shade method calibration procedures that were identical to those employed in the second comparisons.

EXPERIMENTAL

Site and Test Parameters

The facilities are located at DSET Laboratories in New River, Arizona, approximately 20 miles north of the northern city limits of Phoenix. The geography is classed as desert plateau with an elevation of 610 m (2000 ft) at 33° 51'N latitude and 112°10'W longitude. The dates, sky conditions, average temperature, and average humidity are presented in Table 1.

TABLE 1
Pertinent Experimental Test Parameters for Comparisons

	Average Temp. (°C)			Average Humidity (% RH)		
	I	II	III	I	II	III
0° Horizontal	27	33	18	19	7	53
45° South	27	34	20	19	7	49
Normal Incidence	23	30	15	16	8	55

Facilities and Mounting

The pyranometers were affixed to a common platform, and were spaced approximately 15 inches apart center-to-center. They were each leveled with the platform mounted in an exactly horizontal plane on a multiposition, multitilt exposure rack. Leveling was accomplished with the spirit level that is an integral part of each pyranometer. All 0°H (zero degree horizontal) comparisons were made in this position; the 45°S (South) comparisons were performed by tilting the mount table to exactly 45° from the horizontal with the normal to the plane of the table facing exactly south (180°). The platform containing the mounted and exactly coaligned pyranometers was removed from the multitilt exposure rack and placed on a large, precision altazimuth test mount for the normal incident comparisons (on a sun-following rack).

A Data General Nova 30 computer was employed to analyze all comparison data. The data acquisition system utilized consisted of a PD2064 Esterline Angus Datalogger which measured the analog signals and outputed the data to a TCT-300 Three Phoenix tape cartridge transceiver.

Organization of the Comparisons

The intercomparisons were organized into 10-minute data acquisition periods during which 21 instantaneous millivolt output signals were recorded from all pyrhemeters and pyranometers every 30 seconds. The comparisons were performed in compliance with ASTM Standard E 824¹. All channels were measured by the data logger in a 70 millisecond interval, the data were buffered and then recorded on magnetic tape for later retrieval.

Data Reduction

Computer programs have been written for DSET's Nova 3D computer for both the shading disk calibration of pyranometers and the comparison of a large group of instruments. The comparison program essentially computed the instantaneous irradiance measured by each instrument based on the instrument constant furnished by the participant/owner. These irradiance values were averaged for each 21-observation set (standard deviations were computed) and the average irradiance for that set was ratioed to the average irradiance for the set obtained for all instruments and to the average irradiance of the three reference pyranometers chosen. The average ratios and standard deviations were then obtained for all sets within a calibration angle (e.g., at tilts of 0°H, 45°S, and Normal Incidence). New instrument constants were computed. The reference irradiance was the average irradiance of three reference instruments constants calibrated by careful shading disk manipulations against DSET's Eppley Model H-F absolute cavity pyrhemometer (SN 17142)².

Computer plot routines were employed to reduce the comparison results in terms of the ratio of irradiance of each instrument to the mean irradiance of the three reference instruments as a function of angle of incidence.

REFERENCE PYRANOMETERS

Selection

Three Eppley PSP pyranometers were chosen as the reference instruments in all three comparisons: DSET's SN 19129; NOAA/SRL's SN 19917, and the Eppley Laboratory's SN 21017. These instruments were chosen because of their traceability and previous comparison pedigree, and for their comparative lack of deviation from cosine response. The instrument constants for all three reference pyranometers were those determined in the next previous pyranometer comparisons as well as by shade techniques at the time of the comparison. Only results based on shade disk calibrations determined at time of comparison are presented in this paper.

Shading Disk Calibration of Reference Pyranometers

The three reference instruments were calibrated by the shading disk technique in a modification of procedures generally employed for axis vertical and axis tilted. The modification consisted of using a different shade/unshade timing sequence than the usual 50% duty cycle employed. The change was employed as a result of discussions by participants of NRIP V centered upon the relevance of the unshaded (illuminated) duty cycle - the argument being that a 50% duty cycle might be in error.

Accordingly, we analyzed the problem by computing a simple energy balance on an idealized pyranometer. Consider the energy incident on the thermopile's receiver as shown in Figure 1. For the steady state, fully illuminated condition:

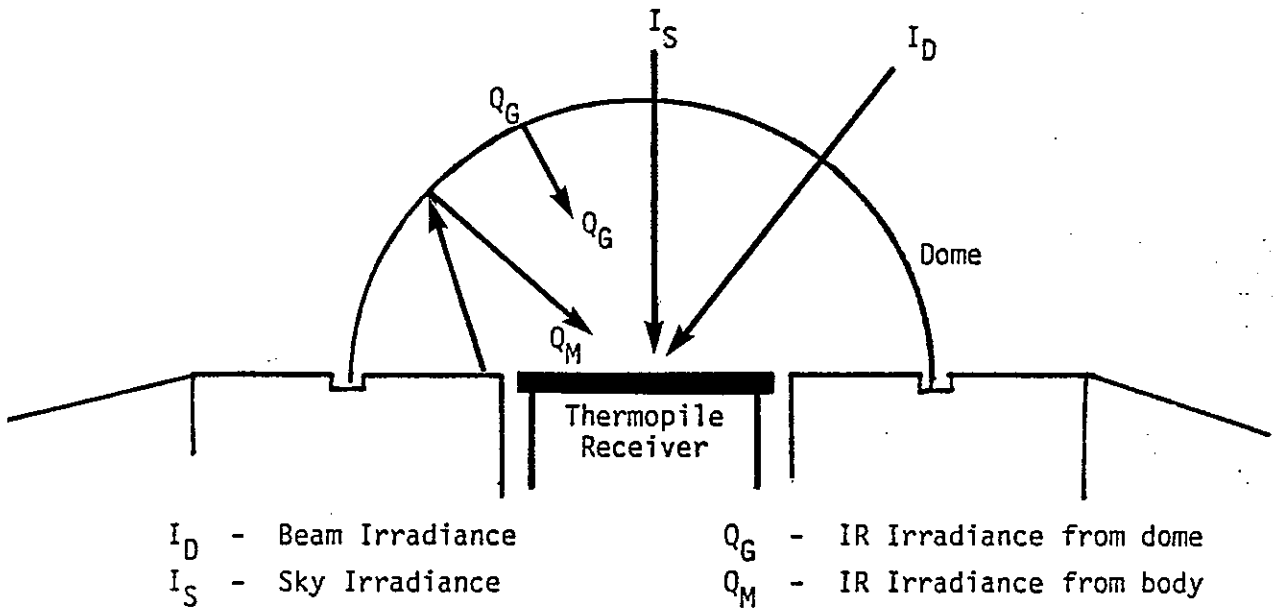


Figure 1. SCHEMATIC OF ENERGY ON A PYRANOMETER'S RECEIVER.

$$V_U = k(I_D + I_S + Q_G + Q_M) \quad \dots (1)$$

where V_U is the response signal generated by the pyranometer, k is its unknown instrument constant, I_D is the beam irradiance measured by the pyranometer, I_S is the unknown contribution to V_U from sky irradiance, Q_G is the unknown infrared irradiance of the receiver due to heating of the glass dome(s), and Q_M is the thermal contribution to the thermopile from solar heating of the pyranometer body. Likewise, for the steady state shaded condition,

$$V_S = k(I_S + Q_G^* + Q_M^*) \quad \dots (2)$$

where Q_G^* and Q_M^* are the corresponding decayed, or residual, thermal contributions. Combining these equations, we obtain

$$kI_B = k(I_D + I_S + Q_G + Q_M) - k(I_S + Q_G^* + Q_M^*) \quad \dots (3)$$

where I_B is the beam irradiance measured by the reference pyrheliometer. Simplifying Equation (3), we obtain

$$I_B = I_D + (Q_G - Q_G^*) + (Q_M - Q_M^*) \quad \dots (4)$$

and we observe that an error is propagated the extent of which is largely dependent on the thermal contribution from the glass domes in the unshaded portion of the sequence. Realizing that a pyranometer, as is true of all thermal devices, possesses multiple time constants, it became obvious that to eliminate the contribution of Q_G in Equation (4), we needed to determine V_S in the nonsteady state condition immediately after the thermopile reaches a steady state defined by 20 time constants, but prior to the onset of linear decay of signal due to the cooling glass dome and thermopile surrounds (and certainly prior to reaching the overall instrument steady state). In other words, one desires that Q_M^* and Q_G^* be as nearly equal to Q_M and Q_G , respectively, as possible (without precluding the development of a steady state thermopile voltage).

The Eppley Laboratory specifies that the time constant of PSP's is approximately 1 second; we have verified that claim for all three reference pyranometers utilized in all three pyranometer comparisons. These were determined as the time required to reach $1/e$ of the final steady state illuminated value after being shaded for about 60 seconds. We then plotted the signal from all four pyranometers as a function of illumination condition (i.e., shaded vs. unshaded), every 10 seconds. A typical plot is shown in Cycle 1 and 2 of Figure 2. It will be observed that the illuminated pyranometer reaches a steady state much more quickly than does the shaded instrument, and even after 3 minutes, the shaded thermopile response is decreasing in a linear fashion. Since 20 time constants will give 99.5% of

the final thermoelectric response value, the shade/unshade sequence presented in the solid curve of Figure 2 was chosen for the shade calibrations performed in support of the May 1982 and November 1983 New River pyranometer calibrations.

On the basis of this analysis and data presented in Table 2 (and presented in a recent publication³), this technique was adopted in the two ASTM Standards dealing with shade calibration of pyranometers with axis vertical and axis tilted, respectively^{4,5}.

RESULTS AND DISCUSSION

Shading Disk Calibration of Reference Pyranometers

For purposes of selecting the proper calibration technique, SN 19129 was calibrated by the timing program presented in Figure 2. The values of B, C and M were selected to provide a range of options. The actual values chosen are presented in Table 2 along with the resultant calibration values.

TABLE 2
Shade Calibration Values for SN 19129 as a
Function of Timing Sequence

Method	Timing (sec)			May 1982 Calibration Value, k ($\mu\text{v}\cdot\text{w}\cdot^{-1}\text{ cm}^2$)
	<u>B</u>	<u>C</u>	<u>M</u>	
A	300	360	30	10.25
B	30	30	2	10.34
C*	20	60	30	10.30
D	10	60	30	10.36
E	30	90	30	10.31

* This is the preferred timing sequence

The preferred timing sequence is given by Method 3 where data are taken in 20 time constants after shading the pyranometer and the pyranometer is unshaded within 30 seconds. The abscissa in Figure 2 gives the preferred sequencing, which is the program employed in both the May 82 and November 83 comparisons.

The temperature-corrected shading disk calibrations of the three reference pyranometers are presented in Table 3, along with the original values that were in use in the summer of 1981. (The calibrations presented are corrected to the comparison temperatures as noted in Table 1). Examination of Table 3 shows two interesting trends: (1) essentially identical values were obtained for each of the three pyranometers at normal incidence in spite of different seasonal tilts and slightly different procedures, and (2) the close agreement between the normal incident values and the values for the seasonal tilt which most closely resembles the mean tilt at normal incidence.

TABLE 3
Temperature-Corrected Shading Disk Calibrations*

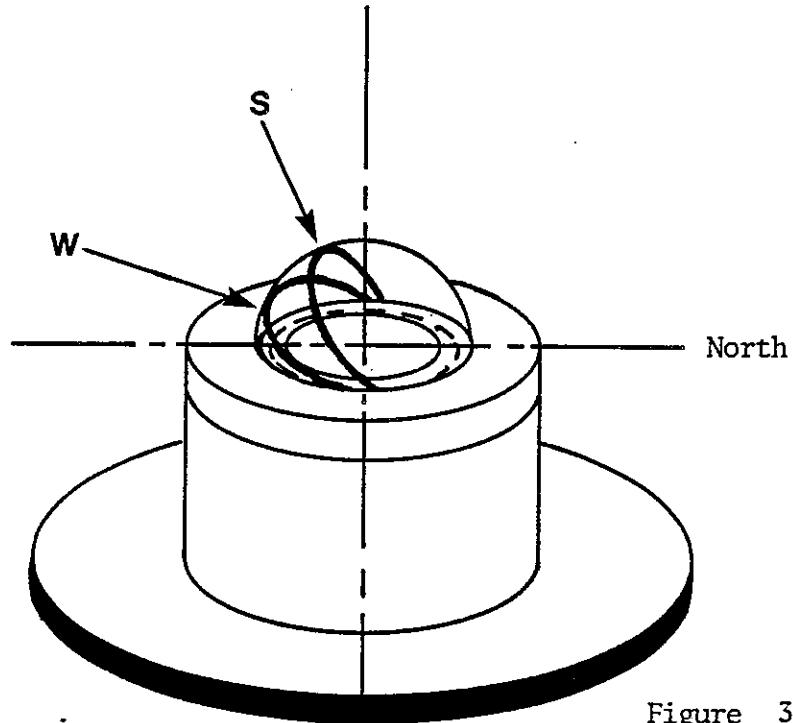
PSP/SN	Cal. Angle	Original Calibration	Nov. '81 I	May '82* II	Nov '83* III
DSET 19129	0°H	--	10.300	10.327	10.152
	45°S	--	10.369	10.299	10.332
	NI	10.386 ¹	10.369	10.335	10.359
NOAA 19917	0°H	10.110 ²	10.204	9.923	9.725
	45°S	--	9.962	9.748	9.897
	NI	--	9.935	9.901	9.905
EPLAB 21017	0°H	--	9.594	9.946	9.490
	45°S	--	9.775	9.632	9.806
	NI	--	9.833	9.803	9.805

- * Normalized to comparison temperatures (see Table 1) except for I, which was 25°C
- + ($\times 10^{-6} \text{ v/w}\cdot\text{m}^{-2}$)
- ¹ At normal incidence October '81 (Label calibration was 10.76 dated January '80)
- ² At horizontal Fall '81 (Label values)
- ³ At horizontal in integrating spheres

These relationships show that tilt effects in all three reference pyranometers are essentially nonexistent through 45° and that the difference must be due to incident angle effects (since temperature differences have been normalized out). This is not at all surprising if one next considers that seasonally different geometrical relationships apply to pyranometers oriented at zero degrees horizontal and at tilts of 45 degrees from the horizontal, as shown in the somewhat exaggerated Figures 3 and 4. These figures show that the "beam track" on the dome is near to normal incidence (at solar noon) in the summertime at horizontal orientation and in the wintertime at a tilt of 45°. Conversely, the greatest angular disparities for the beam component can occur at horizontal orientation in winter months (Trace W in Figure 3); the summer beam trace for pyranometers oriented at 45° tilts occurs entirely in the pyranometer dome's northern hemisphere (Trace S in Figure 4).

PYRANOMETER COMPARISONS

A typical computer printout (for the May '82 comparisons) is presented in Table 4. The averages of the mean ratios to the reference pyranometers were 0.985, 0.984 and 0.941 for the normal incidence, 0° horizontal, and 45° south comparisons, respectively. The respective standard deviations of the mean ratios were 0.016, 0.017 and 0.020, with maximum deviations of 5.0, 5.4 and 6.8% at these three tilts.



S - May 1982 Comparison
W - November 1981 Comparison

Figure 3.
BEAM TRACKS ON DOME OF PYRANOMETER
AT HORIZONTAL ORIENTATION

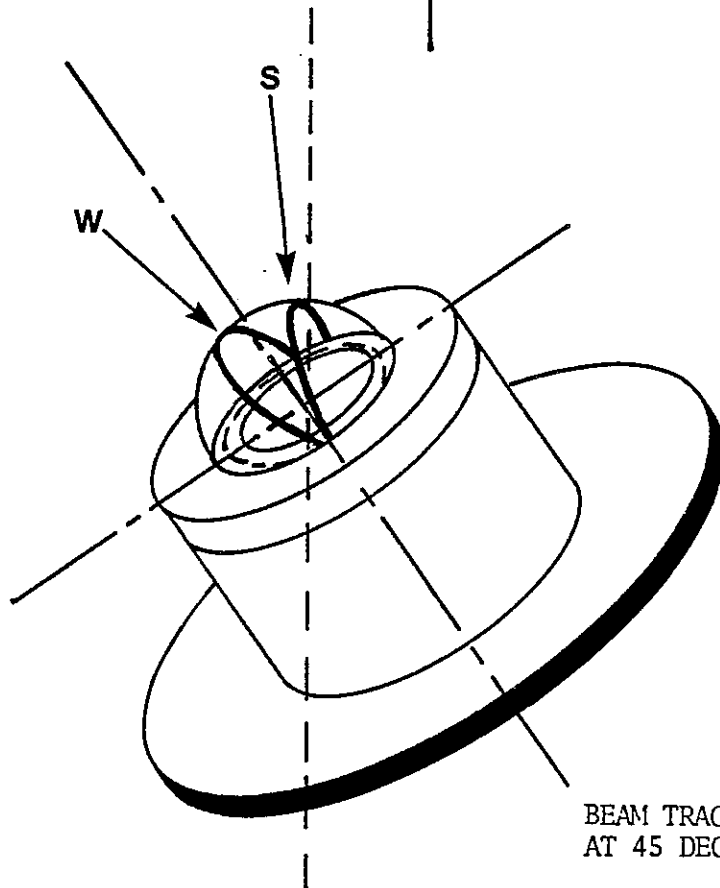


Figure 4.
BEAM TRACKS ON DOME OF PYRANOMETER
AT 45 DEG TILT ORIENTATION

Data for the third comparisons held in November 1983 showed only slightly better calibrations among the participating set. The average of the mean ratios was 0.991, 0.967 and 0.999 for normal incidence, 0° horizontal and 45° south, respectively. The respective standard deviations were 0.013, 0.025 and 0.014.

However, if one examines the data for those pyranometers that participated in all three comparisons and utilized instrument constants derived from the next previous comparison, the results are far superior. These data are presented in Table 5 where it will be observed that the agreement with the reference pyranometers in Comparisons II and III (together) increases to 0.998, 0.994, and 0.994 for normal incidence, 0° horizontal, and 45° south comparisons. The standard deviations drop to 0.005, 0.013 and 0.010, respectively. (It should be noted that three of the six instruments are the reference pyranometers).

Results of twelve pyranometers that participated in at least two inter-comparisons are shown in Tables 6 through 8 for 0° horizontal, 45° south, and normal incidence, respectively.

Special observations are worthy of note: (1) Like the results of shade disk calibrations of the reference pyranometers, the calibration factors for normal incidence were in closer agreement with those of 45° south in the two November comparisons, and with 0° horizontal results for the May comparisons, (2) the November calibrations at all three tilt modes were in closer agreement than either with the May results, (3) the most disparate data were from the November data for 0° horizontal and May data for 45° south comparisons.

A trend that has been observed at DSET - namely, that PSP's that have exhibited increasingly green receivers, begin to suffer greater and greater deviations from the cosine law at low sun angles. This is true for SN 14230, which dropped from a factor of $8.747 \mu\text{v}\cdot\text{w}^{-1}\cdot\text{cm}^2$ to 8.203 at 0° horizontal, and for SN 17860, which dropped from 7.740 to 7.425 also at 0° horizontal.

Incident Angle Response

A plotter program was written that computes the angle of incidence from exact solar time (that is logged as input data) and then plots the ratio of instrument response to the mean response of the three reference pyranometers for the mean angle of incidence of each set.

Figures 5 and 6 are plots of the response of two of the reference instruments, SN 19129 and SN 21017, respective, to the mean of the three reference instruments. Figure 5 is taken from the November 1983 comparisons and Figure 6 is from the May 1982 comparisons. The mean of the three reference instruments plot as a linear line with essentially no cosine deviation. Figure 7 is a plot of the new Eppley absolute cavity pyranometer, showing that it has no cosine deviations and confirming the choice of SN 19129, SN 19197 and 21017 as a reference set.

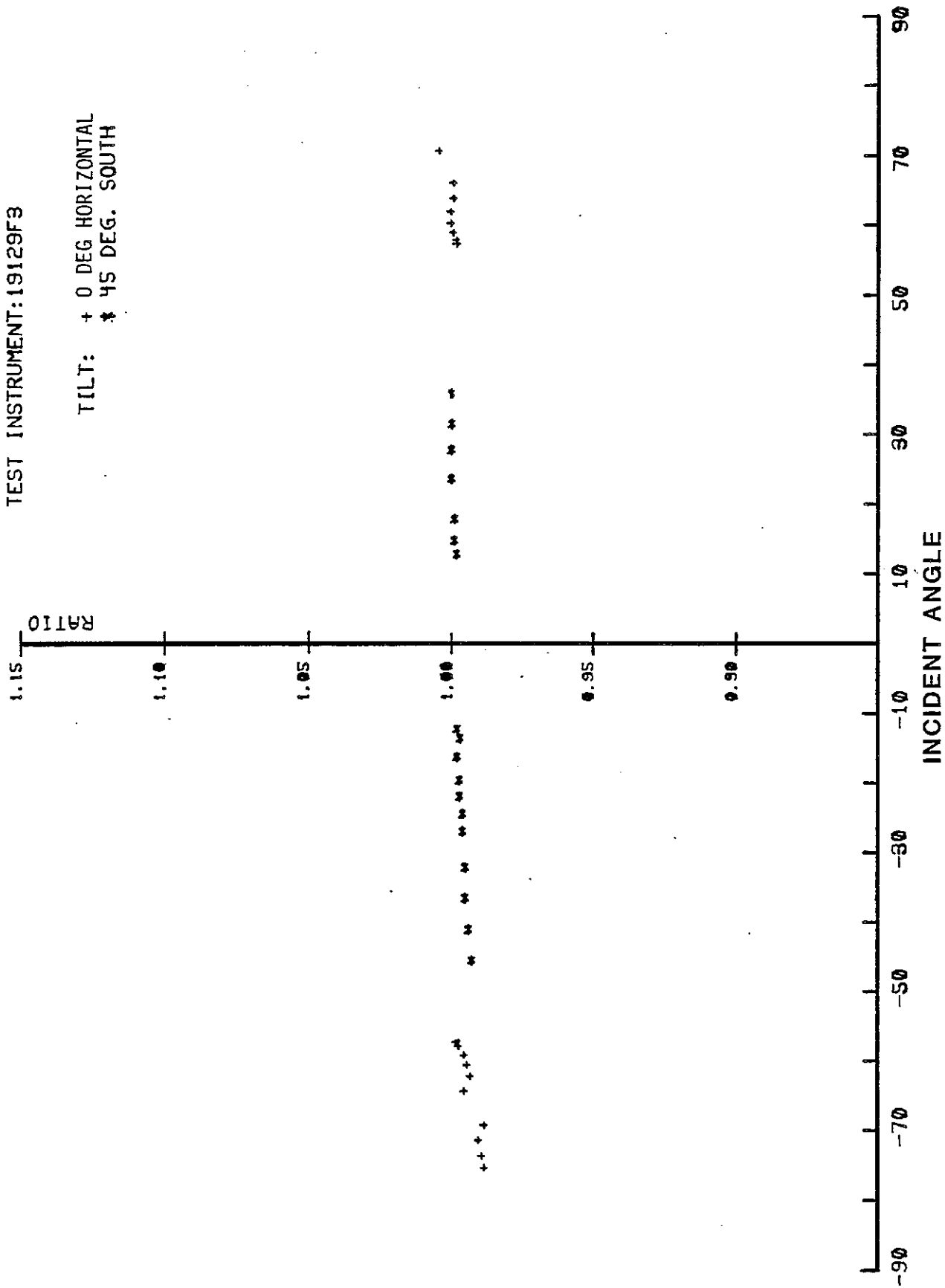


Figure 5. Ratio of response of eppley PSP SN 17322 to reference PSP(S) as a function of angle of incidence (December, 1983, New River, Arizona)

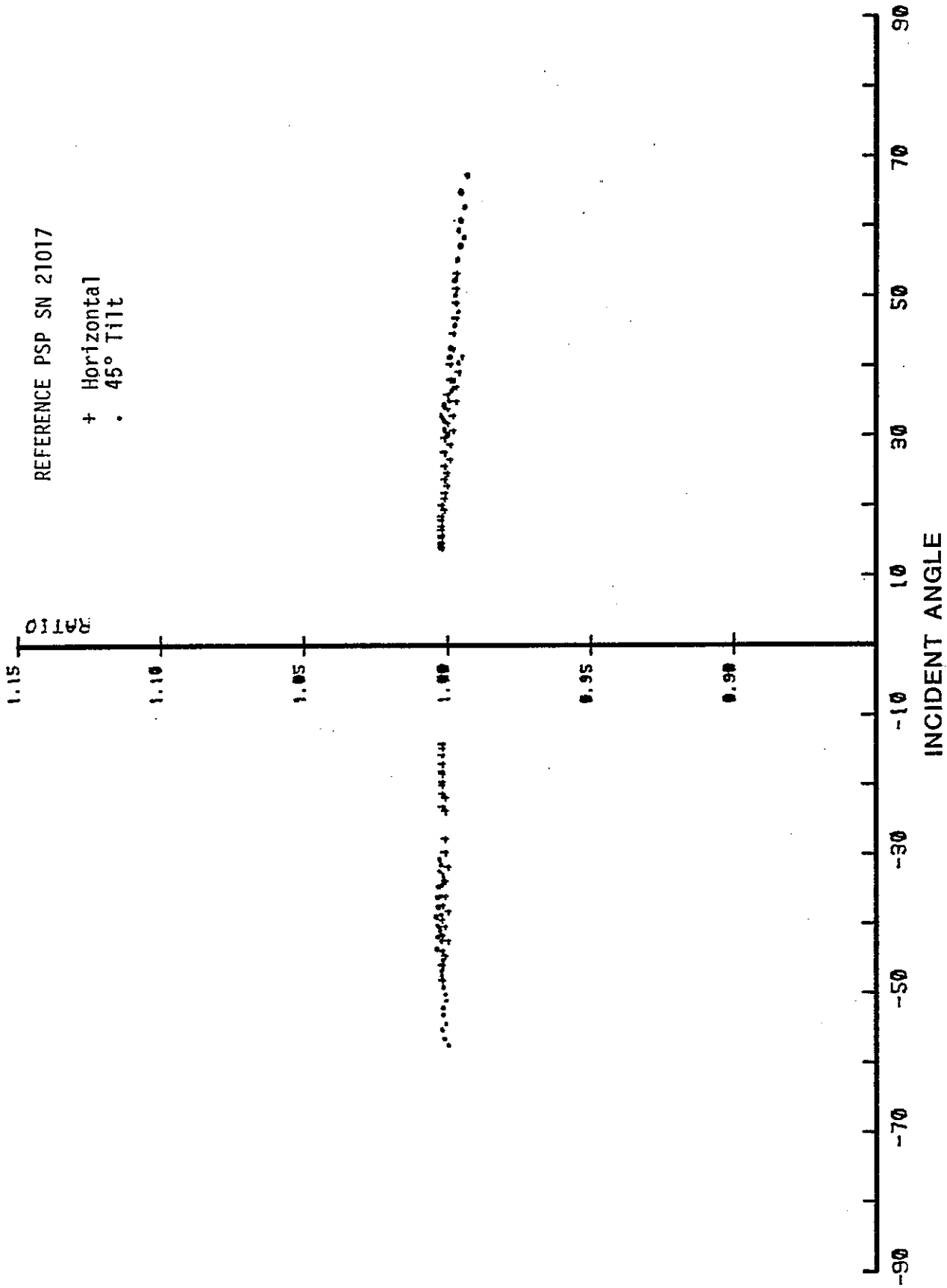


Figure 6. Ratio of response of eppley PSP SN 21017 to reference PSP'S as a function of angle of incidence (May 1982, New River, Arizona)

TEST INSTRUMENT: CAVITY PYRANOMETER
EPLAB

TILT: + 0 DEG HORIZONTAL
* 45 DEG. SOUTH

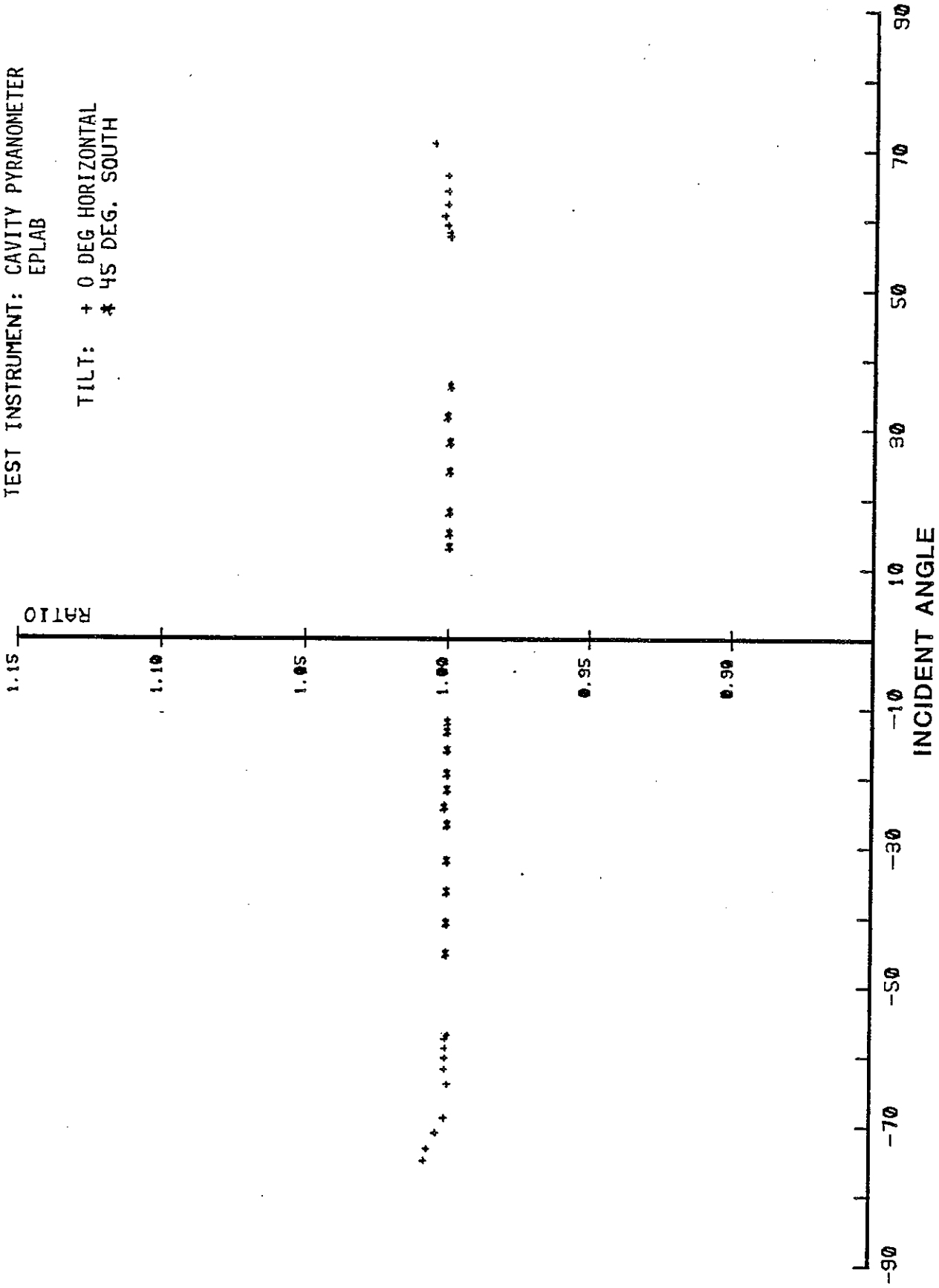


Figure 7. Ratio of response of eppley PSP SN 17322 to reference PSP(S) as a function of angle of incidence (December, 1983, New River, Arizona)

TABLE 4
Comparison of Irradiance of each Pyranometer to Mean Irradiance

(a)

Summary for Group 17 1449 Inst. Meas.
Tilt Normal Incidence

Test Instr.	Mean Ratio	So of Ratio	Old IC #	New IC #	Test Instr.	Mean Ratio	So of Ratio	Old IC #	New IC #
1	0.991	0.001	9.062	8.979	2	1.001	0.002	10.335	10.344
3	0.950	0.001	8.890	8.441	4	1.002	0.001	7.693	7.705
5	0.984	0.001	5.760	5.665	6	1.002	0.001	8.940	8.956
7	0.954	0.001	10.860	10.358	9	0.973	0.001	9.301	9.048
10	0.997	0.002	9.803	9.772	11	0.969	0.004	9.491	9.198
12	0.993	0.002	8.117	8.058	13	0.957	0.002	8.369	8.010
14	0.993	0.002	8.855	8.793	15	0.997	0.001	9.854	9.822
16	0.996	0.001	9.085	9.047	17	0.991	0.001	7.888	7.814
18	0.976	0.003	9.032	8.818	19	0.995	0.001	8.929	8.884
20	1.002	0.001	9.901	9.925	21	0.991	0.002	9.232	9.153
22	0.989	0.002	8.751	8.654	23	0.969	0.012	10.000	9.689

(b)

Summary for Group 18 1470 Inst. Meas.
Tilt Angle 45 Degrees

Test Instr.	Mean Ratio	So of Ratio	Old IC #	New IC #	Test Instr.	Mean Ratio	So of Ratio	Old IC #	New IC #
1	0.982	0.006	8.952	8.795	2	0.990	0.001	10.299	10.191
3	0.932	0.004	8.890	8.282	4	0.980	0.003	7.688	7.535
5	0.978	0.006	5.760	5.632	6	0.979	0.005	8.940	8.753
7	0.936	0.002	10.860	10.163	9	0.949	0.008	9.301	8.827
10	1.000	0.003	9.632	9.632	11	0.962	0.004	9.491	9.127
12	0.976	0.004	8.068	7.876	13	0.937	0.007	8.369	7.838
14	0.968	0.006	8.855	8.568	15	0.973	0.007	9.854	9.593
17	0.982	0.006	7.785	7.647	18	0.973	0.003	0.032	8.787
19	0.977	0.005	8.929	8.727	20	1.010	0.004	9.748	9.850
21	0.968	0.008	9.232	8.936	22	0.964	0.006	8.757	8.444
23	0.975	0.008	10.000	9.746					

(c)

Summary for Group 19 1449 Inst. Meas.
Tilt Angle 0 Degrees (Horizontal)

Test Instr.	Mean Ratio	So of Ratio	Old IC #	New IC #	Test Instr.	Mean Ratio	So of Ratio	Old IC #	New IC #
1	1.006	0.006	8.849	8.899	2	0.998	0.001	10.327	10.303
3	0.946	0.003	8.890	8.409	4	0.999	0.003	7.727	7.721
5	0.986	0.006	5.760	5.678	6	0.997	0.002	8.940	8.909
7	0.954	0.002	10.860	10.363	9	0.970	0.007	9.301	9.018
10	1.000	0.002	9.746	9.751	11	0.969	0.002	9.491	9.200
12	0.992	0.003	8.081	8.013	13	0.957	0.004	8.369	8.013
14	0.978	0.005	8.944	8.747	15	0.989	0.006	9.854	9.745
17	1.009	0.005	7.671	7.740	18	0.976	0.004	0.032	8.816
19	0.993	0.003	8.929	8.863	20	1.002	0.002	9.923	9.942
21	0.987	0.007	9.232	9.110	22	0.987	0.005	8.751	9.638
23	0.977	0.015	10.000	9.773					

TABLE 5
Ratio of Irradiance of Several Instruments to Mean Ratio of
Three Reference Pyranometers (Calibrated by Shade Method)

PSP/SN	Comp. Angle	INTERCOMPARISON		
		Nov '81 I	May '82 II	Nov '83 III
14439	0°H	0.988	0.999	--
	45°S	0.983	0.980	--
	NI	0.984	1.002	--
17860	0°H	0.970	1.009	0.944
	45°S	0.984	0.982	0.984
	NI	0.997	0.991	0.994
19129	0°H	1.005	0.998	0.996
	45°S	0.999	0.990	0.997
	NI	0.996	1.001	0.994
19917	0°H	0.984	1.002	1.006
	45°S	1.000	1.010	1.006
	NI	1.005	1.002	1.005
21017	0°H	1.010	1.000	0.998
	45°S	0.999	1.000	0.996
	NI	0.999	0.997	1.000
21070	0°H	0.966	--	0.978
	45°S	0.959	--	0.999
	NI	0.960	--	0.990

TABLE 6
Instrument Constants at 0° Horizontal Derived by Comparison to
Mean Irradiance of Three Pyranometers Calibrated by Shade Method

Inst. SN	Calibration Value ($\times 10^{-6}$ v/wm ⁻²)		
	Nov. '81 I	May '82 II	May '83 III
573-7	--	8.816	8.524
14230	--	8.747	8.203
14439	7.727	7.721	--
14898	8.849	8.899	--
15659	--	9.745	9.080
17175	--	8.638	8.162
17860	7.761	7.740	7.425
17897	8.081	8.013	--
19129	10.356	10.303	10.111
19917	10.042	9.942	9.779
21017	9.694	9.751	9.476
21070	9.543	--	9.331

TABLE 7
Instrument Constants at 45° South Derived by Comparison to
Mean Irradiance of Three Pyranometers Calibrated by Shade Method

Inst. SN	Calibration Value ($\times 10^{-6}$ v/wm ⁻²)		
	Nov. '81	May '82	May '83
	I	II	III
573-7	--	8.787	8.772
14230	--	8.568	8.618
14439	7.688	7.535	--
14898	8.952	8.795	--
15659	--	9.593	9.669
17175	--	8.444	8.487
17860	7.785	7.647	7.745
17897	8.068	7.876	--
19129	10.300	10.191	10.305
19917	9.964	9.850	9.959
21017	9.765	9.632	9.770
21070	9.478	--	9.485

TABLE 8
Instrument Constants at Normal Incidence Derived by Comparison to
Mean Irradiance of Three Pyranometers Calibrated by Shade Method

Inst. SN	Calibration Value ($\times 10^{-6}$ v/wm ⁻²)		
	Nov. '81	May '82	May '83
	I	II	III
573-7	--	8.818	8.810
14230	--	8.793	8.659
14439	7.693	7.705	--
14898	9.062	8.979	--
15659	--	9.822	9.729
17175	--	8.654	8.520
17860	7.888	7.814	7.824
17897	8.117	8.058	--
19129	10.328	10.344	10.301
19917	9.981	9.925	9.957
21017	9.826	9.772	9.808
21070	9.586	--	9.455

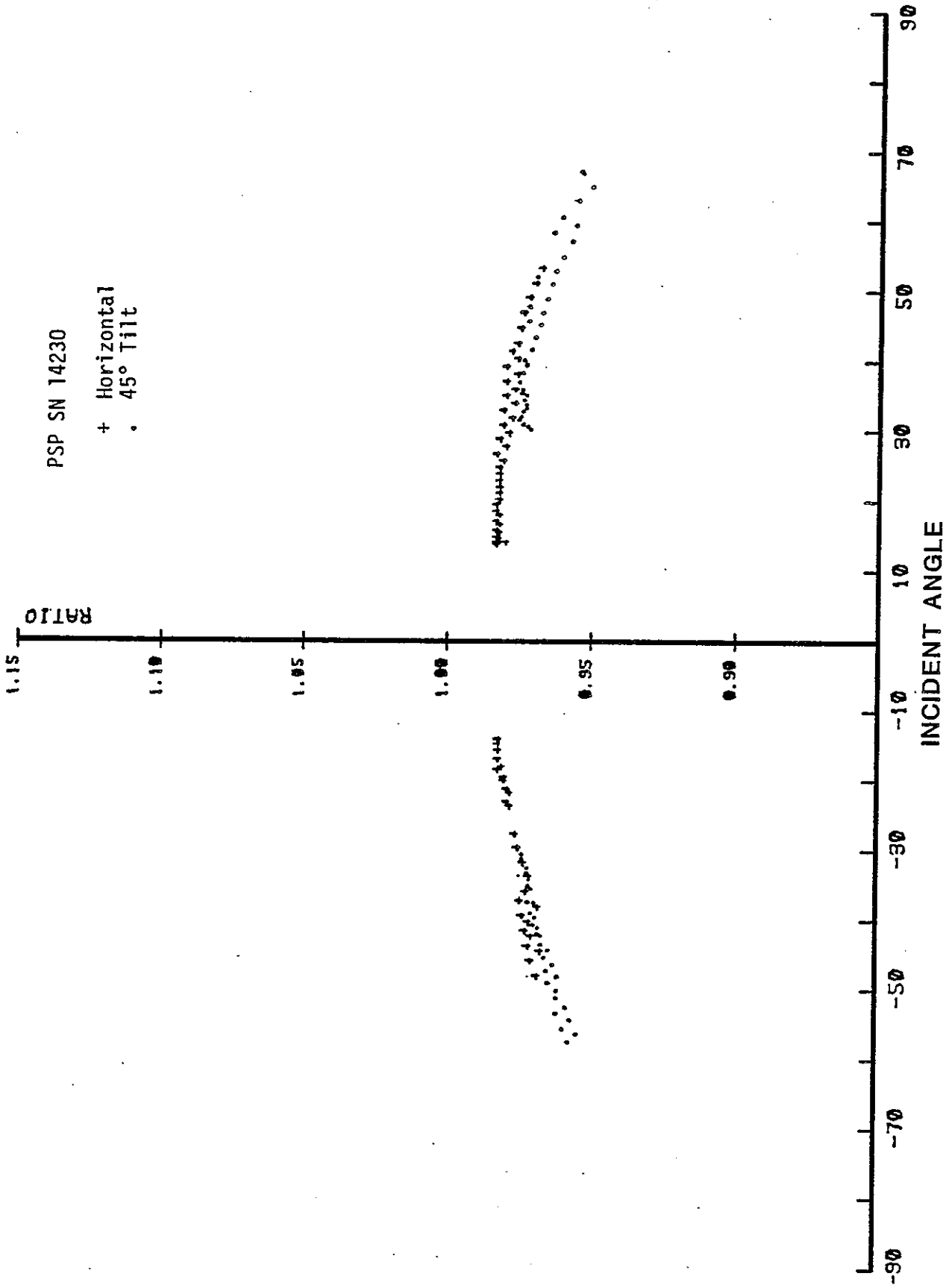


Figure 8. Ratio of response of eppley PSP SN 14230 to reference PSP'S as a function of angle of incidence (May 1982, New River, Arizona)

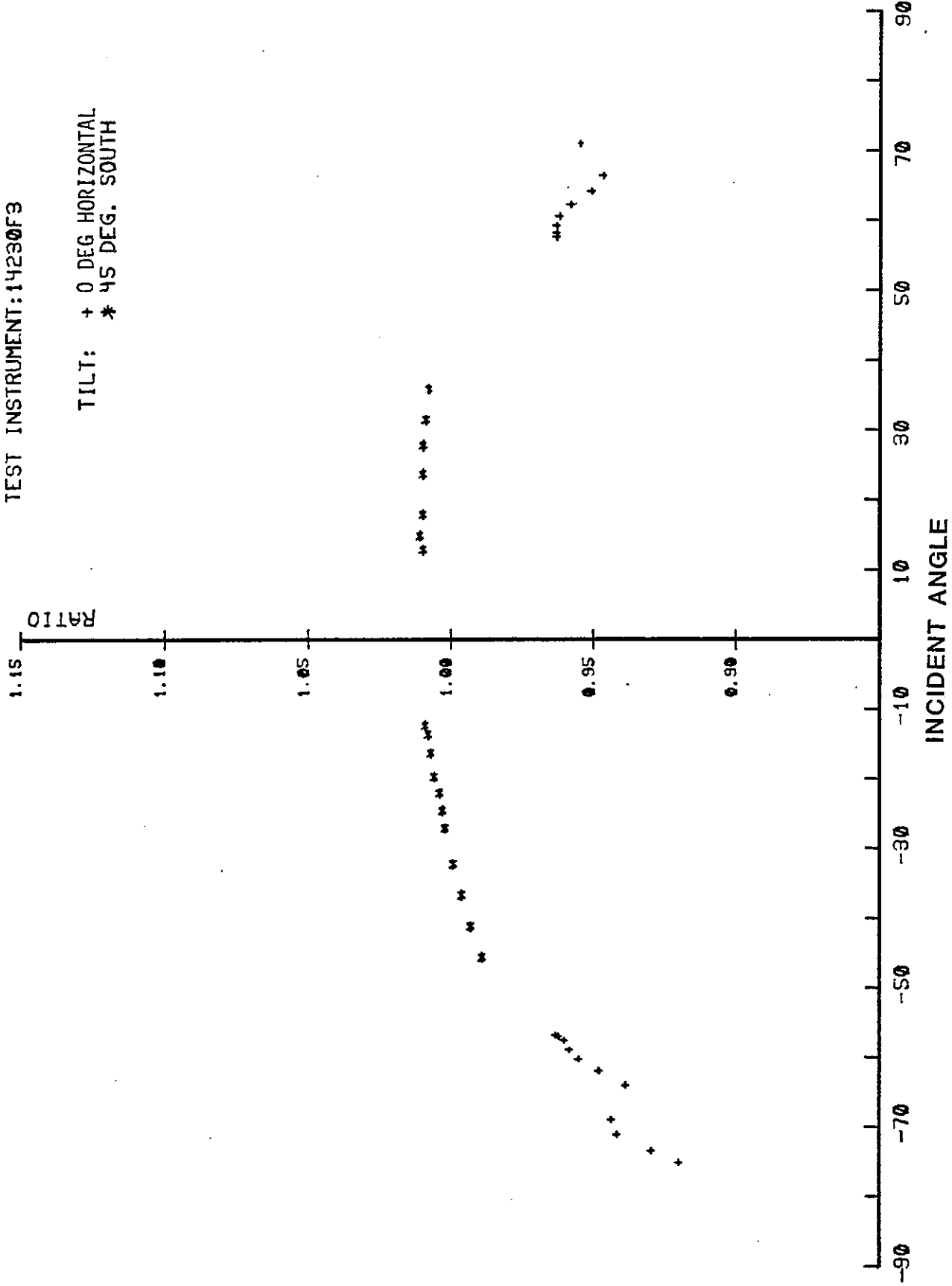


Figure 9. Ratio of response of eppley PSP SN 17322 to reference PSP(S) as a function of angle of incidence (December, 1983. New River Arizona)

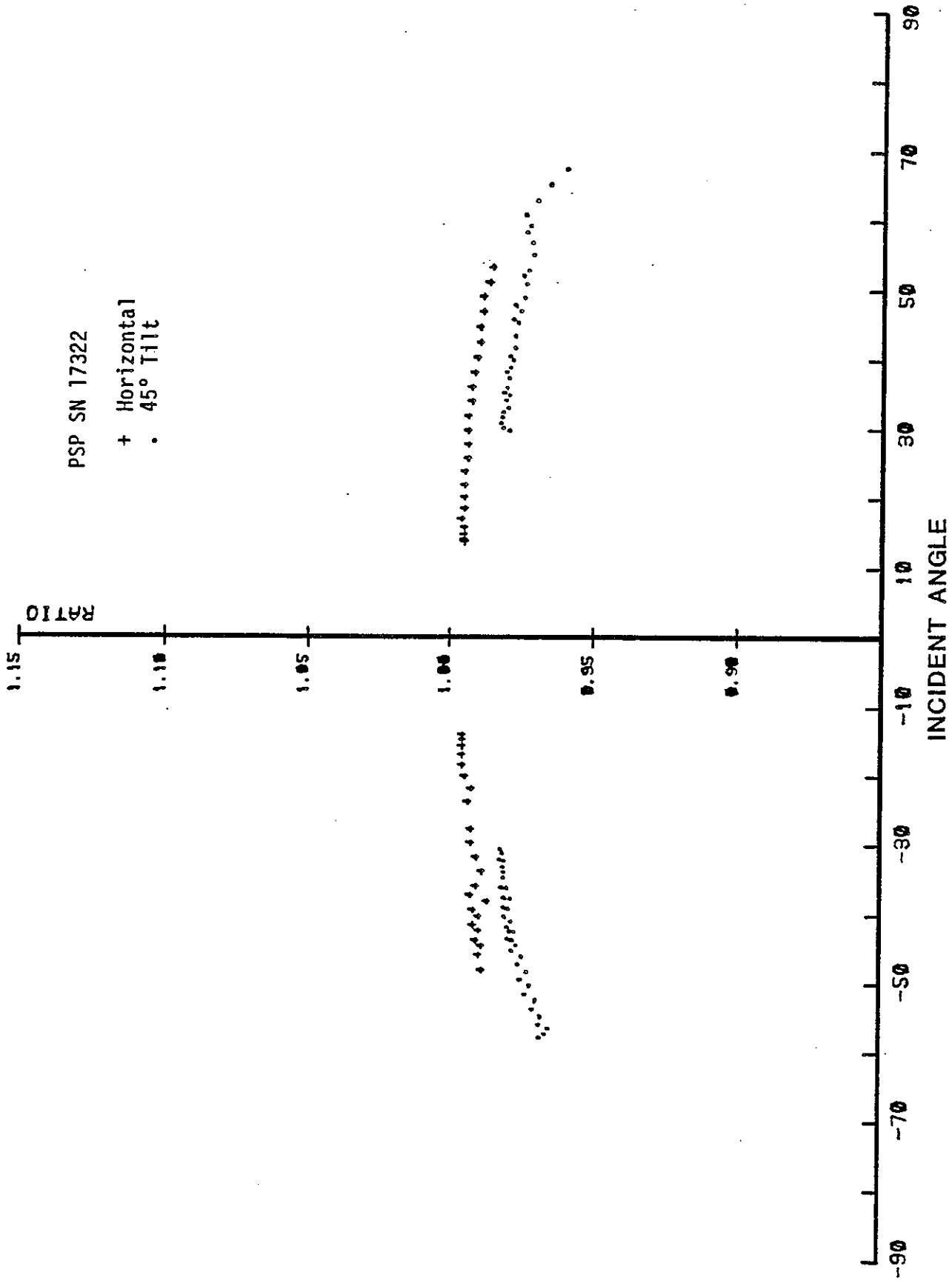


Figure 10. Ratio of response of eppley PSP SN 17322 to reference PSP'S as a function of angle of incidence (May 1982, New River, Ariz.)

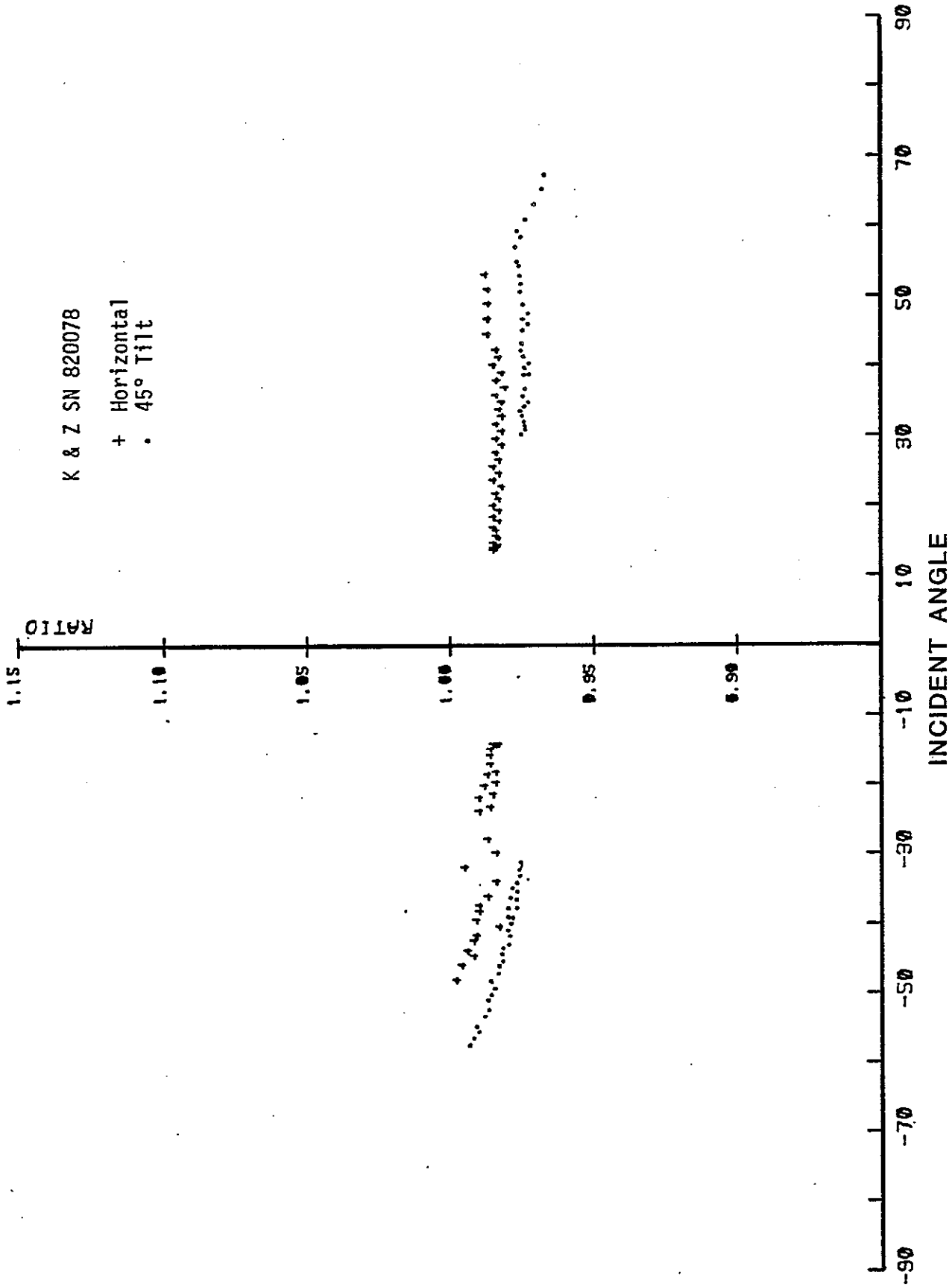


Figure 11. Ratio of response of Kipp & Zonen SN 820078 to reference PSP'S as a function of angle of incidence (May 1982, New River, Arizona)

Figures 8 and 9 are plots of SN 14230 from the May 1982 and November 1983 comparisons, respectively. Obviously, SN 14230 has further deteriorated in one and one-half years of exposure (it is a DSET instrument used for continuous resource assessment and not instantaneous measurements). It is noted that this instrument has exhibited a progressive green coloration of the receiver since May 1982.

Figure 10 is a plot of a PSP (SN 17322) that is more typical of the participants as a whole. Figure 11 is a plot of a Kipp and Zonen CM 10 pyranometer showing a slightly upturned response.

CONCLUSIONS

These results emphasized the notion that pyranometers scheduled for use as physics instruments in the precision measurement of instantaneous solar irradiance must be preselected and then quite thoroughly characterized as to instrument constant and incident angle effects. A case in point is the characteristics of SN 14230 which exhibits a 6% difference in irradiance between near normal incidence and 60° incident angles. This, coupled with disparities between instruments in their basic instrument constants, easily explains why solar hot water collector efficiency values too often differ from lab to lab by as much as 5-6% for the same collector.

At DSET Laboratories, we have established a qualification procedure for pyranometers destined for solar collector testing. It involves examination of the off-angle characteristics by the technique described in this paper (but against SN 19129 only) and then closely watching its calibration stability versus exposure for any signs of deterioration or erratic behaviour. Additionally, for pyranometers utilized in testing collectors on an altazimuth mount, the off-angle characteristics are determined on the altazimuth mount with altitude tracking only (at a fixed orientation to due South). Thus, the cosine response is determined in the exact east-west orthogonal plane of the pyranometer.

The use of three reference pyranometers increases the confidence level of the reference irradiance insofar as the normal scatter in shade disk calibrations tends to be averaged out. Also, we believe the outdoor method of determining the off-angle characteristics of a pyranometer under actual end-use requirements is superior to laboratory characterization. The equation of the response or the actual data may be employed as file information in the computer to provide a series of accurate calibration factors for the test sequence.

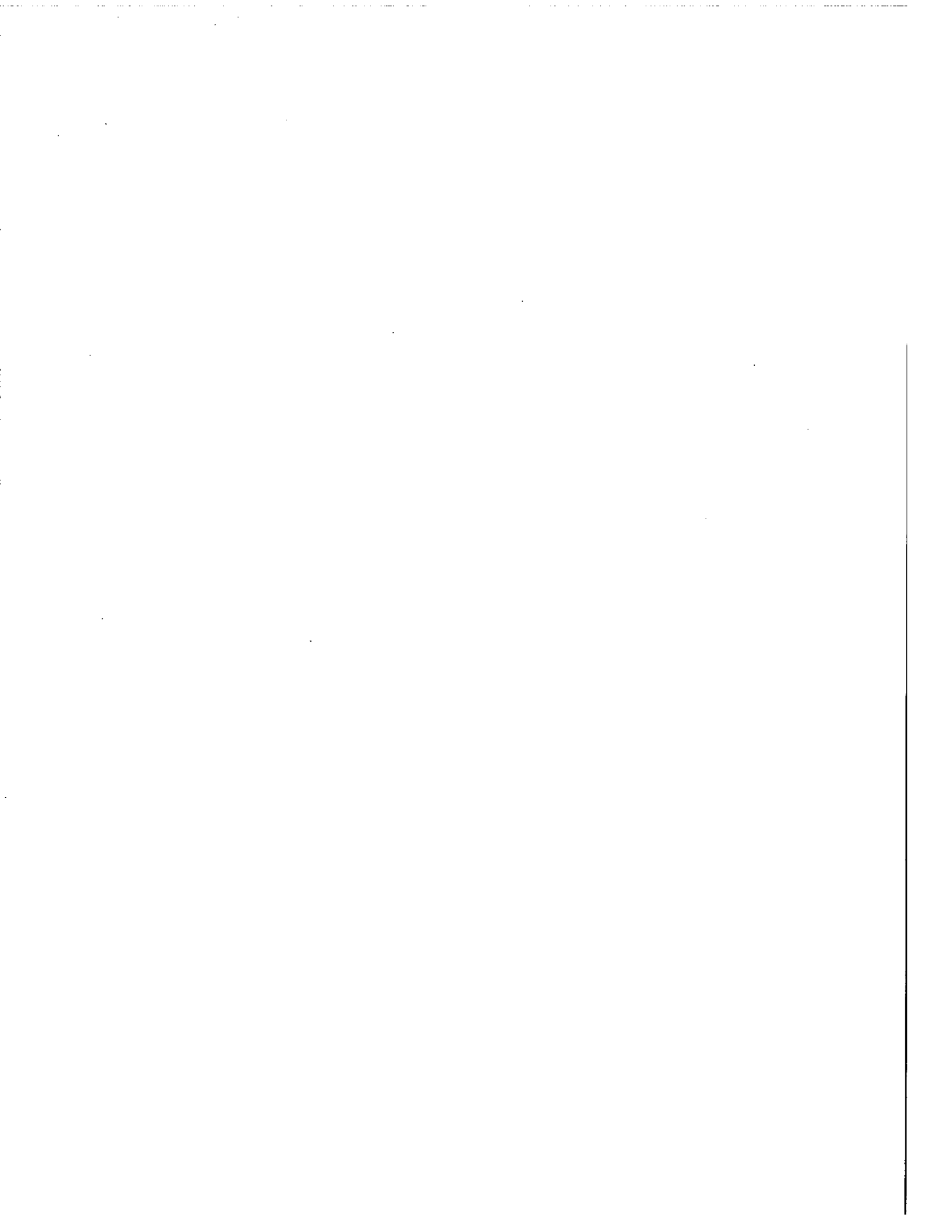
In summary, we recommend the following for pyranometers employed in solar device performance testing:

- Pyranometers used for physics applications, that is, for accurate instantaneous measurement of solar irradiance, should be preselected in a qualification program;

- Temperature-sensitivity functions must be used in precise measurements;
- Single calibration factors, unless utilized in conjunction with an incident angle sensitivity function, are not appropriate for solar collector testing;
- Calibrations should include incident angle response functions for the exact end-use applications of the pyranometer;
- Shading disk calibration transfers from pyrhemometers should take into account the thermodynamic characteristics of pyranometers;
- Calibration transfers should be made from sets of three carefully selected pyranometers.

REFERENCES

1. ASTM Standard E 824, Standard Method for Transfer of Calibration from Reference to Field Pyranometers, American Society for Testing and Materials, 1916 Race St., Philadelphia, PA 19103.
2. Zerlaut, G.A., "The New River Intercomparisons of Absolute Cavity Pyrheliometers (NRIP I-VI), "IEA Symposium, Norrköping, Sweden, January 23-24, 1984.
3. Zerlaut, G.A., "Solar Radiation Measurements: Calibration and Standardization Efforts," pp. 19-60, Advances in Solar Energy, An Annual Review of Research and Development, Volume 1. Karl W. Böer and John A. Duffie, eds., American Solar Energy Society, Inc., 1982.
4. ASTM Standard E 913, Standard Method for Calibration of Reference Pyranometers with Axis Vertical by the Shading Method, American Society for Testing and Materials, 1916 Race St., Philadelphia, PA 19103.
5. ASTM Standard E 941, Standard Test Method for Calibration of Reference Pyranometers with Axis Tilted by the Shading Method, American Society for Testing and Materials, 1916 Race St., Philadelphia, PA 19103.



5.8 ACCURACY CHECKS ON PYRANOMETERS IN THE SWISS ANETZ NETWORK

A. Zelenka

Swiss Meteorological Institute

ACCURACY CHECKS ON PYRANOMETERS IN THE SWISS ANETZ NETWORK

The ANETZ stations have been taken in operation stepwise from 1978 on; routine service has begun 1981.

The 10 min. data are deposited in the original state delivered by central AZEN. Hourly sums (kept in legal zone time), means etc., are gained from these data using interpolation to fill small gaps. Internal consistency tests and cross-checks may lead to rejection of some values. Manipulated values at this level are duly flagged.

The network serves primarily meteorological purposes and, consequently, the main care concerning performance and accuracy is devoted to standard parameters. Controls of horizontal irradiation data have been carried out only when the opportunity was given for comparisons with independently operated and calibrated instruments.

The results of such controls are listed in Table 1. Documented in the last row of Table 1 is another, rougher but larger test, which includes 30 stations with altitude below 1000 m a.s.l.. This test compares the measured daily sums with predictions by a model using METEOSAT II images (visible channel). Clearly, the scatter of individual values must be larger because of model shortcomings. However, large systematic errors resulting from unproper characterisation of the ANETZ pyranometers would be evident, because the model itself is calibrated against the pyranometers of the German network (4). It therefore may be concluded, that the accuracy of the ANETZ irradiation measurements is sufficient for use in solar energy applications.

References

1. Ambrosetti, P.: 1983, measured irradiation (private communication).
2. Ineichen, P.: 1983, "Quatre années de mesures d'ensoleillement à Genève 1978-1982", Thesis No. 2089, Sciences Faculty, Univ. Geneva.
3. Heimo, A.: 1983, "Contrôle de qualité du système RASTA", Internal Rept. Swiss Met. Inst. (in press).
4. Möser, W.: 1983, "Kartierung der Globalstrahlung aus Satellitenbildern", Thesis Univ. Cologne.

TABLE 1

Accuracy evaluations of ANETZ pyranometers

The values of the external instrument is regarded as the independent (X), those of the ANETZ instrument as the dependent (Y) variable

Station	Period	Sums	Cases	Units	Y = aX + b		correl. coeff.	Xmean	MBE	RMSE	Instrument
					a	b			in % of Xmean		
Locarno	30 Sep 81 29 Oct 81	hour	105	MJm ⁻² h ⁻¹	.914	.017	.999	1.13	-7	9	PDI
Locarno	18 Nov 81 4 Feb 82	day	61	MJm ⁻² d ⁻¹	.993	.198	.998	4.95	+3	4	EP (1)
Geneva (+)	1 Jan 80 30 Jun 82	day	848	"	.962	.230	.991	12.05	-2	9	CM5 (2)
Davos	6 Feb 82 23 Feb 82	10 min.	1040	Wm ⁻² (*)	.999	5.334	.997	270.69			EP (3)
30	1 Apr 82 30 Apr 82	day	898	MJm ⁻² d ⁻¹	.924	1.46	.887	17.52	+1	28	Mdel (4)

(+) External instrument 5 km away from ANETZ station

(*) Mean irradiance during 10 minute



5.C SOLAR RADIATION MEASUREMENTS

Edwin Flowers

NOAA/ERL-ARL, R32X2
Solar Radiation Facility
Boulder, CO 80303

SOLAR RADIATION MEASUREMENTS

INTRODUCTION

This paper will present information on pyrhemometers and pyranometers, their characterization, calibration and use as reference instruments and for routine, continuous measurements. The data that is presented have been obtained from experiments and intercomparisons whose main objectives were based on the ultimate end use of the instruments, namely for solar resource monitoring. This report is not intended as a comprehensive review of work of this nature.

ISNTRUMENTATION

This paper is concerned with two basic types of radiation instrumentation:

1. Pyrhemometer - used to measure the direct radiation and some portion of the circumsolar radiation on a surface normal to the beam. The amount of circumsolar is determined by the view geometry; in meteorological practice this is usually between 5 and 6 degrees full view angle.
2. Pyranometer - used to measure the radiation in the hemisphere above the plane of the receiver.

Pyrhemometer

Three kinds of pyrhemometer can be identified: the absolute, self-calibrating pyrhemometer, the thermopile pyrhemometer commonly referred to as the NIP (normal incidence pyrhemometer), and the silicon cell pyrhemometer.

Two older absolute pyrhemometers are the Angström compensation pyrhemometer and the Smithsonian water flow pyrhemometer. The Angström instrument is still in use although in its present configuration it is not used as an absolute instrument, that is, it now requires calibration. The Angström is manufactured in the United States by Eppley Laboratories. The Smithsonian water flow pyrhemometer is seldom used nowadays although one has recently been rebuilt by Eppley Laboratories. This type of instrument has not been used as a standard instrument for perhaps 30 years. Modern absolute instruments of the cavity type are the Kendall (manufactured by Technical Measurements, Inc.), the Eppley HF (manufactured by Eppley Laboratories), the Willson ACR (no longer commercially manufactured) and the PMO designed at the World Radiation Centre, Davos, Switzerland.

Thermopile

Eppley Laboratories: model PSP (B), model 8-48 (B&W)
Hollis Observatories: model MR-1 (B)
Hy-Cal: model P-8405-A (B)
Kipp & Zonen: model CM-6 (B), model CM-11 (B)
Schenk: (B&W)
Swissteco: (B)
Weathertronics: model 3015 (B) (Formerly Spectrolab model SR-75)

Silicon

Dodge Products: model SS-100
Hollis Observatories: model MR-5
Licor: model 220-S
Matrix: model MK-1-G
Rho Sigma: model 1008
Solar Data: model 81B

INSTRUMENT CHARACTERISTICS

All pyrheliometers and pyranometers making measurements in the atmosphere are affected to varying degrees by ambient conditions. For the thermopile detectors, the principal response characteristics are those due to temperature and angle of incidence of the radiation. Lesser effects are those of non-linearity and spectral dependence. For the silicon instruments the greatest effect is usually that of spectral dependence although some of the other characteristics can be equally important if the instrument is poorly constructed.

Figure 1 presents temperature response curves for a group of instruments that have been used as working reference standards at our facility. Although all of the instruments represented by curves have temperature compensation circuits to minimize this effect, it is obvious that for several instruments the compensation is not adequate. The tests for temperature that produced these response curves are essentially static tests and as such indicate the steady state response at any temperature. Figure 2 presents temperature response curves for other kinds of instruments. Neither the Kipp CM-6 or the Schenk is temperature compensated and their curves is a typical shape for this kind of instrument but different numbers of this instrument will have significantly different response values at the same temperature. The Eppley 8-48 is temperature compensated. We have not tested a large enough sample of the Hy-Cal instruments to say whether the shape of the curve is typical. From these curves it is clear that errors as large as 4-5% can occur in measurements at a typical location in the U.S. or when comparing measurements made at two locations which experience large temperature differences. Optimum accuracy can only be had taking account of the instrument temperature response. Composition of the sun plus sky radiation at horizontal exposure may be markedly different than the spectral composition of the sun and sky and ground reflected radiation at tilt. Figure 5 presents tilt response curves for a variety of pyranometers from laboratory, the silicon detectors showed no effects from tilt, the Eppley PSP and Spectrolab instruments showed only small effects. Figure 6 presents the results from a

tilt experiment carried out outdoors with the sun as source. The outdoor results should strictly be considered only relative since an unaffected reference instrument is not available. For the outdoor tests, a silicon sensor was used as reference and for the reasons cited earlier it cannot be assumed that its sensitivity is not affected by tilt in an outdoor test. However, the relative differences in response between the different kinds of instruments should be considered a real feature and as the figure shows these differences are large, particularly between the Eppley PSP, Spectrolab and silicon (reference) group of instruments and the Eppley 8-48 and Schenk pyranometers, both of which are black and white thermopile instruments. Although it is believed that the differences shown Figure 6 are mostly caused by tilt, the individual cosine errors of the different instruments are included in the results as presented.

There is very little experimental data available on the linearity of pyranometers. Eppley Laboratories asserts that their PSP model pyranometer is linear to within $\pm 0.5\%$ over an irradiance range from 0 to 2800 w/m^2 , the limits of their tests. Their tests on specimen samples of a Kipp CM-6 and a Schenk both showed a rather uniform decrease in sensitivity of 4% over the 150-1000 w/m^2 range while a sample Licor 220-S showed an increase of a little less than 3% over the same radiation range.

There is also a dearth of experimental data on the spectral sensitivity of various pyranometer. Nominal spectral curves for various silicon detectors provide some information for these kinds of instruments. Likewise, spectral curves for coating materials used on thermopile pyranometers along with spectral information on the transmission of the glass cover materials provide a certain amount information for these kinds of instruments. The assumption is that the gross effect of over glass and sensor coating for an all black instrument is at the fractions of a percent level. For black and white detectors, the assumption is that the black surface is equally absorptive over all wavelengths and that the white surface is equally reflective over the same wavelengths. The critical part of this assumption is with regard to the white surface not only over all pertinent wavelengths but over all angles of incidence. Experimental evidence shows an increase in sensitivity for black & white pyranometers at low sun angles. Whether this should be listed as a cosine response or a spectral dependence may be a moot point.

Calibration transfers are done from pyrhelimeter to pyranometer and from pyranometer to pyranometer. At NOAA, both transfers are done outdoors, and both are affected in varying degrees of importance by all of the instrumental characteristics, responses due to: cosine, temperature, azimuth, tilt, source spectrum, time and flux intensity.

At our facility, only the reference and control pyranometers are involved in the pyrhelimeter-pyranometer transfers, made by the shading disk method. The transfer is made with the pyranometer mounted horizontal and involves shading the direct solar radiation from the pyranometer so that the difference between the shaded and unshaded pyranometer readings is the vertical component of the absolute radiometer. The method uses 5 minutes of shade and 6 minutes without shade and also uses a second pyranometer which

is not shaded. The test pyranometer is continuously ratioed to the second pyranometer for the purpose of calculating what the test pyranometer unshaded value would be at the final shade sample. The derived calibration values for the test instrument are plotted as a function of the sun's elevation angle. Figure 10 shows such a plot for the current reference pyranometer Eppley 19917F3. In the lower right corner of Figure 10 the data are plotted as a cosine response curve (note that the sun angle is the elevation angle, not the zenith angle). Although the data also contain the azimuthal dependence of the pyranometer, the curve may be used for correcting the direct radiation portion of the observed irradiance. The shape of the curve including the hump near 25° sun elevation is typical for Eppley PSP instruments.

Transfers from pyranometer to pyranometer are done by continuous, side-by-side, comparisons of the test and reference instruments. Instantaneous outputs in millivolts for all instruments are obtained for each minute. Ten-minute averages of the outputs of the two instruments are formed and used to calculate a linear equation by the method of least squares. The initial calculation uses all of the 10-minute values in the daylight period. A second pass on the data is then made in which pair values are discarded where the test value differs by 1.5 times the standard error or more from its predicted value. This screening is to eliminate outliers generally caused by building or people obstructions. The linear equation: $C^*(\text{test}) = a + b [C(\text{reference})]$, where a is the y-intercept, b the slope and C the calibration value for the reference, is solved for C^* , the calibration value for the test instrument. Since C has units of millivolts per 1000 watts/m², the calibration is effectively at an irradiance level of 1000 watts. Regression analyses are performed on each day's data to determine day-to-day variability. The final calibration value, however, is determined from a single regression calculated from the entire period of comparison, usually 14 days for most instruments. Only days with appreciable amounts of rain or snow are eliminated in the final analysis. Day-to-day variations for most.

TABLE 1

I. Transfer: Absolute Radiometer to Eppley PSP		Temp	Cosine(azimuth)	sum			
Source:		0.5%	3% (0.5%)	0-5%			
II. Transfer: Eppley PSP to another pyranometer		Temp	cosine	azimuth	spectral	tilt	Long term comparison
Source:							Rel ABS*
Eppley PSP	<1%	1-2%	0-2%	0	1%	0-2%	0-7%
Spectrolab SR75	0-3%	1-2%	U	0	1%	0-2%	0-7%
Kipp CM-6	0-5%	0-5%	0-4%	0	2%	0-5%	0-10%
HY-Cal	0-5%	U	U	U	(0-3%)	0-9%	0-14%
Eppley 8-48	0-3%	U	U	U	0-12%	0-8%	0-13%
Schenk Star	0-7%	0-7%	0-3%	U	0-5%	0-8%	0-13%
Licor P.C.	U	0-6%	0-2%	0-5%	0	0-6%	0-11%
Matrix P.C.	U	U	U	0-5%	0	0-7%	0-12%
RHO Sigma P.C.	U	U	U	0-5%	U	0-17%	0-22%
Lintronic Dome	0-25%	0-25%	0-5%	U	(0-8%)	0-30%	0-35%

ABS* = Sum of relative error + transfer error absolute radiometer to Eppley PSP

FIGURE 1

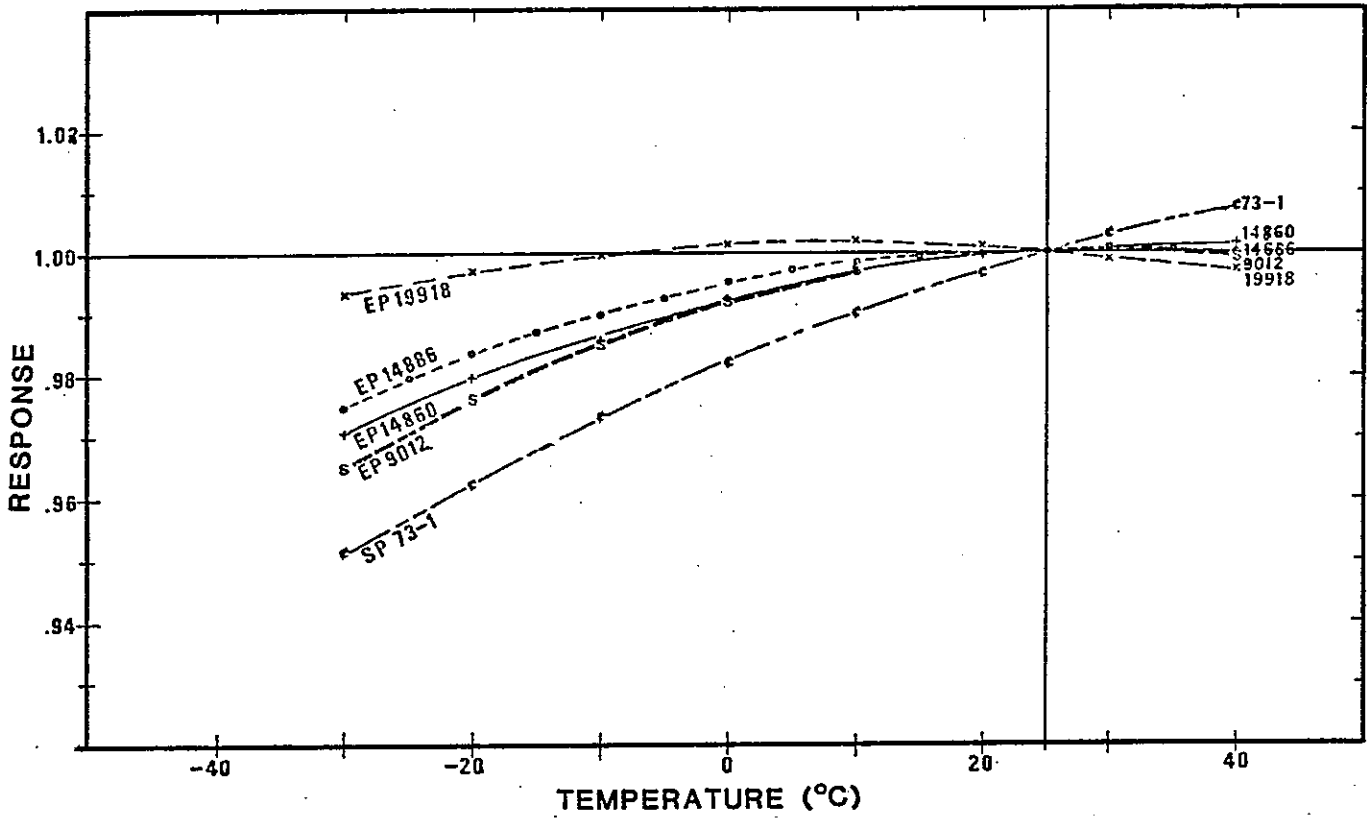


FIGURE 2

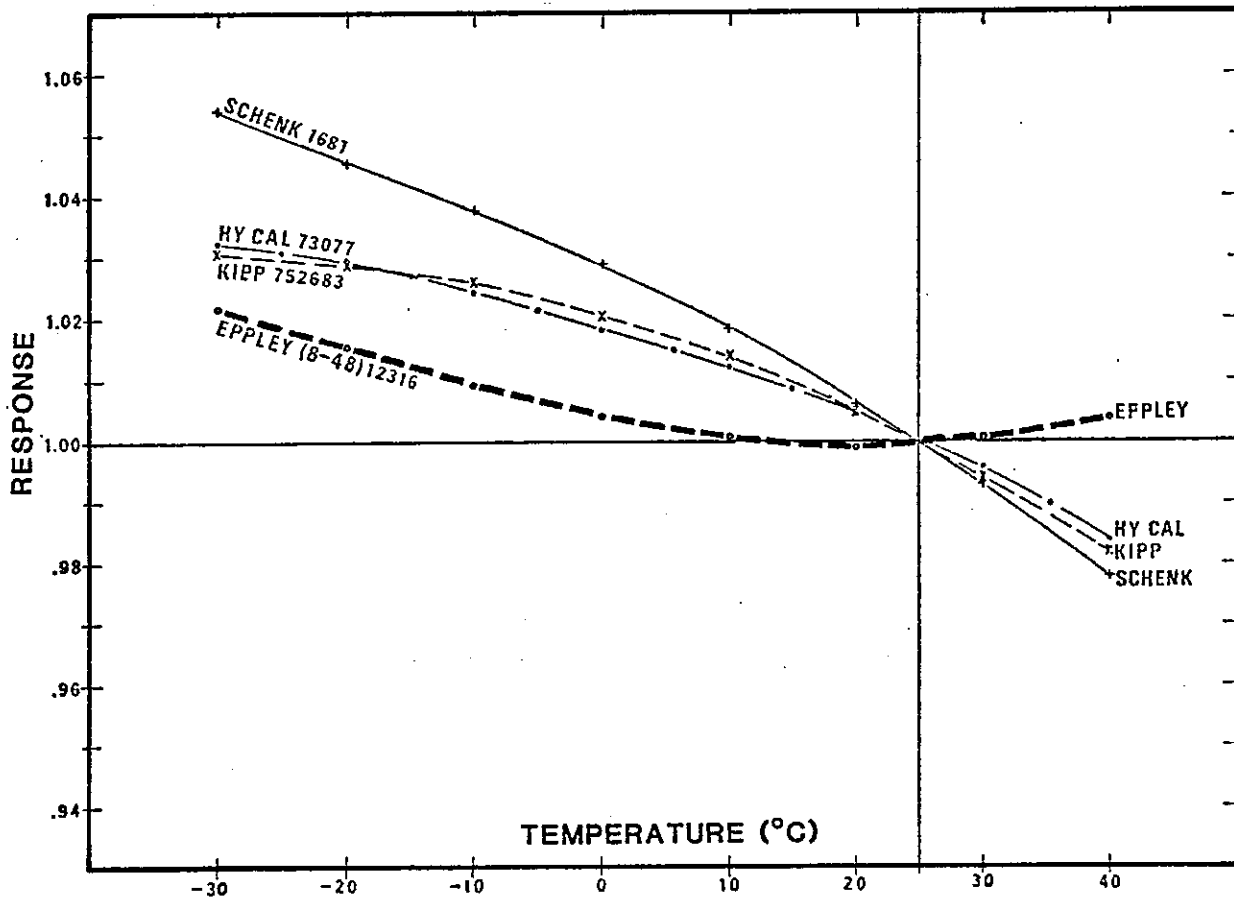


FIGURE 3

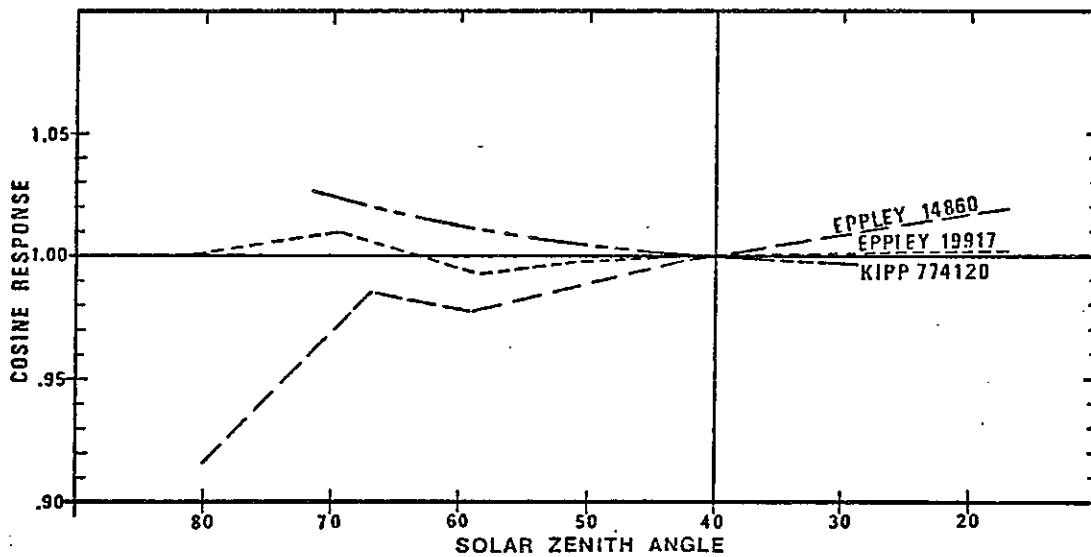
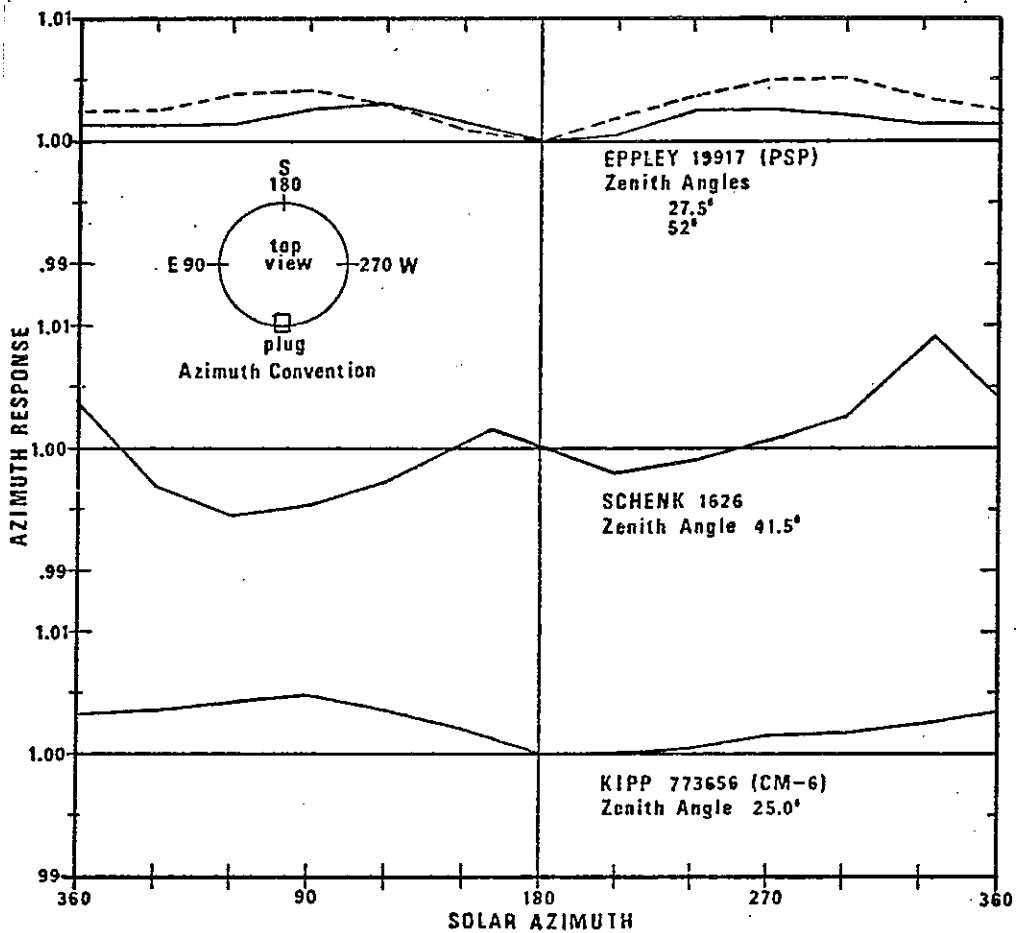


FIGURE 4



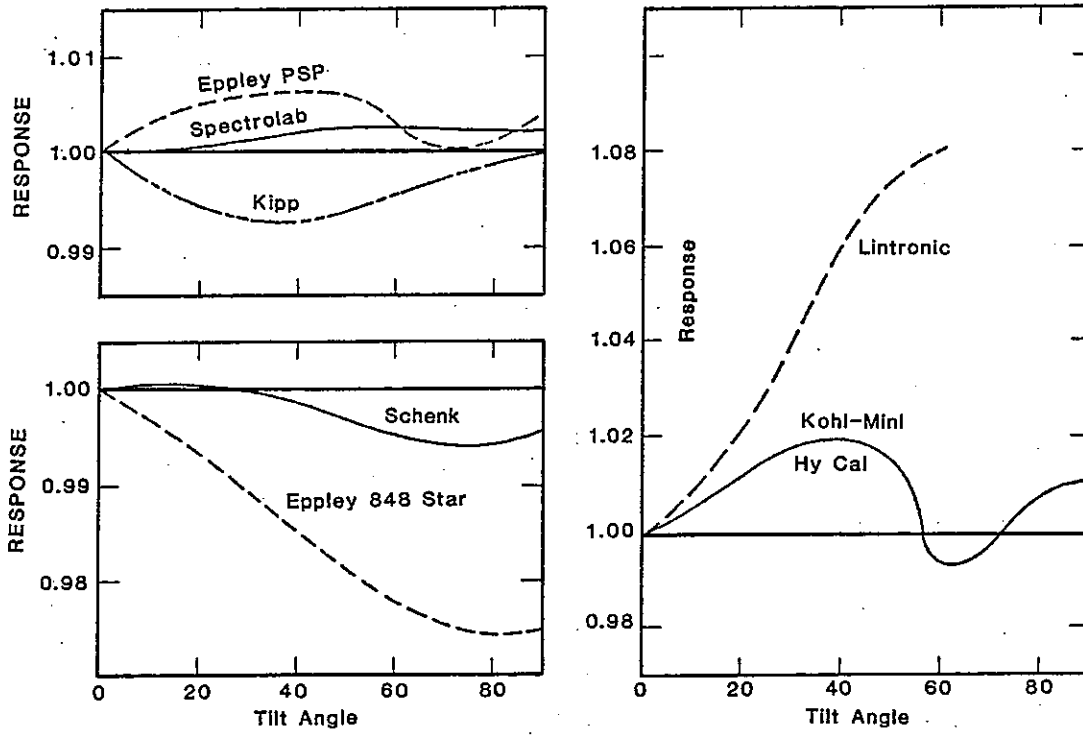


FIGURE 5

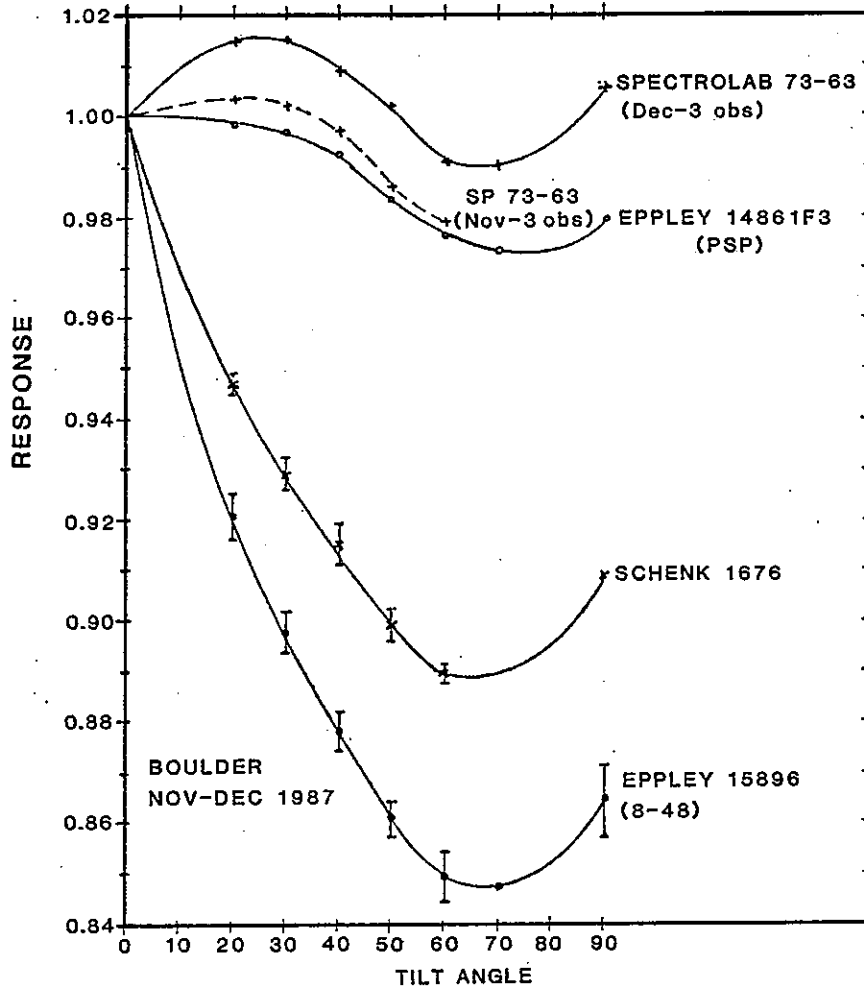


FIGURE 6

NOAA CALIBRATION CHAIN PYRHELIOMETERS

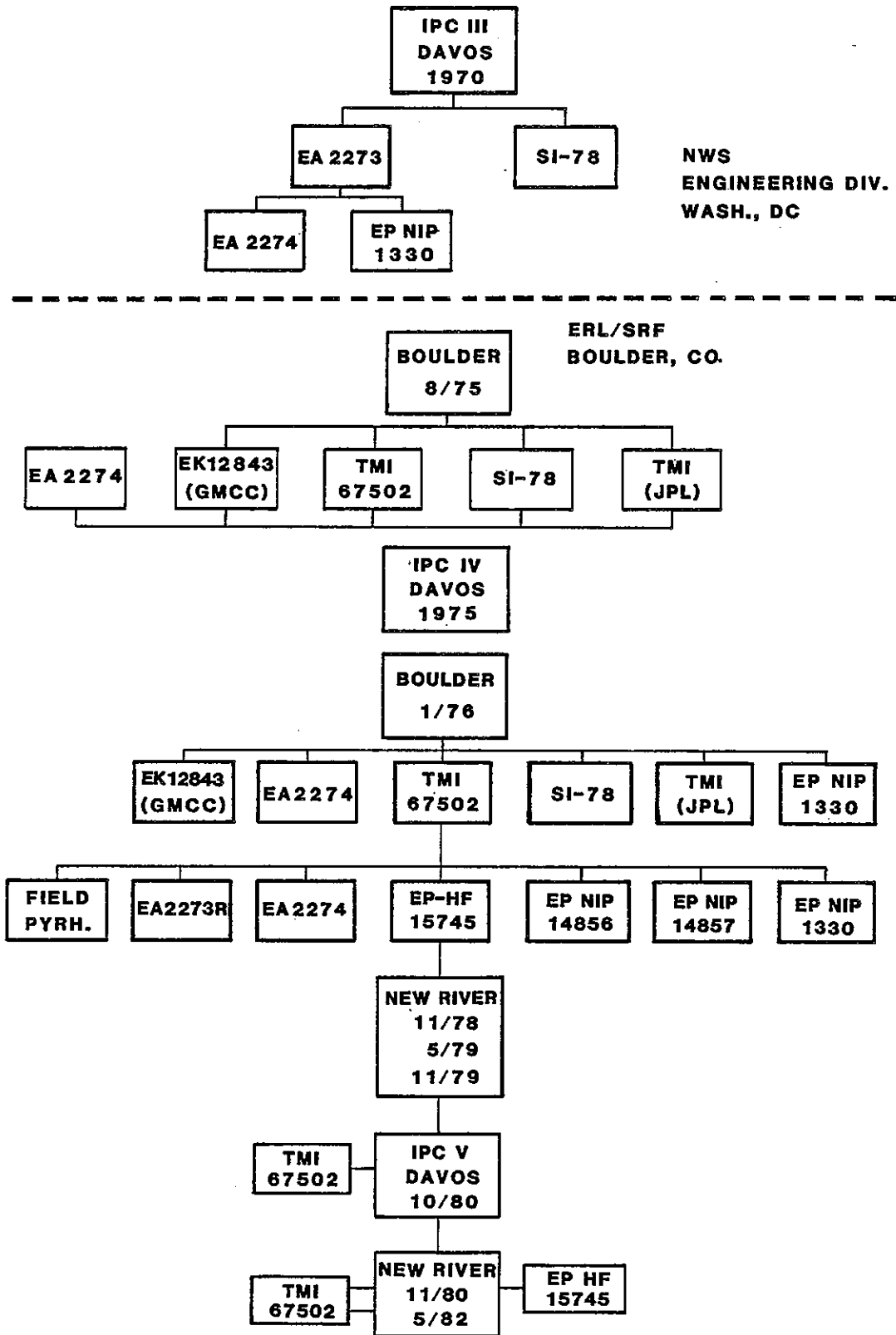


FIGURE 7

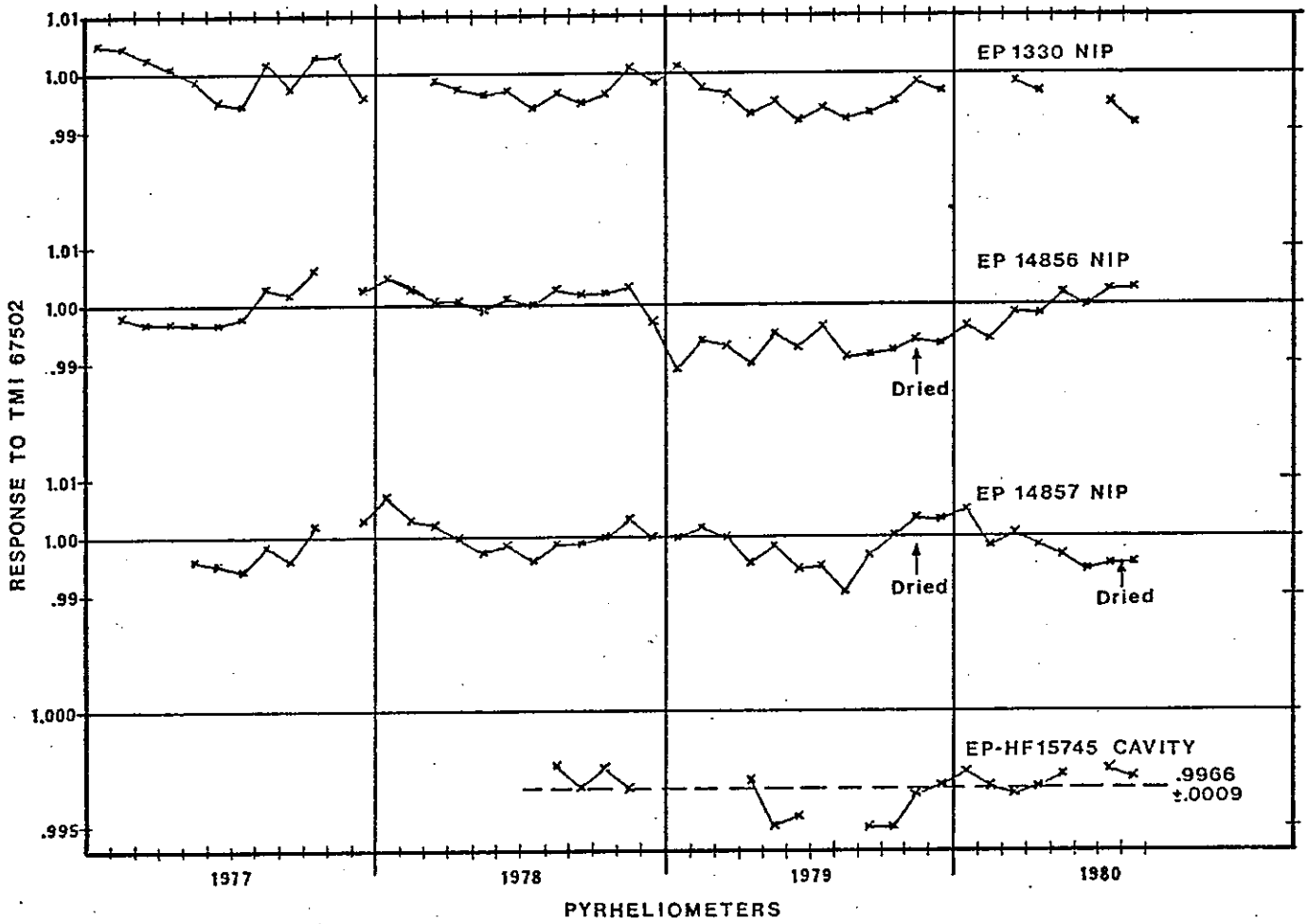


FIGURE 8.

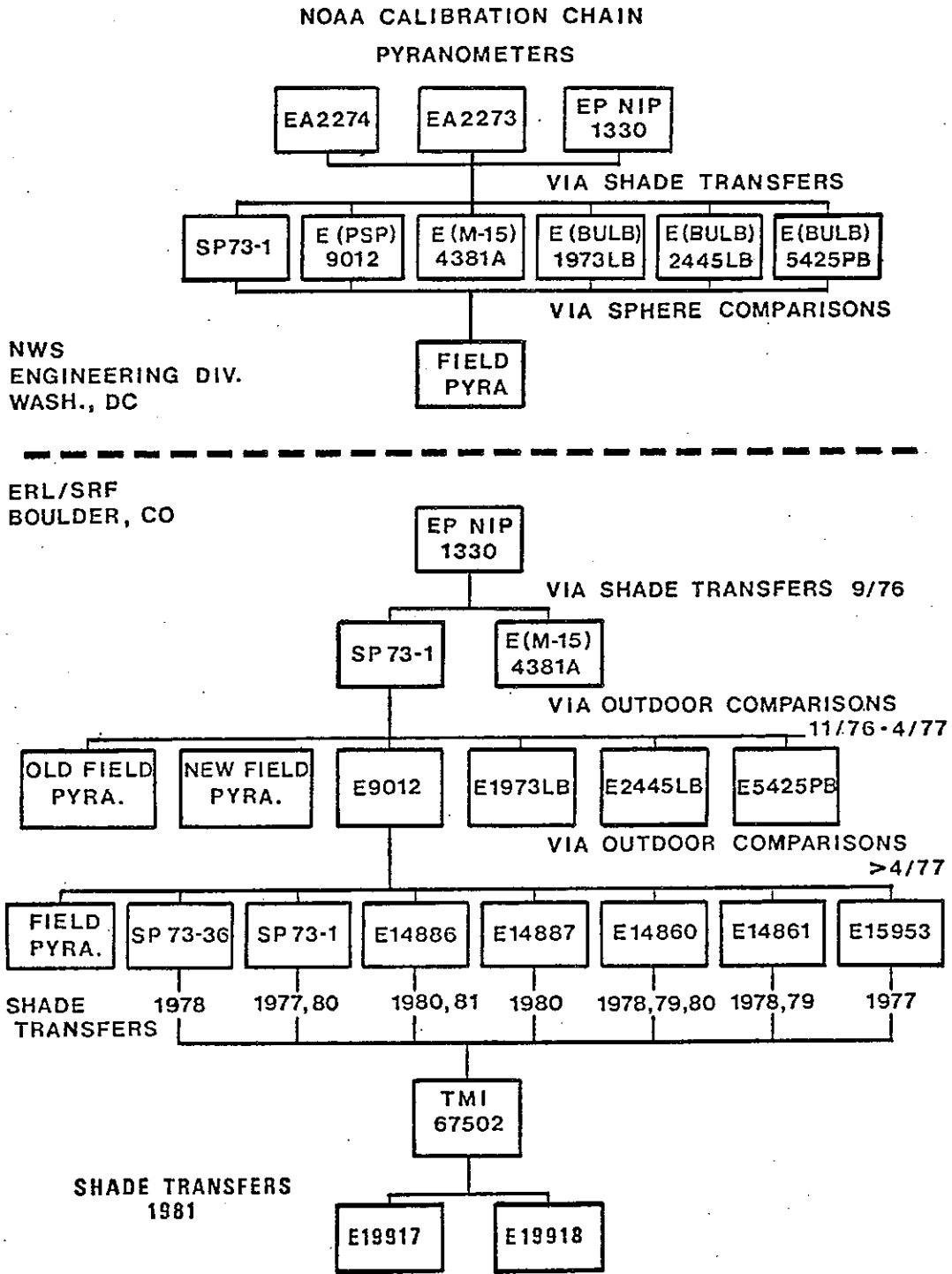


FIGURE 9

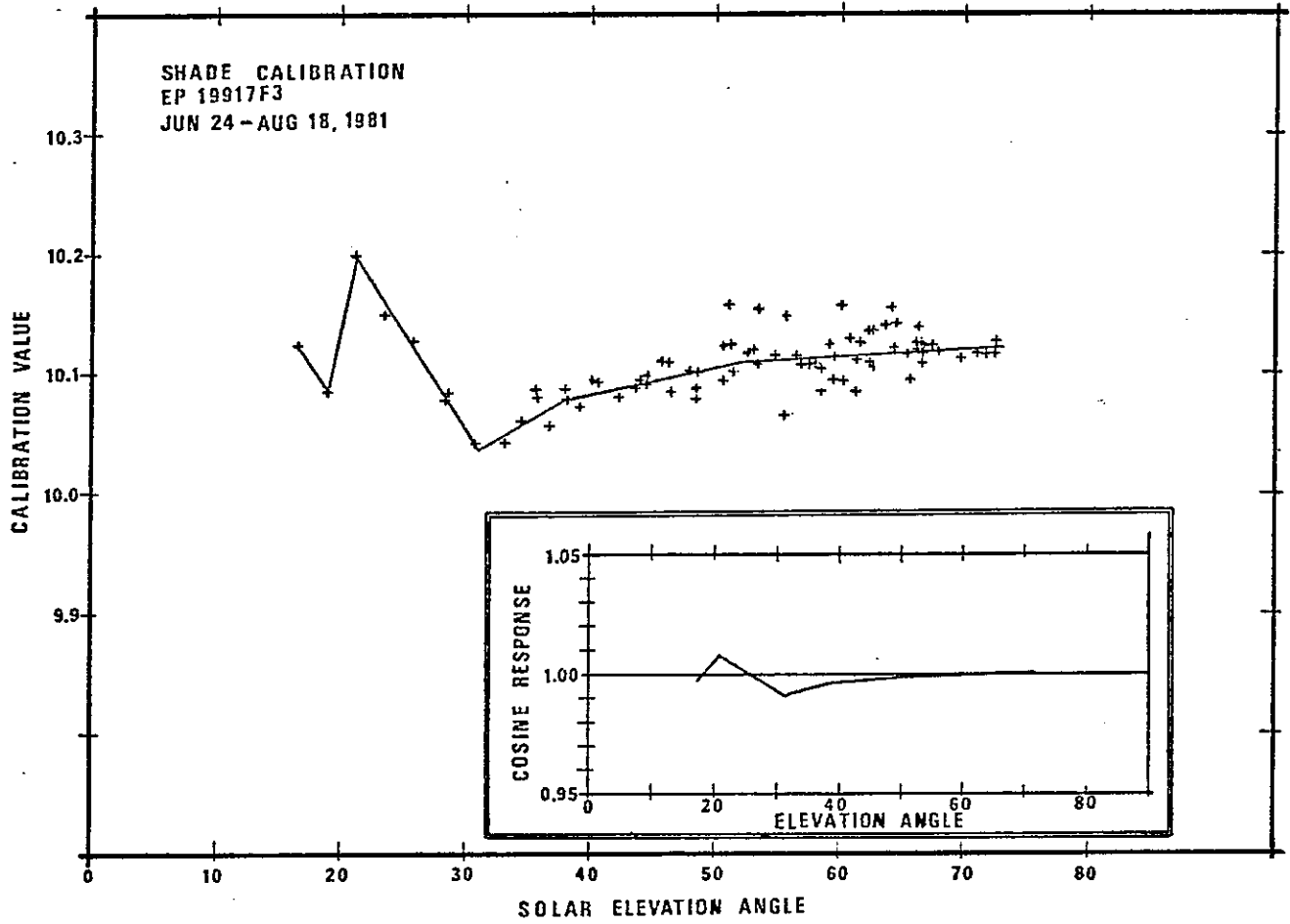


FIGURE 10

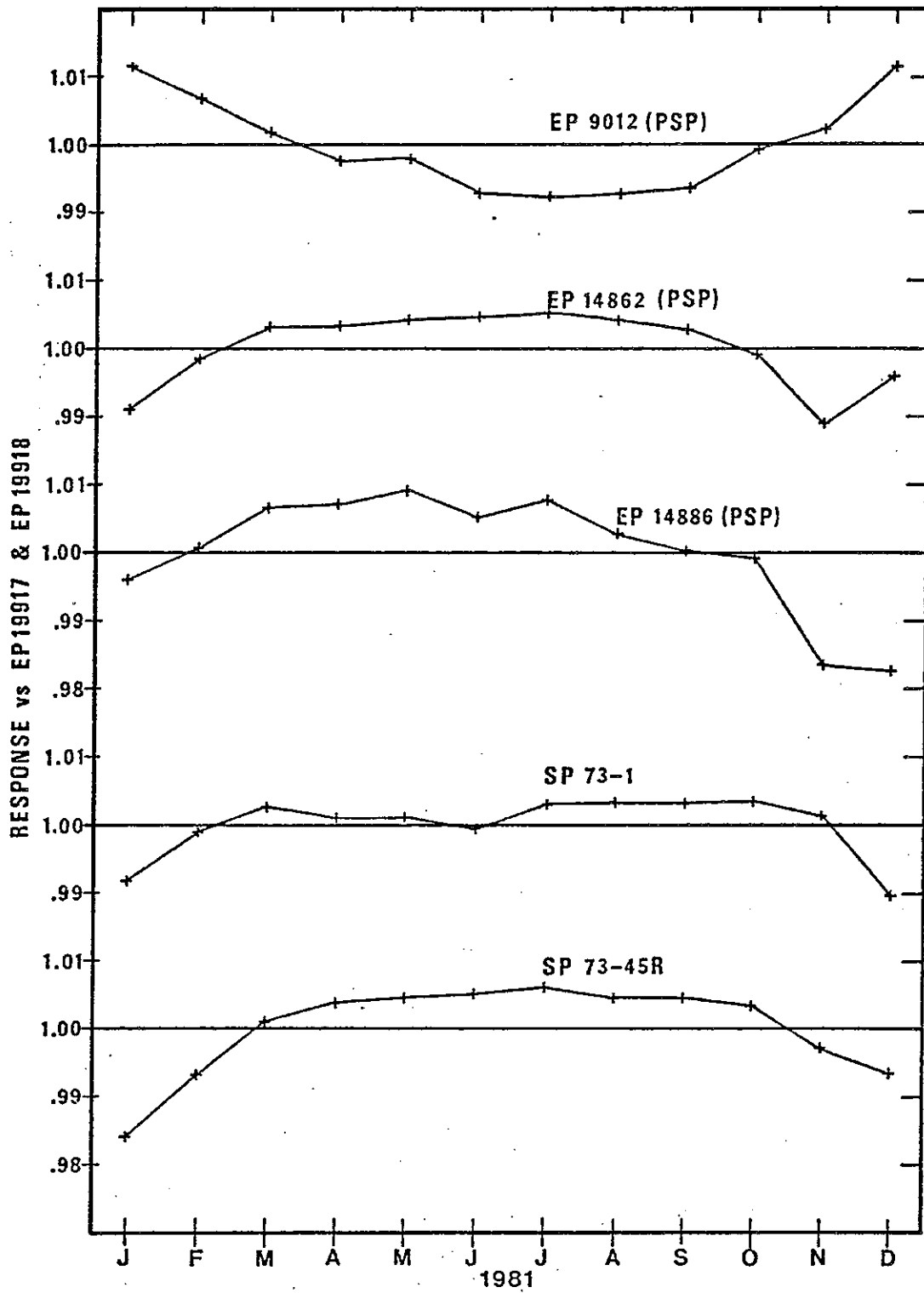


FIGURE 11

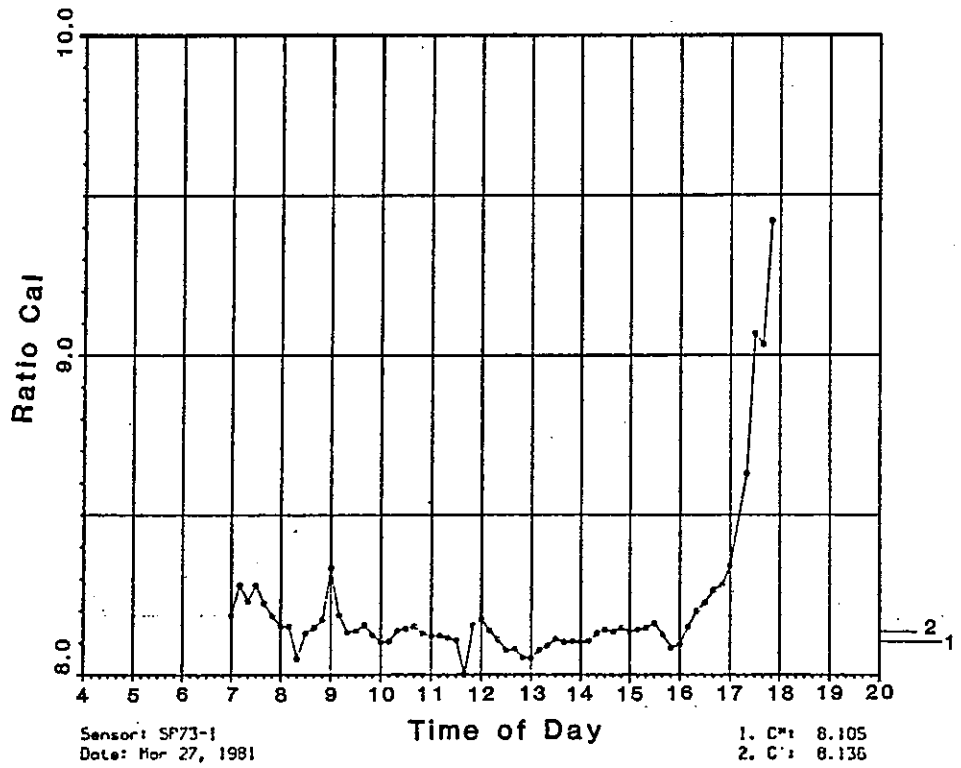
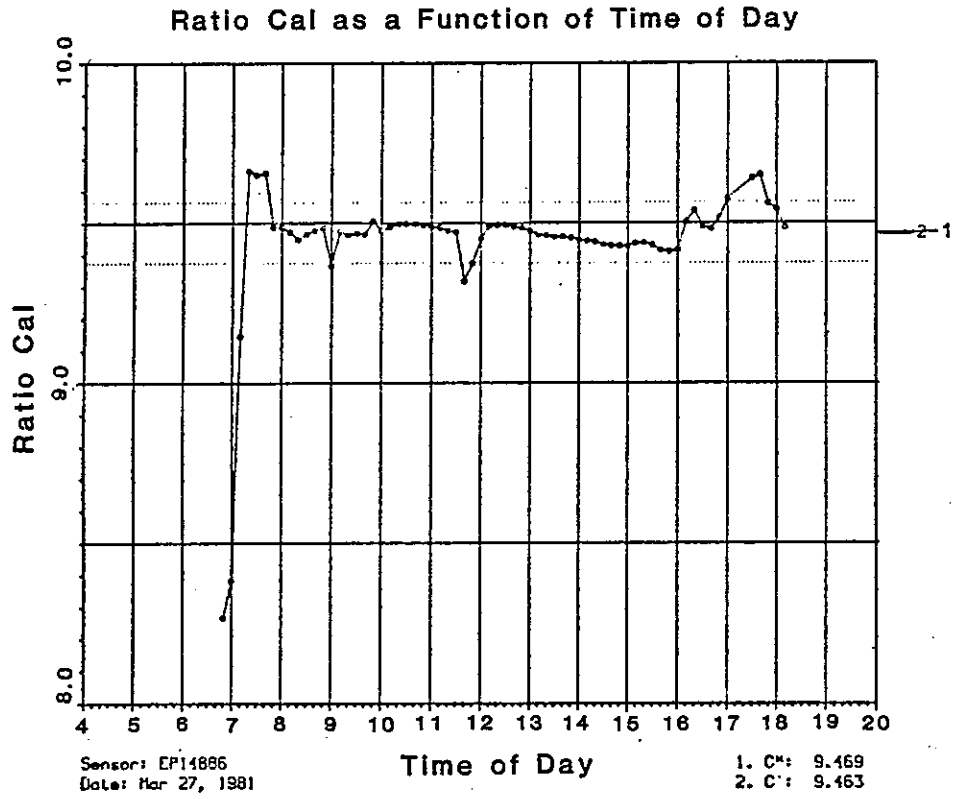


FIGURE 12

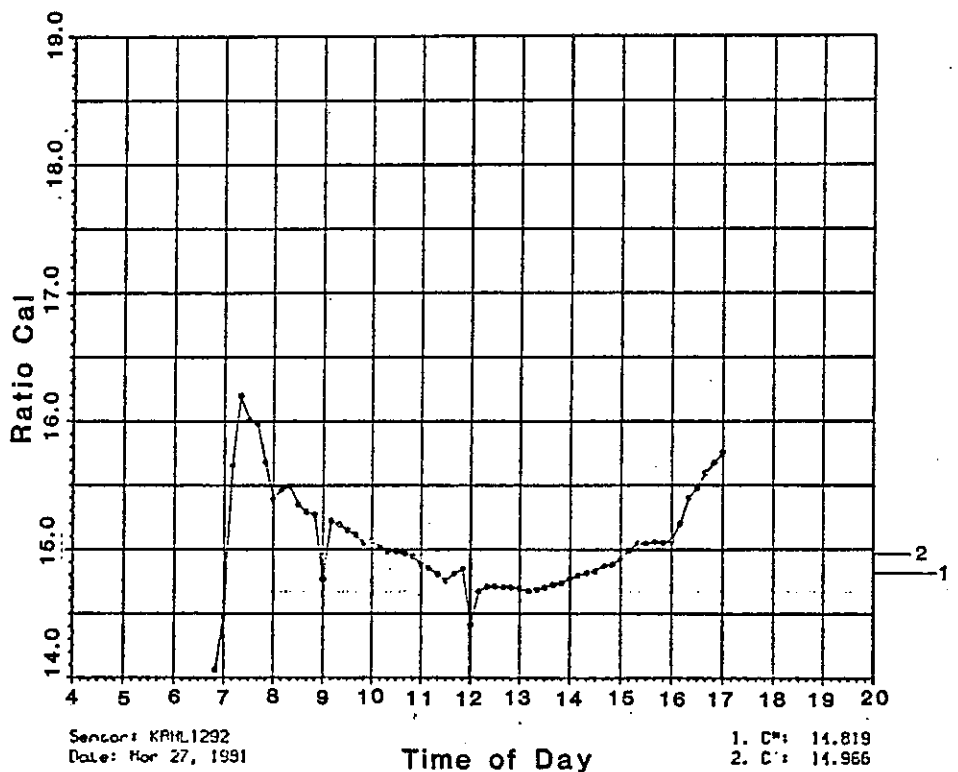
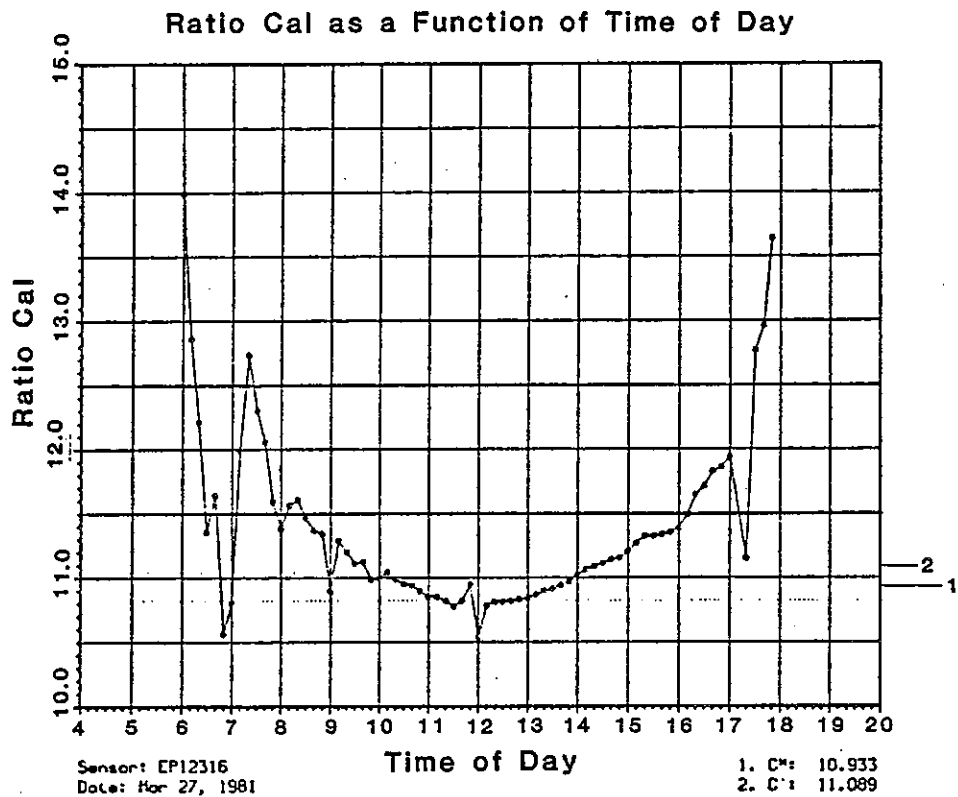


FIGURE 13

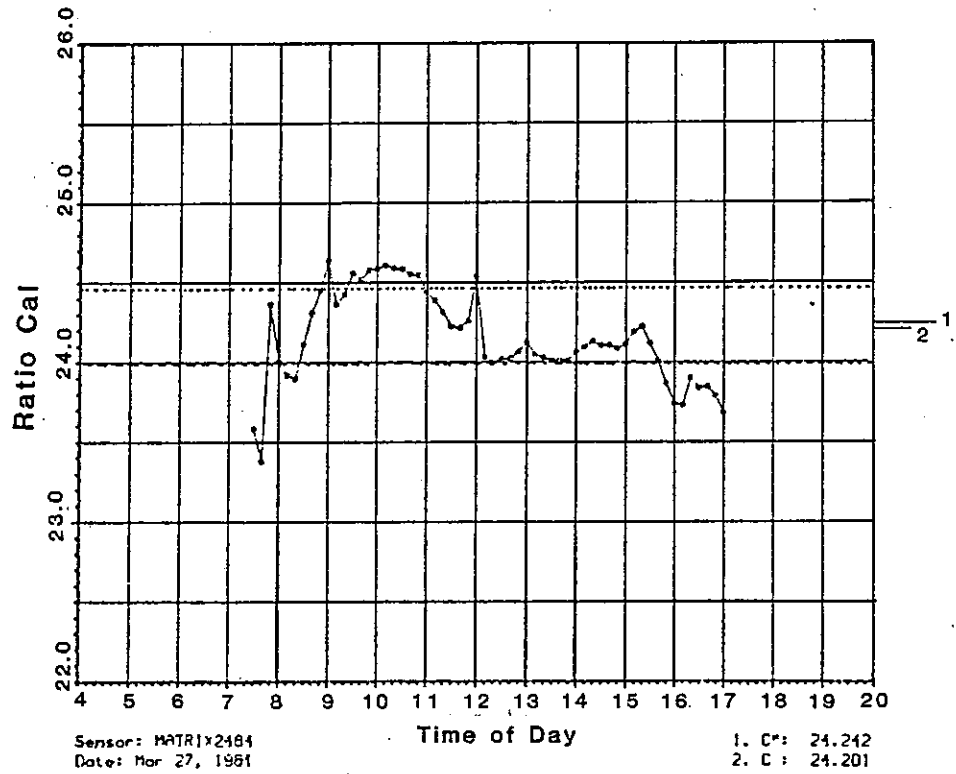
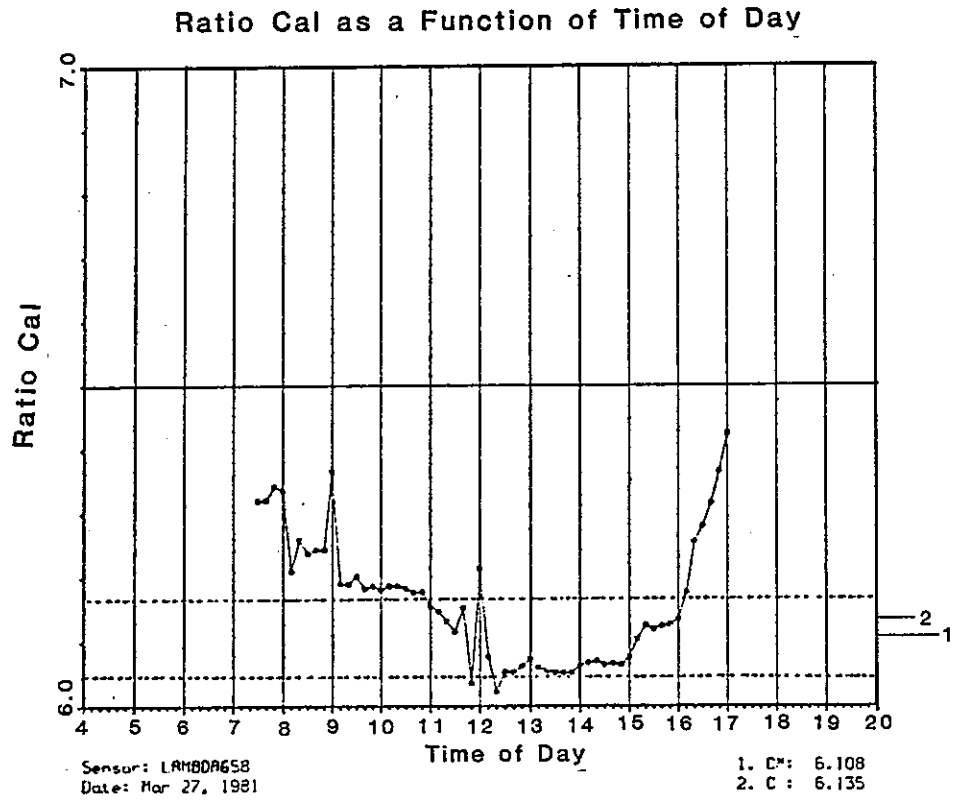


FIGURE 14

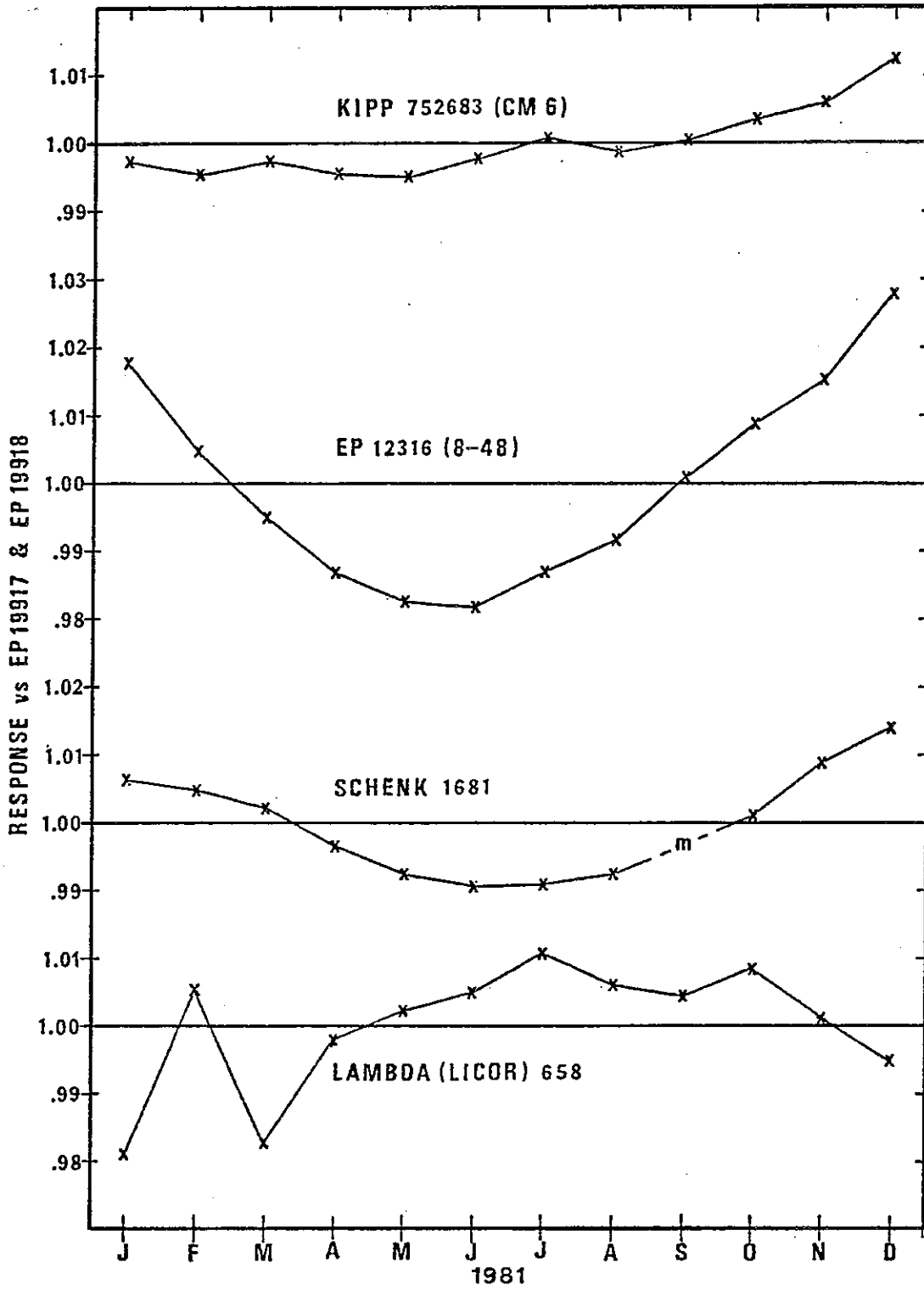
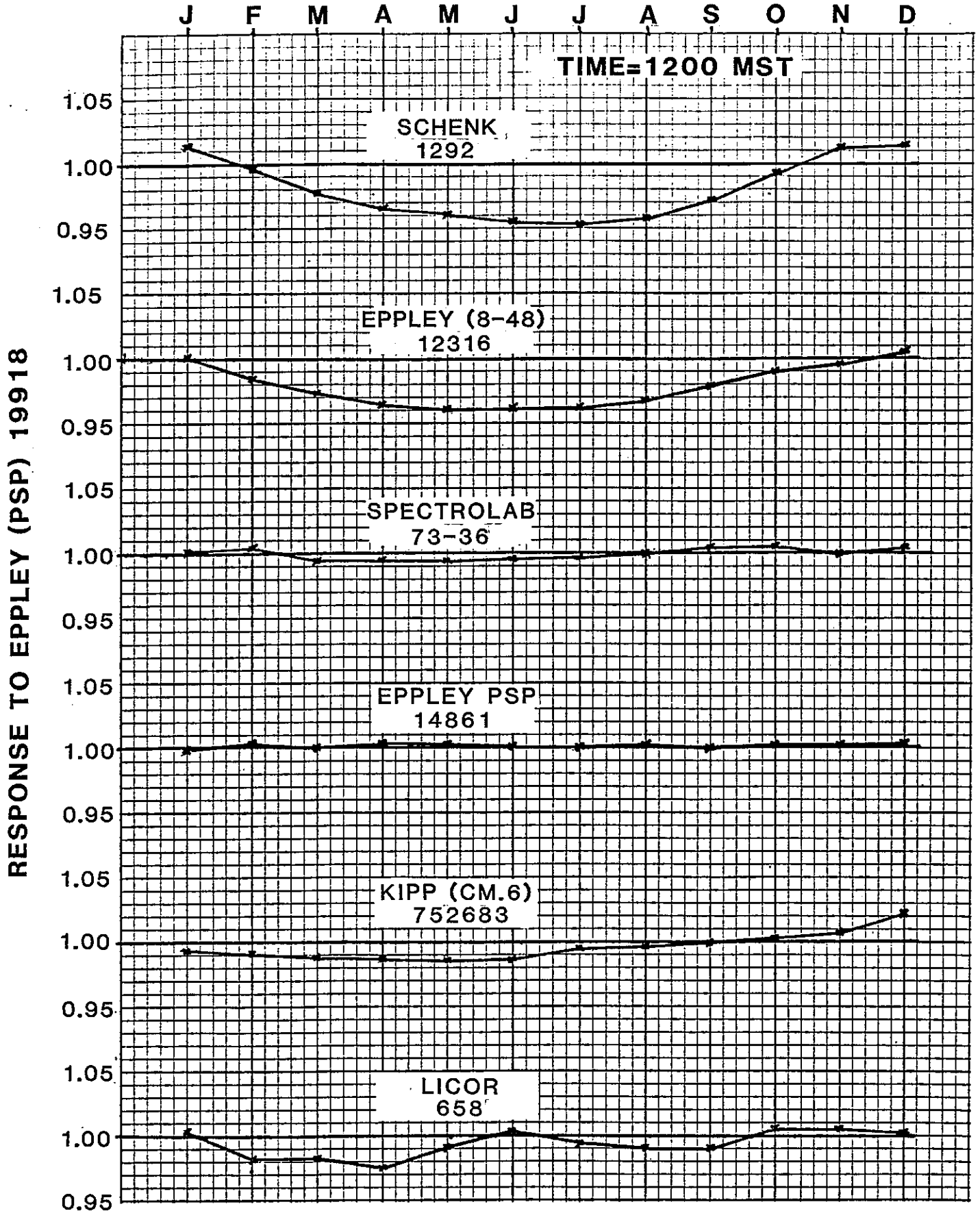


FIGURE 15



SHADED CALIBRATION EP 19917F3 VS TMI 67502 -1983

EP19917F3

8-8-83 A.M.
8-9-83 A.M. }
8-9-83 P.M. }
8-15-83 (1 VALUE)
8-31-83 A.M.
8-31-83 P.M.
9-9-83
9-9-83 A.M. }
9-12-83 P.M. }

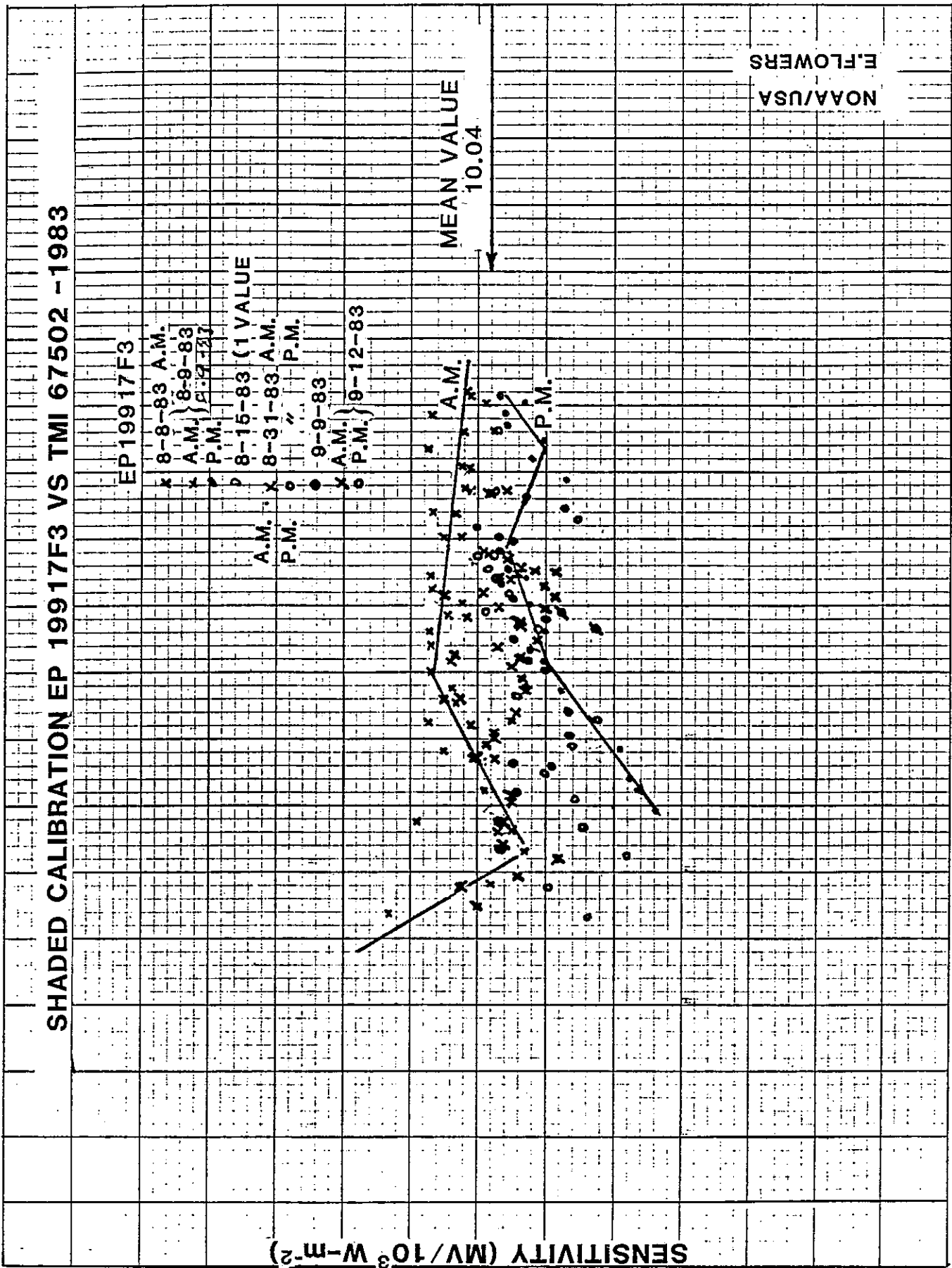
SENSITIVITY (MV/10³ W-m⁻²)

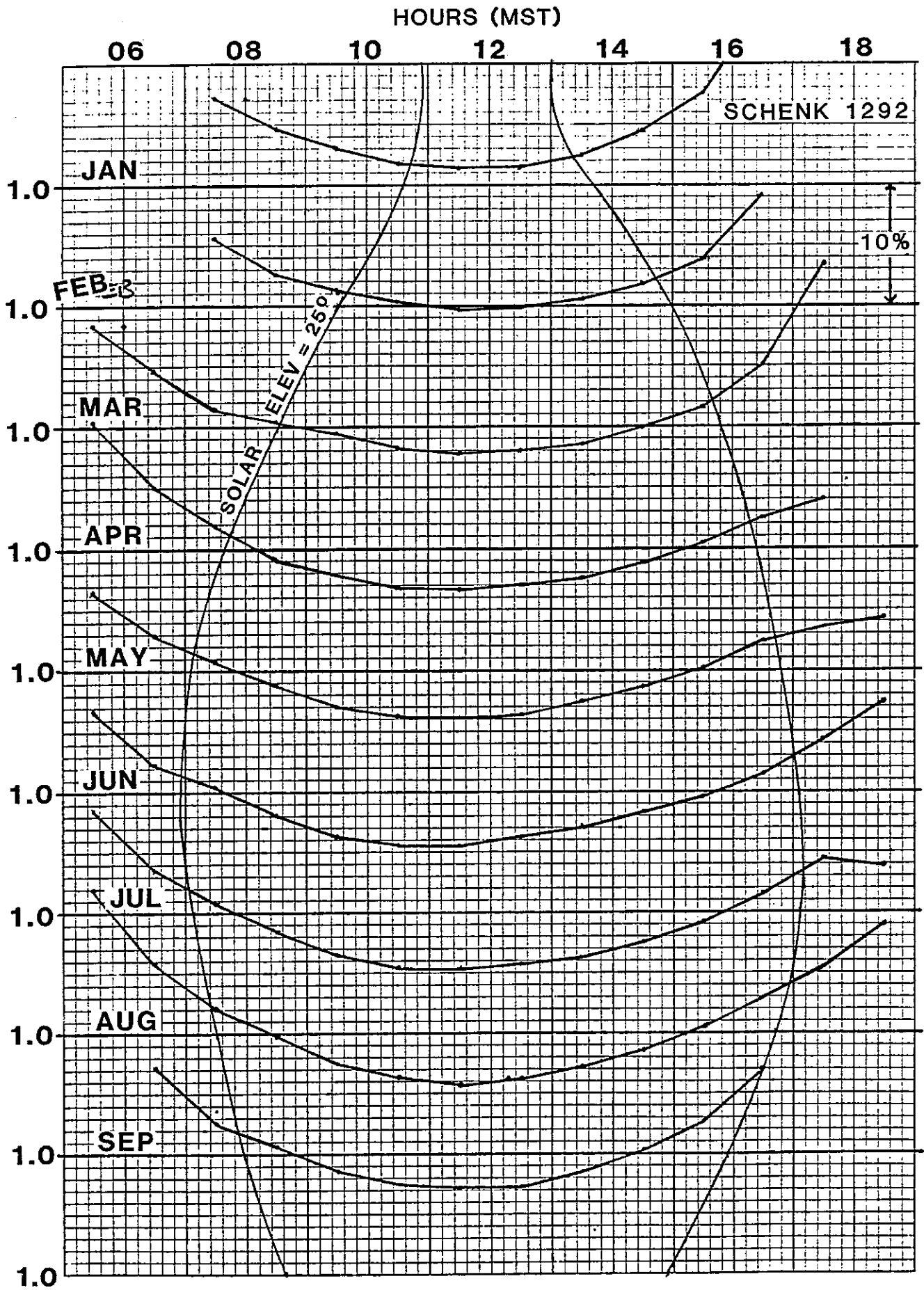
10.2
10.1
10.0
9.9

MEAN VALUE
10.04

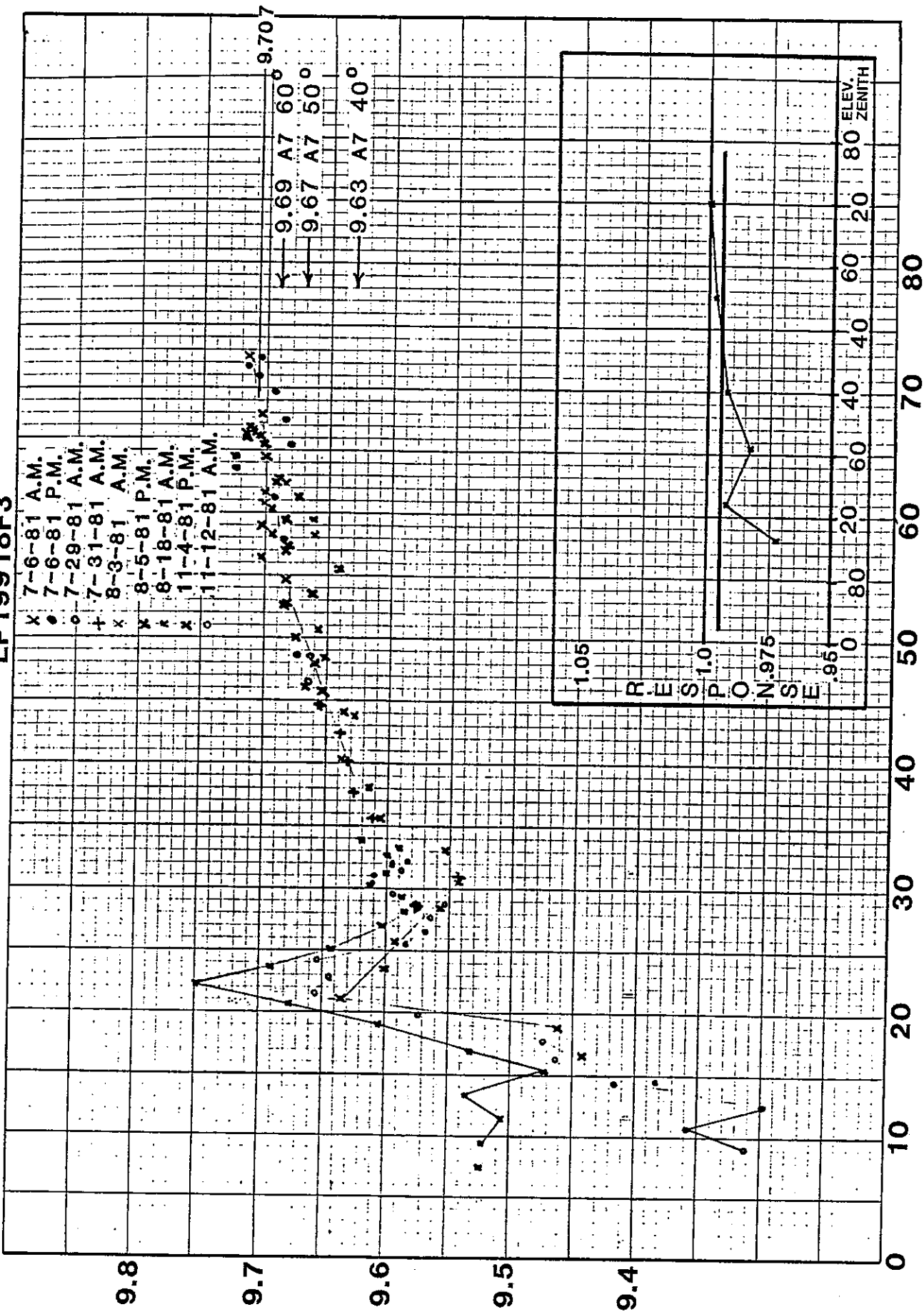
NOAA/USA
E.FLOWERS

0 10 20 30 40 50 60 70
SUN ELEVATION ANGLE

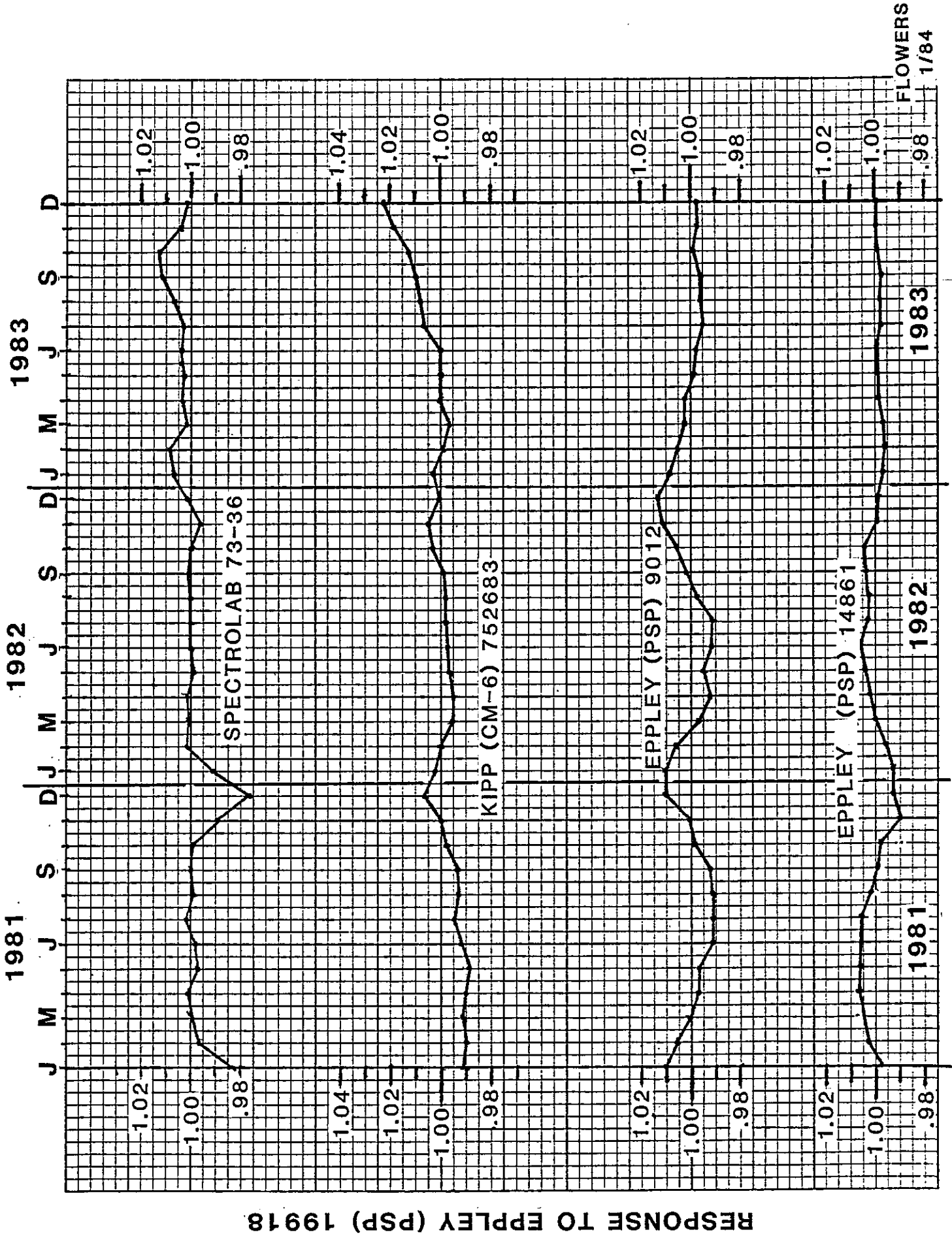


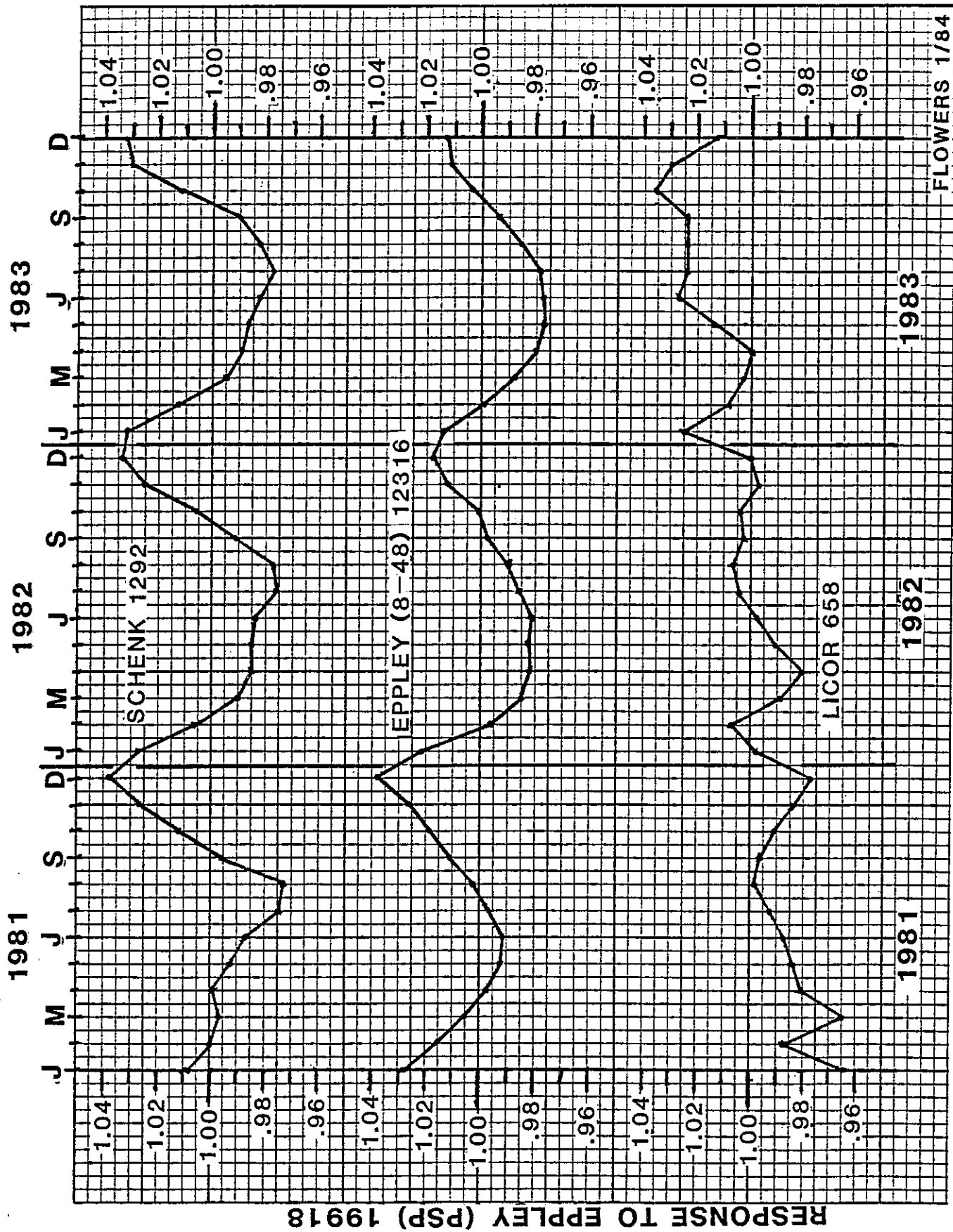


EP 199 18F3

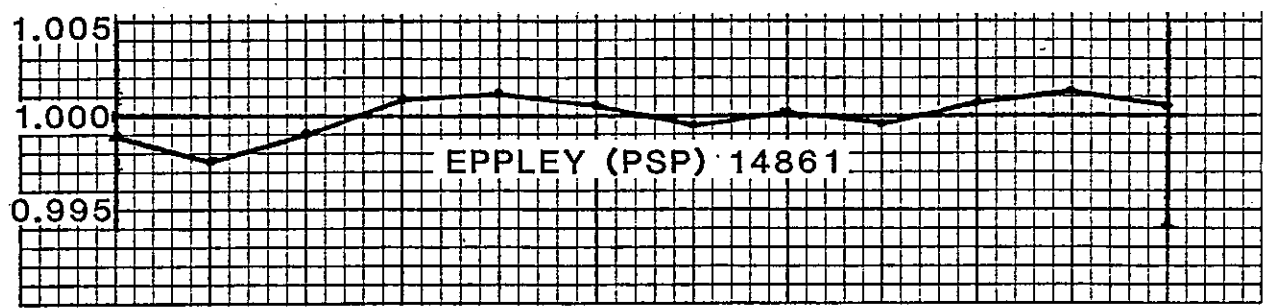
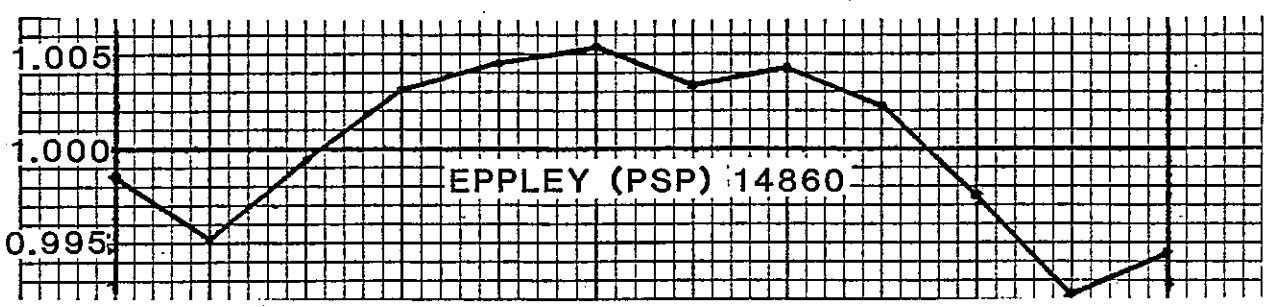
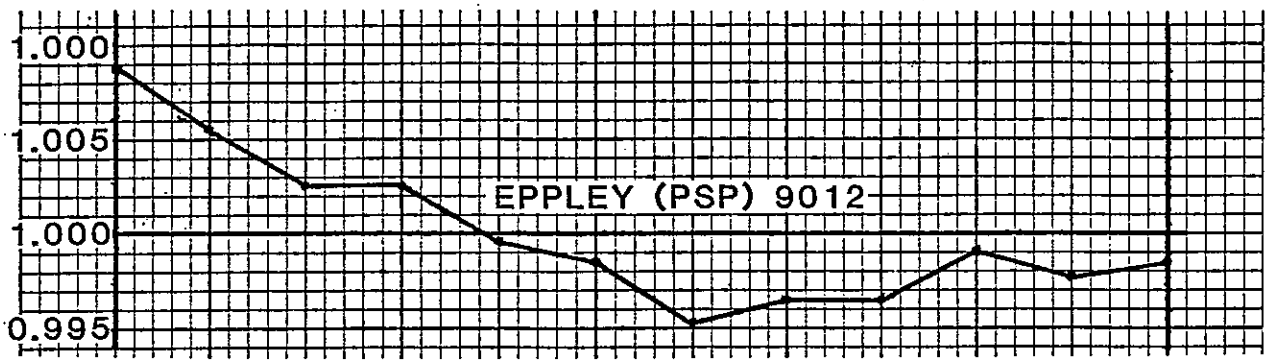
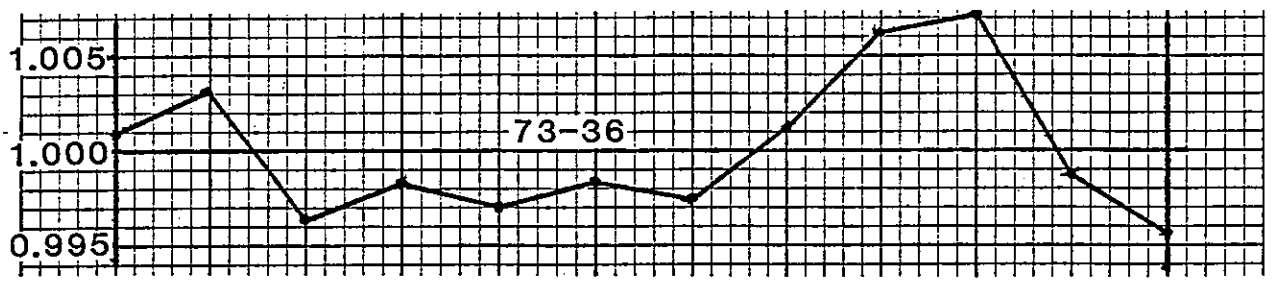
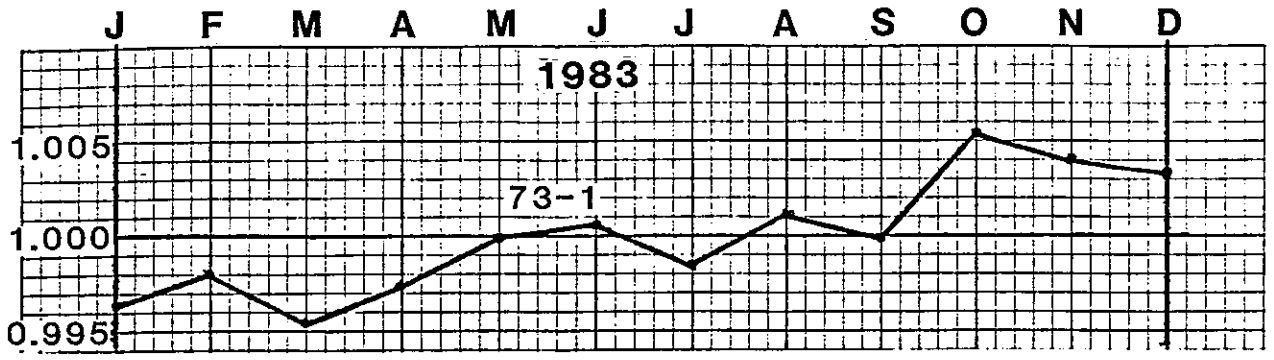


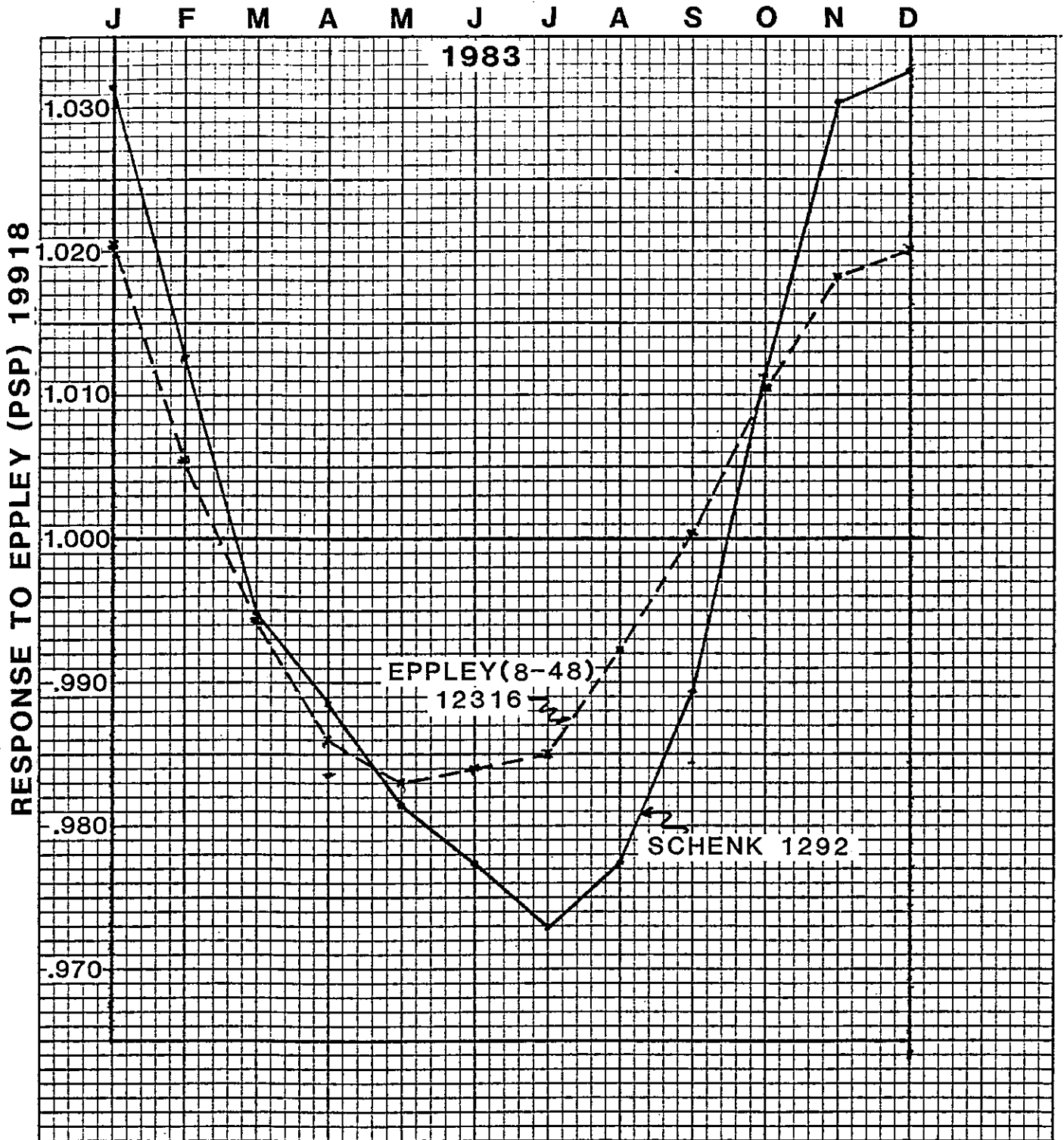
ELEVATION ANGLE



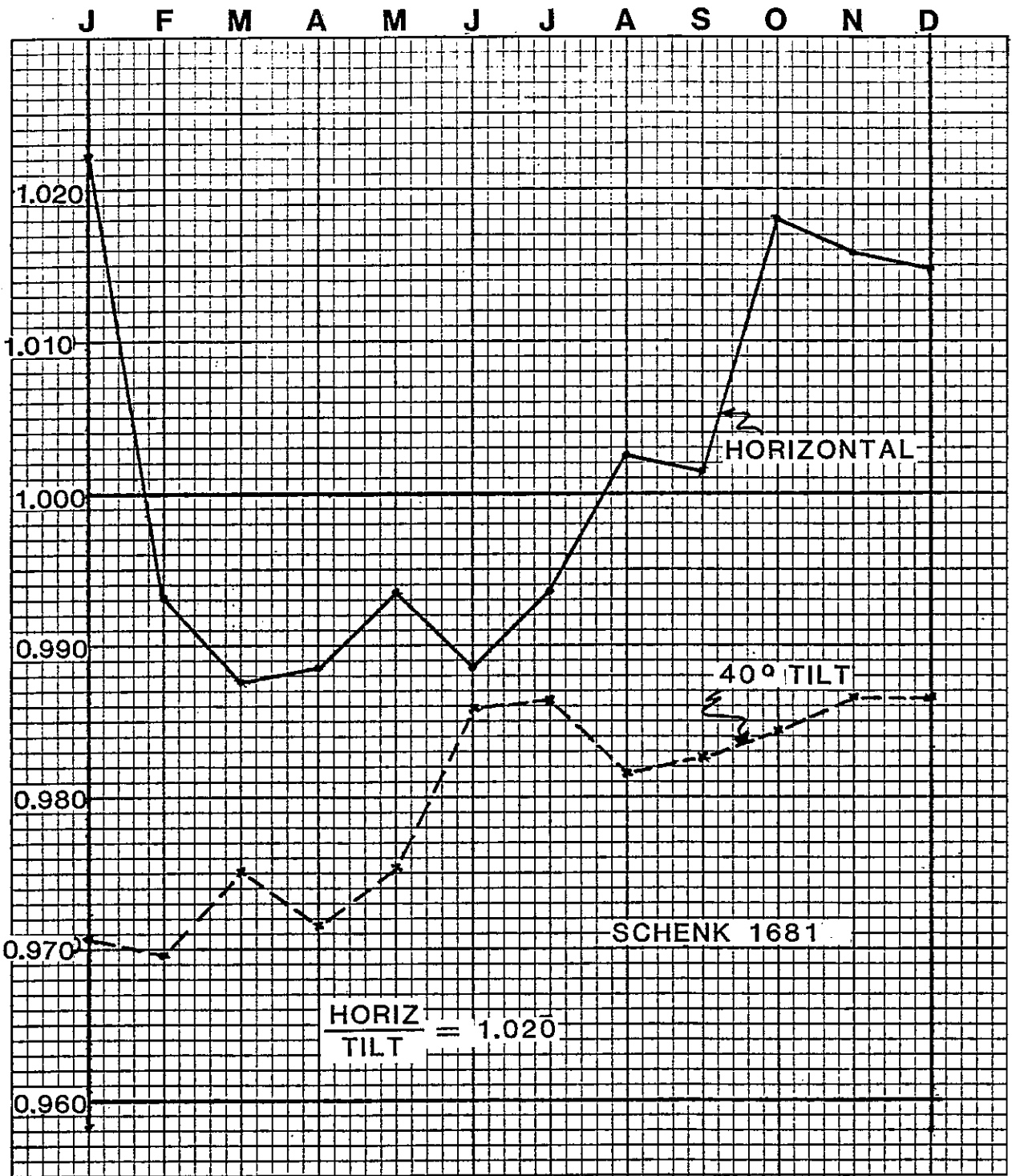


RESPONSE TO EPPLEY (PSP) 19918

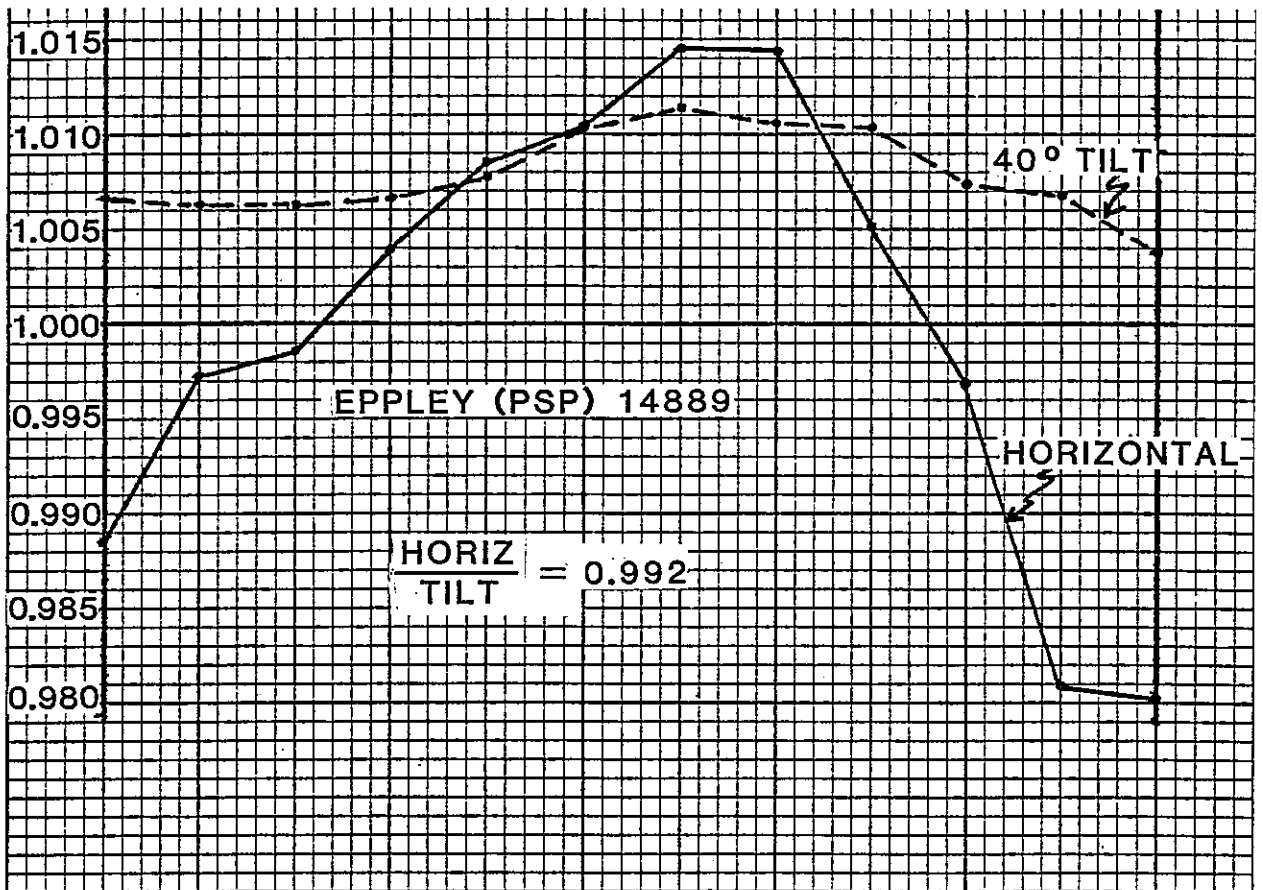
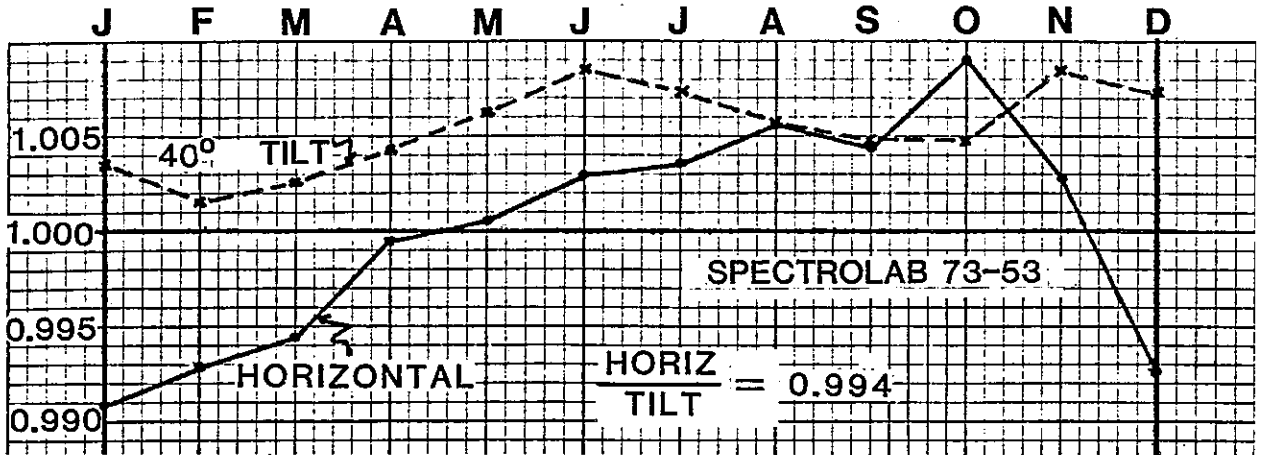


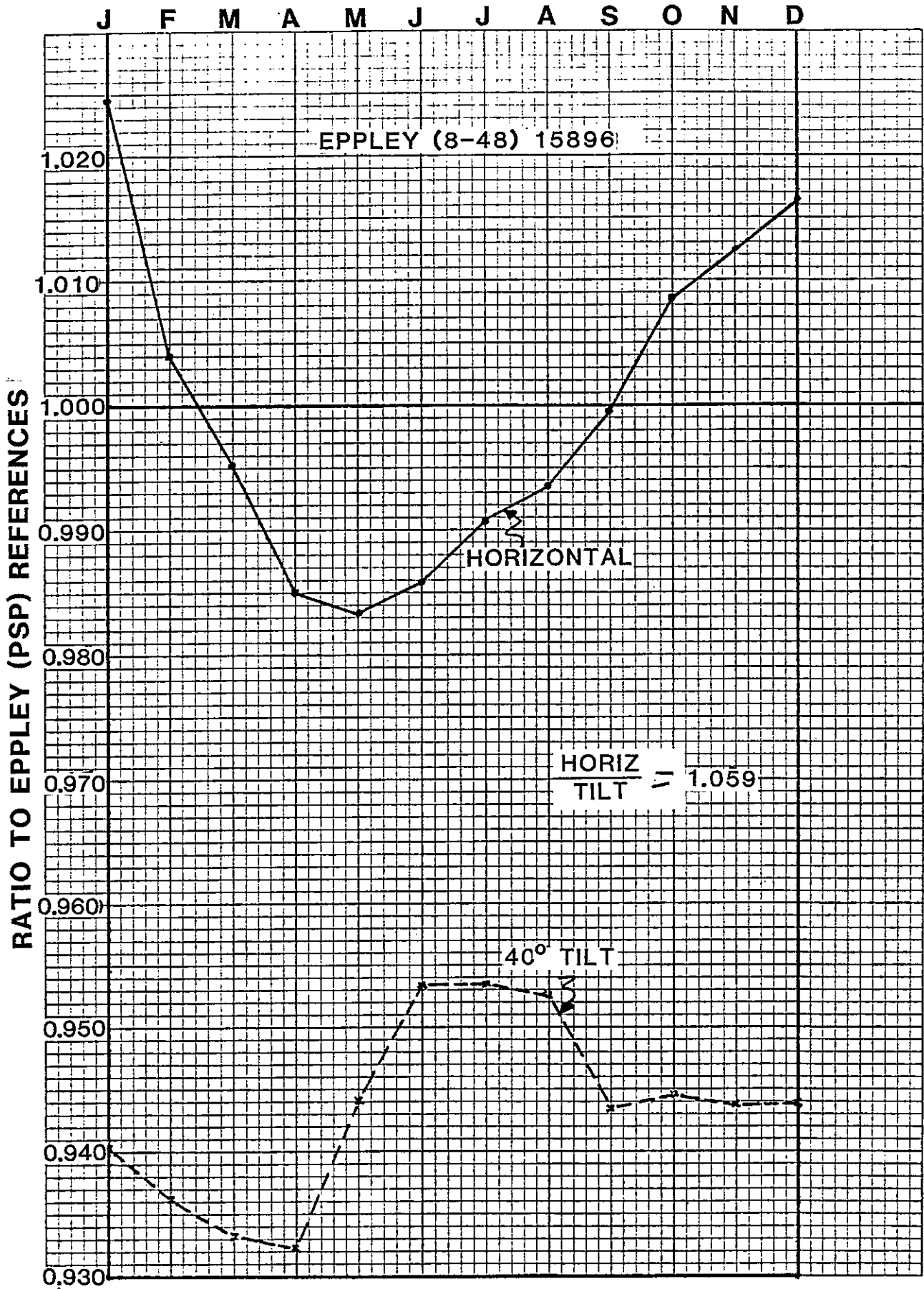


RESPONSE TO EPPLEY (PSP) REFERENCES



RESPONSE TO EPPLEY (PSP) REFERENCES







5.D SOME EXAMPLES OF FIELD EVALUATION OF PYRANOMETERS

L. Dahlgren

Swedish Meteorological & Hydrological Institute
Norrköping, Sweden

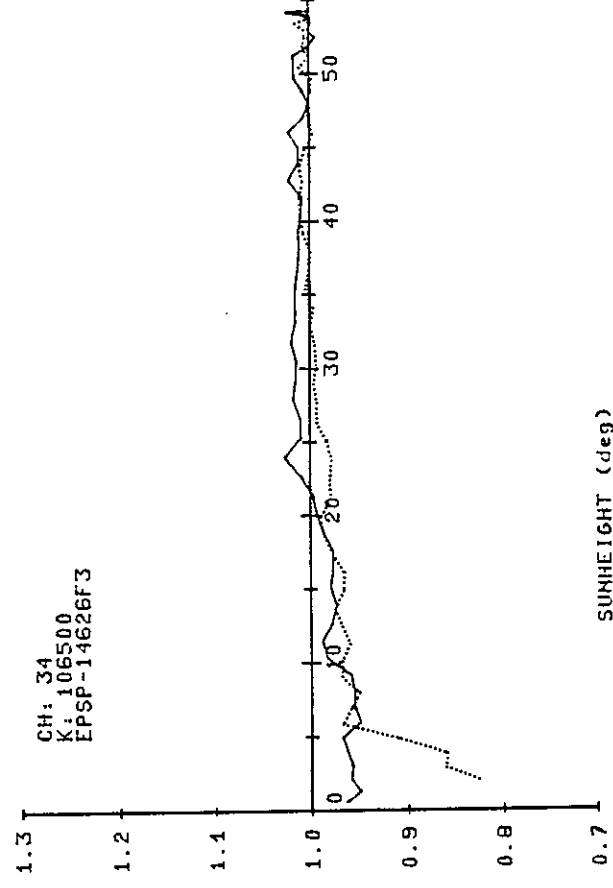
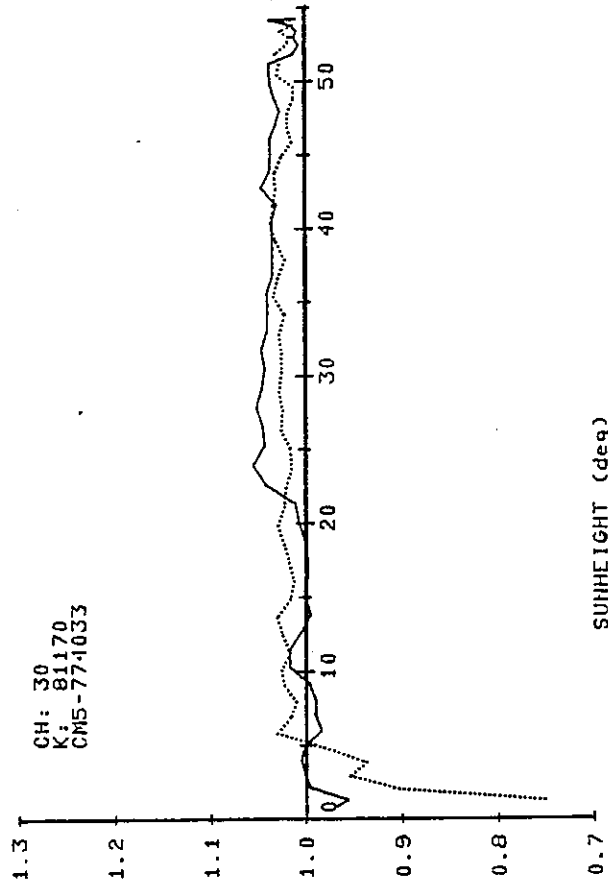
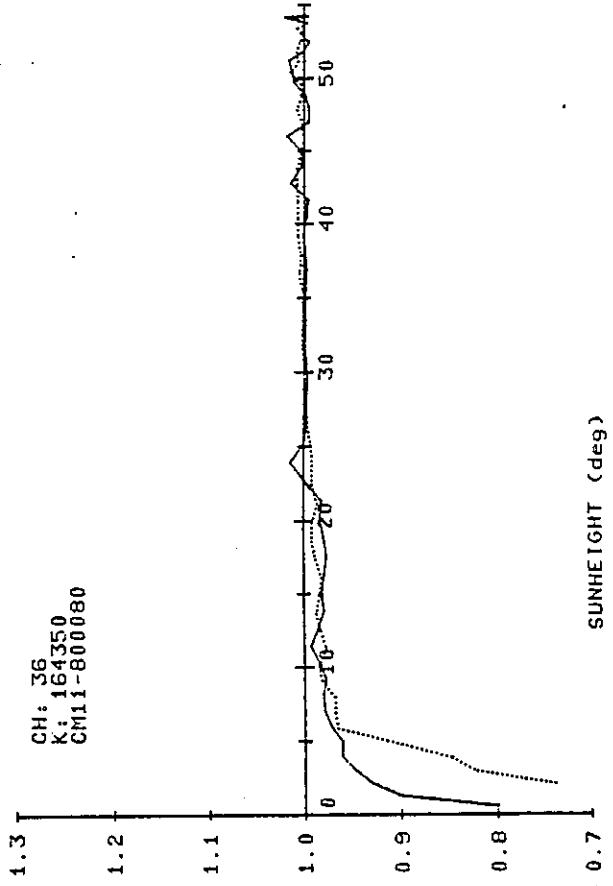
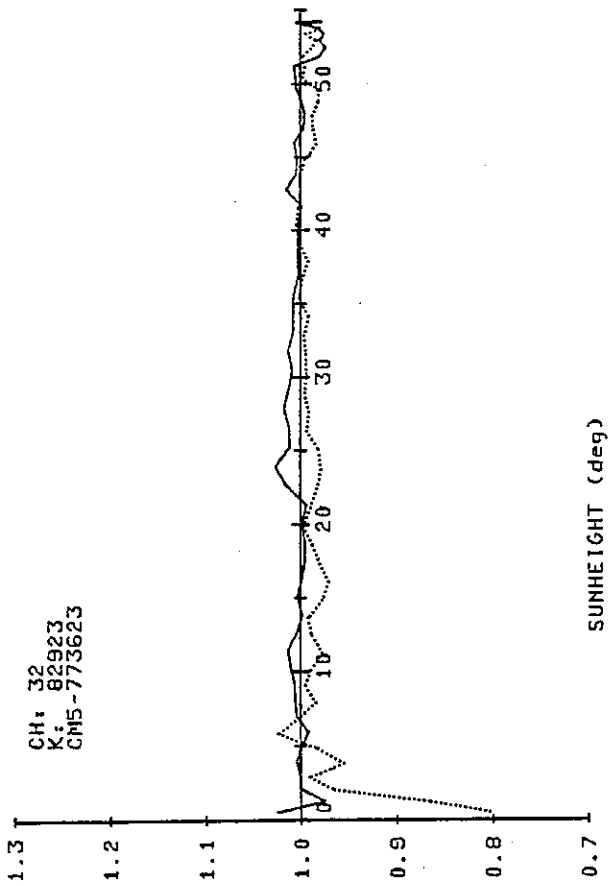
SOME EXAMPLES OF FIELD EVALUATION OF PYRANOMETERS

All the pyranometers in the Swedish network are calibrated at the SMHI roof facility in Norrköping. The values are traced to the World Radiometric Reference currently through the Angstrom pyrhelimeter No. 171; also the standard comparisons at Davos. Recently a PM06 absolute cavity radiometer has been acquired by SMHI.

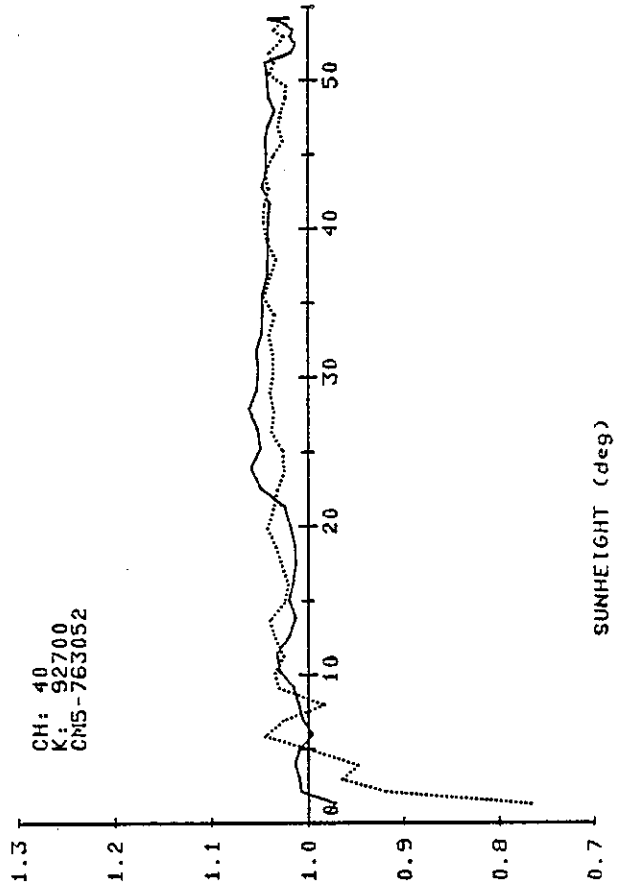
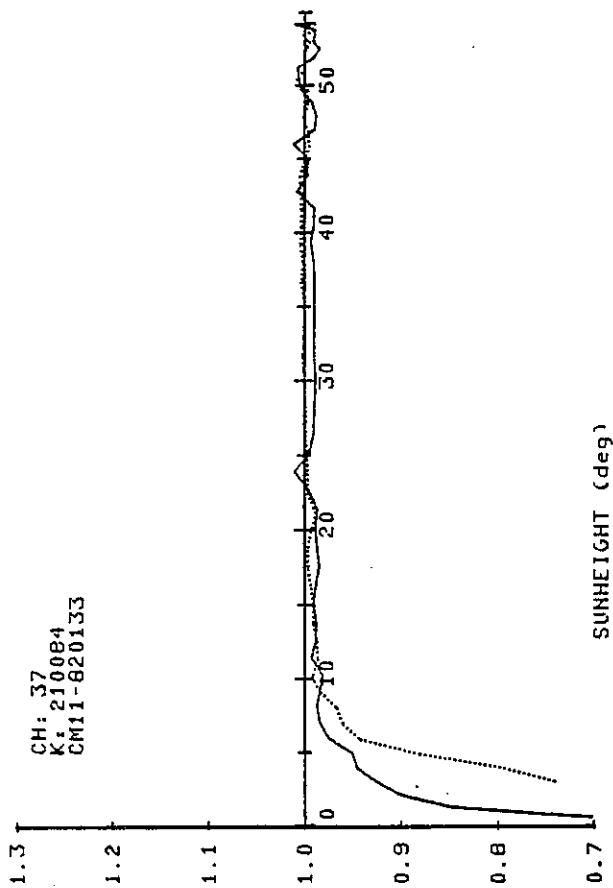
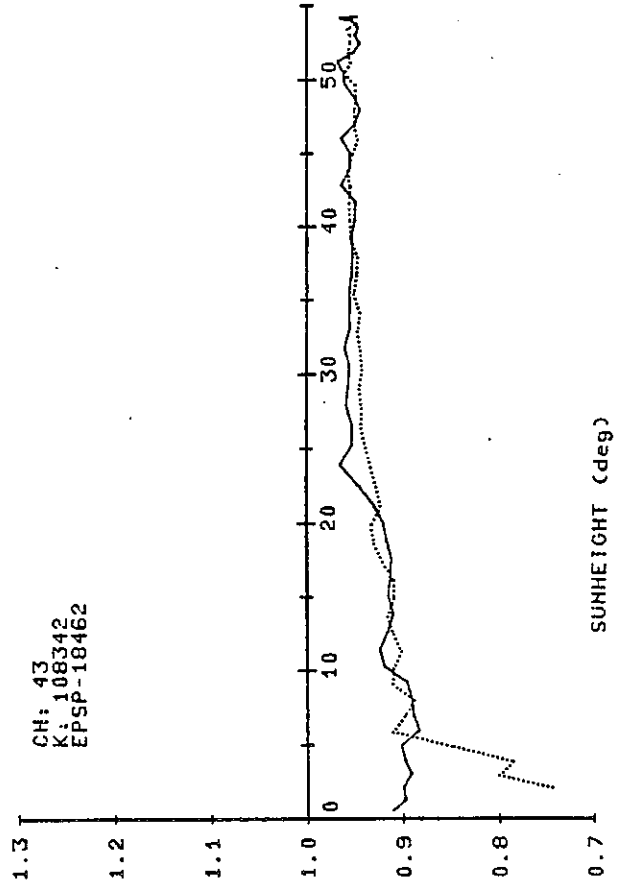
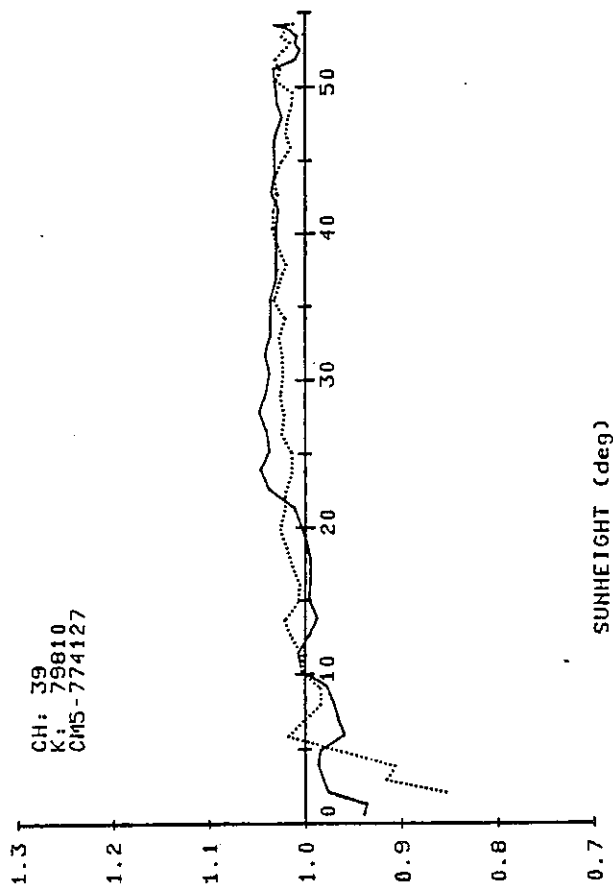
The following figures show an evaluation of several pyranometers during one day in summer at Norrköping and the table gives hourly means of the data. The reference measurement value for global radiation is constructed from an Eppley N.I.P. measurement of the direct beam and a diffuse measurement by a Kipp and Zonen CM-11 equipped with tracking shading disc. The output from any pyranometer being tested is divided by the global reference and the result plotted against solar elevation. Preliminary calibration factors have been used for the pyranometers being investigated. The dotted lines are from afternoon data. The graphs are therefore similar to "cosine error" graphs except that the indicated error here is for global radiation rather than only for direct radiation.

This method will be used extensively to characterize the IEA pyranometers. At present the writer is concerned at the apparent poor stability of the N.I.P. sensitivity as judged from many calibrations against the SMHI Angstroms. In future it may be desirable and possible to use the PM06 pyrhelimeter in place of the N.I.P.

Station: SMHI. Date: 1983-07-05



Station: SMHI. Date: 1983-07-05



5.E COMPARISON OF STANDARD PYRANOMETERS OF EEC MEMBER COUNTRIES

J.L. Plazy, P. Gregoire, R. Coudert and J. Olivieri

French Agency of Energy Development
Valbonne, France

Service radiometrique de Trappe/Carpentras
France

COMPARISON OF STANDARD PYRANOMETERS OF EEC MEMBER COUNTRIES

This is a shortened version of the final report "Comparison des pyranomètres étalons secondaires" contract ESF-005-F of Project F of the EEC Second Programme on Solar Energy. The original report has 88 pages of tables or graphs, of which just 15 are reproduced here. The data given here usually refers to just one of the nine days on which measurements were taken, namely June 24, 1981.

PURPOSE OF EXERCISE

As part of Project F in the solar research and development program of the Commission of the European Communities, the secondary standard pyranometers of the national weather services of the Communities' member states were compared. (The primary standards had been compared at Carpentras, France in 1978). The purpose of these comparisons was to ensure uniformity in the data provided by the solar-radiation observation networks of these countries. This exercise was designed to quantify the instrument error that occurs in actual network observations and to provide a flexible method of reducing this error to acceptable levels.

PARTICIPANTS

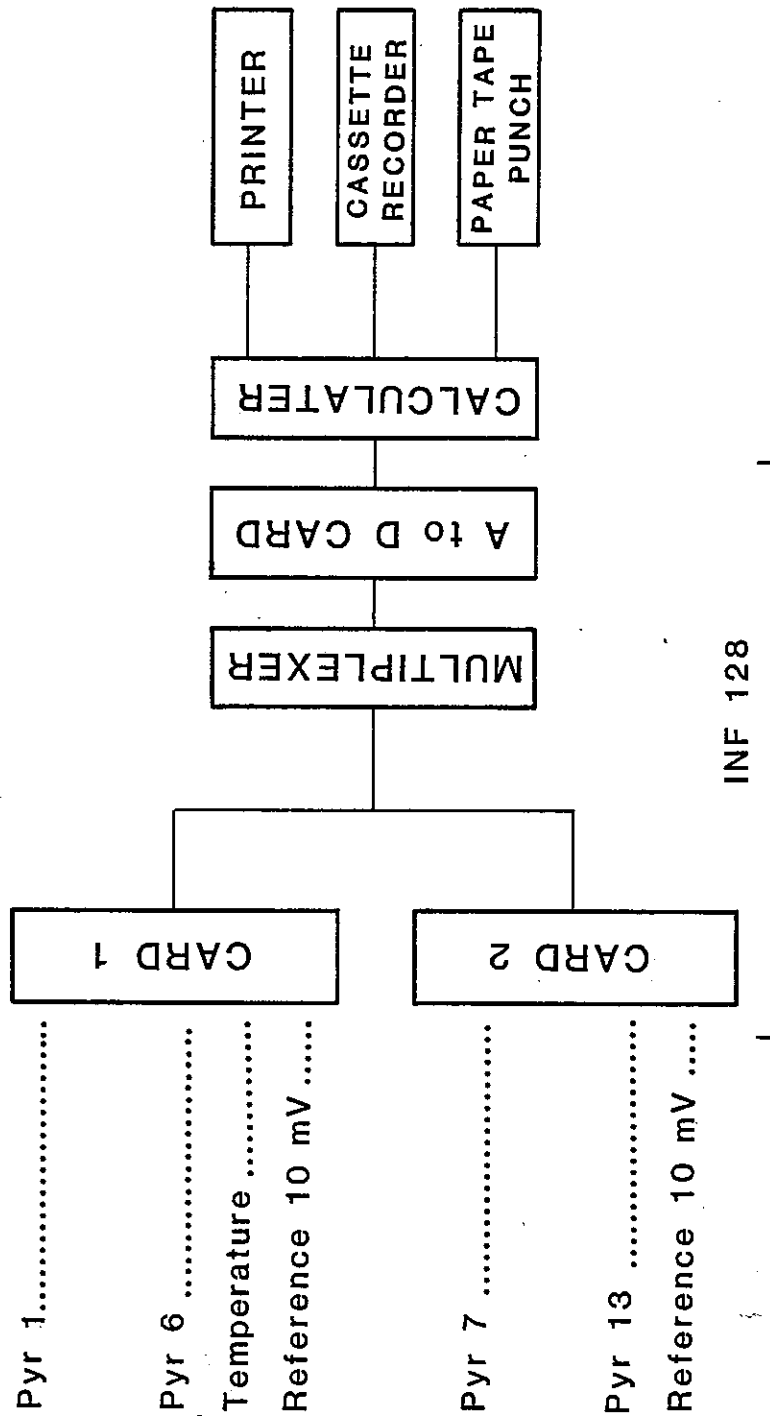
The weather service of each member state was invited to send to the radiometric centre at Trappes-Carpentras at least one pyranometer that it uses to calibrate the instruments in its network. Denmark and Italy were the only countries that did not send instruments. The pyranometer from the Netherlands was delayed by customs and was included in the second week of the comparisons only. The instruments compared are listed in annex 1.

WEATHER CONDITIONS

The comparisons were conducted over the period 15 to 25 June 1981, which included the following types of weather conditions.

- Clear to slightly cloudy, with high temperatures 15 & 16 June
- Clear to slightly cloudy with more moderate temperatures and high winds 17, 18 & 22 June
- Very cloudy 19 & 22 June
- Overcast 25 June

Details of the weather conditions during the comparisons are given in annex 2.



DATA-ACQUISITION SYSTEM

The pyranometers were installed on the roof of the radiometric centre and levelled by means of their built-in spirit levels. The hot junctions of the Kipp and Zonen pyranometers in this group were oriented east-west, except for instrument 1564, which was oriented north-south.

The data-acquisition system, an Aerazur INF 128, was equipped with 2 low-voltage input boards (8 channels each). The data-acquisition software was run on an Intertechnique Multi 20 computer, and the recording devices consisted of a high-speed printer, a mini-cassette recorder, and a tape punch.

The inputs to the first board consisted of the signals from 6 of the pyranometers, a voltage representing the temperature inside one of them, and a 10-mV reference signal. The inputs to the second board consisted of 7 pyranometer signals and another 10-mV reference signal.

COMPUTATIONS AND RESULTS

Reference Values

The reference pyranometer was an Eppley PSP, Serial No. 16542 F3. Its calibration factor was checked both before and after the comparisons. This instrument was selected because its response to varying solar elevations and azimuths had already been characterized through extensive observations using the intermittent-occultation method (with a WRR 1980 pyrhelimeter). The table in annex 3 gives calibration factors (in $\mu\text{V} \cdot \text{mW}^{-1} \cdot \text{cm}^{-2}$) thus determined for this instrument for various solar elevations and azimuths.

The temperature-correction factor for this instrument was taken to be zero. To obtain radiation values to which those from the other instruments could be compared, two different methods were used.

Method 1 The voltage from the reference instrument was divided by a calibration factor of $92.5 \mu\text{V} \cdot \text{mW}^{-1} \cdot \text{cm}^{-2}$, the mean of all the calibration factors previously determined for this instrument.

Method 2 The voltage from the reference instrument was divided by the calibration factor shown in annex 3 to determine the vertical component of direct solar radiation, and by a factor of $91.0 \mu\text{V} \cdot \text{mW}^{-1} \cdot \text{cm}^{-2}$ to determine diffuse solar radiation. This latter factor was derived from the annex 3 table using the assumption of an isotropically radiant sky.

Over the period of the comparisons, the difference between the reference values determined by method 1 and those determined by method 2 ranged from 0.6 to 1.6% depending on sky conditions.

Group No	Pyranometer type	Serial No.
1	Eppley PSP Eppley PSP Eppley PSP Eppley PSP	16542 F3 19682 F3 14899 F3 16540 F3
2	Kipp and Zonen CM 2 Kipp and Zonen CM 5* Kipp and Zonen G 18 Eppley (old 15-junction model)	2508 690187 1564 6217 A
3	Kipp and Zonen CM 5 Kipp and Zonen CM 5 Kipp and Zonen CM 5	796617 795546 796781
4	Kipp and Zonen CM 10 Kipp and Zonen CM 10 Kipp and Zonen CM 10	800082 790057 800070**
<p>* Pre-1972 version ** Instrument belonging to German national atomic energy research agency; comparisons made on 19 June 1981.</p>		

DISCUSSION

Variation in daily ratios

The table in annex 6 shows the ratios between the daily totals for each pyranometer and the daily method-2 reference totals. There is a gap of 9.5% between the instrument that yielded the highest values (Kipp and Zonen CM 10, No. 790057) and the one that yielded the lowest (Kipp and Zonen CM 5, No. 690187). If this latter instrument is not considered, the range of variation narrows to 4.7%. This discrepancy cannot be explained solely by the conditions under which the pyranometers were operated and their differential responses to solar elevation and azimuth. The calibration method was probably partly responsible.

Instrument response to temperature

The days of 15 and 18 June offered an opportunity to study the effects of temperature on the instruments, for though there were clear skies on both days, there was a temperature difference of approximately 14° between them. For some instruments, the results for the two days differed by as much as 1%, even though the Eppley pyranometers have temperature-compensating circuitry and a temperature correction was applied to the Kipp pyranometers. In fact that the temperature-compensating circuitry is accurate only within 1%, and that an Eppley was used as the reference instrument, probably has

something to do with this. Since the differences between the days are thus of the same order of magnitude as the instrument error, the temperature-correction factors used here can be considered reasonable.

Instrument response to solar elevation and azimuth

For determining hourly radiation totals or radiation on inclined surfaces, pyranometers with a relatively flat response to solar elevation and azimuth are recommendable. The graphs in annex 5 indicate that the instruments in group 1, 3 and 4 (i.e., Eppley PSP and Kipp and Zonen CM 5 and CM 10 pyranometers) meet this requirement.

ADJUSTMENT OF CALIBRATION FACTORS FOR ELEVATION AND AZIMUTH EFFECTS

The response of the Eppley PSP, Kipp and Zonen CM 10 and Kipp and Zonen CM 5 pyranometers to variations in solar elevation and azimuth has been characterized at Carpentras through extensive calibration runs. Using the results we have calculated ratios between the radiation that would be measured under clear skies by a hypothetical pyranometer with a flat response to solar elevation and azimuth and by each of these three types of pyranometers. The tables in annex 7 show the following ratios for total daily solar radiation at latitudes between 40° and 55° and solar declinations between $-23^{\circ}27'$ and $+23^{\circ}27'$.

Group	Pyranometer type	Range	Mean	Deviation from mean
1	Eppley PSP	0.961 - 0.986	0.974	$\pm 1.28\%$
2	Kipp & Zonen G 18	1.009 - 1.017	1.013	$\pm 0.4\%$
3	Kipp & Zonen CM 5	0.992 - 0.997	0.995	$\pm 0.25\%$

These results indicate that for measurements of total daily solar radiation at European latitudes with a given type of pyranometer, the calibration factor need not be adjusted for latitude or season if a precision of 0.5% is acceptable. The same does not hold true for measurements to total hourly solar radiation. When different types of pyranometers are being compared, however, their calibration factors must be adjusted for their differential responses to solar elevation and azimuth.

CONCLUSIONS

The results of this exercise show why pyranometric comparisons are necessary. Secondary standard pyranometers must be calibrated especially carefully, and their responses to solar elevation and azimuth taken into account, if they are to provide values suitable for calibrating field instruments. Discrepancies can be reduced by adjusting the calibration factor to account for the pyranometer's particular response curve and the conditions under which the instrument is used.

Further comparisons of this type will be made around the winter solstice to confirm the present results.

Ratios

In order to determine radiation values for each of the other pyranometers, the voltages it transmitted were divided by the calibration factor supplied by the country that sent it. In some cases, a temperature-correction factor also was applied (see annex 1). Hourly totals were determined from 10 instantaneous measurements taken every 6 minutes*. Daily totals were determined from all the measurements taken each day, except that the hours of sunrise and sunset were excluded; and whenever work was done on the system (for example, when a pyranometer was installed or removed), the data from the half of the day were discarded. For each pyranometer, the following ratios were then calculated:

- ratio of each hourly value to corresponding method-1 reference value;
- ratio of each hourly value to corresponding method-2 reference value;
- ratio of each daily value to corresponding method-1 reference value;
- ratio of each daily value to corresponding method-2 reference value.

These ratios are presented in tabular form in annex 4.

Comparisons of hourly ratios

In annex 5, the ratios of hourly values to method-1 and method-2 reference values are graphed for each day of the comparisons. To facilitate analysis, pyranometers of the same type or with similar response curves have been grouped together on the same graph. The four groups thus established are described in the following table.

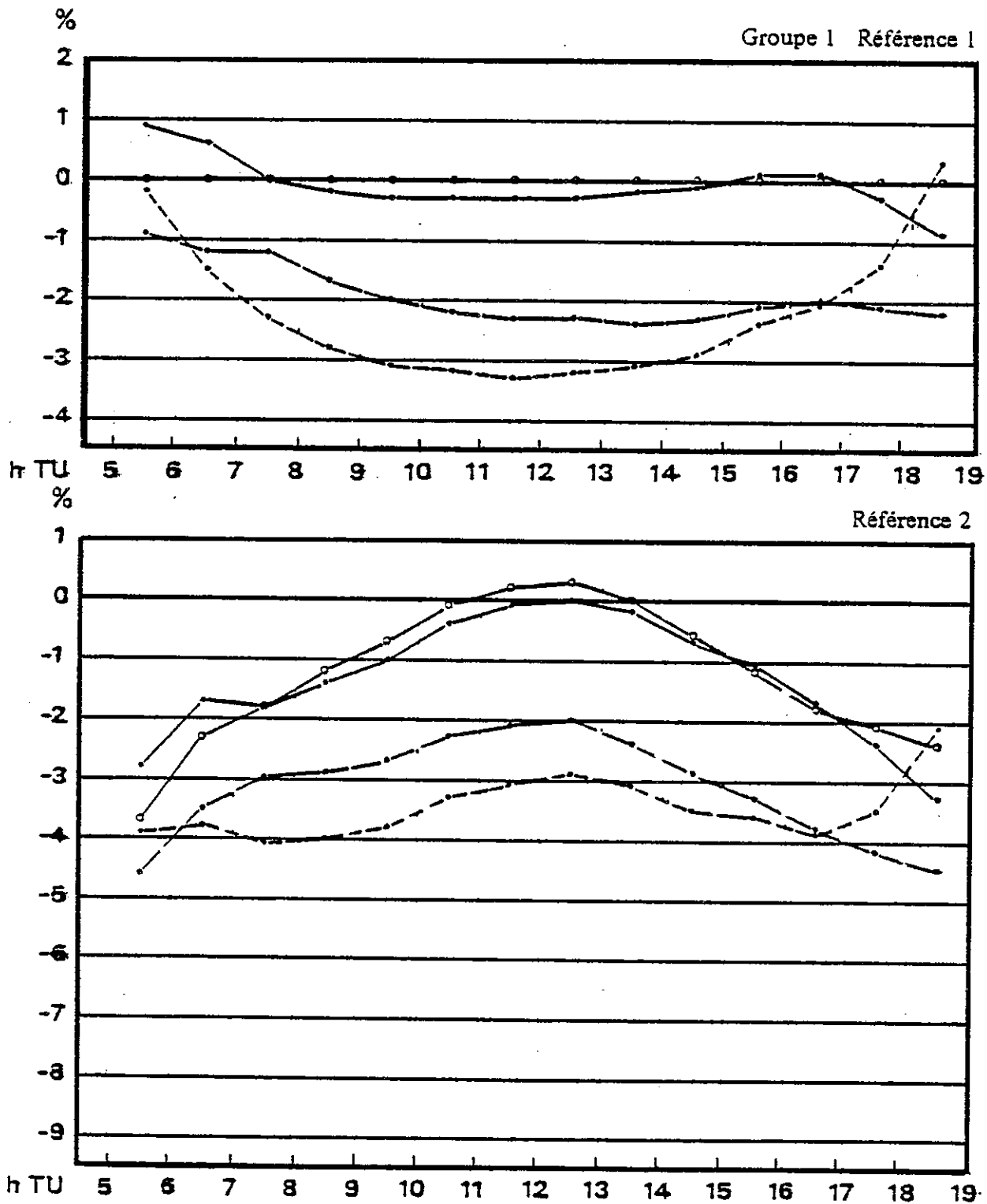
The graphs clearly show that the curves for pyranometers in the same group run parallel to each other. As a first approximation, the response to solar elevation and azimuth may therefore be considered identical for all pyranometers in a given group.

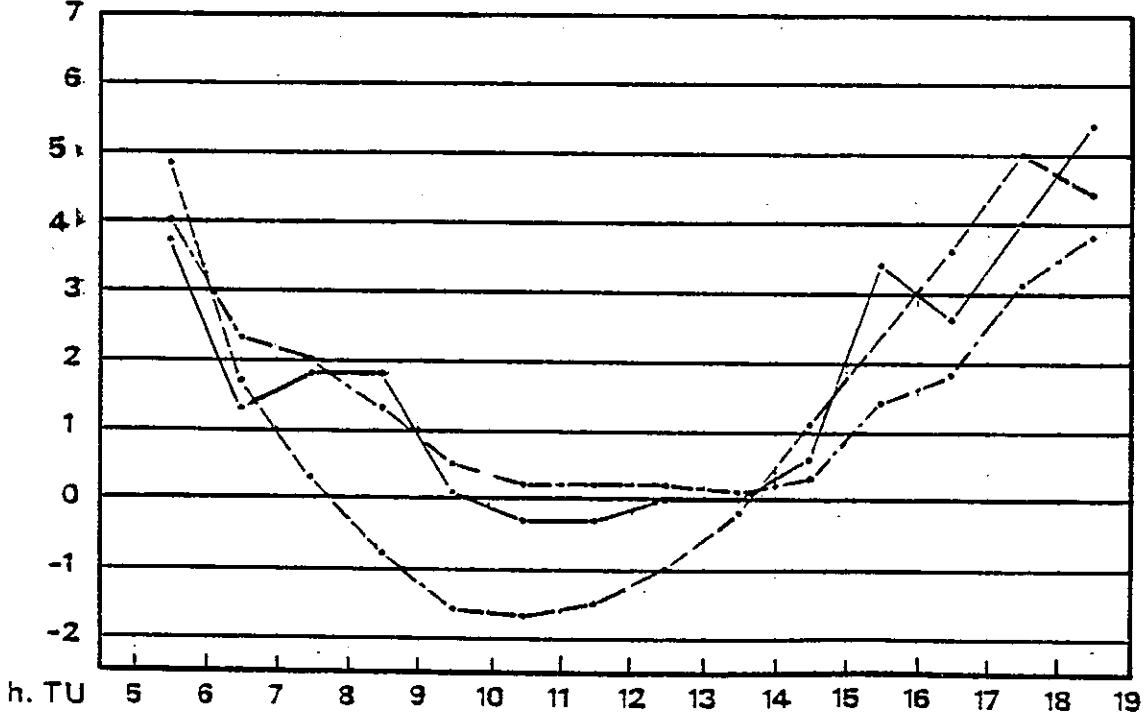
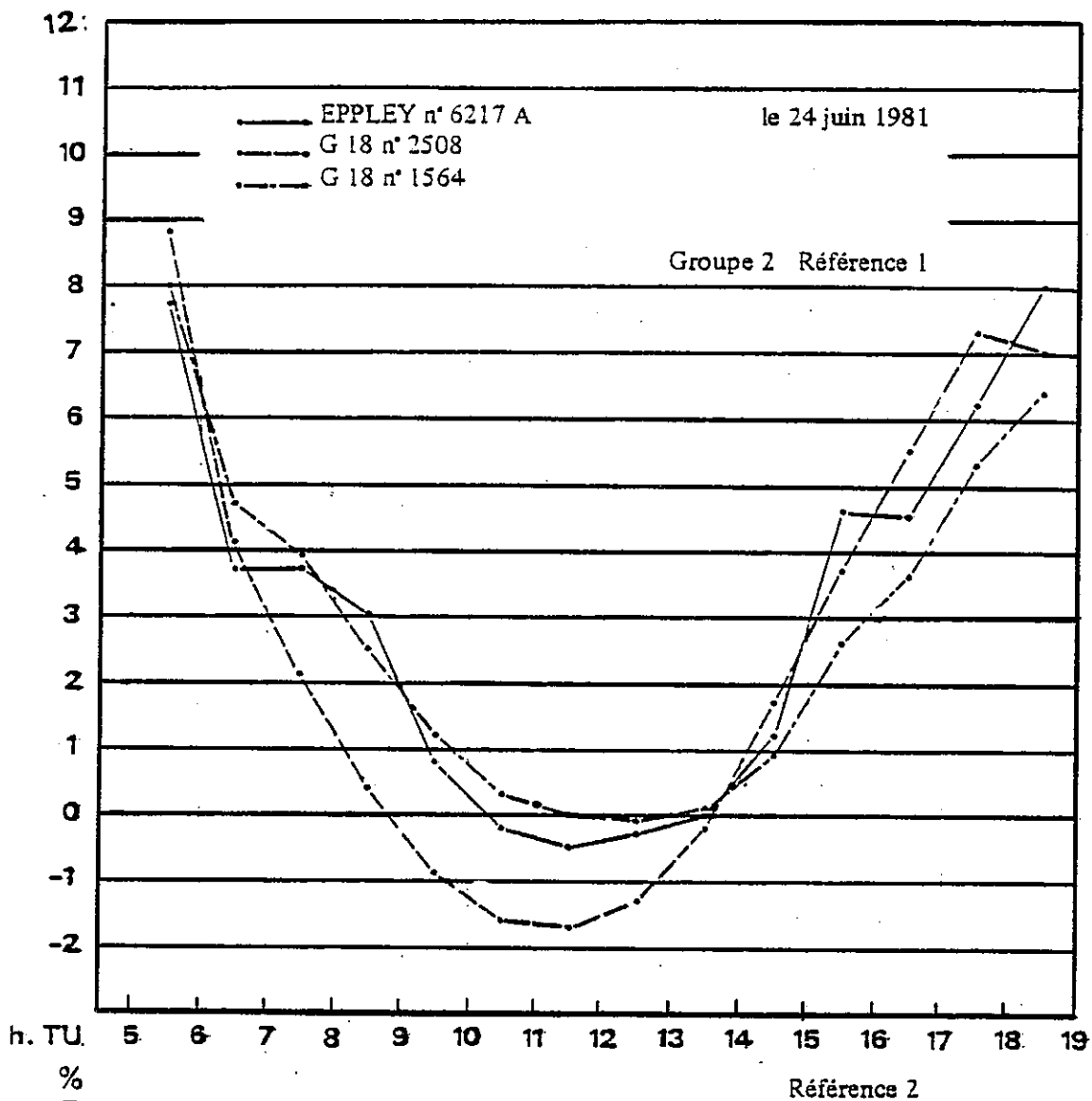
In the comparisons with the method-2 reference values, it is the group-3 pyranometers (Kipp and Zonen CM 5s) whose curves come closest to the ideal, horizontal line. The reason is that in these pyranometers, the effects of elevation are offset by those of azimuth. The group-2 pyranometers, in contrast, have pronounced U-shaped curves, with differences of 6 to 7% between the morning and mid-day values. These instruments are therefore not recommended for determining hourly radiation totals.

PYRANOMETRES EPPLEY PSP

— n° 16 540 F3 - - - n° 19 682 F3
— n° 14 899 F3 ○ — n° 16 542 F3 (étalon)

le 24 juin 1981

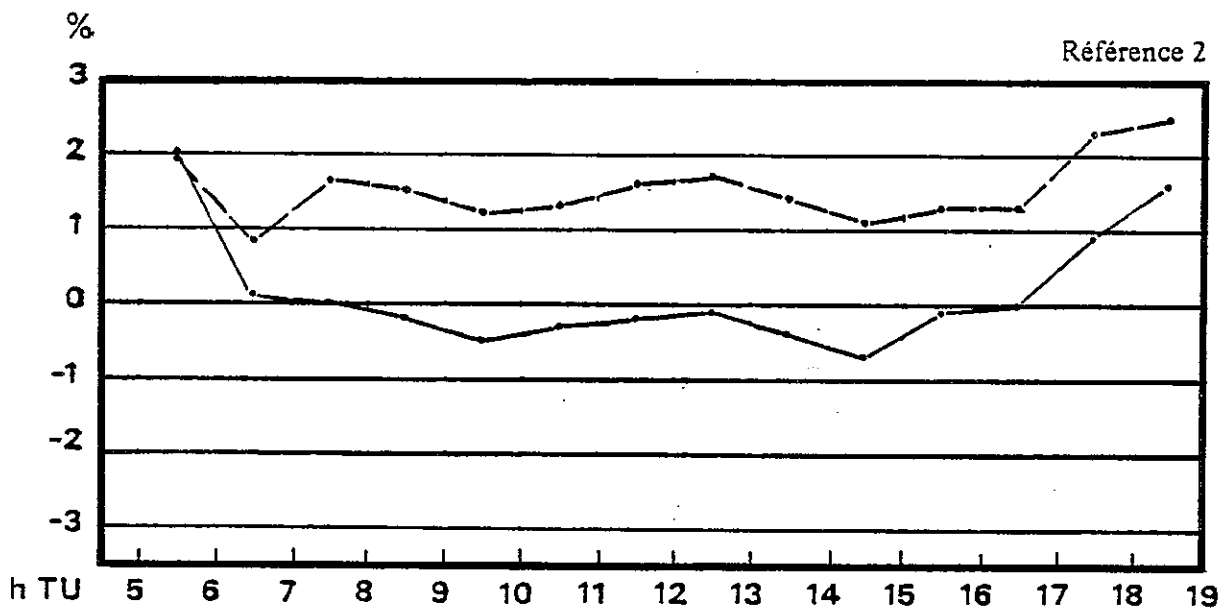
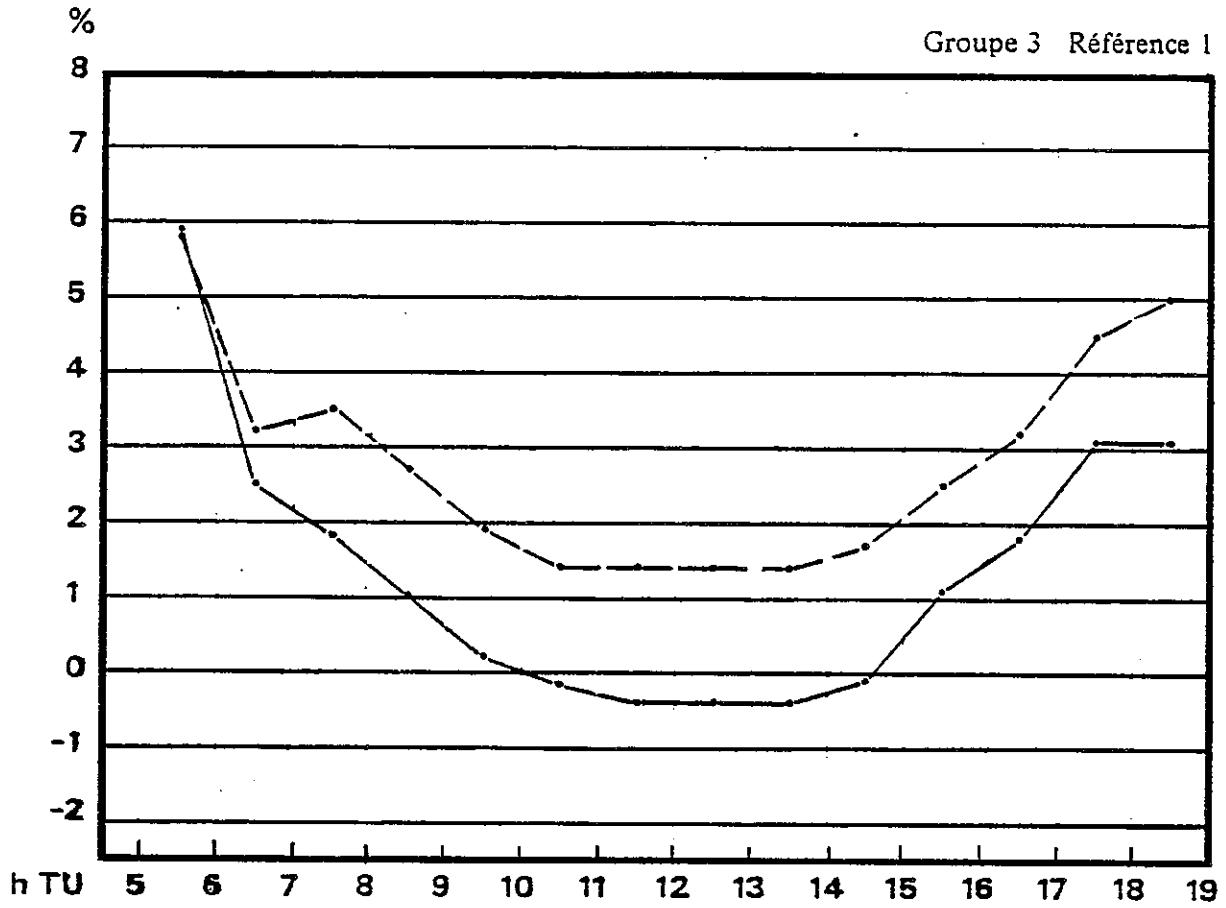


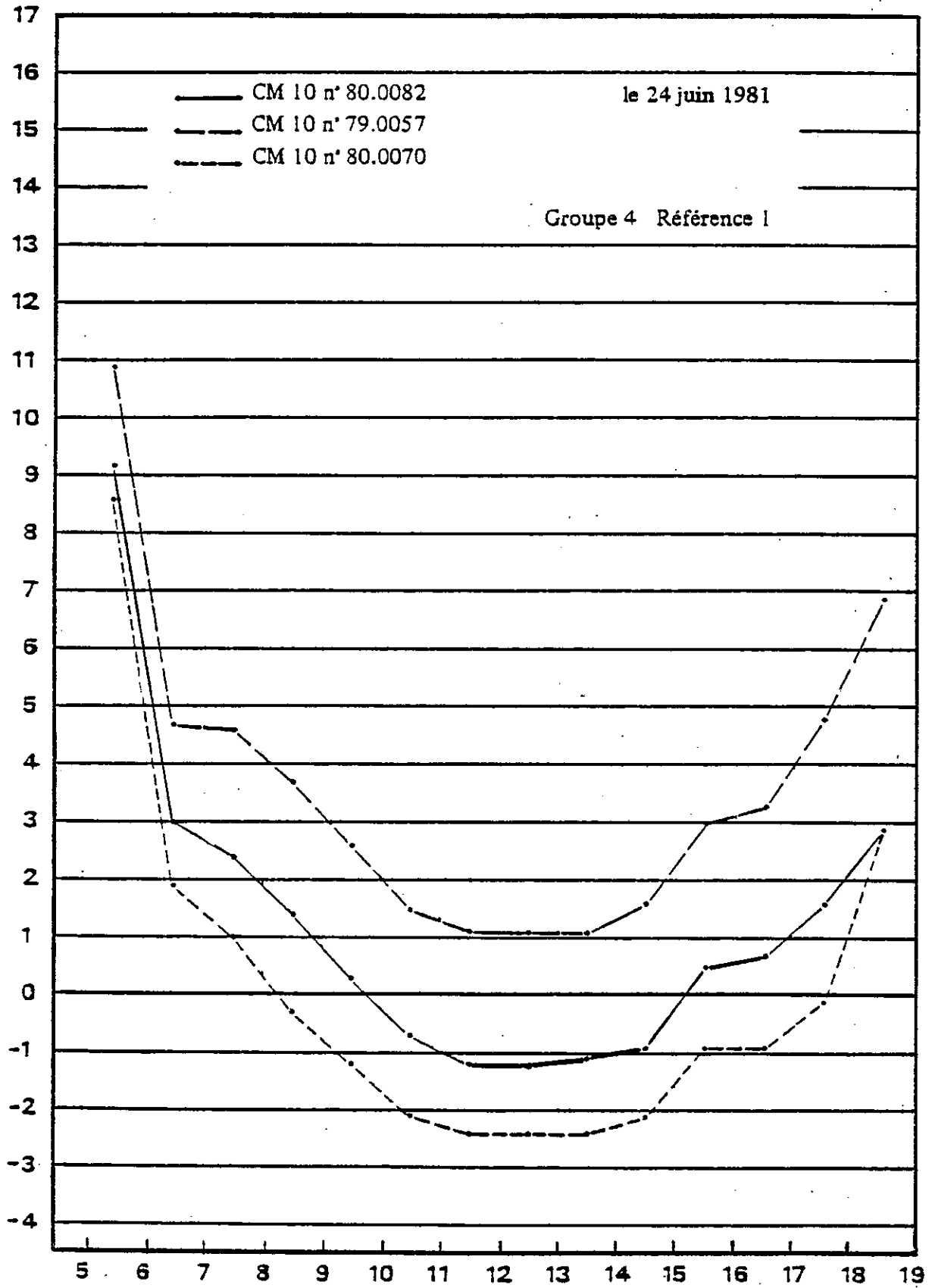


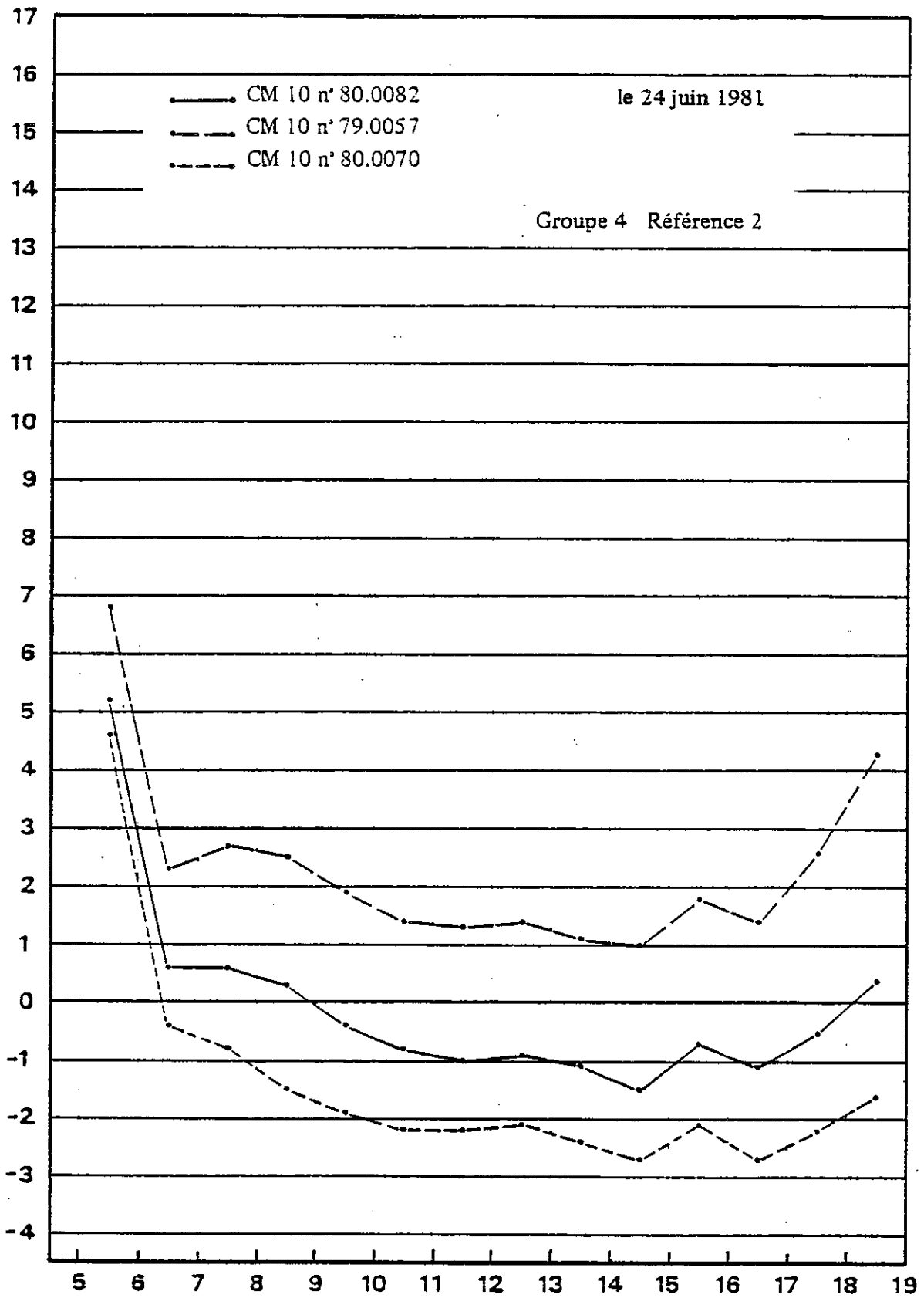
— CM 5 n° 796 617 coef. de temps: -0,12% °C

- - - CM 5 n° 795 546 coef. de temps: -0,12% °C

le 24 juin 1981

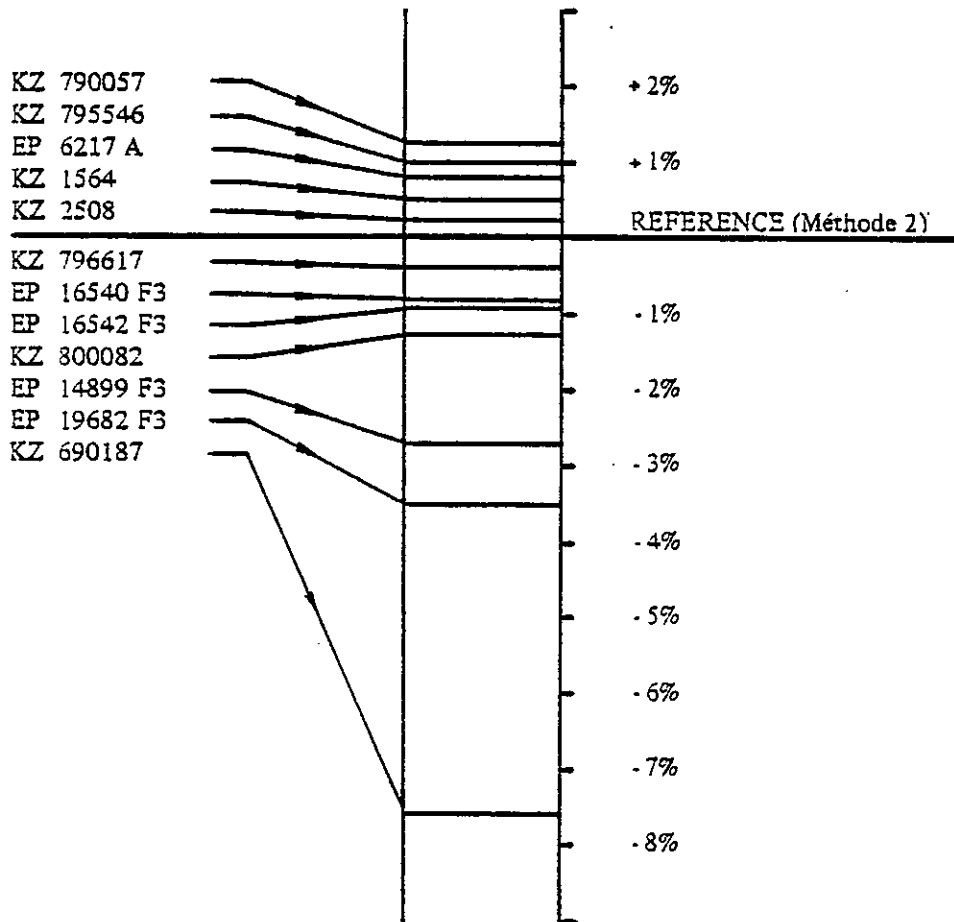






Annexe 6

REPARTITION DES PYRANOMETRES
PAR RAPPORT A LA REFERENCE





5.F PHOTOCHEMICAL MEASUREMENT OF ULTRAVIOLET SOLAR RADIATION

Darwish Lala

The National Swedish Institute for Building Research
Materials and Structures Division

PHOTOCHEMICAL MEASUREMENTS OF ULTRAVIOLET SOLAR RADIATION

INTRODUCTION

The outdoor application of organic materials make them susceptible to ultraviolet solar radiation (UVR) which causes irreversible chemical changes affecting the mechanical properties in these materials in what is called photooxidative degradation. This degradation manifests itself in the form of embrittlement followed by loss of tensile properties, objectional discoloration etc. These negative effects appear in different external building materials such as plastics, paints and wood products.

Degradation mechanism and factors affecting degradation process are well known. UVR, air oxygen, and internal photoactive groups are the most important factors. Various impurities with photoactive groups are introduced in the material during synthesis, processing and storage. These groups absorb UVR and initiate the photooxidative degradation. Qualitative and quantitative analysis of these impurities make it possible to develop and improve effective processes to photostabilize organic materials.

Unfortunately, only few research stations have continuous measurements of the most important degradation factor i.e. UVR. Generally, only global and direct solar radiation are measured at various meteorological stations throughout the world (2-4). In Sweden, for example, solar radiation is measured at 12 stations. UVR is measured at two stations in Gävle (SIB station) for 290-385 nm and in Norrköping (SMHI main station) for 290-320, 306 and 360 nm.

UVR intensity is dependent on several factors such as the state of the atmosphere (clouds, air, impurities), latitude, altitude, weather, time, season etc. These factors can reflect, absorb or scatter UVR and consequently affect the amount of radiation reaching the ground. It is important to measure UVR intensity in different climates and sites in order to be able to forecast the service life of different materials in outdoor uses. With this knowledge it is easier to plan, design and construct the equipment needed for accelerated studies on durability. Data for UVR intensity as a function of time, site and exposure surface are scarce because of the extensive instrumentation involved.

In a previous report (1), different methods for measurement of UVR are reviewed. These methods include physical, biological, chemical and photochemical methods. Measuring UVR intensity photochemically is possible through the use of UV-sensitive polymers such as poly (vinyl chloride) (PVC) and poly (phenylene oxide)(PPO). According to these methods, the degree of photodegradation of the polymer film is measured by IR or UV spectrophotometer. The results are calibrated against data from UVR measurement by instrumental physical methods.

The photochemical methods are developed by Martin et al (PVC method) (13-16) and Davis et al (17-20). Shiota et al (5) used other polymer films, poly methyl methacrylate (PMMA) and polyethylene (PE), to measure radiation intensity in certain accelerated light sources (carbon arc lamp and xenon arc lamp) within standardization working group ISO-Sc6/WG2.

A preliminary investigation to measure UVR photochemically using PVC and PPO started at the national Swedish Institute for Building Research (SIB) in Gävle, Sweden July 1982. This investigation is intended as a first step in a larger Nordic project.

EXPERIMENTAL

PVC films (20 μm) were prepared by dissolving additive free PVC (Pevikon S-689, Kema Nord) in tetrahydrofuran and casting on a plane surface. Films were prepared at SIB laboratory. PPO films (20 μm) were prepared from solution of PPO in chloroform. Films were kindly supplied by Mr. J Lohmeijer, General Electric Plastics B.V., Netherland. The spectrophotometric measurements were carried out by polymer group, department of polymer technology, Chalmers Institute of Technology, Sweden using Perkin-Elmer IR spectrophotometer 399 and UV spectrophotometer 599.

Special film holders made of aluminium sheets (fig. 1) and an exposure element of aluminium to hold both types of film holders mounted in different directions (fig. 2) were made at SIB mechanical workshop. For calibration of data used Eppley ultraviolet radiometer model TUVR.

PHOTODEGRADATION OF POLY (Vinyl Chloride) (PVC)

Photodegradation of PVC can occur through the following mechanism: absorption of UVR, excitation of the internal photoactive groups in the polymer, formation of free radicals chain reactions with air oxygen and formation of functional groups such as CO, CHO, and OH and OOH. Eventually the photodegradation results in chain scission and/or crosslinking of the polymer molecules (6-9).

Carbonyl groups (CO) which are formed during photodegradation have a special IR absorption at 1730 cm^{-1} . The change in this absorption is a function of UVR energy absorbed during exposure independent of temperature (under 60°C) and humidity (13-16).

Calibration of the change in absorption at 1730 cm^{-1} against data from UVR measurement by instrumental method is shown in fig. 3.

Scheme 1 shows photodegradation mechanism of PVC (6-9, 14). Through absorption of UVR, chlorine and hydrogen free radicals are formed, hydrogen chloride evolved through dehydrochlorination, formation of peroxy radicals and hydroperoxides which react to form different segments containing functional groups where carbonyl groups are the most important.

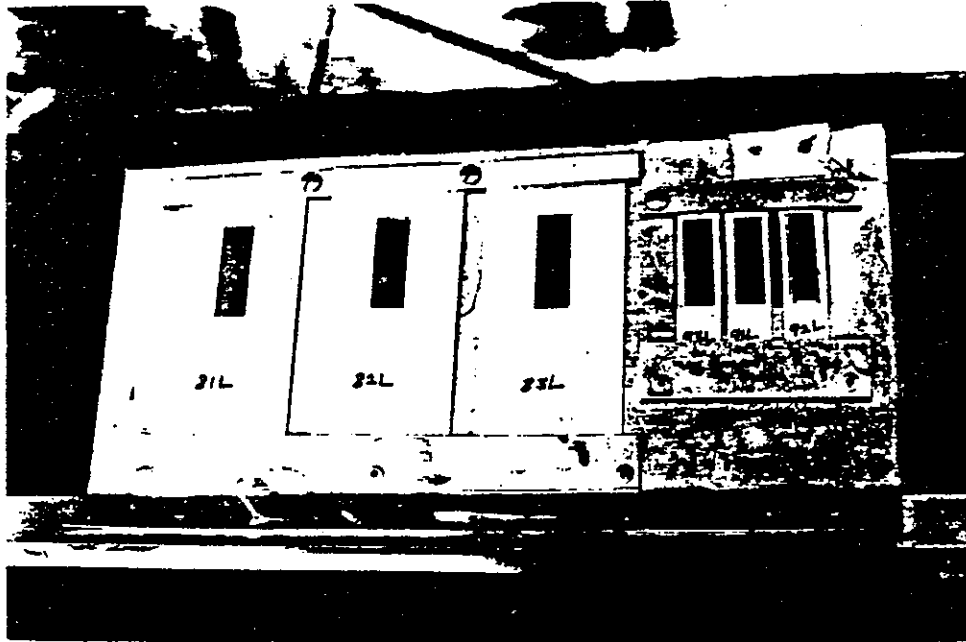


Figure 1. PVC and PPO films mounted on Al holders

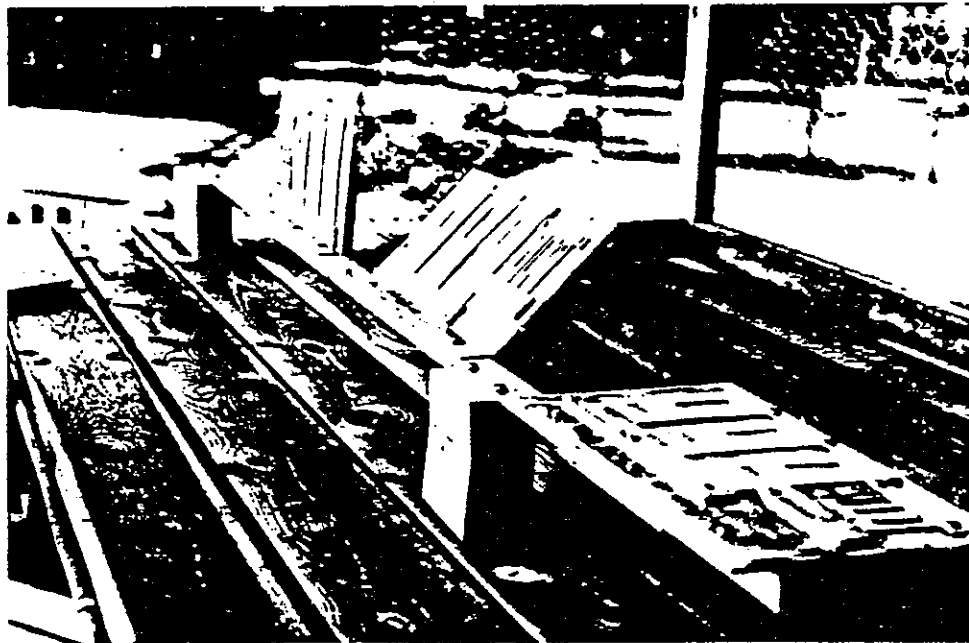
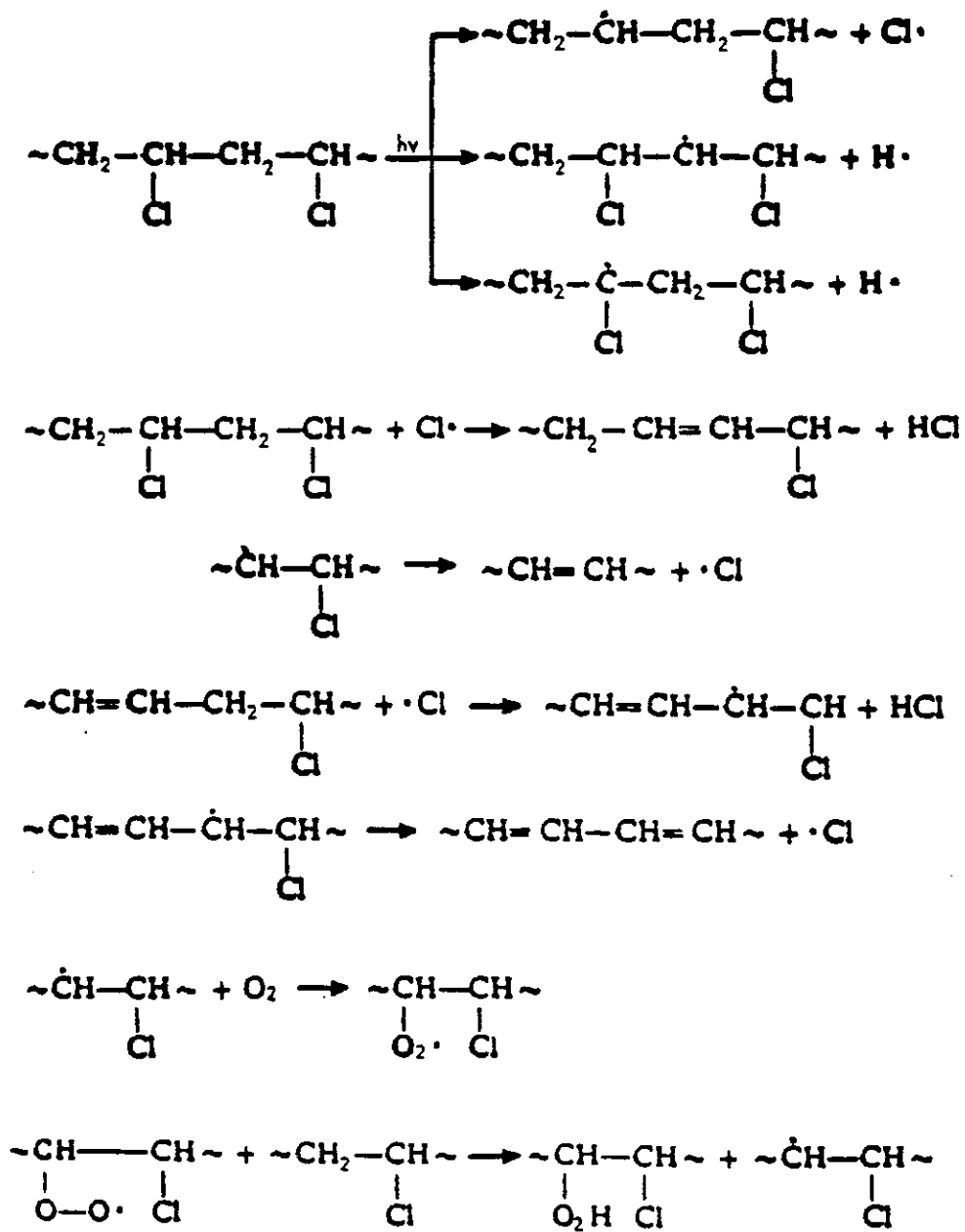


Figure 2. Exposure element for PVC and PPO films



Scheme 1. Photodegradation of PVC

RESULTS AND DISCUSSIONS

Results from UVR measurements on horizontal surface for at least one year is needed in order to get enough correlation between photochemical effect on polymer film and data from instrumental method. Figures 3 and 4 show two calibration curves for PVC and PPO methods respectively. These results are from exposure during the period August 1982-1983. From these curves, the following calibration equations can be derived:

PVC method:

$$UV(KWh/m^2) = 166.75 \Delta A - 1.612 \text{ ----- Fig 3}$$

PPO method:

$$UV(KWh/m^2) = 4.695 \Delta OD \text{ 340 nm ----- Fig 4}$$

From the results of exposure on horizontal, south/45° and south/vertical surfaces and the equations mentioned previously, the intensity of UVR under each exposure period can be estimated. Figure 5 and 6 show the estimated data for PVC and PPC methods respectively. These data are compared to results from UVR measurements by instrumental methods using UV pyranometer.

In case of PPO method, certain degree of photodegradation can be observed during the whole year while with PVC this degradation effect is practically limited to summer time.

Dependence on UVR intensity on exposure direction can be observed from Figures 5 and 6. UVR is highest for exposure on horizontal surface while for exposure on south/45° surface it is 9-37% less than horizontal exposure. For south/vertical surface it is 17-46% less than horizontal exposure. In both cases, the comparison is made for PPO method for the period from January (Figure 6). For PVC method (Figure 5), the same variation tendency can be observed but not as clear.

The quality of polymer films (thickness and composition) is an important factor for the technical application of these methods. It is difficult to evaluate the economic feasibility of these methods at this stage because of that the cost of spectrophotometric measurement of the exposed films is a function of the number of films measured. The more measurements the lower is the unit cost. Even though, it is already clear that these methods are appreciably more economic than the instrumental methods which need UV pyranometer, data collection, processing, registration and storage.

Yamasaki (4) and Nireki (21) investigated UVR intensity by exposure on surfaces with different directions by instrumental physical methods.

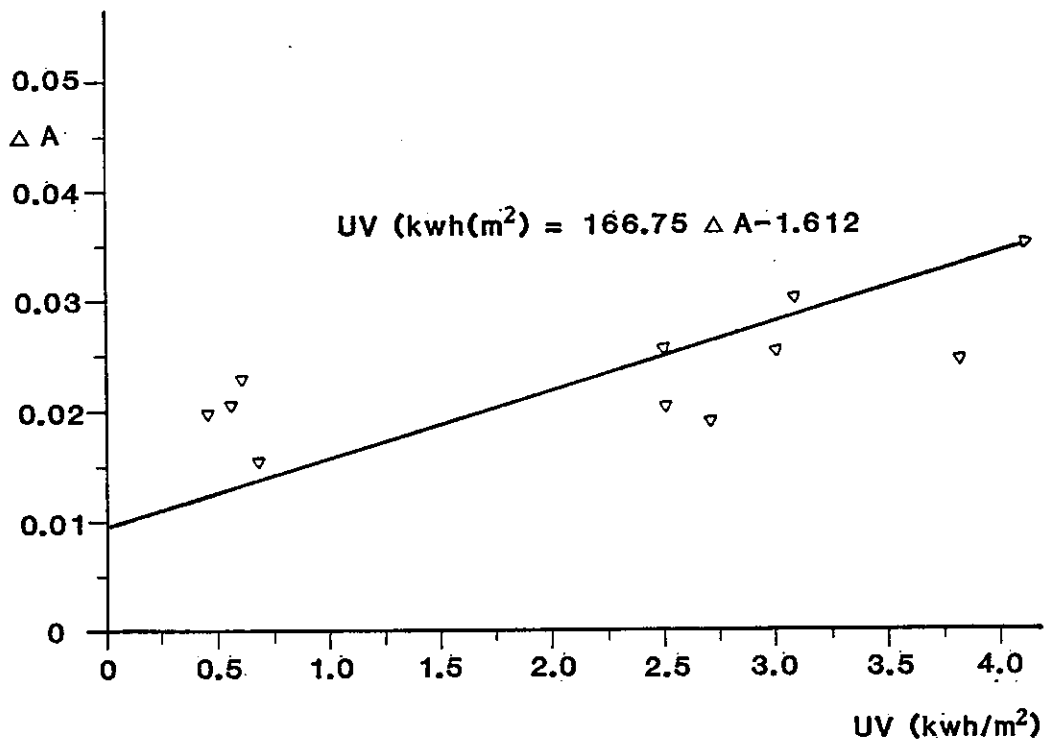
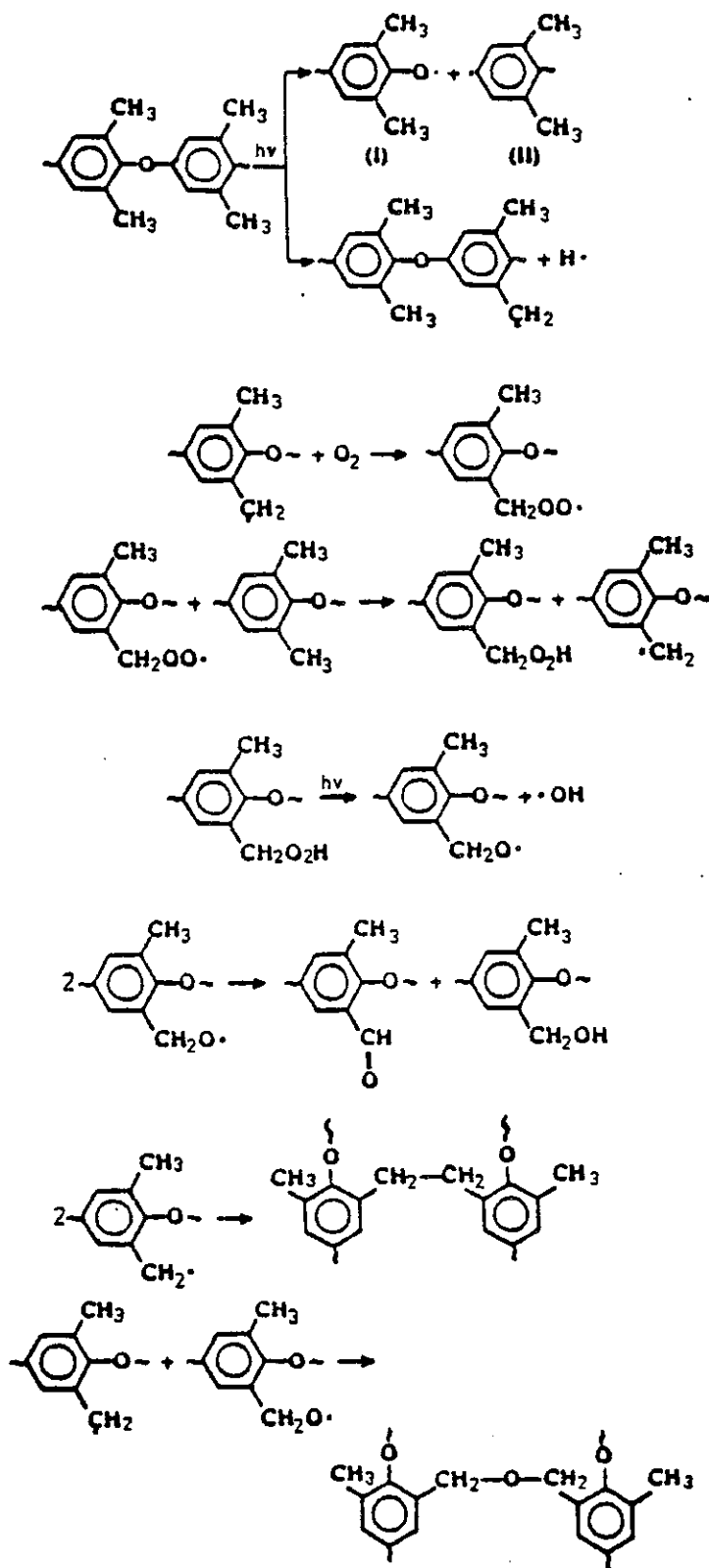


Figure 3. Calibration of PVC films



Scheme 2. Photodegradation of PPO

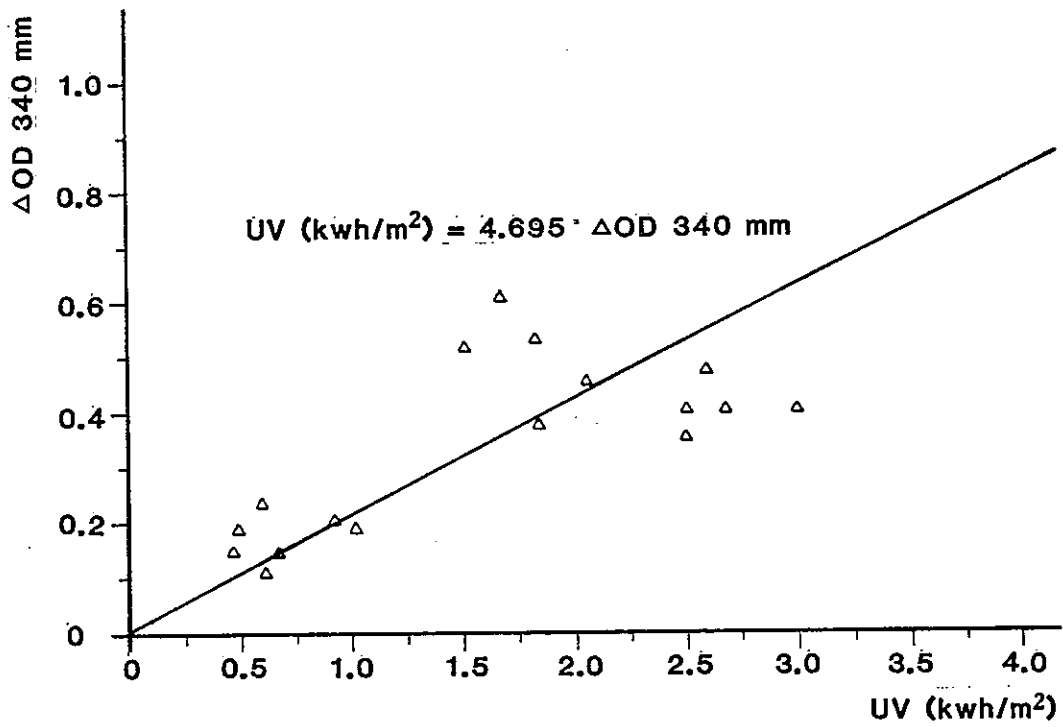


Figure 4. Calibration of PPO films

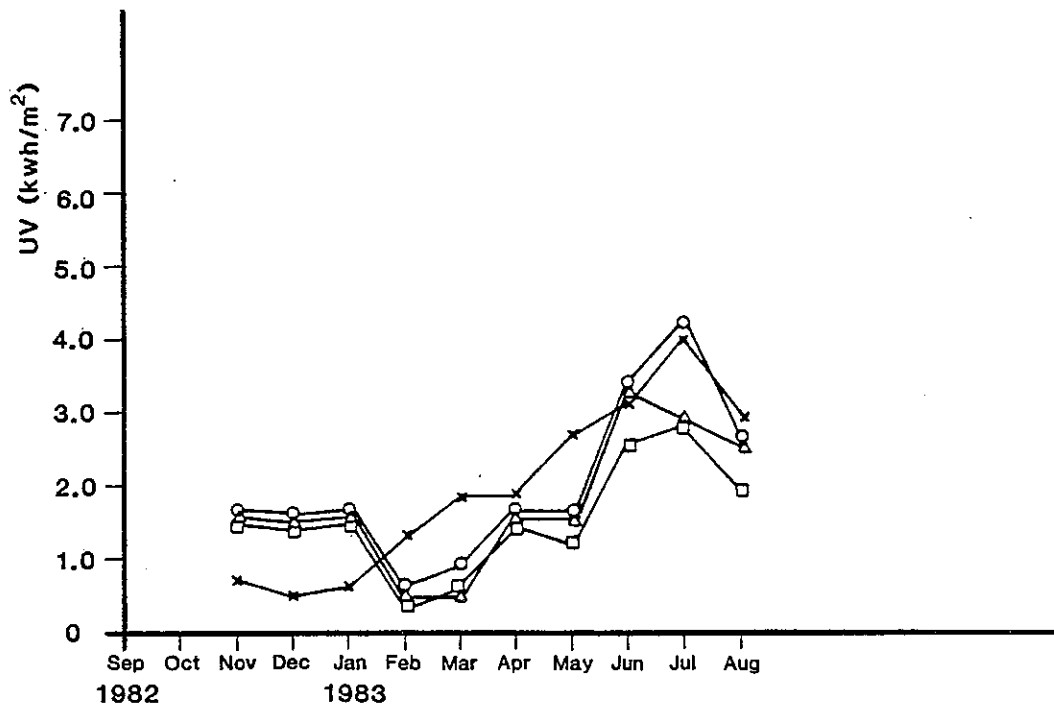


FIGURE 5

Photochemical monitoring of UV solar radiation, (PVC method), (○) exposure on horizontal surface, (△) exposure on south/45° surface. (□) exposure on vertical surface and (×) measurement on horizontal surface with UV pyranometer

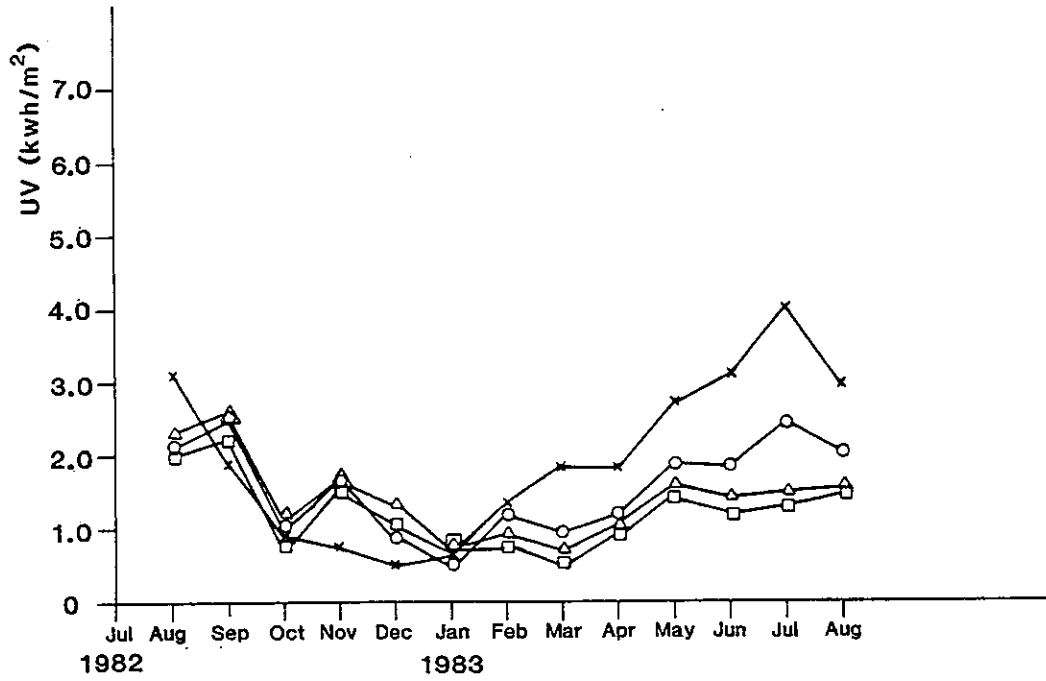


FIGURE 6

Photochemical monitoring of UV solar radiation, (PPO method), (O) exposure on horizontal surface, (Δ) exposure on south/45° surface. (□) exposure on vertical surface and (X) measurement on horizontal surface with UV pyranometer

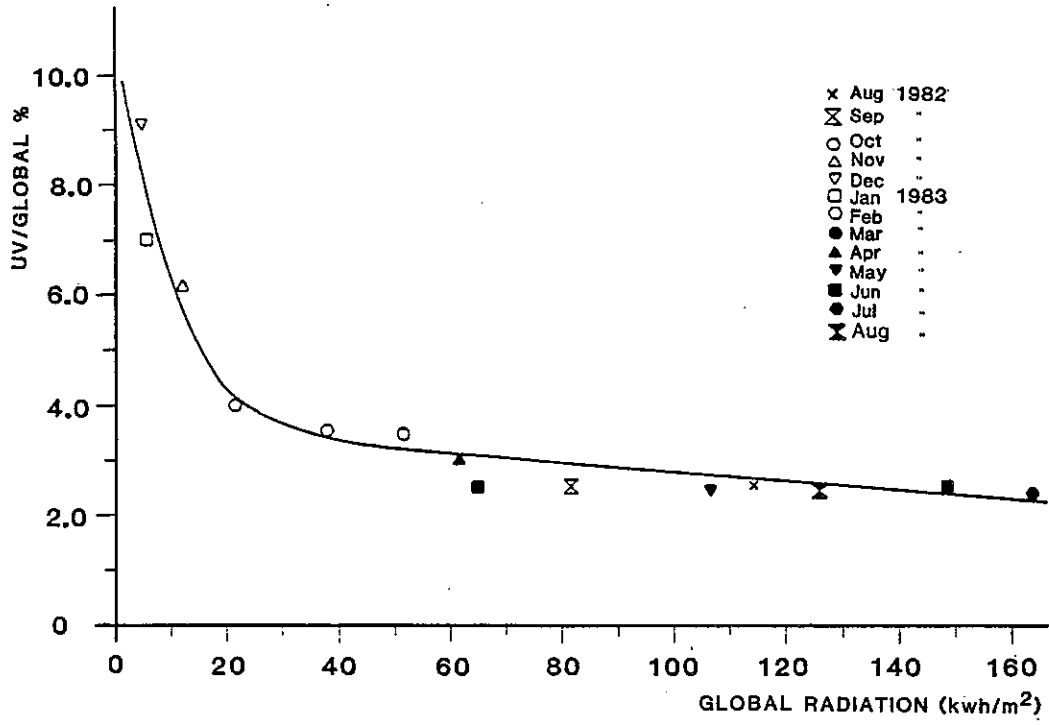


FIGURE 7

Percent UV solar radiation vs. monthly global solar radiation on horizontal surface, Aug. 1982-Aug. 1983.

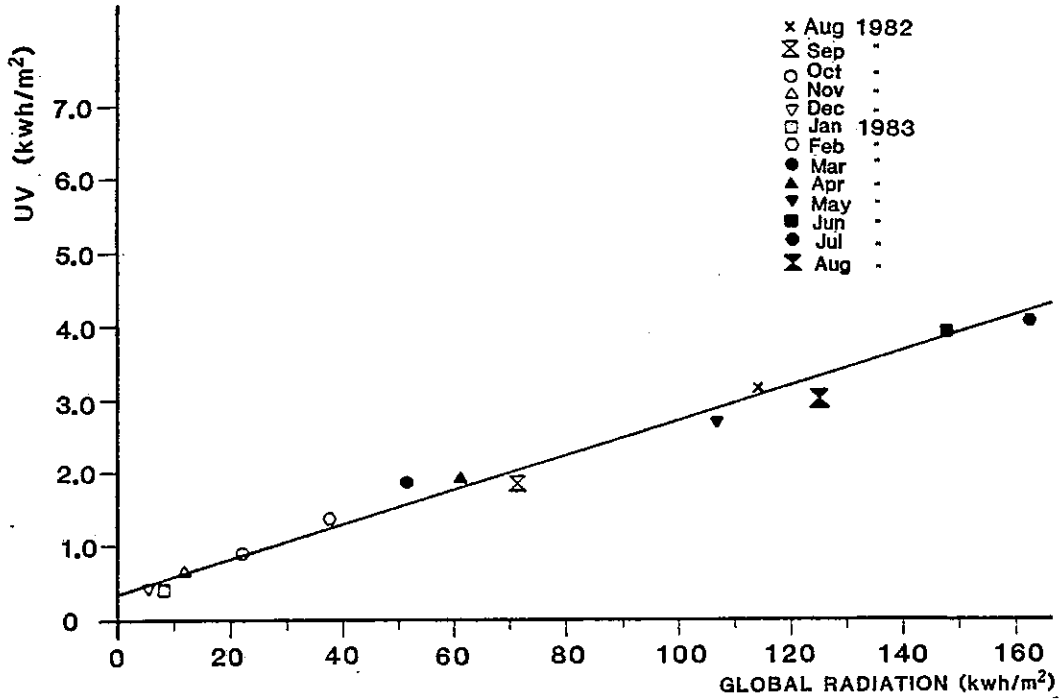


FIGURE 8

Intensity of UV solar radiation vs. monthly global solar radiation on horizontal surface, Aug. 1982-Aug. 1983

A certain correlation between UVR and global solar radiation can be utilized to estimate one component from the other through special calibration curves. The proportion of UVR in solar radiation increases with a decrease in daily global solar radiation (4).

Figure 7 shows the relation between UVR percent of solar radiation and the monthly global solar radiation. A linear relation can be noticed for the interval 2-3.5% UVR% and 25-165 KWh/m² global radiation. In this linear relation, the UVR% increase as global radiation decrease.

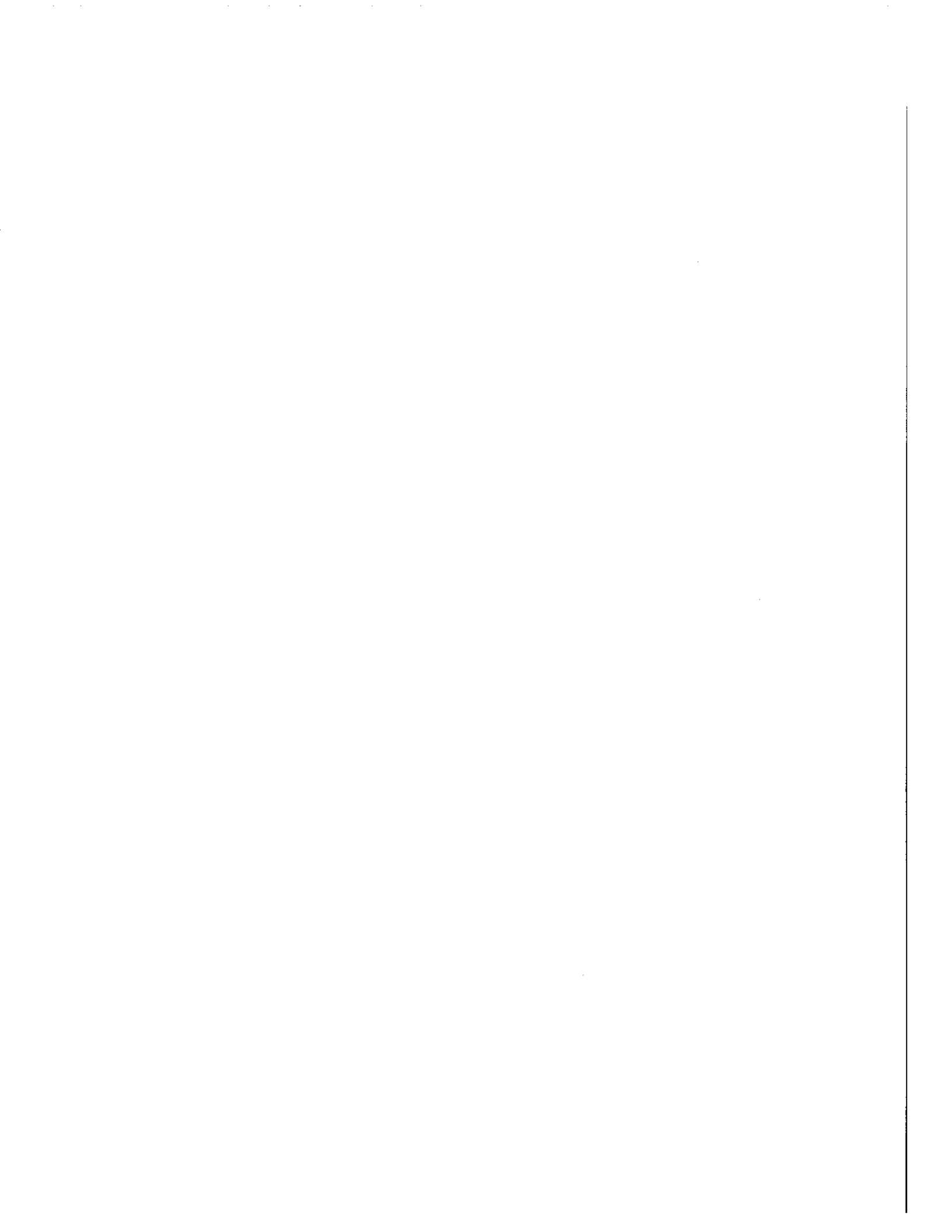
Figure 8 shows another relation between the monthly intensity of UVR and global solar radiation in KWh/m². A direct linear proportionality between both variables can be observed from the figure.

It is important to bear in mind that these relations (Figures 7 and 8) are dependent on time and site of exposure and should be considered as approximate methods for estimation of different component of solar radiation.

REFERENCES

1. Lala, D., "Monitoring of Ultraviolet Solar Radiation", Nordic Seminar on Durability and Service Life of Surface Coatings, Technical Research Centre of Finland, Åbo, May 1982.
2. Ashton, H.E. and P.J. Sereda (1982): "Durability of Building Materials, 1, p. 49-65.
3. Yamasaki, R.S. (1971): "Journal Paint Technology", 43(555), p. 75-83.
4. Yamasaki, R.S. (1983): "Durability of Building Materials", p. 17-26.
5. Shirota, T., Y. Watanabe and K. Yoshikawa (1983): "Report on Round Robin Test on PMMA and PE Standard Reference Materials for Testing Light Exposure, unpublished.
6. Lala, D., J.F. Rabek and B. Rånby (1981): "Polymer Degradation and Stability", 3, p. 307-321.
7. Rånby, B. and J.F. Rabek (1979): Appl. Polym. Symp., No. 35, p. 234-240.
8. Rånby, B. and J.F. Rabek (1977): "ESR Spectroscopy in Polymer Research", Springer Verlag, Berlin.
9. Rånby, B. and J.F. Rabek (1975): "Photodegradation, Photooxidation and Photostabilization of Polymers", Wiley, London.
10. Jerussi, R.A. (1971): Journal Polym. Sci., A1, 9, p. 2009-2015.

11. Kelleher, P.G., L.B. Jassie and P.D. Gesner (1967): *Journal Appl. Polym. Sci.*, 11, p. 137-150.
12. Kelleher, P.G. and P.D. Gesner (1979): *Polym. Eng. Sci.*, 10, p. 38-40.
13. Martin, K.G. (1973): *Br. Polym. Journal*, 5, p. 443-450.
14. Martin, K.G. and R.I. Tilly (1969): *Br. Polym. Journal*, 1, p. 213-216.
15. Martin, K.G. (1971): *Br. Polym. Journal*, 3, p. 36-40.
16. Martin, K.G. (1977): *CSIRO Aust. Div. Building Res., Techn. Pap., (second series) No. 18*, p. 1-33.
17. Davis, A., G.W. Deane, D. Gordon, G.V. Howell and K.J. Ledbury (1976): *Journal Appl. Polym. Sci.*, 20, p. 169-170.
18. Davis, A. and G.W. Deane (1976): *Nature*, 261, p. 169-170.
19. Challoner, A.V.J., M.F. Corbett, A. Davis, B.L. Diffy, J.F. Leach and I.A. Magnus (1978): *National Cancer Institute Monography*, 50, p. 97-100.
20. Davis, A., D. Gordon and G.V. Howell (1973): "Explosives Research and Development Establishment", *Technical Report No. 141*, July 1973.
21. Nireka, T. (1983): "Measurement of Ultraviolet Radiation as the Deterioration Agent for Evaluating Performance over Time of Building Materials and Components", *CIB Congress, Stockholm, August 1983*.



5.G CORRELATION BETWEEN THE PERFORMANCE OF A CONCENTRATING COLLECTOR
AND THE DIRECT RADIATION DERIVED FROM PYRANOMETRIC MEASUREMENTS

Björn Karlsson and Christer Brunström

Alvkarleby Laboratory
S-810 71 Alvkarleby, Sweden

CORRELATION BETWEEN THE PERFORMANCE OF A CONCENTRATING COLLECTOR AND THE DIRECT RADIATION DERIVED FROM PYRANOMETRIC MEASUREMENTS

ABSTRACT

The direct radiation towards a tracking linear parabolic concentrating collector is derived from pyranometric measurements of the global and diffuse radiation. The pyranometers were attached to the tracking mechanisms of the collector with the shadow ring directed along the absorbing tubes. This means that the shadow ring only works properly when the collector is tracking the sun. But it also means that the pyranometers always record the direct radiation useful for the collector. The pyranometric measurements are compared with pyr heliometric measurements and the impact of the width of the shadow ring is discussed.

INTRODUCTION

For a proper evaluation of the thermal efficiency of a concentrating collector it is necessary that the direct component of the radiation can be measured in a convenient way. It is often costly and technically complicated to monitor the direct radiation with a pyr heliometer. Therefore, it is more practical to derive the direct component from pyranometric measurement of the global and diffuse radiation.

In this paper the correlation between the efficiency of the linear parabolic collector shown in Figure 1 and the direct radiation measured with the pyranometers in Figure 2 is presented. The direct radiation measured with the pyranometers is also compared with the beam radiation measured with an Angström-type pyr heliometer and the impact of the width of the shadow ring is discussed. Finally, the possibility of deriving the direct component of the radiation towards the tracking collector, from the direct radiation towards the horizontal surface is evaluated. All measurements were performed in Älvkarleby situated 160 km north of Stockholm at a latitude of 60.57°N and a longitude of 17.45°E.

EXPERIMENTAL

The tested parabolic collector has a ratio of 40 to 1 between the width of the parabol and the diameter of the absorbing tube. It was oriented north-south and tilted 45°. The tracking system was controlled by the sensors in the glass-dome, seen on top of the reflectors in Figure 1. The reflectors and the attached glass-dome moved with the sun in order to balance the radiation on the shadow-plate separated sensors.

This means that the tracking function was activated when the direct radiation was strong enough to generate a difference in the currents generated by the photo-voltaic sensors. Under a clear sky the reflectors were adjusting their position once every minute. The angular dependence of the efficiency of the collector presented in Figure 3 shows that the efficiency

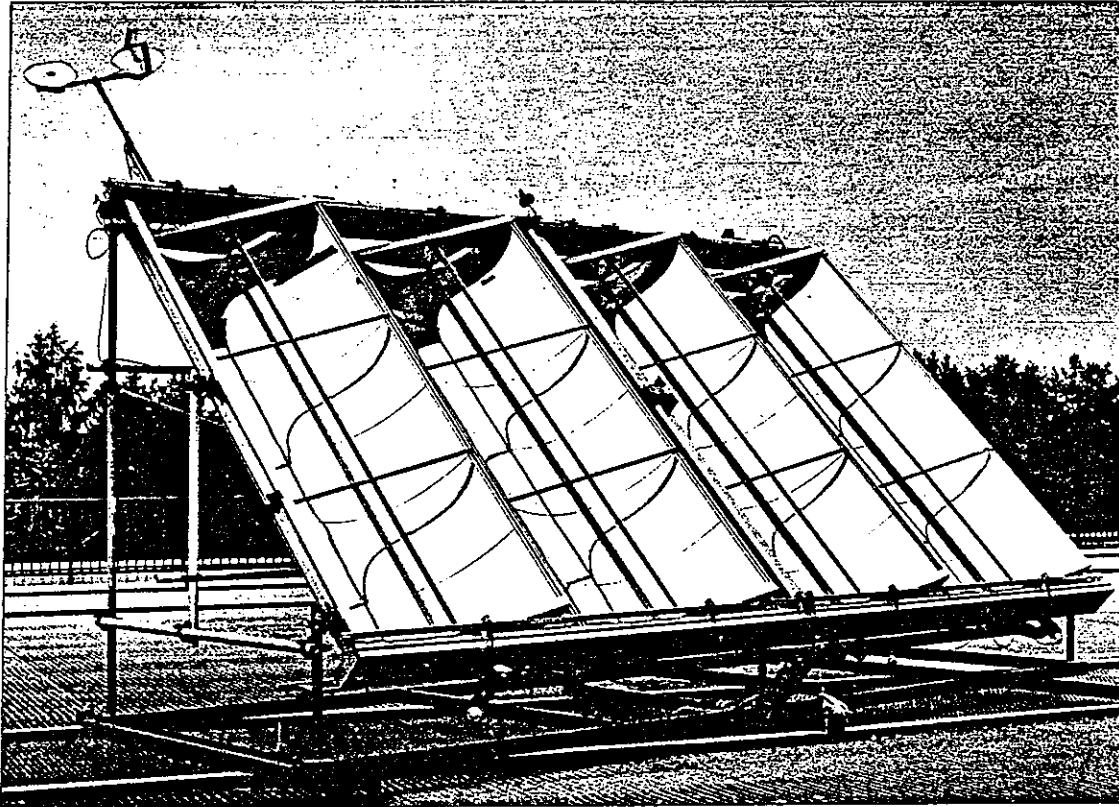


Fig. 1. The linear parabolic collectors with the pyranometers and the globe of the solar-sensor device.

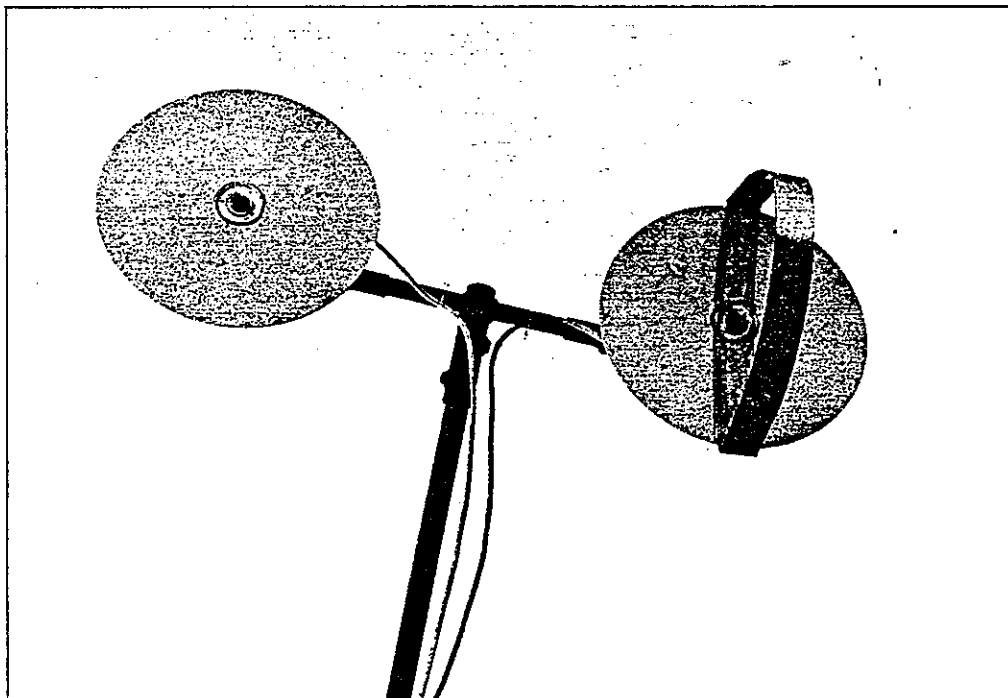


Fig. 2. The Kipp & Zonen CM-5 pyranometers fixed to the tracking paraboles for measuring the global and diffuse radiation towards the collectors.

of a properly aligned collector was not reduced during that minute. This figure was derived by directing the collector on a point to the west of the sun and recording the thermal efficiency of the collector during the time-period when the sun passed that point.

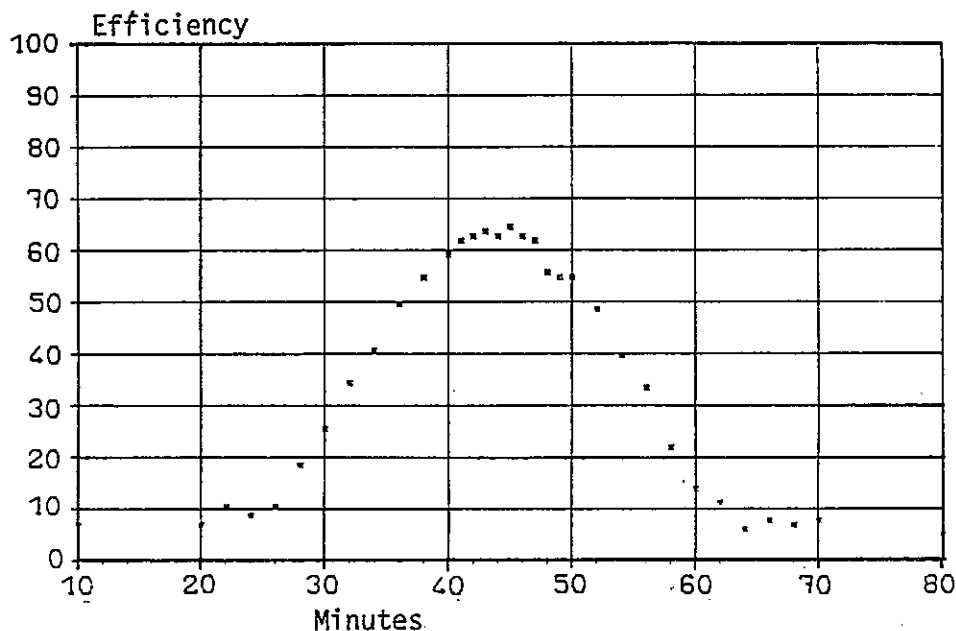


Figure 3 The angular sensitivity of the collector registered as a function of the relative solar time

This figure also indicates that the collector accepts the radiation within an angle corresponding to around 40 minutes which means 10° . This angle should in principle coincide with the acceptance angle of the instruments used for recording the direct radiation.

The global and diffuse radiation towards the parabolic mirrors were monitored by the pyranometers shown in Figure 2. These were mechanically attached to the tracking system and thereby always facing the same direction as the paraboles. The instrument used for recording the diffuse fraction was equipped with a shadow band of a width of 4 cm and radius varying from 15 cm to 19 cm. Its area amounts to 11% of the area of the corresponding half-sphere with an angular aperture of 11° . The shadow ring was mounted in the plane normal to the aperture-plane of the paraboles as seen in Figure 1. This means that the ring only shades the pyranometer when the tracking mechanism is working. But it also means that the pyranometers always monitor the useful direct radiation impinging on the collectors, both in a tracking or a non-tracking state of the system.

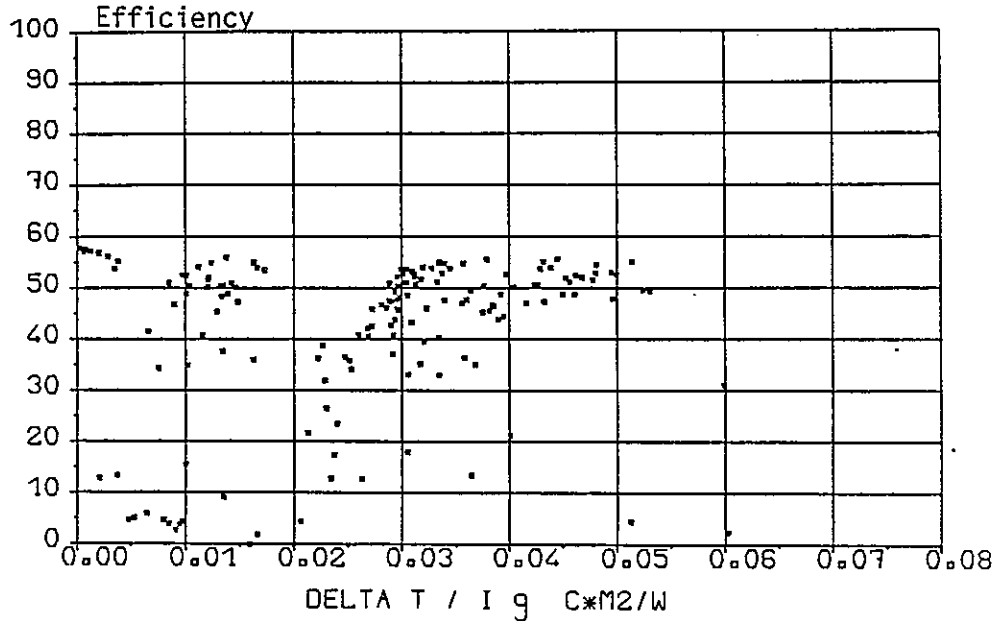


Figure 4 The efficiency curve of the collector correlated by the temperature difference divided by the global radiation.

Figure 4 presents the efficiency of the collector as a function of the global radiation. As expected for this collector, which does not accept diffuse radiation, the correlation is poor with a large scattering in the data.

If however, the efficiency is presented as in Figure 5 as a function of the temperature difference and the direct radiation, given by the difference between the global and diffuse components, a nice correlation is obtained.

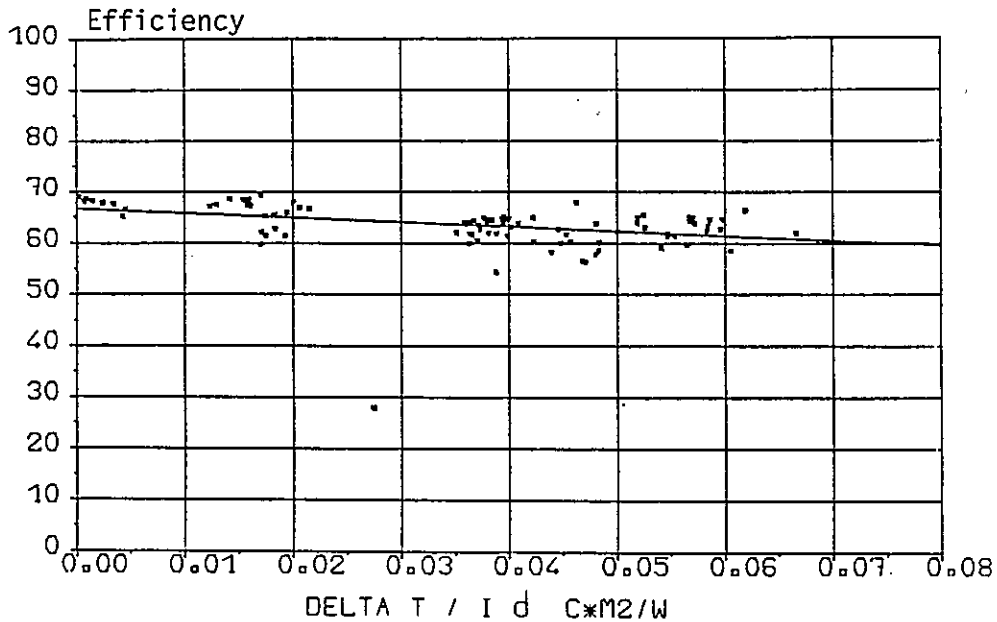


Figure 5 The efficiency of the collector correlated by the temperature difference divided by the direct radiation for radiation-levels above 700 W/m²

This good correlation is further underlined in the next figure, which shows how the efficiency of the collector depends on the intensity of the direct radiation without any compensation for the varying temperatures of the collector and the ambient during the test-period. This temperature compensation is less important for a concentrating collector than for a flat-plate collector, since the concentrating collector has small heat-losses.

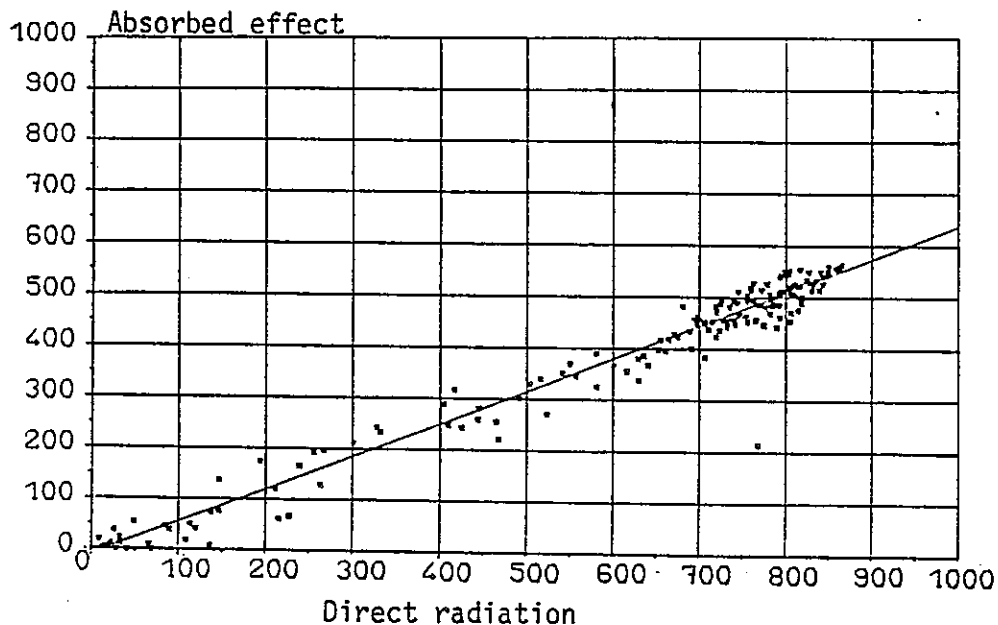


Figure 6 The efficiency of the collector as a function of the intensity of the direct radiation.

DISCUSSION

The nice linear dependence of the efficiency of the collector on the direct radiation measured by the two tracking pyranometers means that this technique forms a useful method for monitoring the direct beam. It works without the complexity of the tracking pyrhemeters and without the frequent adjustments of the shading ring normally required for pyranometers.

This method of monitoring the direct radiation was compared with measurements performed with an Angström pyrhemeter. During these measurements both the pyrhemeter and the pyranometers were manually adjusted towards the sun. The results of these measurements are presented in Figure 7 which illustrates how the direct component measured with the pyrhemeter correlates with the pyranometric measurements for different widths of the shadow ring. The radius of the ring was always 15 cm. The figure shows that the measurements performed with the pyranometers give systematically higher values of the direct radiation. These and the other pyranometric measurements are however presented without any correction for the shadow band (2). If a shadow band correction factor is applied good agreement is obtained.

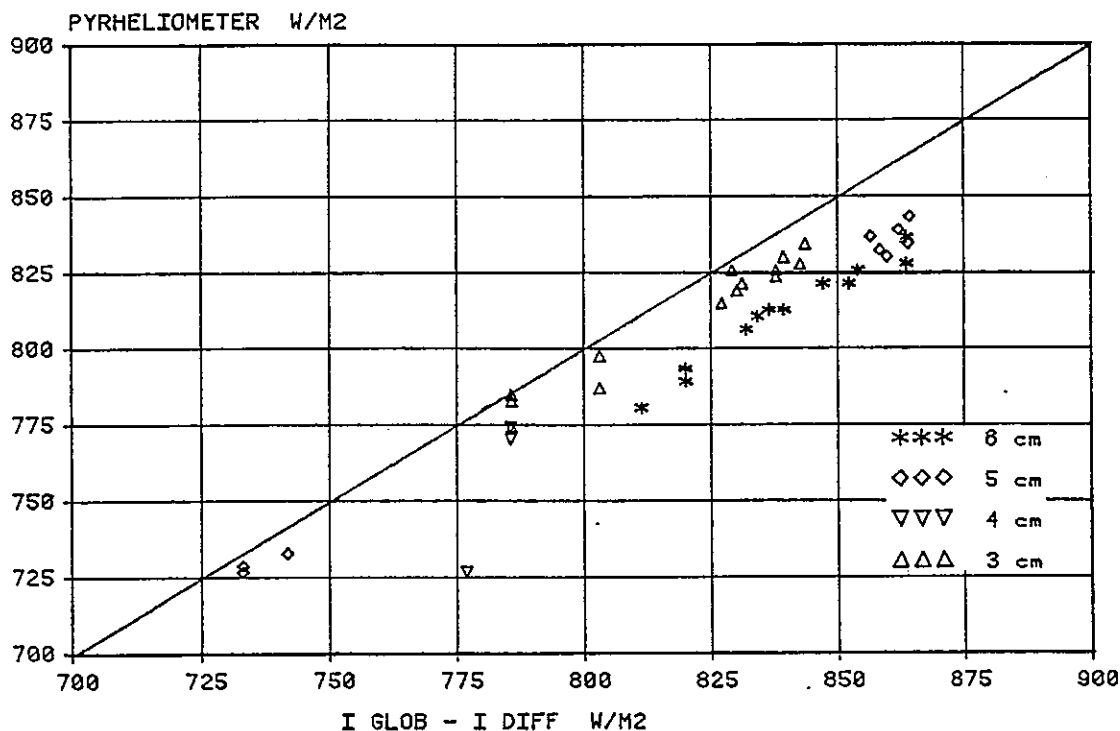


Figure 7 Direct radiation measured with a pyr heliometer and pyranometers with different widths of the shadow ring.

In many radiation models the direct radiation towards an arbitrary surface is calculated from a knowledge of the direct radiation towards a horizontal surface and the angles of incidence towards this surface and the horizontal (1). The use of this method in this application is shown in Figure 8, which shows the correlation between hourly mean-values of the intensity of the direct component on the collector derived from horizontal or tracking pyranometers. These measurements of the radiation on the horizontal surface were performed with Kipp & Zonen CM 11 and CM 12 pyranometers for the global and diffuse components respectively. A large scattering of the data is indicated. If, however, the points are examined in detail it is shown that the data which deviate strongly from the line were recorded when the horizontal shadow ring was misaligned or the tracking system was not activated. If these data are omitted a relatively good correlation between the different methods of deriving the direct radiation is obtained. The horizontal measurements, however, generally result in 5% higher values of the intensity of the direct radiation on the collector. If this method were to be used for deriving the direct radiation for efficiency measurements, large additional experimental errors would be introduced. These errors would occur even if the shadow band was always aligned.

CONCLUSIONS

It is shown that the measurements of the direct radiation incoming on a concentrating collector can be easily carried out by attaching the global and diffuse pyranometers to the tracking mechanism of the collector. If the shadow ring is aligned along the direction of the absorber-tubes the diffuse pyranometer will always record the part of the radiation which can not be

used by the collector. Further, this means that the difference between the global and diffuse pyranometers always represents the part of the radiation which can be focused on the absorbing tubes. This is valid whether the collector is aligned towards the sun or not.

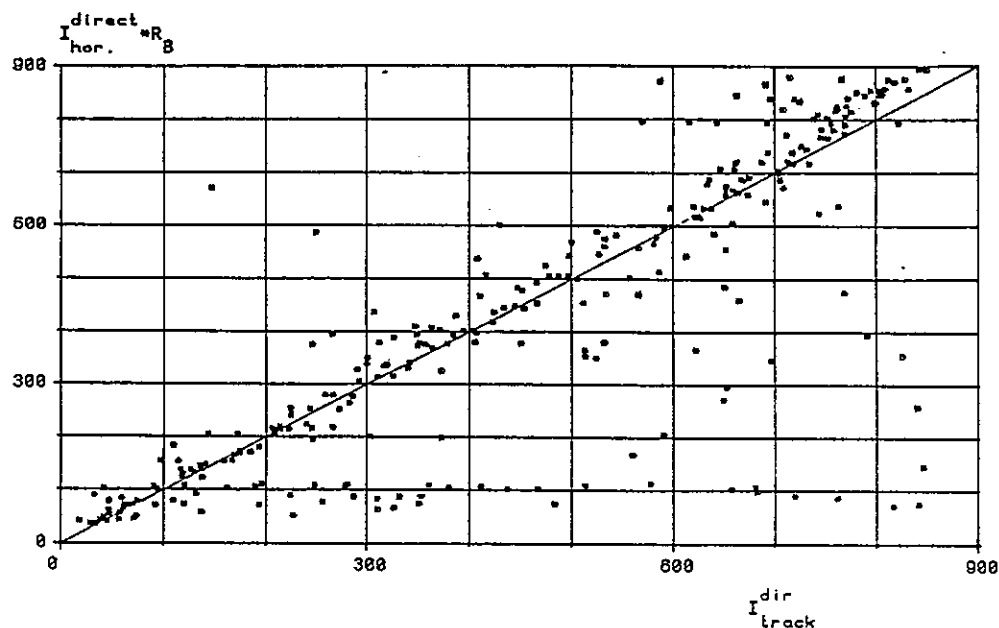


Figure 8 The correlation between the direct radiation on the tracking collector derived from horizontal or tracking measurements

Comparison between pyr heliometric and pyranometric measurements showed good agreement. Calculation of the direct radiation falling on the tracking collector from horizontal measurements involves practical problems and introduces additional errors.

ACKNOWLEDGEMENTS

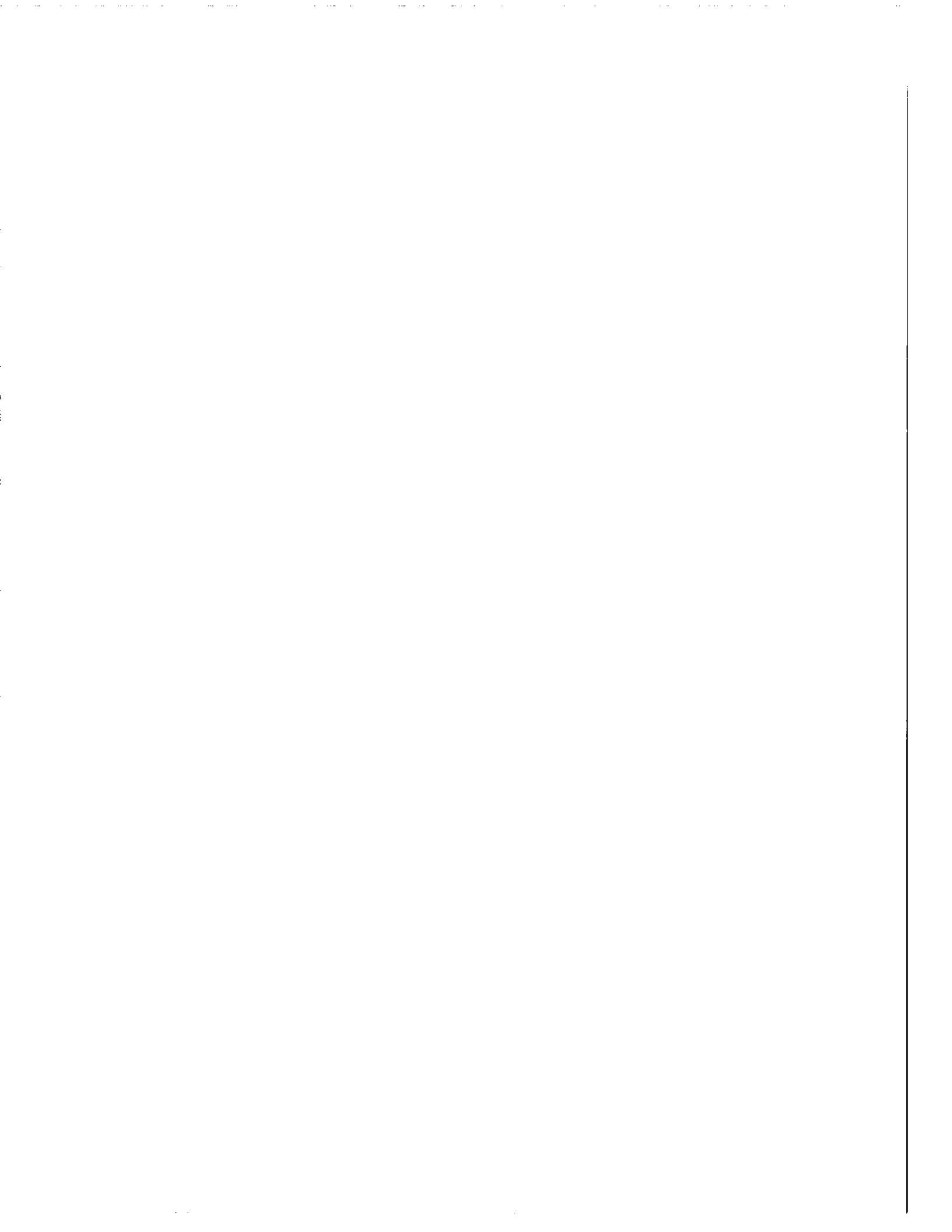
We thank Karin Johansson for typing the manuscript, Monica Löf for computer calculations and Peter Norlin for experimental work. Lars Dahlgren at SMHI is acknowledged for lending us the pyr heliometer and for helpful discussions.

REFERENCES

1. Duffie, J.A. and W.A. Beckman (1980): Solar Engineering of Thermal Processes, John Wiley and Sons, New York, 1980.
2. Turner, W.D. and A. Mujahid (1983): Diffuse Sky Measurements and Determination of Corrected Shadow Band Multiplication Factors, J. of Solar Energy Engineering, V 105, 1983, pp. 305-310.

SESSION 6

General Discussion



6.A SUMMARY OF DISCUSSION

D.C. McKay

Atmospheric Environment Service
Canadian Climate Centre
4905 Dufferin Street
Downsview, Ontario
M3H 5T4

SUMMARY OF DISCUSSION

Question: What do we need to do in pyranometry?

INDIVIDUAL RESPONSES

Participant	Responses
Gert Jaap van den Brink	<ul style="list-style-type: none">- documentation of procedures used in calibration and characterization of pyranometers- common format of reporting the information
C. Wells	<ul style="list-style-type: none">- documentation of procedures and results- transfer function idea a good one
K. Dehne	<ul style="list-style-type: none">- more effort in relating field tests with laboratory tests- problem of ageing of pyranometers- problem of calibration using only one instrument
H.D. Talarek	<ul style="list-style-type: none">- product recommendation for users- defined procedure for the calibration of pyranometers
C. Fröhlich	<ul style="list-style-type: none">- better understanding of pyranometers particularly linearity effects and relationships between outdoor and indoor calibration
L. Liedquist	<ul style="list-style-type: none">- time constant of pyranometers- effect of domes- spectral distribution
H. Andersson	<ul style="list-style-type: none">- cosine response error, suggests this is not large
L. Dalghren	<ul style="list-style-type: none">- need for feedback between laboratory and field investigations regarding characterization- necessary to show the effects of making corrections
E. Flowers	<ul style="list-style-type: none">- need to examine the physical processes involve in pyranometry- need to develop a good experiment to examine physical processes

- J.L. Plazy
 - show users uncertainty of measurement
 - provide guidance on how to use pyranometers, how to calibrate
 - provide a generic transfer function
 - continue work on dynamic behaviour of pyranometers
 - need spectral measurements
- A. Zelinka
 - require feedback to manufacturers
- F. Kasten
 - quality control of data
 - emphasis on care of instrumentation
 - need good documentation
- C. Gandino
 - calibrate on inclined surfaces
 - calibrate instrument in season it will be used
 - provide good documentation
- J. Seymour
 - require two levels of product one for expert and one for user

From the responses I see the following major areas of need:

- i) increased understanding of the physics of pyranometers
- ii) mechanisms for relating field tests to laboratory tests;
- iii) good documentation of calibration procedures and results. This includes a common formatting for reporting characterization of pyranometers.
- iv) set of guidelines which can be used by the solar engineer for calibrating and using pyranometers.



6.B AN OPEN LETTER ON PYRANOMETER CALIBRATION

Edwin Flowers
NOAA/ERL-ARL, R32X2
Solar Radiation Facility
Boulder, Colorado, 80303.

AN OPEN LETTER ON PYRANOMETER CALIBRATION

Dear Colleague:

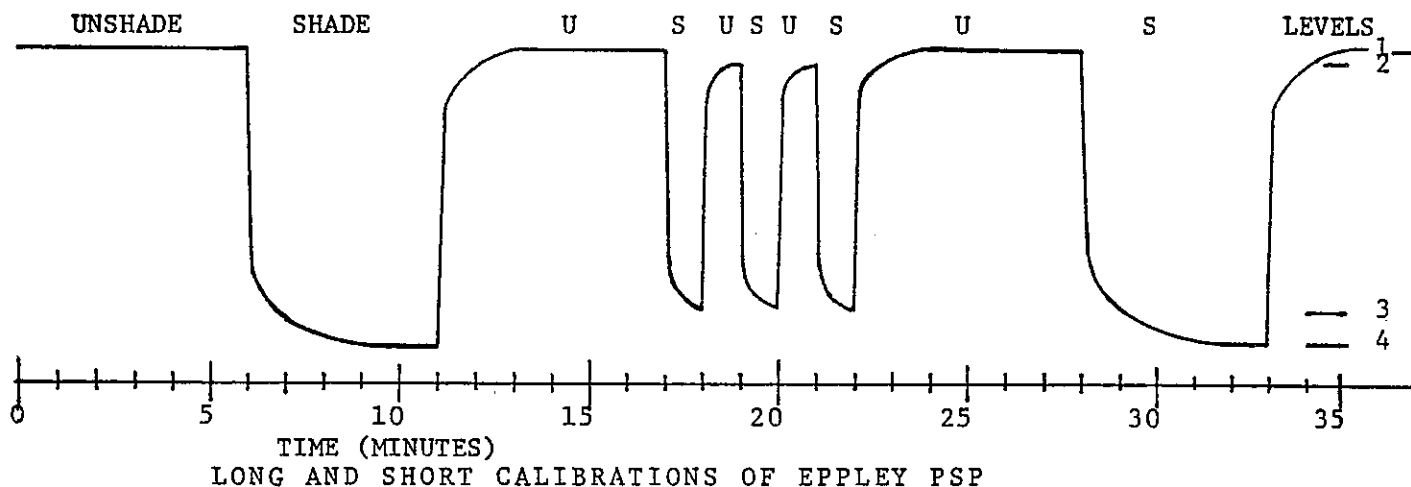
This was first sent as a letter to Gene Zerlaut, Chet Wells, John Hickey, Claus Fröhlich and David Wardle who suggested it should appear here. The purpose is to invite your comments and to pass along some recent experiences which may be of interest to you. There are two subjects:

- (1) the timing sequence for shading pyranometers during transfer calibrations from pyrhemeliometers;
- (2) The "Fröhlich" calibration transfer technique.

Timing Sequence

The timing sequence for shading pyranometers during calibration transfers has historically been assumed to be dependent on the gross time response of the pyranometer. Most experimentors have not measured this response but rather have assumed it to be the time required to reach "steady state" when shaded and unshaded. For the old style Eppley bulb pyranometers this time was between about 5 to 10 minutes depending on the ambient temperature. Thus the shade/unshade cycle was generally 10 minutes (10 shade/unshade). With the introduction of the Eppley model 15 and then the PSP, the time to reach "steady state" was from about 2.5 to 5 minutes with considerable variation from one instrument to another. The cycle I began using some 20 years ago with PSP's was thus 5 minute shade/6 minute unshade. Recently this simple-minded approach has been challenged with the suggestion that the timing should be reduced to as short as 30 seconds to a maximum of 50 seconds shade/90 sec unshade. This is based as I understand it on the measured time response of the naked thermopile/receiver element and a concept referred to as "duty cycle" which involves some multiple of this response. I believe this method presents a paradox: namely, what is the true global radiation? The true diffuse radiation? The true direct component radiation?

Consider the following diagram as an idealization of real data and which shows the analog record of an Eppley PSP undergoing shading by both the long and short cycles.



From the diagram and your own experience the following is true:

1. The total global radiation before any shading, after the 6 minute recovery and following the last shading, is at its highest level (level 1 on the diagram). This is assumed to be "steady state".
2. The unshaded values during a 60 second cycle (level 2) are lower than the "steady state" values.
3. The lowest level of the 5 minute shade ("shade state shade, "level 4) is lower than the shade level (level 3) for the 60 second shades.
4. This pattern, namely the shorter the shade/unshade cycle the smaller the differences between shade and unshade values, prevails with all PSP's as far as I know. Figure 30, p 51 in Zerlaut's article in Advances in Solar Energy, 1982 is incorrect.

The direct radiation component normal to the pyranometer plane as measured by the pyrliometer is equated to the shade/unshade voltage difference from the pyranometer to give the sensitivity figure for the pyranometer. In every case the short cycle will always give a lower pyranometer sensitivity value (e.g. $\text{mv}/10^3\text{w}\cdot\text{m}^{-2}$) than a longer cycle. Table 13, p 54 of Zerlaut's article gives the reverse although there could possibly be other explanations (tests not on the same day, different sun angles). If level 1 (on the diagram) is the true global radiation (if not what is it?) then the true diffuse radiation must be level 3 + (1-2). What then does level 4 represent? If level 2 is the true global and level 3 the true diffuse, is it then necessary when reducing measured data to add an increment (3-4) to diffuse data and subtract another increment (1-2) from global data? Certainly levels 1 and 4 occur during ordinary conditions of exposure and usually it is assumed that the direct radiation component is 1-4 although the short cycle theory would say it is something smaller (2-3). Perhaps not a true paradox but certainly perplexing.

The magnitude of the difference in derived sensitivity (short/long cycle) for the pyranometer from an experiment I did in July 1982 was 3/4% to 1 %. The attached table gives the data and Figure 1 shows plots of 10 second values during the experiment (plotted as a ratio to a second pyranometer which was not shaded). The long cycle was 5 minute shade/6 minute unshade; the short cycle 60 second shade and unshade.

The "Fröhlich" calibration method

It appears to me that this technique is a very powerful tool: (a) to calibrate large numbers of pyranometers simultaneously, (b) to obtain a better measure of the global radiation especially under cloudless skies than can be obtained from any currently available pyranometer, (c) to derive the "response to clear sky global radiation" for types of pyranometers not amenable to direct shade calibrations such as photocell types, black and white types and lower quality types.

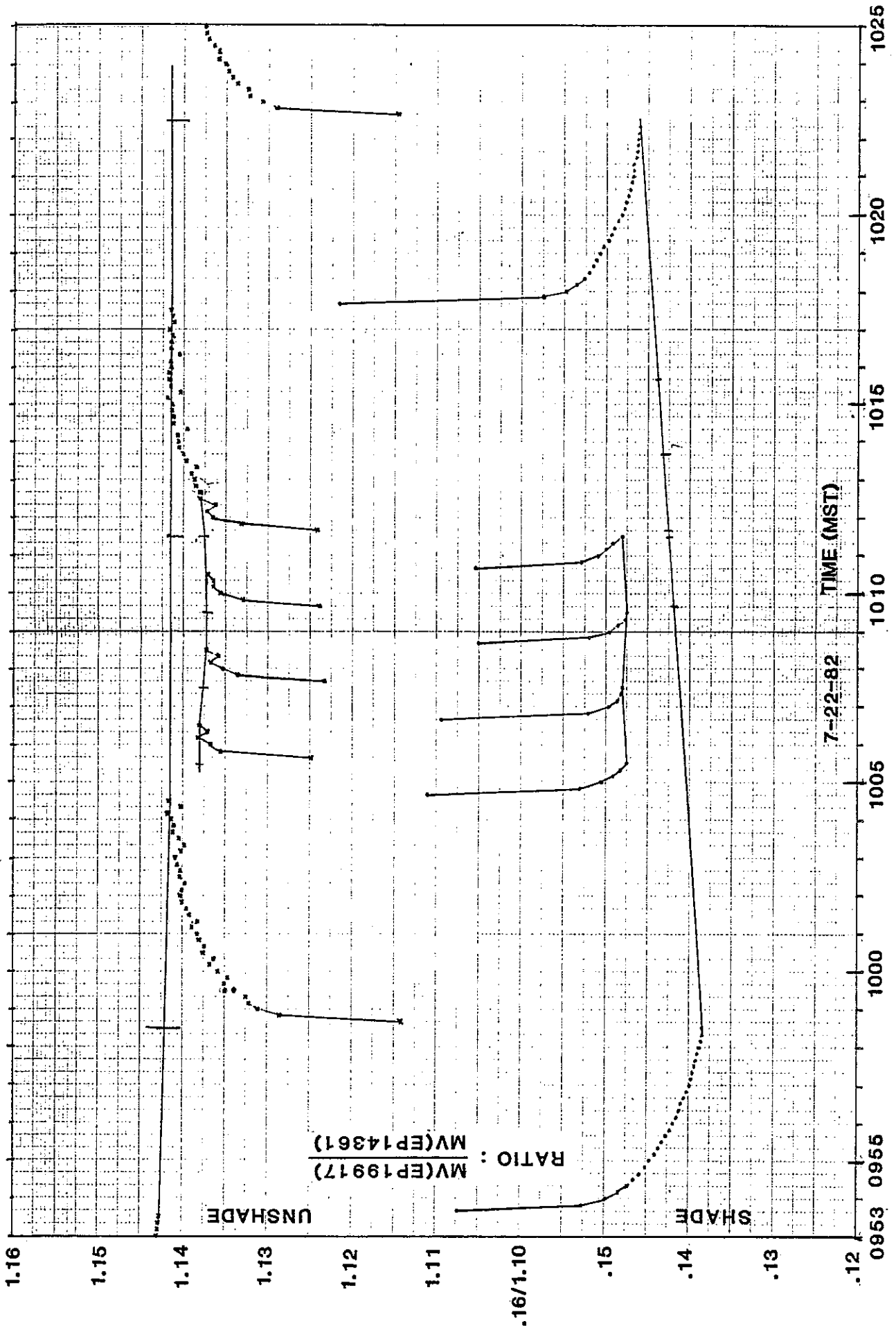


FIGURE 1a

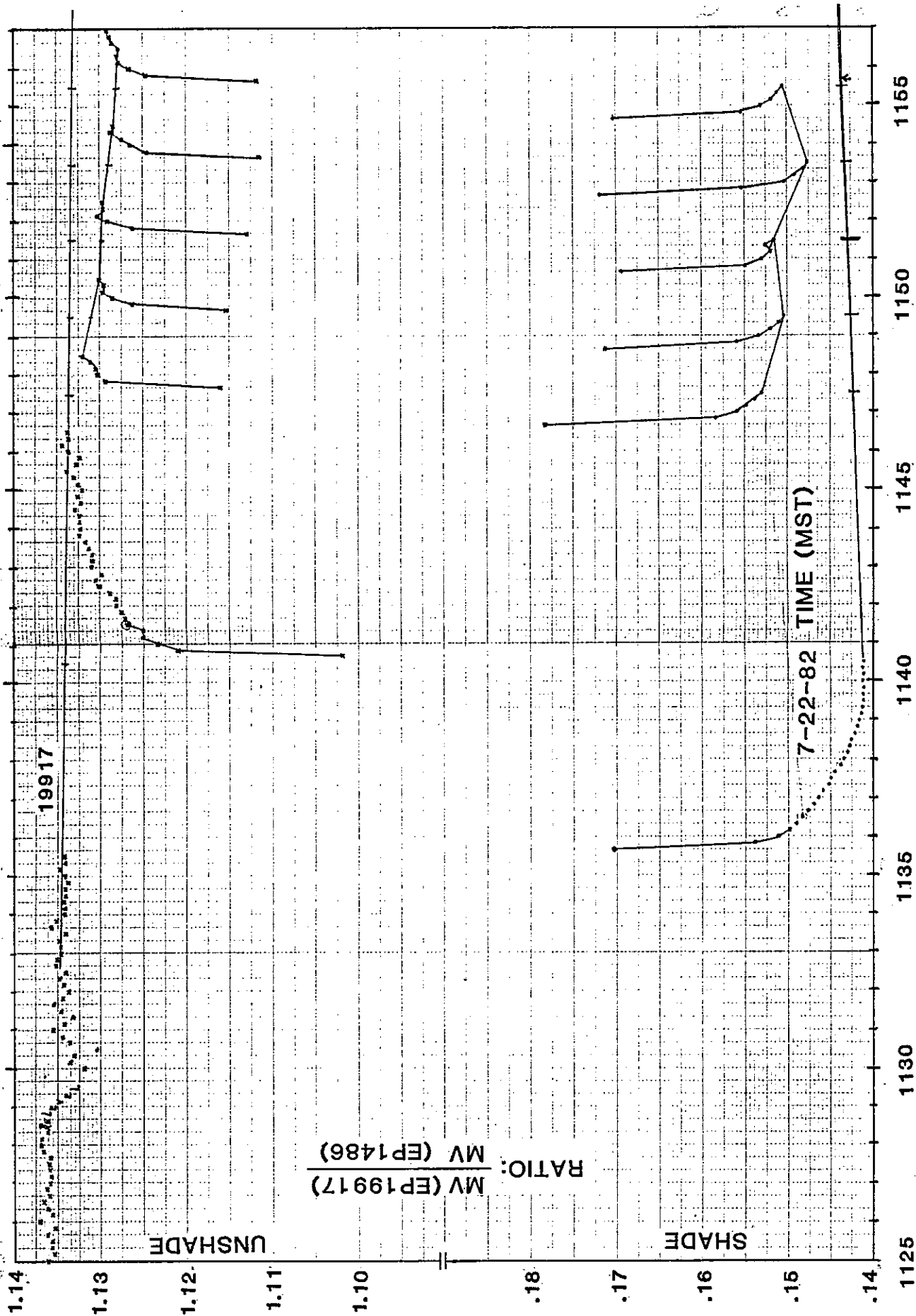


FIGURE 1b

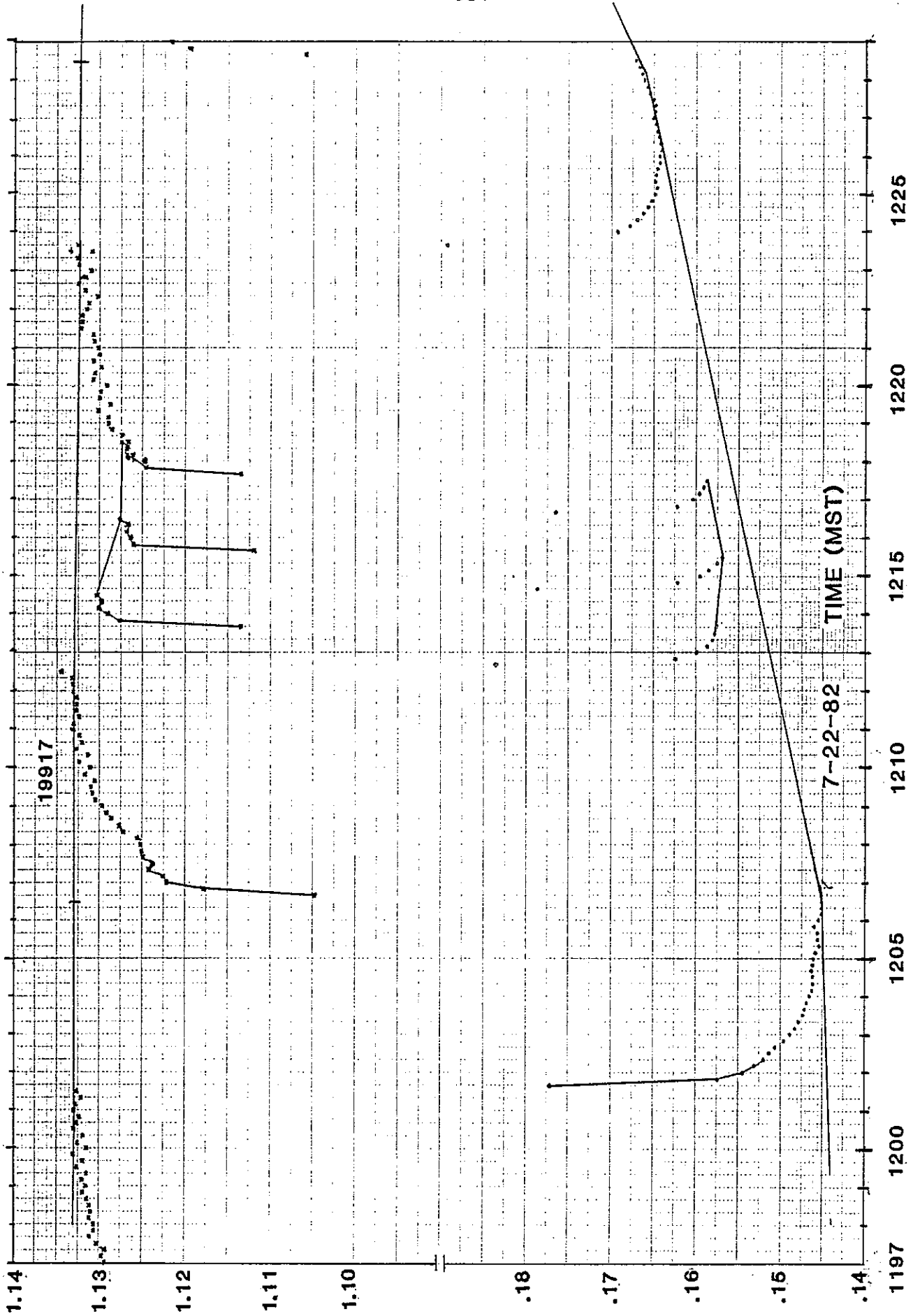


FIGURE 1c

The procedure as you are aware involves obtaining the global radiation from the sun of a disk-shaded pyranometer (diffuse) and a pyr heliometer (direct component). The voltage output from any similarly exposed pyranometer is then equated to this global radiation to yield the sensitivity (calibration) value for the pyranometer. For accurate results, the pyr heliometer should be a cavity instrument and the disk-shaded pyranometer an all-black pyranometer, either an Eppley PSP or Kipp CML1. For continuous measurements the pyr heliometer would need to be all-weather which for the case of the Eppley NIP may introduce an additional $\pm 1\%$ uncertainty.

Since February of this year (1984) at our Facility, each time the primary reference pyranometer was calibrated by the shade method we used the measure of global radiation from the shaded pyranometer and the cavity pyr heliometer to calibrate many of the other pyranometers always in operation in our comparison array. When the shade calibration covered a large range of sun angles both in the morning and afternoon, all of the pyranometers then operating (45 total) were calibrated. If the shade calibrations were limited to smaller parts of the day then only the control and specimen pyranometers were calibrated (10-15 instruments). We have acquired a great amount of data and consequently some new insights into the characteristics of a variety of pyranometer types. Since the greatest numbers of our pyranometers are either Eppley PSP's or Spectrolabs, the data allow us to make some judgments about generic differences in these two kinds of pyranometers. Some of the results (not necessarily new) I believe are worth sharing with you and asking for any opinions you might have about my interpretations or similar or contrary results from your own tests.

- The Eppley PSP's, Kipp (CM6 & CML1) and Spectrolabs give in general repeatable results regardless of season (all data have been corrected for ambient temperature) which indicates that the cosine error is a first order effect and the azimuth error a second order effect. The tests were done on February 6, March 8, April 4 and 16, May 8 and 30, June 27 and 29, July 5, August 27, 29 and 30, 1984, so they cover a wide range of seasonal change in both solar elevation/azimuth and ambient temperature. For these kinds of instruments the average AM and PM sensitivity of 50° sun elevation agrees closely with the sensitivity assigned on the basis of continuous comparisons with the working reference pyranometer, an Eppley PSP whose calibration has been normalized to 50° sun elevation. This simply reflects that these kinds of instruments have similar characteristics and/or their behavior is dominated by their cosine response.
- Few instruments show AM/PM symmetry in the curves of sensitivity versus sun elevation. The asymmetry is repeatable attesting that the spirit level is centred. Several probable causes of this asymmetry are: (a) spirit level does not provide the optical level; (b) sensing surface and/or glass domes are not centred; (c) there are aberrations in the domes or sensor. Without exception, the Spectrolab instruments give steep slopes of sensitivity versus sun angle in the morning, a flattening out around noon and a lesser slope in the afternoon, a shape that

resembles that for air temperature through the day. If this is a temperature effect it is different from the "static" response which we measure in the Lab and apply to the data.

- The Eppley 8-48 and Schenk star pyranometers generally do not give curves which can be repeated through the seasons. The shapes of the curves of sensitivity versus sun angle are similar but absolute values at specific sun angles vary much more than for the all-black instruments. About the most I can deduce from this is that cosine is not the dominant characteristic. Possibly non-linearity and spectral sensitivity play a role.
- Limited data for two LiCor silicon sensors (not temperature corrected) showed surprisingly flat curves of sensitivity versus sun angle with maximum deviations from 15° to 60° sun elevation in the morning of less than 1% for both instruments and in the afternoon from 60° to 15° of $\pm 1.2\%$ for one and $\pm 1.5\%$ for the other. The two predominant characteristics for this instrument - cosine response of the plastic diffuser and spectral response of the photodiode - must cancel each other to produce this effect.
- Visible nicks in the domes (or presumably other aberrations as well) can introduce large excursions in the otherwise smooth curve of sensitivity versus sun angle when the sun tracks over the imperfection. For example, a pinhead size nick in the outer dome of a PSP produced a V shaped depression in the sensitivity with maximum reduction of 2.5% and the total effect from start to recovery lasting one hour.
- Calibrations performed on May 30 during a partial solar eclipse (maximum shadow over the sun about 50%) showed that the Eppley PSP's and a Kipp CM11 were unaffected by the change in radiation amount or the change in diffuse/direct ratio. That is, their sensitivity versus sun angle curves were unaffected. For the Spectrolabs, Kipp CM6's, Schenks and EKO, their curves all showed increased sensitivity exactly covering the period of the eclipse and with maximum increase at maximum of the eclipse (see figures 2-6). For all these instruments excepting perhaps the Spectrolabs, the explanation very likely is non-linearity with higher sensitivity for lower radiation levels. For CM6 and Schenk, Anderson found about a 5% decrease in sensitivity from 200 to 1000W/m²; our curves of sensitivity at low sun angles (low irradiance). At maximum solar eclipse the global irradiance dropped to 400 W/m² (about 50% reduction) and the sensitivities of the three instruments increased by 2.8% for Kipp CM6 S/N 774120, 3.9% for Schenk 1626 and 3.3% for EKO 81907 over their normal sensitivity at this sun elevation angle. Before onset of the eclipse, 400 W/m² occurred at about 25.5° sun elevation. If the eclipse induced change is all due to non-linearity, the non-linearity effect can be removed from the curves for the individual instruments at the comparable irradiance level, that is at 25.5° sun angle both AM and PM. These instruments all show AM/PM asymmetry, particularly the CM6 and Schenk but such corrections to the sensitivity versus sun angle plots would make them flatter. The significance of the

fact that PSP's and CMI1's were not affected during the eclipse is that they very likely are linear and that the cosine effect is the primary characteristic in explaining their behavior.

- Figure 7 shows the "response to clear sky global radiation" for the 4 IEA instruments and Eppley PSP 19918 which serves as our working reference. The curves are taken from the "Fröhlich" calibrations shown in Figures 2-6. The curves clearly show me why continuous outdoor comparisons of these instruments produce markedly different results for comparisons done in Davos in March or July and comparisons in Boulder, or Phoenix at the same or other times of the year. The Davos and U.S. results will differ almost anytime since we use Eppley PSP's for reference while Davos uses a PMO pyranometer. The curves presented here are normalized to 50° sun elevation so any other normalization would produce different results. Figure 8 shows the same data plotted with aspect to out working standard EP 19918. These data relate to cloudless sky conditions that occur during long-term continuous comparisons. All things considered, these and other data collected during these IEA instrument studies seem to offer only small hope that the current crop of pyranometers can produce irradiance data accurate to better than $\pm 1\%$ for use in solar collector testing. However, the "Fröhlich" method of obtaining global radiation for pyranometer calibrations could also produce global irradiance data of the required accuracy for collector testing, providing the pyr heliometer is a cavity type and the pyranometer a PSP, CMI1 or one of similar quality. To assess the accuracy of such a measurement one would need to know the uncertainty in the pyranometer calibration factor for diffuse radiation. An isotropic assumption for the diffuse radiation probably is adequate for a horizontal surface but may not be for a tilted surface where a large portion of the radiation is from a ground surface. However, since the diffuse radiation is usually very small under ideal test conditions, any error in the calibration of the diffuse measuring pyranometer will affect the global radiation only slightly.

If you have any comments I would greatly appreciate hearing from you.

COMPARISON OF LONG AND SHORT TIMING SEQUENCES IN PYRANOMETER CALIBRATIONS
NOAA/SRF, BOULDER, CO. 22 JULY 1982

Timing Shade/unshade	Time (MST)	Solar Elevation	SIN	TMI 67502		EPPLEY 19917		(PSP) Differ.	Sensitivity
				N.I.	VCNI	Unshaded	shaded		
300/360	0958.5	56.135	.8304	888.40	746.17	8.454	1.025	7.429	10.071
30/60	1006	57.41	.8425	885.62	746.17	8.554	1.107	7.447	9.980
30/60	1008	57.75	.8457	883.95	747.58	8.599	1.115	7.484	10.011 9.992
30/60	1010	58.08	.8488	886.50	752.45	8.632	1.119	7.513	9.985
30/60	1012	58.82	.8528	885.44	755.12	8.669	1.124	7.545	9.992
300/360	1022.5	60.12	.8671	881.37	764.21	8.817	1.128	7.689	10.061
RATIO: SHORT CYCLE/LONG CYCLE 9.992/10.066 = 0.9926									
300/360	1140.5	69.39	.9360	896.50	839.13	9.647	1.201	8.446	10.065
30/30	1148	69.78	.9384	890.48	835.60	9.621	1.304	8.317	9.953
30/30	1150	69.87	.9389	894.22	839.60	9.643	1.283	8.360	9.957
30/30	1152	69.94	.9393	887.05	833.24	9.582	1.289	8.293	9.953 9.960
30/30	1154	70.01	.9398	887.23	833.77	9.615	1.296	8.319	9.9775
3/30	1156	70.06	.9401	889.98	836.62	9.622	1.288	8.334	9.9615
300/360	1206.5	70.21	.9409	892.58	839.87	9.686	1.240	8.446	10.057
RATIO: SHORT CYCLE/LONG CYCLE 9.960/10.061 = 0.9900									

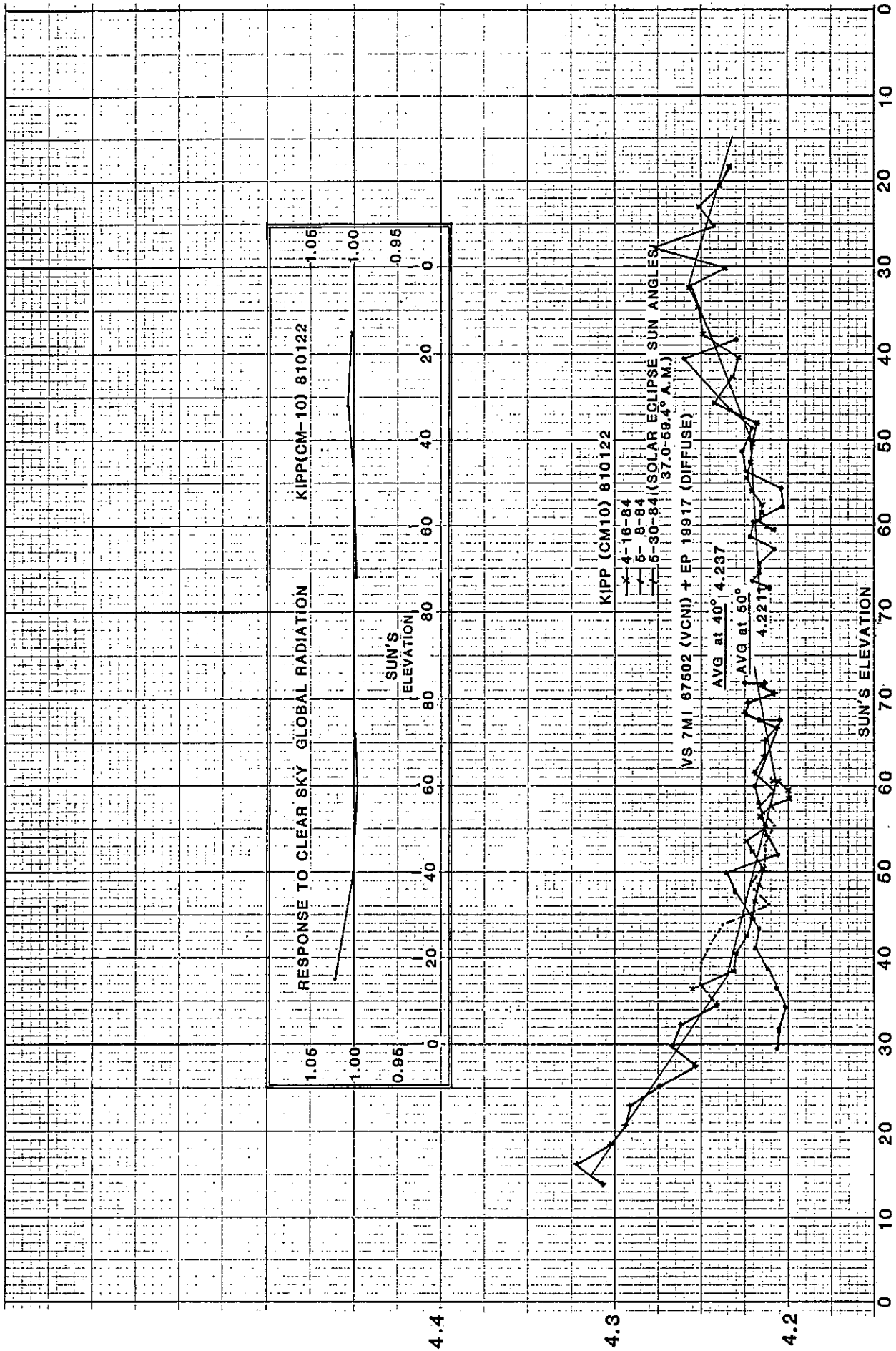


FIGURE 2

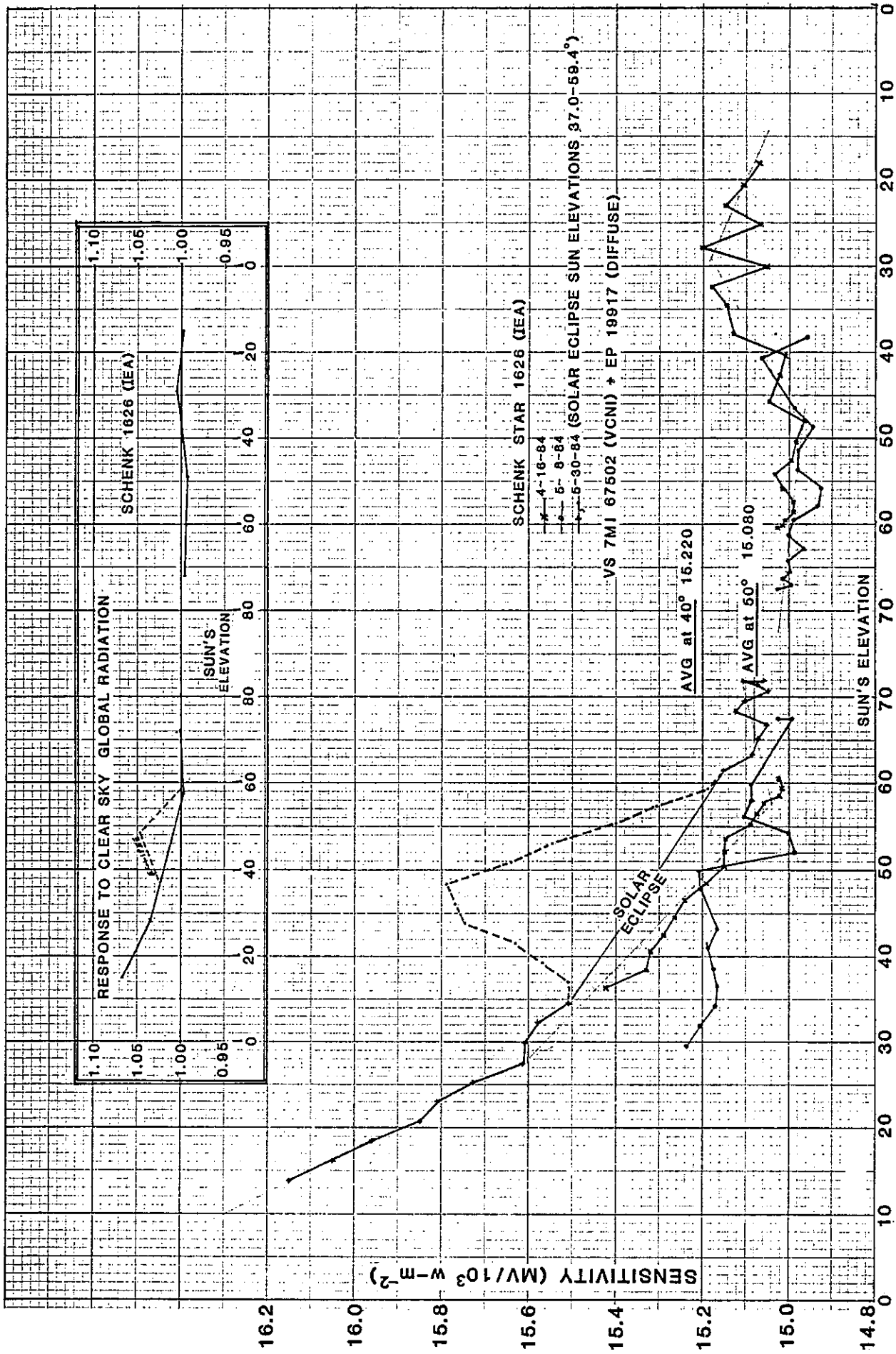


FIGURE 3

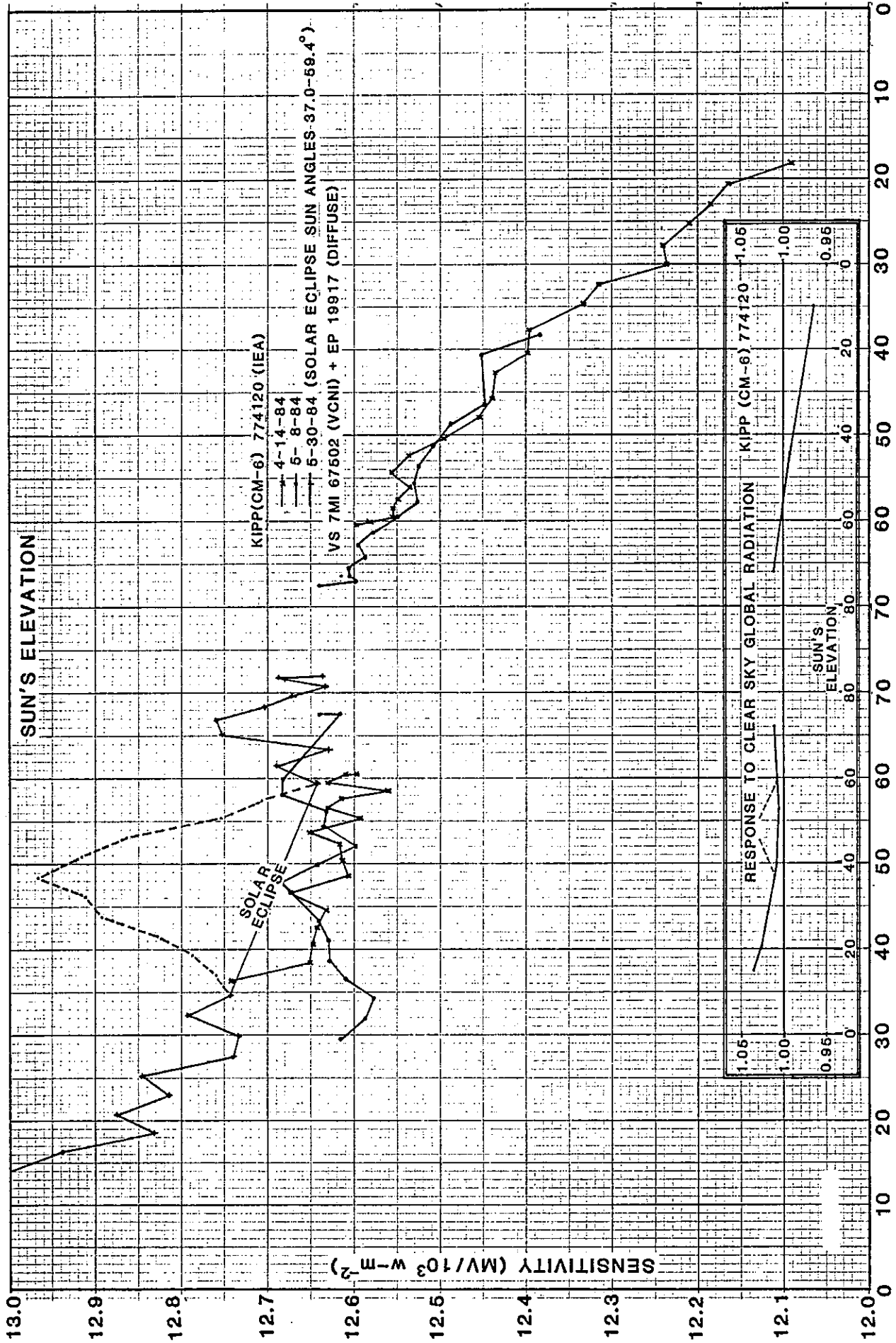


FIGURE 4

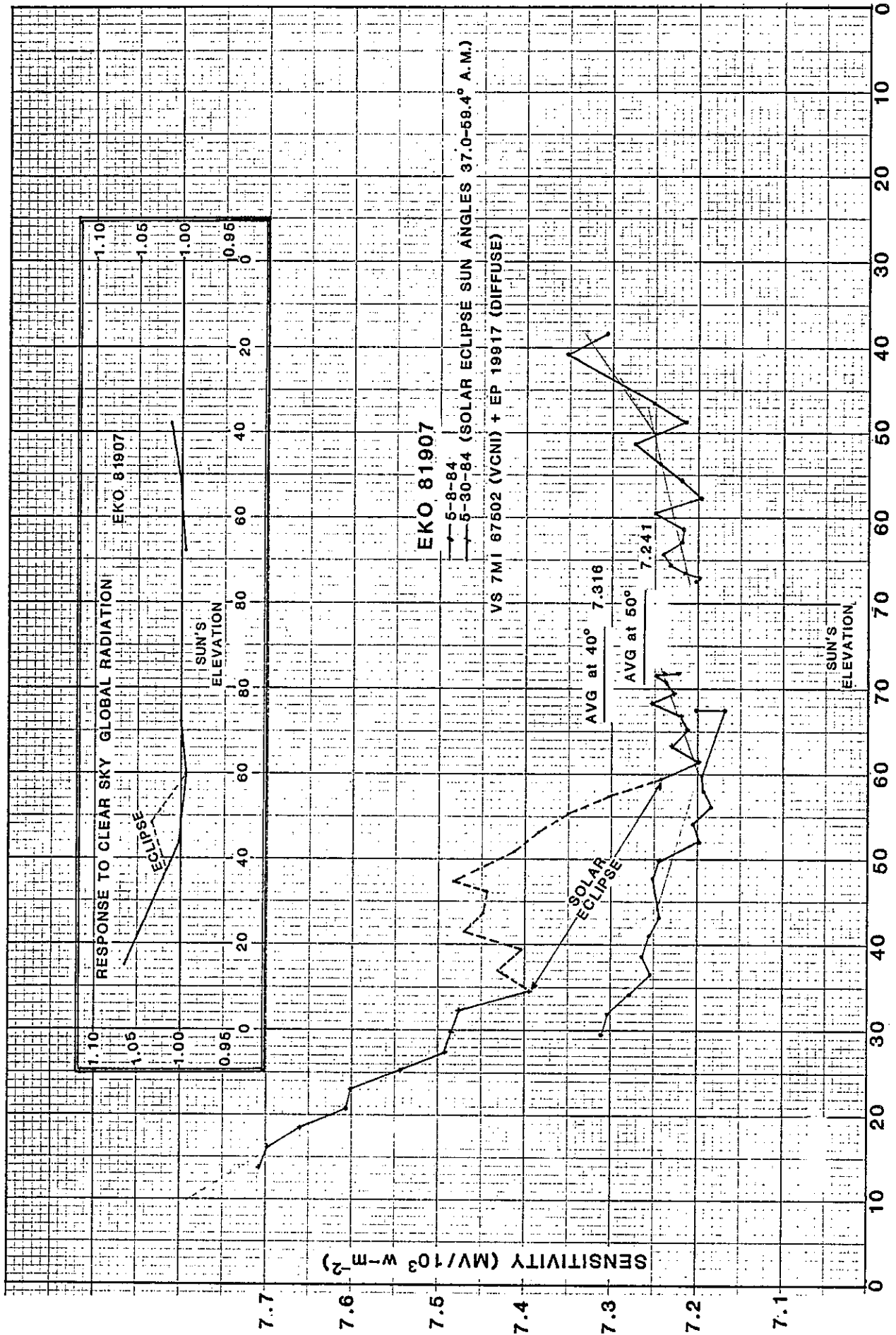


FIGURE 5

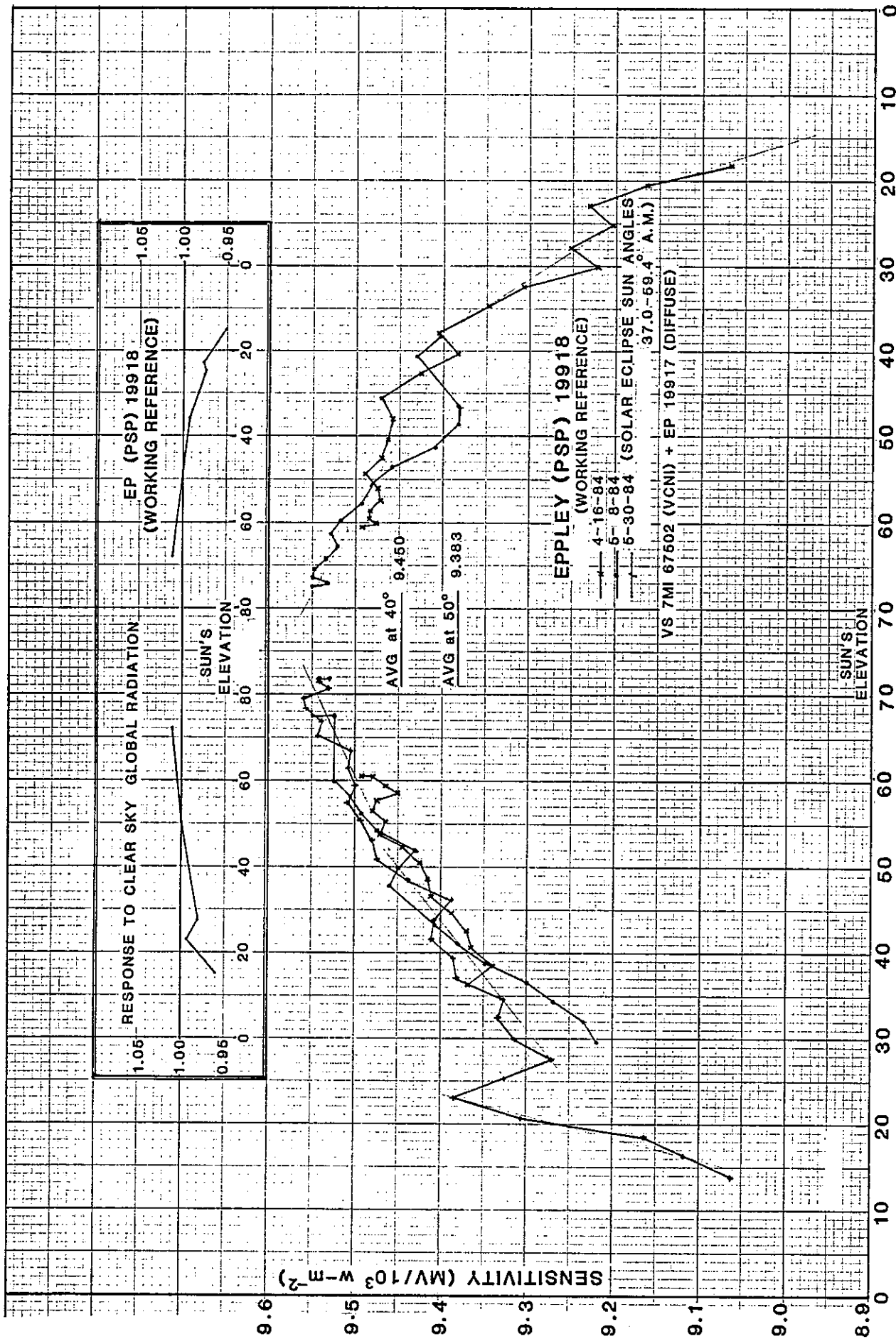


FIGURE 6

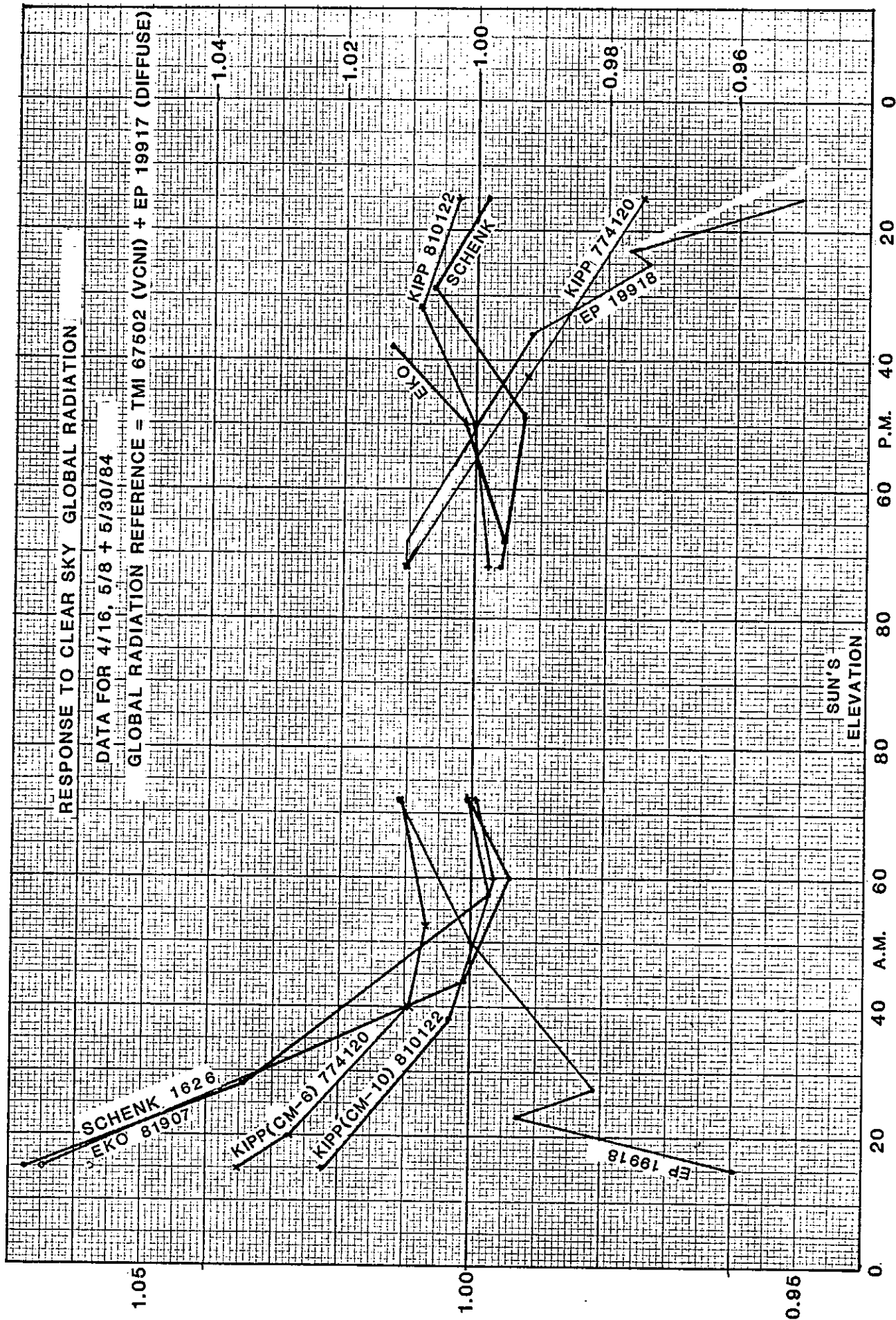


FIGURE 7

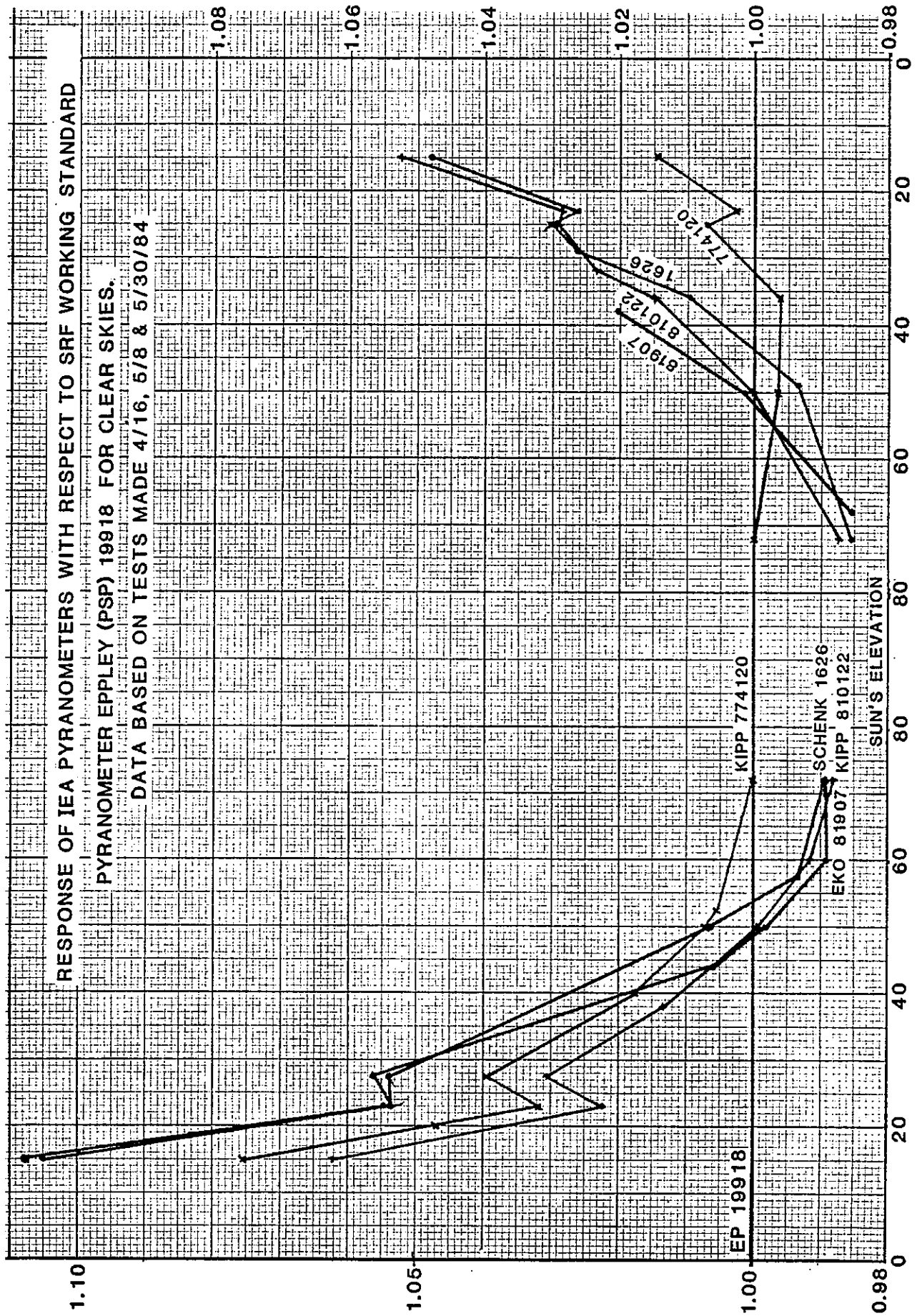


FIGURE 8



6.C CONTRIBUTION TO THE FINAL DISCUSSION AT THE IEA TASK IX
PYRANOMETRY SYMPOSIUM

25 January 1984, Norrköping, Sweden

K. Dehne

CONTRIBUTION TO THE FINAL DISCUSSION AT THE IEA TASK IX
PYRANOMETRY SYMPOSIUM

I have missed a summarizing presentation of the results of the large pyranometer comparisons and test actions started after the Boulder Pyranometry Workshop 1981. These results should deliver the best insight into the state of knowledge about the pyranometer specifications.

The very import review of the physics of thermal radiometers given by C. Fröhlich deserves thorough study and further discussions.

I was most interested in the field of test procedures and I have learned that the results of new "clean" outdoor tests and indoor tests show generally no more large differences. In the problematic case of the cosine response new investigations of the irradiance dependency of the cosine error are required because of the discrepancies between the Davos results and the results of different other indoor tests using lower levels of irradiance. It may be an important success of the symposium if we get results of these investigations from the SP (Borås) in 1984 as promised by H. Andersson and L. Liedquist during the discussions.

6.D CONTRIBUTION TO THE OPEN DISCUSSION AT THE IEA TASK IX
PYRANOMETRY SYMPOSIUM

25 January 1984, Norrköping, Sweden

F. Kasten

CONTRIBUTION TO THE OPEN DISCUSSION AT THE IEA TASK IX
PYRANOMETRY SYMPOSIUM

I have been impressed by the accuracy, achieved by several authors, of pyranometer measurements. But for many applications other than collector testing, the extreme accuracy of less than 1% is not required. This statement particularly holds for meteorological applications including resource assessment of solar energy, and for non-tilted pyranometers. Consequently, a trade-off has to be made between wanted accuracy of data and costs for installation and maintenance of the meteorological radiation network.

In a network, much more emphasis is to be put on correct operation than on precision of the instruments, that means good maintenance and recalibration or recycling of pyranometers, as well as quality control and documentation of data. Nevertheless, the meteorological services owe thanks to the collector testing community for having challenged us to improve pyranometry, and for the advances achieved in the meantime.

6.E PERSONAL PLAN FOR CONTRIBUTION TO PYRANOMETRY
AS ONE OF THE MEMBERS OF TASK IX-C

Yukiharu Miyake
EKO Instruments Trading Co., Ltd.

PERSONAL PLAN FOR CONTRIBUTION TO PYRANOMETRY
AS ONE OF THE MEMBERS OF TASK IX-C

Based on my own long experience in the research and development of pyranometers I would like to contribute to pyranometry improvement in the following three ways:

a) Physics of pyranometer

The characteristics of pyranometer are determined by the result of combined thermal and optical behaviour, so that the individual physical phenomena must be analyzed.

b) Improvement of indoor characterization method

I consider that the characterization itself is insufficient at present especially in respect of accuracy when applying it to an actual use. In addition, other methods which have not yet been established completely, such as the characterization of thermal shock, must be improved and developed as soon as possible.

c) How to express and make use of the characterization

The characteristics discussed in many reports are effective only under limited conditions, resulting in inconvenience in their actual use. Therefore, more suitable expressions of the characteristics must be taken into consideration for a more accurate measurement.

6.F CALIBRATION AND COMPARISON OF PYRANOMETERS

B. Petersen

Kipp & Zonen
Delft-Holland

CALIBRATION AND COMPARISON OF PYRANOMETERS

Calibration of a pyranometer to be used in the "field" involves in most cases at last two steps:

- a) Calibration of a "working standard" pyranometer against a pyr heliometer as a reference.

As it is practically impossible to calibrate every pyranometer for field use against a pyr heliometer, a second step is used:

- b) Transfer of the "working standard" calibration to the pyranometer for field use.

If only one parameter had to be considered this would be a simple matter. However, the output of a pyranometer depends not only on the amount of irradiation by the sun. The well recognized factors to be considered are: intensity (linearity), temperature, elevation and azimuth of the source, tilt of pyranometer, wavelength responsitivity and zero offset (I.R. radiation). Determination of these factors is called "characterization" of a pyranometer. As a starting point to compare pyranometers it would be very useful if some of these factors could be eliminated. If we consider a pyranometer irradiated under normal incidence, not tilted and a "shading - unshading" technique is used only, the parameter intensity, temperature and spectral distribution are left and can easily be determined, unless perhaps spectral distribution. It is sensible to take the sensitivity under these conditions as a base for the calibration factor and calculate from here the sensitivity under working conditions.

However, while calibrating a pyranometer against a pyr heliometer, parameters cannot be set as required. As a consequence a "working standard" pyranometer should be fully characterized to allow the calculation of the sensitivity under normalized conditions. It means also that the calibration certificate of a pyranometer to be used as a "working standard" should include all relevant data. Only if these data are available it is possible to establish the sensitivity under normalized conditions.

Special attention should be given to taking measurements during a whole day and calculating the mean value of this series, while conditions are changing during that day (sun elevation, azimuth and temperature). Theoretically every incremental measurement should be normalized before taking the mean value. As this is not very practical, only comparable increments should be used. If improvements in pyranometry are to be made the characterization is of the utmost importance. It gives pertinent data and these data are indispensable to understand the phenomena and make improvements.

The conclusion to be drawn can be summed up as follows: Characterization of a pyranometer has only sense if it is used in both the calibration process and in actual use.

6.G RECOMMENDED PROCEDURES

C.A. Velds

RECOMMENDED PROCEDURES

As a climatologist I felt myself a user of pyranometer data during this Symposium. From that point of view I should like to extend point 5 "Recommended Procedures" in "Recommendations for Users". We have heard about the results of laboratory characterization and field characterization on the linearity, tilt effect, temperature dependence, etc., but how important are these for routinely measured radiation in a climatological network? Lars Dahlgren mentioned the zero offset due to the temperature difference between the domes and the housing of the instrument. We measured negative zero offset just after sunrise in our network. Can we not correct only these values into zero, or do we have to correct all measured data during the day for this zero offset?

On the other hand as a physicist I am very interested in the physical behaviour of the pyranometer. Therefore, I should like to support Claus Fröhlich's remarks during the open discussion. In De Bilt we have just started to measure the temperatures of the outer and inner dome and of the housing with small thermocouples to test the modelling-error estimates (your point 6).

Summarizing I should like to stress the points 5 Recommended procedures and 6 Results from modelling-error estimates from the list you have given.

SESSION 7

Extra Contributions

7.A OUTDOOR AND LABORATORY TRANSIENT RESPONSE
OF THE EPPLEY PSP - A SHORT NOTE

P.-M. Nast

OUTDOOR AND LABORATORY TRANSIENT RESPONSE
OF THE EPPLEY PSP - A SHORT NOTE

During the Pyranometer Symposium in Norrköping the question was asked whether laboratory measurements of the response time of a pyranometer are reliable. Since then, I have performed some outdoor measurements concerning this question. The results are given in Figures 1 and 2.

The pyranometers were mounted on a tracking device and could be shaded by shading disks. The tested pyranometer PSP 18376 was suddenly shaded (Figure 1) or suddenly unshaded (Figure 2). The difference between the momentary and the "final" value is given. Because of slightly changing radiations the "final" value is determined continuously by a second PSP (SN 18978) which is always shaded (Figure 1) or unshaded (Figure 2). The final difference is not zero because the two pyranometers do not match exactly (calibration factors determined previously are used). Readings from the two voltmeters ($1\mu\text{V}$ resolution) are taken simultaneously by two experimenters. The time for the pretreatment (unchanging conditions) was at least 10 minutes.

Conclusions from the results are:

- a) For stepwise increasing or decreasing radiation the PSP reacts similarly, as laboratory experiments already suggested (in Figure 2 the sign of the y-axis is changed relatively to Figure 1. The greater scatter in Figure 2 is due to greater fluctuations in the global radiation).
- b) The difference to the final value one minute after shading or unshading is a little lower than in laboratory experiments (Figure 3), but it is still about 1% (relative to the width of the step).
- c) For outdoor measurements the greatest time constant is a little lower than in laboratory (2.5 minutes instead of 3 minutes, $1/e$, for PSP 18376), may be because of wind.

For my opinion these results are of importance for choosing the appropriate calibration procedures for PSPs.

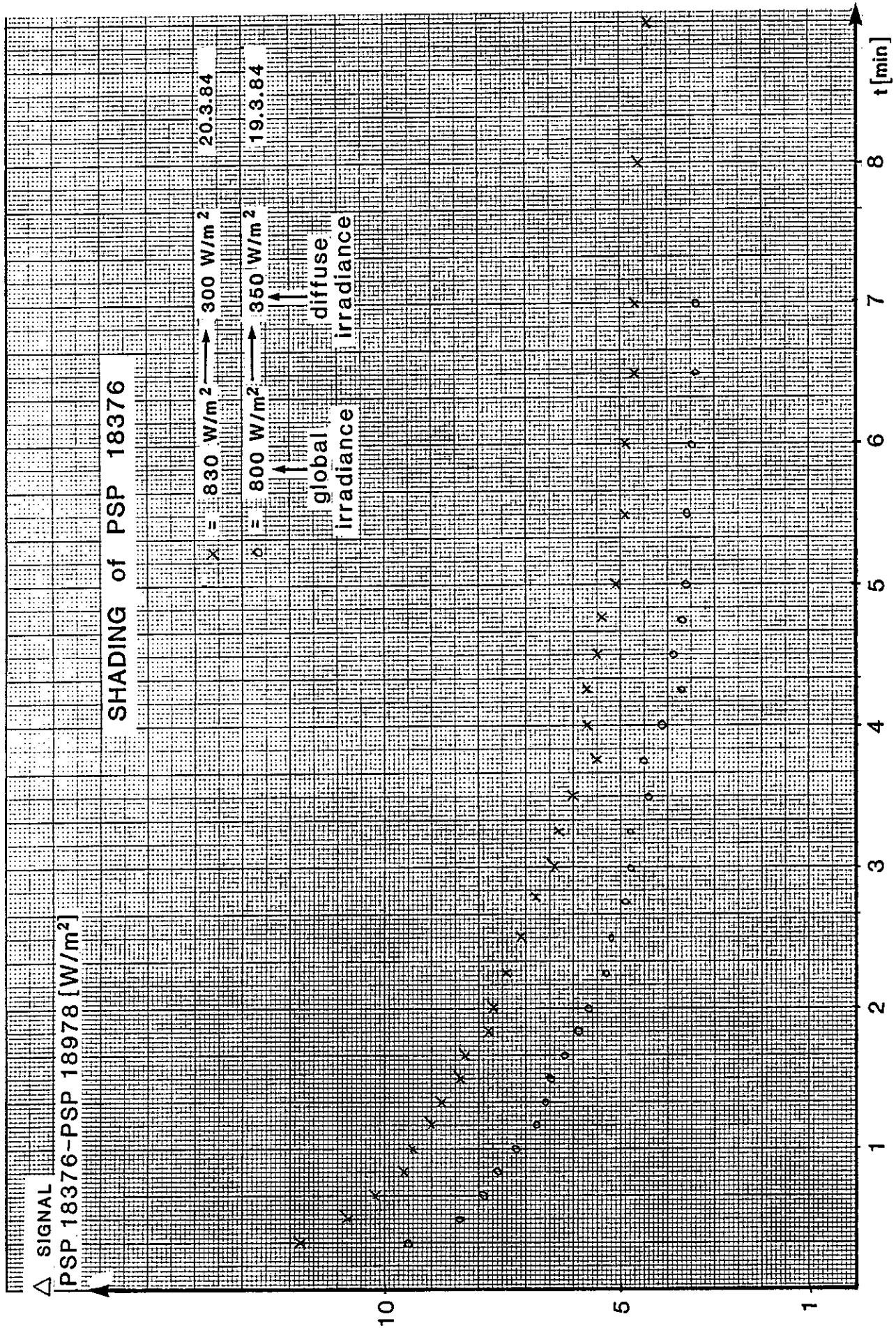


FIGURE 1

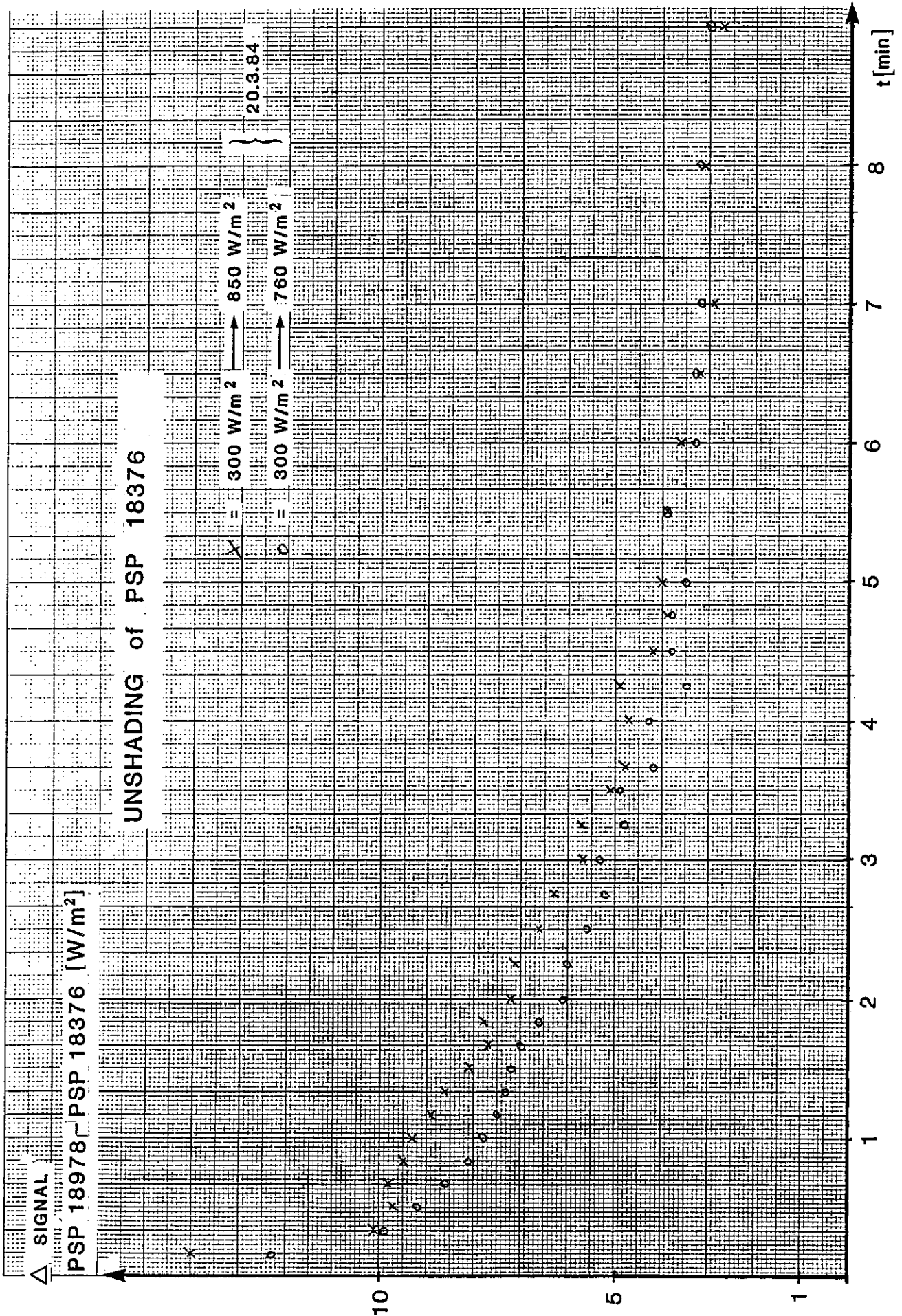


FIGURE 2

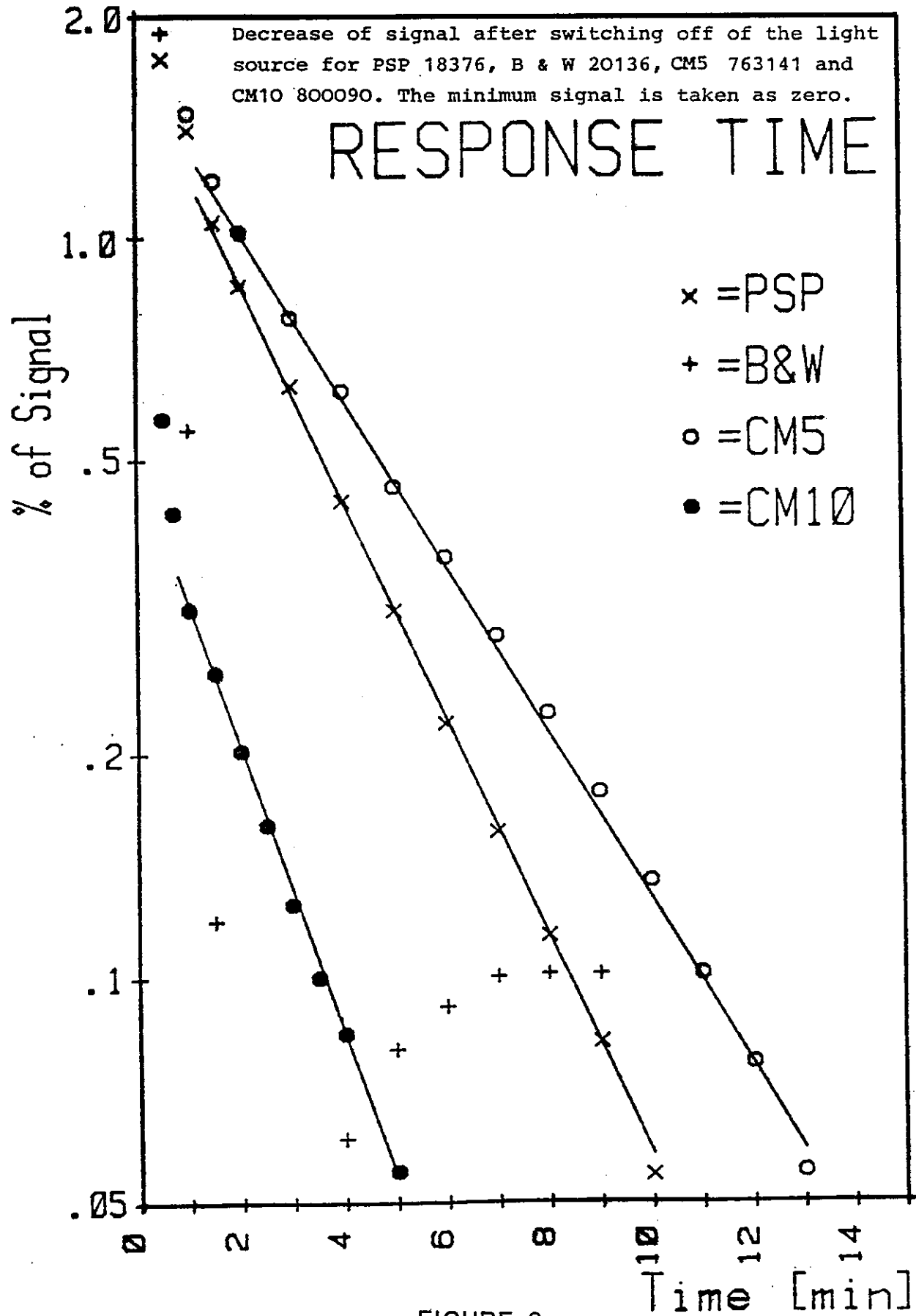
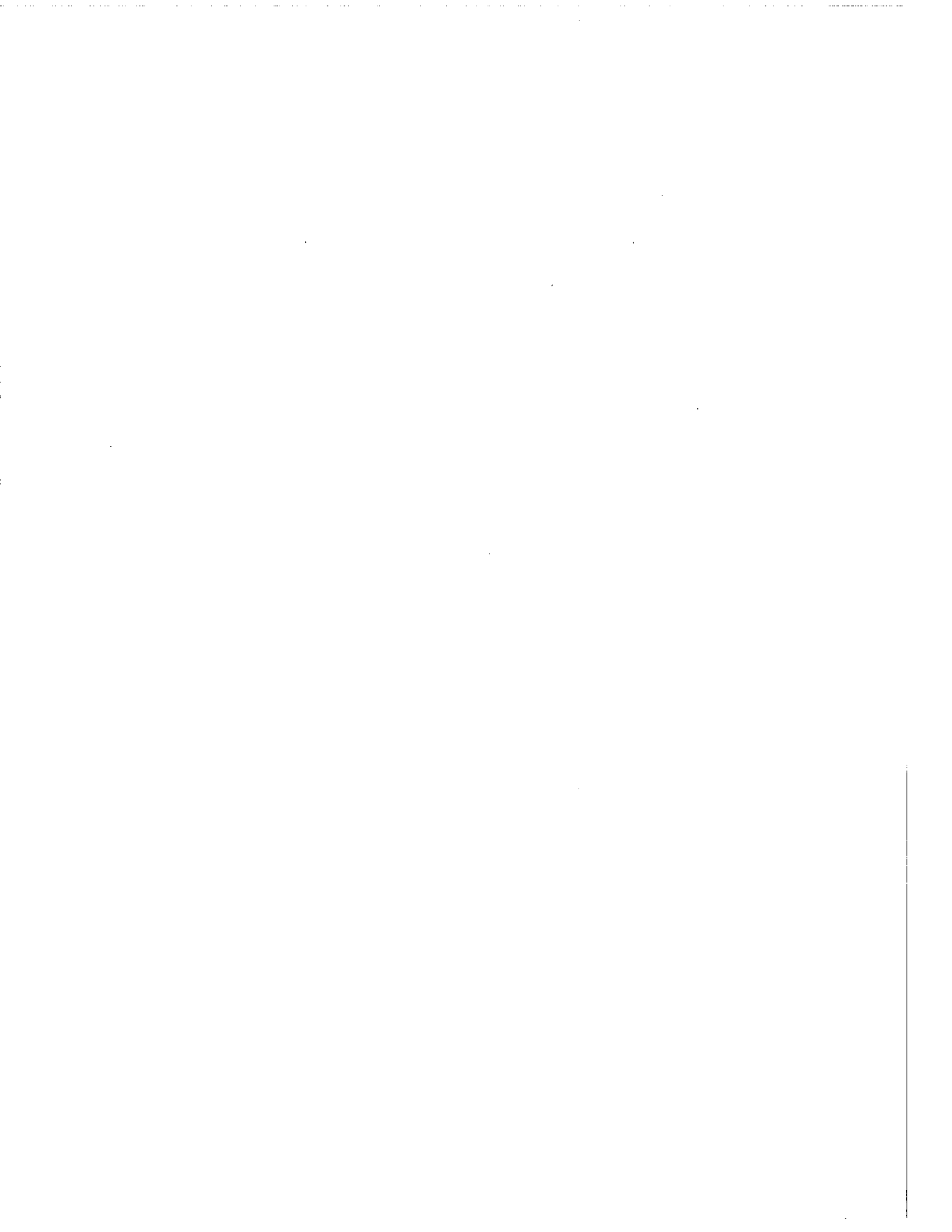


FIGURE 3



7.B PRELIMINARY REPORT ON THE RESULTS OF THE FIRST TEST LOOP
OF 4 PYRANOMETERS WITHIN IEA TASK IX

Dr. K. Dehne and R. Trapp

PRELIMINARY REPORT ON THE RESULTS OF THE FIRST TEST LOOP
OF 4 PYRANOMETERS WITHIN IEA TASK IX

Test Site: Optical laboratories of Meteorologisches Observatorium, Hamburg,
(Deutscher Wetterdienst).

Test Period: May - September 1984

Pyranometers Tested:

- PSP No. 17750 F3 (Eppley)
- CM11 No. 810 119 (Kipp & Zonen)
- CM6 No. 773 992 (Kipp & Zonen)
- MID No. 123 (Middleton Instruments)

Test of Response Time

Test method: shading method.

Test equipment:

- a) Radiation source: Xenon lamp XBO 2.5 kW ofr with condensor and mirror optics. Screen for shading.
- b) Pyranometer mount: vertical position of pyranometer (see 9.2). Ventilator: Type Redmont. Ventilation of dome and body of the pyranometers.
- c) Additional optics: achromatic lens.
- d) Data recorders:
 - Strip chart recorder: type BD9 (Kipp & Zonen)
 - Digital voltmeter: type 195 (Keithley)

Test Procedure:

- a) Zeroing of the recorders after warming-up (30 min).
- b) Irradiating the ventilated pyranometer using a beam irradiance of 1000 Wm^{-2} during 4 min. to 15 min. till a steady state measuring signal has been achieved.
- c) At time 0 s: screening of the lamp.
- d) At time -10 s: switching-on the feed of paper of the strip chart recorder (500 mm/min).

FIGURE 1a. Test of Response Time

PSP No 17750 F3

2 tests from 3 September 1984

x pyran. unventilated $T_1 = 1.25s$ $T_2 = 170s$
● pyran. ventilated $T_1 = 1.25s$ $T_2 = 130s$

100% \wedge 1000 $W \cdot m^{-2}$ (time of exposure: 15min)

0% \wedge 0 $W \cdot m^{-2}$ (10 min after shading)

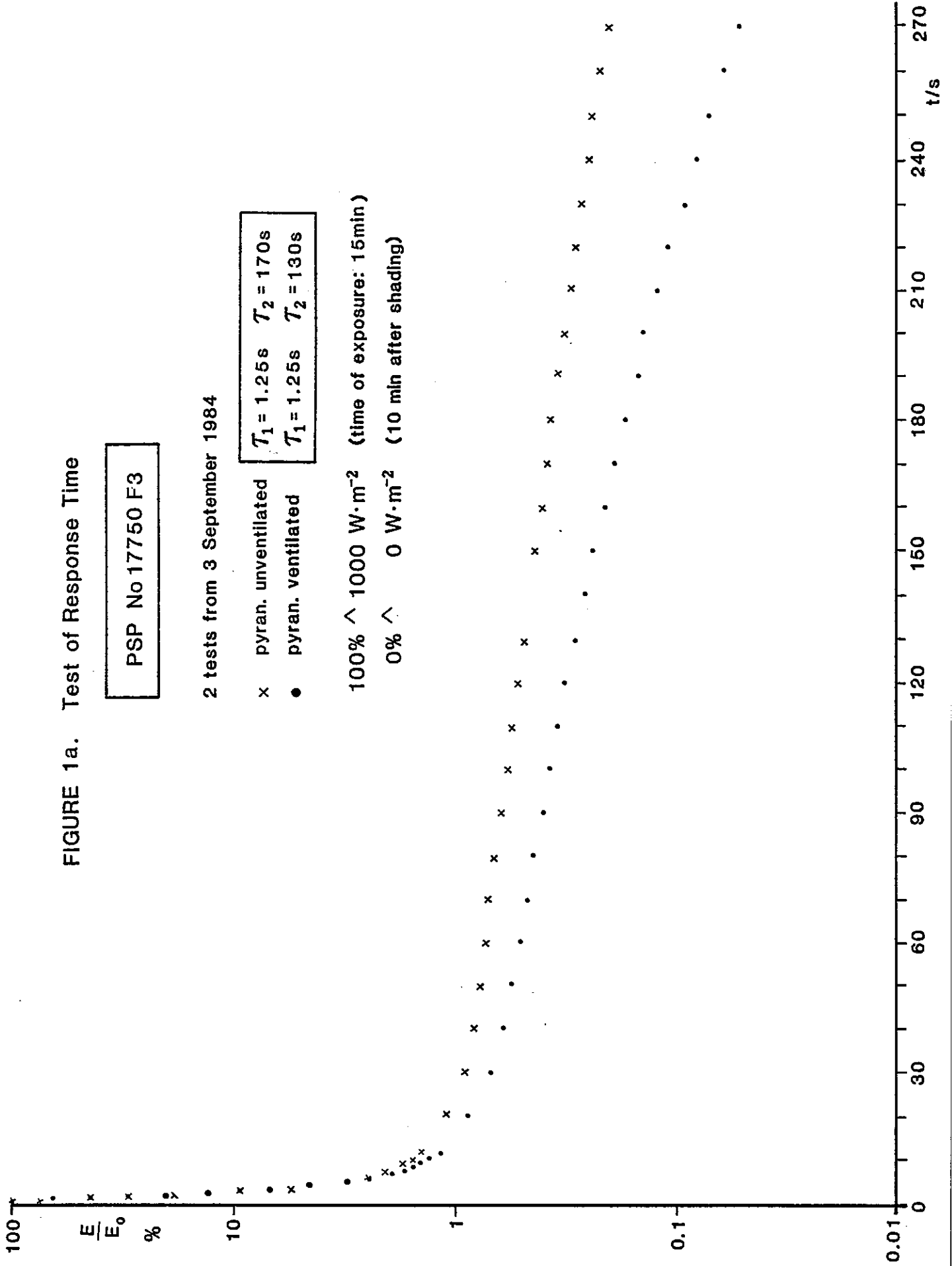


FIGURE 1b. Test of Response Time

CM 11 No 810119

2 tests from 31 August 1984

x: 1. series (pyran. ventilated)

•: 2. series (pyran. ventilated)

$T_1 = 3.5 \text{ s}$ $T_2 = 83 \text{ s}$

$T_1 = 3.3 \text{ s}$ $T_2 = 85 \text{ s}$

100% \wedge 1000 $\text{W}\cdot\text{m}^{-2}$ (time of exposure: 4 min)

0% \wedge 0 $\text{W}\cdot\text{m}^{-2}$ (10 min after shading)

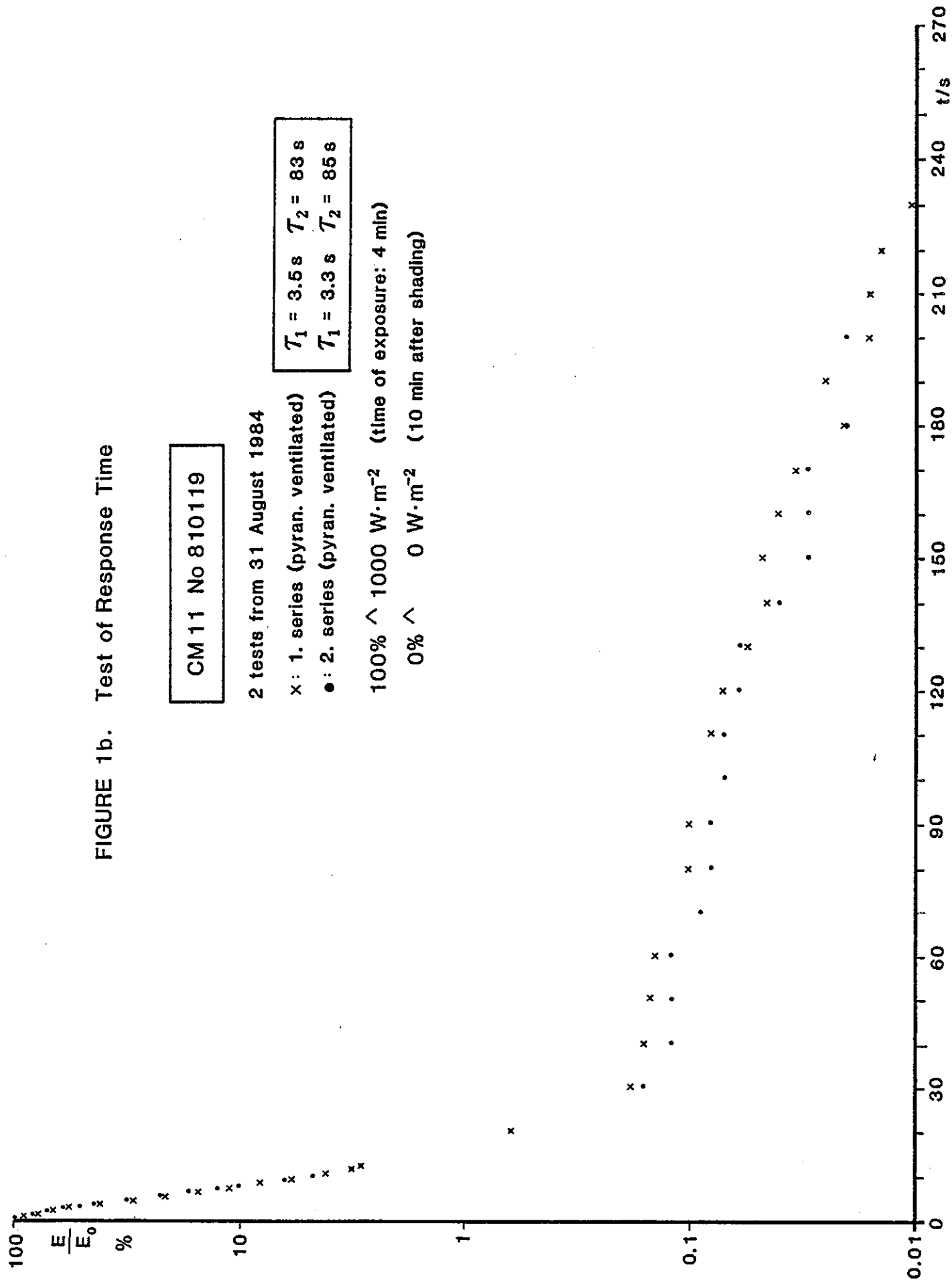


FIGURE 1c. Test of Response Time

CM 6 No 773992

2 tests from 3 September 1985

x pyran. ventilated $T_1 = 2.1s$ $T_2 = 185s$
 ● pyran. ventilated $T_1 = 2.0s$ $T_2 = 150s$

100% $\hat{=}$ 1000 $W \cdot m^{-2}$ (time of exposure: 15min)
 0% $\hat{=}$ 0 $W \cdot m^{-2}$ (10 min after shading)

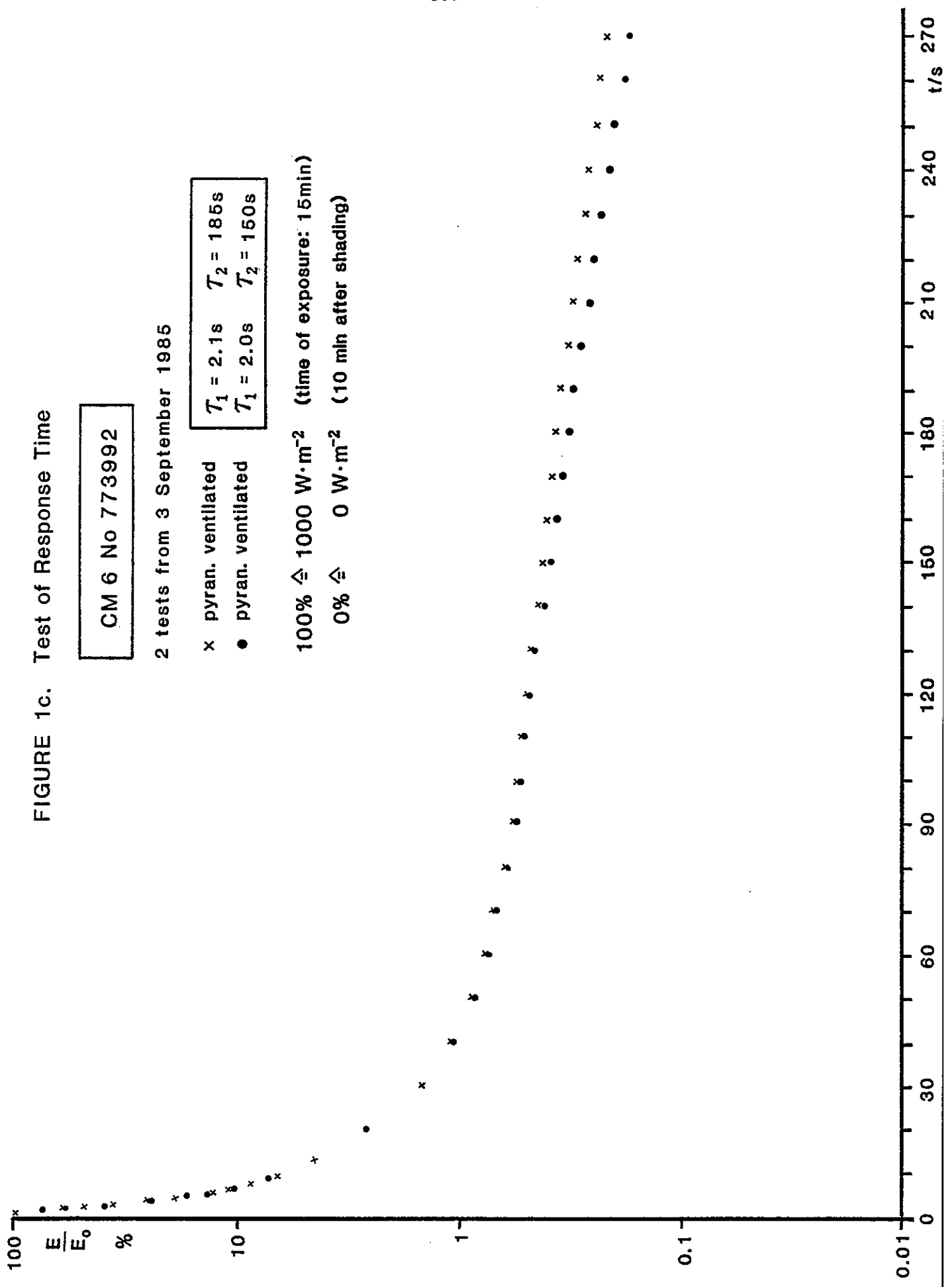


FIGURE 1d. Test of Response Time

MID No 123

2 tests from 4 September 1984

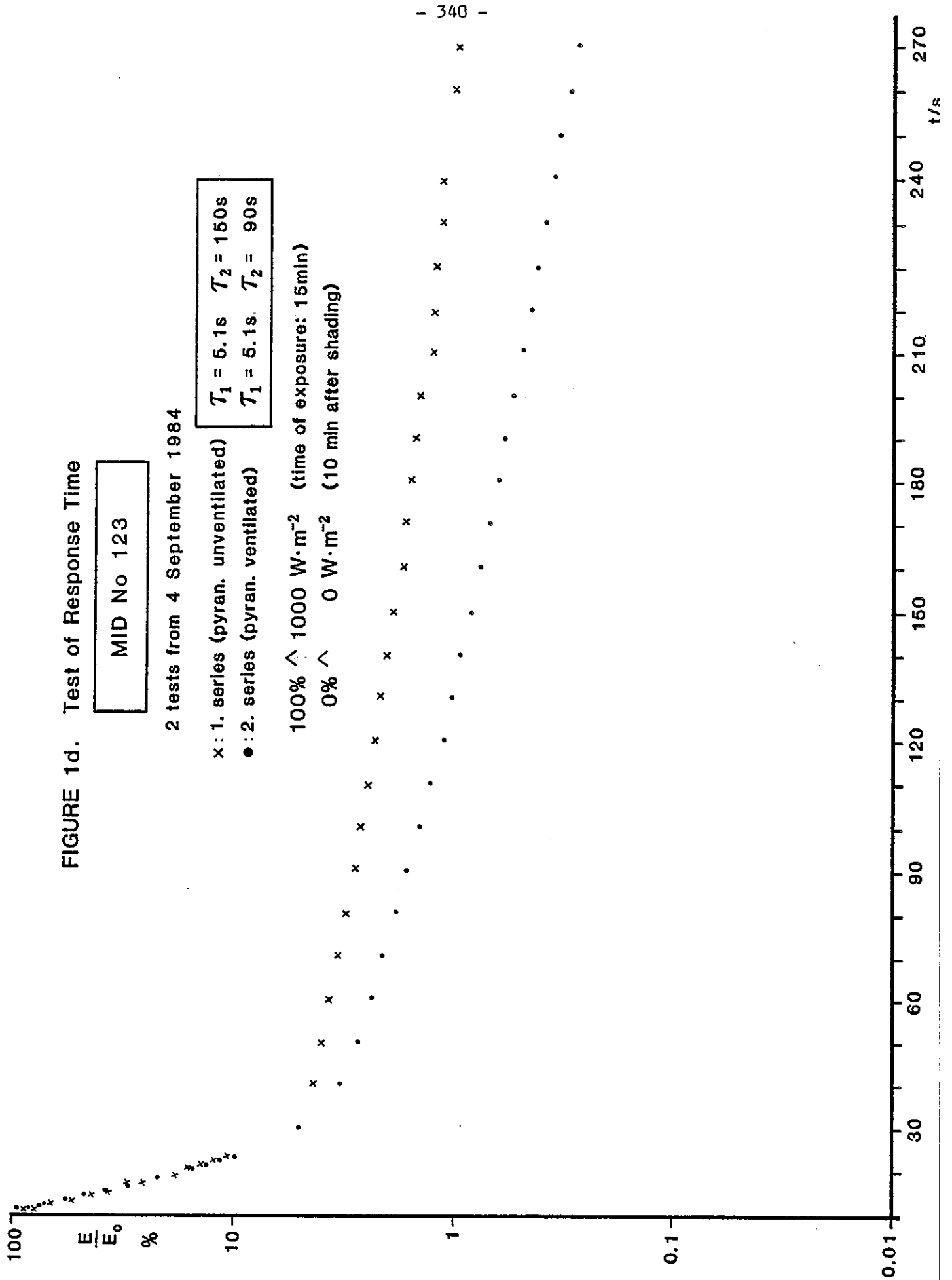
$T_1 = 5.1s$ $T_2 = 150s$
 $T_1 = 5.1s$ $T_2 = 90s$

x : 1. series (pyran. unventilated)

• : 2. series (pyran. ventilated)

100% \wedge 1000 $W \cdot m^{-2}$ (time of exposure: 15min)

0% \wedge 0 $W \cdot m^{-2}$ (10 min after shading)



- e) At time -1 s: start of the sampling of the pyranometer signals $M(t)$ by the DVM 195 (sampling rate approx. 3 s^{-1}). Stop of sampling after storage of 100 readings (appr. 30 s).
- f) At time 40 s: start of visual readings of the DVM display every 10 s over a period of 260 s.
- g) At time 60 s: the strip chart recorder is switched to stand-by.
- h) At time 600 s: reading of the zero value.

Test Results

- a) First time constant derived from the signal decrease of the strip chart curve.
- b) Second time constant and long time response derived from a logarithmic diagram over 4 decades of $M(t)/M(t=0)$ as result of the DVM readings. (see Figure 1a-1d).

TABLE 1
Test Result of Time Response

Pyranometer	1st time constant	2nd time constant	Time for decrease to 5 %	Remarks
PSP 17750 F3	0.9 s	130s (170s)	4 s	
CM11 810 119	3.2 s	84s	9.5 s	
CM 6 773 992	2.0 s	150s 185s	12 s	
MID 123	4.9 s	90s (150s)	20 s	setting time > 10 min

(In brackets: data of the non-ventilated case)

Calibration

Calibration method: Indoor comparison with the reference pyranometer using beam radiation at normal incidence.

Calibration equipment:

- a) Radiation source: Xenon lamp XBO 500 W ofr with condensor and mirror optics. The constancy of radiation output is monitored by a silicon cell.
- b) Pyranometer mount: Rolling platform for mounting reference and test pyranometer side by side. The platform is shifted by means of a control cable to expose the two pyranometers to the beam alternatingly.

The pyranometer mount is installed horizontally on a table in a climatic chamber.

- c) Additional optics:
 - radiation entrance window of suprasil in the wall of the chamber with removable shading screen;
 - "multi-lenses-plate": installed between lamp housing and suprasil window for integrating the radiant fluxes of the beam (increase of homogeneity);
 - turning mirror positioned in the chamber above the platform to turn the beam from horizontal to vertical.
- d) Data recorders: DVM Keithley-model 195 or Digitec model 268.
- e) Reference pyranometers

PSP 16587 F3	(reference for PSP and MID)
CM11 790 057	(" " CM 11)
CM 6 784 805	(" " CM. 6)

Calibration Procedure

- a) Adjustment of the mounting positions of the pyranometers according to the most homogeneous center of the beam (deviations of irradiance within $\pm 2\%$ over a circle of $\varnothing 24$ mm; divergence of the beam: $\pm 1.5^\circ$; irradiance: approx. 70 W.m^{-2}). The centers of the receivers of both pyranometers must have the same coordinates when they are exposed to the beam.
- b) Switching-on the lamp and the recorders as well as the climatic chamber at 30 min. before first reading.
- c) Sequence of readings of the reference pyranometer and the test pyranometer:

First shading at $t = 0$ min.

Time After t=0 min	Reference Pyranometer		Test Pyranometer	
	shaded $M_{R,s}$	unshaded $M_{R,u}$	shaded $M_{T,s}$	unshaded $M_{T,u}$
2 min	x			
4 "		x		
6 "	x			
8 "		x		
10 "	x			
12 "			x	
14 "				x
16 "			x	
18 "				x
20 "			x	
22 "				x
24 "			x	
26 "	x			
28 "		x		
30 "	x			
32 "		x		
34 "	x			

Remark: In the case of the Middleton-Pyranometer, the difference between two readings is 4 min. instead of 2 min.

Evaluation

a) Calculation of measuring values:

for the reference pyranometer:

$$M_R(t) = M_{R,u}(t) - 0.5 [M_{R,s}(t-2 \text{ min}) + M_{R,s}(t+2 \text{ min})];$$

for the test pyranometer:

$$M_T(t) = M_{T,u}(t) - 0.5 [M_{T,s}(t-2 \text{ min}) + M_{T,s}(t+2 \text{ min})];$$

b) Calculation of sensitivity of test pyranometer S_T :

$$S_T = S_R \cdot \bar{M}_T / \bar{M}_R \quad \text{where}$$

S_R : sensitivity of reference pyranometer:

\bar{M}_R : arithmetic mean of all $M_R(t)$

\bar{M}_T : arithmetic mean of all $M_T(t)$

Results

PSP No. 17750 F3 :	S = 9.15 $\mu\text{V}/(\text{W}\cdot\text{m}^{-2})$ (WRR)
CM11 No. 810119 :	S = 4.60 "
CM6 No. 773992 :	S = 12.3 "
MID No. 123 :	S = 10.1 "

Test of Temperature Coefficient

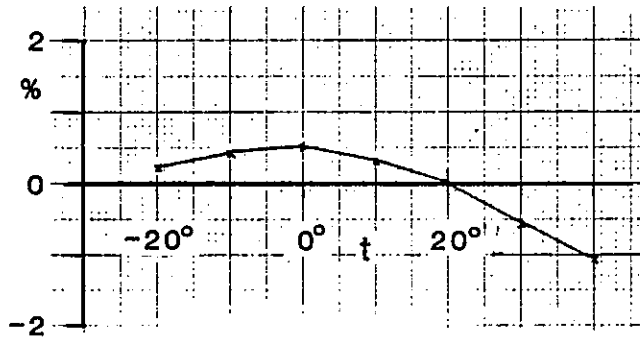
Test Method: Thermostating the pyranometer in a climatic chamber (measurement at steady state)

Test Equipment:

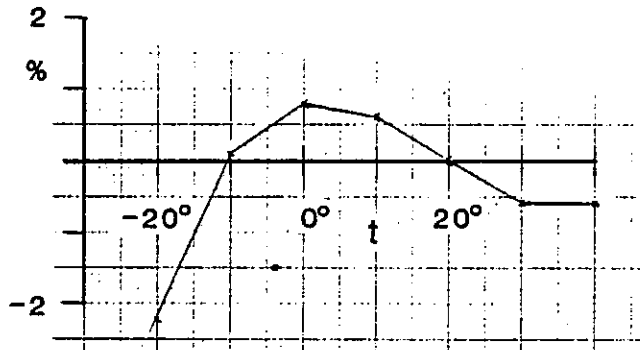
- a) Radiation source: as in 5.2 a)
- b) Pyranometer mount: platform for two pyranometers as in 5.2 b). Additional ventilation during thermostating climatic chamber. Pt-100-sensors at the body of the pyranometers.
- c) Data recorders: DVM model 195 (Keithley). Strip chart recorder for temperatures of pyranometers and of the climatic chamber.
- d) Climatic chamber (Size: 120 cm x 120 cm x 180 cm) with suprasil window. Temperature range: -30°C to $+50^{\circ}\text{C}$.

Test Procedure:

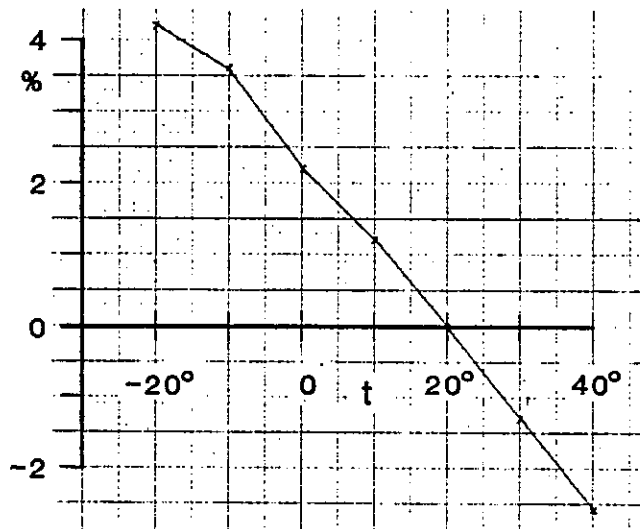
- a) Adjustments
 - Mounting of two pyranometers on the platform (See 5.3 a);
 - Thermostating the chamber to -20°C during the night (dry climate).
- b) Stabilizations
 - Temperature of the test laboratory at 20°C ;
 - Warming-up: of the recorders and the xenon lamp about 30 min. before first reading;
 - Steady state of temperature of the pyranometer body (controlled by the curve of the strip chart recorder).
- c) Sequence of readings
 - Sequence of adjusted temperatures: -20°C to $+40^{\circ}\text{C}$ in steps of 10 K (setting time of the steady state of temperature of the pyranometer body: about 60 min.);
 - to each temperature: determination of the final measuring value of one pyranometer before the other is exposed to the beam;



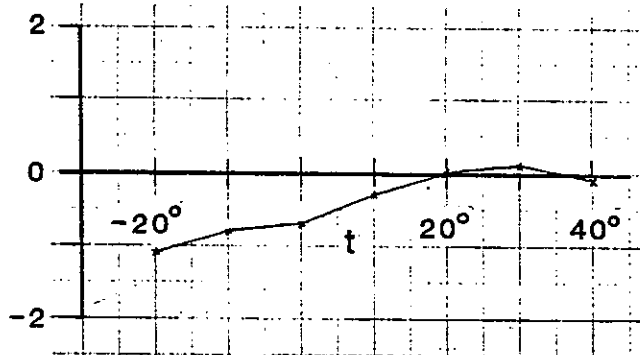
PSP No 17750 F3



CM11 No 810119



CM6 No 773992



MID No 123

FIGURE 2. Percentage deviation of sensitivity at temperature t °C from sensitivity at temperature $t = 20$ °C

- sequence of readings to determine a measuring value of a pyranometer: as given in the time table of 5.3 for the test pyranometer.

Evaluations

- a) Temperature coefficients (in % per K)

For the temperature range T_i to $T_i + 10$ K : $C_i = C(T_i + 5$ K)

$$C_i = \frac{M(T_i) - M(T_i + 1)}{0.5 \cdot (M(T_i) + M(T_{i+1}))} \cdot \frac{100}{(T_i - T_{i+1})} \quad \begin{array}{l} i = 0, 1, 2, \dots 6 \\ T_0 = -20^\circ\text{C} \end{array}$$

- b) Percentage deviation of sensitivity at temperature T_i °C from sensitivity at temperature $T = 20^\circ\text{C}$.

$$\Delta(T_i) = \left(\frac{M(T_i)}{M(20^\circ\text{C})} - 1 \right) \cdot 100 \quad i = 0 \dots 7$$

Results

See Table 2a and 2b as well as Figure 2.

Test of Tilt Effect

Test Method: "Rotating drum" (using diffuse radiation).

Test Equipment:

- Rotating drum: cylindrical drum with two axle arms which allow the drum to rotate around its rotation-symmetrical axis. One of the axle arms is hollow to feed light into the drum. The inner walls are whitened to produce diffuse radiation which is received by the pyranometer flanged to an opening in the jacket of the drum. Through another opening, the interior of the drum is ventilated continuously.
- Radiation source: Xenon lamp XBO 2.5 kW ofr with condensor and mirror optics. Shading screen.
- Additional optics: Two achromatic lenses to guide the radiant flux of the lamp into the drum.
- Silicon photo-voltaic cell (Siemens type TP60) with mount to be flanged to the opening in the jacket.

TABLE 2a
Temperature coefficient in % per K

Mean temperature of 10K interval	Temperature coefficient in % per K			
	PSP S.No. 17750 F3	CM 11 S.No. 810119	CM 6 S.No. 773992	MID S.No. 123
+35°C	-0.049	-0.001	-0.131	-0.019
+25°C	-0.048	-0.059	-0.132	+0.006
+15°C	-0.035	-0.064	-0.116	+0.029
+ 5°C	-0.021	-0.012	-0.103	+0.036
- 5°C	-0.010	+0.062	-0.143	+0.013
-15°C	+0.020	+0.232	-0.060	+0.029

TABLE 2b
Percentage deviation of sensitivity at temperature t °C
from sensitivity at temperature t = 20°C

Temperature t	Percentage deviation of sensitivity at temperature t °C from sensitivity at temperature t=20°C			
	PSP S.No. 17750 F3	CM 11 S.No. 810119	CM 6 S.No. 773992	MID S.No. 123
+40°C	-1.1	-0.6	-2.6	-0.1
+30°C	-0.6	-0.6	-1.3	+0.1
+10°C	+0.3	+0.6	+1.2	-0.3
0°C	+0.5	+0.8	+2.2	-0.7
-10°C	+0.4	+0.1	+3.6	-0.8
-20°C	+0.2	-2.2	+4.2	-1.1

e) Rotating sector: see 8.2a.

f) Data recorders: DVM Model 5000 (PREMA) or Model 174 (Keithley).

Test Procedure

a) Adjustments

- diffuse irradiance of 1000 W m⁻² (by shifting of the achromatic lenses);
- position of the drum (the drum is well adjusted when the signals of the flanged silicon cell TP60 are independent on the turn position of the drum within about ± 0.5%);
- position of rotating section (see 8.3a).

b) Stabilization

- Switching-on the Xenon lamp and recorders about 30 minutes before readings.

c) Sequence of readings

- The following reading times after test starting at $t=0$ min. have been used for each of the three levels of irradiance $E=1000 \text{ W m}^{-2}$, 500 W m^{-2} and 250 W cm^{-2} . (Attenuation to the lower irradiances by means of the rotating sector).

Tilt angle β	Shaded radiation $M_S(E, \beta)$	Unshaded radiation $M_U(E, \beta)$
0° (hor.)	2 min.	4 min.
15° "	6 "	8 "
30° "	10 "	12 "
0° "	14 "	16 "
45° "	18 "	20 "
60° "	22 "	24 "
0° "	26 "	28 "
75° "	30 "	32 "
90° "	34 "	36 "
0° "	38 "	40 "
0° "	42 "	

Evaluations

a) Measuring values $M(E, \beta)$

$$M(E, \beta) = M_U(E, \beta, t_i) - 0.5 \cdot (M_S(E, \beta, t_i - 2) + M_S(E, \beta, t_i + 2))$$

b) Relative deviations $\Delta(E, \beta)$ from:

$$M(E, \beta = 0^\circ):$$

$$\Delta(E, \beta) = \frac{M(E, \beta)}{M(E, 0^\circ)} \cdot \frac{1}{\Delta_{Si}(\beta)} \text{ where}$$

$$\Delta_{Si}(\beta) = \frac{M_{Si}(\beta)}{M_{Si}(0)}$$

delivers the fine correction of unsymmetrical

alignment of the drum from the measuring values of the silicon cell.

$\Delta(E,\beta)-1$ in %

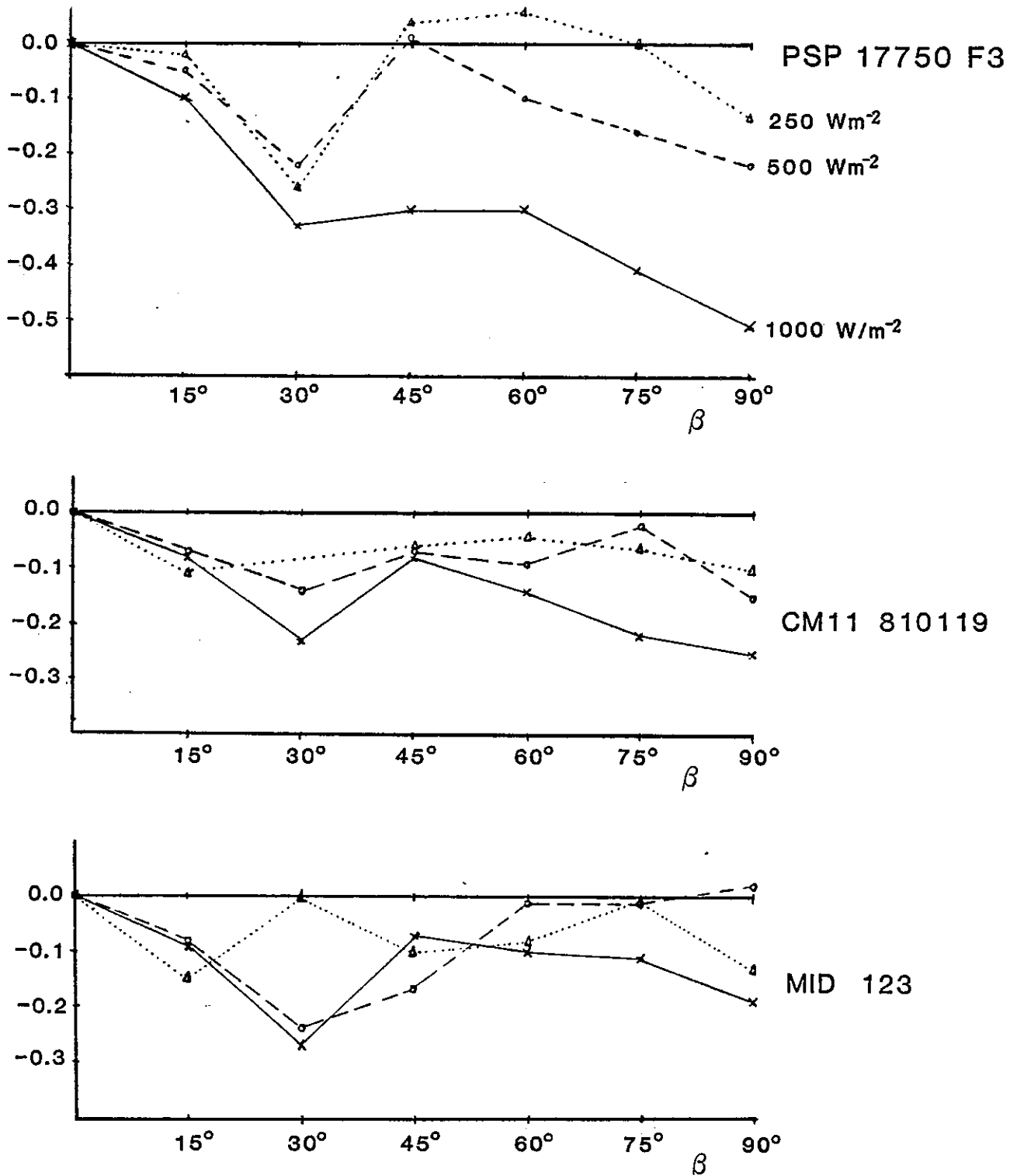


FIGURE 3. Percentage deviation of sensitivity at tilt angle β from sensitivity at tilt angle $\beta=0$

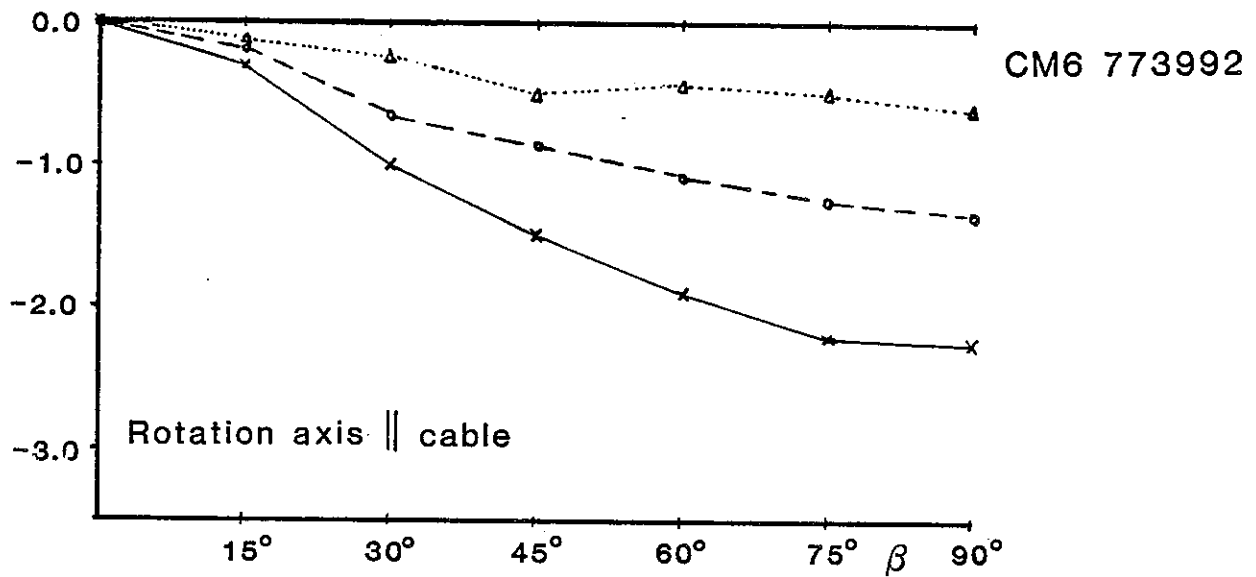
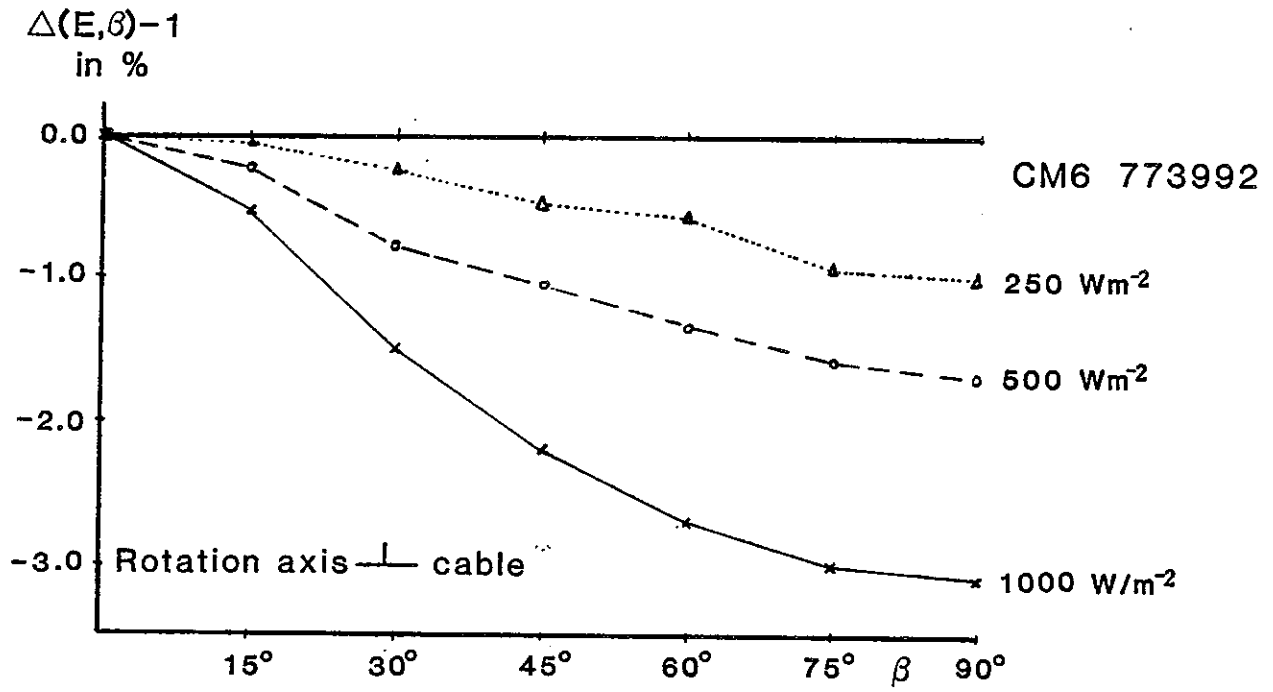


FIGURE 3. (cont.)

TABLE 3
 Percentage deviation of $M(E, \beta)$ from $M(E, 0^\circ)$ for three levels
 of irradiance
 a: 1000 Wm^{-2} b: 500 Wm^{-2} c: 250 Wm^{-2}

Angle of tilt β		PSP S.No. 17750 F3	CM 11 S.No. 810119	CM 6 S.No. 773992 rotations axis		MID S.No. 123
				cable	cable	
15°C	a	-0.10	-0.07	-0.53	-0.30	-0.09
	b	-0.06	-0.07	-0.22	-0.20	-0.08
	c	-0.02	-0.11	-0.06	-0.15	-0.15
30°C	a	-0.33	-0.23	-1.49	-0.98	-0.27
	b	-0.33	-0.14	-0.77	-0.64	-0.24
	c	-0.26	--	-0.23	-0.26	0.00
45°C	a	-0.30	-0.08	-2.19	-1.47	-0.27
	b	+0.01	-0.07	-1.07	-0.87	-0.24
	c	+0.04	-0.06	-0.47	-0.50	0.00
60°C	a	-0.30	-0.14	-2.72	-1.90	-0.10
	b	-0.10	-0.09	-1.35	-1.08	-0.01
	c	+0.06	-0.04	-0.58	-0.42	-0.08
75°C	a	-0.41	-0.22	-3.01	-2.20	-0.11
	b	-0.16	-0.02	-1.57	-1.26	-0.01
	c	0.00	-0.06	-0.93	-0.51	-0.01
90°C	a	-0.51	-0.25	-3.08	-2.27	-0.19
	b	-0.22	-0.15	-1.67	-1.37	+0.02
	c	-0.13	-0.10	-1.02	-0.59	-0.13

Results: See Table 3 and Figure 3.

Test of Non-linearity

Test Method: "rotating sector" (combined with rotating drum in horizontal position).

Test Equipment:

- a) Rotating sector: disk with adjustable ratio of the arc of the open sector to the arc of the closed sector (length of the radius segment of the open sector : 60 mm). The disk is rotated by a motor and delivers a chopped beam of about 80 Hz.

- b) Radiation source: Xenon lamp XBO 2.5 kW ofr with condensor and mirror optics. Screen for shading.
- c) Additional optics: 2 achromatic lenses.
- d) Rotating drum: see 7.2 a (used as diffusing chamber in horizontal position).
- e) Data recorder: DVM Model 5000 (PREMA).

Test Procedure

a) Adjustments

- diffuse irradiance of $1000 \text{ W}\cdot\text{m}^{-2}$ (by shifting the achromatic lenses);
- position of the rotating sector at the site of the smallest diameter of the beam between drum and second lens;
- attenuation factor of the rotating sector (by adjustment of the sector blades).

b) Stabilizations

- Switching-on the lamp and the recorder about 30 minutes before the first reading.

c) Sequence of readings

- Table of reading time (after test starting at $t=0$ minutes).

Attenuation factor f	Shaded Reading M_s	Unshaded Reading M_u
1.00 (= appr. 1000 W m^{-2})	2 min	4 min
0.8	6 "	8 "
0.6	10 "	12 "
0.5	14 "	16 "
1.00	18 "	20 "
0.4	22 "	24 "
0.2	26 "	28 "
0.1	30 "	32 "
1.00	34 "	36 "
1.00	38 "	

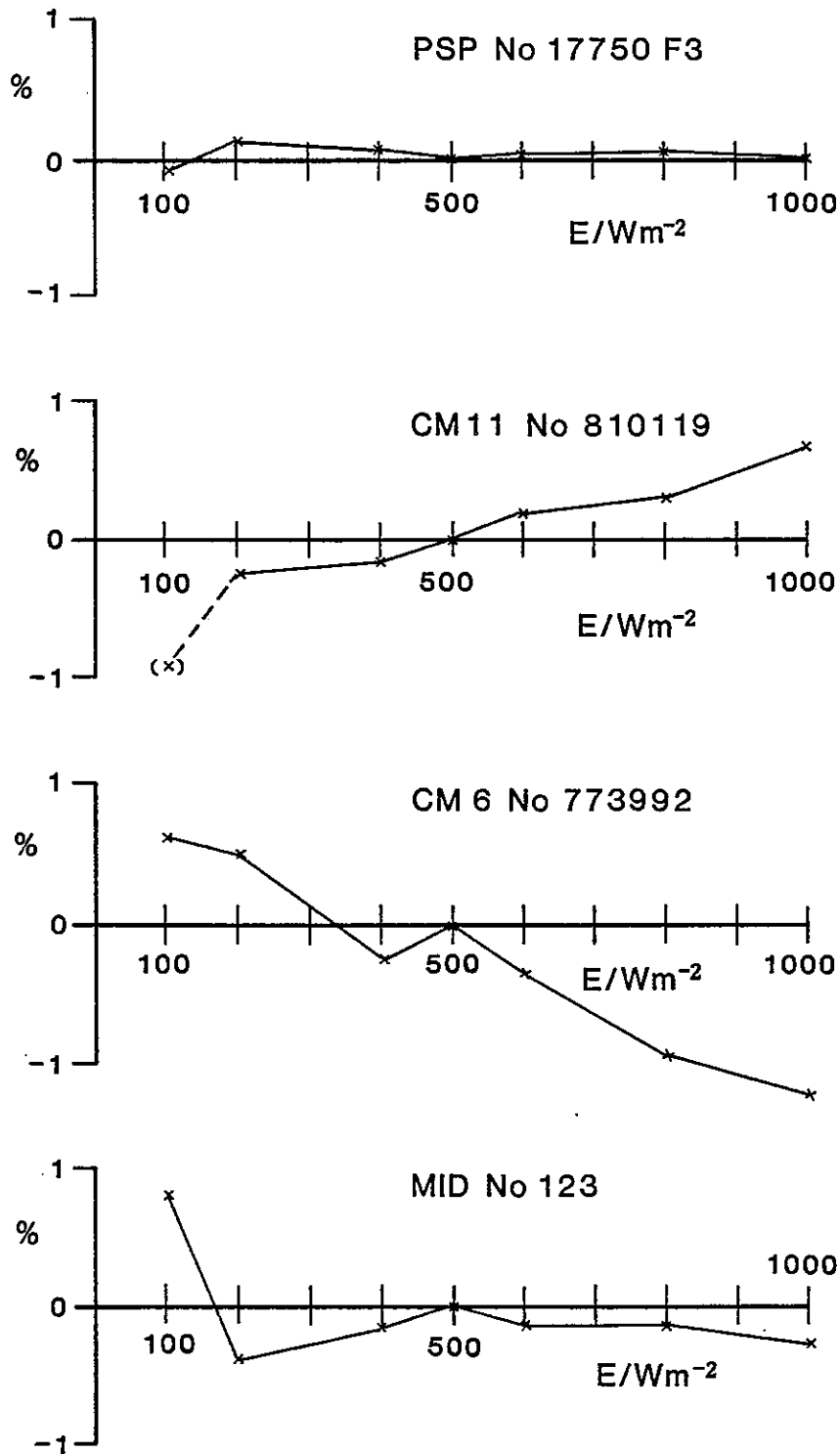


FIGURE 4. Percentage deviation of sensitivity at irradiance E from sensitivity at irradiance 500 Wm^{-2}

Evaluations

a) Measuring values

$$M(f) = M(F(t)) = M_U(t) - 0.5 \cdot [M_S(t-2) + M_S(t+2)]$$

where f corresponds to the reading time of M_U .

b) Percentage deviations $\Delta_1(f)$ of the ratio $M(f)/M(f=1)$ from the attenuation factor f:

$$\Delta_1(f) = \left(\frac{M(f)}{M(1) \cdot f} - 1 \right) \cdot 100\%$$

where $\overline{M(1)}$ in the arithmetic mean of two adjacent $M(1)$ values.

c) Percentage deviation $\Delta_{0.5}(f)$ of the ratio $M(f)/M(f=0.5)$ from the ideal ratio $f/0.5$.

$$\Delta_{0.5}(f) = \left(\frac{M(f) \cdot 0.5}{M(0.5) \cdot f} - 1 \right) \cdot 100\%$$

Results: See Table 4 and Figure 4.

Table 4
Percentage deviation $\Delta_1(f)$ and $\Delta_{0.5}(f)$ for 6 attenuation factors

f	PSP 17750 F3		CM 11 810119		CM 6 773992		MID 123	
	$\Delta_1(f)$	$\Delta_{0.5}(f)$	$\Delta_1(f)$	$\Delta_{0.5}(f)$	$\Delta_1(f)$	$\Delta_{0.5}(f)$	$\Delta_1(f)$	$\Delta_{0.5}(f)$
1	--	+0.01	--	+0.67	--	-1.19	--	-0.27
0.8	+0.03	+0.06	-0.38	+0.29	+0.26	-0.94	+0.12	-0.15
0.6	+0.07	+0.03	-0.61	+0.18	+0.86	-0.35	+0.12	-0.15
0.5	-0.07	--	-0.66	--	+1.18	--	+0.28	--
0.4	-0.04	+0.07	-0.75	-0.17	+1.23	-0.26	+0.05	-0.18
0.2	+0.03	+0.12	-0.90	-0.25	+1.60	+0.50	-0.15	-0.40
0.1	-0.10	-0.10	-1.50	-0.92	+1.75	+0.62	+1.05	+0.81

Test of Cosine Response

Test Method: Turning pyranometer (in vertical position).

Test Equipment:

a) Special turning mount: Combination of two perpendicular turning disks with graduation (incl. vernier). The vertical one serves as

support for the pyranometer to be tested and renders the adjustment of the azimuthal position; the horizontal disk bears the vertical disk and renders the adjustment of the angles of incidence.

- b) Radiation source: Xenon lamp XBO 2.5 kW ofr with condensor and mirror optics. Screen for shading.
- c) Optical bench: Support for the lamp on the one end and the turning mount on the other end (distance: 5 m). Resulting beam (using 4 diaphragmas): diameter: 7 cm; divergence: 0.7° ; irradiance: 180 W m^{-2} ; homogeneity: $< \pm 0.5 \%$ within $\varnothing = 25 \text{ mm}$.
- d) Ventilator for pyranometer: type Redmont.
- e) Data recorders: DVM Model 195 (Keithley) or Model 5000 (PREMA), Resolution : 100 nV.

Test Procedure

- a) Adjustments of the pyranometer
 - installation and levelling of the pyranometer on a plate which is mounted afterwards on the vertical disk;
 - positioning of the pyranometer so that the vertical axis of the horizontal disk lies in the receiver surface;
 - find the normal incidence position ($\theta = 0^\circ$) by means of the reflex of a mirror cup fitted on the head of the pyranometer;
 - azimuthal position: cable outlet downwards.
- b) Stabilizations

switching-on the lamp and the recorder about 30 minutes before first reading.
- c) Sequence of readings

see time table of the readings (at shaded or unshaded beam, resp.) after starting at $t=0$ minutes.

Angle of incidence θ	Shaded reading $M_S(\theta)$	Unshaded reading $M_U(\theta)$
0°	2 min	4 min
40°	6 "	8 "
60°	10 "	12 "
0°	14 "	16 "
70°	18 "	20 "
80°	22 "	24 "
0°	26 "	28 "
-40°	30 "	32 "
-60°	34 "	36 "
0°	38 "	40 "
-70°	42 "	44 "
-80°	46 "	48 "
0°	50 "	52 "
0°	54 "	

Evaluations

- a) Measuring values $M(\theta)$

The $M(\theta)$ are derived as difference between the unshaded readings $M_U(\theta)$ and the arithmetic mean of the adjacent shaded readings

$M_S(\theta)$:

$$M(\theta) = M_U(\theta, t_i) - 0.5 \cdot [M_S(\theta, t_i-2) + M_S(\theta, t_i+2)]$$

- b) Percentage deviations $\Delta(\theta)$ of the measuring values from the ideal cosine response:

$\Delta(\theta)$ has been calculated by:

$$\Delta(\theta) = \left(\frac{M(\theta)}{\overline{M(0)} \cos \theta} - 1 \right) \cdot 100\%$$

where $\overline{M(0)}$ represents the mean of the $M(\theta=0)$ measured before and after $M(\theta)$ (see table in 8.3c).

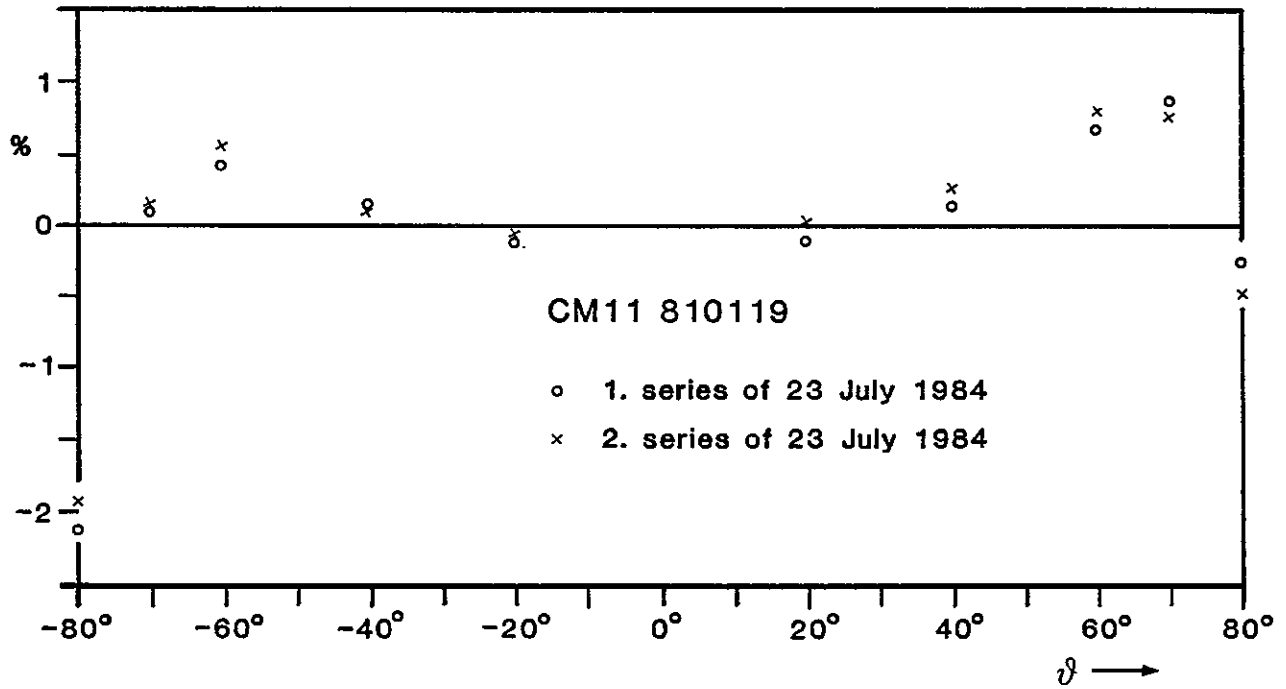
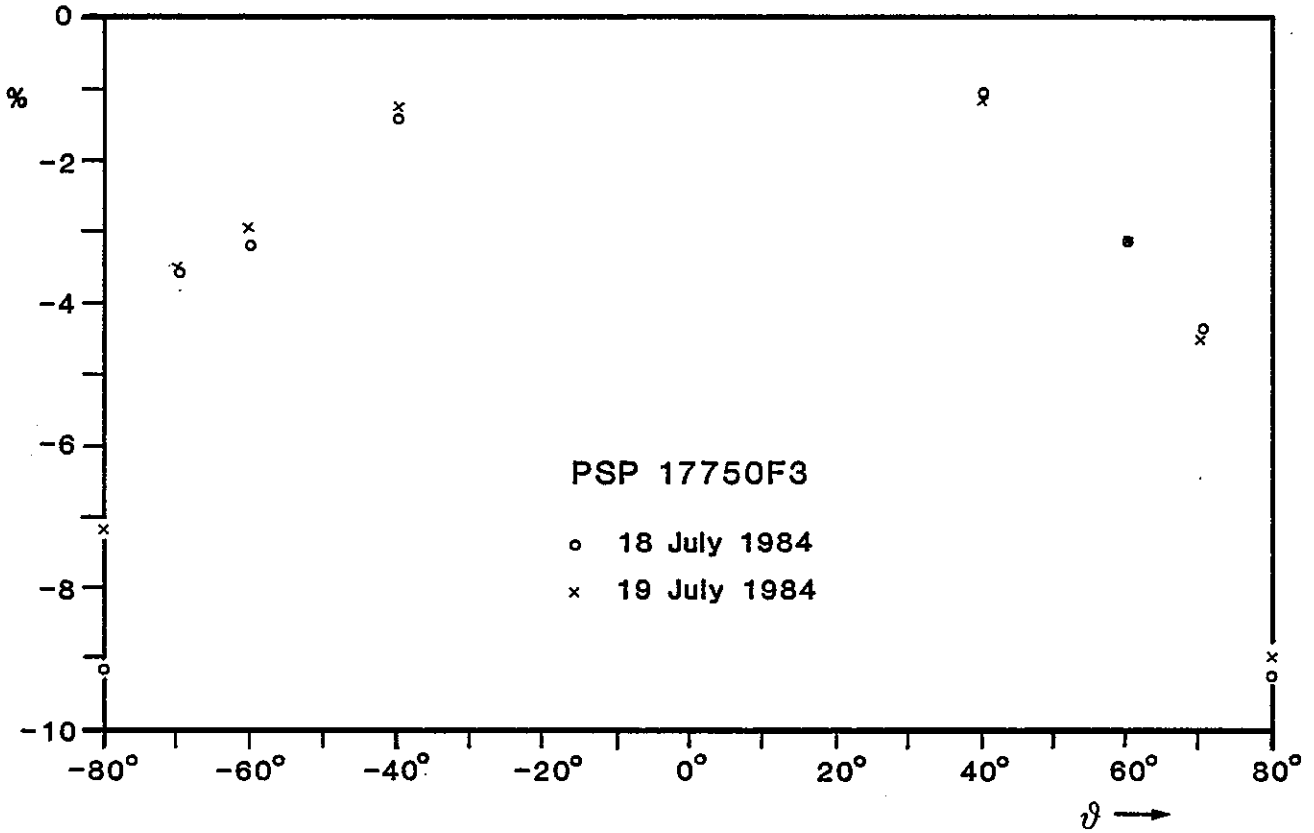
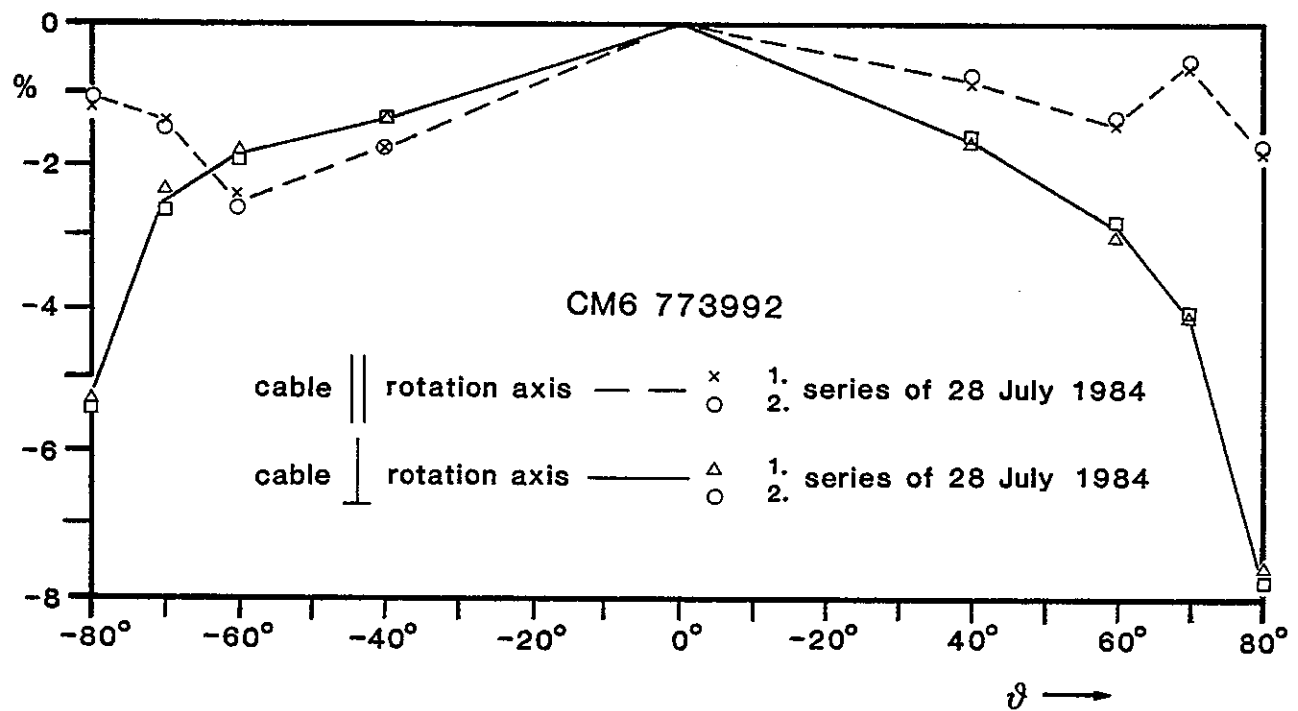
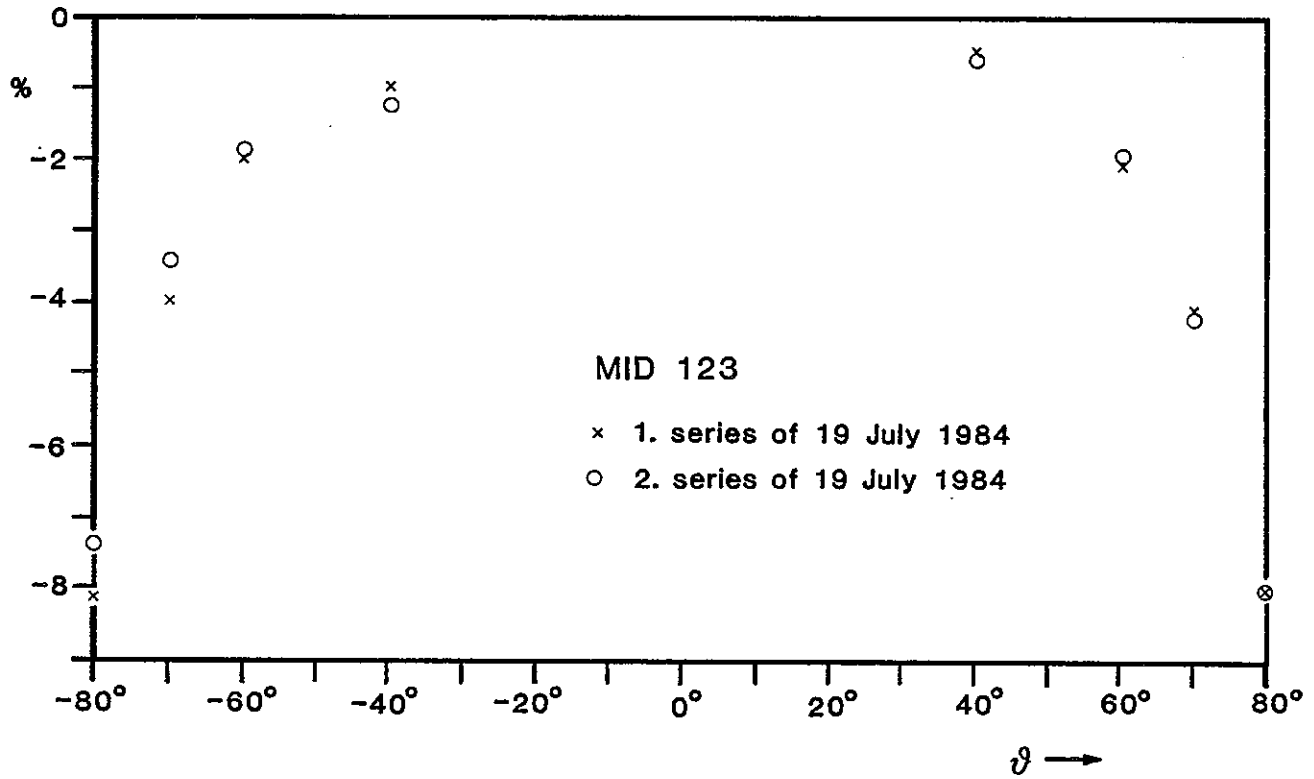


FIGURE 5. Percentage deviations $\Delta(\theta)$ from the ideal cosine response

FIGURE 5. (cont.)



PSP No 17750F3

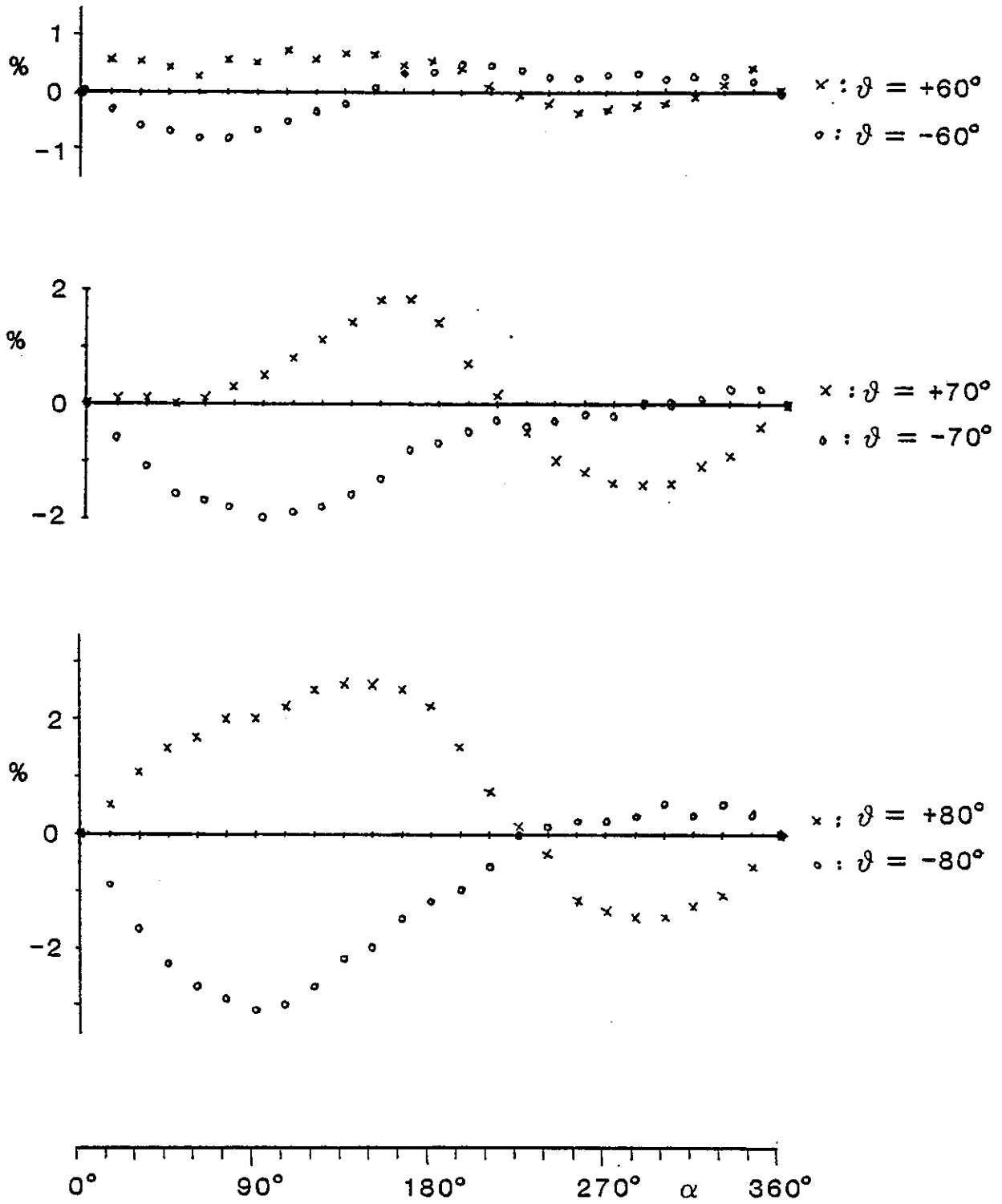


FIGURE 6a. Percentage deviations $\Delta_o(\alpha, \vartheta)$ at azimuth angles α for different incidence angles ϑ

CM 11 No 810119

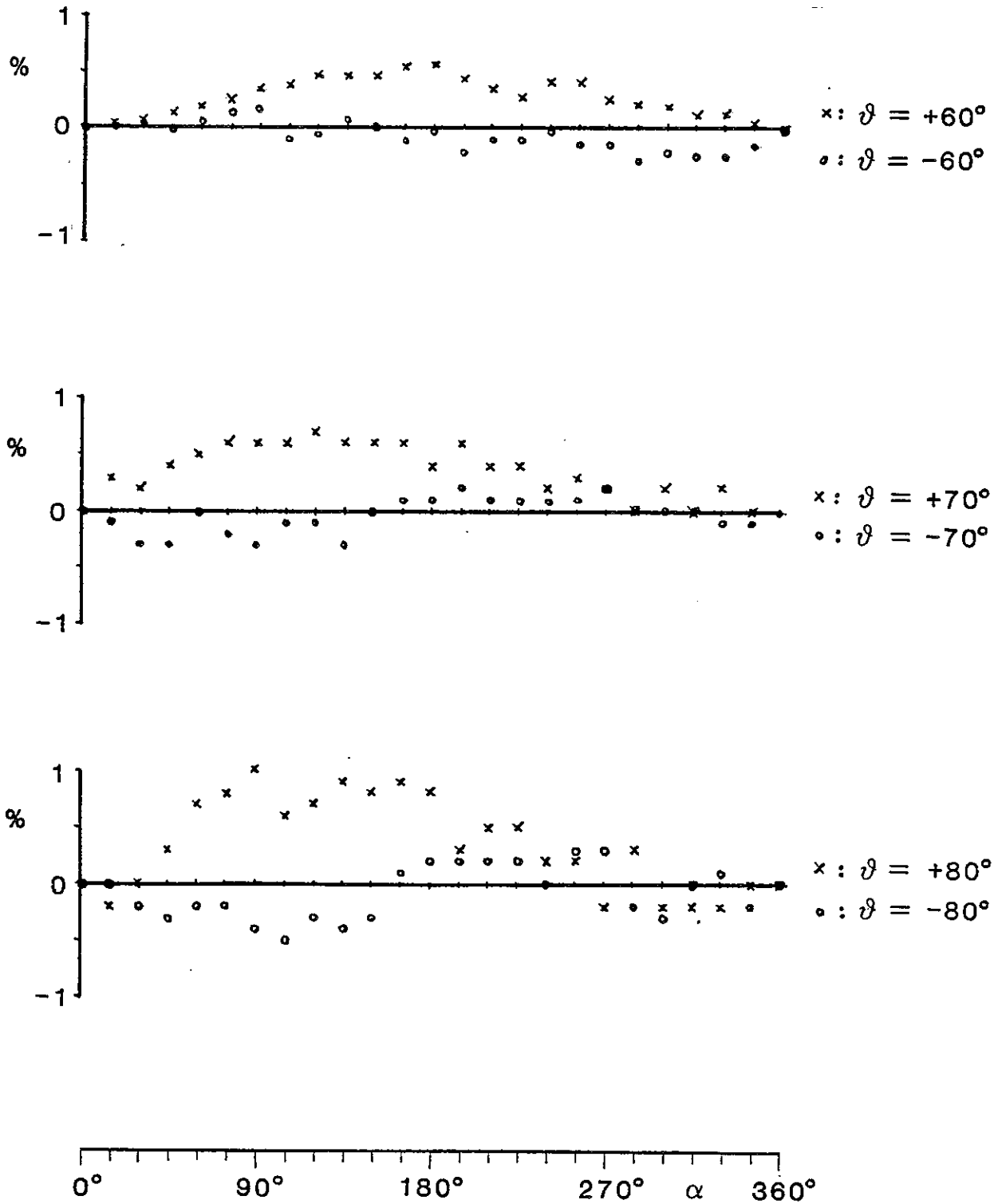


FIGURE 6b. Percentage deviations $\Delta_o(\alpha, \vartheta)$ at azimuth angles α for different incidence angles ϑ

CM 6 No 773992

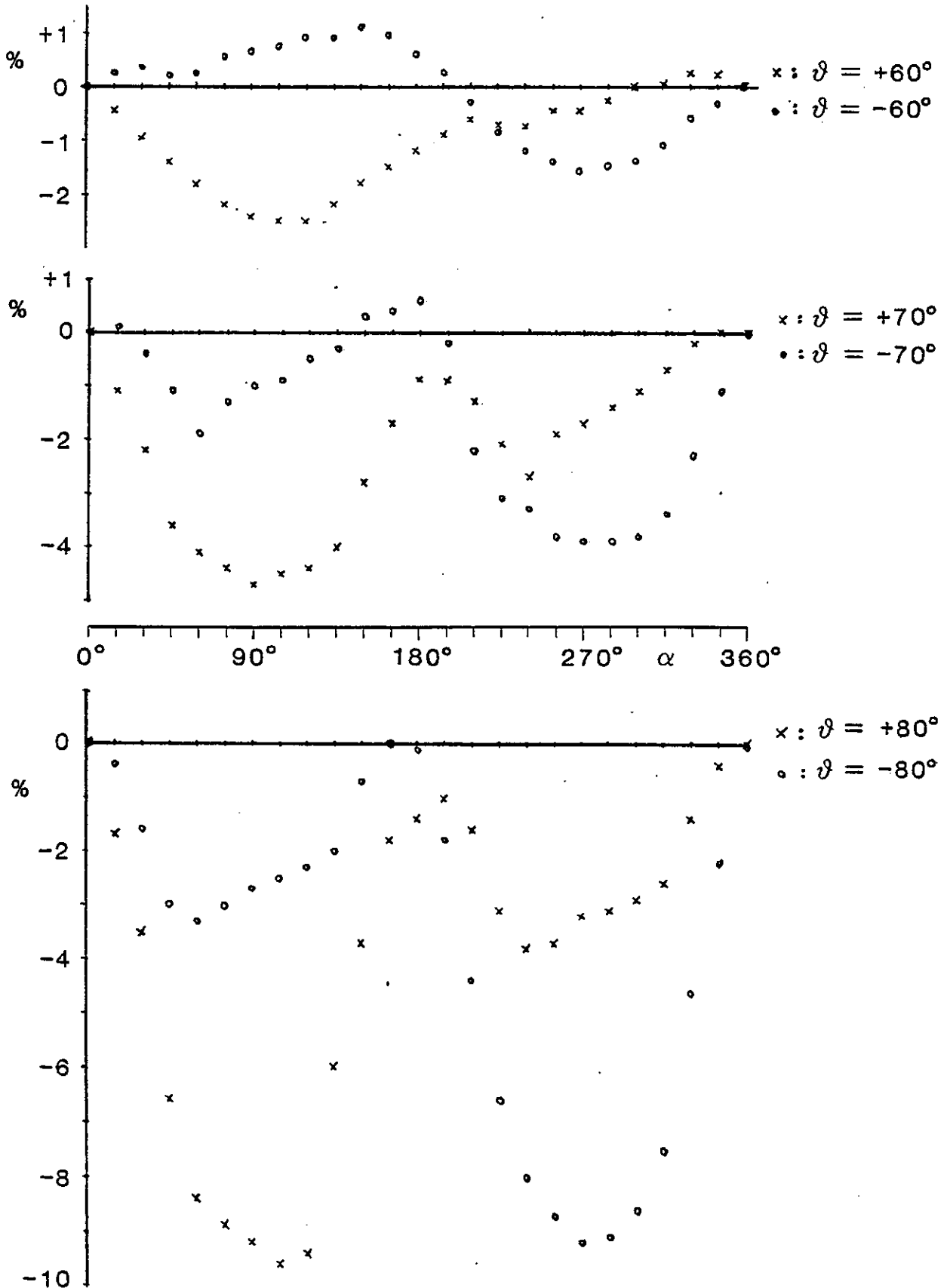


FIGURE 6c. Percentage deviations $\Delta_o(\alpha, \vartheta)$ at azimuth angles α for different incidence angles ϑ

MID 123

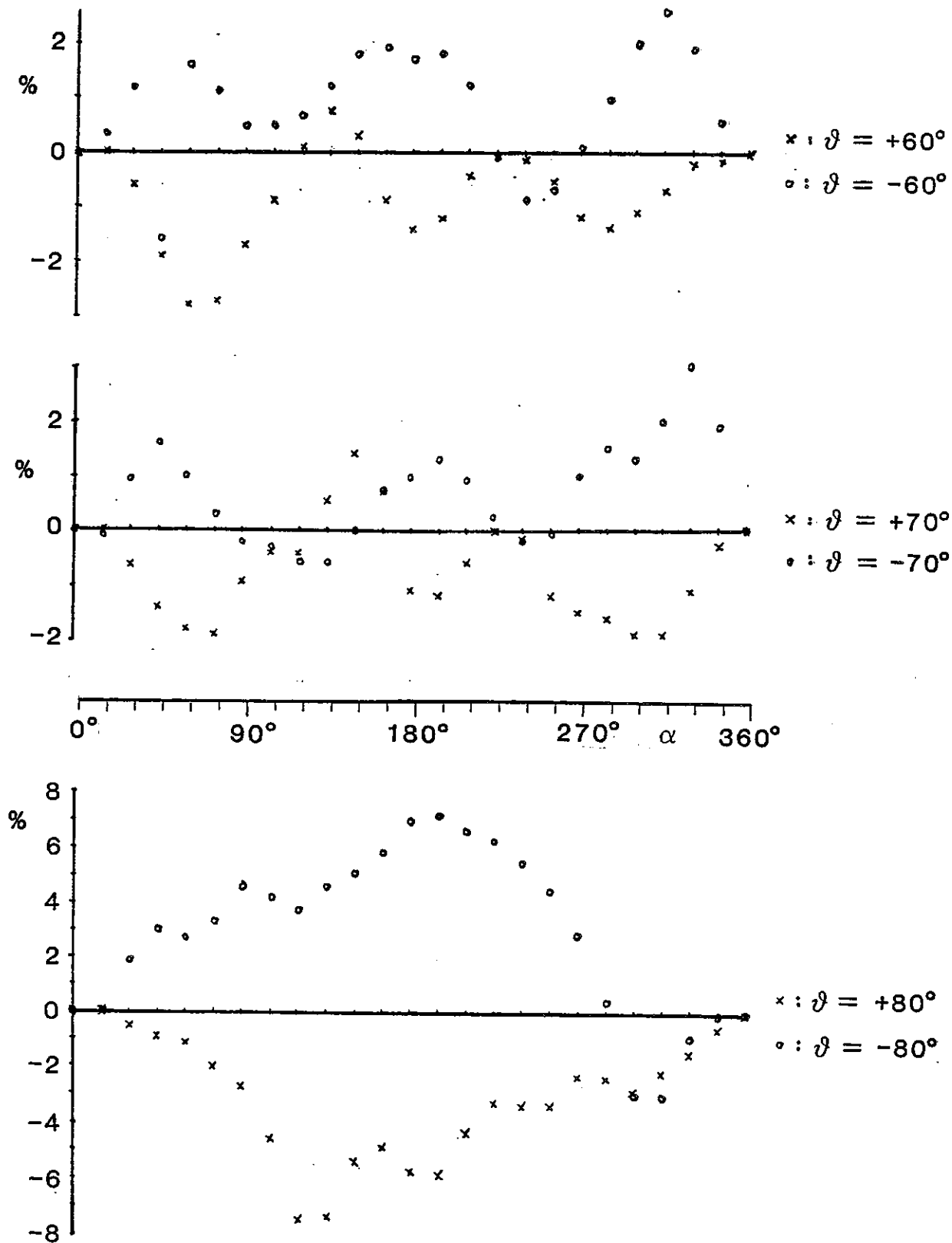


FIGURE 6d. Percentage deviations $\Delta_0(\alpha, \vartheta)$ at azimuth angles α for different incidence angles ϑ

Results of $\Delta(\theta)$: See Table 5 and Figure 5.

Table 5
Percentage deviation from the ideal cosine response
at different angles of incidence θ

θ°	CM 6 773992	CM 11 810119	PSP 17750 F3	MID 123
+40	-0.81 (-1.67)**	+0.17 *	-1.15	-0.45
-40	-1.74 (-1.40)	+0.17 (0.17)	-1.36	-0.99
+60	-1.38 (-3.00)	0.72	-3.15	-2.04
-60	-2.39 (-1.82)	0.42 (0.56)	-3.20	-2.01
+70	-0.64 (-4.06)	0.88 (0.63)	-4.42	-4.12
-70	-1.38 (-2.38)	0.12 (0.35)	-3.55	-4.02
+80	-1.79 (-7.57)	-0.21(-0.69)	-9.24	-7.98
-80	-1.16 (-5.23)	-2.13(-1.65)	-9.10	-8.13

* corrected mathematically by a θ -shift of -0.05°
** cable outlet horizontal

Test of Azimuth Response

Test Method: turning vertical pyranometer by constant angles of incidence.

Test Equipment: See 8.2.

Test Procedures:

a) Adjustments

See 8.3a. Pyranometer position with cable pointing downwards corresponds to the azimuth angle $\alpha = 0$.

b) Stabilizations

See 8.3b.

c) Control measurements

Before and after the test of azimuth response at an fixed angle of incidence θ : readings at normal incidence.

- d) Sequence of readings for $\theta = \pm 20^\circ, \pm 40^\circ, \pm 60^\circ, \pm 70^\circ$ and $\pm 80^\circ$.
- first reading at azimuth angle 0° at time $t=0$ minutes after 5 minutes of continuous irradiating the pyranometer (steady state);
 - after each reading, immediate change of azimuth angle by $\Delta\alpha = 15^\circ$;
 - 0.5 minutes after a reading, the next reading follows (at the next azimuth angle);
 - the last reading is done at azimuth angle $\alpha = 360^\circ = 0^\circ$.

Evaluation

- a) Percentage deviations $\Delta_0(\alpha_i, \theta)$ of the readings at the azimuth positions $\alpha_i = 0^\circ + i \cdot 15^\circ$ ($i = 0, 1 \dots 24$) from the reading at $\alpha = 0^\circ$.

If $M(0^\circ, \theta)$ and $M(360^\circ, \theta)$ differ, then the reference values at the different azimuth angles are determined by linear interpolation between those two readings.

$$\Delta_0(\alpha_i, \theta) = \left(\frac{M(\alpha_i, \theta)}{M_{\text{int}}(0^\circ, \theta)} - 1 \right) \cdot 100\%$$

- b) Percentage deviations $\Delta_m(\alpha_i, \theta)$ of the readings at the azimuthal positions $\alpha_i = 0^\circ + i \cdot 15^\circ$ ($i = 0, 1 \dots 24$) from the arithmetical mean of all 25 readings.

$$\Delta_m(\alpha_i, \theta) = \left(\frac{M(\alpha_i, \theta)}{\frac{1}{25} \sum_{i=0}^{24} M(\alpha_i, \theta)} - 1 \right) \cdot 100\%$$

Results: See Table 6 for the extreme positive, extreme negative and extreme total deviations of $\Delta_0(\alpha_i, \theta)$. $\Delta_0(\alpha_i, \theta)$ for all α_i see Table 6a-6d. $\Delta_0(\alpha_i, \theta)$ for $\theta = 60^\circ, 70^\circ$ and 80° in Figure 6.

TABLE 6
Percentage deviations $\Delta_p(\alpha, \theta)$ at azimuth angles α for
different incidence angles θ

a: extreme positive b: extreme negative c: extreme total deviation

Angle of incidence θ	S.No.				
	PSP 17750 F3	CM 11 810119	CM 6 773992	MID 123	
+20°C	a	0.52 % at 165°	0.19 % at 255°	0.12 % at 345°	0.49 % at 330°
	b	-0.07 % at 330°	-0.15 % at 15°	-0.67 % at 135°	-0.33 % at 90°
	c	0.59 %	0.34 %	0.79 %	0.82 %
-20°C	a	0.41 % at 165°	0.26 % at 195°	0.44 % at 165°	1.33 % at 195°
	b	-0.10 % at 45°	-0.08 % at 285°	-0.07 % at 345°	-0.09 % at 60°
	c	0.51 %	0.34 %	0.51 %	1.42 %
+40°C	a	0.01 % at 150°	0.33 % at 295°	0.00 % at 0°	0.00 % at 0°
	b	-0.39 % at 255°	0.00 % at 0°	-1.24 % at 105°	-3.05 % at 75°
	c	0.40 %	0.33 %	1.24 %	3.05 %
-40°C	a	0.41 % at 270°	0.18 % at 120°	0.44 % at 150°	1.05 % at 180°
	b	-0.27 % at 75°	-0.13 % at 285°	-0.52 % at 285°	-1.45 % at 255°
	c	0.68 %	0.31 %	0.96 ?	2.50 %
+60°C	a	0.71 % at 150°	0.57 % at 180°	0.24 % at 330°	0.75 % at 135°
	b	-0.34 % at 270°	0.00 % at 0°	-2.53 % at 105°	-2.75 % at 60°
	c	1.05 %	0.57 %	2.77 %	3.50 %
-60°C	a	0.45 % at 195°	0.17 % at 90°	1.07 % at 150°	2.57 % at 315°
	b	-0.82 % at 75°	-0.28 % at 285°	-1.55 % at 270°	-0.89 % at 240°
	c	1.27 %	0.45 %	2.62 %	3.46 %
+70°C	a	1.82 % at 150°	0.64 % at 165°	0.01 % at 345°	1.41 % at 150°
	b	-1.39 % at 285°	0.00 % at 0°	-4.69 % at 90°	-1.92 % at 75°
	c	3.21 %	0.64 %	4.70 %	3.33 %
-70°	a	0.32 % at 330°	0.16 % at 270°	0.62 % at 180°	3.03 % at 330°
	b	-1.98 % at 90°	-0.29 % at 90°	-3.91 % at 270°	-0.60 % at 135°
	c	2.30 %	0.45 %	4.53 %	3.63 %
+80°	a	2.61 % at 150°	0.96 % at 90°	0.00 % at 0°	0.00 % at 0°
	b	-1.50 % at 300°	-0.24 % at 315°	-9.58 % at 105°	-7.45 % at 120°
	c	4.11 %	1.20 %	9.58 %	7.45 %
-80°	a	0.49 % at 315°	0.33 % at 255°	0.00 % at 0°	7.23 % at 195°
	b	-3.07 % at 90°	-0.50 % at 150°	-9.19 % at 270°	-3.04 % at 315°
	c	3.56 %	0.83 %	9.19 %	10.27 %

TABLE 6a
Azimuth response of PSP No. 17750 F3
Percentage deviations $\Delta_p(\alpha, \theta)$ at azimuth
angles α for different incidence angles θ

$\alpha^\circ \backslash \theta^\circ$	+20	-20	+40	-40	+60	-60	+70	-70	+80	-80
0	--	--	--	--	--	--	--	--	--	--
15	+0.16	-0.03	-0.10	+0.01	+0.54	-0.31	+0.1	-0.6	+0.5	-0.9
30	+0.23	-0.10	-0.04	-0.05	+0.53	-0.62	+0.1	-1.1	+1.1	-1.7
45	+0.32	-0.10	-0.16	-0.15	+0.42	-0.74	+0.0	-1.6	+1.5	-2.3
60	+0.30	+0.02	-0.17	-0.26	+0.23	-0.81	+0.1	-1.7	+1.7	-2.7
75	+0.21	-0.03	-0.24	-0.27	+0.54	-0.82	+0.3	-1.8	+2.0	-2.9
90	+0.31	+0.02	-0.30	-0.18	+0.50	-0.67	+0.5	-2.0	+2.0	-3.1
105	+0.33	+0.07	-0.24	+0.02	+0.71	-0.52	+0.8	-1.9	+2.2	-3.0
120	+0.38	+0.14	-0.16	-0.01	+0.53	-0.34	+1.1	-1.8	+2.5	-2.7
135	+0.46	+0.18	-0.07	+0.03	+0.67	-0.21	+1.4	+1.6	+2.6	-2.2
150	+0.49	+0.13	+0.01	+0.26	+0.63	+0.07	+1.8	-1.3	+2.6	-2.0
165	+0.52	+0.41	-0.05	+0.28	+0.44	+0.32	+1.8	-0.8	+2.5	-1.5
180	+0.49	+0.36	-0.07	+0.41	+0.42	+0.33	+1.4	-0.7	+2.2	-1.2
195	+0.43	+0.33	-0.13	+0.39	+0.37	+0.45	+0.7	-0.5	+1.5	-1.0
210	+0.40	+0.28	-0.13	+0.32	+0.07	+0.43	+0.1	-0.3	+0.7	-0.6
225	+0.28	+0.21	-0.22	+0.26	-0.05	+0.37	-0.5	-0.4	+0.1	0.0
240	+0.28	+0.17	-0.34	+0.27	-0.26	+0.25	-1.0	-0.3	-0.4	+0.1
255	+0.21	+0.13	-0.39	+0.13	-0.40	+0.22	-1.2	-0.2	-1.2	+0.2
270	+0.18	+0.04	-0.36	+0.11	-0.34	+0.29	-1.4	-0.2	-1.4	+0.2
285	+0.03	+0.05	-0.35	+0.05	-0.30	+0.32	-1.4	+0.0	-1.5	+0.3
300	+0.05	-0.04	-0.28	+0.06	-0.23	+0.22	-1.4	0.0	-1.5	+0.5
315	-0.01	+0.08	-0.08	-0.02	-0.10	+0.27	-1.1	+0.1	-1.3	+0.3
330	-0.07	+0.07	-0.07	-0.04	+0.12	+0.26	-0.9	+0.3	-1.1	+0.5
345	+0.04	+0.03	+0.01	-0.04	+0.42	+0.16	-0.4	+0.3	-0.6	+0.3

TABLE 6b
Azimuth response of CM 11 No. 810119
Percentage deviations $\Delta_p(\alpha, \theta)$ at azimuth
angles α for different incidence angles θ

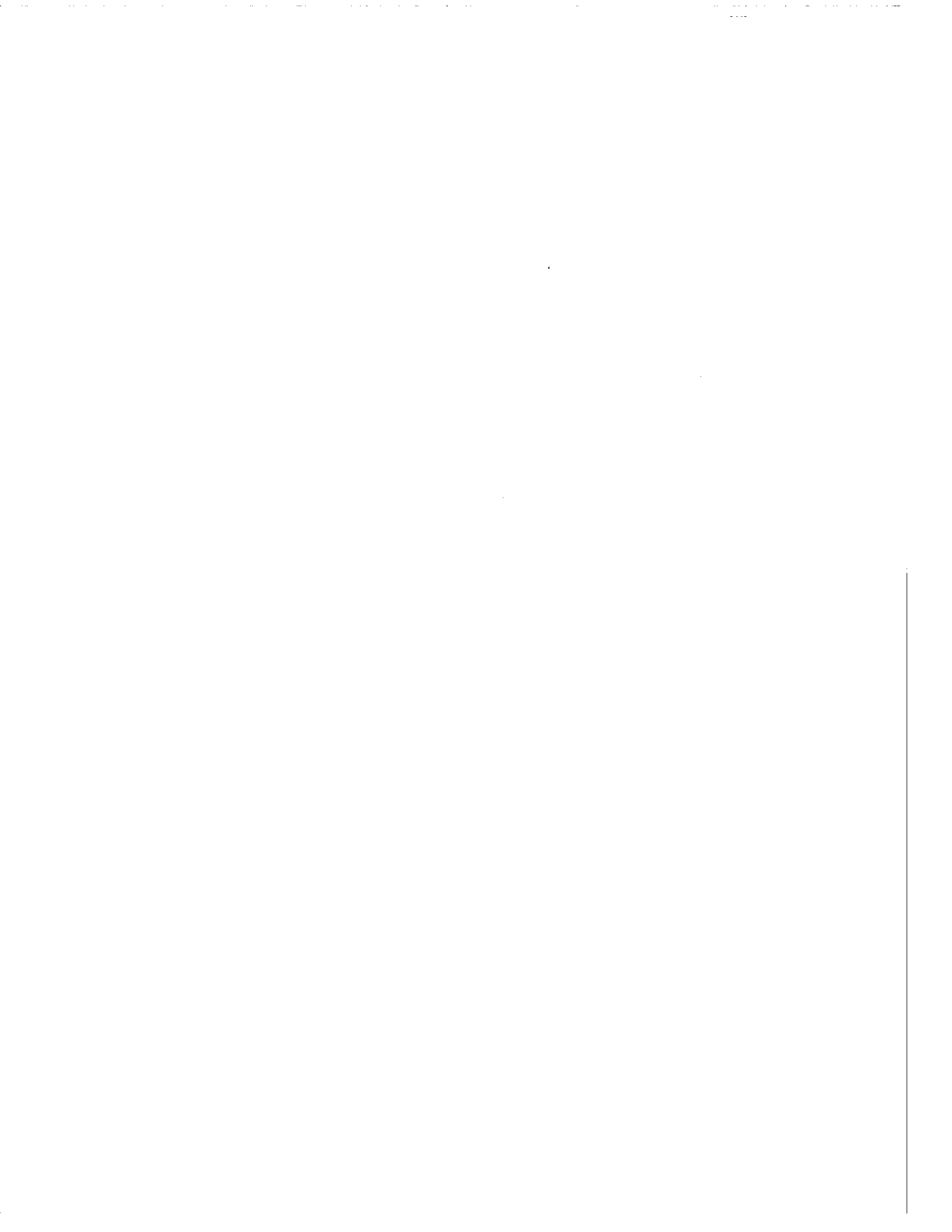
$\alpha^\circ \backslash \theta^\circ$	+20	-20	+40	-40	+60	-60	+70	-70	+80	-80
0	--	--	--	--	--	--	--	--	--	--
15	-.15	+.02	+.04	+.07	+.05	+.03	+0.3	-0.1	-0.2	0.0
30	-.07	+.01	+.05	-.11	+.08	+.06	+0.2	-0.3	0.0	-0.2
45	-.07	+.07	+.04	+.11	+.14	-.03	+0.4	-0.3	+0.3	-0.3
60	-.04	+.10	+.11	+.09	+.19	+.06	+0.5	-0.0	+0.7	-0.2
75	-.01	+.15	+.13	+.11	+.25	+.14	+0.6	-0.2	+0.8	-0.2
90	-.01	+.15	+.27	+.11	+.36	+.17	+0.6	-0.3	+1.0	-0.4
105	+.06	+.24	+.25	+.07	+.38	-.11	+0.6	-0.1	+0.6	-0.5
120	-.04	+.20	+.24	+.18	+.47	-.06	+0.7	-0.1	+0.7	-0.3
135	+.07	+.20	+.22	+.09	+.47	+.08	+0.6	-0.3	+0.9	-0.4
150	+.04	+.13	+.18	+.09	+.47	.00	+0.6	+0.0	+0.8	-0.3
165	-.03	+.17	+.24	+.07	+.55	-.11	+0.6	+0.1	+0.9	+0.1
180	+.06	+.14	+.29	+.14	+.57	-.03	+0.4	+0.1	+0.8	+0.2
195	+.09	+.26	+.33	+.07	+.44	-.22	+0.6	+0.2	+0.3	+0.2
210	+.01	+.24	+.25	.00	+.36	-.11	+0.4	+0.1	+0.5	+0.2
225	+.04	+.24	+.18	+.05	+.27	-.11	+0.4	+0.1	+0.5	+0.2
240	+.06	+.15	+.31	-.04	+.41	-.03	+0.2	+0.1	+0.2	0.0
255	+.19	+.14	+.24	-.04	+.41	-.17	+0.3	+0.1	+0.2	+0.3
270	+.10	+.05	+.20	-.04	+.25	-.17	+0.2	+0.2	-0.2	+0.3
285	+.12	+.07	+.22	-.13	+.22	-.29	+0.0	+0.0	+0.3	-0.2
300	+.10	+.10	+.24	-.05	+.19	-.22	+0.2	+0.0	-0.2	-0.3
315	+.06	-.02	+.22	-.07	+.11	-.25	+0.0	0.0	-0.2	0.0
330	+.03	-.04	+.07	-.09	+.13	-.25	+0.2	-0.1	-0.2	+0.1
345	-.04	-.08	+.07	-.09	+.03	-.14	0.0	-0.1	0.0	-0.2

TABLE 6c
Azimuth response of CM 6 No. 773992
Percentage deviations $\Delta_p(\alpha, \theta)$ at azimuth
angles α for different incidence angles θ

$\alpha^\circ \backslash \theta^\circ$	+20	-20	+40	-40	+60	-60	+70	-70	+80	-80
0	--	--	--	--	--	--	--	--	--	--
15	-.11	+.02	-.19	-.07	-.43	+.29	-1.1	+0.1	-1.7	-0.4
30	-.23	+.04	-.43	+.01	-.96	+.38	-2.2	-0.4	-3.5	-1.6
45	-.39	+.14	-.60	+.04	-1.4	+.22	-3.6	-1.1	-6.6	-3.0
60	-.43	+.14	-.87	+.02	-1.8	+.26	-4.1	-1.9	-8.4	-3.3
75	-.47	+.10	-1.1	+.07	-2.2	+.55	-4.4	-1.3	-8.9	-3.0
90	-.47	+.30	-1.1	+.16	-2.4	+.66	-4.7	-1.0	-9.2	-2.7
105	-.59	+.31	-1.2	+.28	-2.5	+.76	-4.5	-0.9	-9.6	-2.5
120	-.64	+.36	-1.2	+.35	-2.5	+.90	-4.4	-0.5	-9.4	-2.3
135	-.67	+.38	-1.2	+.37	-2.2	+.89	-4.0	-0.3	-6.0	-2.0
150	-.58	+.36	-1.0	+.44	-1.8	+1.1	-2.8	+0.3	-3.7	-0.7
165	-.56	+.44	-1.0	+.38	-1.5	+.94	-1.7	+0.4	-1.8	-0.0
180	-.48	+.43	-.83	+.26	-1.2	+.61	-0.9	+0.6	-1.4	-0.1
195	-.48	+.31	-.74	+.21	-.89	+.27	-0.9	-0.2	-1.0	-1.8
210	-.39	+.05	-.60	-.02	-.62	-.29	-1.3	-2.2	-1.6	-4.4
225	-.33	+.07	-.55	-.10	-.72	-.86	-2.1	-3.1	-3.1	-6.6
240	-.22	+.08	-.51	-.32	-.73	-1.2	-2.7	-3.3	-3.8	-8.0
255	-.27	-.01	-.45	-.45	-.45	-1.4	-1.9	-3.8	-3.7	-8.7
270	-.23	-.03	-.29	-.50	-.45	-1.6	-1.7	-3.9	-3.2	-9.2
285	-.12	-.06	-.10	-.52	-.27	-1.5	-1.4	-3.9	-3.1	-9.1
300	-.09	+.02	-.14	-.45	+.01	-1.4	-1.1	-3.8	-2.9	-8.6
315	+.02	-.06	-.14	-.30	+.04	-1.1	-0.7	-3.4	-2.6	-7.5
330	-.12	-.03	-.01	-.30	+.24	-.60	-0.2	-2.3	-1.4	-4.6
345	+.12	-.07	-.03	-.11	+.22	-.31	+.01	-1.1	-0.4	-2.2

TABLE 6d
Azimuth response of MID 123
Percentage deviations Δ_{θ} (α , θ) at azimuth
angles α for different incidence angles θ

$\alpha^{\circ} \backslash \theta^{\circ}$	+20	-20	+40	-40	+60	-60	+70	-70	+80	-80
0	.00	.00	.00	.00	.00	.00	.00	.00	.00	.00
15	-.01	-.03	-.37	.18	.03	.35	-.03	-.11	-.03	.12
30	-.07	-.06	-1.2	.57	-.62	1.2	-.63	+.95	-.52	1.9
45	-.16	-.06	-2.0	.96	-1.9	-1.6	-1.4	1.6	-.87	3.0
60	-.15	-.09	-2.7	.97	-2.8	+1.7	-1.8	1.0	-1.1	2.7
75	-.25	-.08	-3.1	.61	-2.7	1.1	-1.9	.30	-2.0	3.3
90	-.33	-.07	-2.8	-.05	-1.7	.46	-.94	-.21	-2.7	4.6
105	-.26	+.02	-2.1	-.52	-1.0	.45	-.41	-.32	-4.6	4.2
120	-.26	.23	-1.6	-.58	+.09	.58	-.43	-.58	-7.5	3.8
135	-.17	.53	-1.4	.00	+.75	1.2	+.53	-.60	-7.4	4.6
150	-.06	.86	-1.4	.55	.30	1.8	1.4	-.02	-5.4	5.1
165	+.09	1.1	-1.4	1.0	-.88	1.9	.67	+.73	-4.9	5.9
180	.08	1.3	-1.2	1.1	-1.4	1.7	-1.1	.98	-5.8	7.0
195	.13	1.3	-1.1	.88	-1.2	1.8	-1.2	1.3	-5.9	7.2
210	.09	1.3	-.71	.22	-.45	1.2	-.57	.90	-4.4	6.7
225	.16	1.2	-.35	-.52	-.05	-.08	.00	.23	-3.3	6.3
240	.08	1.1	-.24	-1.2	-.14	-.89	-.16	-.19	-3.4	5.5
255	.14	.90	-.71	-1.5	-.55	-.71	-1.2	-.06	-3.4	4.5
270	.07	.79	-1.3	-1.3	-1.2	+.03	-1.5	+.99	-2.3	2.9
285	.12	.66	-1.8	-.57	-1.4	.97	-1.6	1.5	-2.4	.41
300	.29	.60	-1.7	+.02	-1.1	2.0	-1.9	1.3	-2.9	-3.0
315	.36	.51	-1.2	+.14	-.68	2.6	-1.9	2.0	-2.2	-3.0
330	.49	.29	-.66	-.02	-.22	1.9	-1.1	3.0	-1.5	-.94
345	.24	.23	-.04	+.05	-.17	.54	-.25	1.9	-.57	-.16



7.C PRELIMINARY PRESENTATION OF CHARACTERISTICS OF IEA PYRANOMETERS

G.J. Van den Brink

Institute of Applied Physics TNO-TH
P.O. Box 155
2600 AD Delft
Netherlands

PRELIMINARY PRESENTATION OF CHARACTERISTICS OF IEA PYRANOMETERS

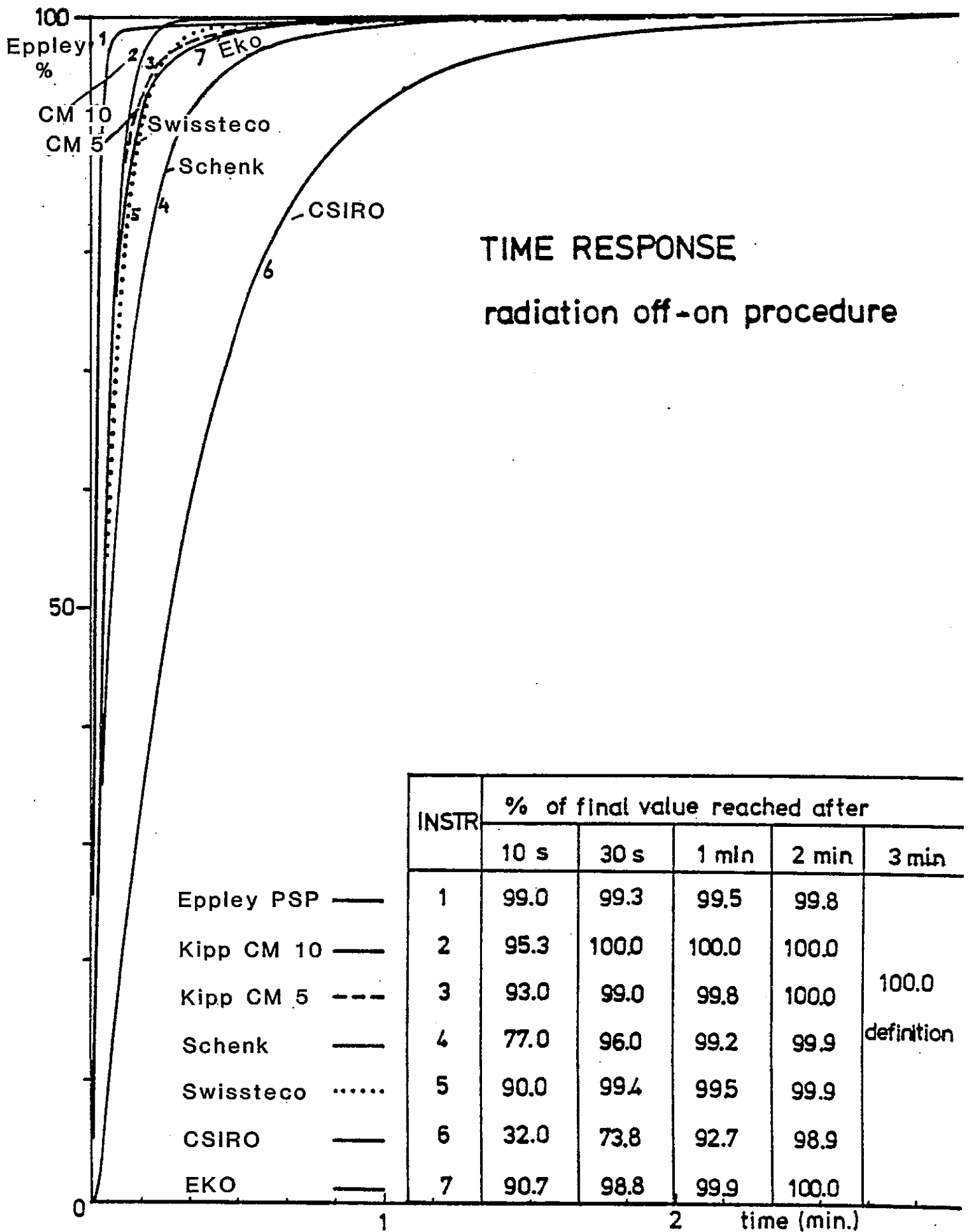
Indoor measurements at:

- Kipp and Zonen
- Technisch Physische Dienst TNO-TH (Institute of Applied Physics)

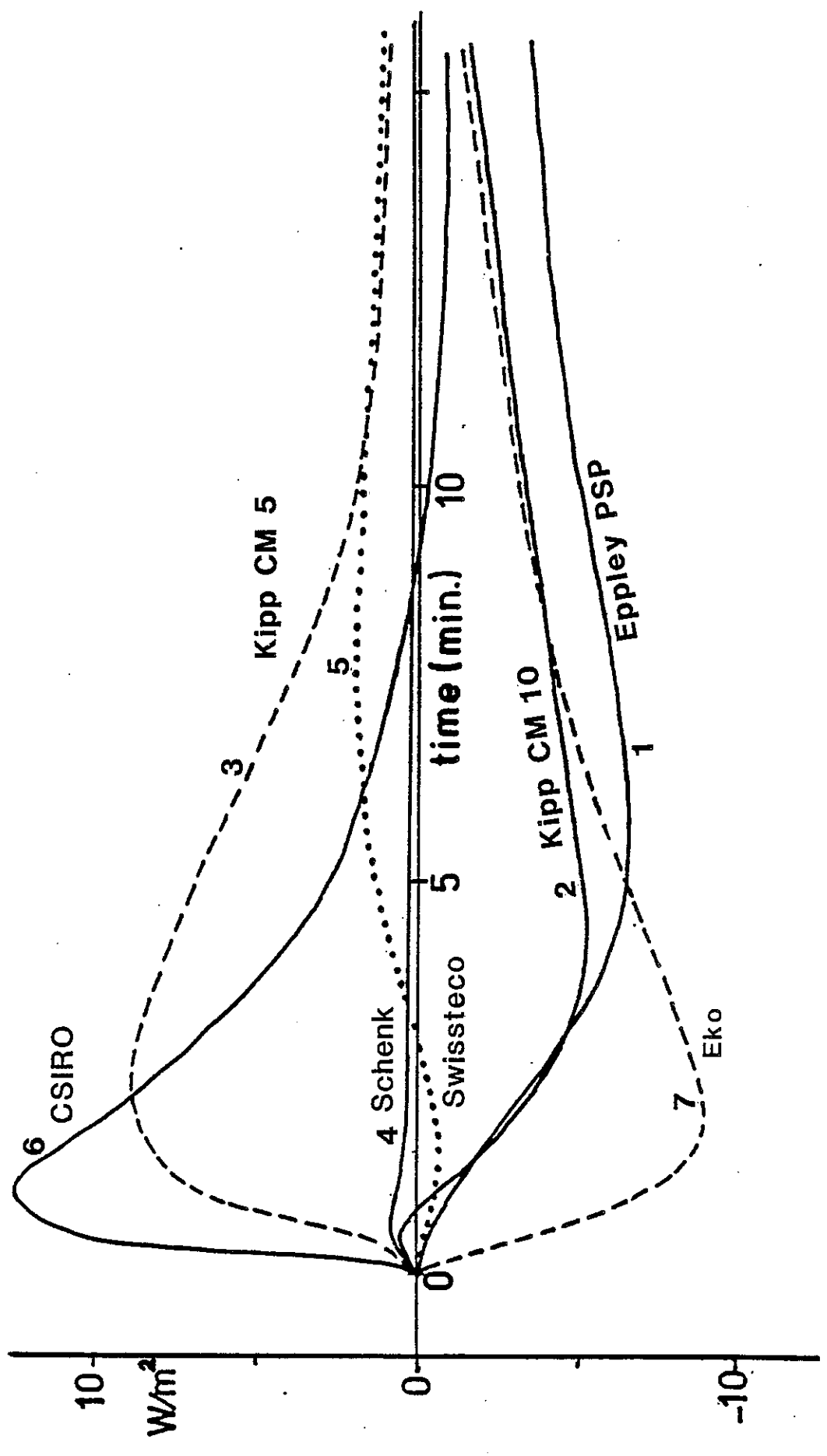
Characteristics:

- Response time*
- Thermal shock*
- Thermal gradient test
- Sky-temperature
- Temperature dependency
- Linearity*
- Tilt dependency*
- Cosine dependency
- Azimuth dependency
- Spectral response*
- Sensitivity

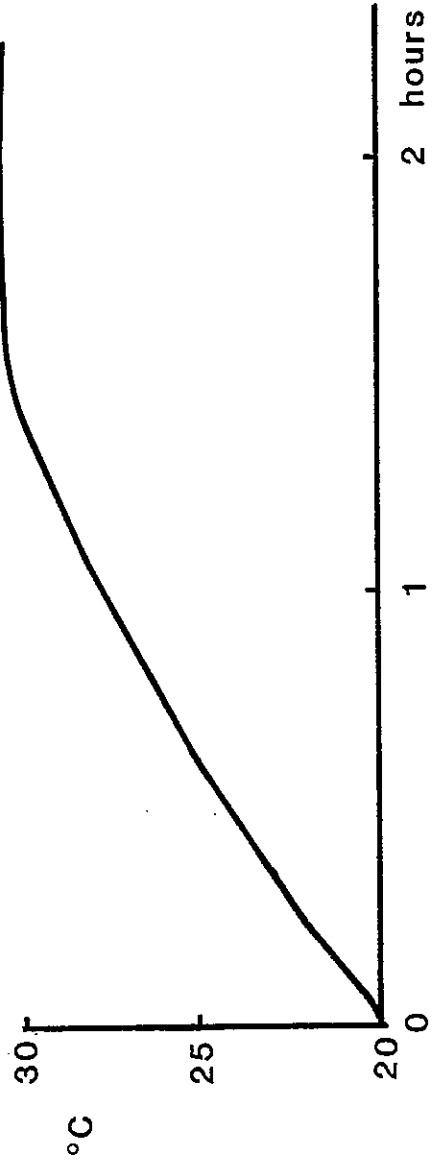
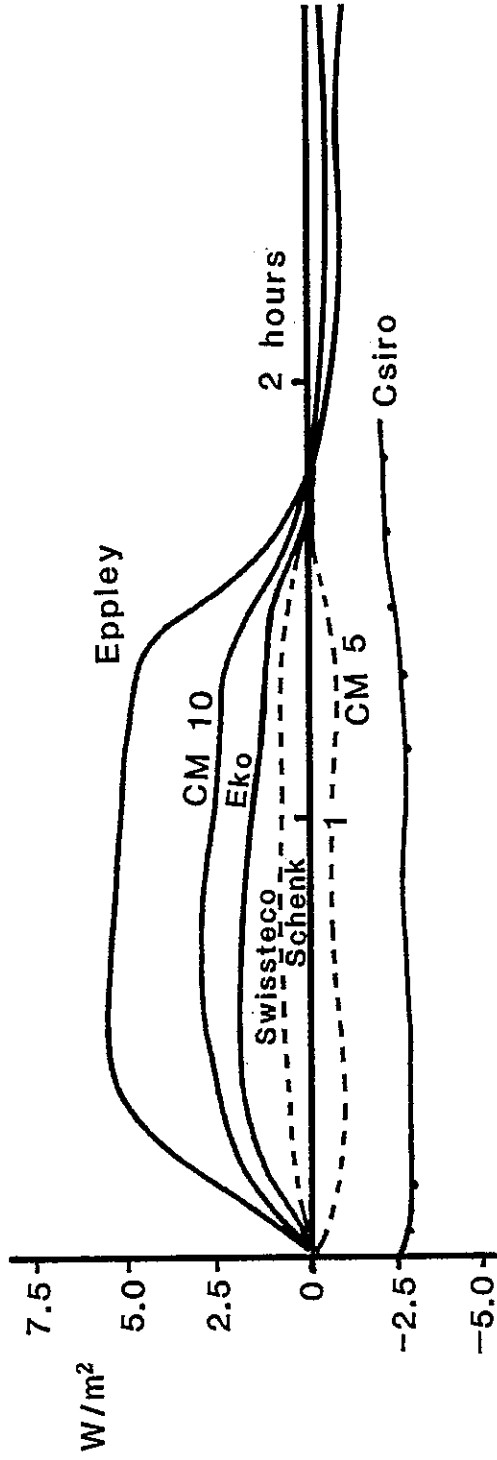
* shown at the Norrköping meeting 1984.



RESPONSE TO AN ABRUPT CHANGE IN AIR TEMPERATURE 25° → 20°C

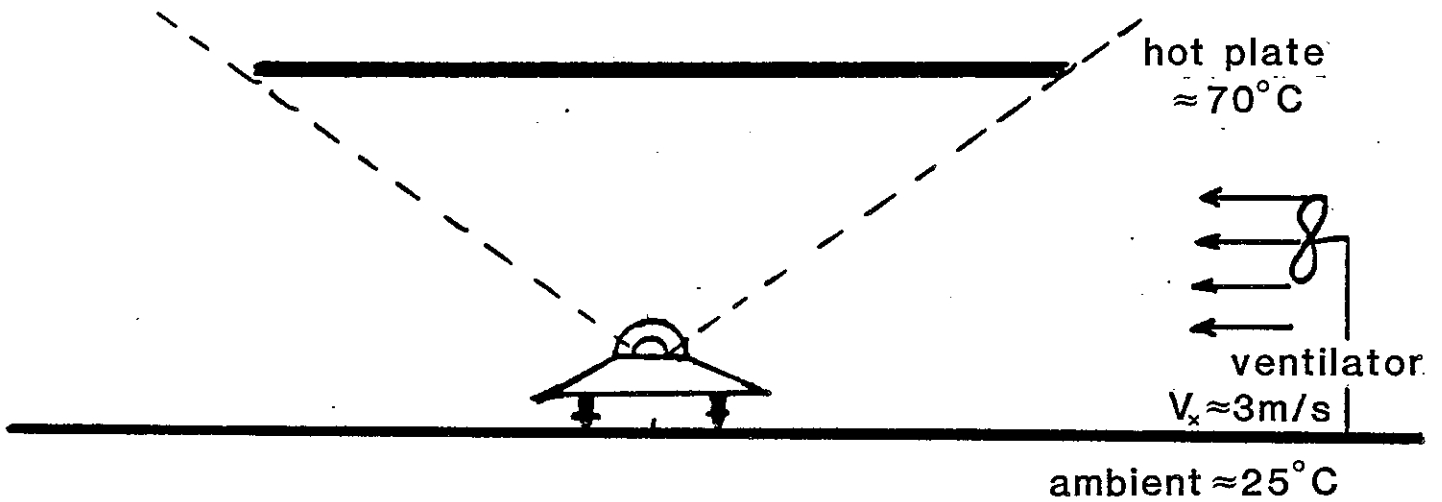


Thermal gradient test (6.7°C /hour) V_{wind} 1m/S



Temperature of climat chamber.

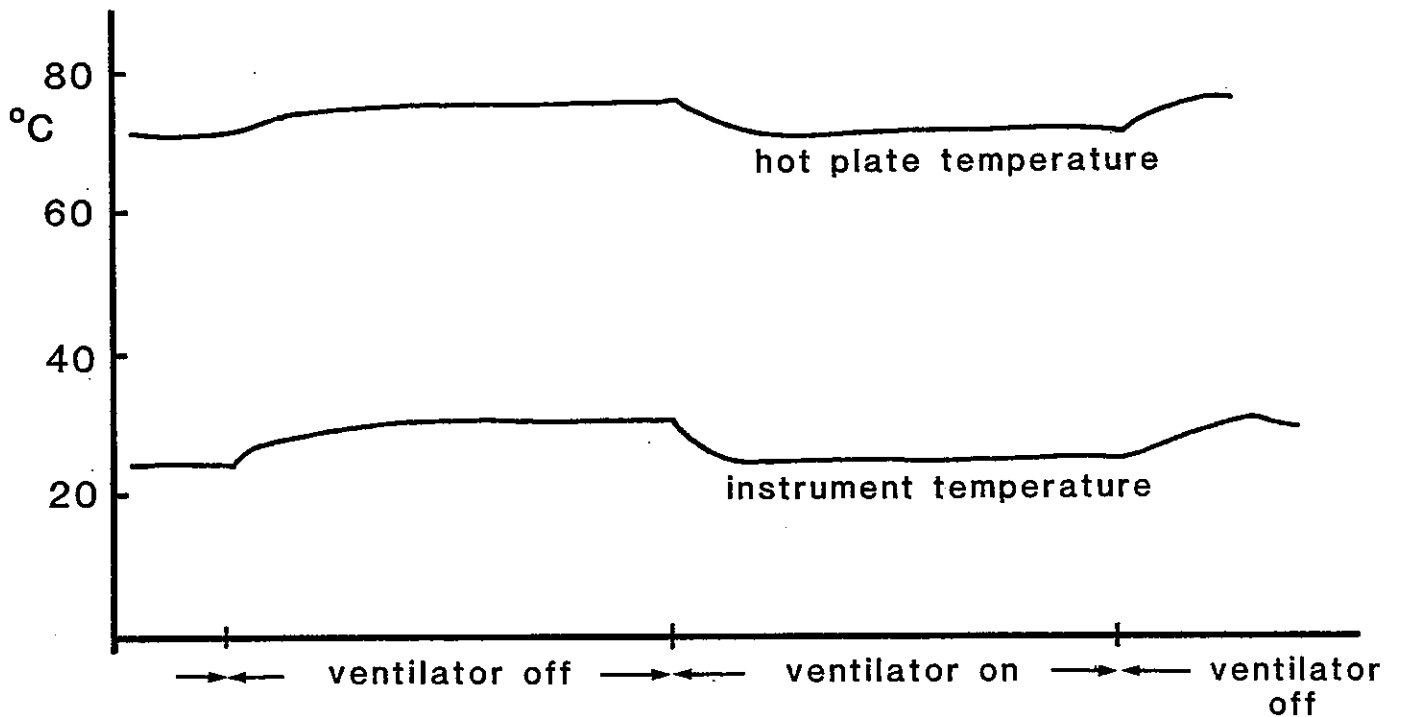
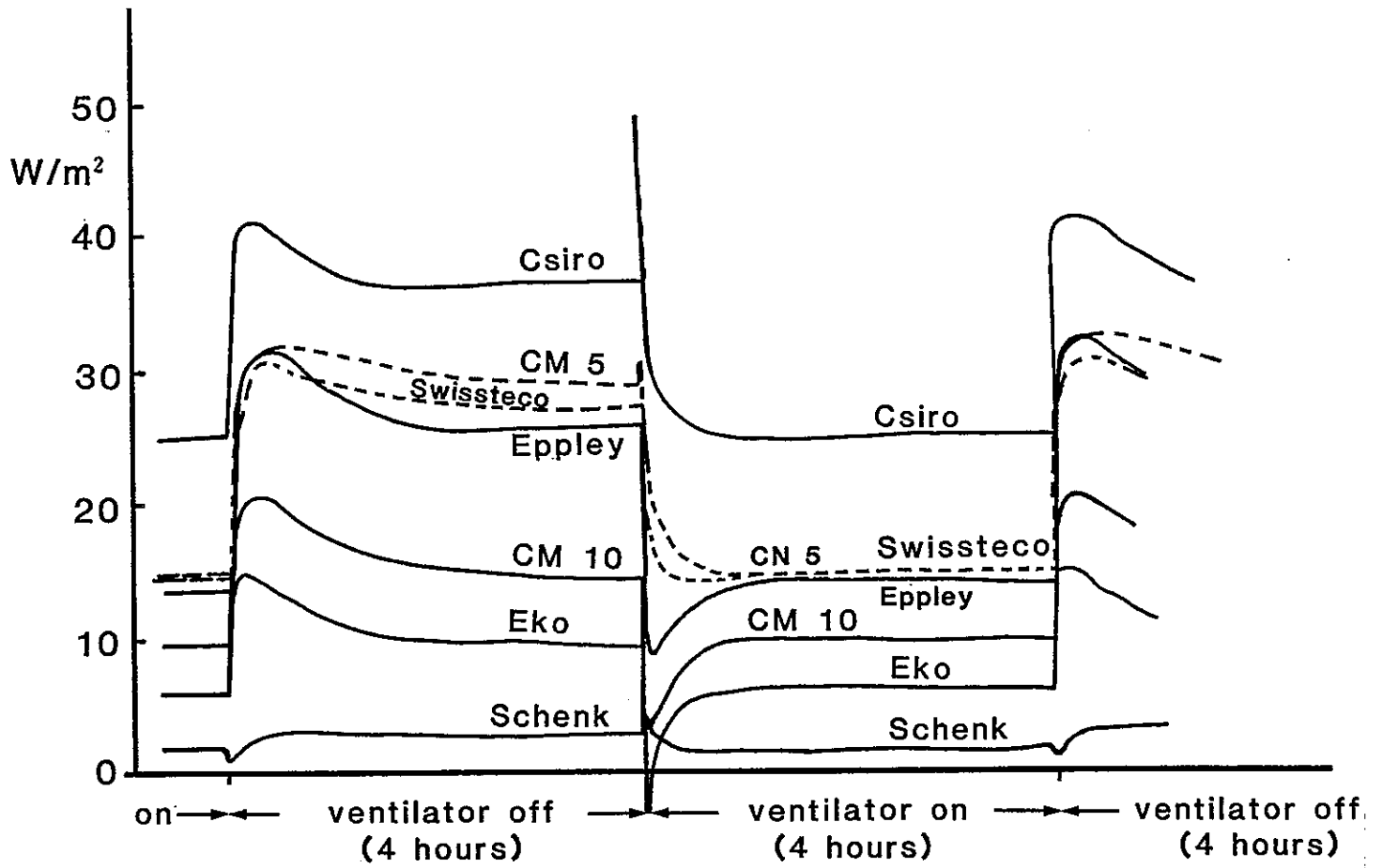
Zero offset – IR. radiation

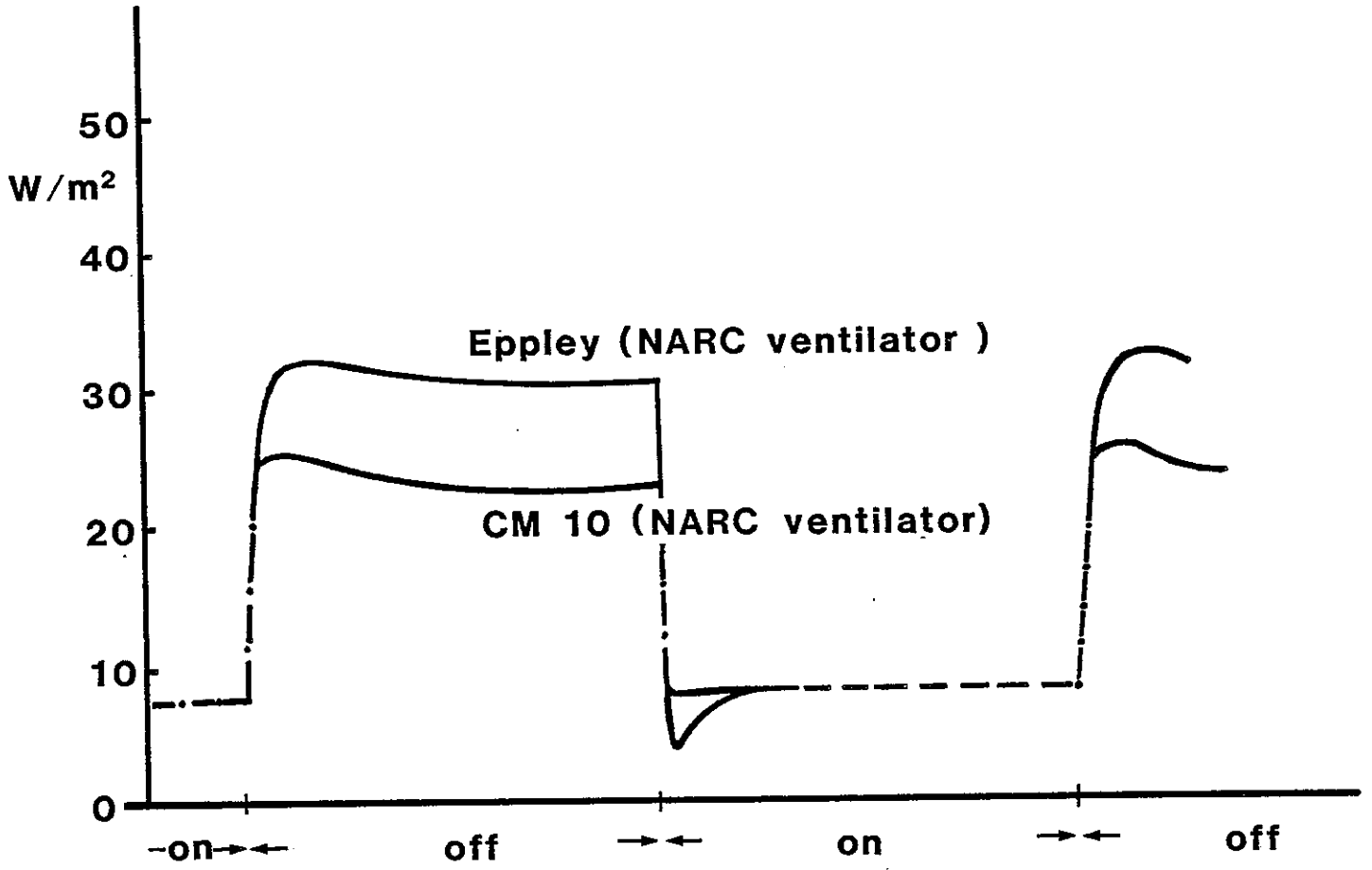


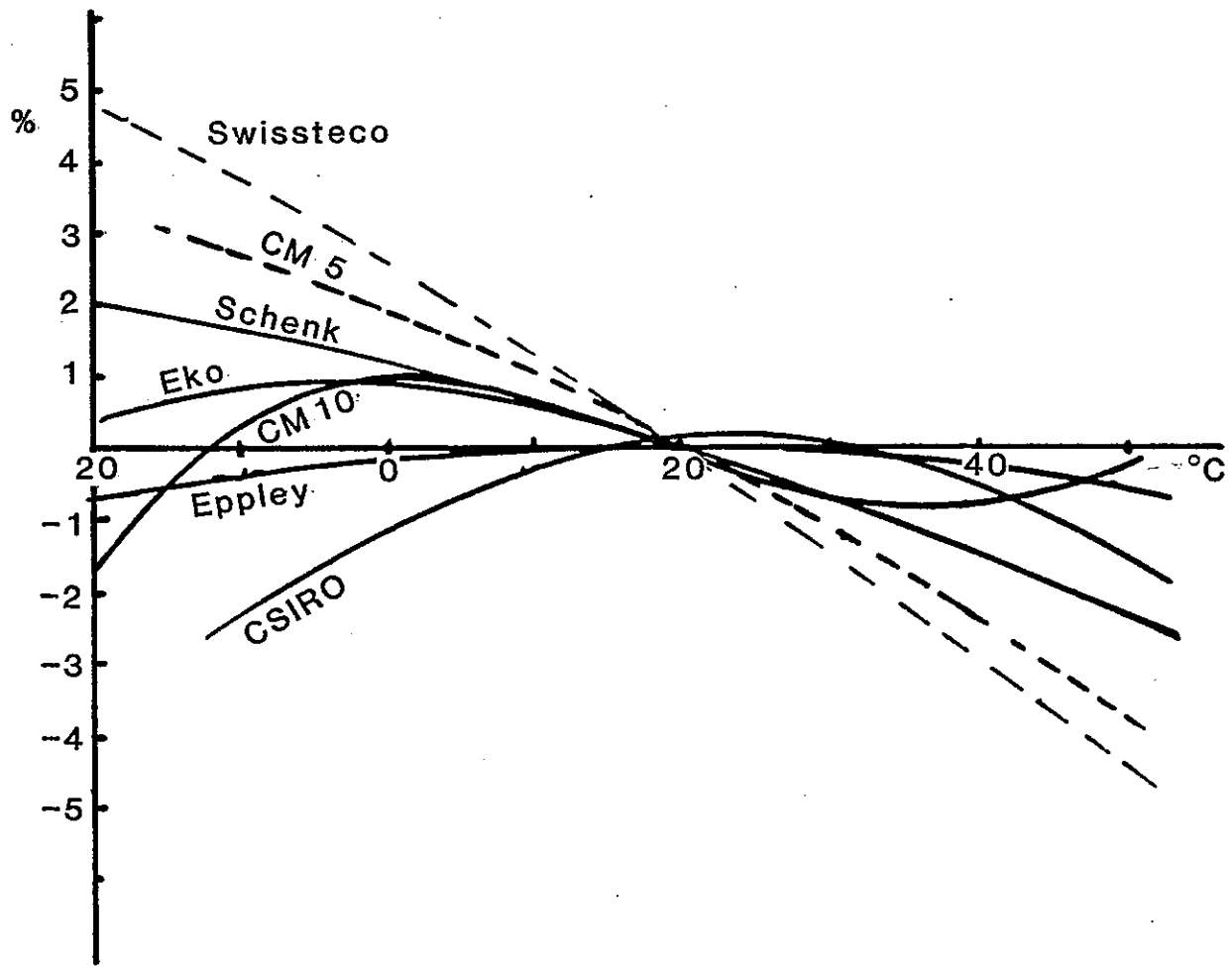
IR radiation on pyranometer (roughly estimated) :

$$(\sigma T_h^4 - \sigma T_a^4) \times \text{vie S} =$$



$$337 \times 0.75 = 250 \text{ W/m}^2$$







Temperature dependency
(relative to 20°C)

Linearity for  HORIZONTAL
 90° TILT

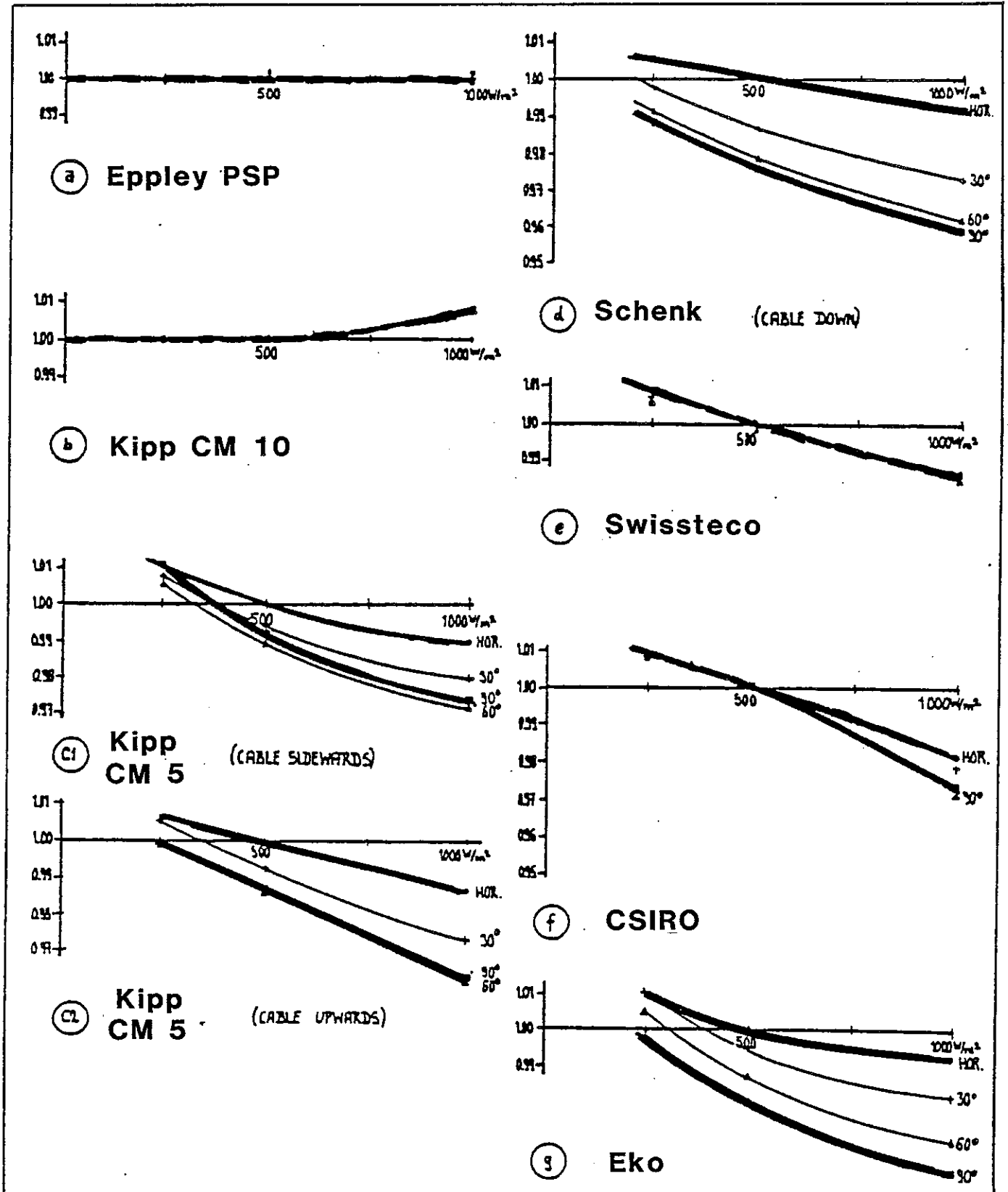


Figure 4

Linearity as a function of irradiance level and tilt angle

Average Cosine Response (% error)

Zenith Angle	20°	40°	60°	70°	80°	85°
Eppley PSP	-0.4	-1.5	-3.7	-4.1	- 9.0	-14.7
Kipp CM 10	-0.2	-0.7	-0.3	-0.3	0.3	1.0
Kipp CM 5	-0.6	-1.8	-4.5	-6.4	-13.7	-20.5
Schenk	-0.6	-1.6	-3.1	-3.9	- 4.4	- 4.9
Swissteco	1.8	1.7	0.7	-0.9	- 4.0	- 7.8
Csiro	0.5	1.4	0.7	0.8	- 5.2	--
Eko	-0.1	-0.5	-0.6	-0.3	- 0.6	--

Azimuth response at 70°-zenith angle relative to south (% error)

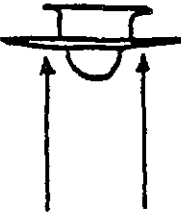





Zenith Angle	East	South	West	North
Eppley PSP	1.8	0	-2.0	-3.0
Kipp CM 10	0.2	0	0.4	0.6
Kipp CM 5	2.5	0	2.9	-1.5
Schenk	0.0	0	3.7	2.7
Swissteco	-0.8	0	1.0	-0.3
Csiro	5.4	0	-0.7	4.7
Eko	-1.1	0	-1.7	-1.8

Relative Sensitivity

as compared with Kipp & Zonen standard pyranometer CM11 820078
(5.65 $\mu\text{V/W m}^{-2}$) under a

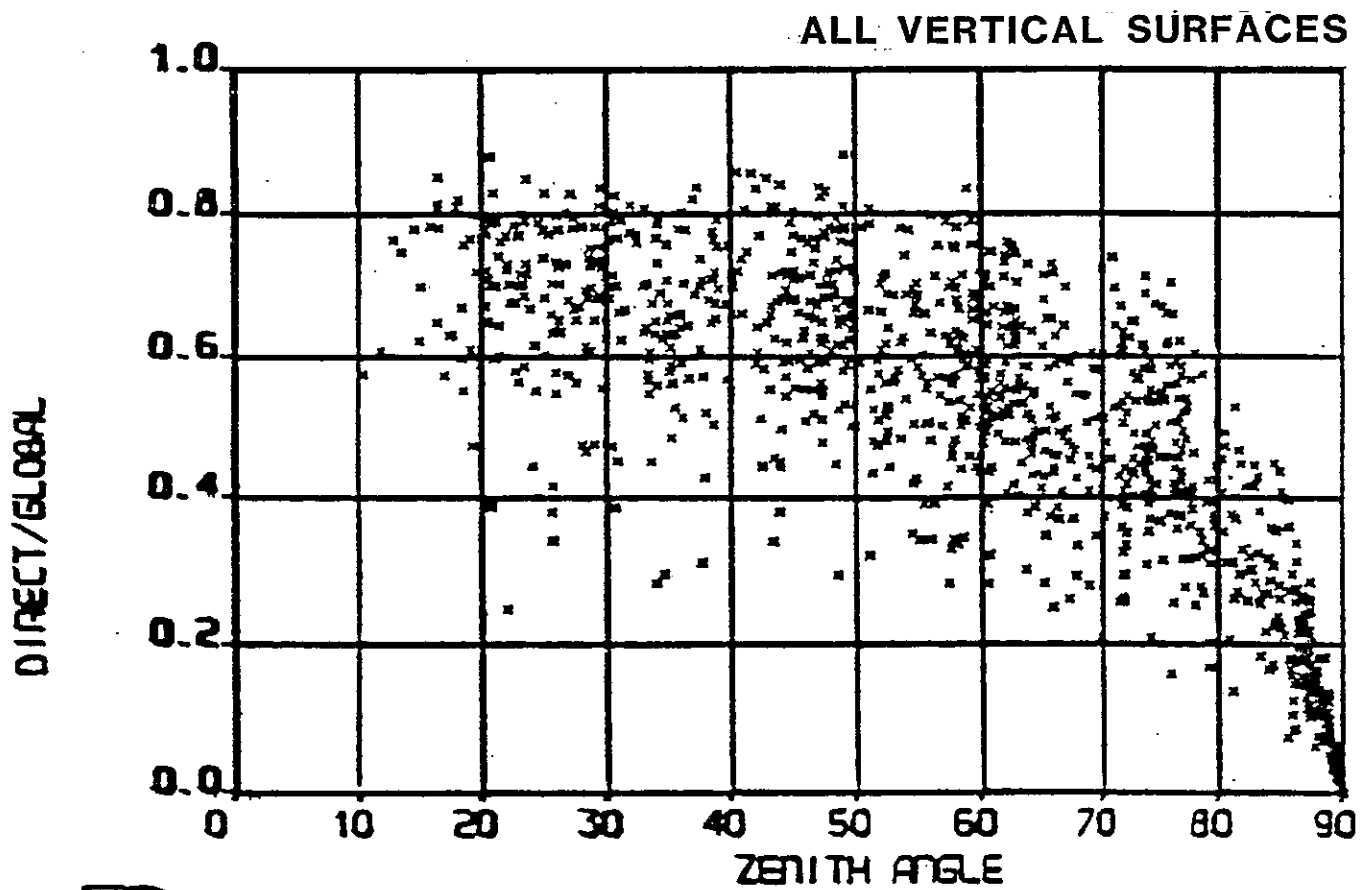
Manufacturer	Type	nr.	Xenonlamp	Tungsten Halogenlamp	Discrepancy
1. Eppley	PSP	20524F3	1.764	1.700	-3.5%
2. Kipp & Zonen	CM10	810121	0.015	0.815	0.0%
3. Kipp & Zonen	CM5	773656	2.061	2.044	-0.9%
4. Schenk		2009	2.699	2.609	-3.4%
5. Swissteco	SS-25	114A	2.725	2.598	-4.4%
6. Csiro	Mk.2	115	0.668	0.626	-6.5%
7. Eko		A81908	1.682	1.534	-9.4%

RELATIVE SENSITIVITY of Eppley PSP 17449 F3 as compared with Kipp & Zonen CM 11 820078 ($5.65 \mu\text{V}/\text{Wm}^{-2}$) under different conditions

Source	INDOORS			OUTDOORS			Oct. 1983
	Xenon lamp	Halogen lamp	Halogen lamp Filter $\lambda < 1.1\mu$	Diffuse sky	Clear sky	Clear sky Normal incid.	
Test set - up							
$\frac{\text{Sensitiv. PSP}}{\text{Sensitiv. CM 11}}$	1.594	1.541	1.606	1.575	1.530	1.578	
Relative to Xenon calibr.	1.000	0.967	1.008	0.988	0.960	0.990	*

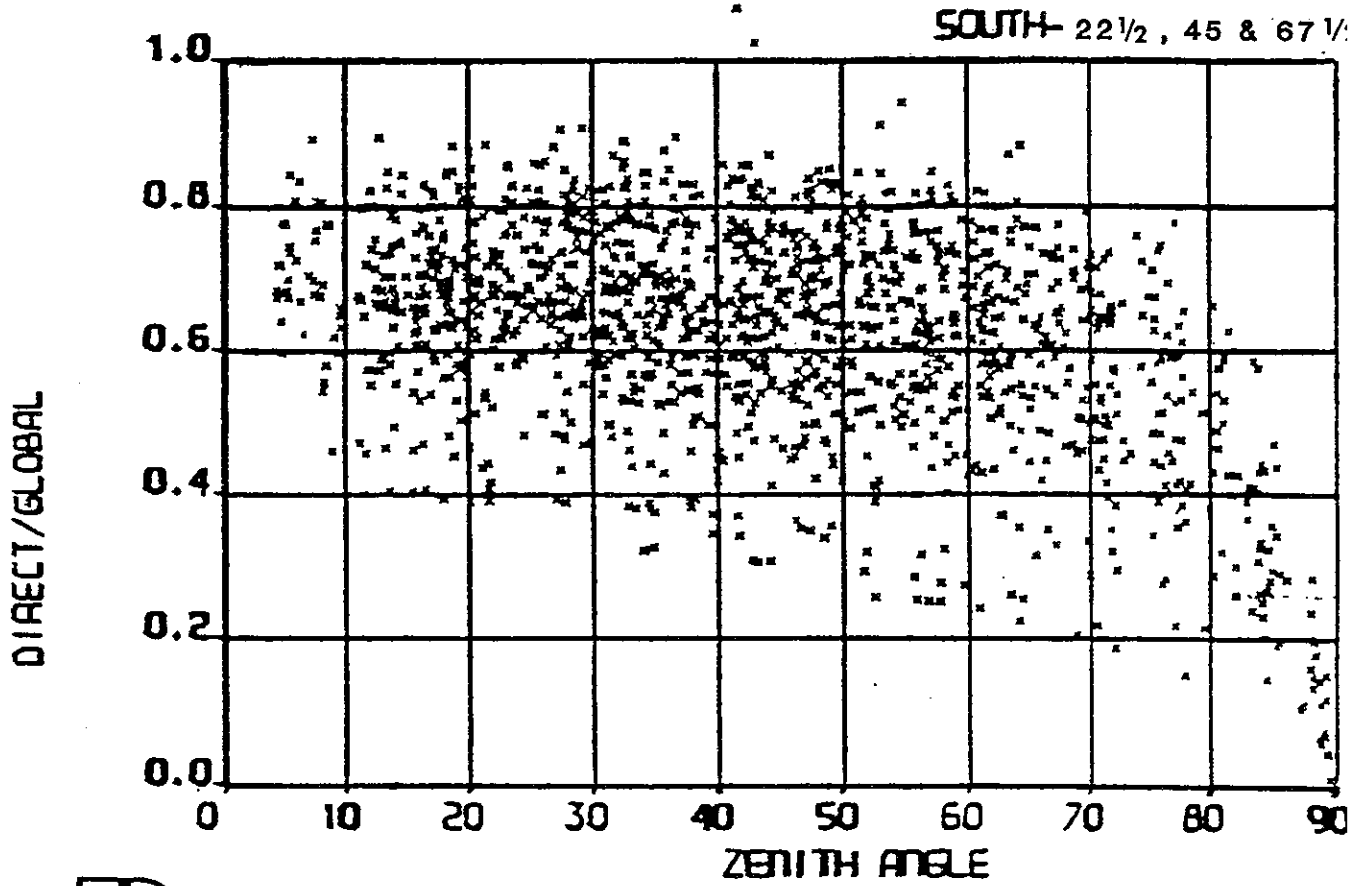
* cosine error

Intensity, temperature and tilt effects cannot be... the sources for these discrepancies

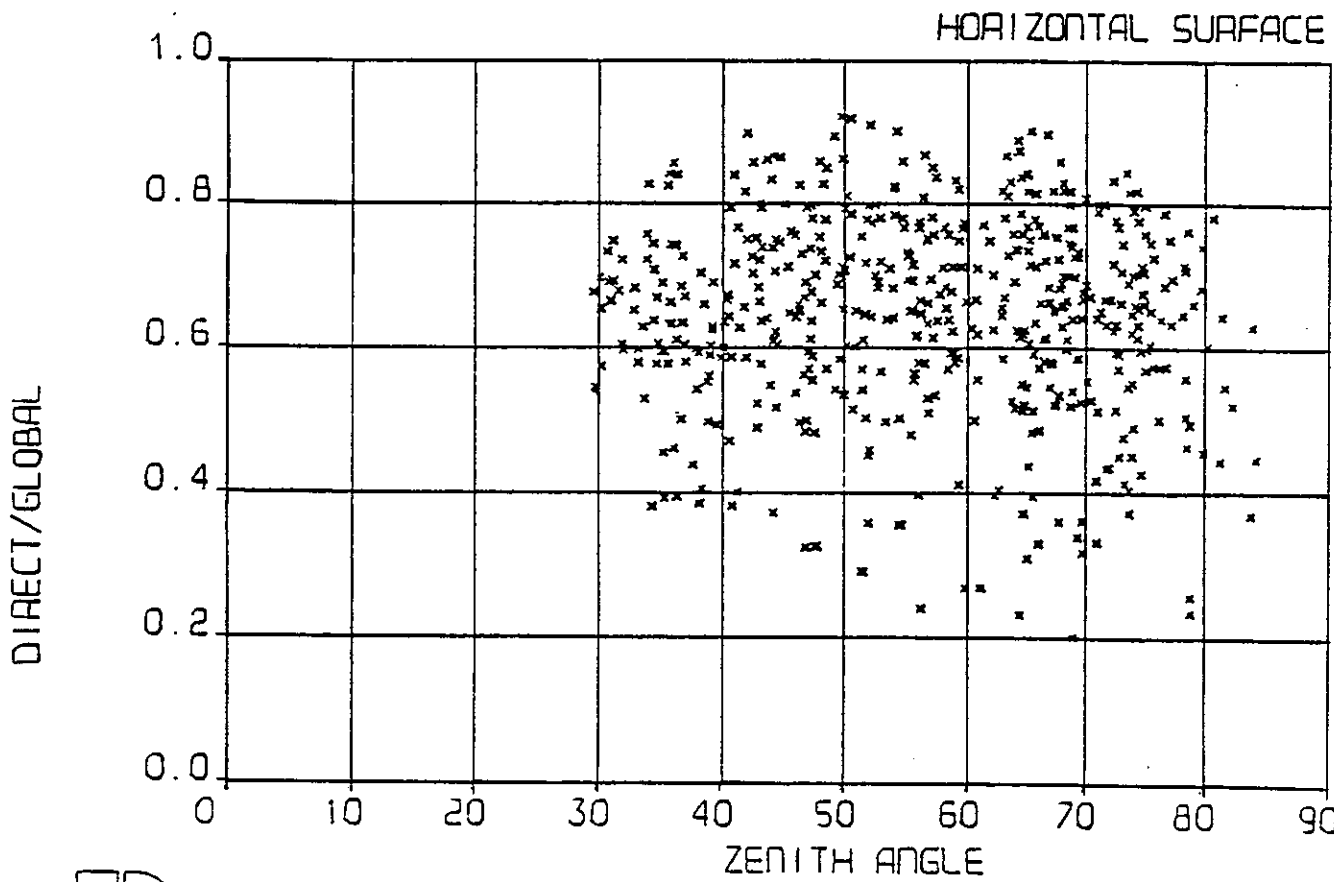


D

DIRECT/GLOBAL VERSUS ZENITH ANGLE

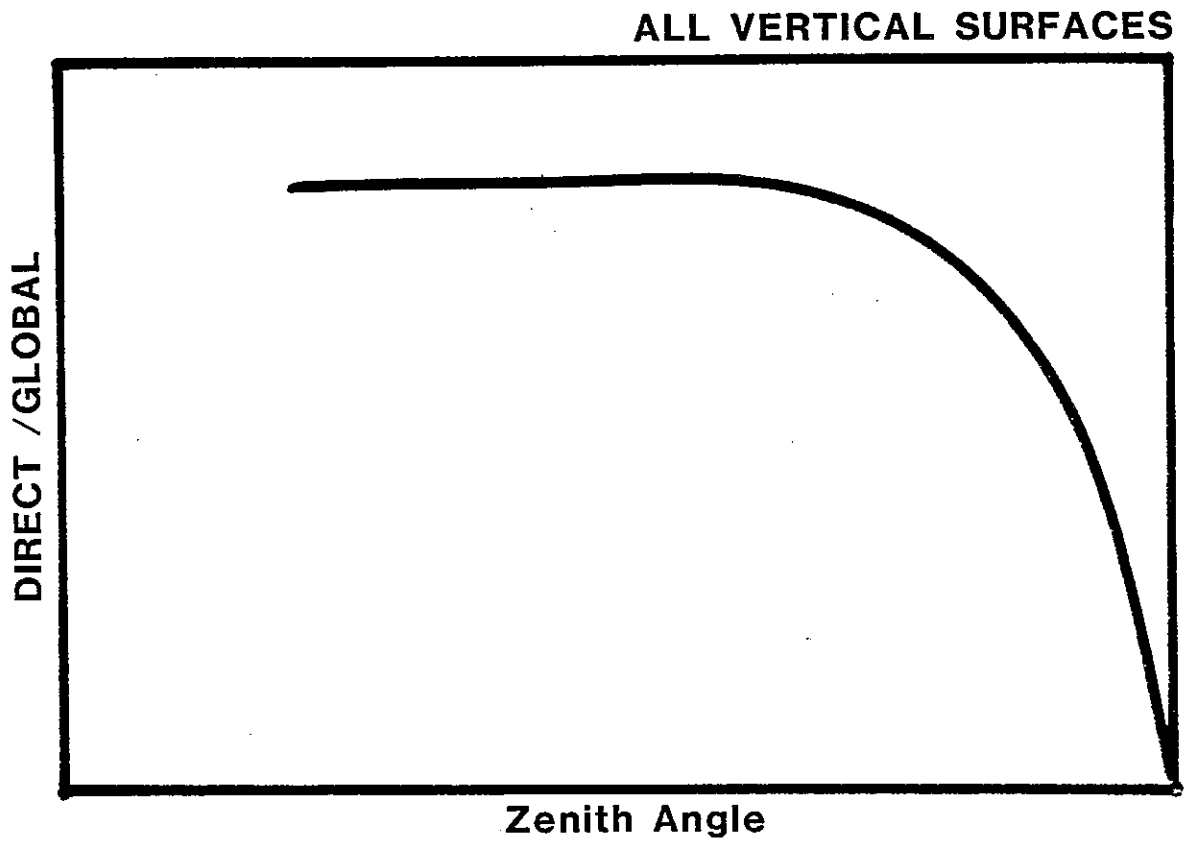


DIRECT/GLOBAL VERSUS ZENITH ANGLE



TD

DIRECT/GLOBAL VERSUS ZENITH ANGLE



(1 - cos. error) for Kipp CM10
(1 - cos. error) for Eppley PSP

$$\text{zenith angle } 80^\circ \frac{G_d}{G_t} = 0.40 \text{ cos. error} = +0.3\% \text{ error in } G_t = +0.1\%$$

$$\text{zenith angle } 80^\circ \frac{G_D}{G_t} = 0.40 \text{ cos. error} = -9.0\% \text{ error in } G_t \approx -3.6\%$$

